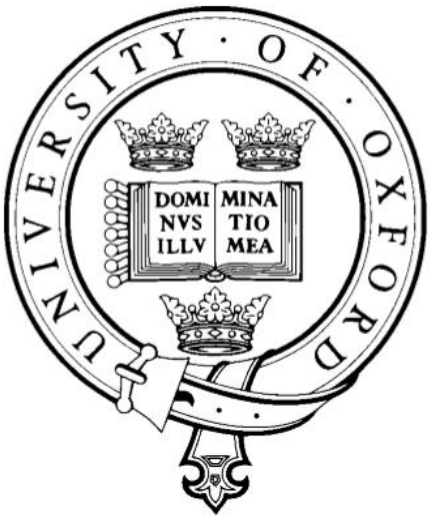
Silyl Radical-Mediated Late-Stage Hydrofunctionalisation of Alkenes



Sandrine Monique Hell

Wolfson College

University of Oxford

Supervised by

Professor Véronique Gouverneur, FRS

December 16, 2020

This thesis is submitted to the Board of the Faculty of Physical Sciences, in partial fulfilment of the requirements for the degree of Doctor of Philosophy at the University of Oxford

Declaration

I hereby declare that the work presented in this thesis was conducted under the supervision of Prof. Véronique Gouverneur FRS FRSC and carried out at the Chemistry Research Laboratory, University of Oxford, and at Janssen CILAG (Toledo, Spain) unless otherwise specified. All the work is my own, except where otherwise stated, and has not been submitted for any other degree at this or any other university.

Sandrine Monique Hell

December 16, 2020

Dedication

This thesis is dedicated in its entirety to my parents Martine and Clément, who always believed in me and supported and supported me throughout all the milestones of my life.

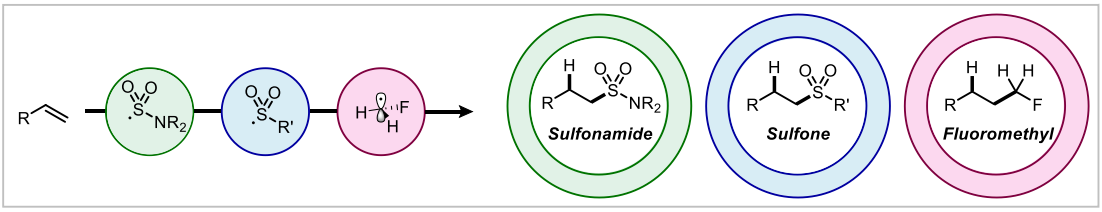
“It always seems impossible until it’s done.”

Nelson Mandela

Sandrine Monique Hell - Wolfson College - DPhil Chemistry - Michaelmas Term 2020

Abstract: Silyl Radical-Mediated Late-Stage Hydrofunctionalisation of Alkenes

In the last decades, photochemistry has been at the forefront of organic chemistry as a modern tool for the synthesis of organic compounds in early- and late-stage functionalisation. This thesis consists of the development of novel methodologies for the late-stage hydrofunctionalisation of alkenes under visible light activation. Specifically, the reactivity of the tris(trimethylsilyl)silyl radical is harnessed for the activation of different organohalides. A general introduction to photochemistry, silyl radicals and hydrofunctionalisation of alkenes is described in **Chapter 1**. In **Chapter 2**, the development of an operationally simple and cost-effective protocol for the late-stage hydrosulfamoylation of electron-deficient alkenes using sulfamoyl chlorides as radical precursors is described. The success of this transformation relies on the generation of a sulfamoyl radical by direct chlorine atom abstraction from a silyl radical. In **Chapter 3**, a facile and robust protocol for the hydrosulfonylation of alkenes is presented. The reaction is amenable to scale-up and allows for the preparation of relevant building blocks for drug discovery in batch and in continuous flow. **Chapter 4** discusses the generation of the fluoromethyl radical from fluoroiodomethane under visible light activation. The application of this protocol has been validated on the ^{18}F-hydrofluoromethylation of alkene-containing biologically active molecules. **Chapter 5** provides experimental data and analysis for the work described in this thesis.



Abbreviations

Å	angström
A	electron acceptor
Ac	acetyl
acac	acetylacetone
Ad	adamantane
ADME	absorption, distribution, metabolism, and excretion
AIBN	2,2′-azobis(2-methylpropionitrile)
Alk	alkyl
Ar	aryl
Asp	aspartic acid
ATRA	atom transfer radical addition
AY	activity yield
B_2mpd_2	4,4,4’,4’,6,6,6’,6’-octamethyl-2,2’-bi(1,3,2-oxaborinane)
b.p.	boiling point
bpy	2,2′-bipyridin
B_2Pin_2	bis(pinacolato)diboron
BDE	bond dissociation energy
BIm	bis(1-imidazolyl)methane
Bn	benzyl
Boc	*tert*-butyloxycarbonyl
BTMG	2-tert-butyl-1,1,3,3-tetramethylguanidine
Bu	butyl
Bz	benzoyl
Cbz	carboxybenzyl
CDK	cyclin-dependent kinase
CNS	Central Nervous system
CV	cyclic voltammetry
Cy	cyclohexyl
Cys	Cysteine
CzlPN	1,2,3,5-tetrakis(carbazol-9-yl)-4,6-dicyanobenzene
D	electron donor
DABCO	1,4-diazabicyclo(2,2,2)octane
DABSO	1,4-diazabicyclo[2.2.2]octane bis(sulfur dioxide)
dap	2,9-bis(4-anisyl)-1,10-phenanthroline
DAST	(diethylamino)sulfur trifluoride
dba	dibenzylideneacetone
DCE	1,2-dichloroethane
DCM	dichloromethane
$dF(CF_3)ppy$	3,5-difluoro-2-[5-(trifluoromethyl)-2-pyridinyl]benzene
DFT	density functional theory
DIBAL-H	diisobutylaluminium hydride
DIPEA	*N*,*N*-diisopropylethylamine
DMA	*N*,*N*-dimethylacetamide
DMAc	*N*,*N*-dimethylacetamide
DME	Dimethoxyethane

DMF	dimethylformamide
DMSO	dimethylsulfoxide
d.r.	diastereomeric ratio
DSC	dynamic Scanning Calorimetry
dtbbpy	4,4′-di-tert-butyl-2,2′-dipyridyl
EDA	electron donor acceptor
e.g.	exempli gratia, “for example”
EPR	electron paramagnetic resonance
ESI-TOF	electrospray ionization-time of flight
Et	ethyl
fac	facial
FCH	fluorocholine
FET	*O*-fluoroethyl-*L*-tyrosine
FDG	2-deoxy-2-fluoroglucose
GC-MS	gas-chromatography coupled mass spectrometry
Gln	Glutamine
HAA	hydrogen atom abstraction
HAD	hydrogen atom donor
HAT	hydrogen atom abstraction
HATU	Hexafluorophosphate azabenzotriazole tetramethyl uronium
HIV	human immunodeficiency viruses
HPLC	high-performance liquid chromatography
HRMS	high resolution mass spectrometry
HTP	hydroxythiophenol
HTS	high throughput screening
i.e.	id est, “that is”
IMes	1,3-dimesitylimidazol-2-ylidene
*i*Pr	isopropyl
IR	infrared
JohnPhos	(2-biphenyl)di-tert-butylphosphine
k	rate constant
K_{222}	4,7,13,16,21,24-Hexaoxa-1,10-diazabicyclo[8.8.8]hexacosane
kq	quenching rate constant
LCMS	liquid chromatography coupled mass spectrometry
LED	light-emitting diode
LSF	late-stage functionalisation
Lys	lysine
MA	molar activity
max	maximum
*m*CPBA	meta-chloroperbenzoic acid
Me	methyl
Mes-Acr	9-mesityl-10-methylacridinium
MLCT	metal to ligand charge transfer
MW	Microwave
n.d.	not detected
NFSI	*N*-fluorobenzenesulfonimide
NMR	nuclear magnetic resonance
NOE	nuclear overhauser effect
NOESY	nuclear overhauser effect spectroscopy
NTf_2	*N*,*N*-bis(trifluoromethylsulfonyl)imide

Nu	nucleophile
OMe	methoxide
OTf	trifluoromethanesulfonate
ox	oxidation
PC	photocatalyst
PEEK	polyether ether ketones
PET	positron emission tomography
Ph	phenyl
Phe	Phenylalanine
Phth	phthaloyl
PIDA	phenyliodine(III) diacetate
ppm	Parts per million
ppy	2-phenylpyridine
pr	propyl
py	pyridine
PRC	polarity reversal catalysis
R	generic substituent
RCP	radiochemical purity
RCY	radiochemical yield
red	reduction
rt	room temperature
S	singlet state
SAR	structure activity relationship
SCE	standard calomel electrode
SET	single electron transfer
SOMO	singly occupied molecular orbitals
SuFEx	sulfur (VI) fluoride exchange
T	triplet state
$t_{1/2}$	half-life
TBS	*tert*-butyldimethylsilyl
t-Bu	*tert*-butyl
TBAF	tetrabutylammonium fluoride
TEAF	tetraethylammonium fluoride
TEMPO	(2,2,6,6-tetramethylpiperidin-1-yl)oxyl or (2,2,6,6-tetramethylpiperidin-1-yl)oxidanyl
TES	triethylsilyl
TFA	trifluoroacetic acid
THF	tetrahydrofuran
Thr	threonine
TLC	thin layer chromatography
TMG	1,1,3,3-tetramethylguanidine
TMS	trimethylsilyl
trig	trigonal
Trp	tryptophan
TRP	transient receptor potential
tyr	tyrosine
UV	ultra-violet
Vis	visible
vs	versus
X	generic substituent or atom

Acknowledgements

First and foremost, I would like to thank my supervisor, Prof. Véronique Gouverneur, for giving me the opportunity to carry out my PhD in her research group, for her guidance and support. Her unwavering enthusiasm for science inspired me all over these years and kept me going with the chemistry. Véronique was always supportive and gave me the freedom to pursue diverse projects. She taught me invaluable lessons during these three years for which I will be always grateful.

I would also like to express my gratitude to Dr. Andrés Trabanco, scientific director at Janssen CILAG (Toledo, Spain), for being extremely supportive over these three years. He taught me the ropes to become a better scientist. I could not have imagined having a better industrial supervisor for my PhD study; I learnt so much from you, thank you Andrés! A deep thanks to Dr. Antonio Misale, senior scientist at Janssen CILAG (Toledo, Spain), who guided me during my stay in Toledo. I am grateful for many insightful discussions/suggestions we had, and I wish him all the best at Janssen in the future. I am also thankful to Dr. Daniel Oehlrich and Dr. Aldo Peschiulli for their guidance during my stay in Janssen (Beerse, Belgium). I am extremely thankful to all Janssen employees with whom it was a pleasure to daily work with, for their warm welcoming and their invaluable advices.

I would like to thank Prof. Benjamin Davis, my co-supervisor, as well as his research group for the really interesting group meetings and chats over coffee breaks. I will never forget the amazing Christmas dinner in Paris!

I would also like to thank Prof. Timothy Noël, Dr. Gabriele Laudadio and Xuanxiao Chen for providing with CV measurements: it was a great collaboration. I would like to thank Prof. Michael Willis for helpful discussions on sulfone chemistry.

I take this opportunity to express my greatest regards to all the Staffs of the Chemistry department of the University of Oxford for their kind help and co-operation. I am also extremely thankful to the Marie-Curie fellowship for their financial support during this PhD. I would like to thank Dr. Manuja Kaluarachchi-Soden for her support over these three years and for organising all the FLUDD events: you did an amazing work!

I am extremely thankful to all the VG group members: working with you all has been a real pleasure! Thank you for all the great moments we shared together. Big thanks to the F11 crew (Rob, Zijun, Konstantinos, Matt, Claudio, Jimmy) with who it was an enormous pleasure to work with. I will never forget the nice musical taste of my labmates (Little Pump, DJ Khaled, Taylor Swift). A special thanks to Jimmy and Matt: the lab is surely in a better place thanks to both of you! I also would like to thank Zijun, my deskmate. You are a talented scientist and musician! Many thanks to Robert Szpera for his unwavering support and valuable comments that guided me at the early stage of my PhD. I truly admire the scientist you are, and I am sure you will have a wonderful and successful career in the pharmaceutical industry or wherever destiny leads you! I will definitely miss the Tikki Tikki parties you organised. Thanks to Konstantinos for your delicious Greek food: you are a real Chef! If you ever get bored from chemistry, please open a restaurant. Thank you, Sebastiano, for joining our team on photochemistry! It was a real pleasure to work with you. You are a talented scientist, and I am sure that you will achieve many good things! I wish you all the best for your PhD in Véronique's group. A

special thanks to Matt, Fra, Jeroen, Claudio, Adeline, Sebastiano and Jimmy for proof reading parts of this thesis.

It is a genuine pleasure to express my deep thanks to the FLUDD students. Giulia, thank you for the nice time in Toledo and Beerse. Tim, thank you for our road trips in France, Switzerland, United-Kingdom and Spain. I will never forget your enthusiasm for the UK! I wish you all the best for your future career. A special thanks to Tobi for making this PhD a really fun adventure. I will keep a really sweet and fun souvenir from Toledo and Beerse with you, laughing and chatting will always be in my memory. I am sure that you will succeed in everything you are doing, and I hope to see you soon again.

Thank you to all the members who regularly joined us for pints (Adeline, Rob, Gianluca, Fra, Claudio, Konstantinos, Tim, Eddie, Natan, Bryan, Ryan, Andrew, Sebastiano, Alex, Myrto, Colm). I am so glad I met so many great persons.

I also would like to thank my housemates, Eddie, Joseph and Linus. I really enjoyed our evenings and dinners! A special thanks to Eddie for the delicious pulled pork.

I am extremely thankful to my parents, Martine and Clément, for their unconditional support and love. Thank you to all my family as a whole for being continuously present for me. Thank you also to my friends from France, Séverine, Camille, Julie, Laurine, Karène, Adèle, Jordan, Jérôme, and Laurent. Your countless support and friendship was a great comfort. A special thanks for those you came to visit me in Oxford, Toledo and Beerse, it was a lot of fun!

The biggest thank you goes to Claudio! I don’t know what I would have done without you, you guided me, motivated me along the whole PhD. I would never be able to write enough to give justice to my gratitude for everything you have done for me. We went

through every milestone together and here we are: submitting our thesis together! I could not wish better partner in life and at work. I am thrilled to pursue this adventure with you in Princeton for our Postdoc and I cannot wait to see where the future will take us.

Contents

Chapter 1 1
1.1 Light-Promoted Transformations 2
1.1.1 Introduction to Photochemistry 2
1.1.2 Photoredox Catalysis 4
1.2 Silyl Radical-Mediated Halogen Atom Abstraction 8
1.2.1 Radical Tin-Mediated Protodehalogenation 8
1.2.2 Silanes as a viable alternative to tin hydrides 10
1.2.3 Properties of silyl radicals 11
1.2.4 Early studies: generation and reactivity of silyl radicals 12
1.3 State-of-the-Art: Photochemical Silyl Radical-Mediated Halogen Atom Abstraction 16
1.3.1 Protodehalogenation of Organohalides 17
1.3.2 Silyl Radical-Mediated $C(sp^2)–C(sp^3)$ Bond Formation 20
1.3.3 Silyl Radical-Mediated $C(sp^3)–C(sp^3)$ Bond Formation 24
1.3.4 Silyl Radical-Mediated Fluorination and (Per)Fluoroalkylation 26
1.4 Hydrofunctionalisation of Alkenes 30
1.4.1 Transition-Metal Catalysed Hydrofunctionalisation of Alkenes 32
1.4.2 Anti-Markovnikov Radical Hydrofunctionalisation of Alkenes 34
1.5 Late-Stage Silyl Radical-Mediated Hydrofunctionalisation of Alkenes 36
1.6 References 39
Chapter 2 41
2.1 Introduction to Sulfonamides 43
2.2 Synthesis of Sulfonamides 44
2.2.1 Traditional Procedures for the Synthesis of Sulfonamides 44
2.2.2 Sulfonamide Synthesis using Sulfur Dioxide Surrogates 45
2.2.3 Synthesis of Aliphatic Sulfonamides 47
2.3 Sulfamoyl Radicals: Properties and Reactivity 49
2.4 Single-Electron Reduction of Sulfamoyl Chlorides 51
2.5 Strategy for the Direct Activation of Sulfamoyl Chlorides 53
2.6 Initial Investigations 56
2.7 Scope of the Hydrosulfamoylation of Electron-Deficient Alkenes 60
2.7.1 Scope of Sulfamoyl Chlorides 60
2.7.2 Scope of Electron-Deficient Alkenes 61
2.7.3 Scale-up Experiment 64
2.7.4 Further Transformations 65

2.8 Preparation of Sulfonamide-Containing Cyclobutanes 66
2.8.1 Hydrosulfamoylation of Cyclobutenes 66
2.8.2 Preparation of Sulfonamide-Containing Cyclobutyl-Spirooxindoles 68
2.9 Mechanistic Investigations 71
2.10 Limitations of this Methodology 76
2.11 Comparison of our Methodology to a Recently Disclosed Radical Sulfamoylation using Sulfamoyl Chloride 77
2.12 Conclusion 79
2.13 Future Work 80
2.14 References 81
Chapter 3 85
3.1 Introduction to Sulfones 87
3.2 Synthesis of Sulfones 88
3.2.1 General Strategies for the Synthesis of Sulfones 88
3.2.2 Radical-Mediated Sulfonylation of Alkenes 91
3.3 Strategy for the Hydrosulfonylation of Alkenes 95
3.4 Optimisation of the Reaction Conditions 97
3.5 Hydrosulfonylation of Electron-Deficient Alkenes 100
3.6 Hydrosulfonylation of Cyclobutenes 106
3.6.1 Scope of Cyclobutenes 106
3.6.2 Scale-up Experiments 107
3.6.3 Quaternisation of the Carbon-Centred Radical Intermediate 112
3.7 Hydrosulfonylation of Alkynes 113
3.8 Hydrosulfonylation of Unactivated Alkenes 116
3.9 Mechanistic Considerations 119
3.9.1 Control Experiments 119
3.9.2 Stern-Volmer Luminescence Quenching 122
3.9.3 Proposed Mechanism 125
3.10 Comparison of this Methodology to a Recently Disclosed Radical Sulfonylation using Sodium Sulfinates 128
3.11 Conclusion 130
3.12 Future Work 131
3.13 References 132
Chapter 4 136
4.1 Introduction to Fluorine 137

4.2 Synthesis of the Fluoromethyl Groups 139
4.2.1 Common Methods 139
4.2.2 Hydrofluoroalkylation of Alkenes 139
4.2.3 Radical Fluoromethylation of Alkenes 142
4.3 Fluoroiodomethane as an Ideal Fluoromethyl Radical Precursor 144
4.4 Optimisation of the Reaction Conditions 147
4.5 Hydrofluoromethylation of Alkenes 151
4.5.1 Scope of Electron-Deficient Alkenes 151
4.5.2 Scale-up Experiment 154
4.5.3 Metallaphotoredox Fluoromethylation of Aryl Bromides 155
4.6 Generation of Fluorinated Ethyl Radicals 157
4.7 Generation of Other Halomethyl Radicals 160
4.8 Competition Experiment 162
4.9 Robustness Screening 163
4.10 ^{18}F-Fluoromethylation of Alkenes 168
4.10.1 Introduction to PET Imaging 168
4.10.2 ^{18}F-Hydrofluoromethylation of Electron-Deficient Alkenes 170
4.11 Mechanistic Investigations 173
4.12 Limitations 176
4.13 Conclusion 177
4.14 Future Work 178
4.15 References 179
Chapter 5 184
5.1 General Informations 185
5.2 Experimental Procedures and Characterisation of Compounds from Chapter 2 186
5.2.1 Synthesis of Starting Materials 187
5.2.2 Optimisation of the Reaction Conditions 189
5.2.3 General Procedures 190
5.2.4 Characterisation: Hydrosulfamoylation of Electron-Deficient Alkenes 192
5.2.5 Scale-up Experiment 207
5.2.6 Further Transformations of Sulfonamide 2.91 208
5.2.7 Hydrosulfamoylation of Cyclobutenes 211
5.2.8 Mechanistic Investigations 223
5.2.9 Limitations 226
5.2.10 Cyclic Voltammetry[b] 227

5.3 Experimental Procedures and Characterisation of Compounds from Chapter 3 229
5.3.1 Synthesis of Starting Materials.....230
5.3.2 Optimisation of the Reaction Conditions 231
5.3.3 General Procedures.....232
5.3.4 Characterisation: Hydrosulfonylation of Electron-Deficient Alkenes 234
3.5.5 Hydrosulfonylation of cyclobutenes.....256
5.3.6 Scale-up experiments.....275
5.3.7 Characterisation: Hydrosulfonylation of alkynes 278
5.3.8 Characterisation: Hydrosulfonylation of unactivated alkenes.....283
5.3.9 Mechanistic investigations 290
5.3.10 X-ray - Crystallographic Data for 3.111.....295
5.4 Experimental procedures and characterisation of compounds from Chapter 4 297
5.4.1 Synthesis of starting materials.....298
5.4.2 Optimisation of the reaction conditions.....298
5.4.3 General procedures 299
5.4.4 Characterisation: Hydrofluoromethylation of Electron-Deficient Alkenes.....300
5.4.5 Scale-up experiment[b] 310
5.4.6 Metallaphotoredox fluoromethylation[a] 311
5.4.7 Generation of Fluorinated Ethyl Radicals 312
5.4.8 Generation of Other Halomethyl Radicals 314
5.4.9 Competition experiments.....317
5.4.10 Robustness screen.....320
5.4.11 [^{18}F]-Hydrofluoromethylation of alkenes[a,c] 321
5.4.12 Mechanistic investigation.....324
5.4.13 Cyclic Voltammetry[d] 325
5.5 References 327

Chapter 1

Introduction

1.1 Light-Promoted Transformations

1.1.1 Introduction to Photochemistry

Recent years have witnessed significant advances in organic chemistry, as endorsed by the multitude of Nobel Prizes awarded in the field. Specifically, synthetic organic chemistry has allowed for major breakthroughs in the pharmaceutical and material industry. The increased demand for processes utilising "green" chemicals, which generate minimal amounts of waste has surged the scientific community to explore the potential of light-promoted transformations.[1] As visible light stands out as a green, non-hazardous, easily-accessible, and traceless energy source, the development of visible light-driven methods has significantly impacted the development of sustainable chemistry.[2–4] The access to the excited-states of molecules upon light irradiation stretches the limits of possibilities to generate reactive intermediates which can participate in novel chemical reactions (**Figure 1.1**).[5]

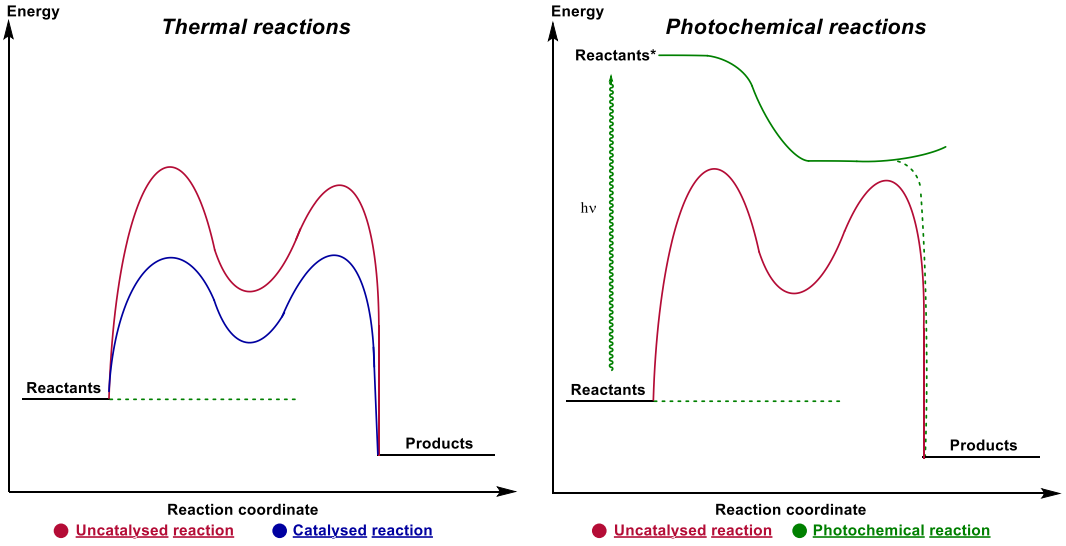


Figure 1.1: Reaction energy profile of thermal and photochemical reactions.

Furthermore, once in the excited state, the remaining process is always energetically favourable (exergonic reaction). Importantly, an excited molecule possesses different

physicochemical properties and different reactivities, with respect to the same molecule in its ground state. This change of properties allows for the formation of thermodynamically disfavoured products by unlocking unconventional reaction pathways and overcoming large kinetic barriers.

In photochemistry, reactions are initiated by the absorption of energy in the form of light (UV or visible light).[6] This process has been well described by Jablonski with a representative energy diagram (**Figure 1.2**).

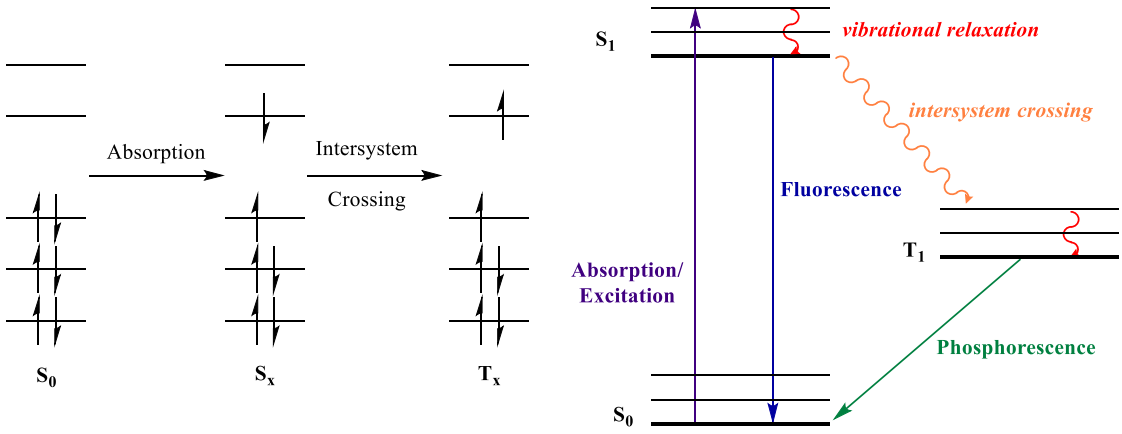


Figure 1.2: Simplified Molecular Orbital and Jablonski-Diagram.

Upon irradiation with light of a specific wavelength, a single-electron transfer promotes an electron from a low energy orbital (ground state S_0) to an excited state S_x (higher energy level). During this process, two electrons become orbitally unpaired. At this stage, the energy release can occur *via* radiationless transitions, such as internal conversion or vibrational relaxation. In these events, the electron transitions between different vibrational levels and thus lowers its energy. Another pathway enabling the excited electron to return from the excited state S_1 to the ground state is through the emission of a photon: this process is called fluorescence (spin allowed). On the other hand, the process involving the loss of energy between two different spin state (e.g. $T_x \rightarrow S_0$) is called phosphorescence (spin forbidden). The interconversion of an electron from a singlet excited state to a triplet excited state is called intersystem crossing. In this event,

the electron spin is flipped to a lower energy orbital and transferred to a long-lived triplet excited state, allowing to reduce overall repulsion between the unpaired electrons. In contrast to the singlet state, the lifetime of a molecule in the triplet state ranges upwards from 10^{-4} seconds, and therefore increases the probability for it to 1) encounter other molecules for chemical reactions, 2) transfer its energy, or 3) undergo molecular rearrangement.[5–7]

1.1.2 Photoredox Catalysis

Photoredox catalysis has witnessed a rapid progress in the last decade, enabling the development of new radical-mediated transformations.[8–11] In these transformations, a chromophore catalyst, such as a metal polyaryl complex or an organic dye sensitiser, absorbs visible light and can further engage in single-electron transfer processes with organic molecules.[12,13] Such photocatalysts are highly reactive and can simultaneously act as an oxidant and a reductant. Furthermore, visible light photoredox reactions are of particular interest since most organic compounds do not absorb visible light, and therefore allows for selective activation of the photocatalyst, avoiding undesired side-reactions.

The concept of photoredox catalysis is similar to the one illustrated in **Figure 1.2**. Upon irradiation with light, an electron from the photocatalyst's metal-centred orbital is promoted from the singlet ground state S_0 to a singlet excited state (ligand centred π^* orbital) by a spin-allowed metal to ligand charge transfer (MLCT) event. This event is followed by rapid intersystem crossing, which generates a stable and long-lived triplet excited state. Importantly, the lifetime of the triplet state (e.g. τ = 1100 ns for $Ru(bpy)_3^{2+}$) is longer than the singlet state, enabling single-electron transfer events to proceed. Once

in the triplet excited state, this highly reactive molecule can undergo intermolecular quenching (kq), which is responsible for the reactivity displayed by these photoexcited catalysts (bimolecular electron transfer, **Figure 1.3**). The excited photocatalyst can act as a reductant (oxidative quenching cycle) and thus reduce an electron acceptor *via* single-electron donation. Upon this electron transfer, a radical anion **A** is formed along with the oxidised form of the photocatalyst. On the other hand, the excited photocatalyst can act as an oxidant (reductive quenching cycle) and accept an electron from an electron donor, generating a radical cation and the reduced form of the photocatalyst. The resulting form of the photocatalyst will then undergo a second single electron transfer (either oxidation or reduction), regenerating the photocatalyst in its original oxidation state (ground state). Importantly, the formation of the radical ion upon single-electron transfer is in direct competition with back-electron transfer reactions, leading to the regeneration of the photocatalyst ground state. This process is often circumvented through the careful design of the ligand framework of the photocatalyst.[14,15]

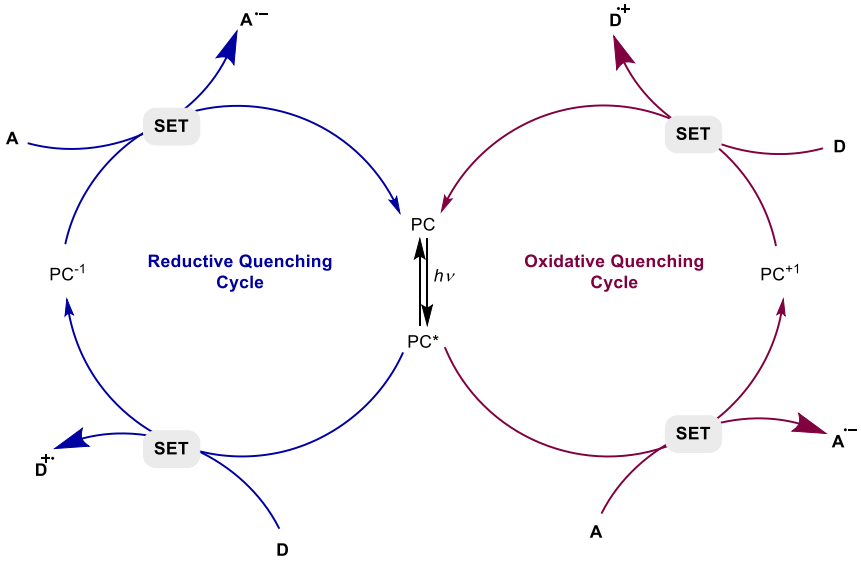


Figure 1.3: Oxidative and reductive quenching cycles. PC = photocatalyst. A = electron acceptor. D = electron donor. PC^{-1} = reductant. PC^{+1} = oxidant.

Two categories of photocatalysts are commonly employed in photoredox catalysis (**Figure 1.4**). Metal-based photocatalysts, ruthenium (**1.1**) and iridium (**1.2**) complexes being the most studied ones; and organic photocatalysts, such as Eosin Y (**1.3**) or Mes-Acr^{+} (**1.4**), which have been recognised as economical and environmentally friendly photocatalysts, as they are metal-free.

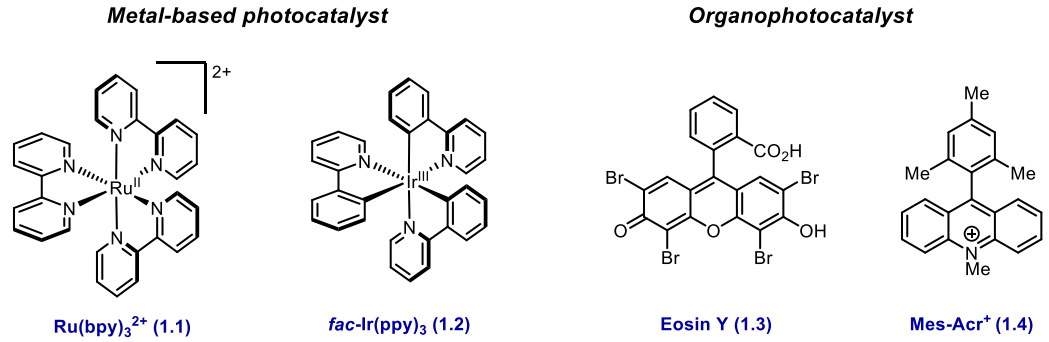


Figure 1.4: Common photocatalysts in photoredox catalysis.

The substitution of the ligands of transition-metal-based photocatalysts can significantly alter their redox properties. Electron-donating substituents (e.g. **1.5**) make them more reducing, whereas electron-withdrawing groups render them more oxidising (e.g. **1.6**, **Figure 1.5**).

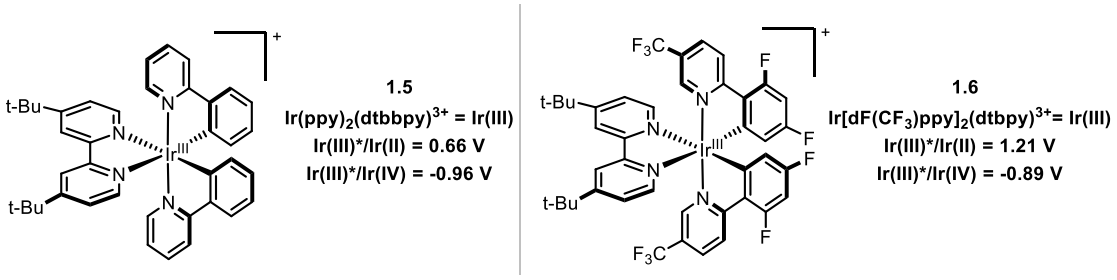


Figure 1.5: Modulation of reduction and oxidation potential depending on the substituent pattern.

The fine-tuning of the ligand framework is essential, as it allows to design novel photocatalysts with unique redox properties and therefore promote the selective activation of an organic molecule. The ability of a photocatalyst to undergo single-electron transfer with another molecule can be estimated with the Rehm-Weller

equation.[16] This equation describes the thermodynamic feasibility of the single-electron transfer process, where ΔG_{ET} is the driving force of the electron transfer reaction; $E(D^+/D)$ and $E(A/A^-)$ are the donor and acceptor ground state potentials; ΔE_{00} is the transition energy between the vibrationally relaxed ground and excited states of the fluorophore; and W_p represents the coulomb stabilisation energy.

$$\Delta G_{ET} = E(D^+/D) - E(A/A^-) - \Delta E_{00} + W_p$$

Until recently, the application of photocatalysts in the context of methodology development remained underexplored. Seminal work in the 1980-1990s furnished the first examples of visible light photoredox catalysis.[17–25] But it was only later, in 2008, that a major breakthrough was achieved by MacMillan, Stephenson and Yoon.[26–28] These early reports are at the origin of a renewed interest in photochemistry. While ruthenium-based photocatalysts have been employed for those seminal reports, the fine-tuning of the ligand backbone of such metal complexes successfully led to the design of new photoactive catalysts, including iridium-, ruthenium- and organophotocatalysts. These straightforward modifications on the ligand framework enabled new reactivities by modulating the catalyst's redox properties. These new discoveries provided unique opportunities for the development of novel synthetic routes previously elusive or unknown, and the interest in the field of photoredox catalysis exploded in the last decade. The efficiency of photochemical processes can be assessed by determining the quantum yield of reactions.[29] The quantum yield represents the moles of reactant decomposed per moles of photons absorbed. Theoretically, in a closed photoredox cycle, the maximal theoretical quantum yield is 1, as one photon absorbed by the photocatalyst can lead to decomposition of one reactant molecule. Contrastingly, in a radical chain propagation often more than one molecule of reactant can be decomposed per photon absorbed, leading to a quantum yield higher than 1.

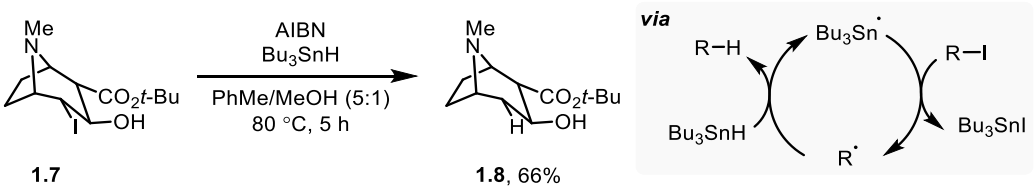
$$\Phi = \frac{moles\ of\ molecules\ decomposed}{moles\ of\ photons\ absorbed}$$

Nowadays, photoredox catalysis is mainly used for the generation of radicals via single-electron transfer processes. The mild reaction conditions provided by the use of a photoredox system pose significant advantages over classical methods relying on radical initiators.[29] Classical methods often require harsh conditions such as high temperatures, strong oxidants or UV light irradiation. Most photoredox catalysts are less toxic than traditional tin-based reagents. Furthermore, photoredox catalysis usually employs commercially available and inexpensive household lightbulbs or blue LED light sources (λ_{max} > 380 nm), which in contrast to UV light (λ_{max} < 380 nm), is lower in energy and prevents the undesired photolysis of chemical bonds.

1.2 Silyl Radical-Mediated Halogen Atom Abstraction

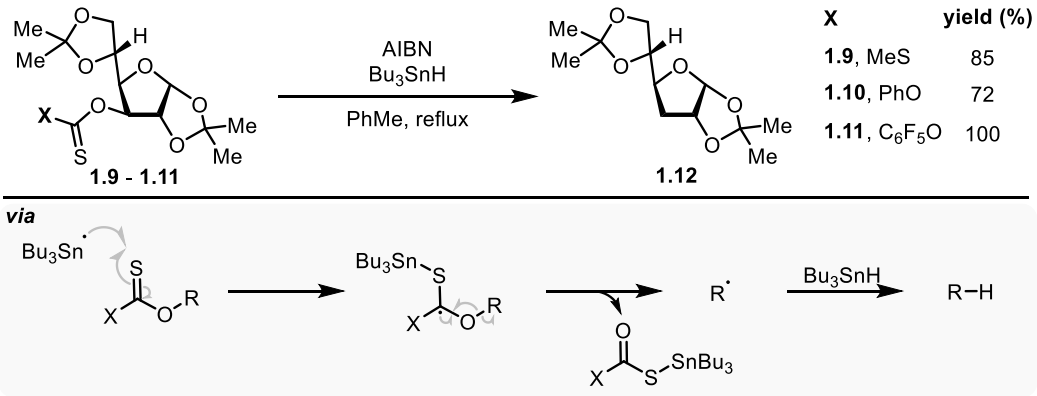
1.2.1 Radical Tin-Mediated Protodehalogenation

Many radical reactions rely on a chain propagation mechanism, enabling the construction of structurally complex molecules. Hydrogenolysis (replacement of a functional group by a hydrogen atom) has been a common transformation in radical chemistry. One of the most prevalent reagents for these transformations is tributyltin hydride. In combination with a radical initiator (e.g. 2,2′-azobis(2-methylpropionitrile), AIBN), a vast set of organohalides can efficiently and chemoselectively be reduced by tin hydrides.[30–34] A representative example is the protodeiodination of compound **1.7** in the context of the synthesis of (+)-Pseudococaine (**Scheme 1.1**).[34]



Scheme 1.1: Use of Bu_3SnH as reducing agent in the synthesis of (+)-Pseudococaine.

Upon radical initiation, the homolytic bond cleavage of the tin-hydrogen bond generates a nucleophilic stannyl radical, which can undergo halogen atom abstraction with an organohalide. The carbon-centred radical intermediate then undergoes hydrogen atom abstraction (HAA) with the tin hydride to form the desired reduced product. For a long time, Bu_3SnH was the reagent of choice for the protodehalogenation of structurally complex molecules, due to its high functional group tolerance. Tin hydrides have also been employed in the Barton-McCombie deoxygenation reaction. This free radical mediated transformation is a landmark reaction in organic synthesis and has been employed in the synthesis of unique molecular architectures, such as **1.12** (**Scheme 1.2**).[30,31,35] The alcohol is initially transformed to a xanthate or a thiocarbonate (**1.9** - **1.11**). Upon radical initiation, the tributyltin radical reacts with the activated alcohol to generate an alkyl radical upon fragmentation. The latter undergoes a hydrogen atom transfer (HAT) with Bu_3SnH to afford the deoxygenated product **1.12**.



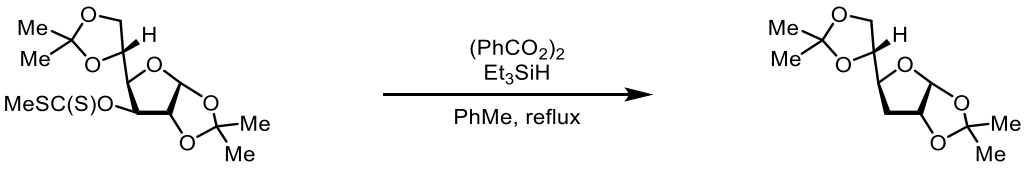
Scheme 1.2: Barton-McCombie reaction with xanthates and thiocarbonates.

Several drawbacks have been associated with the use of organotin compounds including their solubility, purification, cost, and toxicity. To improve their removal/purification from products, alternative tin reagents that can be removed by aqueous work-up were developed.[32] However, the toxicity of these reagents continued to limit the applications of tin-based radical chemistry in the pharmaceutical industry. The identification of alternative routes and reagents directed towards the use of tin-free reagents is therefore an important challenge in radical chemistry.

1.2.2 Silanes as a viable alternative to tin hydrides

More recently, silanes, specifically tris(trimethylsilyl)silane ($(TMS)_3SiH$), have been shown to be powerful alternatives to stannane reagents, particularly from an ecological, practical and safety perspective.[36] They are more tolerant to aqueous and aerobic conditions, which demonstrates their applicability to green chemistry. The use of silane derivatives avoids toxicity and purification issues, commonly encountered with Bu_3SnH-mediated transformations.

Silyl radicals were initially employed for the synthesis of silylated products, a class of building blocks especially valuable to material science.[37,38] The silyl radical-mediated activation of organohalides has emerged as an elegant alternative to stannane reagents. This activation of organohalides relies on a direct HAA from an *in situ* generated silyl radical, leading to the formation of carbon-centred radicals. Similar to tin radicals, silyl radicals can participate in the deoxygenation of xanthate **1.9** in a Barton-McCombie type reaction (**Scheme 1.3**).[39,40]



1.9 **1.12**, 96%

Scheme 1.3: Barton-McCombie deoxygenation using Et_3SiH as reducing agent.

Silyl radicals have been revived by the emergence of visible light photoredox catalysis. Development of strategies for the efficient and selective generation of silyl radicals have therefore become an important topic in photochemistry. The following sections highlight a brief summary of the historical background and properties of silyl radicals in organic chemistry. The advancements over the past decade in the use of silyl radicals in the context of organohalide activation will be discussed, as well as plausible reaction mechanisms for the generation of silyl radicals.

1.2.3 Properties of silyl radicals

The generation of silyl radicals is well documented since the 1940s, although early reports have mainly focused on providing structural, thermodynamic and kinetic properties. Ab initio theoretical studies on silyl radicals revealed that the arrangement of atoms around the silicon atom is essentially tetrahedral, predicting silyl radicals to adopt a pyramidal configuration.[41] However, in the presence of bulky substituents such as tristrimethylsilyl groups (e.g. $(TMS)_3Si$), the substituents adopt a planar configuration with respect to the silicon centre. Pioneering work of Walsh and co-workers revealed that the thermodynamic and kinetic stability of silyl radicals can be modulated with the electronic and steric effects of substituents (**Table 1.1**).[42] The formation of silicon-centred radicals from the corresponding silane depends on the Si−H bond dissociation energy (BDE). Specifically, the introduction of TMS groups decreases the Si−H BDE. The Si−H BDE is significantly weakened when the methyl groups of Me_3SiH (BDE (Si−H) = 397 kJ/mol) are replaced by TMS groups $(TMS)_3SiH$ (BDE (Si− H) = 351

kJ/mol).[42] This result is likely due to hyperconjugation between the bonding (or antibonding) Si−C β-bond and the single occupied molecular orbital (SOMO). It has been also hypothesised that the relief of the steric compression of $(TMS)_3SiH$ upon radical formation might be responsible for the weak Si−H bond. The introduction of pendant TMS groups on silicon atoms allows therefore for an increased stability of the corresponding silyl radical.

Table 1.1: BDE of a variety of silanes.

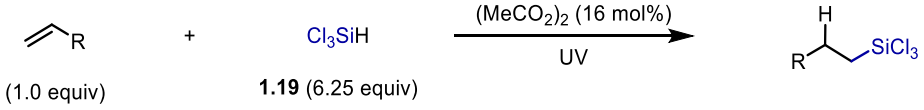
Silane (R_3Si−H)	BDE (kJ/mol)
Me_3Si−H (1.13)	397
$PhSiH_2$−H (1.14)	377
Ph_2SiH−H (1.15)	369
Ph_3Si−H (1.16)	356
$(TMS)Me_2Si$−H (1.17)	357
$(TMS)_3Si$−H (1.18)	351

The most prominent method for the formation of silyl radicals relies on the HAA between a radical intermediate (e.g. carbon-centred radical) and a silane. Rate constants for the reaction between primary alkyl radicals and various silanes demonstrated that the BDE is directly related to the rate constants and increases along the series $Et_3SiH < Ph_3SiH < (TMS)_3SiH$. Silyl radicals have been identified as nucleophilic radicals, that can efficiently undergo halogen atom abstraction with a variety of organohalides (Cl, Br, and I). This is likely due to the favourable p_m-d_n bonding of silicon halides, an interaction that has not been observed for carbon halogen bonds.

1.2.4 Early studies: generation and reactivity of silyl radicals

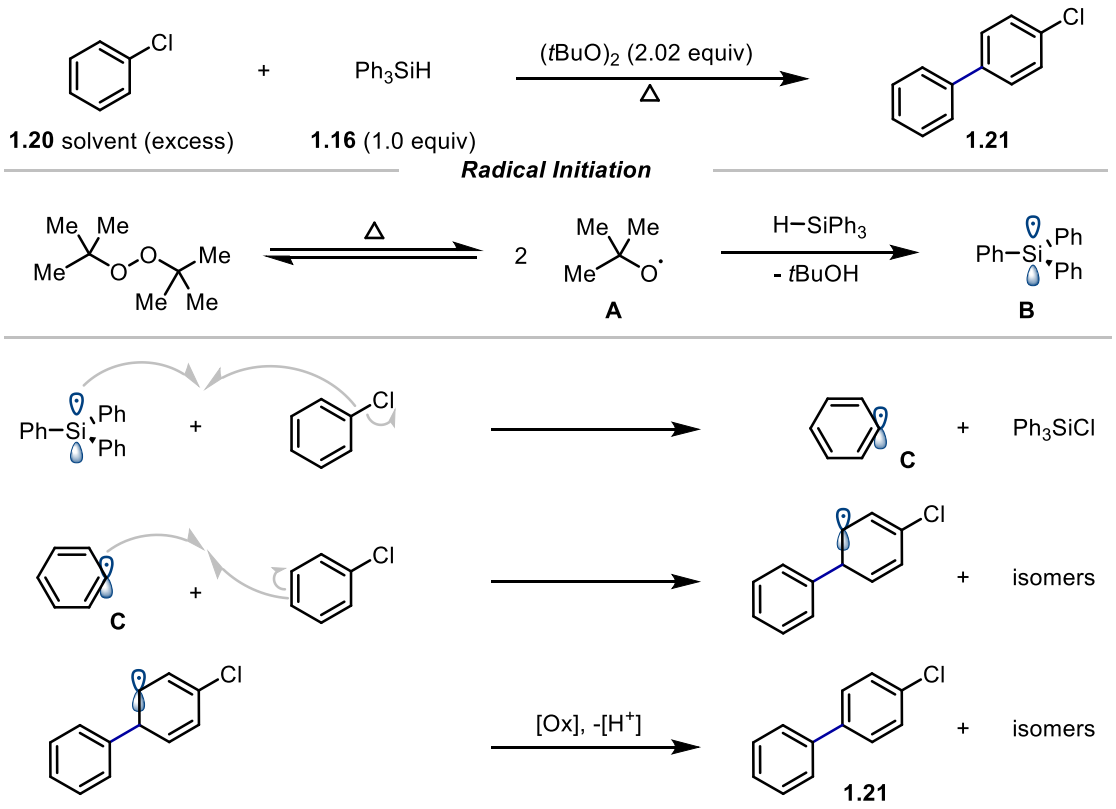
Silyl radicals have been exploited for the hydrosilylation of alkenes, an important transformation in the silicon industry.[43] As early as 1947, Sommer and co-workers

reported the radical hydrosilylation of alkenes using excess trichlorosilane and a peroxide as an initiator (**Scheme 1.4**).[44] To the best of our knowledge, this report represents the first example of a radical hydrosilylation of alkenes. Following this study, other reports focused exclusively on the hydrosilylation of alkenes and alkynes from silanes using peroxides as radical initiators.[45–47] The mechanism involved in these transformations involves a radical chain propagation.



Scheme 1.4: First hydrosilylation of alkenes reported by Sommer and co-workers.

In 1957, Hammond and co-workers described the first silyl radical-mediated HAA of an organochloride (**Scheme 1.5**).[48]



Scheme 1.5: Early example of a silyl-radical mediated halogen atom abstraction.

Upon initiation with a peroxide at high temperature, the triphenylsilyl radical can undergo direct chlorine atom abstraction from chlorobenzene to form an aryl radical. This C(sp^2)-centred radical intermediate can react with another molecule of chlorobenzene to afford the biaryl product. Mechanistic investigations revealed that the absence of oxygen was crucial, due to the formation of triphenylsilanol by-products in presence of oxygen, which inhibited the desired HAA process.

In the 1970s, scientists focused their attention on the use of $(TMS)_3SiH$ as a reducing agent.[49] In combination with a radical initiator, such as AIBN or triethylborane (Et_3B), $(TMS)_3SiH$ enables to achieve chemoselective reduction of a vast set of organohalides.[50] In contrast to previous studies, the use of this silane enabled to drastically broaden the scope of organohalides, and include alkyl bromides, chlorides, iodides, selenides, sulfides and others.[51] Kinetic studies revealed that rate constants for halide atom abstraction from alkyl iodides and bromides by the tris(trimethylsilyl)silyl radical and the tributyltin radical are similar.[52] On the other hand, the rate constants for the reaction with alkyl chlorides are lower for tributyltin radicals than for tris(trimethylsilyl)silyl radicals. This result clearly demonstrates that $(TMS)_3SiH$ ought to be a more efficient reducing agent for alkyl chlorides than tributyltin hydride. Further studies revealed iodine abstraction is favoured over bromine and chlorine with the $(TMS)_3Si$ radical.[53] Furthermore, the ease of abstraction increases from primary, to secondary, tertiary and benzylic C−X bonds, likely due to decreasing C-X bond dissociation energies as well as the stability of the corresponding carbon-centred radical (**Figure 1.6**). $(TMS)_3SiH$ has been identified as a non-hazardous, cost-effective reagent of choice for medicinal chemists, that is tolerated in aqueous media and easy-to-handle.[54] The use of $(TMS)_3SiH$ as a versatile activating agent for organohalides encourages the development of novel silyl radical-mediated transformations. Since the last decade, the field of $(TMS)_3SiH$

radical chemistry has thus tremendously progressed and a plethora of new radical transformations have been developed.

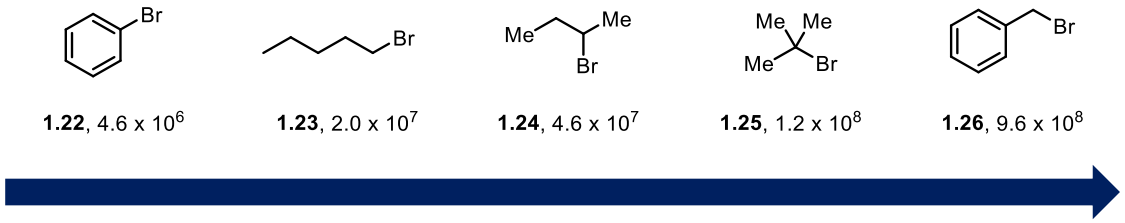


Figure 1.6: Rate constants for the reaction of the $(Me_3Si)_3Si$ radical with various organo bromides.

1.3 State-of-the-Art: Photochemical Silyl Radical-Mediated Halogen Atom Abstraction

The desire to expand the silyl radical-mediated activation mode of organohalides to other transformations has spawned renewed interest within the organic chemistry community. It has been well-recognised that the capacity of silyl radicals to abstract halogens from carbon-halogen bonds at near diffusion-controlled rates could induce new reactivity profiles. This high reactivity could unlock new transformations such as previously challenging cross-coupling reactions.

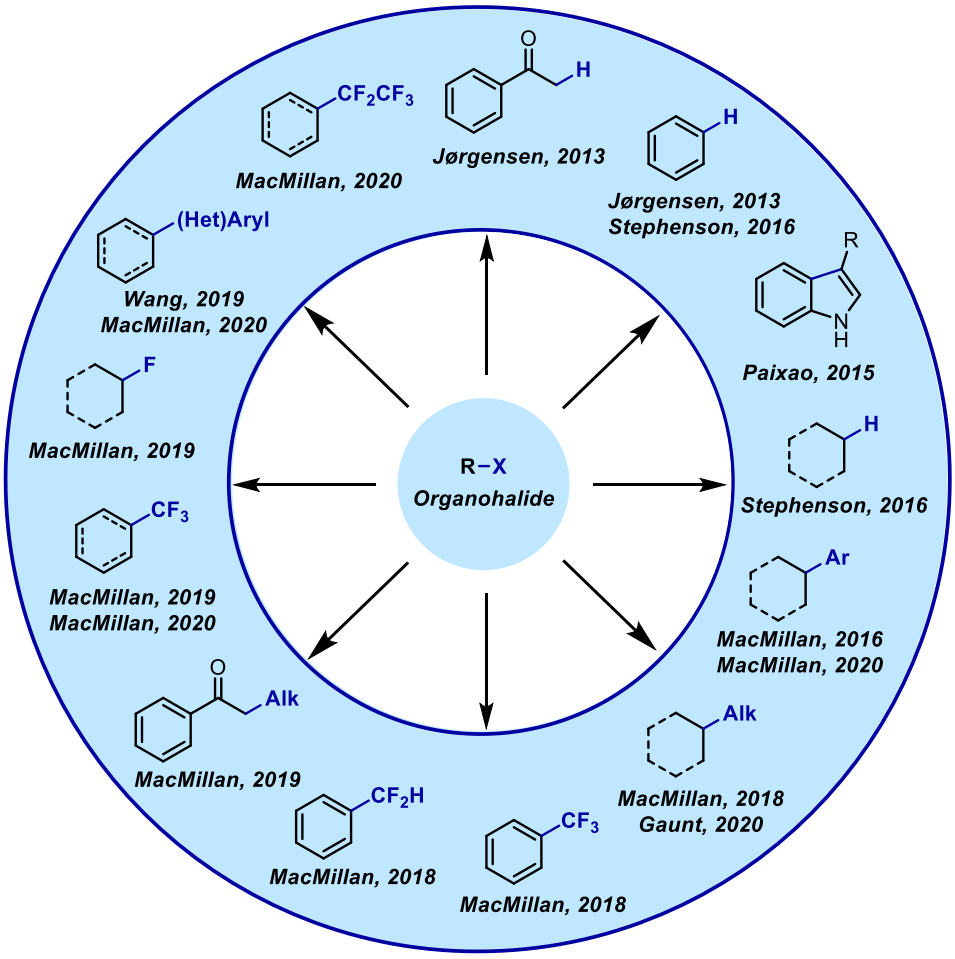


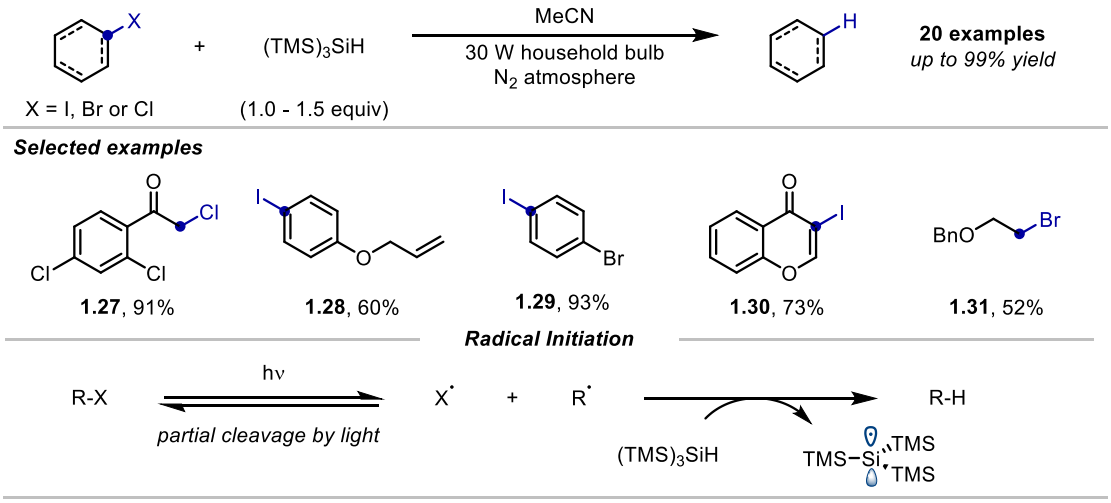
Figure 1.7: Major transformations enabled by silyl radical-mediated HAA of organohalides.

The last decades have seen staggering transformations using silyl radicals, enabling significant advances to the field of synthetic chemistry (**Figure 1.7**). Specifically, silyl radicals allowed for the efficient generation of C(sp^2) and C(sp^3) radicals from the corresponding organohalides. These radicals were used in a plethora of transformations, namely reduction, (hetero)arylation, alkylation, trifluoromethylation, difluoromethylation, (per)fluoroalkylation, and cyclisation, demonstrating the wide applicability of this activation mode. These protocols have found vast application in the medicinal chemistry area and sparked the interest of various research groups. This section provides an overview, perspective and time-lapse of the advances in silyl radical-mediated activation of organohalides over the last decade.

1.3.1 Protodehalogenation of Organohalides

The exchange of a halide with a proton is a chemical process that is routinely utilised in organic synthesis, namely for the construction of saturated hydrocarbon frameworks. Previous reports allowing for radical-mediated protodehalogenation employed harsh thermal conditions in combination with initiators (such as AIBN or by UV-irradiation) to perform similar transformations. The emergence of visible light photochemistry led to the development of milder methods for the radical protodehalogenation of organohalides. In 2013, as part of a growing interest in developing more efficient, more practical, and greener protocols, Jørgensen and co-workers described a facile, metal- and additive-free protodehalogenation of α-halo carbonyls and aryl halides under irradiation from household compact fluorescent light (**Scheme 1.6**).[55] Deiodination, debromination and dechlorination of α-halo carbonyls proceeded smoothly and with good functional group tolerance. In contrast to aryl iodides, the bromine analogues showed lower reactivity, while aryl chlorides remained completely inert. A representative example of an alkyl

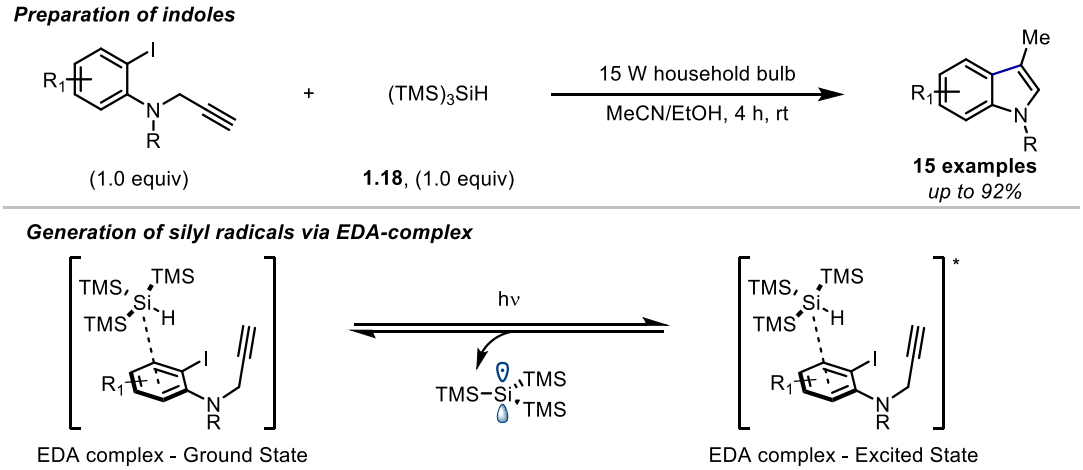
bromide displayed moderate reactivity under these reaction conditions (**1.31**, 52%). Mechanistically, the authors suggest that under light irradiation, the substrate undergoes photodecomposition to form trace amount of an aryl or alkyl radical. This carbon-centred radical can readily undergo HAA from $(TMS)_3SiH$, affording the desired product and regenerating a new silyl radical which can reinitiate the chain propagation mechanism.



Scheme 1.6: Radical-mediated reduction using $(TMS)_3SiH$.

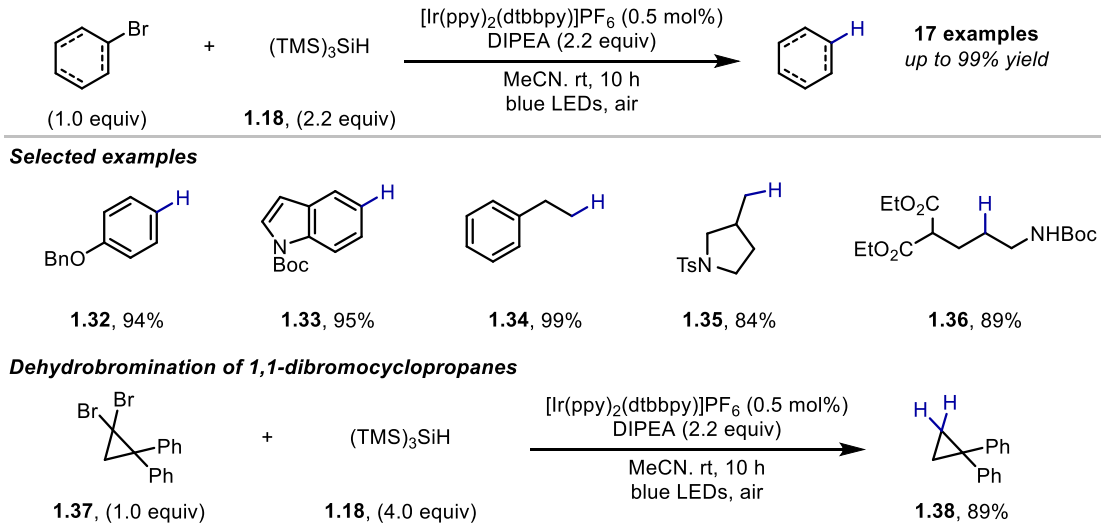
In 2015, Paixão and co-workers employed $(TMS)_3SiH$ under visible light irradiation for the formation of indoles and oxindoles from the corresponding aryl iodides (**Scheme 1.7**).[56] The reaction displays a good functional group tolerance, in which carbonyl and other halogens (Br, Cl, F) remained intact upon this transformation. UV-Vis experiments revealed a new absorption band when mixing the substrate and the silane, suggesting the formation of a transient Electron Donor Acceptor (EDA) complex. The authors suggest that the silicon-centred radical is formed upon an energy transfer step. The silyl radical undergoes iodine atom abstraction to generate an aryl radical. Subsequent 5-exo-dig cyclisation followed by aromatisation provides the desired product in good yields. Furthermore, distinctively to previous reports, deuteration experiments revealed that the primary carbon-centred radical intermediate reacts with the solvent to form the desired

product, demonstrating that the silane does not act as an HAD in this transformation. This method has been later expended to the synthesis of indolines and 2,3-dihydrobenzofurans.[57]



Scheme 1.7: Generation of the silyl radical *via* energy transfer of the EDA complex.

Alternatively, Stephenson and co-workers combined photoredox catalysis and silyl radical-mediated atom transfer chemistry under visible light activation for the hydrodebromination of unactivated aryl and alkyl organobromides (**Scheme 1.8**).[58]



Scheme 1.8: Photoredox-catalysed hydrodebromination of aryl- and alkyl derivatives.

The reaction proceeds smoothly for electron-rich arenes, heteroarenes as well as alkyl derivatives, affording the desired products in good to excellent yields. The authors demonstrated that this protocol can be used for the hydrodebromination of

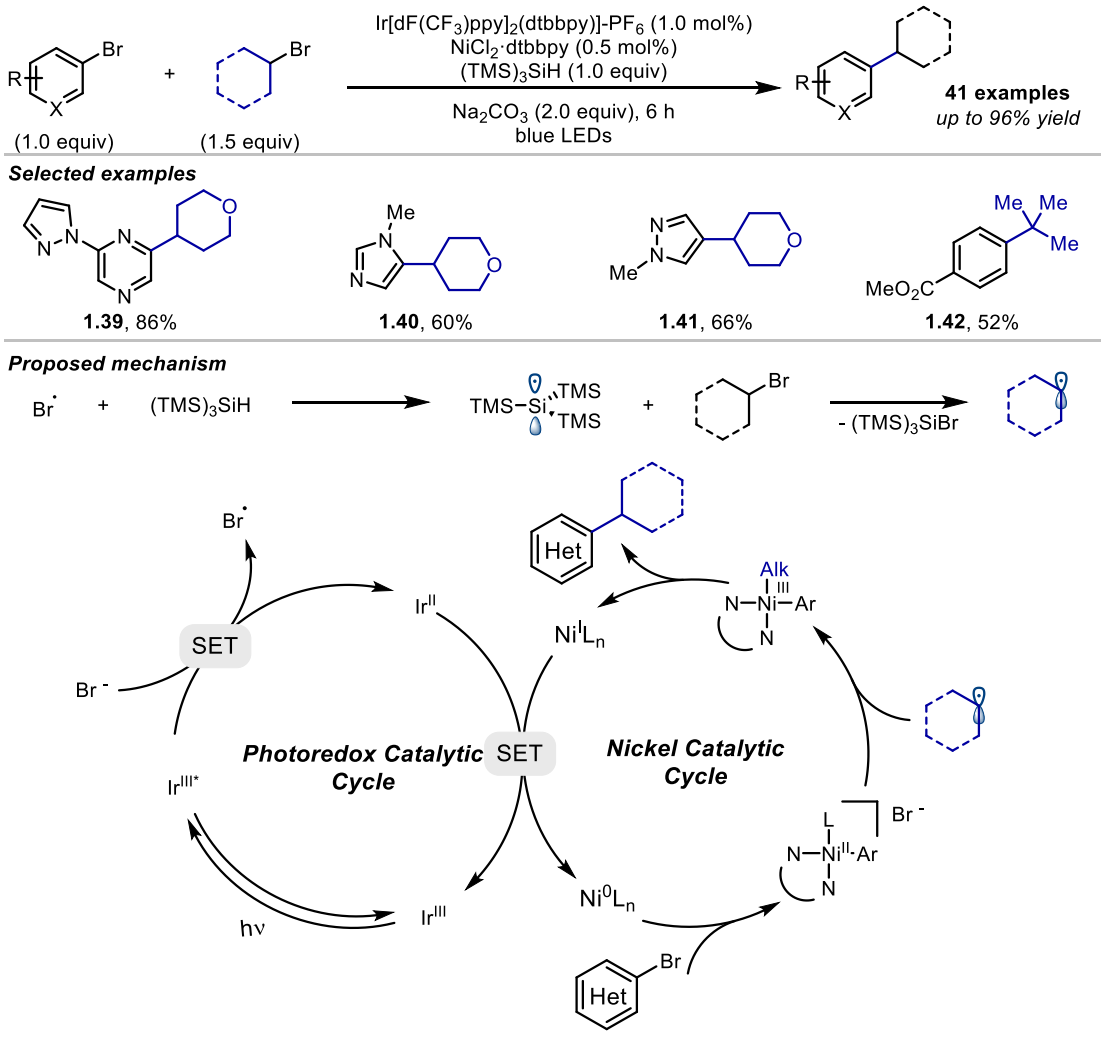
dibromocyclopropane with an excess of $(TMS)_3SiH$, whereas traditional methods were limited to the removal of a single bromide atom. As previously described, this method is also suitable to radical cyclisation cascades.

Mechanistically, the authors suggest that the generation of the silyl radical can arise from two different pathways under these reaction conditions: by HAA from an alkyl or aryl radical; or in presence of oxygen by HAA from a peroxyl radical.

1.3.2 Silyl Radical-Mediated $C(sp^2)$–$C(sp^3)$ Bond Formation

More recently, silyl radicals have been extended to transformations other than reduction. In the last decade, the MacMillan group pioneered the synergistic merger of photoredox chemistry and transition-metal catalysis. More specifically, a key area of their research relies on the development of novel transformations arising from the silyl radical-mediated activation of organohalides. In 2016, MacMillan and co-workers designed a novel silyl radical/halogen abstraction/nickel capture mechanism for the cross-electrophile coupling of (hetero)aryl bromides and alkyl bromides to construct $C(sp^3)$–$C(sp^2)$ bonds under mild reaction conditions (**Scheme 1.9**).[59] This new method represents a significant advance in the field of cross-coupling reactions, as alkyl bromides were previously considered inert. The authors demonstrated that the combination of $(TMS)_3SiH$ with metallaphotoredox catalysis (employing nickel catalyst and an iridium-based photocatalyst) under blue-light irradiation resulted in the successful construction of $C(sp^3)$–$C(sp^2)$ bonds. The reaction was initiated *via* the single-electron oxidation of bromide [dissociable ligand on nickel; $E_{1/2}^{red}$ = +0.80 V vs saturated calomel electrode (SCE) in DME] by the triplet excited state of the photocatalyst $[Ir[dF(CF_3)ppy]_2(dtbbpy)]$-$PF_6$ [$E_{1/2}^{red}$ [$Ir^{III}*/Ir^{II}$] = +1.21 V vs SCE in MeCN], leading to the formation of a bromine radical. Subsequent HAA with $(TMS)_3SiH$ affords the silyl

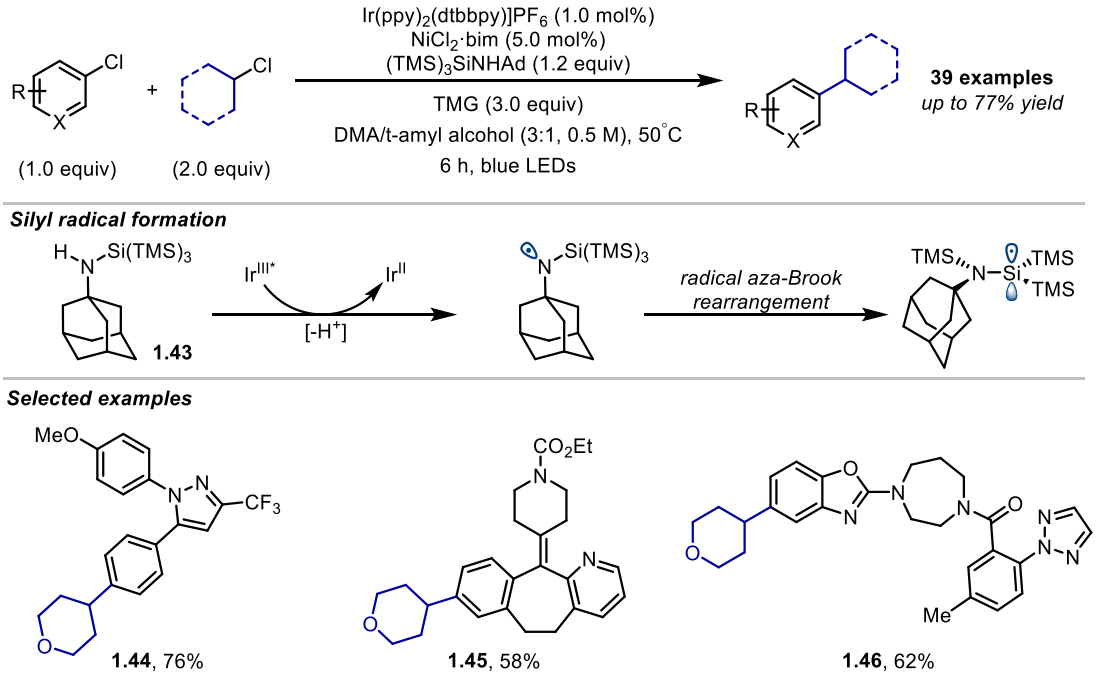
radical. The tris(trimethylsilyl)silyl radical can undergo bromine atom abstraction from an alkyl bromide, generating the corresponding alkyl radical. Simultaneously, a Ni^0 complex will undergo oxidative addition into the aryl bromide C–Br bond, forming L_nAr-Ni^{II}-Br. Upon oxidative capture of the alkyl radical, a high valent Ni^{III} species is formed. Reductive elimination affords the desired product alongside the reduced Ni^I catalyst. The Ni^I can be reduced back to Ni^0 by single-electron reduction from the reduced photocatalyst. Initially, the authors screened different silanes. They observed a strong correlation between the BDE of the silane and the outcome of the reaction. When using silanes with higher silicon-hydrogen BDE, a significant decrease of the yield was observed (e.g. Ph_3SiH, $Me_2(TMS)SiH$).



Scheme 1.9: Merger of photoredox- and nickel catalysis for the cross-electrophile coupling of (hetero)aryl bromides and alkyl bromides.

The success of this transformation relied on the selective bromine atom abstraction of the weaker C(sp^3)-Br bond as well as the facile oxidative addition of nickel into the C(sp^2)−Br bond. The extended scope demonstrated the robustness of this coupling. A recent analysis comparing different C(sp^2)−C(sp^3) cross-coupling methods in the context of drug-like library synthesis, revealed that this novel nickel/photoredox catalysed protocol is as powerful and efficient as traditional cross-coupling methods using organometallic nucleophiles.[60,61] Limitations of this method have been identified, such as the presence of basic amines as well as the direct installation of benzylic groups. This procedure has been recently applied to the late-stage introduction of tritium and carbon-11 radioisotopes, employing a metallaphotoredox-catalysed methylation strategy of pharmaceuticals and PET radiotracers.[62]

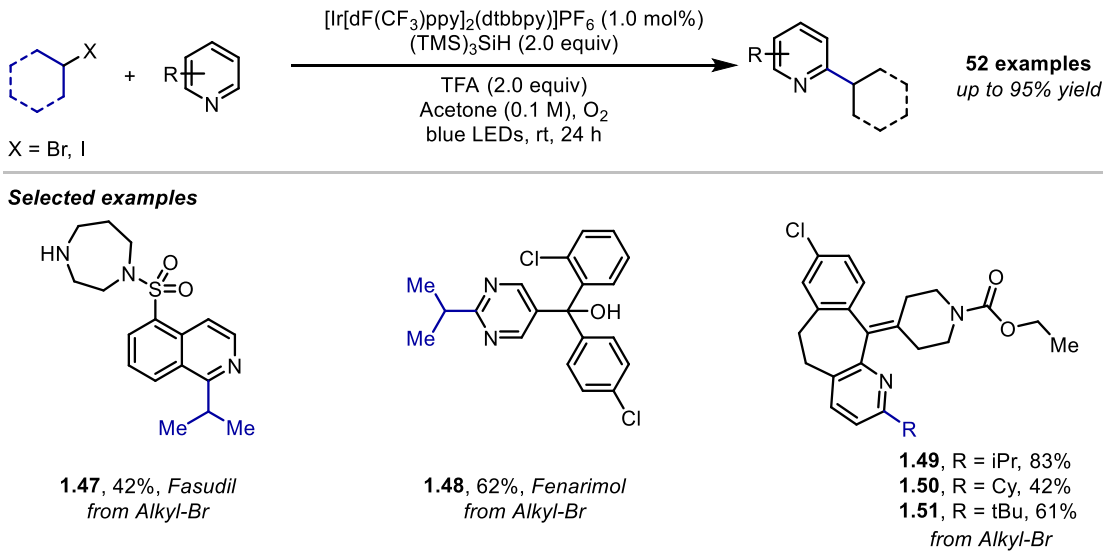
Most cross-electrophile couplings disclosed in the literature employ alkyl bromides, iodides or sulfonates as viable reaction partners. On the other hand, the use of simple alkyl chlorides remains unknown. This is likely due to the intrinsic chemical stability of alkyl chlorides (C−Cl BDE = 397 kJ/mol) making them particularly challenging to activate. Recent studies from the MacMillan group revealed that the rate of chlorine abstraction by the tris(trimethylsilyl)silyl radical is several orders of magnitude slower than for the corresponding bromine analogue.[63] In response to these challenges, the MacMillan group designed a new silane reagent bearing an amino substituent (**Scheme 1.10**, **1.43**). This π-donating group renders the silyl radical more nucleophilic allowing for a more efficient chlorine atom abstraction. As such, the development of a 1-adamantylamine-substituted supersilyl reagent enabled the kinetically challenging chlorine atom abstraction from various unactivated alkyl chlorides.



Scheme 1.10: C(sp^2)−C(sp^3) cross-electrophile coupling of organochlorides.

Measurement of the oxidation potential of the aminosilane (E_{ox} = +0.66 V vs SCE in MeCN) revealed that a direct single-electron oxidation from the excited state of the photocatalyst [Ir(ppy)$_2$(dtbbpy)](PF$_6$) ($E_{red}[Ir^{III*}/Ir^{II}]$ = +0.76 V vs SCE in DMA/*tert*-amyl alcohol) was viable, affording a *N*-centred radical intermediate, which undergoes fast aza-Brook rearrangement to generate the corresponding reactive silyl radical. The merge of nickel and photoredox catalysis allowed for the late-stage formation of a broad range of C(sp^2)−C(sp^3) coupled products (**1.44** - **1.46**). The use of organochlorides is highly beneficial as they are less toxic, less expensive and more abundant than other organohalides. This strategy has been later extended to the cross-electrophile coupling of a wide range of α-chloro carbonyls with aryl halides using (TES)$_3$SiH as silyl radical precursor.[64]

Inspired from MacMillan's work, Wang and co-workers explored the activation of alkyl bromides and alkyl iodides in a Minisci-type C−H alkylation of heteroarenes (**Scheme 1.11**).[65]



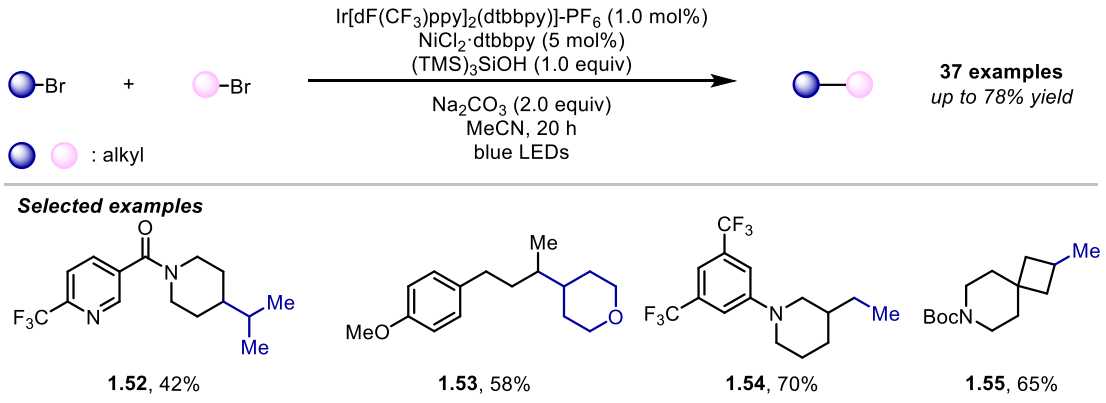
Scheme 1.11: Minisci C−H alkylation of heteroarenes with unactivated alkyl halides.

Aiming at using green reagents, the protocol employs oxygen as an environmentally benign stoichiometric oxidant. The generation of the silyl radical follows a similar mechanism as previously described (**Scheme 1.6**),[59] whereby an *in situ* generated bromine radical from the alkyl bromide abstracts the hydrogen from the silane. Both alkyl bromides and iodides were suitable alkyl radical precursors for the alkylation of a wide range of different electron-deficient heteroarenes. Interestingly, primary, secondary, and tertiary alkyl radicals were efficiently generated under the reaction conditions. This transformation is scalable and has been validated on the late-stage alkylation of different biologically active molecules (**1.47 - 1.51**).

1.3.3 Silyl Radical-Mediated C(sp^3)–C(sp^3) Bond Formation

In 2018, MacMillan and co-workers expanded the cross-electrophile coupling to the formation of C(sp^3)–C(sp^3) bonds (**Scheme 1.12**).[66] This elusive transformation remains a long-standing challenge in organic chemistry. An important design criterion for this transformation relies on the oxidative addition of small alkyl groups by transition-metal

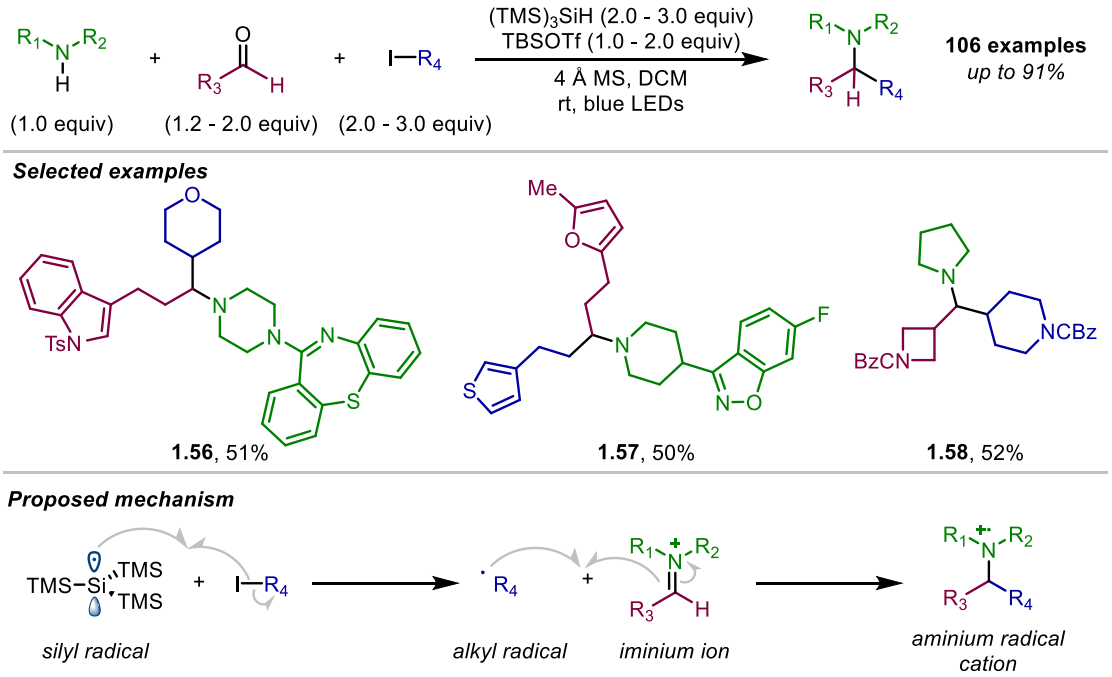
catalysis, whereas the second coupling partner, structurally more complex, would be activated by a silyl radical-mediated HAA process. In this transformation, supersilanol has shown better reactivity than $(TMS)_3SiH$, which gave predominantly protodehalogenation byproducts. Using these mild reaction conditions, the metallaphotoredox-catalysed coupling of simple aliphatic electrophiles with various complex aliphatic bromides was achieved in good to excellent yields. Mechanistically, the silyl radical is generated upon single-electron transfer and Brook rearrangement, as already described in **Scheme 1.10**. Notably, the authors achieved the methylation of aliphatic bromides using a combination of methyl tosylate and tetrabutylammonium bromide. For example, both secondary and primary alkyl bromides underwent methylation in good yields (**1.54**, **1.55**). These cross-electrophile technologies are synthetically attractive for the incorporation of drug-like molecular complexity with high chemoselectivity and exquisite functional group tolerance.



Scheme 1.12: $C(sp^3)–C(sp^3)$ cross-electrophile coupling of aliphatic bromides

In 2020, Gaunt and co-workers harnessed the reactivity of the tris(trimethylsilyl)silyl radical for the preparation of complex tertiary alkylamines employing secondary amines, aldehydes and alkyl-halides as feedstock precursors under visible light activation (**Scheme 1.13**).[67] This transformation is triggered by the addition of an alkyl radical to alkyliminium ions, leading to the formation of an aminium radical cation. The authors

suggest a silyl radical-mediated chain propagation mechanism, whereby an alkyl radical is generated upon iodine atom abstraction by the tris(trimethylsilyl)silyl radical. In this transformation $(TMS)_3SiH$ is serving both as a silyl radical source capable of activating alkyl iodides and the HAD to generate an ammonium salt. This novel radical-mediated strategy allows for the streamlined synthesis of complex tertiary amines (**1.56** - **1.58**) of high interest to the pharmaceutical sector.

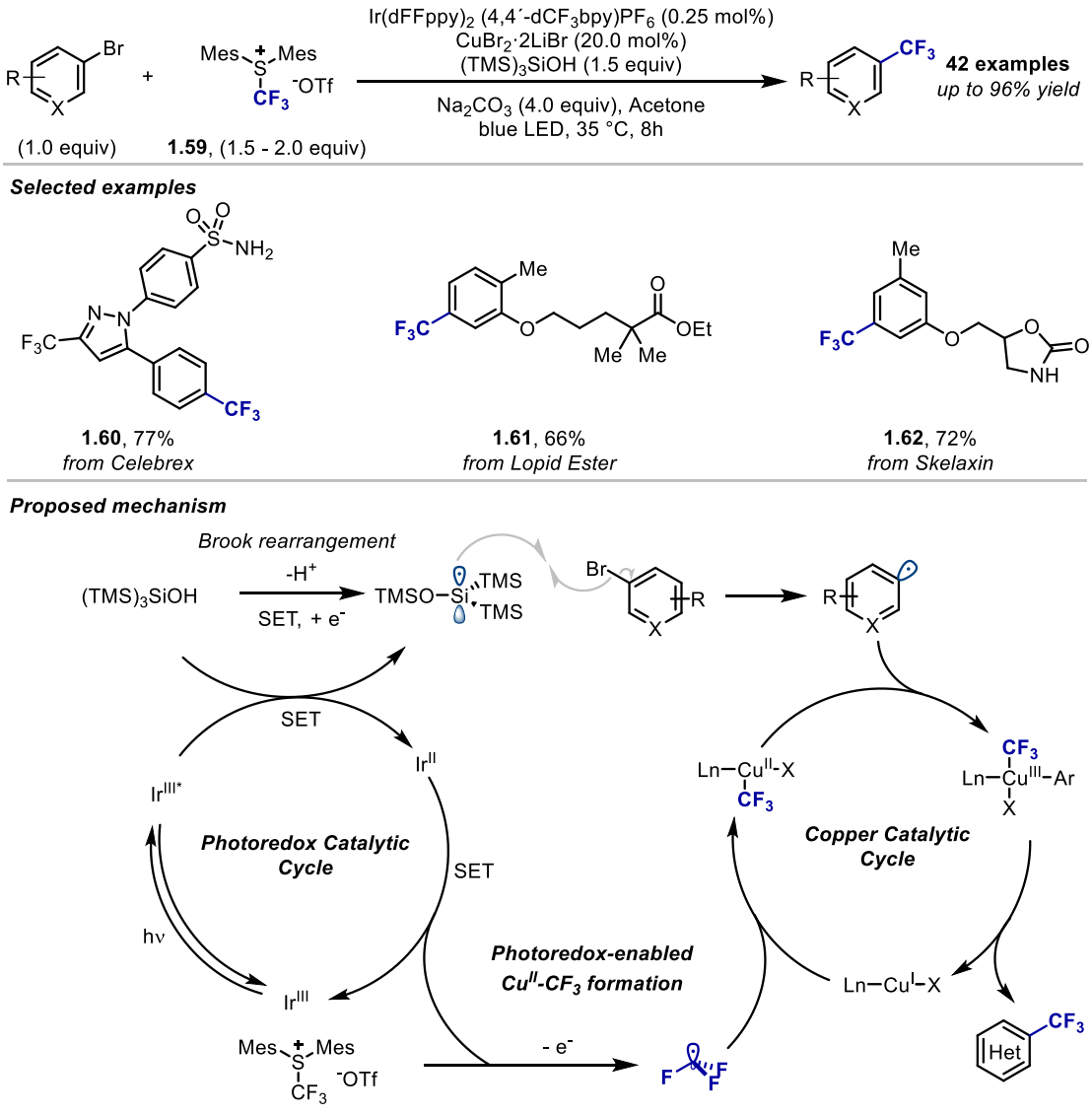


Scheme 1.13: Visible light catalysed formation of complex tertiary alkylamines.

1.3.4 Silyl Radical-Mediated Fluorination and (Per)Fluoroalkylation

Owing to the extraordinary potential of fluorine-containing molecules in medicinal chemistry, new methods that construct C−R_f (R_f = CF_3, CF_2H, F, CF_2CF_3) bonds in an efficient and selective fashion are highly sought after.[68,69] Copper has attracted many interests in cross-coupling reactions for the incorporation of fluorine-containing motifs, as high-valent Cu^{III} complexes are well-known to undergo favourable and facile reductive elimination with electronegative groups such as trifluoromethyl groups. Given

its economical and operational benefits, the development of novel methodologies employing copper would be beneficial for the exploration of new chemical spaces. In this context, the MacMillan group applied a silyl radical-mediated activation mode of aryl halides for the facile introduction of fluorinated motifs into organic molecules. In 2018 they have reported a copper-catalysed trifluoromethylation of aryl bromides using dMesSCF$_3$ (**1.59**, **Scheme 1.14**).[70]

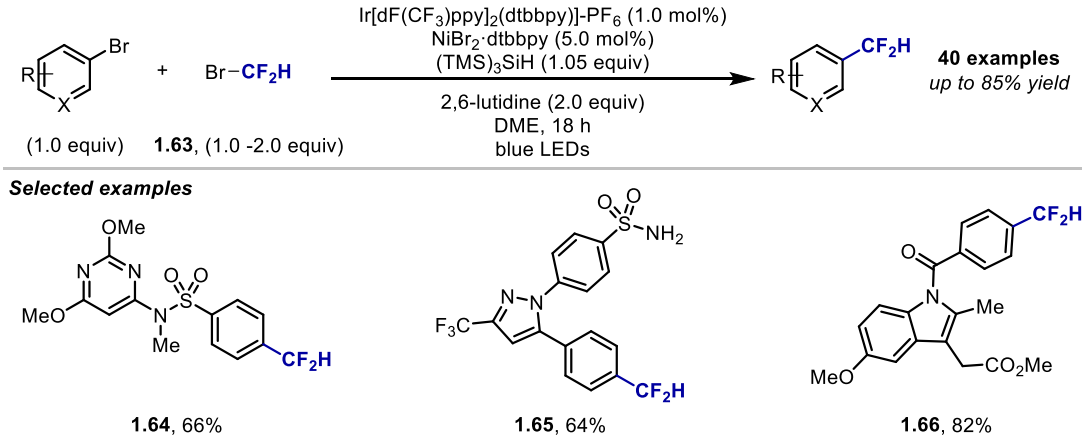


Scheme 1.14: A metallophotoredox strategy for the trifluoromethylation of aryl bromides.

This transformation uses a silyl radical/halogen abstraction/copper capture mechanism. Mechanistically, an aryl radical, formed by silyl radical-mediated bromine atom

abstraction undergoes addition to an *in-situ* generated Cu^{II}–CF_3 complex. Upon reductive elimination from a high valent Cu^{III} intermediate, the desired trifluoromethyl (hetero)arene is formed. This transformation displays a wide functional group tolerance as well as an extended (hetero)arene scope. The efficiency of this transformation was demonstrated on biorelevant molecules, where trifluoromethylated derivatives of Celebrex, Lopid, and Skelaxin were successfully synthesised (**1.60** - **1.63**). The generation of aryl radicals using $(TMS)_3SiOH$ has been later exploited in a copper metallaphotoredox protocol allowing for the $C(sp^2)$–N_{het} coupling of aryl halides and *N*-heterocycles.[71] In 2019, the MacMillan group achieved the introduction of the trifluoromethyl group onto aliphatic scaffolds employing a similar strategy. [72] One year later, the same group demonstrated that Ruppert-Prakash type reagents were also suitable radical precursors, allowing for the introduction of trifluoromethyl, pentafluoroethyl and heptafluoropropyl groups.[73]

Today, the introduction of the difluoromethyl group has attracted many interests in drug discovery.[74] In 2018, MacMillan and co-workers merged nickel and photoredox catalysis for the radical difluoromethylation of (hetero)aryl bromides (**Scheme 1.15**).[75]

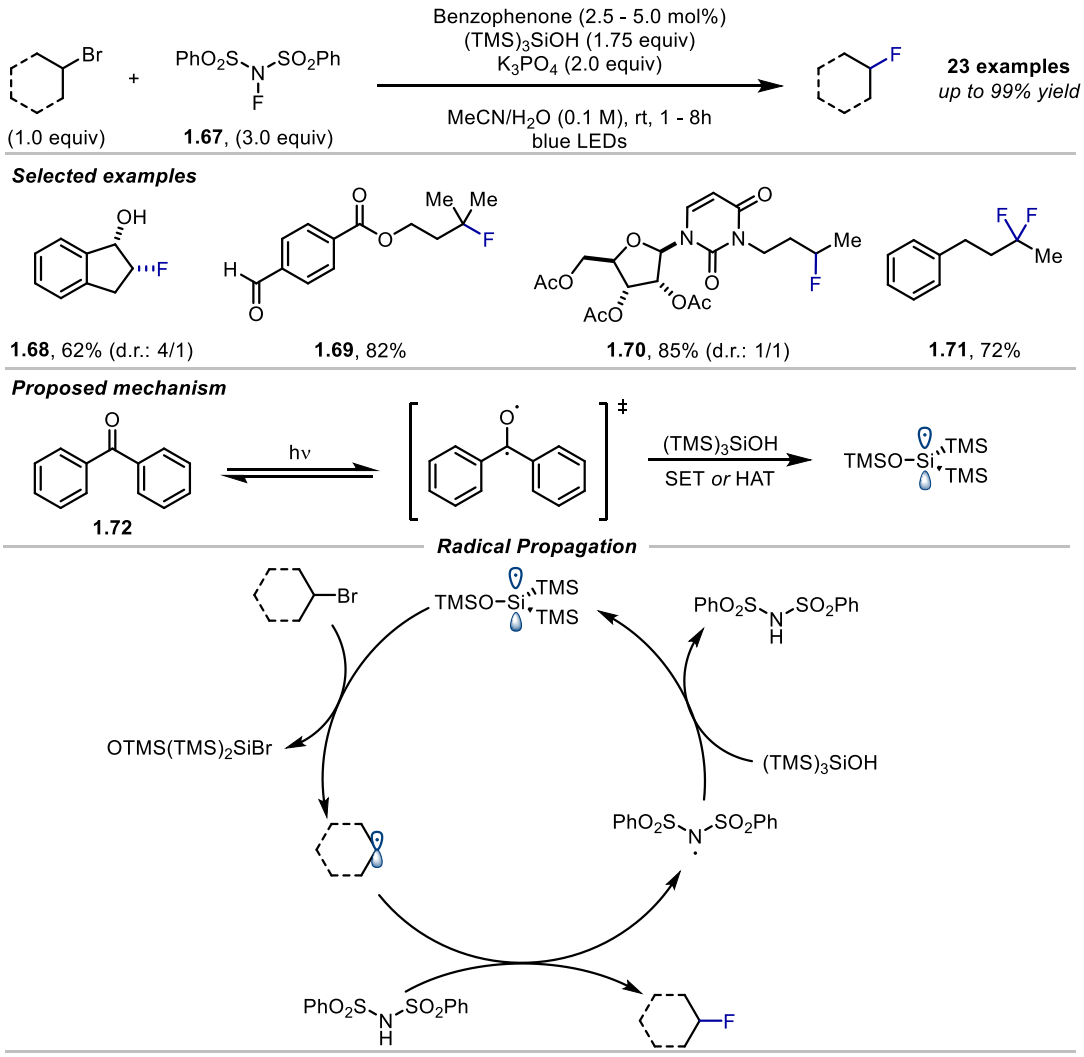


Scheme 1.15: Late-stage difluoromethylation of pharmaceutical agents.

The difluoromethyl radical was generated upon bromine atom abstraction of bromodifluoromethane (**1.63**) by the tris(trimethylsilyl)silyl radical. The applicability of

this protocol has been showcased with the efficient late-stage difluoromethylation of numerous pharmaceutically relevant heterocycles (e.g. pyrimidines, pyrazoles and indoles) and biologically active molecules (**1.64**- **1.66**).

Simultaneously, the MacMillan group developed a metal-free protocol for the fluorination of aliphatic bromides, employing a silyl radical-mediated chain process (**Scheme 1.16**).[76]



Scheme 1.16: Fluorination of alkyl bromides under visible light activation.

In this report, the silyl radical is generated by HAT between the triplet excited state of benzophenone (**1.72**) and $(TMS)_3SiH$ upon irradiation with light. After HAA from the alkyl bromide, the carbon-centred radical intermediate undergoes fluorine atom

abstraction from NFSI. The resulting amino radical undergoes HAT with the silane to regenerate the silyl radical and close the radical chain propagation cycle. This metal-free fluorination protocol is a viable alternative to deoxyfluorination reagents, where alcohols, ketones, and aldehydes are usually not tolerated under the reaction conditions. Primary, secondary, tertiary, benzylic bromides and saccharides derivatives were all suitable for this transformation (**1.68** - **1.71**).

In the last decade, advances in silyl-radical mediated metallaphotoredox catalysis has led to an explosion in novel transformations. These new methods have enabled the creation of new bond disconnections, which will provide the medicinal chemists with a new broad toolbox in retrosynthetic analysis. The seminal contributions from MacMillan and co-workers described above have had significant impacts within the realm of the broader field of photocatalysis and cross-coupling reactions.

1.4 Hydrofunctionalisation of Alkenes

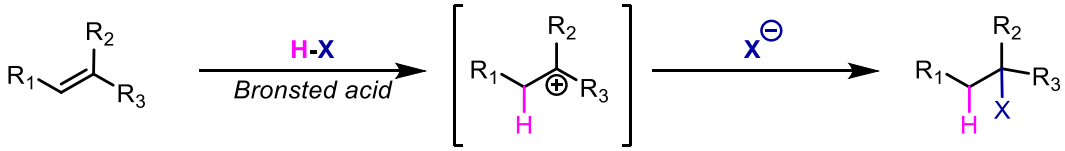
The preparation of C(sp^3)-enriched fragments is the subject of many studies in the field of synthetic organic chemistry. A straightforward strategy to access aliphatic structures is the reductive functionalisation of alkenes, as alkenes represent one of the most abundant classes of organic molecules. This area has been tremendously explored in modern organic synthesis and allowed for the introduction of a plethora of different functionalities. Perhaps, one of the most important transformations in this field, is the hydrofunctionalisation of readily available alkenes, namely the introduction of a hydrogen atom and another functional group. Traditionally, the reaction of a strong acid with an alkene provides the net addition product with high atom-economy. However, the use of strong acids limits the functional group tolerance of these reactions.

Hydrofunctionalisation reactions can be classified in two categories depending on the regioselectivity of the addition: 1) the Markovnikov addition, where the hydrogen atom adds to the carbon containing more hydrogen substituents; 2) the anti-Markovnikov addition, where the hydrogen atom adds to the carbon with less hydrogen substituents (**Figure 1.8**).



Figure 1.8: Markovnikov and anti-Markovnikov regioselectivity.

The addition of an acid (e.g. H−X) to an alkene (polar pathway) results in the exclusive formation of Markovnikov products. This regioselectivity is due to the formation of an energetically more stable carbocation intermediate, in compared to the anti-Markovnikov addition (**Scheme 1.17**).



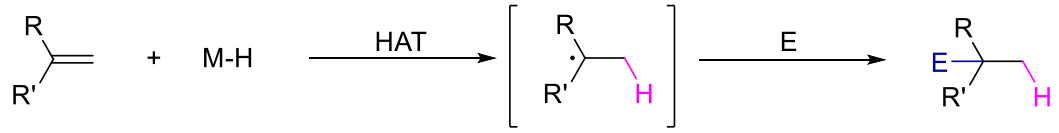
Scheme 1.17: Simplified representation of a hydrofunctionalisation of alkenes with Brønsted acids.

More recently, numerous radical approaches have been reported for the hydrofunctionalisation of alkenes. The milder reaction conditions involved in radical transformations, compared to ionic methods come with an important advantage, namely increased functional group tolerance. Furthermore, anti-Markovnikov selectivity can easily be obtained under radical conditions. The radical hydrofunctionalisation of alkenes with Markovnikov selectivity often relies on a metal-hydride hydrogen atom transfer (MHAT) employing transition metals, such as manganese, iron or cobalt. The opposite selectivity (anti-Markovnikov) can be achieved in free radical reactions. A brief overview

of these two regioselective additions to C=C double bonds will be discussed in this section.

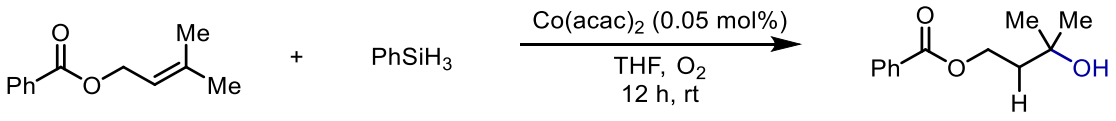
1.4.1 Transition-Metal Catalysed Hydrofunctionalisation of Alkenes

In contrast to Brønsted acid catalysed-hydrofunctionalisation of alkenes, the initial MHAT results in the formation of a carbon-centred radical intermediate instead of a carbocation. This free radical can further engage with a radical acceptor, providing the corresponding Markovnikov hydrofunctionalised product (**Scheme 1.18**).[77]



Scheme 1.18: Simplified representation of a MHAT-catalysed hydrofunctionalisation of alkenes.

The metal hydrides (M−H) are often generated *in situ* using silanes (e.g. $PhSiH_3$) as reductants. A representative example of MHAT reactions is the Drago-Mukaiyama hydration, which has been extensively employed in more than 38 total syntheses (**Scheme 1.19**).[78]



1.73, (1.0 equiv) **1.14**, (2.0 equiv) **1.74**, 93%

Scheme 1.19: Drago-Mukaiyama hydration of alkenes.

The combination of cobalt(II) acetylacetonate and a suitable hydride donor allowed for the hydration of alkenes in excellent yields. This strategy has been later extended to other abundant first-row transition metals, such as manganese and iron catalysts. Whilst traditional Markovnikov hydration reactions require harsh conditions (e.g. strong acids),

the catalytic oxidation/reduction Drago-Mukaiyama hydration of alkenes is performed under mild conditions, demonstrating the compatibility of this method with the late-stage functionalisation (LSF) of complex molecules.

Since then, novel variants of this alkene hydrofunctionalisation utilising cobalt-, manganese-, and iron-based catalysts, for the construction of C−O, C−N, C−S, C−C, C−H, C−X (X = halogens) bonds and others, have been disclosed (**Figure 1.9**).[78–87] As witnessed by the plethora of methods that have been developed in the past decades, MHAT represents a powerful and general tool for the Markovnikov hydrofunctionalisation of alkenes in synthetic chemistry.[78,88,89]

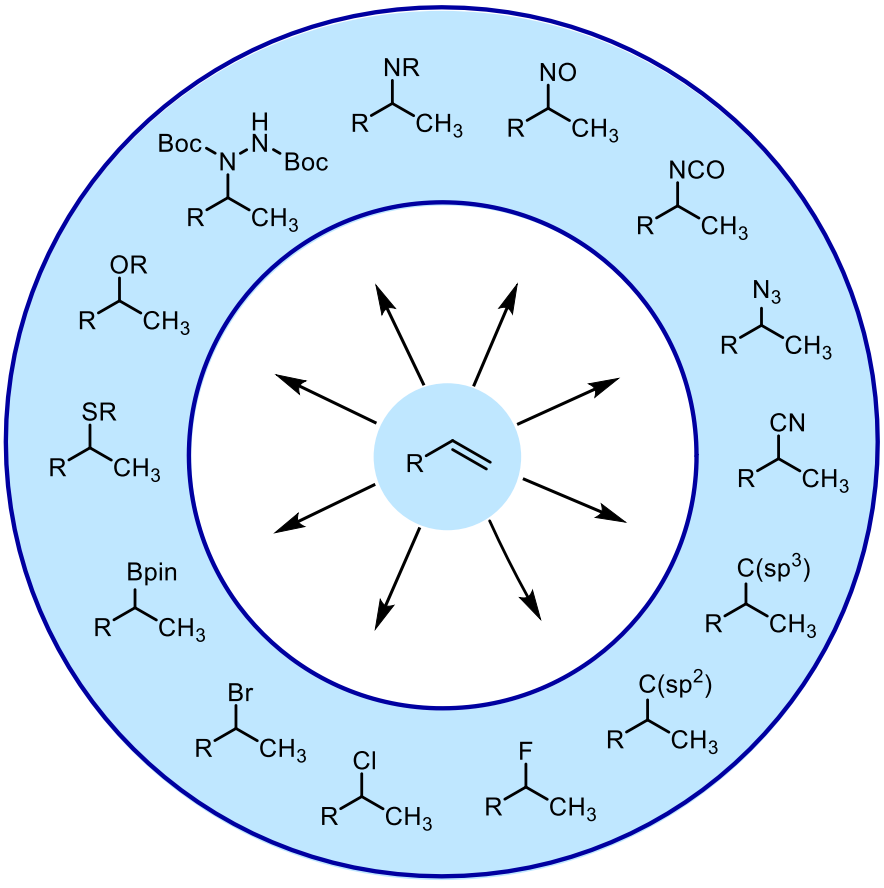
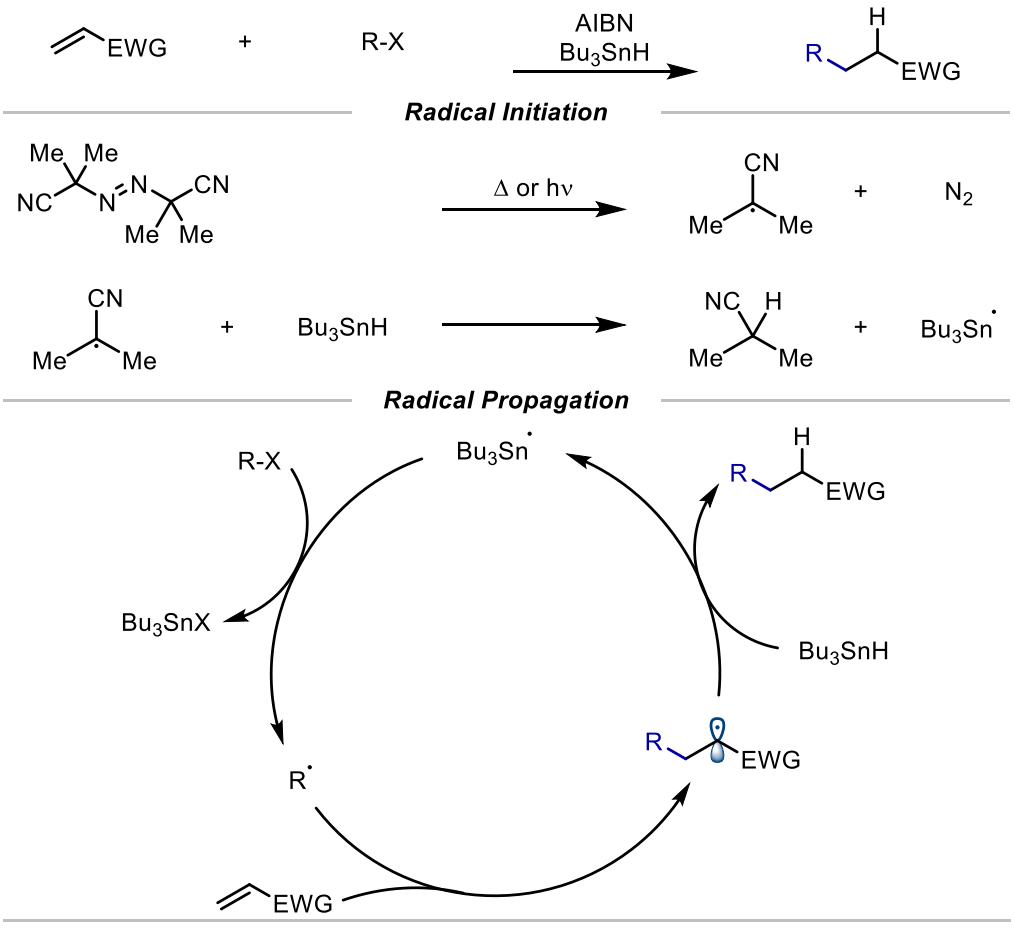


Figure 1.9: MHAT-catalysed Markovnikov hydrofunctionalisation of alkenes.

1.4.2 Anti-Markovnikov Radical Hydrofunctionalisation of Alkenes

Whilst the formation of Markovnikov products has been well-documented, the access to anti-Markovnikov adducts long remained underdeveloped. The free radical chain propagation addition to alkenes utilising organotin and organomercury hydrides, has appeared as an alternative to the Markovnikov regioselectivity.[90] Specifically, Giese and co-workers demonstrated at the onset, that nucleophilic alkyl radicals can undergo Giese addition (1,4 radical addition to Michael acceptor) using trialkyltin hydrides (**Scheme 1.20**).[91]



Scheme 1.20: Radical chain propagation for the hydrofunctionalisation of alkenes.

Traditionally, such reactions are often initiated by peroxides or diazo-compounds (e.g. AIBN) under thermal activation or photoinitiation. The addition of the desired radical to

the alkene generally takes place on the less substituted carbon of the alkene to produce a more stable carbon-centred radical intermediate (anti-Markovnikov selectivity). This radical intermediate further reacts upon HAT with tin hydrides to form the corresponding hydrofunctionalised product. A representative simplified example of a radical tin-mediated hydrofunctionalisation of alkene is shown in **Scheme 1.20**. More recently, synthetic advancements in the field of photochemistry enabled major breakthroughs in the design of elegant and diversified anti-Markovnikov hydrofunctionalisation of alkenes using milder reaction conditions. Considering the numerous reports that have been recently developed, only the major transformations that have been achieved are highlighted (**Figure 1.10**).

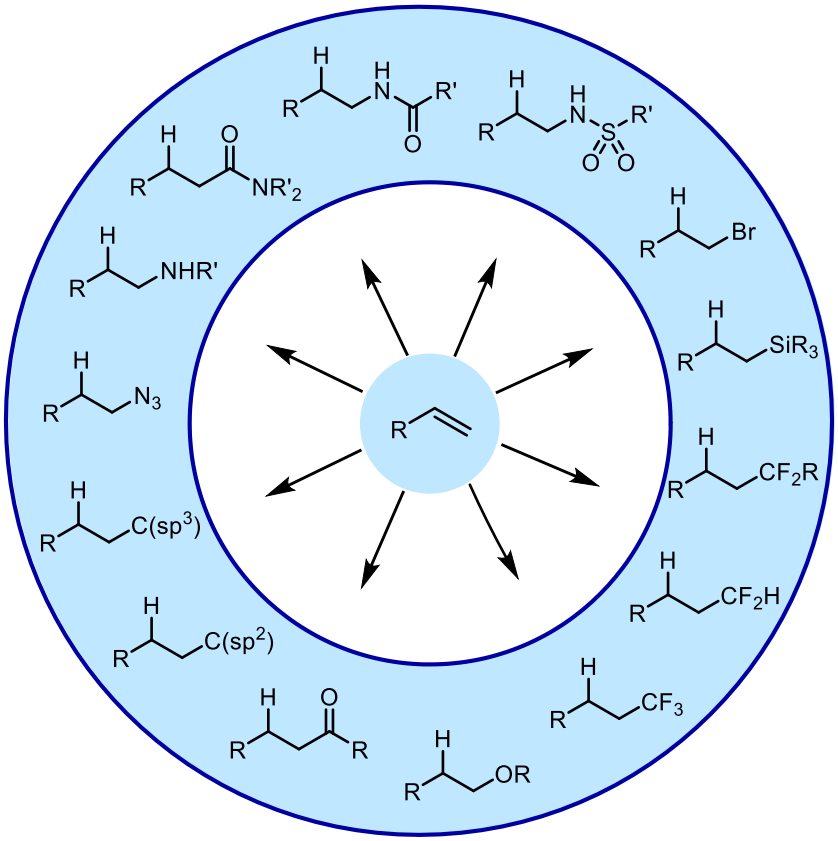


Figure 1.10: Anti-Markovnikov hydrofunctionalisation of alkenes.

The development of novel modes of activation in the field of photoredox catalysis allowed to expand these transformations to readily available starting materials, such as

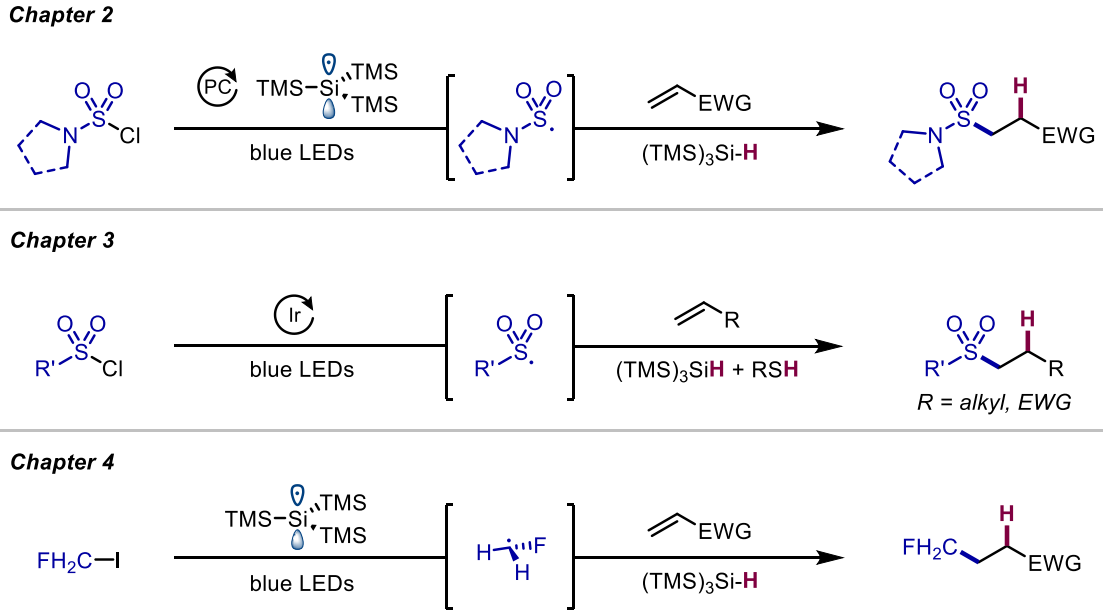
carboxylic acids,[92–94] alcohols,[95,96] amines,[97–99] thiols,[100–104] organohalides,[105] volatile alkanes[106] and others.[107,108] More recently, the synergistic merger of photoredox catalysis and organocatalysis has allowed the translation of these methods towards a stereocontrolled pattern, enabling the asymmetric hydrofunctionalisation of alkenes (e.g. enantioselective α- and β-alkylation of aldehydes utilising simple olefins).[109–114] The successful application of these protocols to a myriad of applications towards drug discovery has been demonstrated with the development of novel methods enabling photocatalytic peptide modification and site selective protein bioconjugation.[115,116]

1.5 Late-Stage Silyl Radical-Mediated Hydrofunctionalisation of Alkenes

Late-stage functionalisation (LSF) represents an attractive strategy to rapidly introduce important functional groups in the last steps of a chemical synthesis.[117] Specifically, the late-stage hydrofunctionalisation of alkenes constitutes the ideal scenario for the rapid installation of aliphatic fragmentsin drug discovery.[118,119] This process would allow for the generation of diversified chemical libraries, which results in a faster exploration of structure-activity relationship (SAR).[120,121] Furthermore, the development of new late-stage methodologies employing photochemistry is of particular interest, as light stands out as a green, non-hazardous, and traceless energy source.

In the last decade, the generation of silyl radicals for cascade transformations has been of particular interest. Surprisingly, silyl radicals have been employed exclusively in the activation of alkyl and aryl halides for the generation of carbon-centred radical

intermediates. However, silyl radicals have never been exploited for the activation of other organohalides in the context of methodology development. Whilst late-stage introduction of pharmaceutically relevant fragments using photochemistry is a growing field of interest within organic chemistry, methods which can incorporate sulfonamide, sulfone, and fluoromethyl fragments in complex drug manifolds are underrepresented. Recent developments of light-driven generation of silyl radicals and their subsequent applications in organic synthesis encouraged us to investigate this activation pathway for the functionalisation of alkenes, an area of research which remained underexplored before our work. Within our collaboration with Janssen, we focused on developing "minimalistic" procedures for the efficient generation of small fluorine- and sulfone-containing radicals for the LSF of complex biologically active molecules (**Scheme 1.21**). Specifically, in the context of hydrofunctionalisation, the addition of sulfamoyl, sulfonyl, and fluoromethyl radicals to a broad range of different alkenes will be discussed in **Chapters 2**, **3** and **4**.



Scheme 1.21: Hydrofunctionalisation of alkenes.

All approaches described in this thesis employ commercial, cost-effective and easy-to-handle reagents. The utility of these methods has been validated on the multigram-synthesis of pharmaceutically relevant building blocks and the preparation of structurally complex fragments for drug discovery. These procedures display a broad functional group tolerance and have found applicability for the LSF of a diverse set of drug molecules and natural products.

1.6 References

[1] P. Anastas, N. Eghbali, *Chem. Soc. Rev.* **2010**, *39*, 301–312.
[2] G. E. M. Crisenza, P. Melchiorre, *Nat. Commun.* **2020**, *11*, 1–4.
[3] W. Liu, C. J. Li, *Synlett* **2017**, *28*, 2714–2754.
[4] D. Ravelli, D. Dondi, M. Fagnoni, A. Albini, *Chem. Soc. Rev.* **2009**, *38*, 1999–2011.
[5] A. B. Beeler, *Chem. Rev.* **2016**, *116*, 9629–9630.
[6] G. S. Hammond, N. J. Turro, *Science* **1963**, *142*, 1541–1553.
[7] L. Marzo, S. K. Pagire, O. Reiser, B. König, *Angew. Chem. Int. Ed.* **2018**, *57*, 10034–10072.
[8] M. H. Shaw, J. Twilton, D. W. C. MacMillan, *J. Org. Chem.* **2016**, *81*, 6898–6926.
[9] C. K. Prier, D. A. Rankic, D. W. C. MacMillan, *Chem. Rev.* **2013**, *113*, 5322–5363.
[10] F. T. Iers, *Inorg. Chem. Front.* **2015**, *2*, 687–712.
[11] N. A. Romero, D. A. Nicewicz, *Chem. Rev.* **2016**, *116*, 10075–10166.
[12] B. M. Hockin, C. Li, N. Robertson, E. Zysman-Colman, *Catal. Sci. Technol.* **2019**, *9*, 889–915.
[13] S. Paria, O. Reiser, *ChemCatChem* **2014**, *6*, 2477–2483.
[14] P. J. DeLaive, T. K. Foreman, C. Giannotti, D. G. Whitten, *J. Am. Chem. Soc.* **1980**, *102*, 5627–5631.
[15] S. Ruccolo, Y. Qin, C. Schnedermann, D. G. Nocera, *J. Am. Chem. Soc.* **2018**, *140*, 14926–14937.
[16] K. Henk, D. REHM, A. WELLER, *Berichte der Bunsengesellschaft für Phys. Chemie* **1968**, *72*, 257–263.
[17] H. Cano-Yelo, A. Deronzier, *Tetrahedron Lett.* **1984**, *25*, 5517–5520.
[18] H. Cano-Yelo, A. Deronzier, *J. Photochem.* **1987**, *37*, 315–321.
[19] C. Pac, Y. Miyauchi, O. Ishitani, M. Ihama, M. Yasuda, H. Sakurai, *J. Org. Chem.* **1984**, *49*, 26–34.
[20] T. J. van Bergen, D. M. Hedstrand, W. H. Kruizinga, R. M. Kellogg, *J. Org. Chem.* **1979**, *44*, 4953–4962.
[21] S. Fukuzumi, S. Mochizuki, T. Tanaka, *J. Phys. Chem.* **1990**, *94*, 722–726.
[22] C. Pac, M. Ihama, M. Yasuda, Y. Miyauchi, H. Sakurai, *J. Am. Chem. Soc.* **1981**, *103*, 6495–6497.
[23] O. Ishitani, M. Ihama, Y. Miyauchi, *J. Chem. Soc. Perkin Trans. I* **1985**, 1527–1531.
[24] D. M. Hedstrand, W. H. Kruizinga, R. M. Kellogg, *Tetrahedron Lett.* **1978**, 1255–1258.
[25] K. Hironaka, S. Fukuzumi, T. Tanaka, *J. Chem. Soc. Perkin Trans. II* **1984**, 1705–1709.
[26] J. M. R. Narayanam, J. W. Tucker, C. R. J. Stephenson, *J. Am. Chem. Soc.* **2009**, *131*, 8756–8757.
[27] D. A. Nicewicz, D. W. C. MacMillan, *Science* **2008**, *322*, 77–80.
[28] M. A. Ischay, M. E. Anzovino, J. Du, T. P. Yoon, *J. Am. Chem. Soc.* **2008**, *130*, 12886–12887.
[29] V. Balzani, P. Ceroni, A. Juris, *Photochemistry and Photophysics*, **2014**.
[30] D. H. R. Barton, Mcco. Stuart W., *J. C. S. Perkin I* **1975**, 1574–1585.
[31] D. H. R. Barton, J. C. Jaszberenyi, *Tetrahedron Lett.* **1989**, *30*, 2619–2622.
[32] J. Light, R. Breslow, *Tetrahedron Lett.* **1990**, *31*, 2957–2958.
[33] A. Studer, S. Amrein, *Synthesis* **2002**, 835–849.
[34] E. A. Brock, S. G. Davies, J. A. Lee, P. M. Roberts, J. E. Thomson, *Org. Lett.* **2012**, *14*, 4278–4281.
[35] R. M. Lopez, D. S. Hays, G. C. Fu, *J. Am. Chem. Soc.* **1997**, *119*, 6949–6950.
[36] C. Chatgilialoglu, C. Ferreri, Y. Landais, V. I. Timokhin, *Chem. Rev.* **2018**, *118*, 6516–6572.
[37] K. J. Shea, D. A. Loy, *Chem. Mater.* **2001**, *13*, 3306–3319.
[38] P. G. Harrison, *J. Organomet. Chem.* **1997**, *542*, 141–183.
[39] D. H. R. Barton, D. O. Jang, J. C. Jaszberenyi, *Tetrahedron Lett.* **1991**, *32*, 7187–7190.
[40] D. M. Hodgson, L. H. Winning, *Beilstein J. Org. Chem.* **2008**, *4*, 4–11.
[41] C. Chatgilialoglu, V. I. Timokhin, *Adv. Organomet. Chem.* **2008**, *57*, 117–181.
[42] R. Walsh, *Acc. Chem. Res.* **1981**, *14*, 246–252.
[43] L. N. Lewis, J. Stein, Y. Gao, R. E. Colborn, G. Hutchins, *Platin. Matals Rev.* **1997**, *41*, 66–75.
[44] L. H. Sommer, E. W. Pietrusza, F. C. Whitmore, *J. Am. Chem. Soc.* **1947**, *69*, 188.
[45] H. Merten, H. Gilman, *J. Am. Chem. Soc.* **1954**, *76*, 5798–5799.
[46] F. W. Pietrusza, L. H. Sommer, F. C. Whitmore, *J. Am. Chem. Soc.* **1948**, *70*, 484–486.
[47] C. A. Burkhard, R. H. Krieble, *J. Am. Chem. Soc.* **1947**, *69*, 2687–2689.
[48] J. Curtice, H. Gilman, G. S. Hammond Vol, L. P. Hammett, E. Grunwald, R. W. Taft, *J. Am. Chem. Soc.* **1957**, *79*, 4754–4759.
[49] C. Chatgilialoglu, C. Ferreri, Y. Landais, V. I. Timokhin, *Chem. Rev.* **2018**, *118*, 6516–6572.
[50] C. Chatgilialoglu, J. Lalevée, *Molecules* **2012**, *17*, 527–555.
[51] C. Chatgilialoglu, *Chem. Eur. J.* **2008**, *14*, 2310–2320.
[52] C. Chatgilialoglu, D. Griller, M. Lesage, *J. Org. Chem.* **1989**, *54*, 2492–2494.
[53] C. C. Icocea, C. Nazionale, D. Ricerche, O. Emilia, *Acc. Chem. Res* **1992**, *25*, 188–194.

[54] A. Postigo, S. Kopsov, C. Ferreri, C. Chatgilialoglu, *Org. Lett.* **2007**, *9*, 5159–5162.
[55] H. Jiang, J. R. Bak, F. J. López-Delgado, K. A. Jørgensen, *Green Chem.* **2013**, *15*, 3355–3359.
[56] G. P. Da Silva, A. Ali, R. C. Da Silva, H. Jiang, M. W. Paixão, *Chem. Commun.* **2015**, *51*, 15110–15113.
[57] C. A. D. Caiuby, A. Ali, V. T. Santana, F. W. S. De Lucas, M. S. Santos, A. G. Corrêa, O. R. Nascimento, H. Jiang, M. W. Paixão, *RSC Adv.* **2018**, *8*, 12879–12886.
[58] J. J. Devery, J. D. Nguyen, C. Dai, C. R. J. Stephenson, *ACS Catal.* **2016**, *6*, 5962–5967.
[59] P. Zhang, C. C. Le, D. W. C. MacMillan, *J. Am. Chem. Soc.* **2016**, *138*, 8084–8087.
[60] J. Boström, D. G. Brown, R. J. Young, G. M. Keserü, *Nat. Rev. Drug Discov.* **2018**, *17*, 709–727.
[61] P. Li, J. A. Terrett, J. R. Zbieg, *ACS Med. Chem. Lett.* **2020**, *11*, 2120–2130.
[62] R. W. Pipal, K. T. Stout, P. Z. Musacchio, S. Ren, T. J. A. Graham, S. Verhoog, L. Gantert, T. G. Lohith, A. Schmitz, H. S. Lee, et al., *Nature* **2020**, ttps://doi.org/10.1038/s41586-020-3015-0.
[63] H. A. Sakai, W. Liu, C. Le, D. W. C. MacMillan, *J. Am. Chem. Soc.* **2020**, *142*, 11691–11697.
[64] T. Q. Chen, D. W. C. MacMillan, *Angew. Chem. Int. Ed.* **2019**, *131*, 14726–14730.
[65] J. Dong, X. Lyu, Z. Wang, X. Wang, H. Song, Y. Liu, Q. Wang, *Chem. Sci.* **2019**, *10*, 976–982.
[66] R. T. Smith, X. Zhang, J. A. Rincón, J. Agejas, C. Mateos, M. Barberis, S. García-Cerrada, O. De Frutos, D. W. C. MacMillan, *J. Am. Chem. Soc.* **2018**, *140*, 17433–17438.
[67] R. Kumar, N. J. Flodén, W. G. Whitehurst, M. J. Gaunt, *Nature* **2020**, *581*, 415–420.
[68] P. Shah, A. D. Westwell, *J. Enzyme Inhib. Med. Chem.* **2007**, *22*, 527–540.
[69] T. Liang, C. N. Neumann, T. Ritter, *Angew. Chem. Int. Ed.* **2013**, *52*, 8214–8264.
[70] C. Le, T. Q. Chen, T. Liang, P. Zhang, D. W. C. MacMillan, *Science* **2018**, *360*, 1010–1014.
[71] M. N. Lavagnino, T. Liang, D. W. C. MacMillan, *Proc. Natl. Acad. Sci. U. S. A.* **2020**, *117*, 21058–21064.
[72] D. J. P. Kornfilt, D. W. C. MacMillan, *J. Am. Chem. Soc.* **2019**, *141*, 6853–6858.
[73] X. Zhao, D. W. C. MacMillan, *J. Am. Chem. Soc.* **2020**, *142*, 19480–19486.
[74] Y. Zafrani, D. Yeffet, G. Sod-Moriah, A. Berliner, D. Amir, D. Marciano, E. Gershonov, S. Saphier, *J. Med. Chem.* **2017**, *60*, 797–804.
[75] V. Bacauanu, S. Cardinal, M. Yamauchi, M. Kondo, D. F. Fernández, R. Remy, D. W. C. MacMillan, *Angew. Chem. Int. Ed.* **2018**, *130*, 12723–12728.
[76] G. H. Lovett, S. Chen, X. S. Xue, K. N. Houk, D. W. C. MacMillan, *J. Am. Chem. Soc.* **2019**, *141*, 20031–20036.
[77] J. Choi, L. Tang, J. R. Norton, *J. Am. Chem. Soc.* **2007**, *129*, 234–240.
[78] S. W. M. Crossley, C. Obradors, R. M. Martinez, R. A. Shenvi, *Chem. Rev.* **2016**, *116*, 8912–9000.
[79] S. W. M. Crossley, R. M. Martinez, S. Guevara-Zuluaga, R. A. Shenvi, *Org. Lett.* **2016**, *18*, 2620–2623.
[80] S. A. Green, S. Vásquez-Céspedes, R. A. Shenvi, *J. Am. Chem. Soc.* **2018**, *140*, 11317–11324.
[81] S. A. Green, J. L. M. Matos, A. Yagi, R. A. Shenvi, *J. Am. Chem. Soc.* **2016**, *138*, 12779–12782.
[82] J. L. M. Matos, S. Vásquez-Céspedes, J. Gu, T. Oguma, R. A. Shenvi, *J. Am. Chem. Soc.* **2018**, *140*, 16976–16981.
[83] S. A. Green, T. R. Huffman, R. O. McCourt, V. Van Der Puyl, R. A. Shenvi, *J. Am. Chem. Soc.* **2019**, *141*, 7709–7714.
[84] T. Okamoto, K. Kobayashi, S. Oka, S. Tanimoto, *J. Org. Chem.* **1988**, *53*, 4897–4901.
[85] M. Takeuchi, H. Shimakoshi, K. Kano, *Organometallics* **1994**, *13*, 1208–1213.
[86] H. Shigehisa, E. Nishi, M. Fujisawa, K. Hiroya, *Org. Lett.* **2013**, *15*, 5158–5161.
[87] H. Shigehisa, H. Kikuchi, K. Hiroya, *Chem. Pharm. Bull.* **2016**, *64*, 371–374.
[88] S. L. Shevick, C. V. Wilson, S. Kotesova, D. Kim, P. L. Holland, R. A. Shenvi, *Chem. Sci.* **2020**, DOI 10.1039/d0sc04112b.
[89] S. A. Green, S. W. M. Crossley, J. L. M. Matos, S. Vásquez-Céspedes, S. L. Shevick, R. A. Shenvi, *Acc. Chem. Res.* **2018**, *51*, 2628–2640.
[90] B. Giese, *Angew. Chem. Int. Ed.* **1985**, *24*, 553–565.
[91] D. P. Curran, *Synthesis* **1988**, *6*, 417–439.
[92] L. Chu, C. Ohta, Z. Zuo, D. W. C. MacMillan, *J. Am. Chem. Soc.* **2014**, *136*, 10886–10889.
[93] E. De Pedro Beato, D. Mazzarella, M. Balletti, P. Melchiorre, *Chem. Sci.* **2020**, *11*, 6312–6324.
[94] A. J. Perkowski, D. A. Nicewicz, *J. Am. Chem. Soc.* **2013**, *135*, 10334–10337.
[95] C. C. Nawrat, C. R. Jamison, Y. Slutskyy, D. W. C. MacMillan, L. E. Overman, *J. Am. Chem. Soc.* **2015**, *137*, 11270–11273.
[96] D. S. Hamilton, D. A. Nicewicz, *J. Am. Chem. Soc.* **2012**, *134*, 18577–18580.
[97] T. M. Nguyen, N. Manohar, D. A. Nicewicz, *Angew. Chem. Int. Ed.* **2014**, *53*, 6198–6201.
[98] D. C. Miller, J. M. Ganley, A. J. Musacchio, T. C. Sherwood, W. R. Ewing, R. R. Knowles, *J. Am. Chem. Soc.* **2019**, *141*, 16590–16594.
[99] Q. Zhu, D. E. Graff, R. R. Knowles, *J. Am. Chem. Soc.* **2018**, *140*, 741–747.

[100] E. L. Tyson, M. S. Ament, T. P. Yoon, *J. Org. Chem.* **2013**, *78*, 2046–2050.
[101] V. T. Bhat, P. A. Duspara, S. Seo, N. S. B. Abu Bakar, M. F. Greaney, *Chem. Commun.* **2015**, *51*, 4383–4385.
[102] G. Zhao, S. Kaur, T. Wang, *Org. Lett.* **2017**, *19*, 3291–3294.
[103] E. L. Tyson, Z. L. Niemeyer, T. P. Yoon, *J. Org. Chem.* **2014**, *79*, 1427–1436.
[104] R. O. McCourt, E. M. Scanlan, *Chem. Eur. J.* **2020**, *26*, https://doi.org/10.1002/chem.202002542.
[105] R. A. Aycock, H. Wang, N. T. Jui, *Chem. Sci.* **2017**, *8*, 3121–3125.
[106] G. Laudadio, Y. Deng, K. Van Der Wal, D. Ravelli, M. Nunõ, M. Fagnoni, D. Guthrie, Y. Sun, T. Noël, *Science* **2020**, *369*, 92–96.
[107] D. J. Wilger, J. M. M. Grandjean, T. R. Lammert, D. A. Nicewicz, *Nat. Chem.* **2014**, *6*, 720–726.
[108] J. A. Terrett, M. D. Clift, D. W. C. MacMillan, *J. Am. Chem. Soc.* **2014**, *136*, 6858–6861.
[109] A. G. Capacci, J. T. Malinowski, N. J. McAlpine, J. Kuhne, D. W. C. MacMillan, *Nat. Chem.* **2017**, *9*, 1073–1077.
[110] P. Bonilla, Y. P. Rey, C. M. Holden, P. Melchiorre, *Angew. Chem. Int. Ed.* **2018**, *57*, 12819–12823.
[111] D. Mazzarella, G. E. M. Crisenza, P. Melchiorre, *J. Am. Chem. Soc.* **2018**, *140*, 8439–8443.
[112] C. Verrier, N. Alandini, C. Pezzetta, M. Moliterno, L. Buzzetti, H. B. Hepburn, A. Vega-Peñaloza, M. Silvi, P. Melchiorre, *ACS Catal.* **2018**, *8*, 1062–1066.
[113] G. Goti, B. Bieszczad, A. Vega-Peñaloza, P. Melchiorre, *Angew. Chem. Int. Ed.* **2019**, *58*, 1213–1217.
[114] M. Silvi, C. Verrier, Y. P. Rey, L. Buzzetti, P. Melchiorre, *Nat. Chem.* **2017**, *9*, 868–873.
[115] S. Bloom, C. Liu, D. K. Kölmel, J. X. Qiao, Y. Zhang, M. A. Poss, W. R. Ewing, D. W. C. MacMillan, *Nat. Chem.* **2018**, *10*, 205–211.
[116] Y. Yu, L. K. Zhang, A. V. Buevich, G. Li, H. Tang, P. Vachal, S. L. Colletti, Z. C. Shi, *J. Am. Chem. Soc.* **2018**, *140*, 6797–6800.
[117] J. Börgel, T. Ritter, *Chem* **2020**, *6*, 1877–1887.
[118] F. Lovering, *Med. Chem. Commun.* **2013**, *4*, 515–519.
[119] F. Lovering, J. Bikker, C. Humblet, *J. Med. Chem.* **2009**, *52*, 6752–6756.
[120] T. Cernak, K. D. Dykstra, S. Tyagarajan, P. Vachal, S. W. Krska, *Chem. Soc. Rev.* **2016**, *45*, 546–576.
[121] M. Moir, J. J. Danon, T. A. Reekie, M. Kassiou, *Expert Opin. Drug Discov.* **2019**, *14*, 1137–1149.

Chapter 2

Activation of Sulfamoyl Chlorides: The Development of a Novel Route to Access Aliphatic Sulfonamides

This chapter discloses a new methodology to access aliphatic sulfonamides from cost-effective, commercial, and easy-to-handle reagents. Specifically, this process utilises sulfamoyl radicals generated *in situ* by a silyl radical-mediated halogen atom abstraction strategy in combination with a suitable hydrogen atom donor. This operationally simple one-step method tolerates numerous functional groups, thereby allowing access to a broad range of novel alkylsulfonamides including complex sulfonamide-containing cyclobutyl-spirooxindoles, which are potentially valuable building blocks for drug discovery.

This work has been published in *The Journal of the American Chemical Society* in 2020.

S. M. Hell, C. F. Meyer, G. Laudadio, A. Misale, M. C. Willis, T. Noël, A. A. Trabanco, V. Gouverneur, Silyl Radical-Mediated Activation of Sulfamoyl Chlorides Enables Direct Access to Aliphatic Sulfonamides from Alkenes, *J. Am. Chem. Soc.* **2020**, *142*, 720-725.

Author contributions: Reactions were designed by Sandrine M. Hell, Dr. Andrés A. Trabanco and Prof. Véronique Gouverneur. The reaction conditions were optimised by Sandrine M. Hell. Scope and mechanistic experiments were performed by Sandrine M.

Hell and Claudio F. Meyer. Cyclic voltammetry measurements of sulfamoyl chlorides were performed by Dr. Gabriele Laudadio (former PhD student in the research group of Prof. Timothy Noël, Eindhoven University, Netherlands). Dr. Antonio Misale, Prof. Michael C. Willis and Prof. Timothy Noël provided helpful comments.

A detailed description of the experimental work has been published in *the Journal of Visualized Experiments* in 2020.

S. M. Hell, C. F. Meyer, A. A. Trabanco, V. Gouverneur, Easy Access to Aliphatic Sulfonamides using Sulfamoyl Chlorides Under Visible Light Activation, *J. Vis. Exp.* (161), e61384, doi:10.3791/61384 (**2020**).

This manuscript describes a step-by-step explanation of the reaction set-up and the manipulations required to reproduce these experiments successfully in any laboratory.

2.1 Introduction to Sulfonamides

In the last century, sulfonamides have garnered significant interests in the pharmaceutical industry because of their powerful antibacterial properties, which were discovered in the 1930s with the antibacterial agent Prontosil (**Figure 2.1**, **2.1**).[1] Nowadays, amongst all sulfur-containing FDA approved drugs, nearly 30% contain a sulfonamide moiety, demonstrating the ubiquity of this fragment in drug discovery (**2.2-2.6**).[2–7] Sulfonamide-containing drugs were initially utilised to combat bacterial infections, but their clinical applications have later been extended to the treatment of a plethora of other diseases, such as cancer, CNS disorder, diabetes, dementia, HIV, high blood pressure, and malaria.[6,8–10] In medicinal chemistry, the sulfonamide group is often used as a bioisostere of various functional groups such as carboxylic acids, phenols and amides.[11–15] Nowadays, the incorporation of sulfonamides into pharmaceuticals has become a common strategy for the improvement of drug potency and efficacy.[5,16]

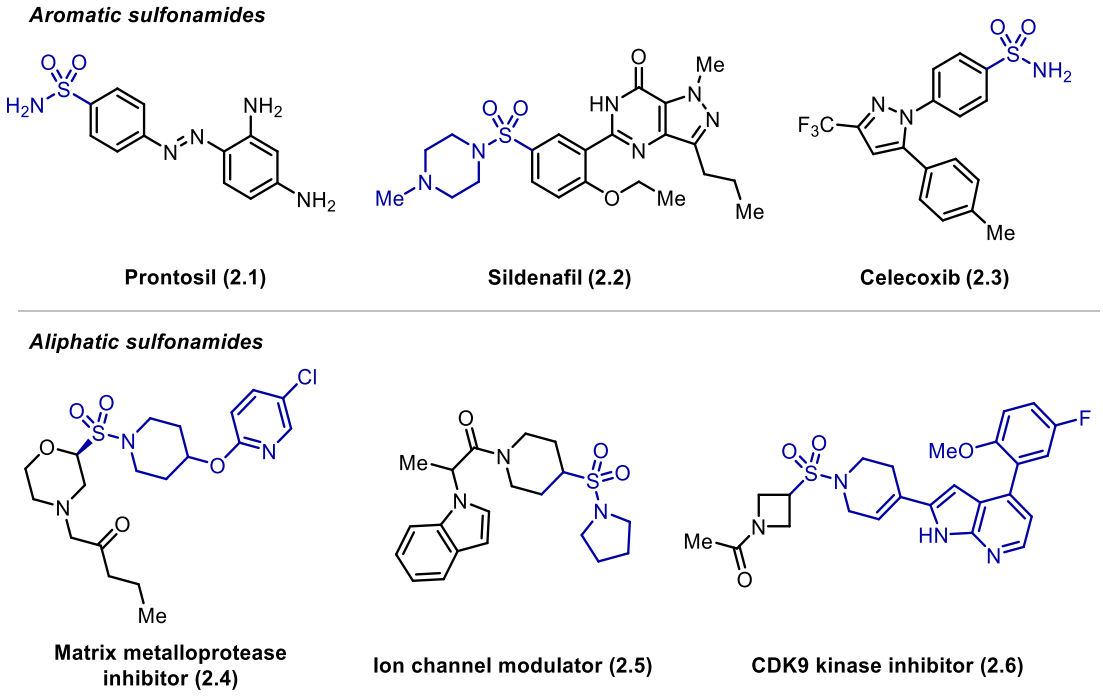
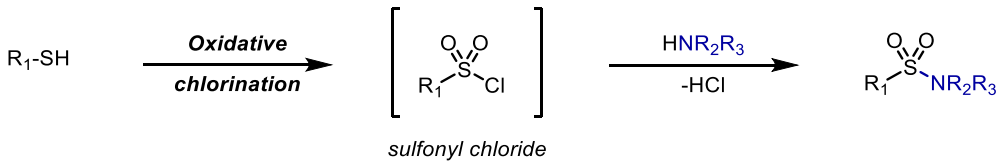


Figure 2.1: Selected examples of sulfonamide-containing biologically active molecules.

2.2 Synthesis of Sulfonamides

2.2.1 Traditional Procedures for the Synthesis of Sulfonamides

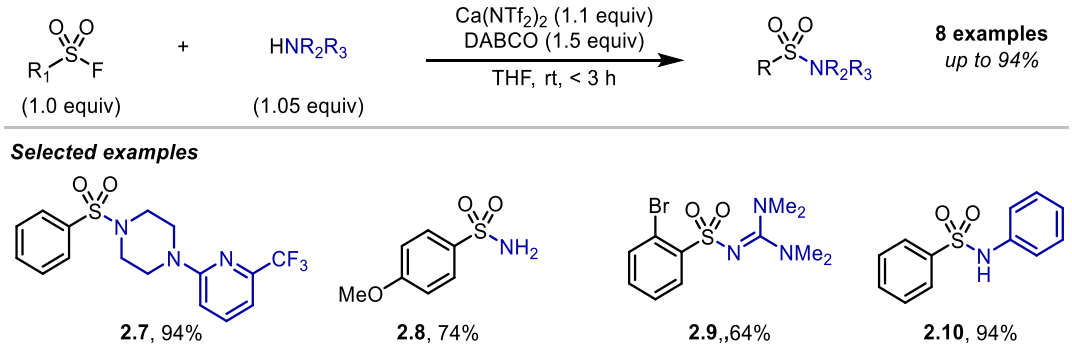
Most syntheses reported to date for the preparation of sulfonamides require a multi-step reaction sequence, whereby a sulfonyl chloride reacts with a primary or a secondary amine (**Scheme 2.1**).[17–20] Sulfonyl chlorides are often not readily available and require preparation beforehand. They are traditionally synthesised by the oxidative chlorination of a thiol with strong oxidising agents, such as hydrogen peroxide in combination with chlorine gas or sodium hypochlorite. This two-step process is routinely used for the synthesis of sulfonamides.[20,21] The harsh reaction conditions employed for the generation of sulfonyl chlorides,[19–26] as well as their difficulty in handling can hamper their suitability for use in the late-stage functionalisation of complex molecules.



Scheme 2.1: Traditional two-step approach for the synthesis of sulfonamides.

Other sulfonyl halides, such as sulfonyl fluorides, have also been employed as precursors in the synthesis of sulfonamides.[27,28] Owing to the increased stability of sulfonyl fluorides over sulfonyl chlorides, their reactivity is relatively diminished. An excess of amines, strong bases or nucleophiles, or extensive heating is usually required for the reaction to proceed.[29–31] More recently, milder reaction conditions have been reported by am Ende, Ball and co-workers, whereby sulfonyl fluorides are activated using a Lewis-acid (**Scheme 2.2**).[27,28] This new sulfur (VI) fluoride exchange (SuFEx) activation mode provided access to a variety of sulfonamide-containing building blocks

(**2.7** - **2.10**) at ambient conditions with only slight excess of amine used (1.05 equivalents).

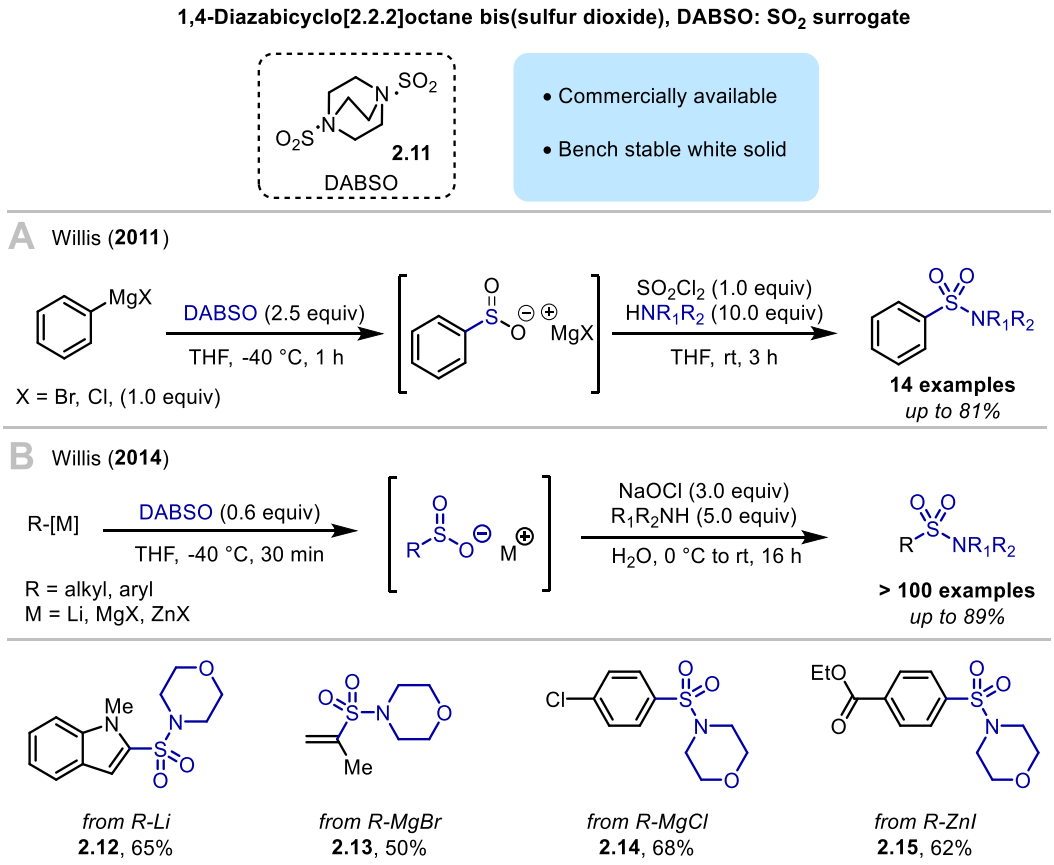


Scheme 2.2: Calcium-triflimide activation of sulfonyl fluorides.

2.2.2 Sulfonamide Synthesis using Sulfur Dioxide Surrogates

With the aim of avoiding operationally complex procedures, scientists focused on the development of one-pot procedures for the introduction of sulfonamide fragments. In the past decades, the design of new reagents used as sulfur dioxide surrogates has enabled a surge in method development for the synthesis of sulfonamides. The Willis research group identified DABCO·$(SO_2)_2$ (DABSO, **2.11**), as a versatile surrogate for the preparation of sulfonamides (**Scheme 2.3**). Initially reported by Santos and co-workers in 1988,[32] this bench-stable and easy-to-handle white solid was overlooked until 2011, when Willis and co-workers demonstrated an efficient one-pot preparation of sulfonamides from organometallic reagents (**Scheme 2.3A**). In this transformation, a reactive sulfinate salt is formed upon reaction of an organometallic and DABSO **2.11**.[33] This sulfinate intermediate can readily react *via* oxidative amination to afford a wide selection of sulfonamides. This work has later been extended to a wider range of organometallic reagents, including organolithium and organozinc reagents (**Scheme 2.3B**).[34] This new strategy employs milder reaction conditions for the *in situ* generation

of the sulfonyl chloride, specifically by replacing sulfuryl chloride with an aqueous solution of sodium hypochlorite.

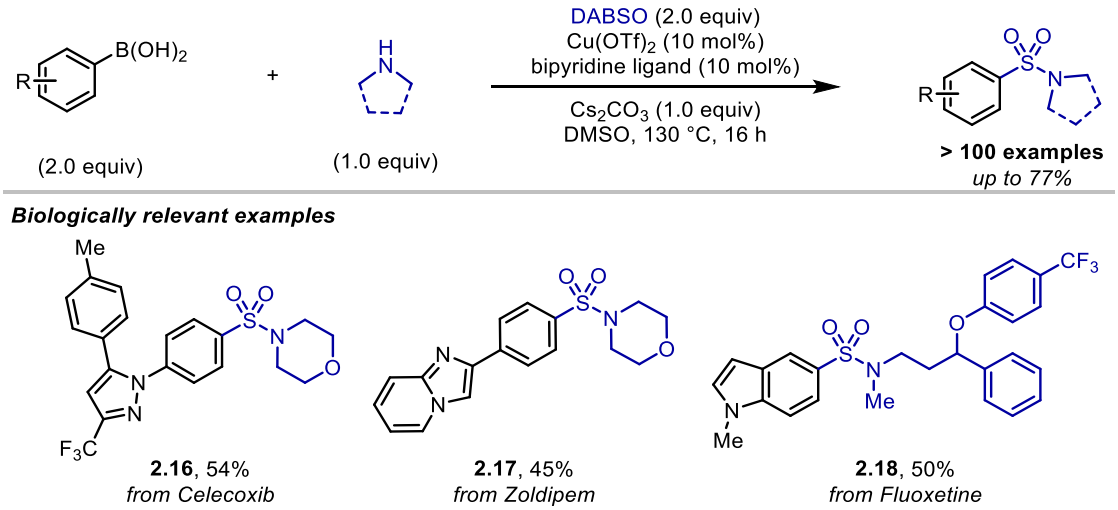


Scheme 2.3: One-pot process for the synthesis of sulfonamides using DABSO.

In the past years, DABSO (**2.11**) has been employed in numerous transition metal-catalysed cross-coupling reactions, employing copper or palladium catalysts, enabling to extend the scope to aryl halides and aryl boronic acids.[35–39] Alternative sulfur dioxide surrogates, such as potassium metabisulfite ($K_2S_2O_5$), were also successful in the sulfination of aryl and heteroaryl halides.[39,40] These novel methodologies allowed access to a collection of pharmacophores in good to excellent yields. Notably, all methods described above consist of one-pot two steps procedures.

More recently, the Willis research group described a single-step copper-catalysed protocol allowing the attachment of a sulfonamide functionality to (hetero)aryl and alkenyl boronic acids using commercially available reagents (**Scheme 2.4**).[41] This

transformation displays a wide functional group tolerance resulting in a broad scope, including highly desirable biologically active molecules (**2.16** - **2.18**). This three-component procedure represents a robust methodology for the installation of sulfonamide groups onto drug-fragments.

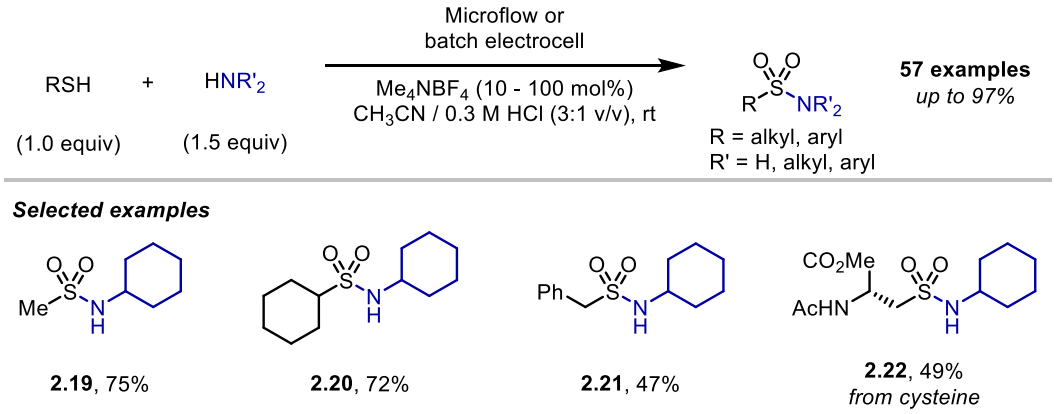


Scheme 2.4: Copper-catalysed synthesis of arylsulfonamides.

2.2.3 Synthesis of Aliphatic Sulfonamides

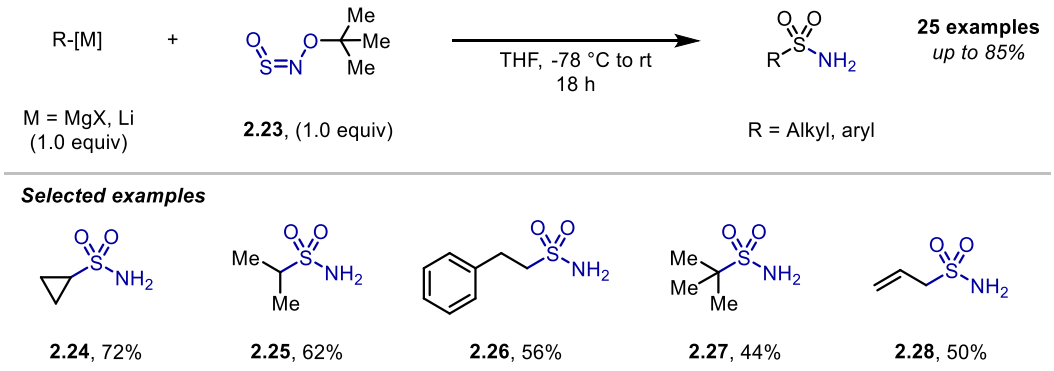
As shown above, powerful strategies for the preparation of (hetero)aryl sulfonamides have been developed in the last century. However, these methodologies are often not amenable to aliphatic substrates. An exceptional advance in the field of aliphatic sulfonamide synthesis, is the electrochemical oxidative coupling of readily available and inexpensive amines and thiols described by Noël and co-workers in 2019 (**Scheme 2.5**).[42] This methodology addresses a longstanding challenge of employing readily available thiols and amines as feedstock starting materials for the preparation of sulfonamides. The reaction displays a broad substrate scope, including aryl- and alkylsulfonamides and operates under mild reaction conditions. Interestingly, this transformation was successful for the preparation of aliphatic sulfonamides by

employing aliphatic thiols and amines (**2.19** - **2.21**). Furthermore, cysteine was also suitable for this transformation affording the desired product in 49% yield (**2.22**).



Scheme 2.5: Electrochemical oxidative coupling of amines and thiols.

More recently, Willis and co-workers developed a novel sulfinylamine reagent, *N*-sulfinyl-*O*-(*tert*-butyl)-hydroxylamine (**Scheme 2.6**, **2.23**; *t*BuONSO) for the preparation of primary sulfonamides from organometallic reagents.[43] Although most of the examples described in this work focused on aryl sulfonamides, several examples of aliphatic sulfonamides were reported. This transformation offers a straightforward way for the introduction of polar primary sulfonamides.

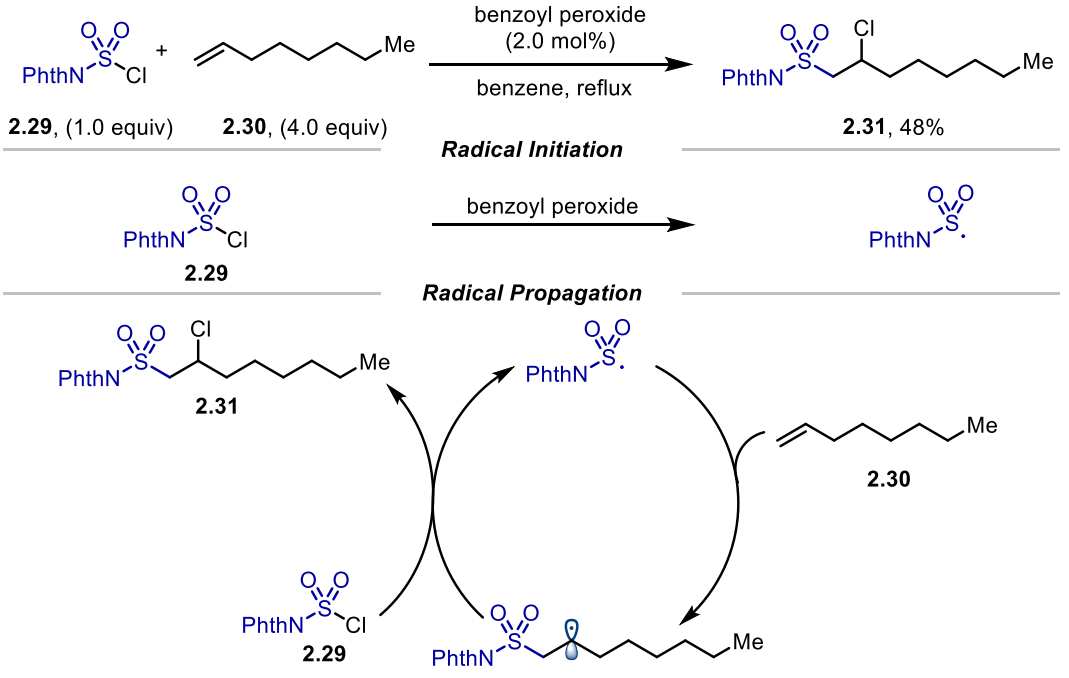


Scheme 2.6: Preparation of primary sulfonamides using *t*BuONSO as sulfonamide precursor.

2.3 Sulfamoyl Radicals: Properties and Reactivity

Owing to the increasing demand from the pharmaceutical sector for C(sp^3)-rich molecules, facile access to alkylsulfonamides from cost-effective, commercial and easy-to-handle sulfonylating reagents is highly desirable.[44–47] The use of sulfamoyl chlorides as sulfamoyl radical precursors, for the direct introduction of the SO_2NR_2 motif is an attractive strategy. The study of this class of radicals remains scarce and only few reports described their use in organic synthesis. In 1988, Chatgilialoglu and co-workers provided evidence by electron spin resonance (ESR) spectral studies of *N*,*N*-dimethylsulfamoyl radicals that sulfamoyl radicals are pyramidal with respect to the sulfur atom.[48]

As early as 1951, Kharash and co-workers reported for the first time the use of sulfamoyl radicals in organic synthesis (**Scheme 2.7**).[49]

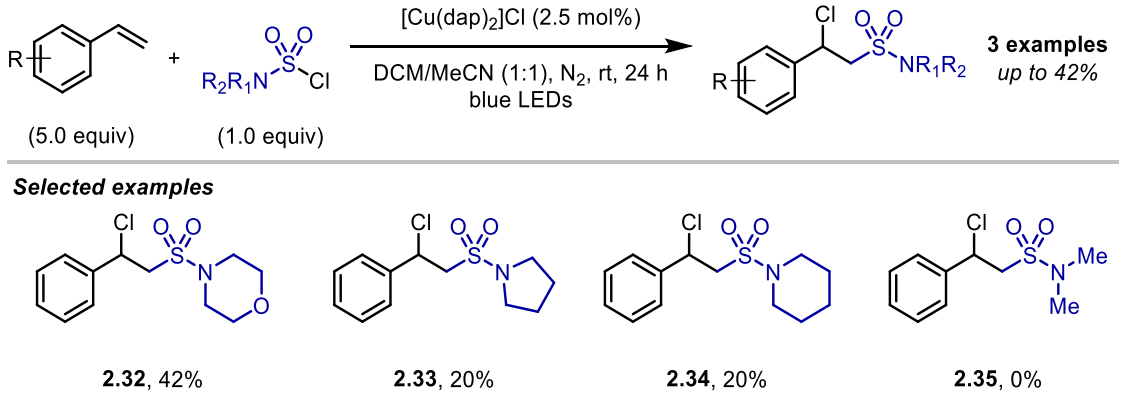


Scheme 2.7: Radical-mediated synthesis of chlorosulfonamides.

In this report, *N*-chlorosulfonylphthalimide **2.29** reacts with alkene **2.30**, yielding the net chlorosulfonamide adduct **2.31**. Mechanistically, the sulfamoyl radical is generated by initiation with benzoyl peroxide under thermal conditions. The sulfamoyl radical

regioselectively adds to the alkene to generate a carbon-centred radical intermediate. The ATRA product is finally formed by chlorine atom abstraction from the sulfamoyl chloride, whereby a new sulfamoyl radical is generated. These seminal results demonstrated the feasibility of the generation of sulfamoyl radicals from sulfamoyl chlorides. Importantly, no product was observed either using styrene, indene, vinyl acetate or allyl chloride as alkene. Furthermore *N*,*N*-dimethylsulfamoyl chloride or *N*,*N*-dimethylcarbamoyl chloride were not suitable for the generation of the corresponding sulfamoyl radicals. Whilst the generation of sulfamoyl radicals has been described in seminal reports from various precursors,[50–52] their reactivity in methodology development has not been fully exploited.

Recently, Hu and co-workers investigated the activation of sulfamoyl chlorides with visible light photoredox catalysis (**Scheme 2.8**).[53]



Scheme 2.8: Copper-catalysed chlorosulfonylation under visible light activation.

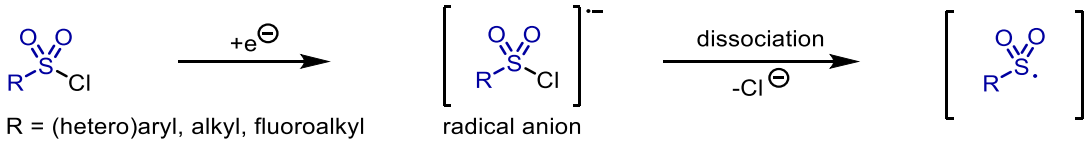
This procedure features an ATRA leading to vicinal chlorosulfamoylated motifs (**2.32** - **2.35**). Whilst most of the examples reported in this work focused on chlorosulfonylation, select examples of chlorosulfamoylation are also described. An important drawback of this methodology is that five equivalents of styrene were required for the reaction to proceed in low yield (20 - 42%). Furthermore, no reactivity was observed for *N*,*N*-

dimethylsulfamoyl chloride, demonstrating the challenges associated with the efficient activation of sulfamoyl chlorides under photoredox catalysis.

Overall, the employment of sulfamoyl chlorides as sulfamoyl radical precursors for the functionalisation of small molecules remains underdeveloped. The underlying reason for the challenging generation of sulfamoyl radicals from sulfamoyl chlorides will be discussed in the following section.

2.4 Single-Electron Reduction of Sulfamoyl Chlorides

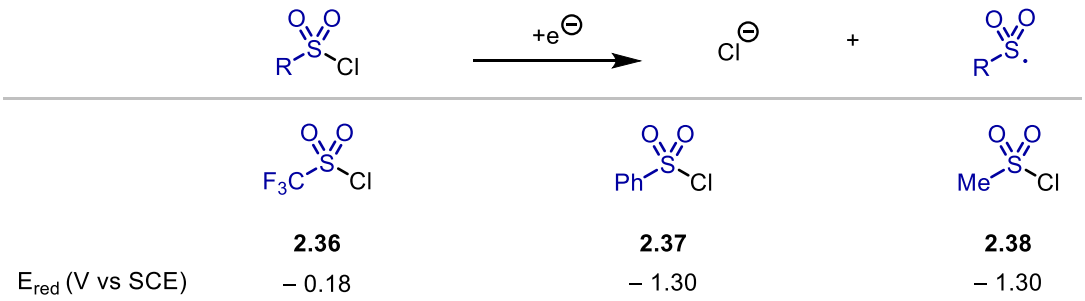
In the context of photoredox-catalysis, the direct activation of sulfonyl chlorides *via* single-electron reduction has already been achieved.[54–58] Generally, upon SET, a sulfonyl chloride radical anion $[RSO_2Cl]^{\bullet-}$ is formed, which spontaneously undergoes heterolytic bond cleavage to the free sulfonyl radical (**Scheme 2.9**). This process is dependent on the energy barrier of the electron transfer as well as the stability of the radical generated upon dissociation.



Scheme 2.9: Single-electron reduction of sulfonyl chlorides.

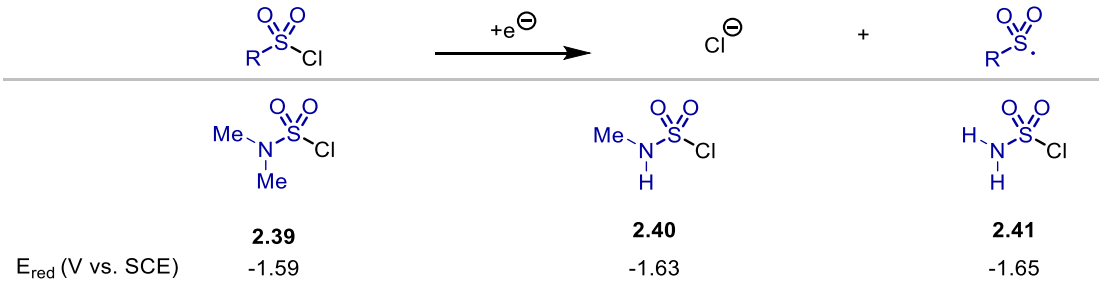
The success of radical generation relies on a redox match between the reduction potential of the photocatalyst in the excited state and the sulfonyl chloride substrate. As such, a wide range of sulfonyl chlorides, including fluoroalkyl- (E_{red} (CF_3SO_2Cl, **2.36**) = − 0.18 V vs SCE in MeCN),[54] aryl (E_{red} ($PhSO_2Cl$, **2.37**) = − 1.30 V vs SCE in MeCN)[59] and alkylsulfonyl chlorides (E_{red} ($MeSO_2Cl$, **2.38**) = − 1.30 V vs SCE in MeCN),[60] have been

successfully activated by single-electron reduction under photoredox catalysis (**Scheme 2.10**).[53,61–67]



Scheme 2.10: Reduction potentials of sulfonyl chlorides.

On the other hand, the photoredox-catalysed generation of sulfamoyl radicals in the context of methodology development has attracted comparatively very little attention.[68] To the best of our knowledge, no data for the reduction potential of sulfamoyl chlorides has been disclosed. Therefore, our collaborators at the University of Eindhoven (Prof. Timothy Noël and Dr. Gabriele Laudadio) performed cyclic voltammetry measurements of *N*,*N*-dimethylsulfamoyl chloride (**2.39**, E_{red} (Me_2NSO_2Cl = − 1.59 V vs SCE in MeCN), *N*-methylsulfamoyl chloride (**2.40**, E_{red} ($MeHNSO_2Cl$ = − 1.63 V vs SCE in MeCN) and sulfamoyl chloride (**2.41**, E_{red} (H_2NSO_2Cl = − 1.65 V vs SCE in MeCN).



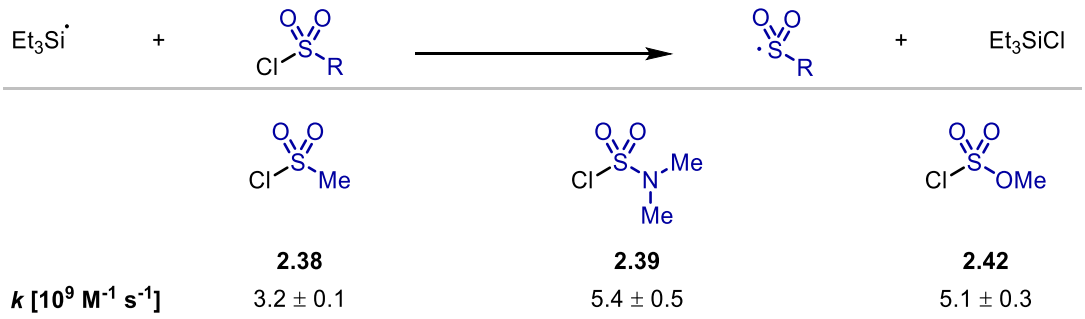
Scheme 2.11: Reduction potential of sulfamoyl chloride derivatives.

These initial data revealed that the reduction potentials of sulfamoyl chlorides are higher (absolute value) than for (fluoro)alkyl and aryl- or alkylsulfonyl chlorides (**Scheme 2.11**). These values indicated that the direct activation of sulfamoyl chlorides by SET is more challenging compared to sulfonyl chlorides. Therefore, we were interested in developing

an alternative mode of activation for sulfamoyl chlorides, whereby the generation of the sulfamoyl radical would be independent from its reduction potential.

2.5 Strategy for the Direct Activation of Sulfamoyl Chlorides

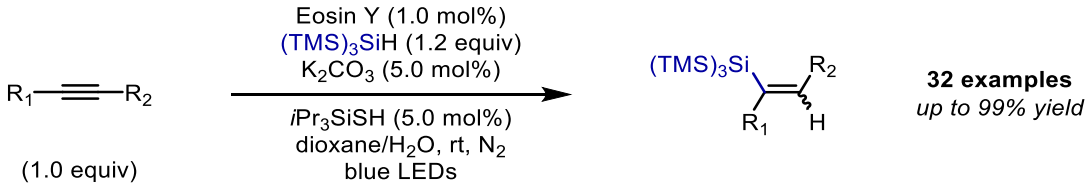
We were initially inspired by early studies from Chatgilialoglu's and other groups describing the numerous advantages in terms of selectivity, and functional group tolerance of silyl radical-mediated activation of organohalides.[69–78] Silyl radicals are usually generated either by initiation with additives (e.g. peroxides or AIBN) or by direct UV-photolysis (see **Chapter 1** for more details). In 1988, Chatgilialoglu and co-workers reported the generation of alkyl, alkoxy and sulfamoyl radicals by direct chlorine atom abstraction of the sulfonyl chloride by a silyl radical (**Scheme 2.12**).[48]



Scheme 2.12: Rate constants for chlorine atom abstraction by triethylsilyl radicals from sulfonyl chloride derivatives.[a] *k*: rate constants (M^{-1} s^{-1}).

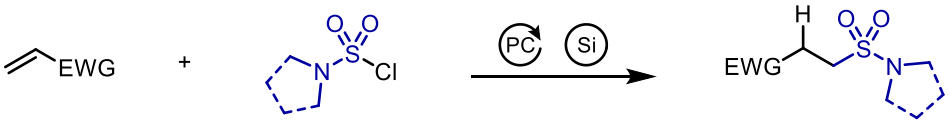
In this study, Electron Paramagnetic Resonance (EPR) studies demonstrated that this HAA is independent of the substitution pattern on the sulfur. As such, *N*,*N*-dimethylsulfamoyl, methylsulfonyl as well as methoxysulfonyl radicals were generated *via* direct chlorine atom abstraction from a triethylsilyl radical with similar reaction rates ($3 - 6 \times 10^9$ M^{-1} s^{-1}). Encouraged by this study, we speculated that this mode of activation could be employed for the efficient generation of sulfamoyl radicals from sulfamoyl chlorides and applied in methodology development. Given the synthetic power of

photoredox catalysis for the functionalisation of C(sp^3)-centers, we were interested in the use of visible light, as a clean and traceless energy source for the activation of the silane. Interestingly, previous reports revealed that $(TMS)_3SiH$, a privileged reagent for "green" free radical chemistry, has been activated under photoredox catalysis using the organophotocatalyst Eosin Y.[79] In the context of hydrosilylation of alkynes, Yao and co-workers demonstrated that upon irradiation with light, the triplet excited state of the organophotocatalyst Eosin Y can activate $(TMS)_3SiH$ *via* single-electron oxidation for the generation of a silyl radical (**Scheme 2.13**). This radical can be efficiently added to an alkyne to form the corresponding alkene.

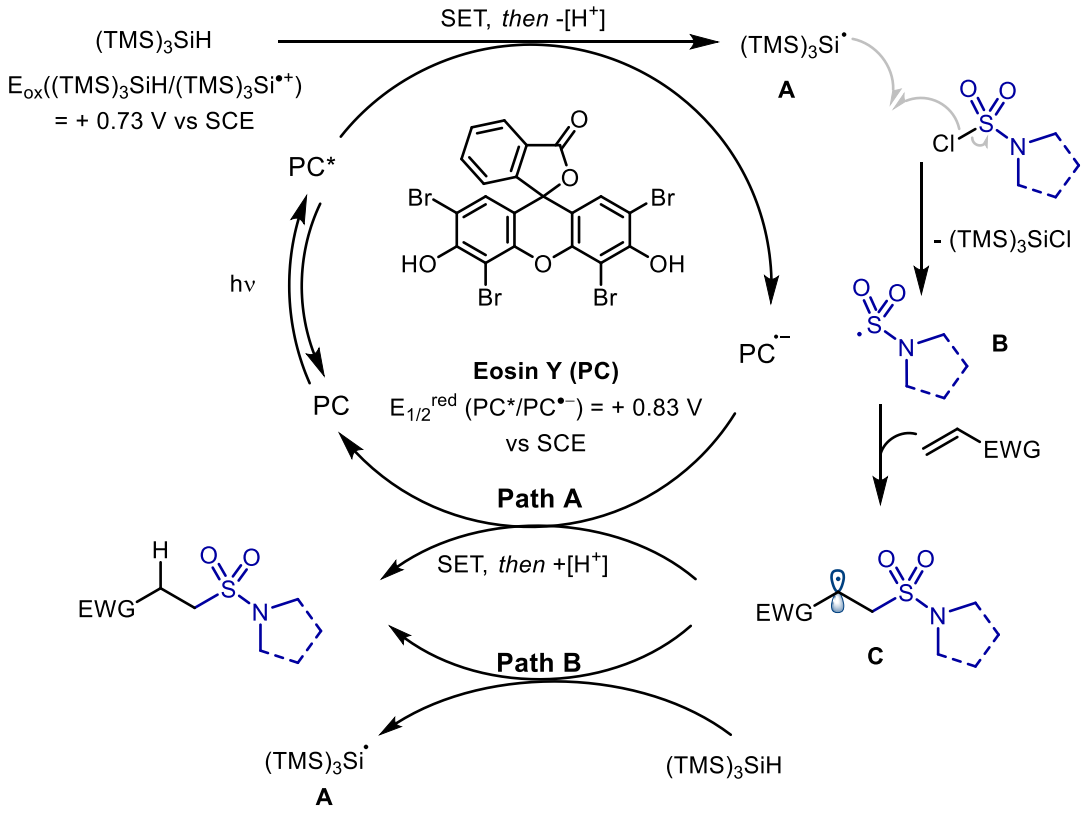


Scheme 2.13: Hydrosilylation of alkynes under photoredox catalysis.

Encouraged by this report, we hypothesised a mechanistic scenario enabling the activation of sulfamoyl chlorides for the net hydrosulfamoylation of alkenes (**Scheme 2.14**). In this scenario, the excited triplet state Eosin Y* [$E_{1/2}^{red}$ ($PC^*/PC^{\bullet-}$) = + 0.83 V vs SCE], generated upon exposure to visible light, undergoes SET with $(TMS)_3SiH$ [E_{ox} ($(TMS)_3SiH/(TMS)_3SiH^{\bullet+}$) = + 0.73 V vs SCE]. Upon single-electron oxidation and loss of a proton, the corresponding silyl radical **A** is formed.



Reaction design



Scheme 2.14: Reaction design for the photoredox-catalysed hydrosulfamoylation of electron-deficient alkenes.

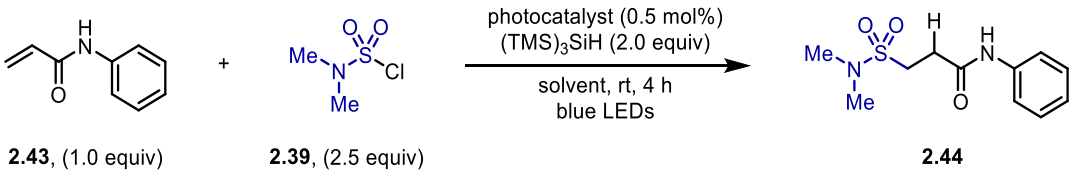
Subsequent chlorine atom abstraction of the sulfamoyl chloride by the silyl radical **A** affords a sulfamoyl radical **B**, and the byproduct $(TMS)_3SiCl$. Next, sulfamoyl radical **B** can undergo regioselective Giese-addition to the alkene, whereby an electrophilic carbon-centred radical **C** is generated. The desired hydrosulfamoylated product can be obtained upon a second SET followed by protonation (**Path A**). In this event, the PC returns in its native oxidation state. Alternatively, a chain propagation reaction mechanism, involving the direct HAT between radical **C** and $(TMS)_3SiH$ is also viable (**Path B**). In this scenario, a new silyl radical would be generated, enabling the activation of a new sulfamoyl chloride to close the chain reaction.

2.6 Initial Investigations

To test the viability of this mechanistic scenario, *N*-phenylacrylamide (**2.43**) was chosen as the model substrate. The structure and purity of the product, resulting from hydrosulfamoylation, were assessed by ^{1}H and ^{13}C NMR spectra. Specifically, disappearance of characteristic alkene peaks [**^{1}H NMR** (500 MHz, $CDCl_3$) δ 6.45 (dd, J = 16.9, 9.8 Hz, 1H), 6.37 (dd, J = 17.0, 2.0 Hz, 1H), 5.63 (dd, J = 9.8, 2.0 Hz, 1H); **^{13}C NMR** (126 MHz, $CDCl_3$) δ 131.4, 127.8] and appearance of aliphatic peaks [**^{1}H NMR** (500 MHz, $CDCl_3$) δ 3.35 (t, J = 7.5 Hz, 1H), 2.91 (t, J = 7.5 Hz, 1H); **^{13}C NMR** (126 MHz, $CDCl_3$) δ 43.5, 37.5, 30.5] are characteristic for the addition of the *N*,*N*-dimethyl sulfamoyl radical to alkene **2.43**.

Initial efforts showed that the combination of alkene **2.43** with Eosin Y (0.5 mol%), $(TMS)_3SiH$, *N*,*N*-dimethylsulfamoyl chloride **2.39** and MeCN as solvent under blue light irradiation (λ_{max} = 470 nm), afforded the desired hydrosulfamoylated product **2.44** in good yield (83% yield; **Table 2.1**, **entry 1**) after 4 hours. Further screening of catalyst loading (5.0 mol%, 1.0 mol%, 0.1 mol%) did not improve the yield (**Table 2.1**, **entries 2-4**). Next, a variety of solvents were tested (**Table 2.1**, **entries 5-9**). Amongst those solvents, MeCN was optimal for this transformation giving the highest yield. DMSO was not compatible with our reaction conditions. Other solvents, such as water, DCE, DMF or toluene were not beneficial, affording the desired product in significantly lower yield.

Table 2.1: Screening of catalyst loading and solvents for the hydrosulfamoylation of *N*-phenylacrylamide (**2.43**).[a]



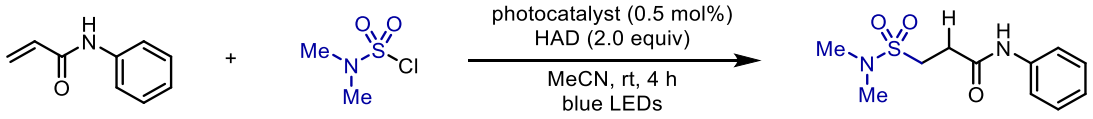
2.43, (1.0 equiv) **2.39**, (2.5 equiv) **2.44**

entry	photocatalyst	solvent	yield[b]
1	Eosin Y	MeCN	83%
2	Eosin Y (5.0 mol%)	MeCN	64%
3	Eosin Y (1.0 mol%)	MeCN	69%
4	Eosin Y (0.1 mol%)	MeCN	73%
5	Eosin Y	H_2O	21%
6	Eosin Y	DMSO	0
7	Eosin Y	DCE	14%
8	Eosin Y	DMF	45%
9	Eosin Y	Toluene	14%

[a] Reaction conditions: alkene **2.43** (0.5 mmol), *N*,*N*-dimethylsulfamoyl chloride **2.39** (1.25 mmol), Eosin Y (0.5 mol%), $(TMS)_3SiH$ (1.0 mmol), solvent (3.0 mL), blue light (λ_{max} = 470 nm) irradiation for 4 hours. [b] Yields of isolated products.

Interestingly, no other silane-containing HAD was found to be suitable for this transformation, demonstrating the unique properties of $(TMS)_3SiH$ (BDE (Si−H = 84 kcal/mol)[80] (**Table 2.2**, **entries 1-5**). Other HAD, such as Hantzsch ester, a thiol, or THF were not effective under our reaction conditions (**Table 2.2**, **entries 6-8**). A wide range of different photocatalysts were suitable and afforded the desired product in moderate to excellent yield (**Table 2.2**, **entries 9-12**). Specifically, iridium-based $[Ir\{dF(CF_3)ppy\}_2(dtbbpy)]PF_6$: Ir(III)*/Ir(II) = + 1.21 V vs. SCE in MeCN) and ruthenium-based $(Ru(bpy)_3(PF_6)_2$: Ru(II)*/Ru(I) = + 0.77 V vs. SCE in MeCN) photocatalysts were found to be high yielding (**Table 2.2**, **entries 9**, **10**). As a metal-free alternative, the organophotocatalyst Eosin Y was selected for further studies.

Table 2.2: Screening of HAD and photocatalysts for the hydrosulfamoylation of *N*-phenylacrylamide (**2.43**).[a]



2.43, (1.0 equiv) **2.39**, (2.5 equiv) **2.44**

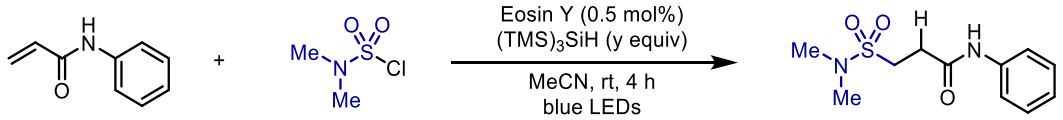
entry	photocatalyst	HAD	yield[b]
1	Eosin Y	$(TMS)_3SiH$	83%
2	Eosin Y	$(TMS)_3SiOH$	0%
3	Eosin Y	Et_3SiH	0%
4	Eosin Y	Ph_3SiH	0%
5	Eosin Y	Ph_2SiH_2	0%
6	Eosin Y	Hantzsch ester	9%
7	Eosin Y	4-HTP	0%
8	Eosin Y	THF	0%
9	$[Ir\{dF(CF_3)ppy\}_2(dtbbpy)]PF_6$	$(TMS)_3SiH$	88%
10	$Ru(bpy)_3(PF_6)_2$	$(TMS)_3SiH$	74%
11	Rose Bengal	$(TMS)_3SiH$	33%
12	$(Mes\text{-}Acr)BF_4$	$(TMS)_3SiH$	35%

[a] Reaction conditions: alkene **2.43** (0.5 mmol), *N*,*N*-dimethylsulfamoyl chloride **2.39** (1.25 mmol), photocatalyst (0.5 mol%), HAD (1.0 mmol), MeCN (3.0 mL), blue light (λ_{max} = 470 nm) irradiation for 4 hours. [b] Yields of isolated products. 4-HTP = 4-Hydroxythiophenol, $[Ir\{dF(CF_3)ppy\}_2(dtbbpy)]PF_6$ = [4,4′-Bis(1,1-dimethylethyl)-2,2′-bipyridine-*N*1,*N*1′]bis[3,5-difluoro-2-{5-(trifluoromethyl)-2-pyridinyl-*N*}phenyl-C]Iridium(III) hexafluorophosphate, $Ru(bpy)_3(PF_6)_2$ = Tris(2,2′-bipyridine)ruthenium(II) hexafluorophosphate, $(Mes\text{-}Acr)BF_4$ = 10-Methyl-9-(2,4,6-trimethylphenyl)acridinium tetrafluoroborate.

Running the reaction at lower concentrations or modulating the reagents equivalents did not influence the reaction outcome (**Table 2.3**, **entries 1-4**). Control experiments revealed that no product was obtained when the reaction was performed in the absence of light or in absence of $(TMS)_3SiH$ (**Table 2.3**, **entries 5**, **6**). Strict oxygen and water free conditions are not necessary for the reaction to proceed in good yield (**Table 2.3**, **entry 7**). In the absence of sulfamoyl chloride, the hydrosilylated product was isolated in good yield, which is in accordance with our mechanistic design, whereby a silyl radical is generated under our reaction conditions (**Table 2.3**, **entry 8**). The reaction can also be

performed without photocatalyst, although this process requires significantly longer reaction time (**Table 2.3**, **entry 9**; 16 hours instead of 4 hours). Furthermore, a fluctuation of the temperature (depending on the distance between the vial and the lamp), did not impact the outcome of the reaction, which should enable reproducibility of the results in different photochemical reactors (homemade or commercial).

Table 2.3: Further experiments for the hydrosulfamoylation of *N*-phenylacrylamide (**2.43**).[a]



2.43, (1.0 equiv) **2.39,** (x equiv) **2.44**

entry	2.39 (equiv)	$(TMS)_3SiH$ (equiv)	yield[b]
1	2.0	2.0	62%
2	2.0	2.5	65%
3	2.5	2.5	82%
4[c]	2.5	2.0	82%
5[d]	2.5	2.0	0
6	2.5	-	0
7[e]	2.5	2.0	79%
8	-	2.0	0%[f]
9[g]	2.5	2.0	0 (80%)[h]

[a] Reaction conditions: alkene **2.43** (0.5 mmol), *N*,*N*-dimethylsulfamoyl chloride **2.39** (1.25 mmol), Eosin Y (0.5 mol%), $(TMS)_3SiH$ additive (1.0 mmol), MeCN (3.0 mL), blue light (λ_{max} = 470 nm) irradiation for 4 hours. [b] Yields of isolated products. [c] Reaction was performed in 5.0 mL of MeCN. [d] Reaction performed in the absence of light. [e] Reaction performed under nitrogen atmosphere and in degassed solvent. [f] 76% of hydrosilylated product was isolated (see mechanistic investigation). [g] No photocatalyst was added. [h] After 16 hours, 80% of **2.44** was isolated.

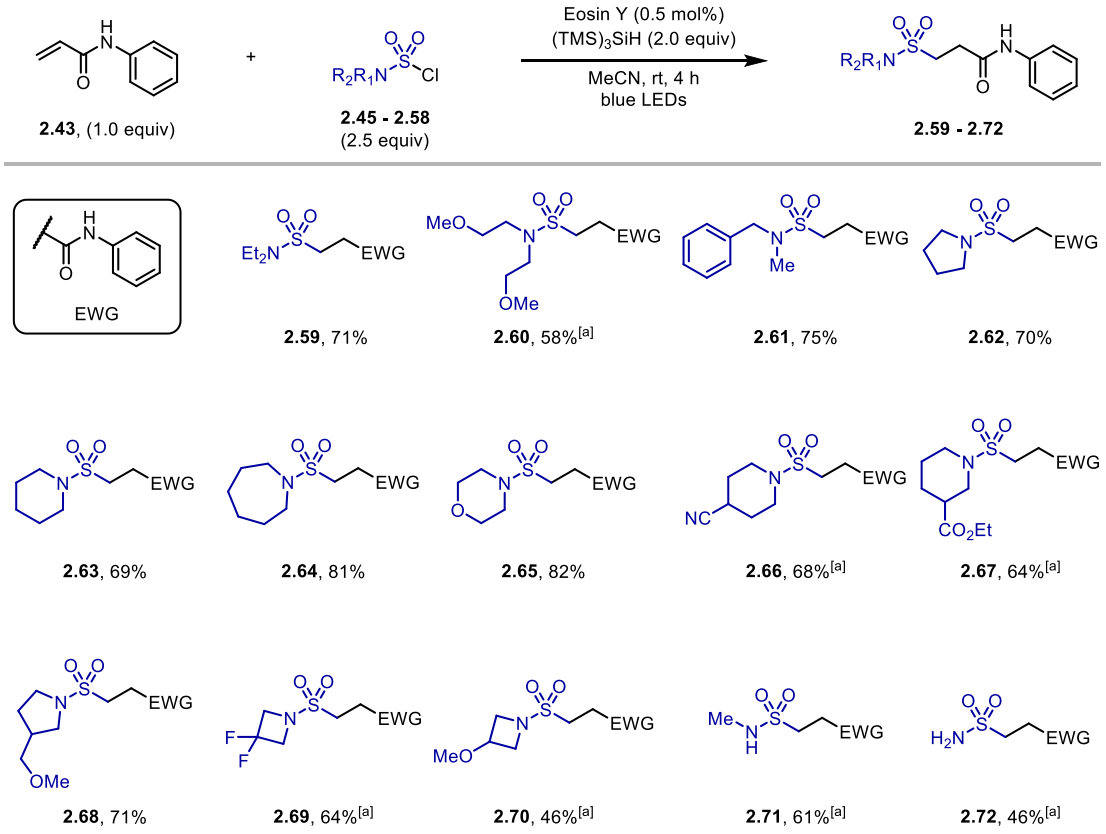
2.7 Scope of the Hydrosulfamoylation of Electron-Deficient Alkenes

With the optimised conditions in hand, we sought to investigate the scope of our hydrosulfamoylation with respect to sulfamoyl chlorides and electron-deficient alkenes (**Schemes 2.15** and **2.16**).

2.7.1 Scope of Sulfamoyl Chlorides

As shown in **Scheme 2.15**, a wide range of electronically different sulfamoyl chlorides were found to be suitable for the hydrosulfamoylation of alkene **2.43**. Initial investigations showed that linear sulfamoyl chlorides such as diethyl and bis(2-methoxyethyl)sulfamoyl chloride were suitable precursors for this transformation (**2.59**, **2.60**). A benzylmethylsulfamoyl choride was also successfully used in this transformation and afforded sulfonamide **2.61** in 75% yield. Interestingly, cyclic sulfonamides, a motif often encountered in biologically active molecules, were readily obtained. Five-, six- and seven-membered sulfamoyl chlorides afforded pyrrolidine, piperidine and azepane sulfonamides in good to excellent yields (**2.62**-**2.64**). Morpholine-4-sulfonyl chloride was compatible with this protocol allowing access to **2.65** in 82% yield. Piperidine derivatives with a pending ester, nitrile, or a 3-methoxymethylpyrrolidine furnished valuable building blocks containing vectors for further functionalisation (**2.66**-**2.68**). Given the unique properties of fluorine to improve bioavailability and adsorption of drug candidates, as well as the importance of azetidines in drug discovery, a sulfamoyl chloride containing fluorine atoms were investigated.[81–83] Pleasingly, fluorine-containing sulfonamide **2.69** could be accessed in moderate yield. The methoxy analogue was also a suitable substrate (**2.70**). Additionally, a secondary

sulfonamide was obtained in moderate yield (**2.71**). Unprotected sulfamoyl chloride was more challenging and furnished the primary sulfonamide **2.72** in 46% yield. The late-stage conversion of primary sulfonamides to several other functional groups has been well documented over the years.[84,85]

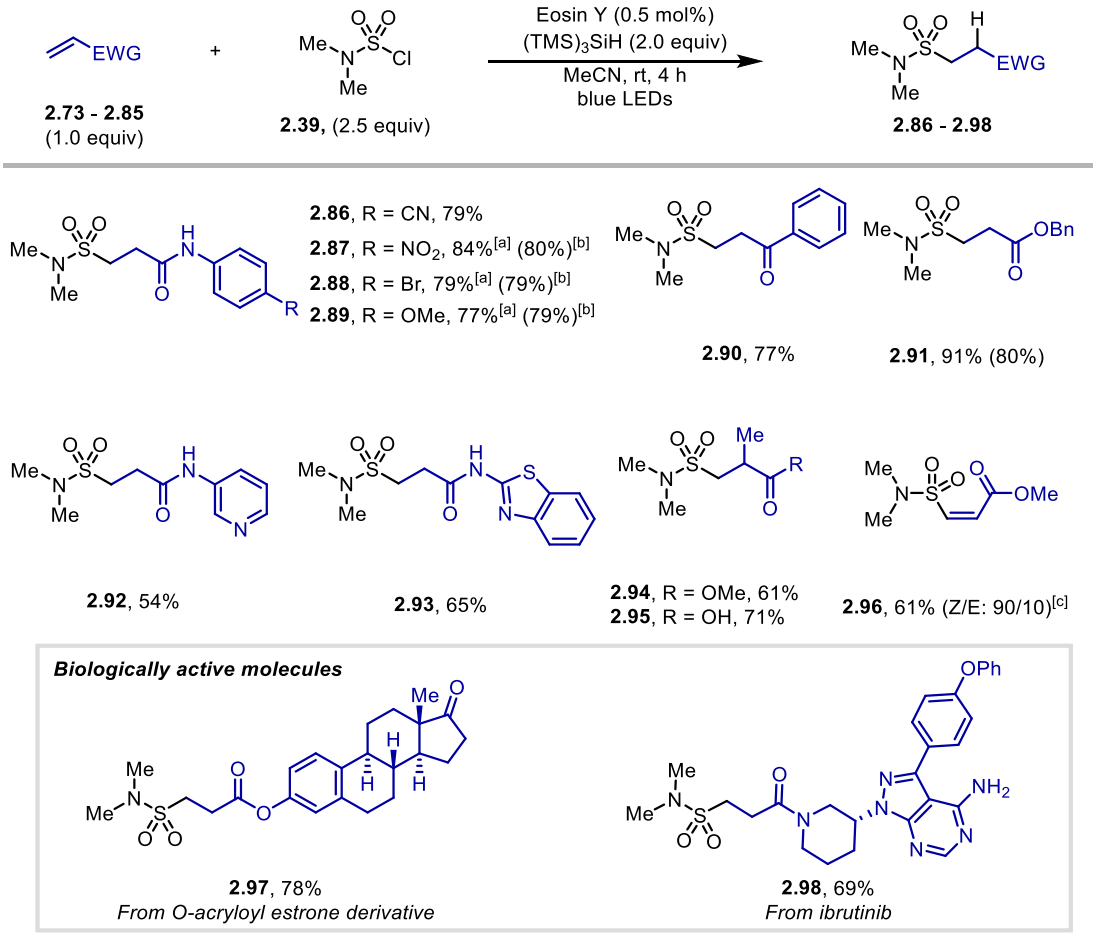


Scheme 2.15. Substrate scope of sulfamoyl chlorides. Reaction conditions: alkene **2.43** (0.5 mmol), sulfamoyl chlorides **2.45**-**2.58** (1.25 mmol), $(TMS)_3SiH$ (1.0 mmol), Eosin Y (0.5 mol%), MeCN (3.0 mL), blue light irradiation (λ_{max} = 470 nm), room temperature, 4 h. Yields of isolated products. [a] 16 h reaction time. EWG = C(O)NHPh.

2.7.2 Scope of Electron-Deficient Alkenes

We next evaluated the scope of electron-deficient alkenes that are amenable to this new hydrosulfamoylation protocol using *N*,*N*-dimethylsulfamoyl chloride **2.39** (**Scheme 2.16**). The reaction is efficient on a variety of *N*-phenylacrylamides bearing different substituents on the arene, including both electron-withdrawing and -donating groups. More specifically, nitrile, nitro, bromo, and methoxy groups were tolerated and provided

a wide range of different aliphatic sulfonamides in good yields (**2.86**-**2.89**). The synthesis of **2.87**-**2.89** required longer reaction time (16 hours). Nevertheless, the use of [Ir{dF(CF$_3$)ppy}$_2$(dtbbpy)]PF$_6$ as photocatalyst instead of Eosin Y was more effective and allowed the reaction to proceed within 4 hours. Notably, no side-product resulting from competitive silyl-radical mediated bromine atom abstraction was observed using *N*-(4-bromophenyl)acrylamide.[86,87]



Scheme 2.16: Substrate scope of electron-deficient alkenes. Reaction conditions: alkene **2.73**-**2.85** (0.5 mmol), **2.39** (1.25 mmol), (TMS)$_3$SiH (1.0 mmol), Eosin Y (0.5 mol%), MeCN (3.0 mL), blue light irradiation (λ_{max} = 470 nm), room temperature, 4 h. Yields of isolated products. [a] 16 h reaction time. [b] [Ir{dF(CF$_3$)ppy}$_2$(dtbbpy)]PF$_6$ was used instead of Eosin Y and full conversion was observed within 4 hours. [c] The minor isomer was not isolated.

Other electron-withdrawing groups, such as ketone and ester derivatives were transformed to the desired sulfonamide products in good yields (**2.90**, **2.91**). We were delighted to observe that heteroarenes, such as a pyridine and a benzothiazole derivative

were suitable for this transformation, affording the desired products in moderate yields (**2.92**, **2.93**). Geminal disubstituted alkenes provided the hydrosulfamoylated products in good yields (**2.94**, **2.95**). We were able to extend this novel mode of activation to an electron-deficient alkyne, which allowed for the synthesis of a vinyl sulfonamide with high *Z*-selectivity (Z/E: 90/10) and good yield (**2.96**). The major stereoisomer was separated by silica gel chromatography. The stereochemistry of vinyl sulfonamide **2.96** was assigned by ^{1}H NMR analysis of the coupling constants of both hydrogens of the double bond δ $^{3}J_{H\text{-}H}$ = 11.6/11.7 Hz, **Figure 2.2**).

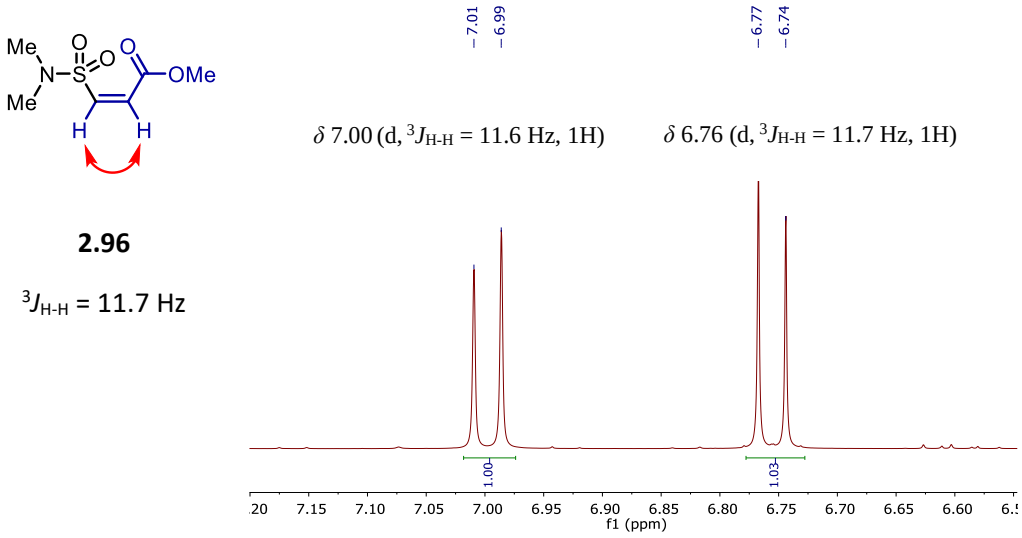
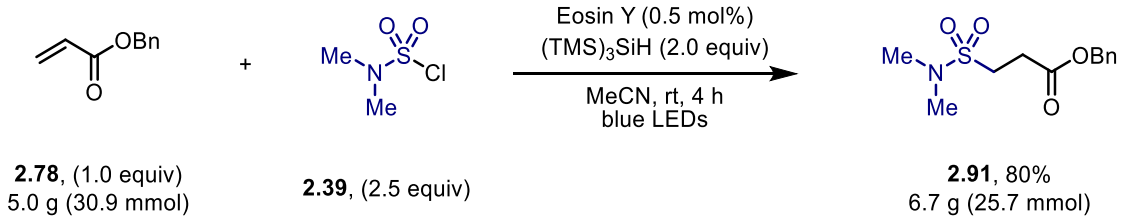


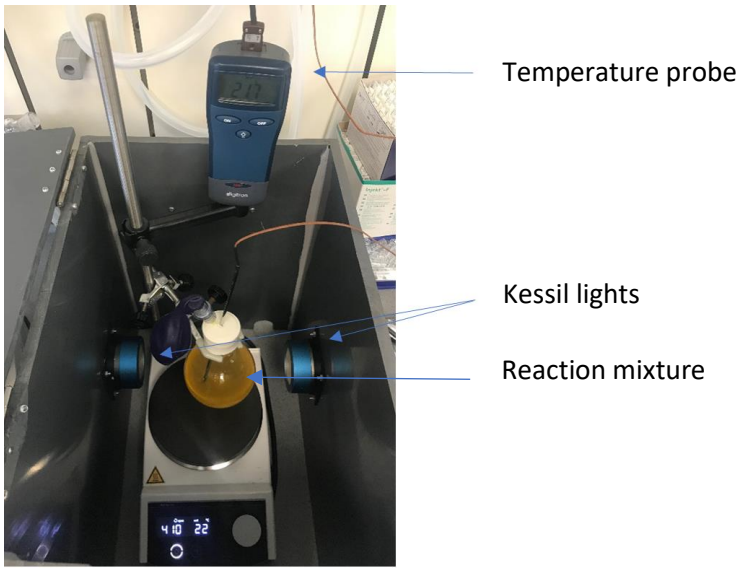
Figure 2.2: Assignment of stereochemistry for compound **2.96**.

We were able to extend this hydrosulfamoylation methodology to the late-stage functionalisation of biologically active molecules. A sulfonamide-containing estrone derivative was isolated in 78% (**2.97**). Furthermore, the anti-cancer drug ibrutinib was subjected to the reaction conditions, furnishing the hydrosulfamoylated product in 69% yield (**2.98**). These results demonstrate the robustness of this transformation with all functional groups present in the molecule remaining intact.

2.7.3 Scale-up Experiment

To further display the utility and the scalability of this transformation, we applied our optimised reaction conditions to a five-gram scale synthesis of sulfonamide **2.91** (**Scheme 2.17**).



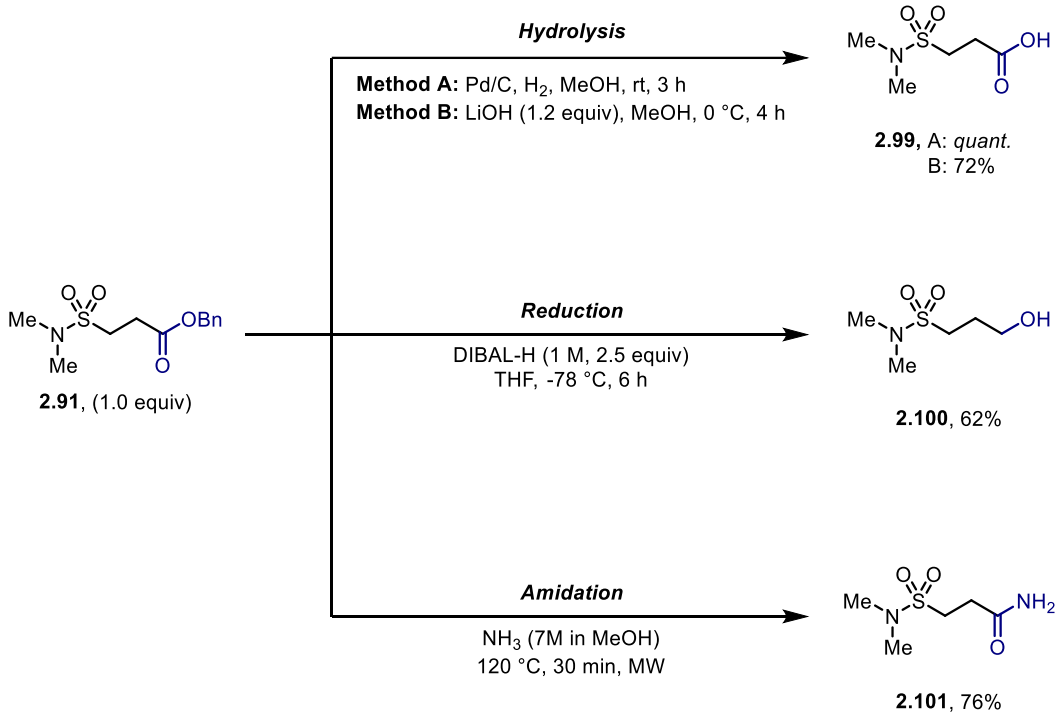


Scheme 2.17: Setup for the five-gram scale-up experiment of sulfonamide **2.91**.

The hydrosulfamoylation of benzyl acrylate **2.78** was accomplished in one step on a 5 g scale affording the desired product **2.91** in 80% yield (6.7 g). Importantly, previous methodologies enabling access to those molecules would require a multi-step sequence using harsher reaction conditions.[88]

2.7.4 Further Transformations

Given the importance of sulfonamides in drug discovery, we explored the robustness of those aliphatic scaffolds towards typical reaction conditions used in medicinal chemistry such as hydrolysis, reduction and amidation. Sulfonamide **2.91** was efficiently converted to various derivatives (**Scheme 2.18**).



Scheme 2.18: Further transformations of sulfonamide **2.91**.

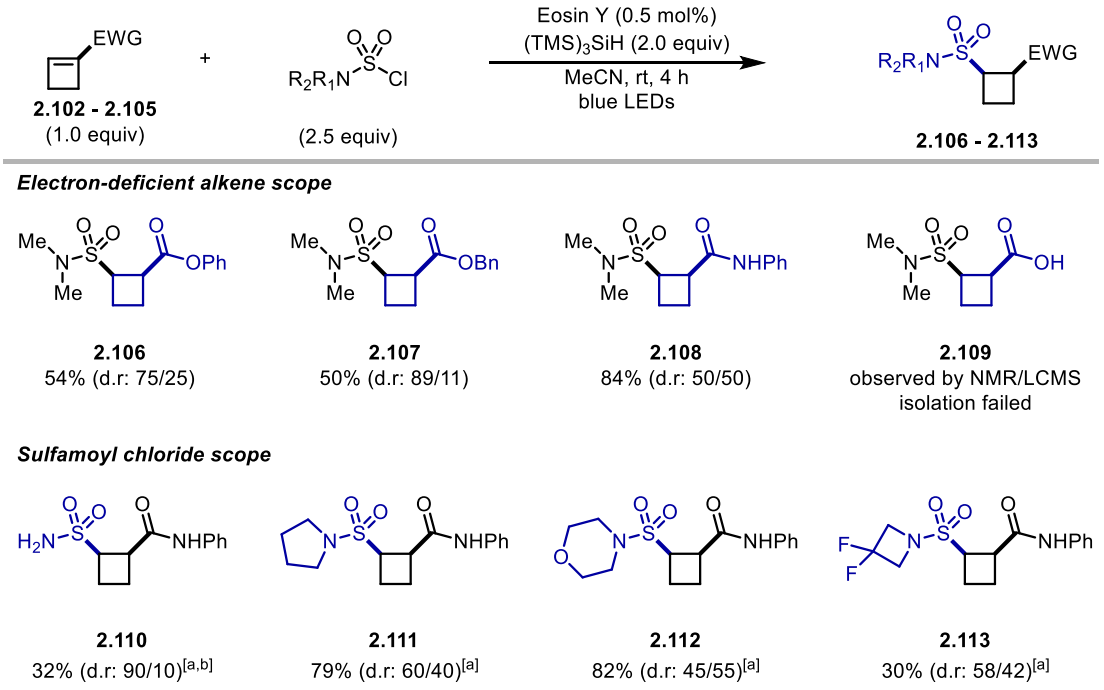
Hydrolysis of the benzyl ester using either Pd/C, H_2 or LiOH provided the corresponding carboxylic acid **2.99** in good to excellent yields. Next, reduction of the ester with diisobutylaluminium hydride (DIBAL-H) at room temperature furnished the desired alcohol **2.100** in moderate yield. A primary amide could be accessed by treating sulfonamide **2.91** with ammonia (7M in MeOH) to afford the amide **2.101** in good yield.

2.8 Preparation of Sulfonamide-Containing Cyclobutanes

Four-membered rings, such as cyclobutanes, have played a considerable role in the development of modern organic chemistry and attracted many interests in medicinal chemistry.[89–92] The incorporation of these scaffolds can significantly improve the efficiency of drugs, due to their unique structural properties. Owing to the increased bond angle strain (88º C-C-C bond angle), cyclobutanes adopt a puckered conformation, enabling the reduction of the torsional interaction between adjacent methylene groups. This results in a strain energy of 26 kcal mol^{-1}, leading to an increase in reactivity compared to larger rings (e.g. cyclohexane).[93]

2.8.1 Hydrosulfamoylation of Cyclobutenes

We investigated the introduction of sulfonamide fragments into cyclobutenes. Using the standard reaction conditions **(Table 2.1, entry 1)**, we isolated highly valuable 1,2-disubstituted cyclobutanes in moderate yield and diastereomeric ratio. Conveniently, the diastereoisomers could be separated by silica gel column chromatography. As shown in **Scheme 2.19**, esters and amides were suitable electron-withdrawing groups and afforded the corresponding sulfonamide-containing cyclobutanes in moderate to good yields (**2.106 - 2.108**). Although the corresponding carboxylic acid could be engaged in this transformation (**2.109**, product observed by crude NMR and LCMS), isolation by normal or reverse phase HPLC failed to afford the desired product. This is likely due to the instability of the product, which led to decomposition upon purification *via* elimination of the sulfonamide. Furthermore, different linear, cyclic and heterocyclic sulfamoyl chlorides, were suitable and afforded interesting building blocks for drug discovery (**2.110**-**2.113**).



Scheme 2.19: Substrate scope of cyclobutene derivatives. Reaction conditions: cyclobutene **2.102** - **2.105** (0.5 mmol), sulfamoyl chloride (1.25 mmol), $(TMS)_3SiH$ (1.0 mmol), Eosin Y (0.5 mol%), MeCN (3.0 mL), blue light irradiation (λ_{max} = 470 nm), room temperature, 4 h. Yields of isolated products. [a] 16 h reaction time. [b] The minor isomer was not isolated.

The diastereoselectivity in this transformation likely stems from the steric hindrance of the bulky HAD ($(TMS)_3SiH$). Therefore, the HAT takes place on the less hindered face (exo face), leading favourably to the *cis*-product (**Figure 2.3**).[93] The approach from the endo face is more challenging due to the steric clash with the sulfonamide.

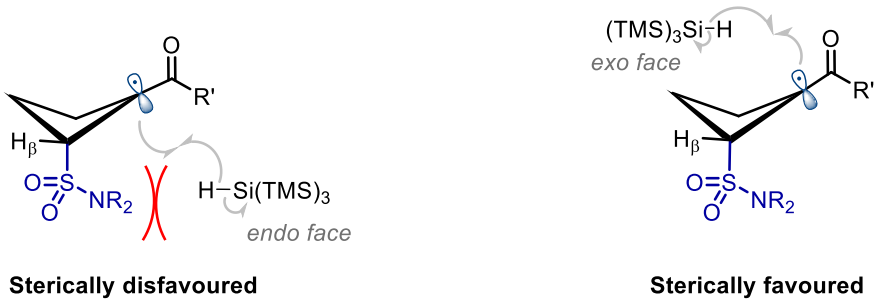


Figure 2.3: Stereoselectivity of the HAT of cyclobutyl radicals.

The substitution pattern on the sulfonamide and the electron-withdrawing group might also influence the stereochemical outcome of the transformation.

The relative stereochemistry of 1,2-disubstituted cyclobutanes was assigned by 2D-NOESY NMR (**Figure 2.4**). A strong NOE between H_α and H_β was observed for the *cis*-diastereoisomer. On the other hand, no interaction between H_α and H_β was observed for the corresponding *trans*-diastereoisomer (**Figure 2.4**).

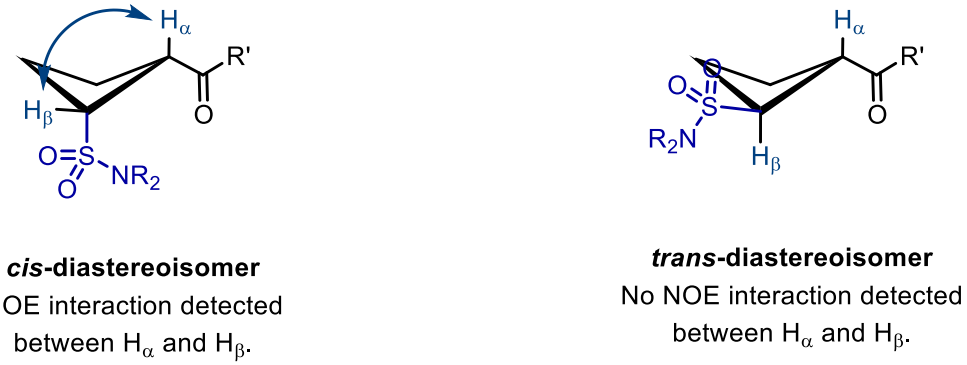
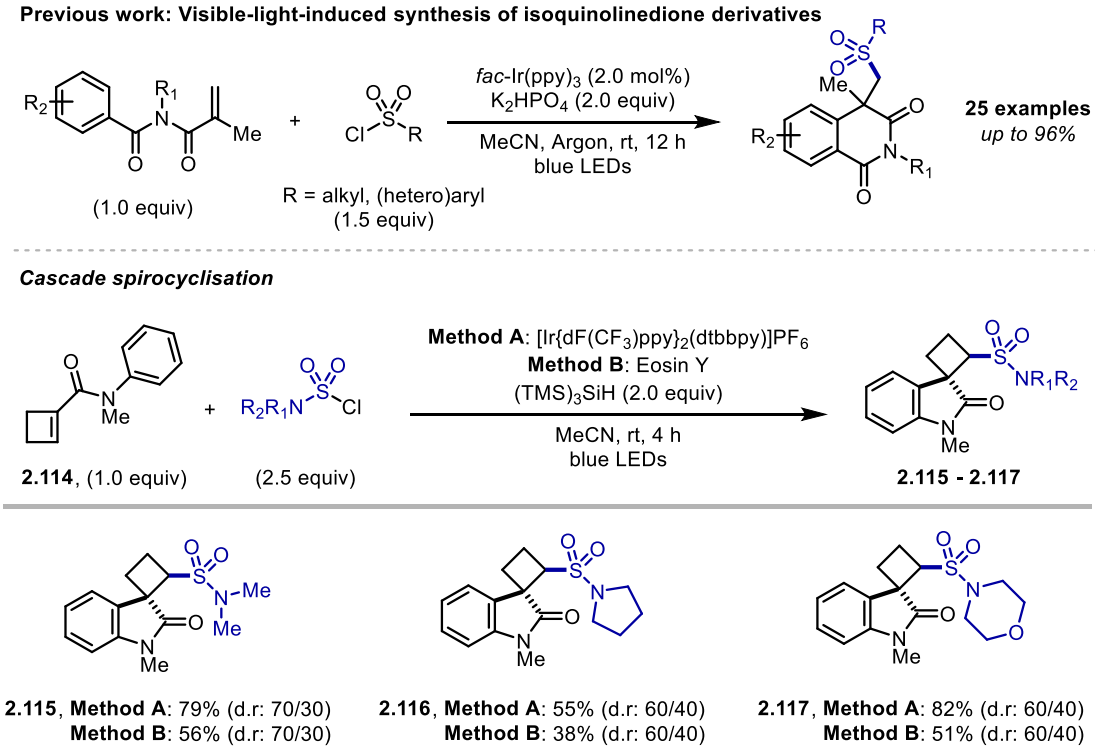


Figure 2.4: Determination of the stereochemistry of 1,2-disubstituted cyclobutanes.

2.8.2 Preparation of Sulfonamide-Containing Cyclobutyl-Spirooxindoles

Owing to the prevalence of spirocyclic oxindoles in numerous natural products and biologically active molecules, we next turned our attention to the synthesis of sulfonamide-containing cyclobutyl-spirooxindoles.[94–96] Encouraged by previous studies from Sun and co-workers, whereby isoquinolinedione derivatives were synthesised *via* a tandem radical cyclisation and sulfonylation reaction, we speculated that intramolecular quaternization of the *α*-carbonyl radical intermediate would allow us to build molecular complexity (**Scheme 2.20**).[97] *N*-methyl-*N*-phenylcyclobutene carboxamide **2.114** underwent a cascade spirocyclisation to afford sulfonamide-containing cyclobutyl-spirooxindoles in moderate yields and diastereoselectivities (**Method A**). Linear (**2.115**), cyclic (**2.116**) and heterocyclic (**2.117**) sulfonamides could be easily introduced. Both diastereoisomers were separated by silica gel column chromatography. Further

optimisation of the reaction conditions showed that the use of Ir{dF(CF_3)ppy}$_2$(dtbbpy)]PF_6 instead of Eosin Y allowed to afford higher yields, with similar diastereomeric ratios (**Scheme 2.20**, **Method B**).



Scheme 2.20: Substrate scope of sulfonamide-containing cyclobutyl-spirooxindoles. Reaction conditions: cyclobuten **2.114** (0.5 mmol), sulfamoyl chloride (1.25 mmol), $(TMS)_3SiH$ (1.0 mmol), photocatalyst (0.5 mol%, Method A or Method B), MeCN (3.0 mL), blue light irradiation (λ_{max} = 470 nm), room temperature, 4 h. Yields of isolated products.

This transformation allowed the synthesis of unprecedented scaffolds which could be valuable building blocks for medicinal chemistry. The relative stereochemistry of sulfonamide-containing cyclobutyl-spirooxindoles could be assigned by 2D-NOESY NMR: a strong NOE between H_A and H_B was observed for the *cis*-diastereoisomer. On the other hand, no interaction between H_A and H_B was observed for the corresponding *trans*-diastereoisomer (**Figure 2.5**).

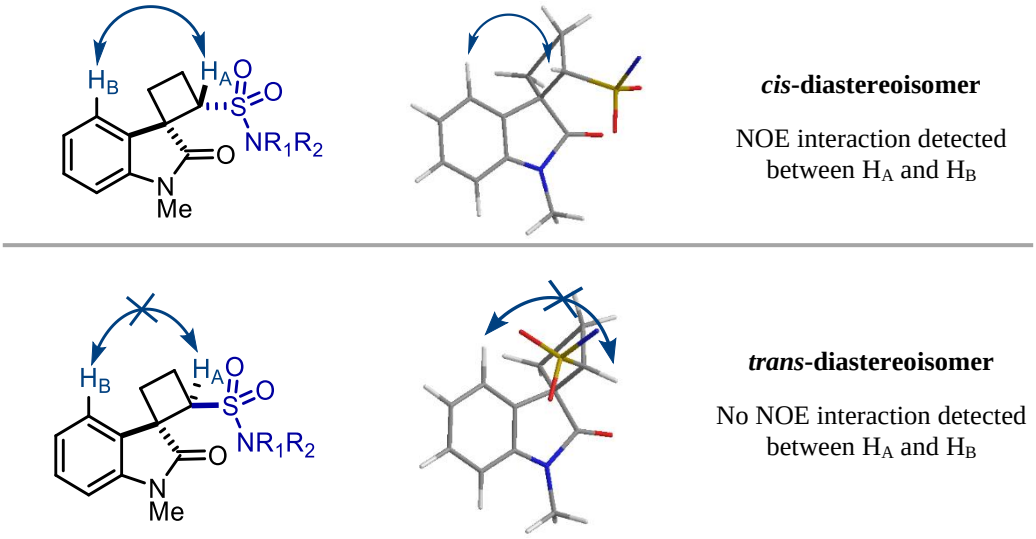
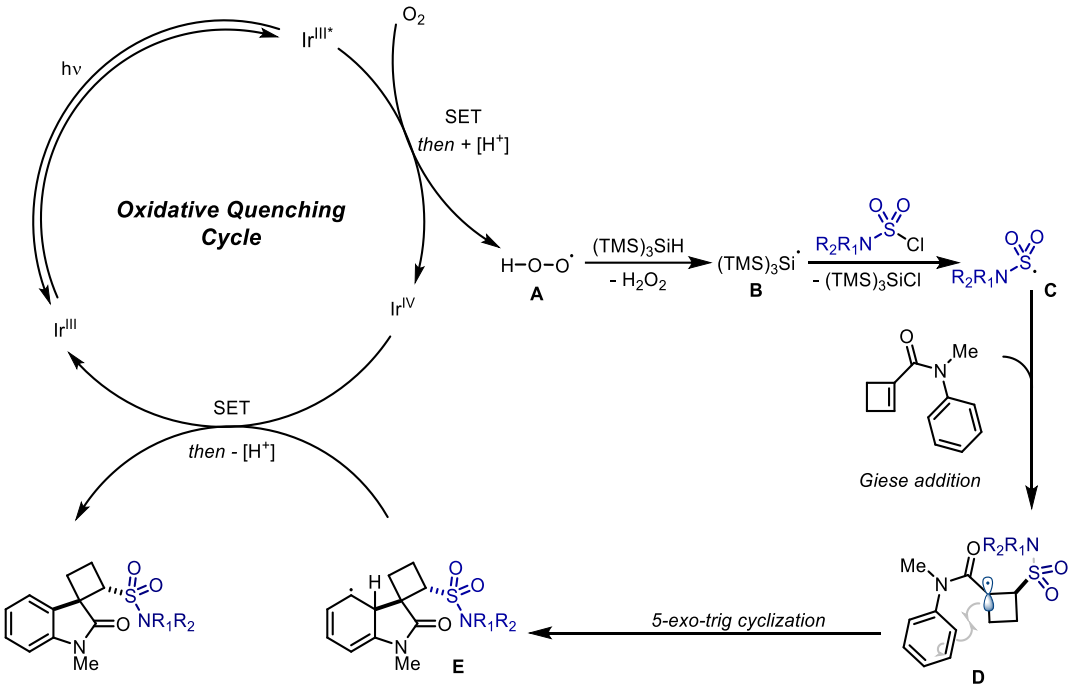


Figure 2.5: Determination of the diastereoselectivity of spirocyclic oxindoles.

Next, we were interested in the mechanism involved in this cascade spirocyclisation. We observed that the reaction does not proceed under a rigorously controlled nitrogen atmosphere. The need for oxygen is consistent with an oxidative quenching cycle (**Scheme 2.21**).[98,99] In this scenario, upon blue-light irradiation, superoxide **A** is formed upon SET between O_2 and the triplet excited state of the iridium-based photocatalyst. This peroxyl radical **A** can abstract a hydrogen atom from $(TMS)_3SiH$ to generate hydrogen peroxide and the corresponding silyl radical **B**. The latter can efficiently activate a sulfamoyl chloride and generate a sulfamoyl radical **C**. Upon Giese-addition, the carbon-centred radical intermediate **D** is formed. Radical **D** undergoes intramolecular addition to the aromatic ring *via* a 5-exo-trig cyclisation. The conformation of the amide functional group and more specifically of intermediate **D** is crucial for this cyclisation step. Tertiary amides adopt a *cis*-folded conformation which facilitates the reaction between the carbon-centred radical intermediate and the pendant aryl group.[100] On the other hand, secondary amides adopt a *trans*-conformation, which hamper this cyclisation and promotes the hydrosulfamoylation of the four-membered ring. The cyclic radical

intermediate **E** is thereafter oxidised *via* a second single-electron transfer and the desired sulfonamide-containing building block is formed upon deprotonation.



Scheme 2.21: Suggested mechanism for the formation of sulfonamide containing cyclobutyl-spirooxindoles.

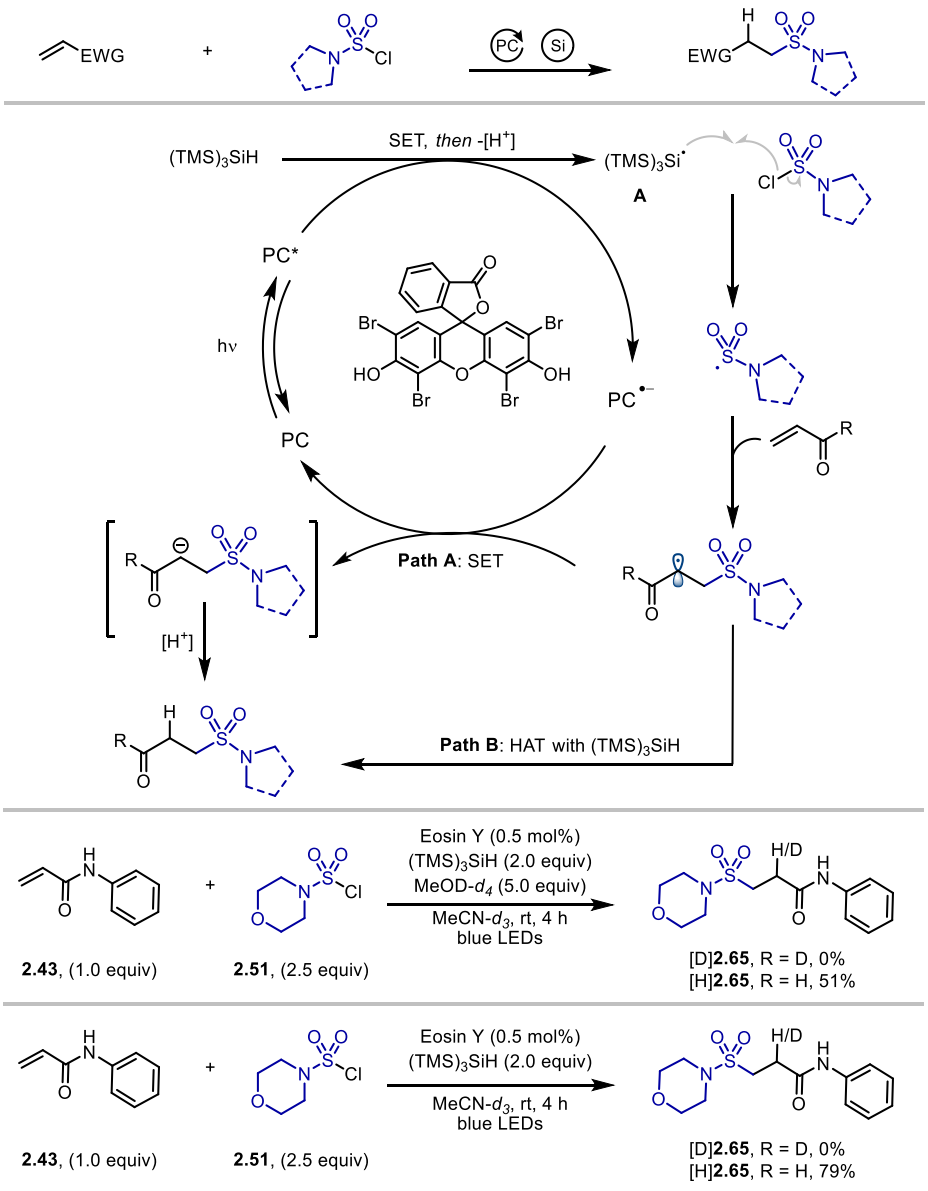
2.9 Mechanistic Investigations

To elucidate the mechanism of this transformation, we conducted several control experiments. We initially investigated the formation of radical species under our reaction conditions. Upon addition of 4.0 equivalents of the radical scavenger TEMPO (2,2,6,6-tetramethylpiperidin-1-yl)oxyl, no conversion to the desired hydrosulfamoylated product **2.65** was observed (**Scheme 2.22**). Analysis of the crude reaction mixture by LCMS revealed that all reagents remained untouched upon reaction. This initial experiment advocates in favour of a radical mechanism.



Scheme 2.22: Radical-trapping experiment with TEMPO.

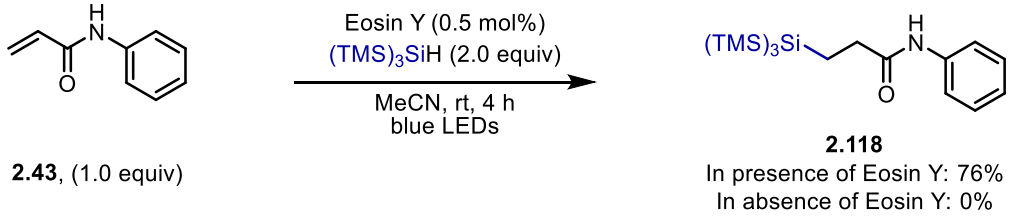
In our reaction design (**Scheme 2.14**) the desired hydrosulfamoylated product could arise from an enol-type intermediate. In this scenario, the carbon-centred radical intermediate would be reduced to an anion (**Scheme 2.23**, **Path A**).



Scheme 2.23: Deuteration experiments to probe for an enol-type intermediate.

Upon protonation, the anion would react to form the desired hydrosulfamoylated product. To probe the formation of such an anion, deuteration experiments with MeOD-d_4 in MeCN-d_3 were performed (**Scheme 2.23**). Addition of deuterated solvents/additives did not result in deuterium incorporation; selective formation of [H]**2.65** was observed over [D]**2.65**. This result combined with the efficacy of the reaction in the absence of a photocatalyst suggest that no anion is formed under our reaction conditions and that $(TMS)_3SiH$ acts as the HAD (**Scheme 2.23, Path B**).

Next, the activation mode of sulfamoyl chlorides under visible light activation was investigated. In the absence of sulfamoyl chloride, the hydrosilylated product **2.118** was isolated in 76% yield (**Scheme 2.24**).[101–103] As hypothesised in our reaction design, the excited state of Eosin Y* is likely oxidising $(TMS)_3SiH$ to the silyl radical, which can undergo Giese addition to the alkene. In the absence of photocatalyst Eosin Y, the hydrosilylated product was not observed, suggesting that a photocatalyst is required for the efficient formation of this silyl radical.



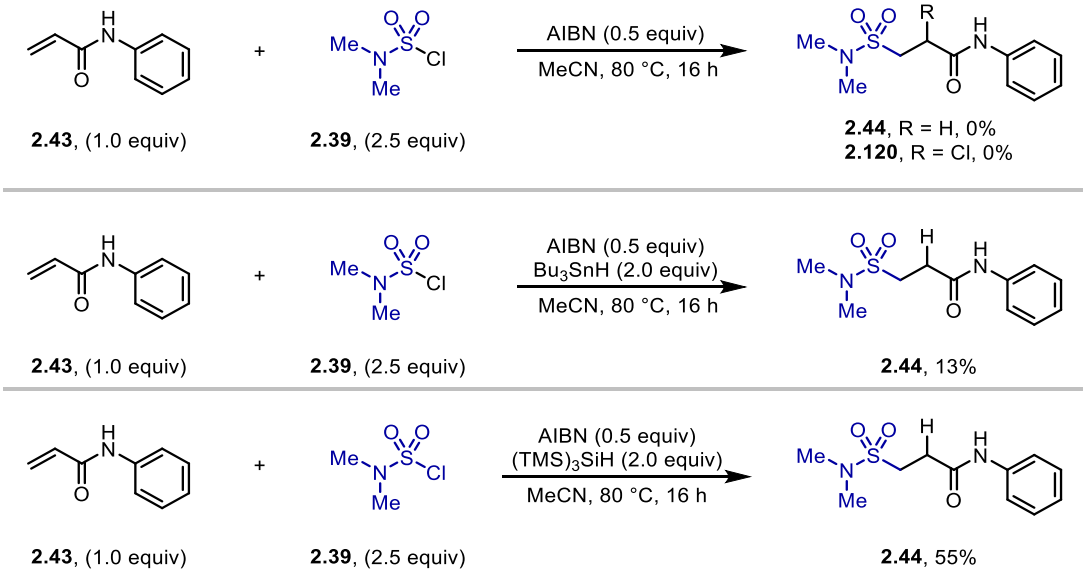
Scheme 2.24: Hydrosilylation of electron-deficient alkenes.

Furthermore, $(TMS)_3SiCl$ (**2.119**) was isolated as a byproduct of the reaction under the standard reaction conditions, which is consistent with a direct chlorine atom abstraction of the sulfamoyl chloride by the silyl radical (**Scheme 2.25**).



Scheme 2.25: Formation of $(TMS)_3SiCl$ under the standard reaction conditions.

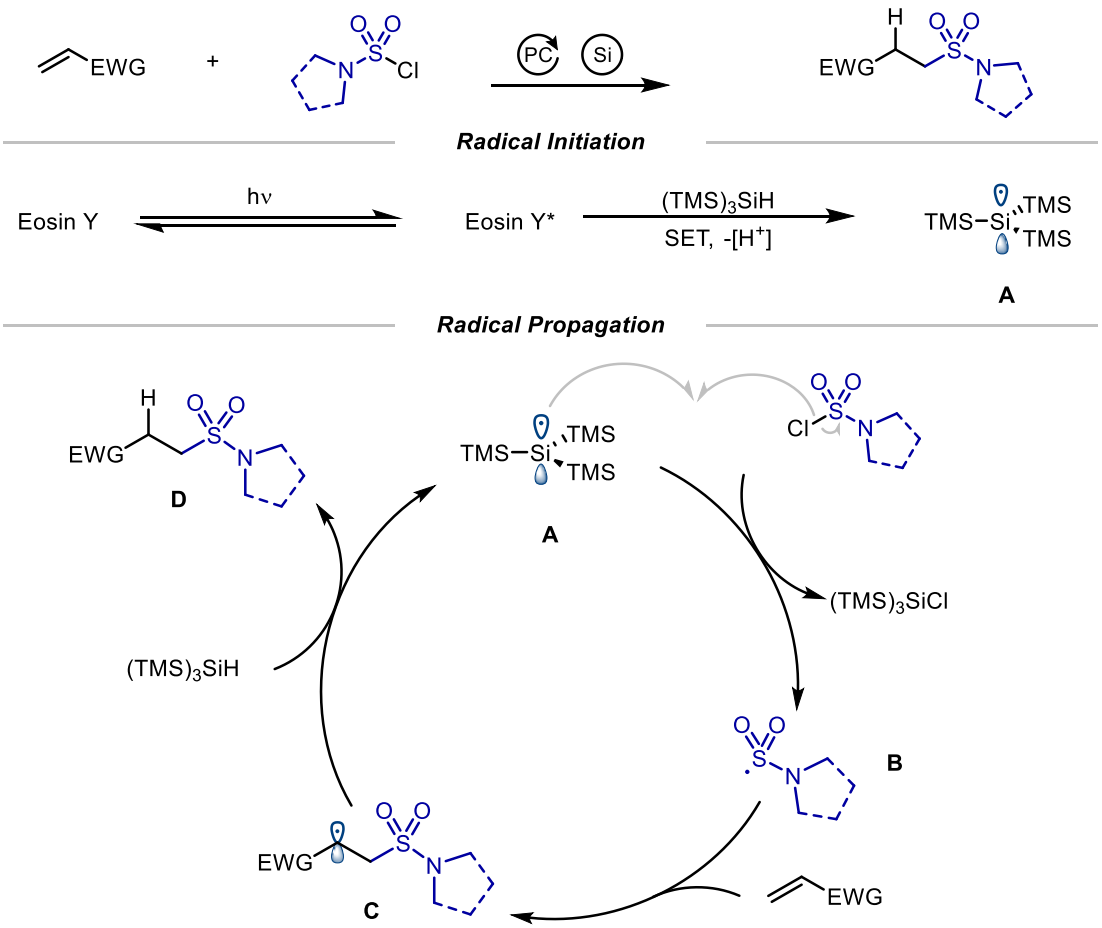
Further experiments employing AIBN as a radical initiator demonstrated that the sulfamoyl radical cannot be generated under classical initiation reaction conditions (**Scheme 2.26**). The addition of Bu_3SnH afforded the desired product in 13% yield. The combination of AIBN and $(TMS)_3SiH$ enables net hydrosulfamoylation in 55% yield. This result is in accordance with the ability of silyl radicals to activate efficiently sulfamoyl chlorides under these reaction conditions. This result could be of interest to process chemists for large scale hydrosulfamoylation in absence of light, but would require further optimisation.



Scheme 2.26: Hydrosulfamoylation of alkenes using AIBN as radical initiator.

This result combined with the deuteration experiments corroborate our proposed photoinitiation-chain propagation mechanism (**Scheme 2.14**, **Path B**). In this process,

Eosin Y acts as an initiator for the chain propagation reaction, whereby a silyl radical **A** is generated (**Scheme 2.27**). The silyl radical abstracts the chlorine atom from the sulfamoyl chloride to form the corresponding sulfamoyl radical **B**. Subsequent Giese-addition of radical **B** to the electron-deficient alkene furnishes radical intermediate **C**. HAT between **C** and $(TMS)_3SiH$ affords the desired hydrosulfamoylated product **D**, along with the silyl radical **A**, which can reinitiate the chain reaction.



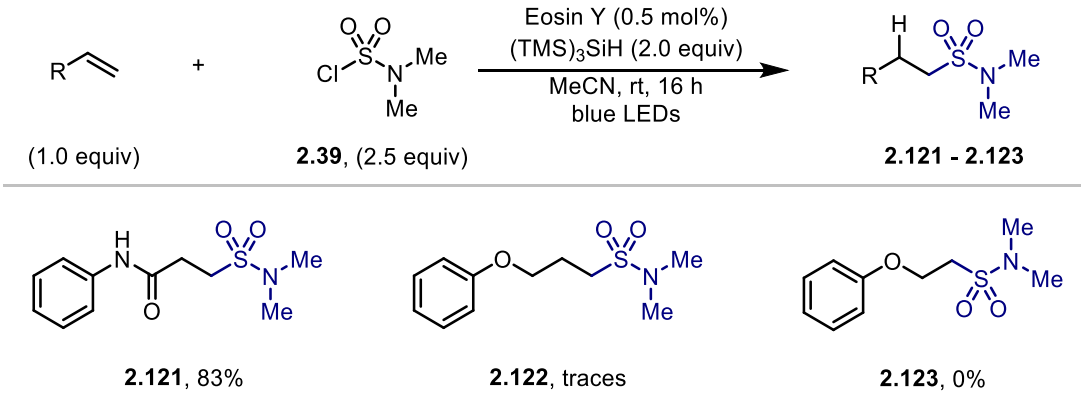
Scheme 2.27: Proposed radical chain propagation mechanism for the hydrosulfamoylation of alkenes.

The efficacy of the reaction in absence of photocatalyst suggests that a partial homolytic cleavage of the sulfur-chlorine bond of the sulfamoyl chloride is possible, generating the sulfamoyl radical **B**. A longer reaction time is required in this case likely due to a less efficient initiation period for this activation mode. The presence of a chain propagation pathway could also be assessed by quantum yield experiment. However, at the time of

this study no suitable equipment for the determination of the quantum yield was available.

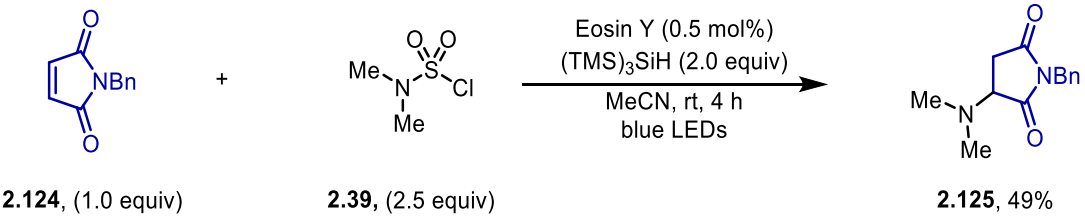
2.10 Limitations of this Methodology

Aiming to broaden the scope of this transformation, we investigated the hydrosulfamoylation of a range of alkenes with different electronic properties. As shown in **Scheme 2.16**, the sulfamoyl radical can be added efficiently to electron-deficient alkenes; nevertheless, no conversion was observed with unactivated or electron-rich alkenes (**Scheme 2.28**).



Scheme 2.28: Hydrosulfamoylation of alkenes of different electronic profile. Yields of isolated products.

We speculated that this lack of reactivity might be due to a polarity mismatch between the carbon-centred radical intermediate and the HAD. Efforts to address these limitations and to expand the scope of this process to include unactivated and electron-rich alkenes will be discussed in **Chapter 3**.

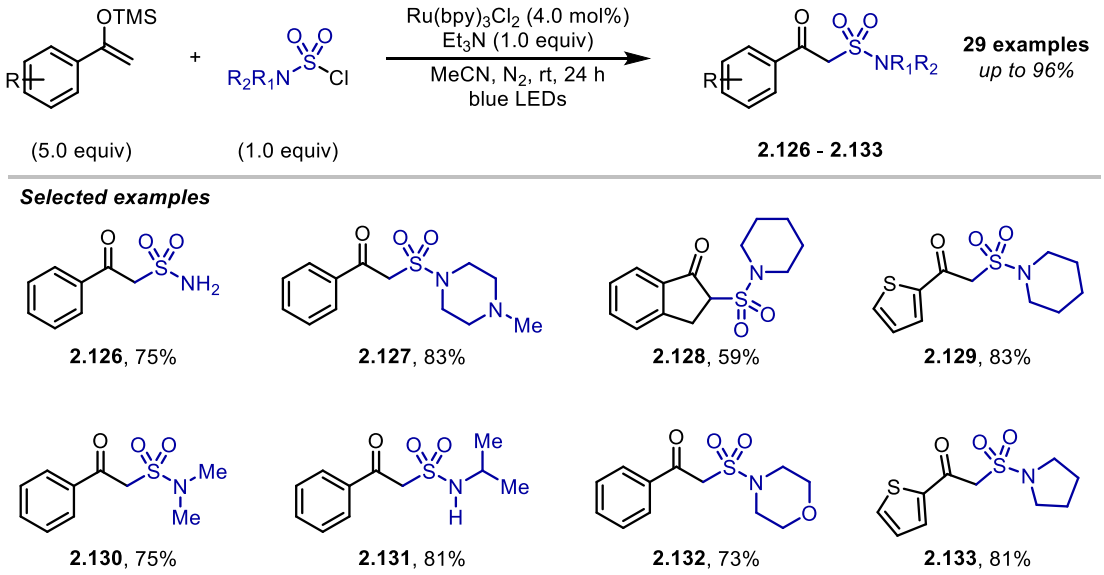


Scheme 2.29: Desulfonylative amination of *N*-benzylmaleimide under standard reaction conditions.

Furthermore, we noted competitive desulfonylation when *N*-benzylmaleimide **2.124** was treated under our standard reaction conditions (**2.125**, **Scheme 2.29**). Sulfur dioxide extrusion from sulfamoyl radicals has previously been reported.[104,105]

2.11 Comparison of our Methodology to a Recently Disclosed Radical Sulfamoylation using Sulfamoyl Chloride

During the preparation of our manuscript, Wang and co-workers reported a photoredox-catalysed synthesis of *β*-ketosulfonamides using sulfamoyl chlorides (**Scheme 2.30**).[68] This report described the addition of different sulfamoyl chlorides to silyl enol ethers.



Scheme 2.30: Introduction of sulfonamides to silyl enol ethers using sulfamoyl chlorides.[68]

Notably, five equivalents of silyl enol ethers are required to afford the desired products in good yields. In comparison to our protocol, a metal-catalysed photocatalyst, nitrogen atmosphere, longer reaction times, as well as additional reagents are required for this transformation. The authors suggest that sulfamoyl radicals are generated by a direct single-electron reduction process between the triplet excited state of the photocatalyst

($Ru(bpy)_3(PF_6)_2$: Ru(II)*/Ru(III) = − 0.81V vs. SCE in MeCN) and the sulfamoyl chloride (*N*,*N*-dimethylsulfamoyl chloride: E_{red} = −1.59V vs. SCE in MeCN). This process is unlikely and an alternative mechanism might be at play.

2.12 Conclusion

In conclusion, we developed a practical, scalable, rapid, robust, and cost-effective protocol for the one-step preparation of aliphatic sulfonamides, using inexpensive olefins, tris(trimethylsilyl)silane (acting both as the activator and the HAD) and the organophotocatalyst Eosin Y. In our study, we established that single-electron reduction is more challenging for sulfamoyl chlorides than for other sulfonyl chloride derivatives. An efficient solution to activate sulfamoyl chlorides was provided, whereby the direct chlorine atom abstraction by a silyl radical generates the corresponding sulfamoyl radical. Prior to our study, sulfamoyl chlorides have not been activated by silyl radicals in the context of reaction development.

Numerous functional groups are tolerated, allowing access to a broad range of novel alkylsulfonamides that are valuable building blocks for drug discovery. Notably, this methodology is also applicable to the late-stage functionalisation of complex biologically active molecules. Mechanistic studies and cyclic voltammetry analysis corroborates with a silyl radical-mediated activation mode for the sulfamoyl chlorides. Furthermore, we report for the first time the synthesis of structurally complex sulfonamide-containing cyclobutyl-spirooxindoles that are novel building blocks of interest to our industrial collaborators and for which no other routes existed.

To the best of our knowledge, our protocol is the first method which allows the one-step late-stage introduction of sulfonamides to aliphatic substrates. Considering the importance of sulfonamides in medicinal chemistry, we believe that this methodology will find wide applications for both building block synthesis and late-stage functionalisation.

2.13 Future Work

Future work on this project will aim at expanding the scope of this transformation to other substrates of different electronic properties, including unactivated and electron-rich alkenes. Owing to the importance of (hetero)aromatics in biologically active molecules, the introduction of sulfamoyl radicals onto heteroaryl substrates, enabling Minisci-type chemistry would open a new avenue for the formation of $C(sp^2)$-sulfonamide fragments. Ideally, distinct reaction conditions would allow the chemoselective addition of a sulfamoyl radical to an alkene or an aromatic group.

Furthermore, we are interested in applying this methodology to other sulfonyl chloride derivatives, such as alkyl or (hetero)aryl sulfonyl chlorides. Such a transformation would render a net hydrosulfonylation product, a reaction which remains underdeveloped. This project will be discussed in **Chapter 3**.

Owing to the importance of fluorine in drug discovery, the silyl radical-mediated activation of fluoroiodomethane for the generation of the fluoromethyl radical will be investigated in the context of the hydrofluoromethylation of alkenes, an unknown transformation to date (**Chapter 4**).

2.14 References

[1] L. Zaffiri, J. Gardner, L. H. Toledo-Pereyra, *J. Investig. Surg.* **2012**, *25*, 67–77.
[2] M. Feng, B. Tang, S. H. Liang, X. Jiang, *Curr Top Med Chem* . **2016**, *16*, 1200–1216.
[3] K. A. Scott, J. T. Njardarson, *Top. Curr. Chem.* **2018**, *376*, 5–39.
[4] J. Drews, *Science* **2000**, *287*, 1960–1964.
[5] A. S. Kalgutkar, R. Jones, A. Sawant, *RSC Drug Discov. Ser.* **2010**, *1*, 210–274.
[6] S. Shoaib, A. Shah, G. Rivera, M. Ashfaq, *Rev. Med. Chem.* **2013**, *13*, 70–86.
[7] S. A. Zhersh, O. P. Blahun, I. V. Sadkova, A. A. Tolmachev, Y. S. Moroz, P. K. Mykhailiuk, *Chem. Eur. J.* **2018**, *24*, 8343–8349.
[8] S. Bag, R. Tulsan, A. Sood, H. Cho, H. Redjeb, W. Zhou, H. Levine, B. Török, M. Török, *Bioorganic Med. Chem. Lett.* **2015**, *25*, 626–630.
[9] E. A. Ilardi, E. Vitaku, J. T. Njardarson, *J. Med. Chem.* **2014**, *57*, 2832–2842.
[10] D. Schelz, *Dye. Pigment.* **1990**, *12*, 1–20.
[11] C. Ballatore, D. M. Huryn, A. B. Smith, *ChemMedChem* **2013**, *8*, 385–395.
[12] P. Lassalas, B. Gay, C. Lasfargeas, M. J. James, V. Tran, K. G. Vijayendran, K. R. Brunden, M. C. Kozlowski, C. J. Thomas, A. B. Smith, et al., *J. Med. Chem.* **2016**, *59*, 3183–3203.
[13] T. Pinter, S. Jana, R. J. M. Courtemanche, F. Hof, *J. Org. Chem.* **2011**, *76*, 3733–3741.
[14] G. A. Patani, E. J. Lavoie, *Chem. Rev.* **1996**, *96*, 3147− 3176.
[15] J. V. Alegre-Requena, S. Grijalvo, D. Sampedro, J. Mayr, C. Saldías, J. J. Marrero-Tellado, R. Eritja, R. P. Herrera, D. D. Díaz, *RSC Adv.* **2020**, *10*, 11481–11492.
[16] N. Şanli, S. Şanli, G. Özkan, A. Denizli, *J. Braz. Chem. Soc.* **2010**, *21*, 1952–1960.
[17] Y. Joyard, C. Papamicaël, P. Bohn, L. Bischoff, *Org. Lett.* **2013**, *15*, 2294–2297.
[18] A. Shavnya, S. B. Coffey, K. D. Hesp, S. C. Ross, A. S. Tsai, *Org. Lett.* **2016**, *18*, 5848− 5851.
[19] O. Chantarasriwong, D. O. Jang, W. Chavasiri, *Tetrahedron Lett.* **2006**, *47*, 7489–7492.
[20] A. G. Beaman, R. K. Robins, L. R. Lewis, C. W. Noell, G. R. Revankar, G. R. Greenberg, N. B. Hanna, N. Imamura, A. F. Lewis, S. B. Larson, et al., *J. Med. Chem.* **1990**, *33*, 1220–1225.
[21] P. J. Dunn, S. Galvin, K. Hettenbach, *Green Chem.* **2004**, *6*, 43–48.
[22] J. D. Bonk, D. T. Amos, S. J. Olson, *Synth. Commun.* **2007**, *37*, 2039–2050.
[23] H. Veisi, R. Ghorbani-Vaghei, S. Hemmati, J. Mahmoodi, *Synlett* **2011**, *16*, 2315–2320.
[24] F. E. Scully, K. Bowdring, *J. Org. Chem.* **1981**, *46*, 5077–5081.
[25] K. N. H. Stephen W. Wright, *J. Org. Chem.* **2006**, *71*, 1080–1084.
[26] T. Kataoka, T. Iwama, T. Setta, A. Takagi, *Synthesis* **1998**, 423–426.
[27] S. Mahapatra, C. P. Woroch, T. W. Butler, S. N. Carneiro, S. C. Kwan, S. R. Khasnavis, J. Gu, J. K. Dutra, B. C. Vetelino, J. Bellenger, et al., *Org. Lett.* **2020**, *22*, 4389− 4394.
[28] P. Mukherjee, C. P. Woroch, L. Cleary, M. Rusznak, R. W. Franzese, M. R. Reese, J. W. Tucker, J. M. Humphrey, S. M. Etuk, S. C. Kwan, et al., *Org. Lett.* **2018**, *20*, 3943–3947.
[29] R. Zelli, S. Tommasone, P. Dumy, A. Marra, A. Dondoni, *Eur. J. Org. Chem.* **2016**, *2016*, 5102–5116.
[30] C. Li, Y. Zheng, K. P. Rakesh, H.-L. Qin, *Chem. Commun.* **2020**, *56*, 8075–8078.
[31] A. Dondoni, A. Marra, *Org. Biomol. Chem.* **2017**, *15*, 1549–1553.
[32] P. S. Santos, M. T. S. Mello, *J. Mol. Struct.* **1988**, *178*, 121–133.
[33] H. Woolven, C. González-Rodríguez, I. Marco, A. L. Thompson, M. C. Willis, *Org. Lett.* **2011**, *13*, 4876–4878.
[34] A. S. Deeming, C. J. Russell, M. C. Willis, *Angew. Chem. Int. Ed.* **2015**, *54*, 1168–1171.
[35] E. F. Flegeau, J. M. Harrison, M. C. Willis, *Synlett* **2016**, *27*, 101–105.
[36] Y. Chen, M. C. Willis, *Chem. Sci.* **2017**, *8*, 3249–3253.
[37] H. Zhu, Y. Shen, Q. Deng, C. Huang, T. Tu, *Chem. Asian J.* **2017**, *12*, 706–712.
[38] J. R. Debergh, N. Niljianskul, S. L. Buchwald, *J. Am. Chem. Soc.* **2013**, *135*, 10638–10641.
[39] A. Shavnya, S. B. Coffey, A. C. Smith, V. Mascitti, *Org. Lett.* **2013**, *15*, 6226–6229.
[40] M. W. Johnson, S. W. Bagley, N. P. Mankad, R. G. Bergman, V. Mascitti, F. D. Toste, *Angew. Chem. Int. Ed.* **2014**, *126*, 4493–4496.
[41] Y. Chen, P. R. D. Murray, A. T. Davies, M. C. Willis, *J. Am. Chem. Soc.* **2018**, *140*, 8781–8787.
[42] G. Laudadio, E. Barmpoutsis, C. Schotten, L. Struik, S. Govaerts, D. L. Browne, T. Noël, *J. Am. Chem. Soc.* **2019**, *141*, 5664–5668.
[43] T. Q. Davies, M. J. Tilby, D. Skolc, A. Hall, M. C. Willis, *Org. Lett.* **2020**, doi.org/10.1021/acs.orglett.0c03505.

[44] F. W. Goldberg, J. G. Kettle, T. Kogej, M. W. D. Perry, N. P. Tomkinson, *Drug Discov. Today* **2015**, *20*, 11–17.
[45] F. Lovering, *Med. Chem. Commun.* **2013**, *4*, 515–519.
[46] K. Kingwell, *Nat. Rev. Drug Discov.* **2009**, *8*, 931.
[47] F. Lovering, J. Bikker, C. Humblet, *J. Med. Chem.* **2009**, *52*, 6752–6756.
[48] C. Chatgilialoglu, D. Griller, S. Rossini, *J. Org. Chem.* **1989**, *54*, 2734–2737.
[49] M. S. Kharasch, R. A. Mosher, *J. Org. Chem.* **1952**, *17*, 453–456.
[50] M. L. E. N. Da Mata, W. B. Motherwell, F. Ujjainwalla, *Tetrahedron Lett.* **1997**, *38*, 141–144.
[51] F. L. Scott, J. A. Barry, *Tetrahedron Lett.* **1968**, *9*, 513–517.
[52] F. Montermini, E. Lacôte, M. Malacria, *Org. Lett.* **2004**, *6*, 921–923.
[53] M. Alkan-Zambada, X. Hu, *J. Org. Chem.* **2019**, *84*, 4525–4533.
[54] C. K. Prier, D. A. Rankic, D. W. C. MacMillan, *Chem. Rev.* **2013**, *113*, 5322–5363.
[55] R. C. McAtee, E. J. McClain, C. R. J. Stephenson, *Trends Chem.* **2019**, *1*, 111–125.
[56] G. E. M. Crisenza, P. Melchiorre, *Nat. Commun.* **2020**, *11*, 1–4.
[57] M. K. Bogdos, E. Pinard, J. A. Murphy, *Beilstein J. Org. Chem.* **2018**, *14*, 2035–2064.
[58] N. A. Romero, D. A. Nicewicz, *Chem. Rev.* **2016**, *116*, 10075–10166.
[59] L. B. Johansson, P. Bjorn, *Acta Chem. Scand. B* **1978**, *32*, 431–436.
[60] N. Ignat'ev, A. Kucherina, S. P., *Acta Chem. Scand.* **1999**, *53*, 1110–1116.
[61] H. Jiang, Y. Cheng, Y. Zhang, S. Yu, *Eur. J. Org. Chem.* **2013**, 5485–5492.
[62] C.-J. Wallentin, J. D. Nguyen, P. Finkbeiner, C. R. J. Stephenson, *J. Am. Chem. Soc.* **2012**, *134*, 8875–8884.
[63] C. S. Gloor, F. Dénès, P. Renaud, *Angew. Chem. Int. Ed.* **2017**, *129*, 13514–13517.
[64] A. Hossain, S. Engl, E. Lutsker, O. Reiser, *ACS Catal.* **2019**, *9*, 1103–1109.
[65] S. K. Pagire, S. Paria, O. Reiser, *Org. Lett.* **2016**, *18*, 2106–2109.
[66] X.-J. Tang, W. R. Dolbier, *Angew. Chem. Int. Ed.* **2015**, *54*, 4246–4249.
[67] X. Zeng, L. Ilies, E. Nakamura, *Org. Lett.* **2012**, *14*, 954–956.
[68] Q. Luo, R. Mao, Y. Zhu, Y. Wang, *J. Org. Chem.* **2019**, *84*, 13897–13907.
[69] D. J. P. Kornfilt, D. W. C. MacMillan, *J. Am. Chem. Soc.* **2019**, *141*, 6853–6858.
[70] B. Chen, Q. Long, Y. Zhao, Y. Wu, S. Ge, P. Wang, C. G. Yang, Y. Chi, B. Song, S. Yang, *J. Agric. Food Chem.* **2019**, *67*, 6962–6969.
[71] G. H. Lovett, S. Chen, X. S. Xue, K. N. Houk, D. W. C. MacMillan, *J. Am. Chem. Soc.* **2019**, *141*, 20031–20036.
[72] P. Zhang, C. C. Le, D. W. C. MacMillan, *J. Am. Chem. Soc.* **2016**, *138*, 8084–8087.
[73] J. R. Robalo, S. Huhmann, B. Koksch, A. Vila Verde, *Chem* **2017**, *3*, 881–897.
[74] V. Bacauanu, S. Cardinal, M. Yamauchi, M. Kondo, D. F. Fernández, R. Remy, D. W. C. MacMillan, *Angew. Chem. Int. Ed.* **2018**, *130*, 12723–12728.
[75] X. Fan, P. Xiao, Z. Jiao, T. Yang, X. Dai, W. Xu, J. Da Tan, G. Cui, H. Su, W. Fang, et al., *Angew. Chem. Int. Ed.* **2019**, *131*, 12710–12714.
[76] W. Yu, Y. Luo, L. Yan, D. Liu, Z. Wang, P. Xu, *Angew. Chem. Int. Ed.* **2019**, *131*, 11057–11061.
[77] J. Lalevée, X. Allonas, J. P. Fouassier, *J. Org. Chem.* **2007**, *72*, 6434–6439.
[78] J. J. Devery, J. D. Nguyen, C. Dai, C. R. J. Stephenson, *ACS Catal.* **2016**, *6*, 5962–5967.
[79] J. Zhu, W. C. Cui, S. Wang, Z. J. Yao, *Org. Lett.* **2018**, *20*, 3174–3178.
[80] C. Chatgilialoglu, C. Ferreri, Y. Landais, V. I. Timokhin, *Chem. Rev.* **2018**, *118*, 6516–6572.
[81] P. Shah, A. D. Westwell, *J. Enzyme Inhib. Med. Chem.* **2007**, *22*, 527–540.
[82] S. Purser, P. R. Moore, S. Swallow, V. Gouverneur, *Chem. Soc. Rev.* **2008**, *37*, 320–330.
[83] J. Wang, M. Sánchez-Roselló, J. L. Aceña, C. Del Pozo, A. E. Sorochinsky, S. Fustero, V. A. Soloshonok, H. Liu, *Chem. Rev.* **2014**, *114*, 2432–2506.
[84] T. Kim, S. J. McCarver, C. Lee, D. W. C. MacMillan, *Angew. Chem. Int. Ed.* **2018**, *130*, 3546–3550.
[85] P. S. Fier, K. M. Maloney, *J. Am. Chem. Soc.* **2019**, *141*, 1441–1445.
[86] X. Zhao, D. W. C. MacMillan, *J. Am. Chem. Soc.* **2020**, *142*, 19480–19486.
[87] C. Le, T. Q. Chen, T. Liang, P. Zhang, D. W. C. MacMillan, *Science* **2018**, *360*, 1010–1014.
[88] J. N. Freskos, D. P. Getman, J. J. Talley, J. A. Sikorski, *Bis-Sulfonamide Hydroxyethylamino Retroviral Protease Inhibitors*, **2007**, WO 1996/022287.
[89] V. M. Dembitsky, *J. Nat. Med.* **2008**, *62*, 1–33.
[90] Q. Liu, N. Li, Y. Yuan, H. Lu, X. Wu, C. Zhou, M. He, H. Su, M. Zhang, J. Wang, et al., *J. Med. Chem.* **2012**, *55*, 250− 267.
[91] C. M. Marson, *Chem. Soc. Rev.* **2011**, *40*, 5514–5533.
[92] A. Sergeiko, V. V Poroikov, L. O. Hanu, V. M. Dembitsky, *Open Med. Chem. J.* **2008**, *2*, 26–

37.
[93] J. F. Liebman, *The Chemistry of Cyclobutanes Patai Series : The Chemistry of Functional Groups*, **2005**.
[94] E. M. Carreira, T. C. Fessard, *Chem. Rev.* **2014**, *114*, 8257–8322.
[95] G. S. Singh, Z. Y. Desta, *Chem. Rev.* **2012**, *112*, 6104–6155.
[96] M. M. M. Santos, *Tetrahedron* **2014**, *70*, 9735–9757.
[97] X. Liu, T. Cong, P. Liu, P. Sun, *Org. Biomol. Chem.* **2016**, *14*, 9416–9422.
[98] J. Dong, X. Lyu, Z. Wang, X. Wang, H. Song, Y. Liu, Q. Wang, *Chem. Sci.* **2019**, *10*, 976–982.
[99] J. J. Devery, J. D. Nguyen, C. Dai, C. R. J. Stephenson, *ACS Catal.* **2016**, *6*, 5962–5967.
[100] H. Masu, T. Okamoto, T. Kato, K. Katagiri, M. Tominaga, H. Goda, H. Takayanagi, I. Azumaya, *Tetrahedron Lett.* **2006**, *47*, 803–807.
[101] A. Postigo, S. Kopsov, S. S. Zlotsky, C. Ferreri, C. Chatgilialoglu, *Organometallics* **2009**, *28*, 3282–3287.
[102] J. Zhu, W. C. Cui, S. Wang, Z. J. Yao, *Org. Lett.* **2018**, *20*, 3174–3178.
[103] H. Qrareya, D. Dondi, D. Ravelli, M. Fagnoni, *ChemCatChem* **2015**, *7*, 3350–3357.
[104] T. M. Monos, R. C. McAtee, C. R. J. Stephenson, *Science* **2018**, *361*, 1369–1373.
[105] W. B. Motherwell, A. M. K. Pennell, *Chem. Commun* **1991**, 877–879.

Chapter 3

Synthesis of Aliphatic Sulfones with Sulfonyl Chlorides under Visible Light Activation

This chapter discloses a robust and operationally simple methodology for the hydrosulfonylation of alkenes using sulfonyl chlorides as inexpensive sulfonyl radical precursors. Sulfonyl chlorides are suitable reagents for atom transfer radical addition reactions to alkenes, leading to chlorosulfonylation. However, re-routing this process towards hydrosulfonylation of alkenes has not been accomplished prior to the work outlined in this chapter. This late-stage functionalisation strategy permits direct attachment of sulfones onto a wide range of feedstock olefins allowing access to a broad range of novel alkylsulfones including biologically active molecules and complex sulfone-containing cyclobutyl-spirooxindoles, which are valuable building blocks for drug discovery. Furthermore, the use of polarity reversal catalysis allowed us to expand the generality of this transformation to a wide range of alkenes with different electronic profiles.

The contents of this chapter have been published in *Angewandte Chemie* in 2020.

S. M. Hell*, C. F. Meyer*, A. Misale, J. B. I. Sap, K. E. Christensen, M. C. Willis, A. A. Trabanco, V. Gouverneur, Hydrosulfonylation of Alkenes with Sulfonyl Chlorides under Visible Light Activation. *Angew. Chem. Int. Ed.* **2020**, *59*, 11620-11626.

*These authors contributed equally to this work.

Author contributions: Reactions were designed by Sandrine M. Hell, Claudio F. Meyer, Dr. Andrés A. Trabanco and Prof. Véronique Gouverneur. The reaction conditions were optimised by Sandrine M. Hell. Scope and mechanistic experiments were performed by Sandrine M. Hell and Claudio F. Meyer. Stern-Volmer fluorescence quenching experiments were performed by Claudio F. Meyer and Dr. Jeroen B. I. Sap. Dr. Antonio Misale and Prof. Michael C. Willis provided helpful comments.

3.1 Introduction to Sulfones

Sulfones have been identified as privileged functionalities, and are therefore widely present in marketed drugs,[1] agrochemicals,[2] and polymers.[3,4] Sulfone-containing molecules have especially attracted many interests from the pharmaceutical industry, due to the unique electronic and structural properties of the SO_2 group (**3.1**-**3.5**; **Figure 3.1**).[1,5,6] The distinctive ability of sulfones to participate in intra- and intermolecular hydrogen bonding interactions, along with their strong electron-withdrawing nature, stability against hydrolysis, and resistance to reduction at sulfur, have made them a powerful functional group in medicinal chemistry.[7,8]

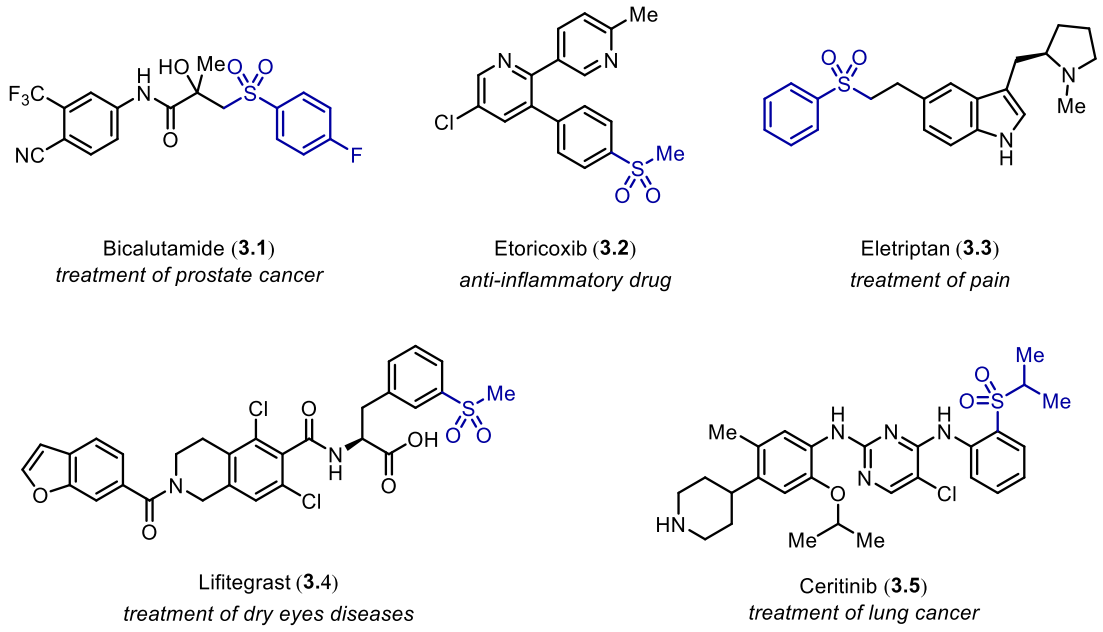
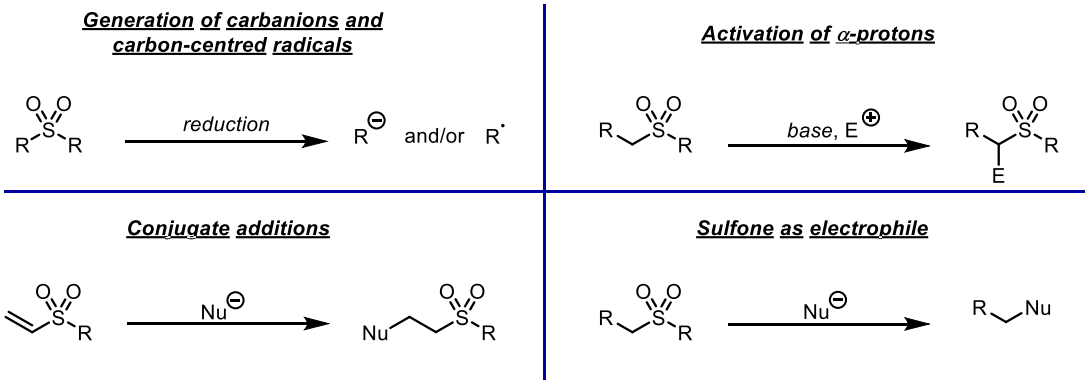


Figure 3.1: Marketed drugs featuring sulfone motifs.

Nowadays, the synthesis of novel structurally complex sulfones is an active area of research in organic chemistry, specifically in the context of late-stage functionalisation of structurally complex molecules.[5,6,9,10]

3.2 Synthesis of Sulfones

Also known as "chameleons", sulfones are attractive motifs due to their remarkable reactivity profile.[11,12] Depending on the reaction conditions, sulfones can act as nucleophiles, electrophiles, or radicals, demonstrating their versatility in organic synthesis (**Scheme 3.1**).

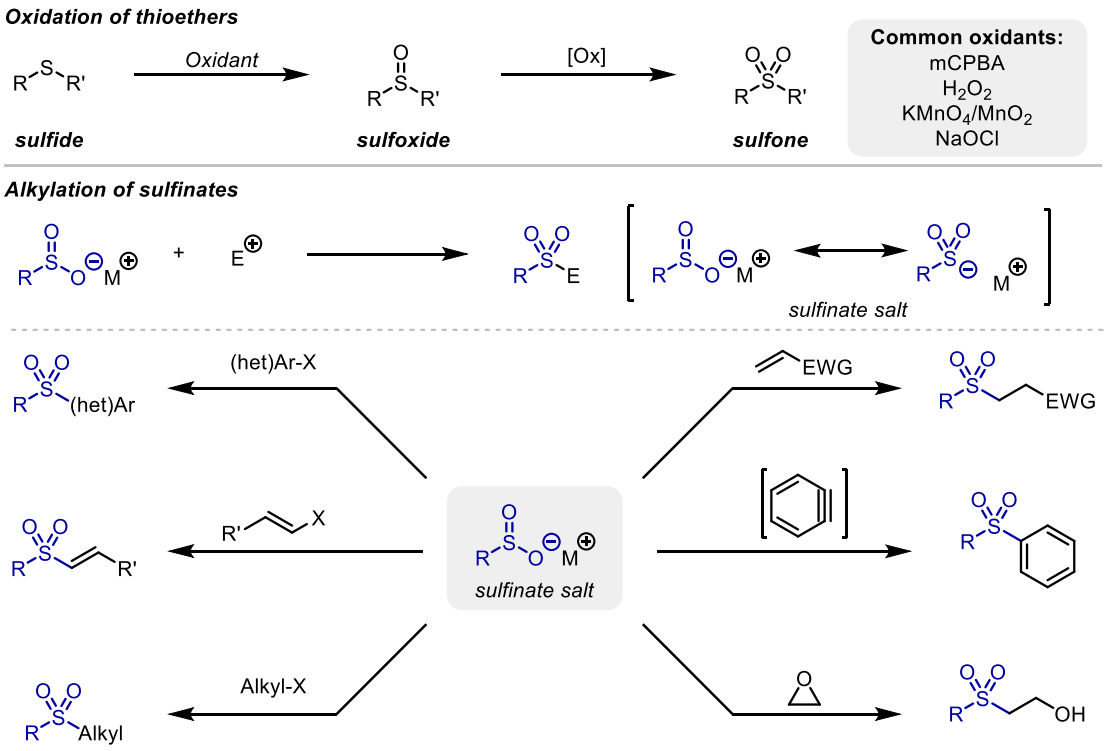


Scheme 3.1: Sulfones as chemical "chameleons".

3.2.1 General Strategies for the Synthesis of Sulfones

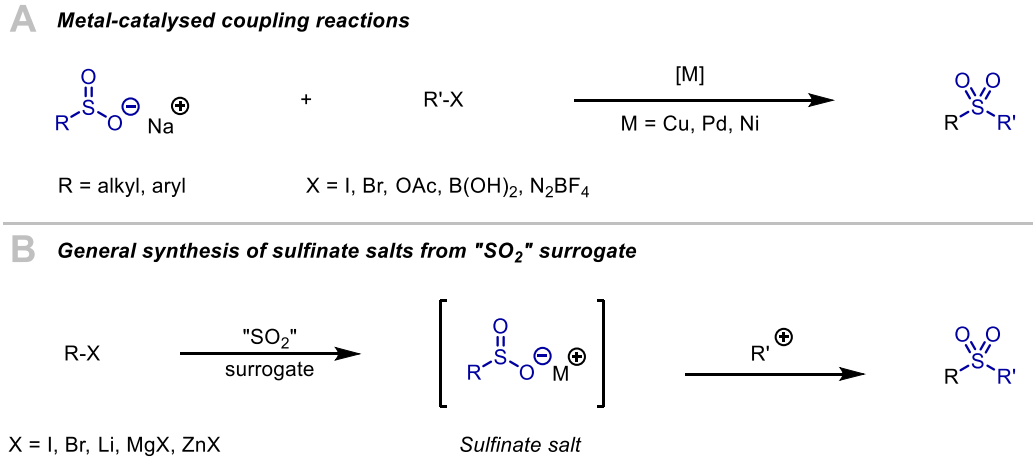
Owing to their wide spectrum of reactivity, it is therefore no surprise that a plethora of methods have been developed for the synthesis of this motif. The most common route to access sulfones is the oxidation of a sulfide or sulfoxide with strong oxidants such as peracids or hydrogen peroxide (**Scheme 3.2**).[13–18] Although milder oxidation conditions have been developed more recently,[19–26] these strategies are limited in scope and functional group tolerance. Sulfides or sulfoxides are often synthesised from odorous and toxic thiols, which is a drawback of this synthetic strategy. Another limitation stems from the incomplete oxidation of the sulfide to the sulfone, affording the sulfoxide product. Furthermore, the use of harsh reaction conditions (strong oxidising agents, high temperatures, long reaction times) limits the application of these strategies in terms of late-stage functionalisation of complex scaffolds. Other common synthetic methods to

access sulfones include the alkylation/arylation of sulfinate salts with alkyl halides, epoxides,[27] Michael acceptors[27], (hetero)aryl halides[27], vinyl halides,[28] arynes intermediates[29] and others. Sulfinate salts are privileged reagents for the preparation of sulfones; they are easy to prepare, bench-stable for several months, easy to handle, and non-odorous.



Scheme 3.2: Traditional methods for the preparation of sulfones.

Whilst most of these protocols have been developed in the 20th century, new methods have emerged in the last decades. The use of sulfinate salts has been extended to transition metal-catalysed coupling reactions for the regioselective and stereoselective introduction of sulfones into C(sp^2)-fragments.[30–35] With the aim of diversifying this transformation to a wide range of coupling partners, new ligands, diverse metals and milder reaction conditions were utilised (**Scheme 3.3A)**. Furthermore, the use of chiral ligands allowed for the development of enantioselective protocols.[36,37]



Scheme 3.3: A. Transition metal-catalysed cross-coupling of sulfinate salts. B. One-pot synthesis of sulfones employing SO_2 surrogates.

Another strategy for the preparation of a wider scope of sulfones relies on the direct incorporation of the SO_2 fragment (**Scheme 3.3B**). Although several reports described the use of sulfur dioxide gas for the installation of the sulfone motif,[38–40] the high toxicity and difficult handling of sulfur dioxide gas led scientists to develop new methodologies using solid and bench-stable sulfur dioxide surrogates such as DABSO and potassium metabisulfite ($K_2S_2O_5$).[41–47] A key step in these transformations is the *in situ* generation of a sulfinate salt by reacting a nucleophile with DABSO, which can subsequently react with carbon electrophiles (e.g. organohalides, epoxides, (hetero)aryliodonium salts) to form a diverse set of sulfones.[41,44,45] Compared to the traditional synthesis of sulfinate salts, these novel approaches led to a considerable improvement of substrate scope and functional group tolerance, as they are typically performed under mild reaction conditions. Overall, a plethora of other methods have been reported for the introduction of the sulfone group (e.g. *via* C−H activation[48–55]); these methods have been addressed in several reviews and will not be the focus of this chapter.[27,56–58]

3.2.2 Radical-Mediated Sulfonylation of Alkenes

Most of the protocols described above are well suited for the construction of C(sp^2)-linked sulfones, but the construction of sulfones substituted with two alkyl groups remains underexplored. Given the contemporary challenges faced by industry at increasing the C(sp^3) character in complex molecules,[59–62] a myriad of radical processes for the synthesis of C(sp^3)-sulfonylated fragments have been reported. The most common synthetic methods rely on the addition of a sulfonyl radical to alkenes and alkynes. Sulfonyl halides are the most common sulfonyl radical precursors.[63–71] Other sulfonyl radical precursors include metal sulfinates,[72–75] sulfonyl selenides,[76,77] sulfonyl hydrazides,[78–80] sulfonyl azides[81] as well as allyl sulfones (**Figure 3.2**).[82]

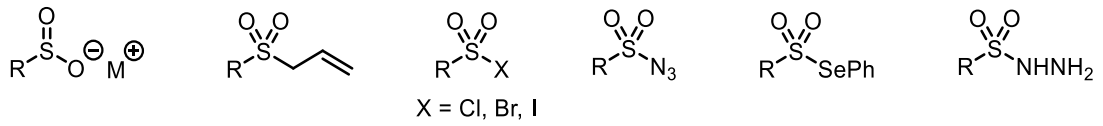
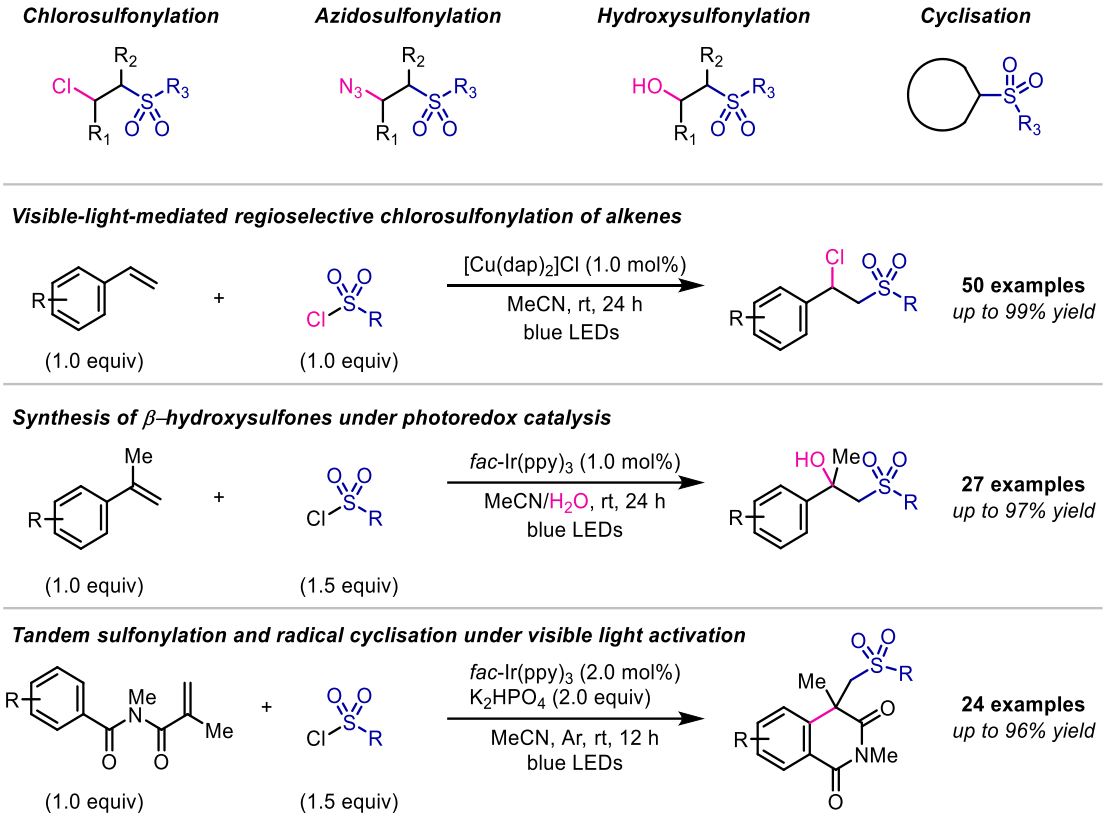


Figure 3.2: Sulfonyl radical precursors.

Classical conditions for their activation rely on the use of a radical initiator, such as peroxides or AIBN. However, these sulfonyl radical precursors are often less stable, not readily available and/or require harsher reaction conditions to generate the corresponding sulfonyl radical compared to sulfonyl halides.

More recently, redox processes employing copper, iridium, ruthenium, and others enabled the direct single-electron reduction of sulfonyl halides, specifically sulfonyl chlorides, for the generation of sulfonyl radicals.[67,69,83] Most of these methods have found applications in the addition of sulfonyl radicals to alkenes, generating vicinal difunctionalised products, including *β*-chlorosulfones, *β*-hydroxysulfones, *β*-azidosulfones and sulfone-containing cyclic structures (**Scheme 3.4**). Sulfonyl chlorides

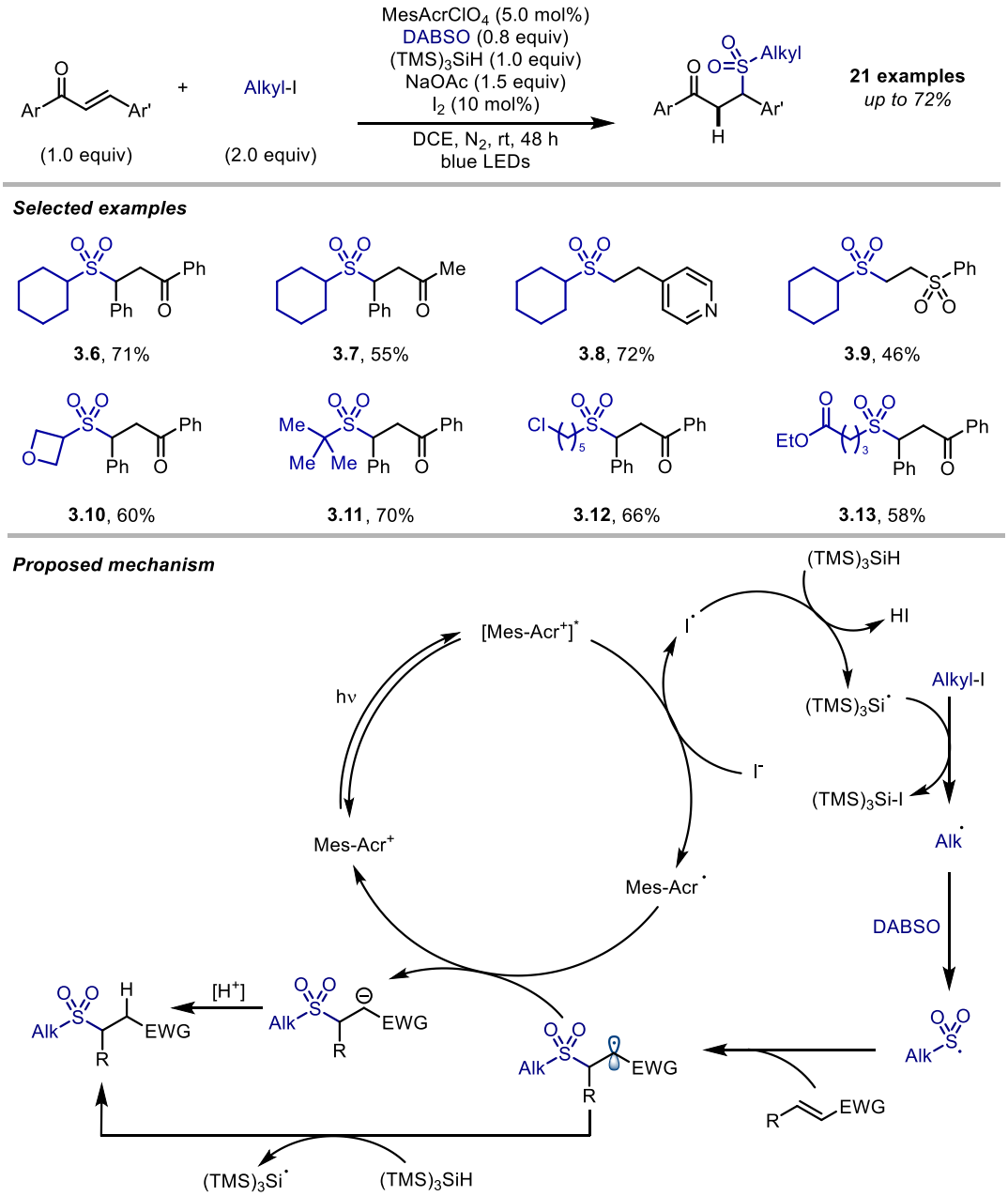
offer many advantages over other reagents with respect to price, commercial availability, and ease of handling. These protocols also offer unique opportunities for the one-step incorporation of two functional groups, increasing the structural complexity of a molecule.



Scheme 3.4: Selected examples of vicinal difunctionalisation of alkenes.

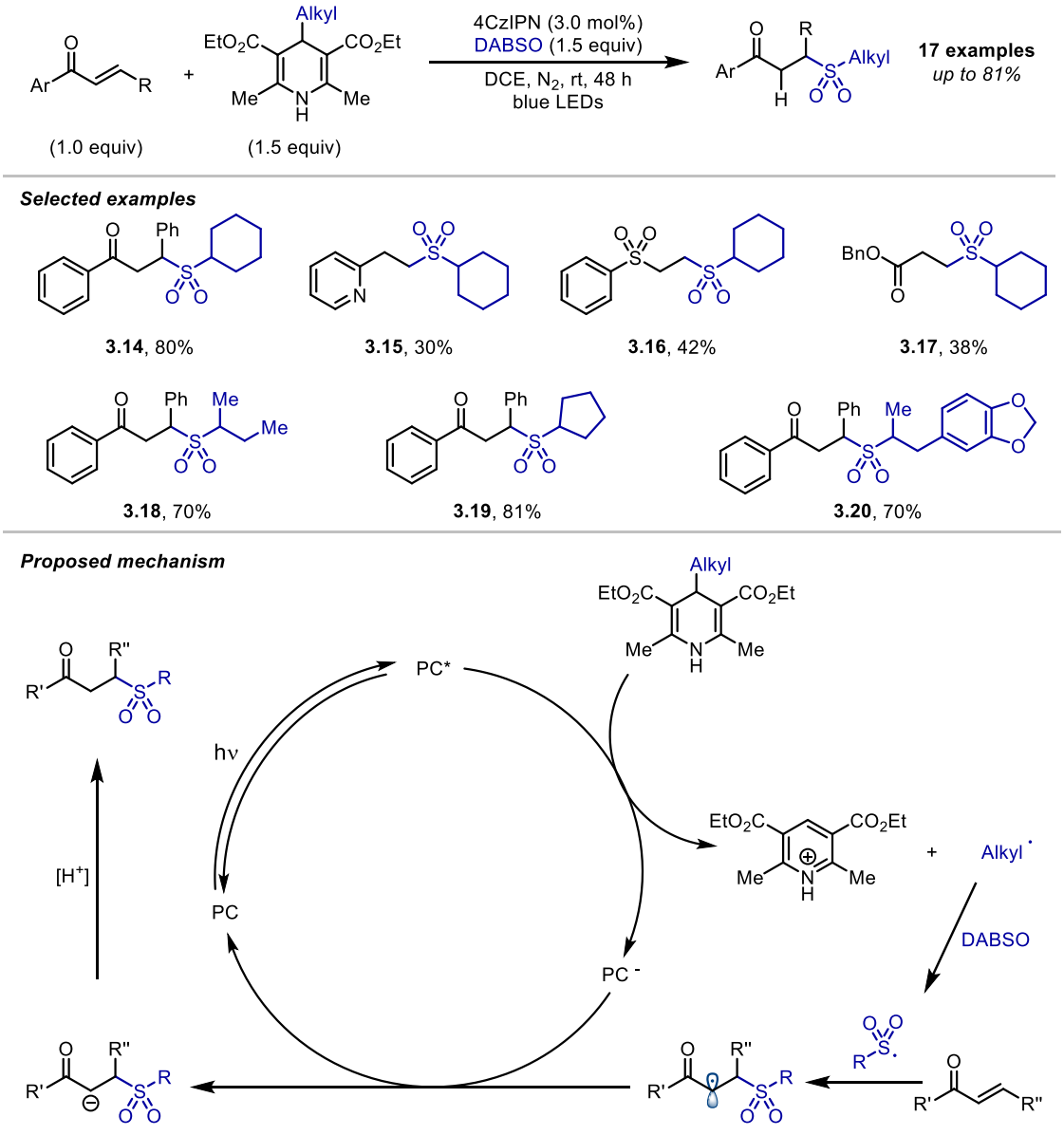
In contrast to the aforementioned methods, processes enabling the introduction of a sulfonyl radical and a hydrogen atom (hydrosulfonylation) to form alkylsulfones are less common.[84] It is only in 2019, that advances in the hydrosulfonylation of 1,2-disubstituted electron-deficient alkenes, giving rise to alkyl sulfones, have been reported. Qiu and co-workers described the hydrosulfonylation of electron-deficient alkenes under photoredox conditions (**Scheme 3.5**).[85] In this transformation, alkyl radicals react with DABSO to form sulfonyl radicals. Mechanistically, the organophotocatalyst undergoes single-electron oxidation with iodide to form the corresponding iodine radical, which can

subsequently undergo HAA with $(TMS)_3SiH$. The hereby generated silyl radical activates various alkyl iodides by HAA, leading to alkyl radicals. The latter reacts with DABSO to provide sulfonyl radicals, which can regioselectively add to the electron-deficient alkene (Giese addition). The carbon-centred radical intermediate is further reduced to an anionic intermediate *via* SET, yielding the desired product upon protonation. An alternative pathway involving the direct HAT between the radical intermediate and the silane was also suggested by the authors.



Scheme 3.5: Photoredox-catalysed hydrosulfonylation of electron-deficient alkenes with alkyl iodides.

Simultaneously, Wu and co-workers reported the photoredox hydrosulfonylation of electron-deficient alkenes employing 4-susbtituted Hantzsch esters as alkyl radical precursors in combination with DABSO as an SO_2 source (**Scheme 3.6**).[86]



Scheme 3.6: Photoredox-catalysed hydrosulfonylation of electron-deficient alkenes with Hantzsch esters.

The alkyl radical is generated upon single-electron transfer between the 4-substituted Hantzsch ester and the excited state of the photocatalyst. Next, this radical is trapped by DABSO to form the corresponding sulfonyl radical, which undergoes Giese addition to the electron-deficient alkene. The authors suggest a single-electron reduction of the

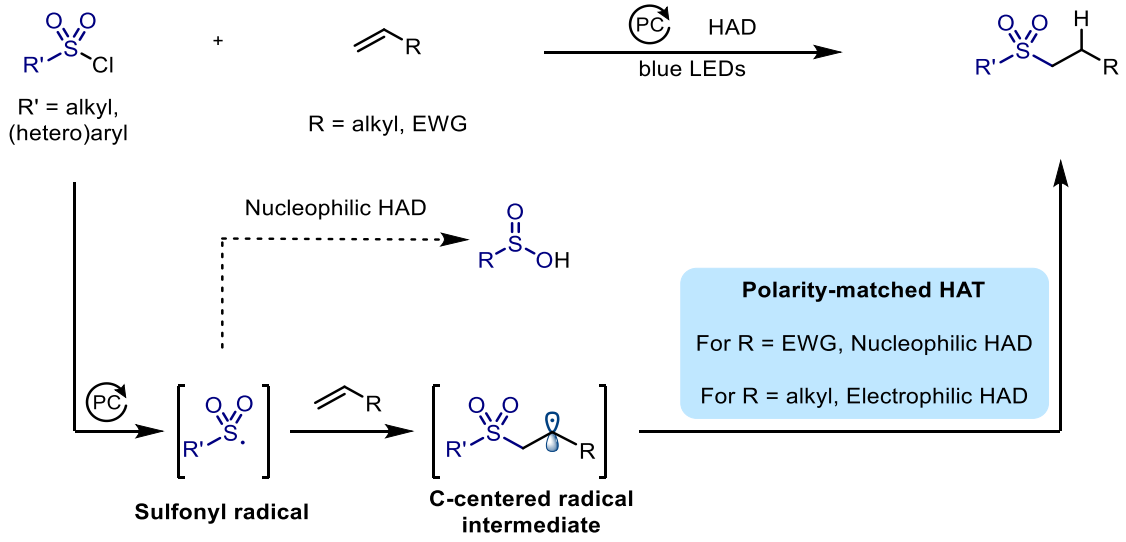
carbon-centred radical to form an anion, which yields the desired hydrosulfonylated product upon protonation. Importantly, both methodologies described above (**Scheme 3.5** and **3.6**) are best suited to highly activated chalcone derivatives (**3.6**-**3.20**), which limits their application in terms of late-stage functionalisation of biologically relevant molecules. Furthermore, in the context of Wu's report, only few 4-substituted Hantzsch esters are commercially available, which hampers the use of this methodology to the introduction of complex sulfone fragments.

Although few hydrosulfonylation methodologies have emerged in 2019, the development of a more general procedure employing commercially available starting materials is highly desirable. Specifically, the application of such a methodology to a wider range of alkenes with varying electronics and to the late-stage introduction of sulfones into complex biologically active molecules would be particularly beneficial for medicinal chemists.

3.3 Strategy for the Hydrosulfonylation of Alkenes

Based on the recently disclosed visible light promoted hydrofunctionalisations of alkenes by our group,[71,87–89] we were encouraged to develop a novel methodology for the incorporation of sulfone moieties onto alkenes. As shown is **Chapter 2**, the reduction potentials of sulfonyl chlorides (E_{red} ($MeSO_2Cl$: -1.30 V vs. SCE;[90] E_{red} ($PhSO_2Cl$): -1.30 V vs. SCE)[91] are in range with commercially available photocatalysts, and their direct activation by single-electron reduction with the excited state of a photocatalyst has been already demonstrated in numerous reports.[92–96] We aimed to design a process that would render hydrosulfonylated products by employing commercially and readily available sulfonyl chlorides, as well as alkenes as feedstock building blocks. Although

sulfonyl chlorides have been extensively used as radical precursors for the ATRA of alkenes affording chlorosulfonylation[63–70,83,97], re-routing this process towards hydrosulfonylation of alkenes has never been accomplished. To this end, we felt compelled to develop a novel protocol for the net hydrosulfonylation of alkenes (**Scheme 3.7**).



Scheme 3.7: Reaction design for the hydrosulfonylation of alkenes.

Such a strategy would require the anti-Markovnikov addition of a sulfonyl radical to the alkene. This step would furnish a carbon-centred radical intermediate, which would undergo HAT with a HAD to afford the hydrosulfonylated product. Although sulfonyl radicals have been described as electrophilic radicals, previous reports describing processes other than hydrosulfonylation,[98] demonstrated the ability of this radical to add to both electron-rich and deficient alkenes.[67,84,99] Therefore, we expected that the remaining challenge relies on a polarity match between a suitable HAD and the carbon-centred radical intermediate. We speculated that the nature of the HAD would be essential depending on the electronic profile of the alkene. As such, electrophilic radicals (e.g. α-carbonyl radicals) will require a nucleophilic HAD for a polarity matched HAT. The *in situ* generated electrophilic sulfonyl radical could also undergo competitive HAT

in presence of a nucleophilic HAD. We believe that an extensive screening of HAD would be required to promote HAT on the carbon-centred radical. In contrast, in the case of a nucleophilic radical intermediate (e.g. alkyl radicals), an electrophilic HAD would be required to afford the desired hydrosulfonylated product.

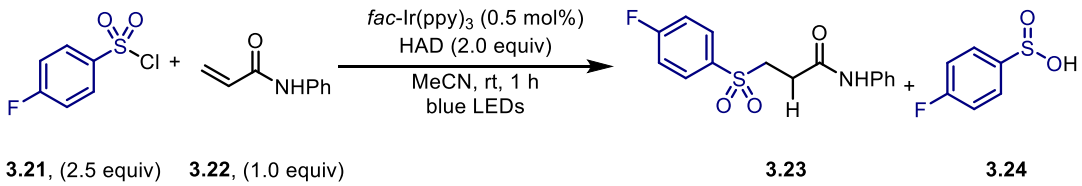
3.4 Optimisation of the Reaction Conditions

To explore this concept, we investigated the reaction of an electron-deficient alkene with a sulfonyl chloride as radical precursor under photoredox catalysis. Central to our reaction design, we believed that a strong reducing photocatalyst would be suitable for the activation of sulfonyl chlorides *via* single-electron reduction. Specifically, the triplet excited state of the photocatalyst *fac*-Ir(ppy)$_3$ [$E(Ir^{III*}/Ir^{IV}) = -1.73$ V vs SCE in MeCN)[94] could undergo SET with alkyl and arylsulfonyl chlorides (E_{red} ($MeSO_2Cl$: -1.30 V vs. SCE;[172] E_{red} ($PhSO_2Cl$): -1.30 V vs. SCE)[171], allowing for the efficient generation of a wide range of sulfonyl radicals. Therefore, we reasoned that 4-fluorobenzenesulfonyl chloride (**3.21**) as sulfonyl radical source, *N*-phenylacrylamide (**3.22**) as the model alkene, and *fac*-Ir(ppy)$_3$ in MeCN, were suitable conditions to initiate our investigation. The use 4-fluorobenzenesulfonyl chloride (**3.21**) enabled to assess the yield of the product by quantitative ^{19}F NMR spectroscopy [Product: **^{19}F NMR** (471 MHz, $CDCl_3$) δ -102.5 (m, 1F)]. The structure and purity of the desired product (**3.23**) were assessed by ^{1}H and ^{13}C NMR spectra. Specifically, disappearance of characteristic alkene peaks [**^{1}H NMR** (500 MHz, $CDCl_3$): δ 6.45 (dd, J = 16.9, 9.8 Hz, 1H), 6.37 (dd, J = 17.0, 2.0 Hz, 1H), 5.63 (dd, J = 9.8, 2.0 Hz, 1H); **^{13}C NMR** (126 MHz, $CDCl_3$): δ 131.4, 127.8] and appearance of aliphatic peaks [**^{1}H NMR** (500 MHz, $CDCl_3$): δ 3.58 (t, J = 8.1 Hz, 2H),

2.95 (t, J = 8.1 Hz, 2H); **^{13}C NMR** (126 MHz, $CDCl_3$): δ 52.2, 29.8] are characteristic for the addition of **3.21** to **3.23**.

At the onset, a screening of different HAD was performed (**Table 3.1**). No reactivity was observed in absence of HAD (**Table 3.1**, **entry 1**). As envisioned in our reaction design, the *in situ* generated sulfonyl radical can undergo competitive HAA to form the corresponding sulfinic acid **3.24** [**^{19}F NMR** (471 MHz, $CDCl_3$) δ − 107.0 (m, 1F)]. The use of THF, triphenylmethane or the electrophilic HAD thiophenol, led to traces or low yields of hydrosulfonylated product **3.23** and sulfinic acid **3.24** (**Table 3.1**, **entries 2-4**).

Table 3.1: Screening of HAD for the hydrosulfonylation of *N*-phenylacrylamide (**3.22**).[a].



entry	HAD	yield[b] (3.23)	yield[b] (3.24)
1	-	-	2%
2	THF (solvent)	traces	4%
3	Ph_3CH	traces	traces
4	PhSH	26%	3%
5	Bu_3SnH	28%	59%
6	Hantzsch ester	34%	3%
7	Et_3SiH	traces	traces
8	Ph_3SiH	traces	4%
9	$(TMS)_3SiH$	90% (82%)[c]	11%

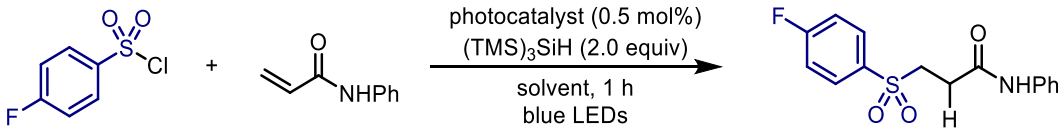
[a] Reaction conditions: sulfonyl chloride **3.21** (0.25 mmol), alkene **3.22** (0.1 mmol), *fac*-Ir(ppy)$_3$ (0.5 mol%), HAD (0.2 mmol), MeCN (0.6 mL) under blue light (λ_{max} = 450 nm) irradiation for 1 h. [b] Yields determined by quantitative ^{19}F NMR using α,α,α-trifluorotoluene as the internal standard. [c] Yield of isolated product.

Screening of other nucleophilic HAD revealed that Hantzsch ester and tributyltin hydride were slightly more efficient, allowing access to the desired hydrosulfonylated product

3.23 in moderate yield (**Table 3.1**, **entries 5-6**). Interestingly, tributyltin hydride (BDE = 74 kcal/mol),[100] resulted in the formation of the sulfinic acid **3.24** as the major product. Screening of different silanes such as triethylsilane or triphenylsilane afforded traces of the hydrosulfonylated product (**Table 3.1**, **entries 7-8**). Owing to its favourable Si−H bond dissociation energy (BDE = 84 kcal/mol),[101,102] $(TMS)_3SiH$ afforded the desired hydrosulfonylated product **3.23** in 90% yield along with only 11% yield of sulfinic acid **3.24** (**Table 3.1**, **entry 9**). Although tributyltin hydride allowed for efficient consumption of the sulfonyl chloride, the weak BDE of the Sn−H bond led to the quenching of the sulfonyl radical before addition to the alkene.

Further screening revealed that the yield was not improved when alternative solvents such as DMF, DMSO or MeOH were used (**Table 3.2**, **entries 1-3**).

Table 3.2: Optimisation of the reaction conditions for the hydrosulfonylation of *N*-phenylacrylamide (**3.22**)[a].



3.21, (2.5 equiv) **3.22**, (1.0 equiv) **3.23**

entry	catalyst	solvent	yield
1	*fac*-Ir(ppy)$_3$	DMF	65%
2	*fac*-Ir(ppy)$_3$	DMSO	traces
3	*fac*-Ir(ppy)$_3$	MeOH	49%
4	[Ir(ppy)$_2$(dtbby)$_2$)PF$_6$]	MeCN	55%
5	Ir[dCF$_3$(ppy)$_2$](dtbbpy)PF$_6$	MeCN	88%
6	Eosin Y	MeCN	78%
7[b]	*fac*-Ir(ppy)$_3$	MeCN	81%
8[c]	*fac*-Ir(ppy)$_3$	MeCN	55%
9[d]	*fac*-Ir(ppy)$_3$	MeCN	72%

10[e]	*fac*-Ir(ppy)$_3$	MeCN	nd
11[f]	-	MeCN	23%
12[g]	*fac*-Ir(ppy)$_3$	MeCN	81%

[a] Reaction condition: sulfonyl chloride **3.21** (0.25 mmol), alkene **3.22** (0.1 mmol), photocatalyst (0.5 mol%), $(TMS)_3SiH$ (0.2 mmol), solvent (0.6 mL) under blue light (λ_{max} = 450 nm) irradiation for 1 hour. The yield was determined by quantitative ^{19}F NMR using α,α,α-trifluorotoluene as the internal standard. [b] 1.5 equiv of $(TMS)_3SiH$ was used. [c] 2.5 equiv of $(TMS)_3SiH$ was used. [d] 1.5 equiv of **3.21** [e] In the dark. [f] In the absence of photocatalyst, the reaction was yielding an inconsistent complex mixture of products; [g] Reaction performed under nitrogen atmosphere and in degassed solvent.

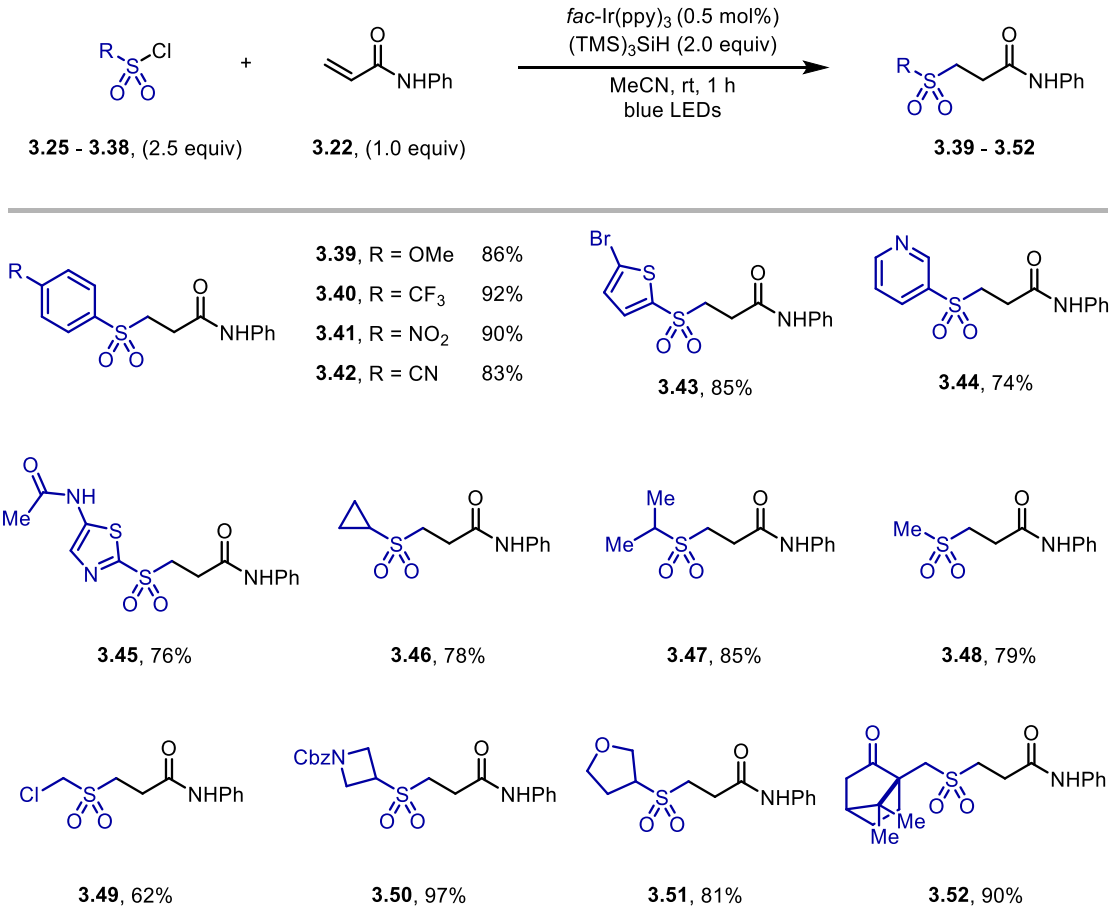
MeCN was therefore retained as solvent. Interestingly, several iridium-based photocatalysts were suitable for this transformation (**Table 3.2, entries 4 and 5**). The organophotocatalyst Eosin Y was also suitable but afforded the desired hydrosulfonylated **3.23** in slightly lower yield (**Table 3.2, entry 6**).

Varying the equivalents of silane or sulfonyl chloride in the reaction mixture did not improve the yield (**Table 3.2, entries 7-9**). Control experiments revealed that no conversion was observed in the absence of light (**Table 3.2, entry 10**). Furthermore, the reaction proceeded with significantly lower yield in the absence of photocatalyst (**Table 3.2, entry 11**). Performing the reaction under nitrogen atmosphere and in degassed solvent did not improve the yield of the transformation, demonstrating the practicality of this reaction (**Table 3.2, entry 12**).

3.5 Hydrosulfonylation of Electron-Deficient Alkenes

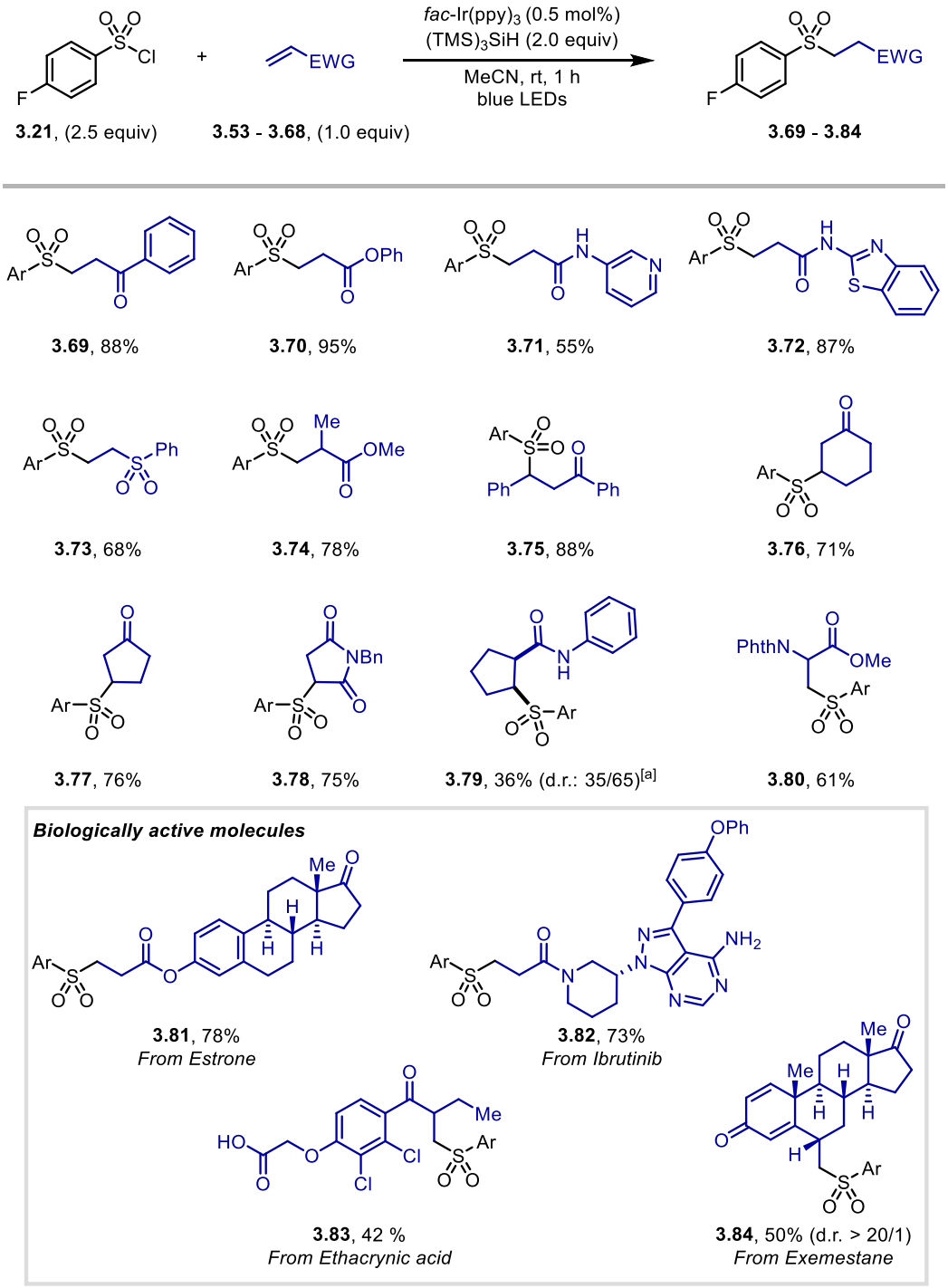
Having successfully developed reaction conditions for the hydrosulfonylation of alkene **3.22**, we explored the generality of the reaction on a wide range of sulfonyl chlorides, containing (hetero)aryl and alkyl substituents. Numerous functional groups were tolerated in this transformation, including trifluoromethyl, nitro, nitrile, halide,

ketone, ether, amide and carbamate groups (**Scheme 3.8**, **3.39**-**3.52**). Arylsulfonyl chlorides bearing electron-donating and electron-withdrawing groups afforded the desired products in moderate to excellent yields (**3.39**-**3.42**). Heteroarylsulfonyl chlorides yielded the hydrosulfonylated products in good yields, enabling the incorporation of thiophene, thiazole and pyridine motifs (**3.43**-**3.45**). Furthermore, alkyl sulfonyl chlorides were subjected to our reaction conditions and delivered the corresponding sulfones in good yields (**3.46**-**3.52**). Sulfones containing heterocycles, such as an azetidine and a tetrahydrofuran group, were introduced in excellent yields (**3.50**, **3.51**); and a camphor derivative was isolated in excellent yield (**3.52**).



Scheme 3.8: Substrate scope of sulfonyl chlorides. Reaction conditions: sulfonyl chloride **3.25**-**3.38** (1.25 mmol), alkene **3.22** (0.5 mmol), $(TMS)_3SiH$ (1.0 mmol), *fac*-$Ir(ppy)_3$ (0.5 mol%), MeCN (3.0 mL), under blue light (λ_{max} = 450 nm) irradiation for 1 hour, room temperature. Yields of isolated products.

Next, the scope of electron-deficient alkenes was investigated (**Scheme 3.9**). Linear terminal alkenes, containing an ester or a ketone moiety afforded the corresponding hydrosulfonylated products **3.69** and **3.70** in excellent yields. Acrylamides containing pyridyl or benzothiazyl functional groups were tolerated and yielded the desired hydrosulfonylated products in moderate to excellent yields (**3.71**, **3.72**). Other electron-withdrawing groups, such as sulfones afforded product **3.73** in 68%. 1,2-Disubstituted or geminal disubstituted alkenes such as chalcone or methyl methacrylate were suitable substrates for this protocol (**3.74**, **3.75**).



Scheme 3.9: Substrate scope of electron-deficient alkenes. Reaction conditions: sulfonyl chloride **3.21** (1.25 mmol), alkene **3.53-3.68** (0.5 mmol), $(TMS)_3SiH$ (1.0 mmol), *fac*-$Ir(ppy)_3$ (0.5 mol%), MeCN (3.0 mL), under blue light (λ_{max} = 450 nm) irradiation for 1 hour, room temperature. Yields of isolated products. [a] The isomers were separated by silica gel column chromatography. Ar = 4-Fluorobenzene.

Notably under our reaction conditions, cyclic alkenes such as cyclohexenone, cyclopentenone, *N*-benzylmaleimide, and a cyclopentene derivative were well tolerated and the desired products were obtained in moderate to good yields (**3.76-3.79**). Although

a cyclopentene derivative afforded the hydrosulfonylated product **3.79** in lower yield (starting material remaining) and low diastereoselectivity, both diastereoisomers could be separated by silica gel column chromatography, affording highly desirable 1,2-disubstituted cyclopentane building blocks. The relative stereochemistry of **3.79** was assigned by 2D-NOESY NMR: a strong NOE between H_α (δ = 3.16 ppm) and H_β (δ = 4.10 ppm) was observed for the *cis*-diastereoisomer. No interaction between H_α and H_β was observed for *trans*-**3.79** (**Figure 3.3**).

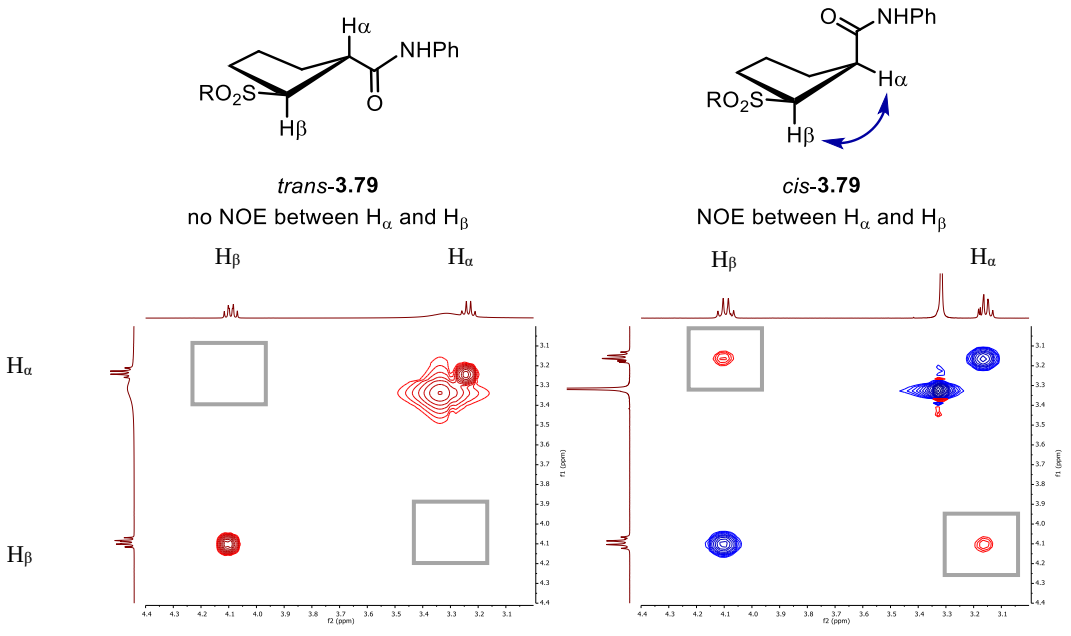


Figure 3.3: Assignment of stereochemistry for compound **3.79**.

The hydrosulfonylation of a dehydroalanine derivative was achieved in 61% yield, demonstrating the potential use of this methodology for the site-selective incorporation of sulfone moieties into peptides (**3.80**).[103–105] In order to demonstrate the robustness of this protocol, the late-stage functionalisation of a range of biologically active molecules was investigated. The hydrosulfonylation of an estrone derivative, ibrutinib and ethacrynic acid was successful (**3.81**-**3.83**). Furthermore, exemestane, a drug employed for the treatment of breast cancer,[106] underwent hydrosulfonylation in moderate yield

(starting material remaining), affording the product with complete diastereoselectivity and regioselectivity for the exo-1,6-system (**3.84**).

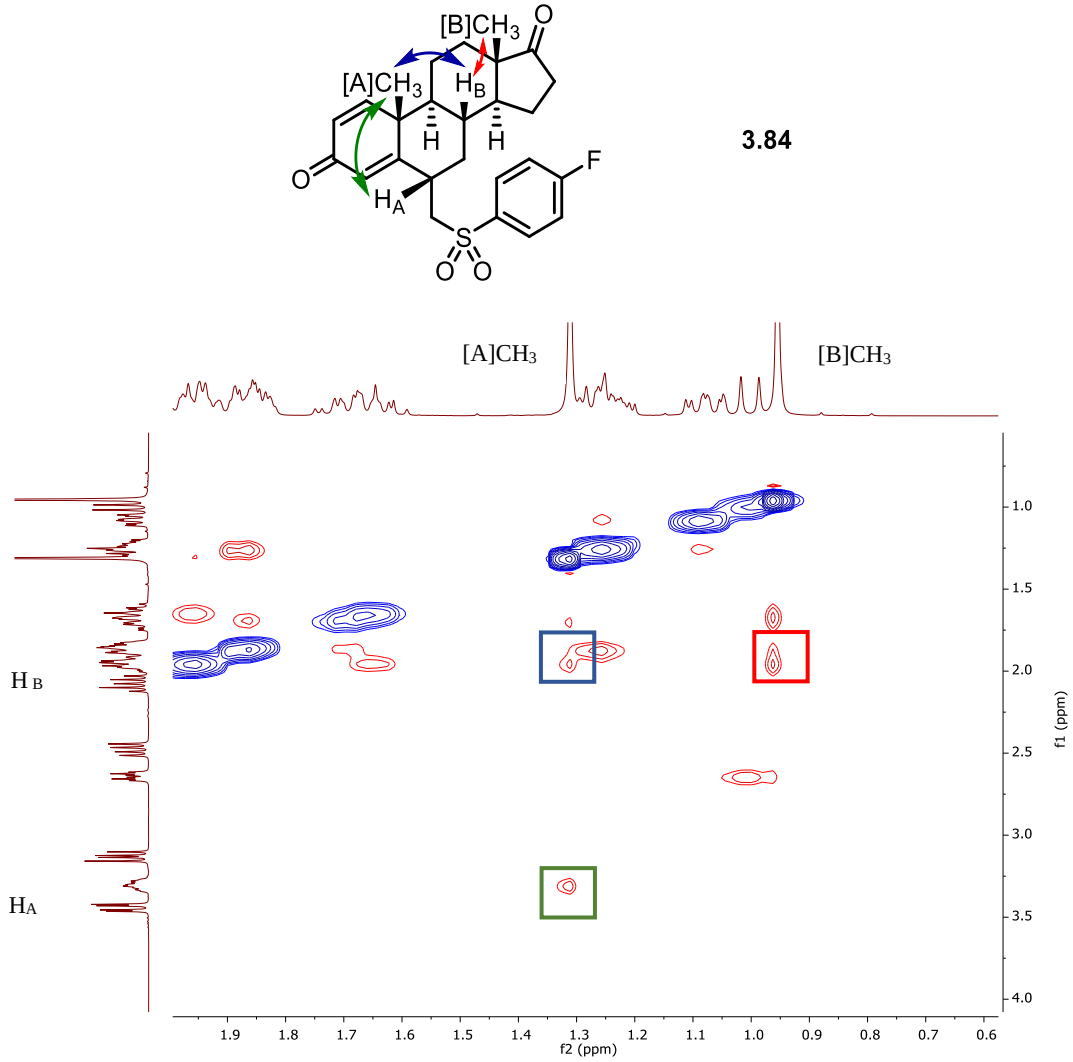


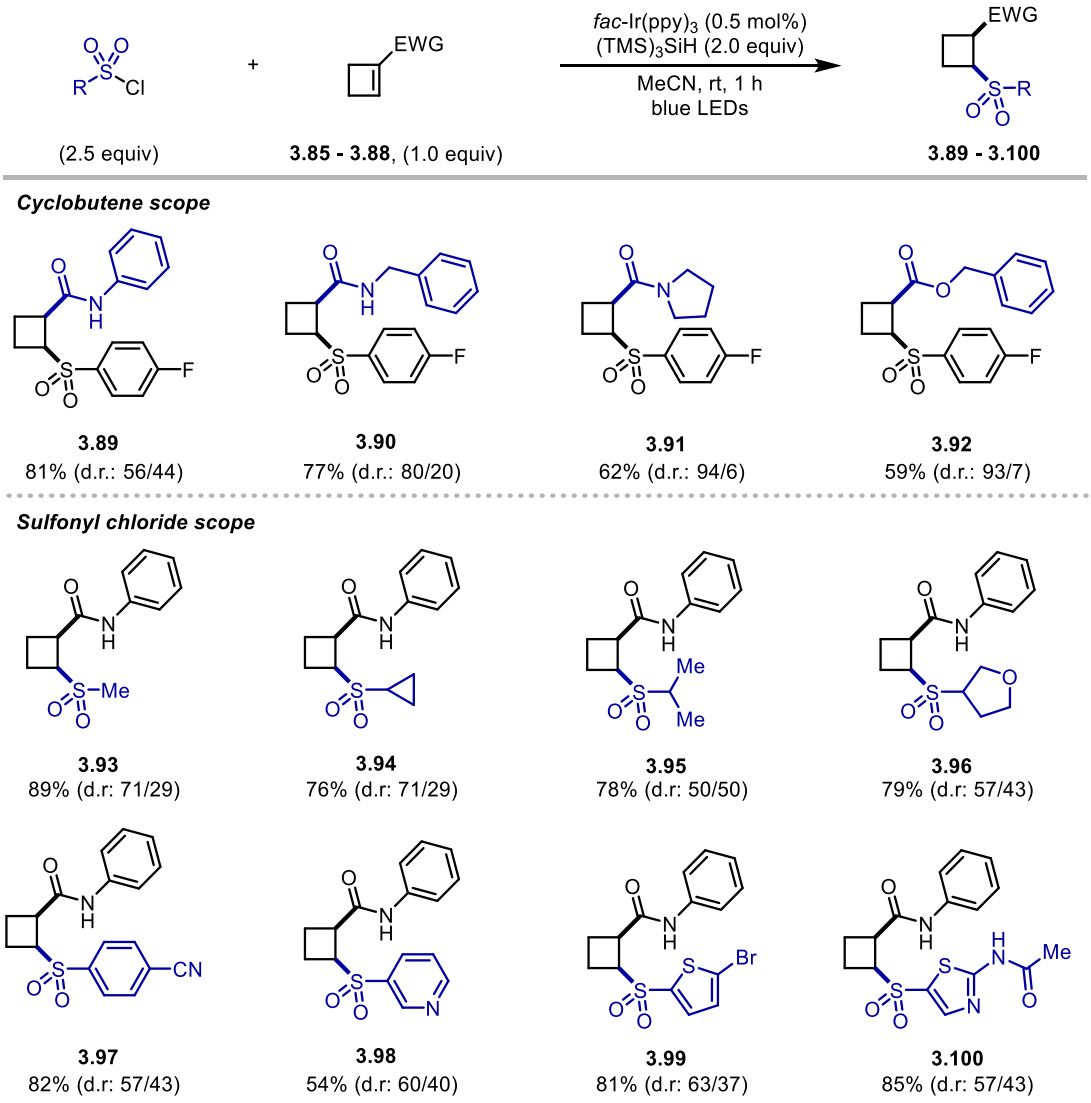
Figure 3.4: Assignment of the stereochemistry for compound **3.84**.

The diastereoselectivity of product **3.84** was determined by 2D-NOESY NMR, where a strong NOE between [A]CH_3 (δ = 1.31 ppm) and H_A (δ = 3.31 ppm) was observed. This was further confirmed by the observation of other strong NOEs between [A]CH_3 (δ = 1.31 ppm) and H_B (δ = 1.98 ppm) as well as between H_B (δ = 1.98 ppm) and [B]CH_3 (δ = 0.96 ppm) (**Figure 3.4**).

3.6 Hydrosulfonylation of Cyclobutenes

3.6.1 Scope of Cyclobutenes

As part of our ongoing collaboration with industry, we were interested in a series of 2´-sulfonyl- and sulfonamide-cyclobutyl carboxamides for HTS exploration. Thus, the reactivity of cyclobutene derivatives was explored towards the novel hydrosulfonylation protocol (**Scheme 3.10**).



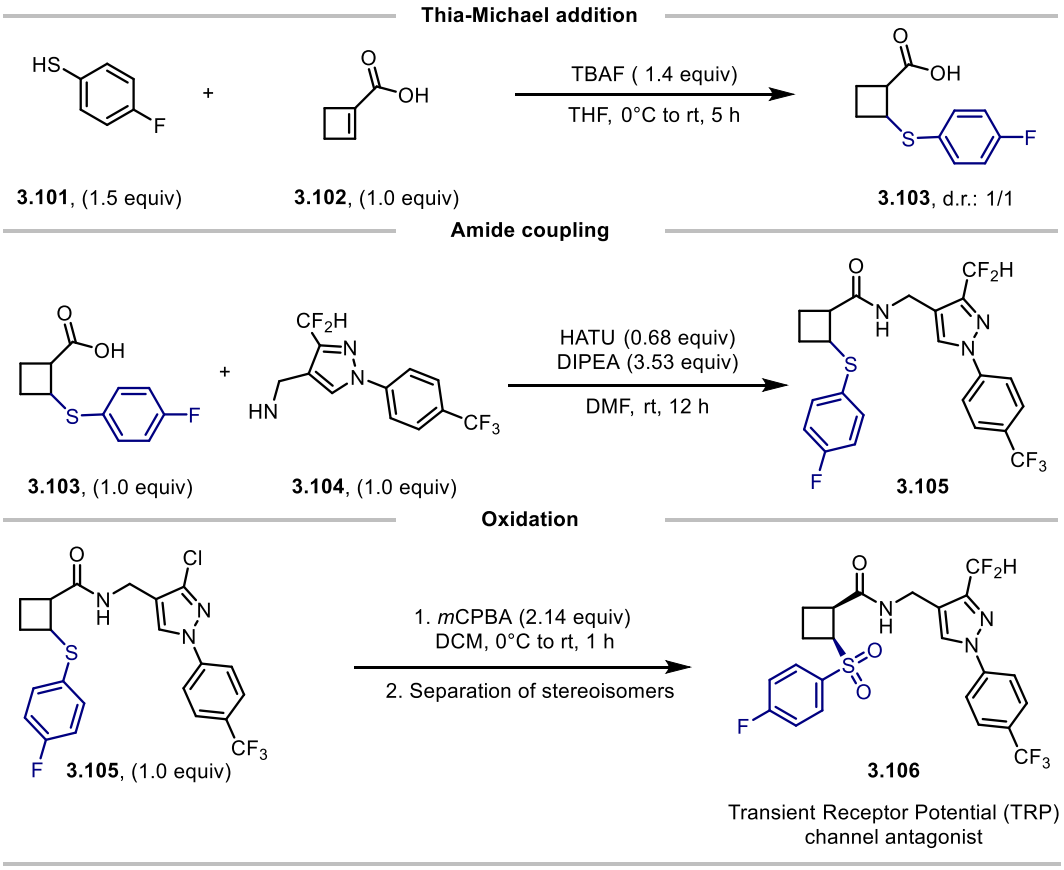
Scheme 3.10: Substrate scope of 1,2-disubstituted cyclobutanes. Reaction conditions: sulfonyl chloride (1.25 mmol), cyclobutene **3.85**-**3.88** (0.5 mmol), $(TMS)_3SiH$ (1.0 mmol), *fac*-$Ir(ppy)_3$ (0.5 mol%), MeCN (3.0 mL), under blue light (λ_{max} = 450 nm) irradiation for 1 hour, room temperature. Yields of isolated products. The isomers were separated by silica gel column chromatography.

Under the standard reaction conditions, phenyl, benzyl, and pyrrolidinyl cyclobutene carboxamides yielded the 1,2-disubstituted cyclobutanes in good yields (**3.89**-**3.91**). A benzyl ester was also well tolerated in this transformation (**3.92**). Apart from phenyl carboxamide, all substrates afforded predominantly the *cis*-diastereoisomer in moderate yield (starting material remaining). As discussed in **Chapter 2** (**Section 2.8**), the *cis*-diastereoselectivity can be explained by the steric hindrance in the HAT step. Nonetheless, the bulkiness of the electron-deficient group or internal hydrogen-bond interactions may also influence the selectivity outcome. Given that both diastereoisomers can easily be separated by silica gel column chromatography, *N*-phenyl cyclobutene carboxamide was selected as an ideal model substrate to determine sulfonyl chloride tolerance. The ease of separation and purification of both diastereoisomers allowed for the synthesis of a compound library for our collaborators at Janssen. A variety of sulfonyl chlorides readily engaged in the hydrosulfonylation of *N*-phenyl cyclobutene carboxamide. The introduction of simple alkyl sulfonyl groups was successful and gave the desired products in good to excellent yields (**3.93**, **3.94**). Furthermore, azetidine- and tetrahydrofuran-containing cyclobutanes could be isolated in good yields (**3.95**, **3.96**). Finally, (hetero)aryl sulfonyl chlorides were successful and enabled the preparation of a collection of 1,2-disusbtituted cyclobutane compounds with structural diversity and complexity (**3.97**-**3.100**).

3.6.2 Scale-up Experiments

In 2019, Genentech reported the synthesis of sulfone-containing cyclobutyl carboxamide compounds for the treatment of diseases and conditions mediated by TRPA1 (Transient Receptor Potential channel antagonist 1), such as pain.[17] The introduction of the sulfone

fragment into the four-membered ring relied on a multi-step procedure (**Scheme 3.11**). First, the Michael addition of 4-fluorobenzenethiol (**3.101**) to cyclobutene carboxylic acid **3.102** yielded the 2-thio-adduct **3.103** as a mixture of diastereomers (d.r.:1/1). They next performed an amide coupling, using HATU as coupling agent to give **3.105**. Finally, oxidation of the thioether with *m*CPBA afforded the corresponding sulfone. HPLC separation of stereoisomers gave the TRP channel antagonist **3.106**.



Scheme 3.11: Synthesis of sulfonylcycloalkyl carboxamide compounds - Genentech (2019).

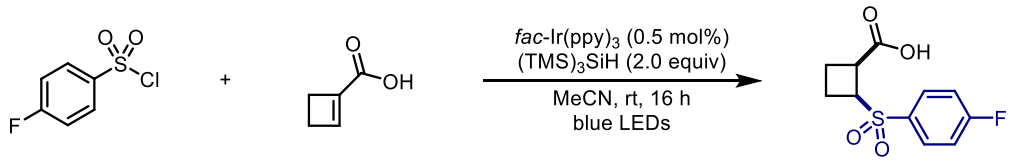
Although successful, this synthetic route has significant drawbacks, namely the need for a multi-step sequence, the use of harsh reaction conditions, the lack of selectivity as well as poor overall atom economy. Therefore, we considered applying our one-step hydrosulfonylation protocol to the synthesis of a potential precursor of these TRP channel antagonist compound. If successful, this would provide a new route for the rapid access of **3.106**. It has been well recognised that scalability is a limiting factor in photochemical

processes. As dictated by the Beer-Lambert law, light penetration decreases exponentially as the distance from the light source increases.[107] Given that a bigger reaction vessel is often required for scale-up experiments, the distance between the centre of the reaction mixture and the light source increases drastically, leading to intermittent light distribution. Flow chemistry has been identified as a powerful alternative in which this challenge can easily be overcome. Based on these considerations, the multigram hydrosulfonylation of cyclobutene carboxylic acid **3.102** was investigated in two set-ups: batch and continuous flow.

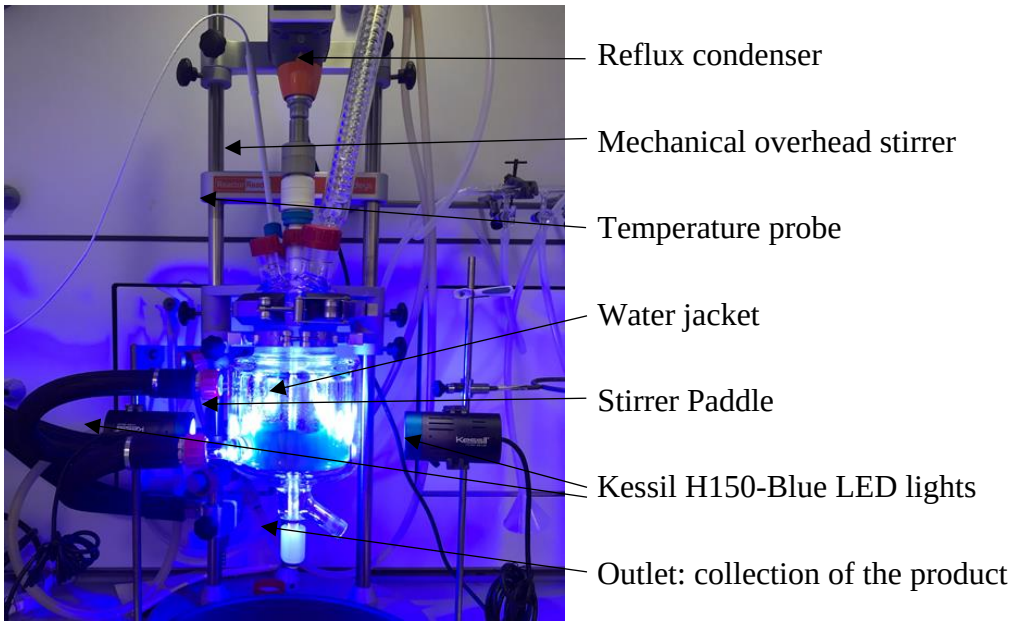
3.6.2.1 Scale-up Experiment in Batch

Scaling-up a chemical process can be accompanied with several challenges. Exothermic runaways, pressure, side-product formation, solubility or stirring issues are amongst the most prominent ones. In order to prevent such risks, the scale-up experiment was performed in batch using a 1 Litre Radleys Reactor Ready (**Scheme 3.12**). This reactor is equipped with a reflux condenser, a water jacket and a mechanic stirring paddle. The control unit allows the real-time monitoring of the reaction temperature and pressure. These functionalities allowed us to perform the experiment in a safer manner, where thermal runaways (temperature and pressure) can easily be controlled. The reaction mixture was irradiated with two Kessil H150-Blue LED lights (34 W, 5 cm distance, **Scheme 3.12**) for 16 hours. Hydrosulfonylation of **3.102** was successfully accomplished on a 5 g scale affording the desired hydrosulfonylated product **3.107** in good yield (10.7 g, 81%) and high *cis*-diastereoselectivity (89/11). Although the use of such reactors has shown to be practical to perform scale-ups, it is important to mention that some

limitations can be observed due to intermittent light intensity within the reactor. This leads to slower reactions (16 h vs 1 h), and therefore a lower productivity (0.67g/h).



3.21, (2.5 equiv) **3.102**, (1.0 equiv) **3.107**
81% (d.r.: 89/11)
10.7 g isolated product

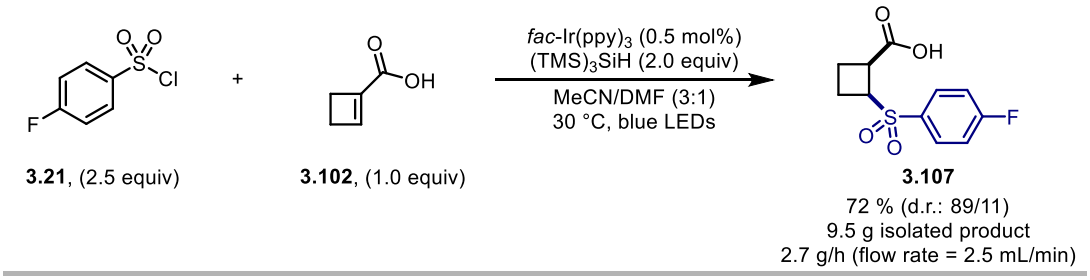


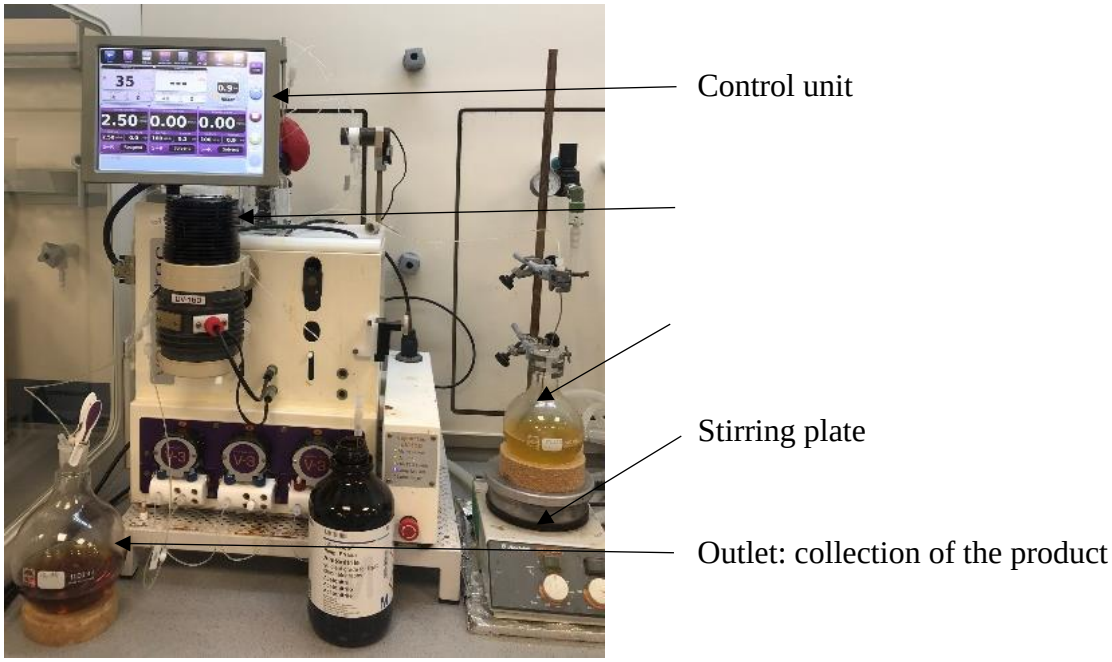
Scheme 3.12: Scale-up experiment in batch performed in a 1 Liter Radleys Reactor Ready.

3.6.2.2 Scale-up Experiment in Continuous Flow

Given the importance of continuous flow processes for the large-scale production of building blocks, we were also interested in the benefits of performing this photochemical protocol in continuous processing (**Scheme 3.13**).[107–110] Continuous-flow photochemistry is a powerful platform to perform reactions quicker and with better reproducibility. In contrast to batch reactors, the irradiation distribution can be kept

uniform in a continuous-flow system. The microtubings allow for a more homogenous and efficient photon flux, leading to increased surface area-to-volume ratios.





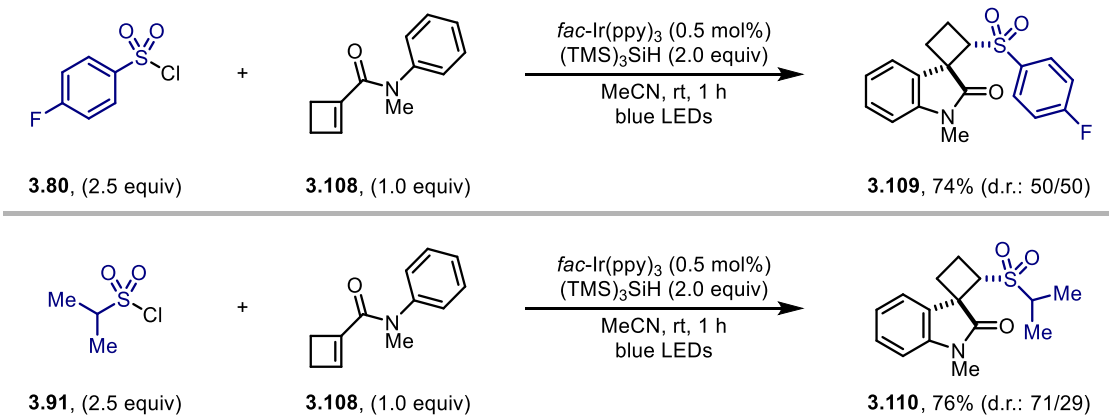
Scheme 3.13: Scale-up experiment performed in continuous flow.

This is of particular interest to the pharmaceutical industry in order to achieve reliable scale-ups. A requirement for flow chemistry is the solubility of all reaction components in the reaction solvent. Given the partial insolubility of *fac*-Ir(ppy)$_3$ and (TMS)$_3$SiH in MeCN, the addition of a co-solvent was required; a solvent mixture of MeCN/DMF (3:1) was suitable. The mixture was pumped through a Vapourtec photoreactor (fluoropolymer tube, 1.3 mm internal diameter, 10 mL) and the flow rate was set at 2.5 mL/min (4 min residence time, 10 mL reactor volume). The reactor was irradiated with 54W blue LEDs (410 nm, total power 24 W) at 30 °C (internal temperature of the photoreactor: 35 °C).

Starting from 5 g of cyclobutene **3.102**, the desired hydrosulfonylated product **3.107** was isolated in good yield (9.5 g, 72%) and in identical level of diastereocontrol (compared to batch set-up) within a shorter reaction time (3.5 h). Collectively, these results suggest that this methodology could be applicable to large-scale production in batch, or under continuous flow conditions with an increased productivity (2.7 g/h in continuous flow vs 0.67g/h in batch).

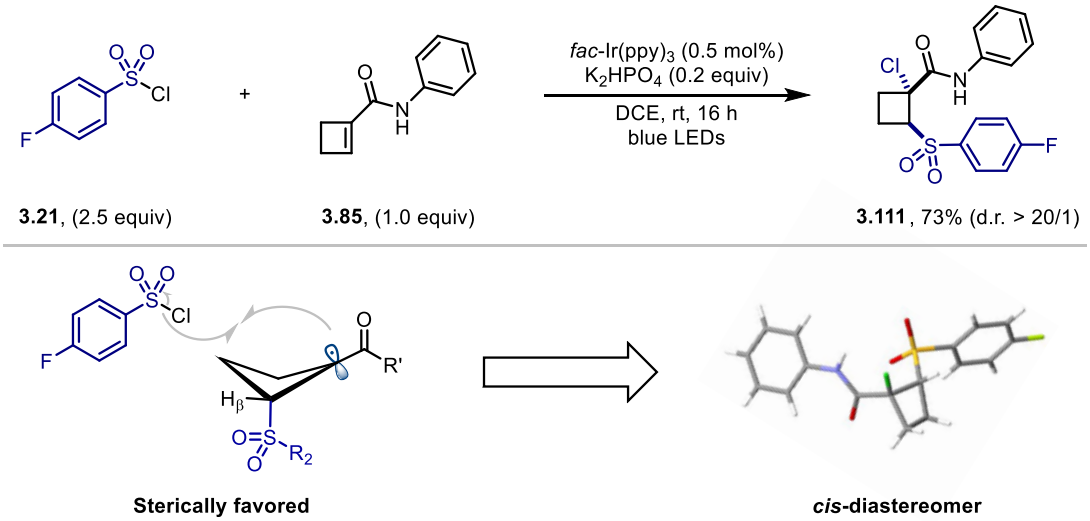
3.6.3 Quaternisation of the Carbon-Centred Radical Intermediate

Next, the concomitant quaternisation of the α-carbonyl radical intermediate was investigated. Similarly to the synthesis of sulfonamides (**Chapter 2**, **Section 2.8**), the sulfonyl radical addition to the tertiary cyclobutene carboxamide **3.108** led to a cascade spirocyclisation to afford sulfone-containing cyclobutyl spirooxindoles (**Scheme 3.14**). Aryl and alkylsulfonyl chlorides were suitable for this transformation, affording the desired products **3.109** and **3.110** in good yields and moderate diastereomeric ratio. Both diastereoisomers could be easily separated and isolated by silica gel column chromatography. The mechanism of this transformation has already been discussed in **Chapter 2** (**Section 2.8**).



Scheme 3.14: Cascade spirocyclisation leading to sulfonyl-containing cyclobutyl spirooxindoles.

Additionally, ATRA leading to net chlorosulfonylation has been investigated on cyclobutene **3.85** (**Scheme 3.15**).[68]



Scheme 3.15: Chlorosulfonylation of cyclobutene **3.85**.

In absence of $(TMS)_3SiH$ and by using 1,2-dichloroethane as solvent, the ATRA product (**3.111**) was obtained in high yield and excellent diastereoselectivity (d.r. > 20/1). The stereochemistry was assigned by single-crystal X-ray diffraction analysis, as NOESY NMR was not conclusive. Similarly to the hydrosulfonylation of cyclobutenes, the chlorine atom transfer occurs on the less sterically hindered face, affording selectively the *cis*-diastereoisomer. The introduction of a chlorine atom adds structural complexity to the four-membered ring and can be used as a handle for further functionalisation (e.g. cross-coupling reactions, substitution, etc.).[111,112]

3.7 Hydrosulfonylation of Alkynes

The direct functionalisation of alkynes offers unique opportunities for the construction of versatile building blocks.[113] More specifically, the functionalisation of alkynes to generate vinyl sulfones is highly desirable, due to the prevalence of these motifs in biologically active molecules.[84,114,115] In these transformations, upon additon

of a free radical to the alkyne, a vinyl radical intermediate is generated. Vinyls radicals can have different structures: bent or linear, depending on the substitution pattern of the alkyne (**Figure 3.5**).[116]

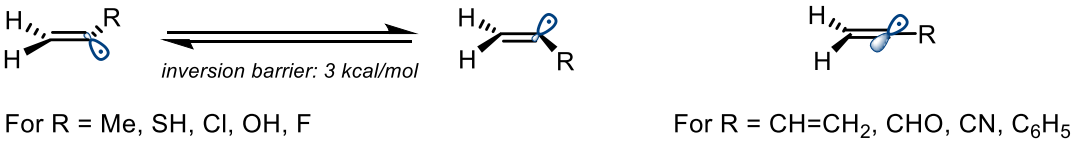
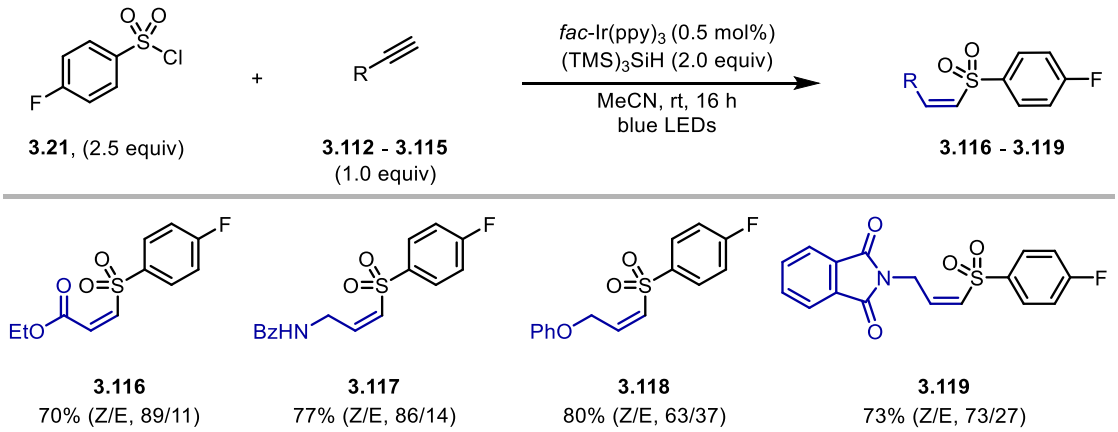


Figure 3.5: Structure of vinyl radicals.

DFT calculations revealed that vinyl radicals bearing methyl, thiol, chlorine, hydroxyl or fluorine groups were predominantly bent. [117] The inversion barrier between the two sp^2 bent structures was estimated to be as low as 3 kcal/mol. The two isomeric bent forms can rapidly interconvert *via* the linear π-radical intermediate. This inversion barrier increases significantly as the electronegativity of the substituent increases. In contrast, vinyl radicals bearing $CH=CH_2$, CHO, CN, or C_6H_5 groups are linear. This is due to the stabilised delocalisation of the radical by the adjacent π-system of the α-substituent. As such, the SOMO can be stabilised by the coplanar π-system of the susbtituent.

The potential of this methodology was further explored for the hydrosulfonylation of a set of different alkynes (**Scheme 3.16**).



Scheme 3.16: Hydrosulfonylation of alkynes. Reaction conditions: sulfonyl chloride **3.21** (1.25 mmol), alkyne **3.112-3.115** (0.5 mmol), $(TMS)_3SiH$ (1.0 mmol), *fac*-$Ir(ppy)_3$ (0.5 mol%), MeCN (3.0 mL under

blue light (λ_{max} = 450 nm) irradiation for 16 hour, room temperature. Yields of isolated products. The isomers were separated by silica flash column chromatography.

The electron-deficient alkyne **3.112** was suitable for this transformation and afforded the desired product **3.116** in 70% yield and high *Z*-selectivity. This result is in accordance with previous results, where HAT to the vinyl radical preferably occurs *anti* to the sulfone substituent, generating the *Z*-alkene (**3.116**).[118]

Alkynes substituted with alkyl groups were also reactive and led to the corresponding hydrosulfonylated alkenes in good yields, and moderate to high *Z*-selectivity (**Scheme 3.16**, **3.117**-**3.119**). Both isomers could be isolated by silica gel column chromatography. Therefore, this methodology offers a mild and efficient way to access vinyl sulfones.

The stereoselectivity of the HAT-step is likely dependent on the bulkiness of the HAD $(TMS)_3SiH$. We speculated that the HAT occurs on the less sterically hindered face, affording favourably the *Z*-isomer (**Figure 3.6**).

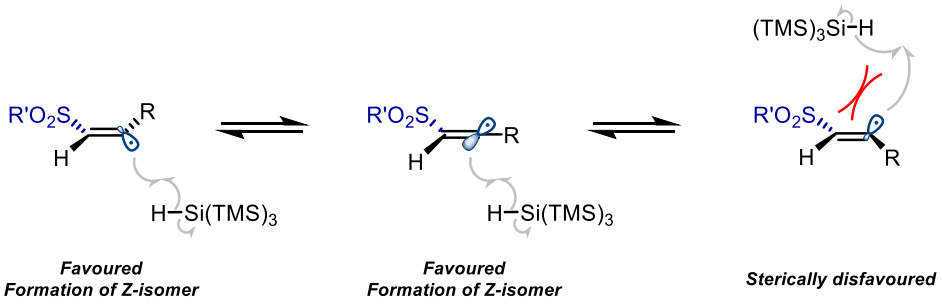


Figure 3.6: Stereoselectivity of the HAT to the vinyl radical.

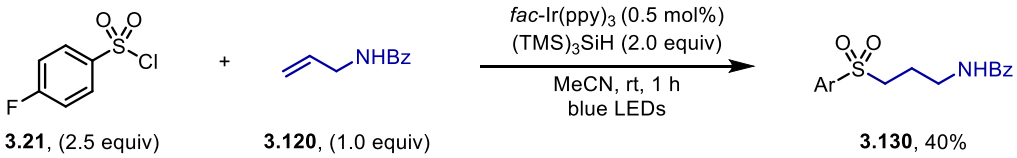
The stereoselectivity of the vinyl sulfones was assigned by ^{1}H NMR analysis of the coupling constants of both alkynyl hydrogens (**Figure 3.7**). The coupling between both alkynyl hydrogens of the *E*-isomer is greater ($^3J_{H\text{-}H}$ = 11 - 18 Hz), than for the corresponding *Z*-isomer ($^3J_{H\text{-}H}$ = 6 - 14 Hz).



Figure 3.7: Assignment of stereochemistry for compounds **3.116** - **3.119**.

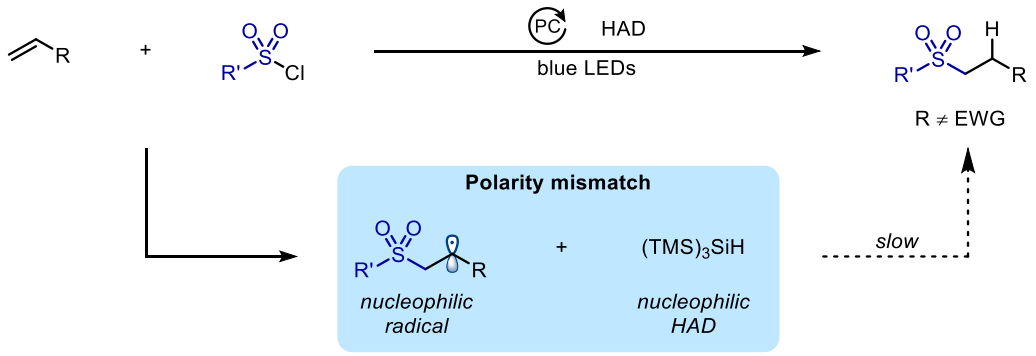
3.8 Hydrosulfonylation of Unactivated Alkenes

Due to the availability of unactivated alkenes as feedstock precursors for organic synthesis, we were interested in expanding the scope of this hydrosulfonylation protocol to these substrates.[119] Unactivated alkenes are bench stable, inexpensive, often commercially available and represent attractive handles for late-stage functionalisation. Initial investigation on *N*-allylbenzamide, revealed that unactivated alkenes are less reactive under our standard reaction conditions. The desired hydrosulfonylated product was only obtained in 40% yield after 16 h reaction time with starting material remaining (**Scheme 3.17**).



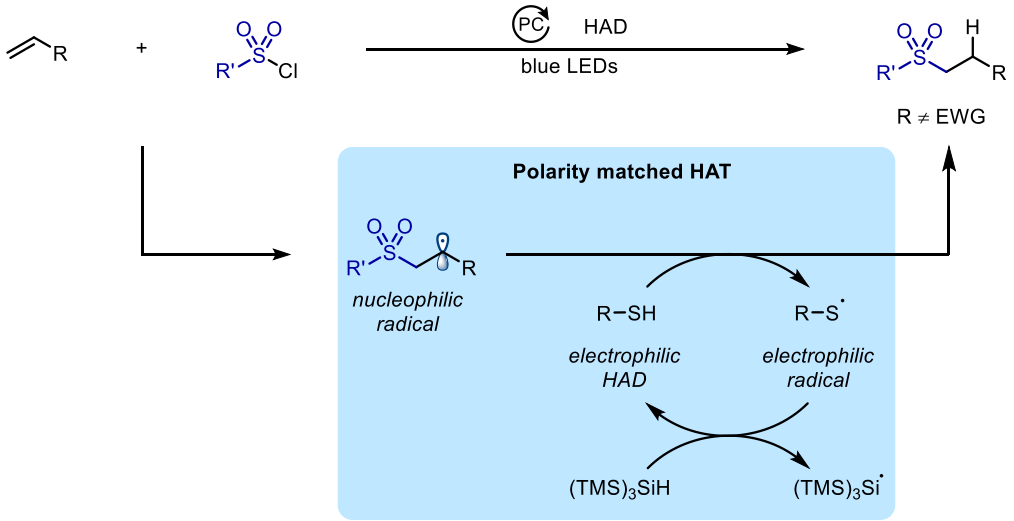
Scheme 3.17: Hydrosulfonylation of *N*-allylbenzamide **3.120**.

This low reactivity is likely due to a poor polarity match between the nucleophilic carbon-centred radical intermediate and the nucleophilic HAD $(TMS)_3SiH$ (**Scheme 3.18**).



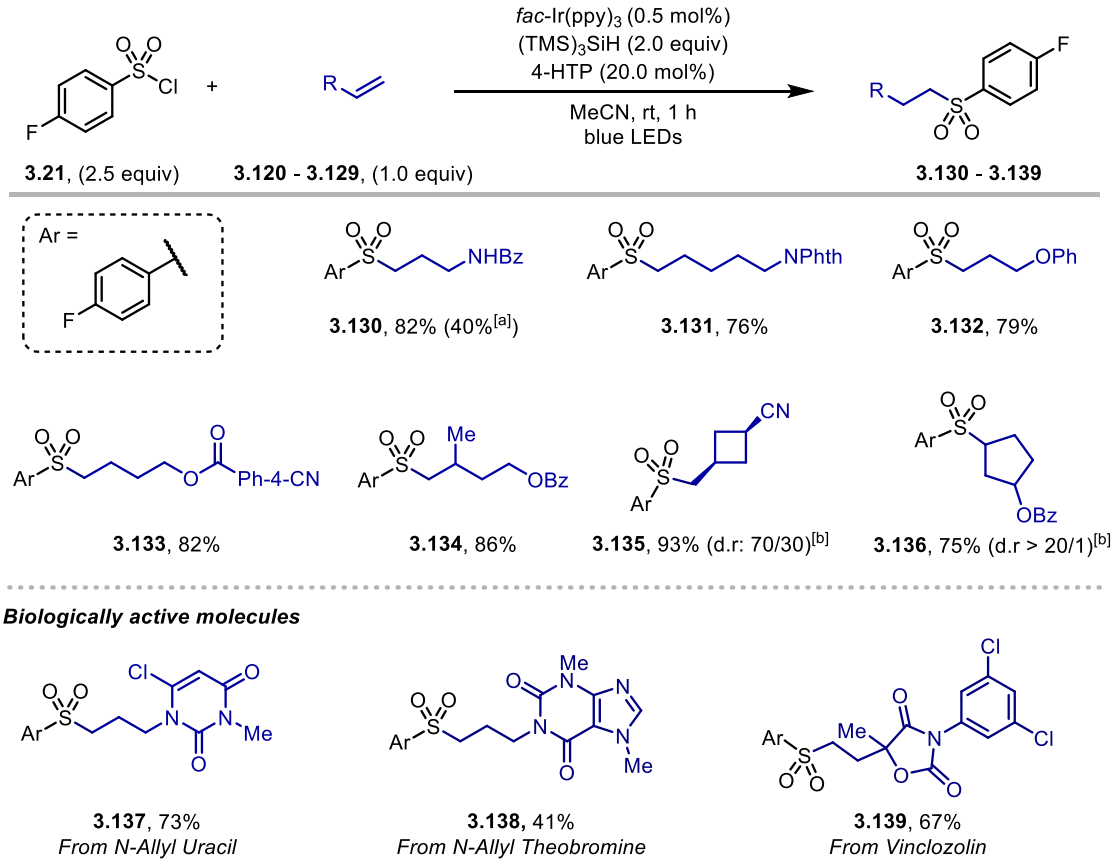
Scheme 3.18: Polarity mismatch for the hydrosulfonylation of unactivated alkenes.

On this basis, we questioned whether polarity-reversal catalysis (PRC)[120,121] could be implemented for alkenes bearing alkyl substituents (**Scheme 3.19**). PRC is a concept that replaces a single-step HAT (which is inefficient due to polarity mismatch) by a two-step process (two polarity matched HAT) using an HAT catalyst. Previous reports demonstrated that challenges associated to the slow HAT have been solved by fine-tuning the polarity of the HAD. As such, the addition of a polarity reversal catalyst can significantly accelerate HAT and extend the scope of a given transformation. Based on this, we hypothesised that the addition of a polarity reversal catalyst, such as a thiol, would enlarge the spectrum of reactivity for the novel hydrosulfonylation protocol.



Scheme 3.19: Polarity reversal catalysis applied to the hydrosulfonylation of unactivated alkenes.

The addition of a catalytic amount of 4-hydroxythiophenol (4-HTP, 20 mol%) as a polarity reversal catalyst (electrophilic HAD) enabled the formation of the desired sulfone **3.130** in high yield (82%, **Scheme 3.20**). Under these modified conditions, the hydrosulfonylation of a variety of unactivated alkenes was investigated. Terminal, *gem*-disubstituted, internal alkenes, as well as biologically active molecules were tolerated and afforded the desired hydrosulfonylated products in good to excellent yields (**3.130**-**3.139**). More specifically, terminal alkenes containing amide, phthalimide, ether and ester functional groups were suitable for this transformation (**3.130 - 3.133**). Representative examples of both a geminal disubstituted and cyclic geminal disubstituted alkenes afforded the corresponding hydrosulfonylated products in high yields (**3.134**, **3.135**). A 1,2-disubstituted alkene such as a cyclopentene derivative was reactive towards our protocol, affording the hydrosulfonylated product in good yield and excellent diastereomeric ratio (d.r. >20/1, **3.136**). However, the exact stereochemistry of the major product could not be assessed using 2D-NMR analysis. This modified protocol was also validated on alkene-containing biologically relevant molecules. The reaction was successful on an uracil derivative leading to the corresponding hydrosulfonylated product in 73% yield (**3.137**). *N*-Allyl theobromine yielded the corresponding product in moderate yield and excellent chemoselectivity without C−H sulfonylated side product arising from Minisci-type chemistry (**3.138**).[95] Vinclozolin was also suitable and afforded the desired product in 67% yield (**3.139**).

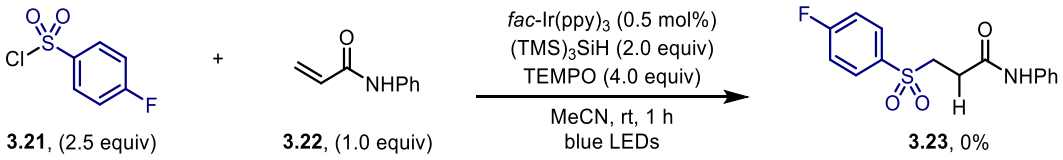


Scheme 3.20: Substrate scope of unactivated alkenes. Reaction conditions: sulfonyl chloride **3.21** (1.25 mmol), alkene **3.120**-**3.129** (0.5 mmol), $(TMS)_3SiH$ (1.0 mmol), 4-hydroxythiophenol (0.1 mmol), *fac*-$Ir(ppy)_3$ (0.5 mol%), MeCN (3.0 mL), blue LED irradiation (λ_{max} = 450 nm), room temperature, 16 h. Yields of isolated products. 4-HTP = 4-Hydroxythiophenol. [a] Without thiol catalyst. [b] The minor isomer was not isolated.

3.9 Mechanistic Considerations

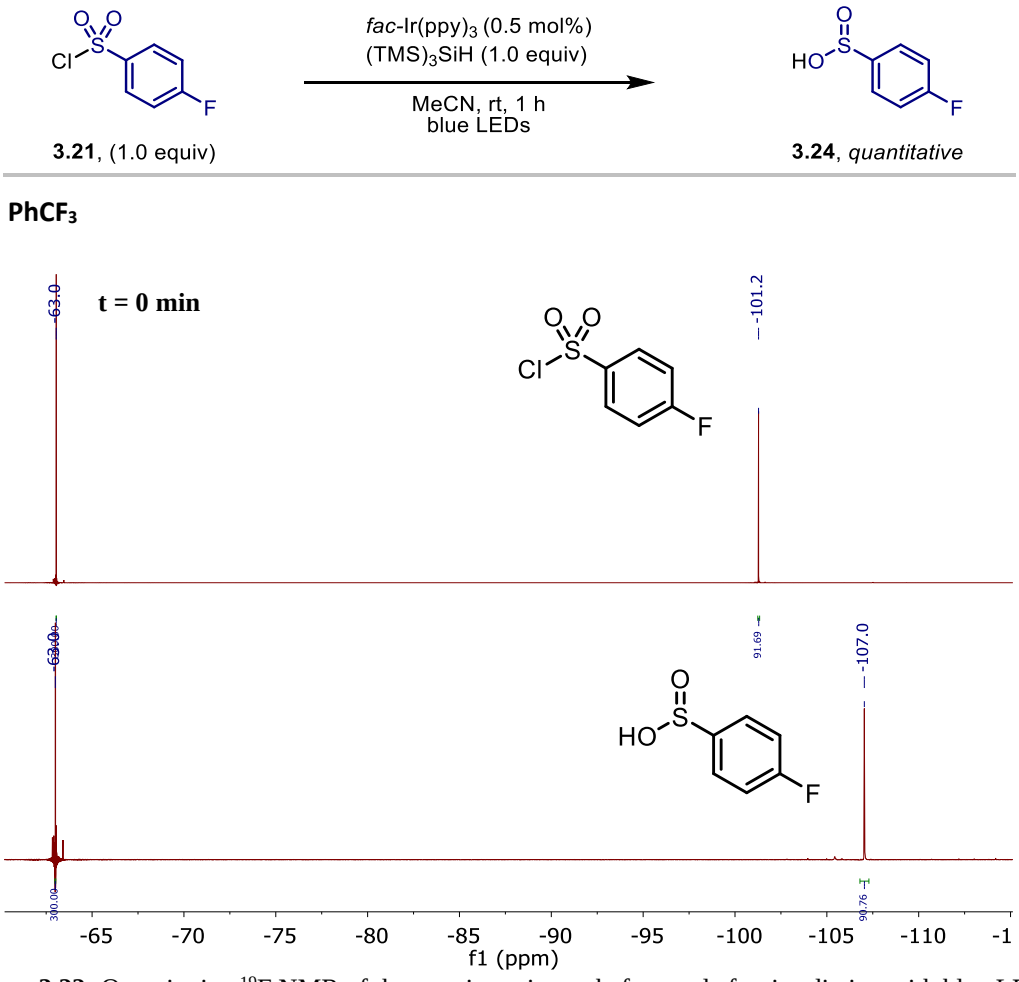
3.9.1 Control Experiments

In order to gain more insight into the mechanism of this transformation, a range of experiments was performed. First, we sought to investigate whether this transformation relied on a radical mechanism. As such, 4.0 equivalents of the radical scavenger TEMPO was added to the reaction. After 1 h, no desired hydrosulfonylated product **3.23** was formed, and the starting material was fully recovered (**Scheme 3.21**). This result advocates in favour of a radical pathway for the hydrosulfonylation of alkenes.



Scheme 3.21: Addition of TEMPO as a radical scavenger.

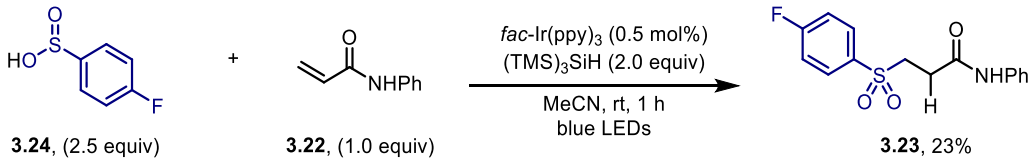
As described in **Table 3.1**, sulfinic acid **3.24** was identified as a byproduct in this transformation. In the absence of alkene, sulfonyl chloride **3.21** was quantitatively reduced to the corresponding sulfinic acid **3.24** in presence of $(TMS)_3SiH$ in MeCN (**Scheme 3.22**).



Scheme 3.22: Quantitative ^{19}F NMR of the reaction mixture before and after irradiation with blue LEDs.

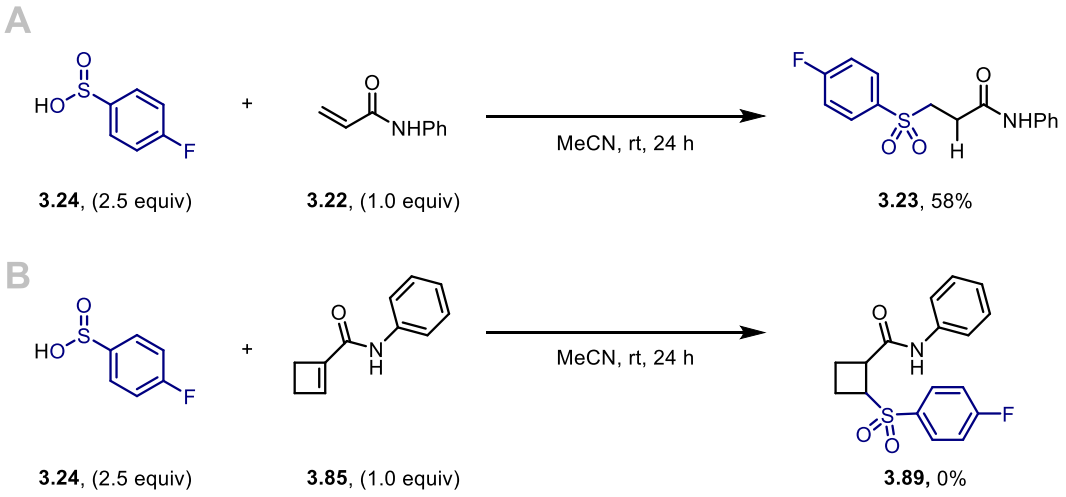
Quantitative ^{19}F NMR using α,α,α-trifluorotoluene as the internal standard revealed that after 1 hour irradiation, the fluorine peak fully shifted from δ −101.2 ppm (sulfonyl chloride **3.21**) to δ − 107.0 ppm (sulfinic acid **3.24**).

A control experiment using **3.24** revealed that sulfinic acids can be used as sulfonyl radical precursors under the same reaction conditions, affording the desired hydrosulfonylated product **3.23**, albeit in significantly lower yield (**Scheme 3.23**).



Scheme 3.23: Use of sulfinic acid as a sulfonyl radical precursor.

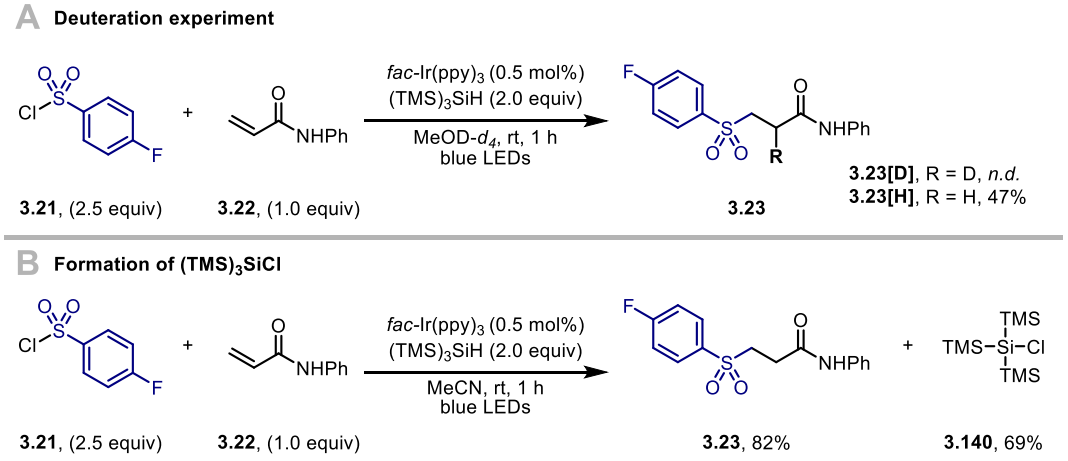
The Michael-addition of sulfinic acids has been described in the literature.[122] Treating alkene **3.22** with sulfinic acid **3.24** at room temperature in MeCN for 24 h, yielded the desired hydrosulfonylated product in 58% (**Scheme 3.24A**).



Scheme 3.24: Michael-addition of sulfinic acids to electron-deficient alkenes.

Although some conversion for the linear substrate **3.22** was observed, no hydrosulfonylated product has been identified using alternative substrates such as yclobutene **3.85** (**Scheme 3.24B**). This result demonstrates that the 1,4-addition of sulfinic acids is dependent on the nature of the alkene, and therefore cannot be used as a reliable route for the preparation of these compounds.

Next, deuteration experiments were performed to illustrate whether solvents or additives could participate in a HAT process with the carbon-centred radical intermediate. When the reaction was performed in MeOD-d_4, no deuterium incorporation was observed (**Scheme 3.25A**).



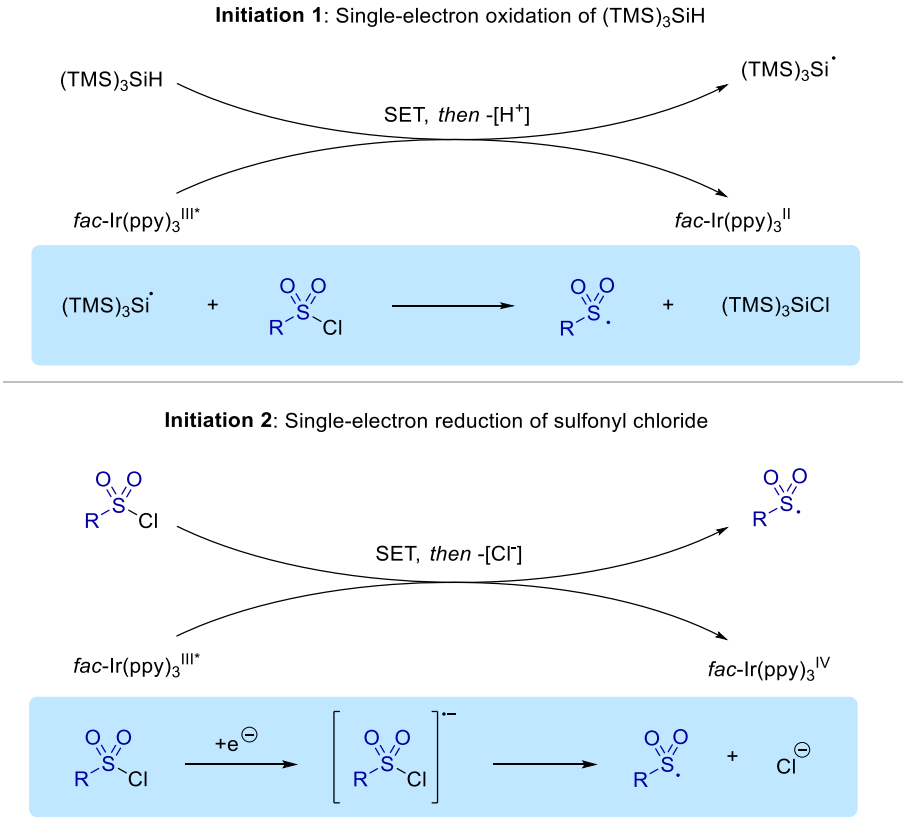
Scheme 3.25: A. Deuteration experiment; B. Formation of $(TMS)_3SiCl$. n.d. = not detected.

The selective formation of [H]**3.23** over [D]**3.23** suggests that no enol-type intermediate is formed, but that a direct HAT between $(TMS)_3SiH$ and the carbon-centred radical intermediate is more likely with no direct involvement of the solvent in the reaction mechanism.

Collectively, these data demonstrate that the formation of an enol-type intermediate, resulting from the Michael-addition of a sulfinic acid can be ruled out under our reaction conditions. Furthermore, the formation of the sulfone-containing cyclobutyl spirooxindoles (**Scheme 3.14**), as well as the formation of the chlorosulfonylated product (**Scheme 3.15**) is consistent with a radical-based mechanism and advocates against an ionic pathway. Finally, the byproduct $(TMS)_3SiCl$ (**3.140**, **Scheme 3.25B**) was isolated. This observation is consistent with a radical chain propagation mechanism or with the oxidation of the silyl radical upon SET.

3.9.2 Stern-Volmer Luminescence Quenching

By comparing this methodology with our previously disclosed hydrosulfamoylation of alkenes[71] (**Chapter 2**), one could envision the single-electron oxidation of $(TMS)_3SiH$ to form the corresponding silyl radical, able to abstract the chlorine atom of the sulfonyl chloride (**Scheme 3.26**). To elucidate the nature of the initiation process, Stern-Volmer luminescence quenching experiments were performed.



Scheme 3.26: Two viable pathways for the generation of sulfonyl radicals.

The Stern Volmer experiment was performed in a spectrofluorometer. In this experiment, the fluorescence of a sample, containing both the photocatalyst and a reaction component is analysed upon irradiation at a specific wavelength. The emitted light reaches a detector, placed at 90 degrees to the incident light (to prevent interference with the transmitted excitation light), whereby the fluorescence intensity is measured. Upon irradiation of the sample, the triplet excited state of the photocatalyst is generated, leading to the luminescence of the sample (emission of light). At this stage, two pathways can be

envisioned: 1) the reaction component does not react with the excited state of the photocatalyst and the fluorescence does not vary; 2) if the reaction component quenches the excited state of the photocatalyst, the intensity of the emitted light is reduced depending on the concentration of the quencher. A simplified setup for this experiment in shown in **Figure 3.8**.

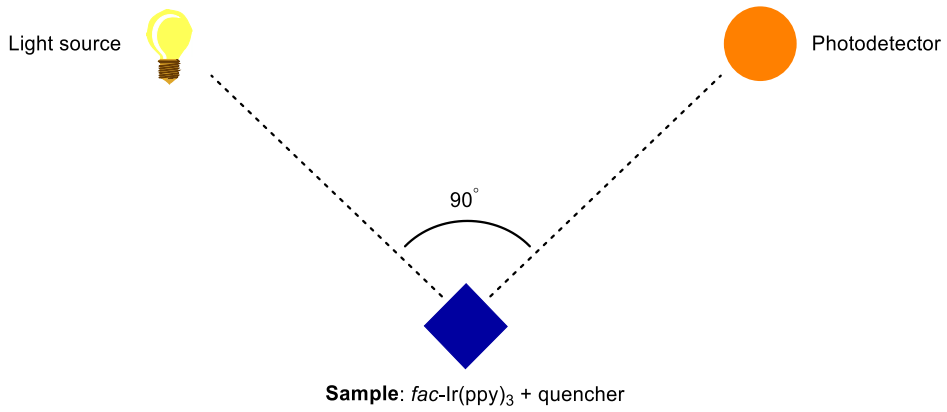


Figure 3.8: Simplified setup of the spectrofluorometer for the Stern-Volmer analysis.

In this experiment, quenching of the excited state of *fac*-Ir(ppy)$_3$ was observed in the presence of 4-fluorobenzenesulfonyl chloride, but not with *N*,*N*-dimethylsulfamoyl chloride (**Figure 3.9**). This result indicates that direct single-electron reduction of the sulfonyl chloride by the triplet excited state of *fac*-Ir(ppy)$_3$ is plausible to initiate the hydrosulfonylation of alkenes; the same initiation scenario is unlikely for the hydrosulfamoylation of alkenes with sulfamoyl chlorides. Furthermore, the excited state of *fac*-Ir(ppy)$_3$ is not quenched by the addition of (TMS)$_3$SiH, a result indicating that SET between the excited state of this photocatalyst and (TMS)$_3$SiH leading to (TMS)$_3$SiH$^{\bullet+}$ is unlikely [$E_{1/2}^{red}$ (Ir(III)*/Ir(II)) = + 0.31 V vs SCE in MeCN;[123] E^{ox} ((TMS)$_3$SiH/(TMS)$_3$SiH$^{\bullet+}$) = + 0.73 V vs SCE in MeCN].[101] However, one cannot rule out such a scenario when Eosin Y is used instead of *fac*-Ir(ppy)$_3$ [$E_{1/2}^{red}$ (EosinY*/EosinY$^{\bullet-}$) = + 0.83 V vs SCE in MeCN;[123] E^{ox} ((TMS)$_3$SiH/(TMS)$_3$SiH$^{\bullet+}$) = + 0.73 V vs SCE in MeCN].[101] The Stern-Volmer

luminescence quenching experiments demonstrated unambiguously that the reactivity profile of sulfonyl chlorides contrasts with the one of sulfamoyl chlorides.

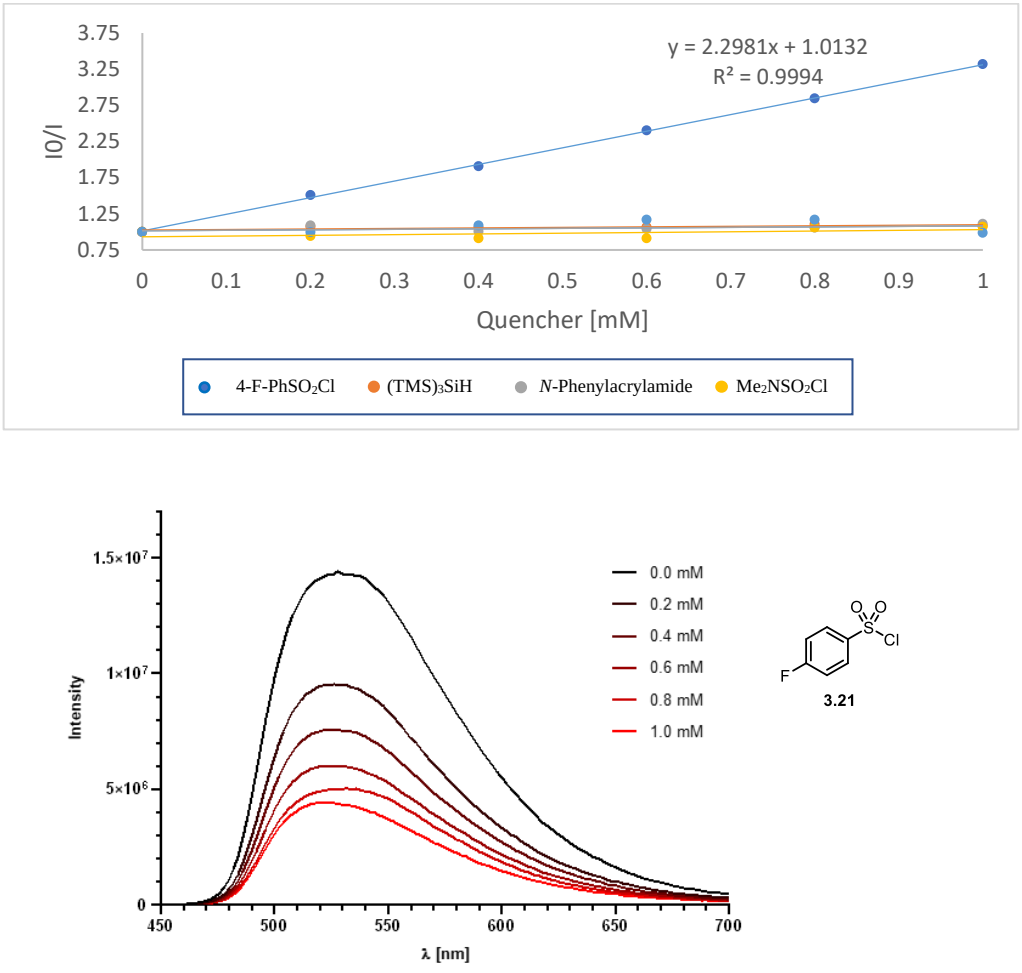
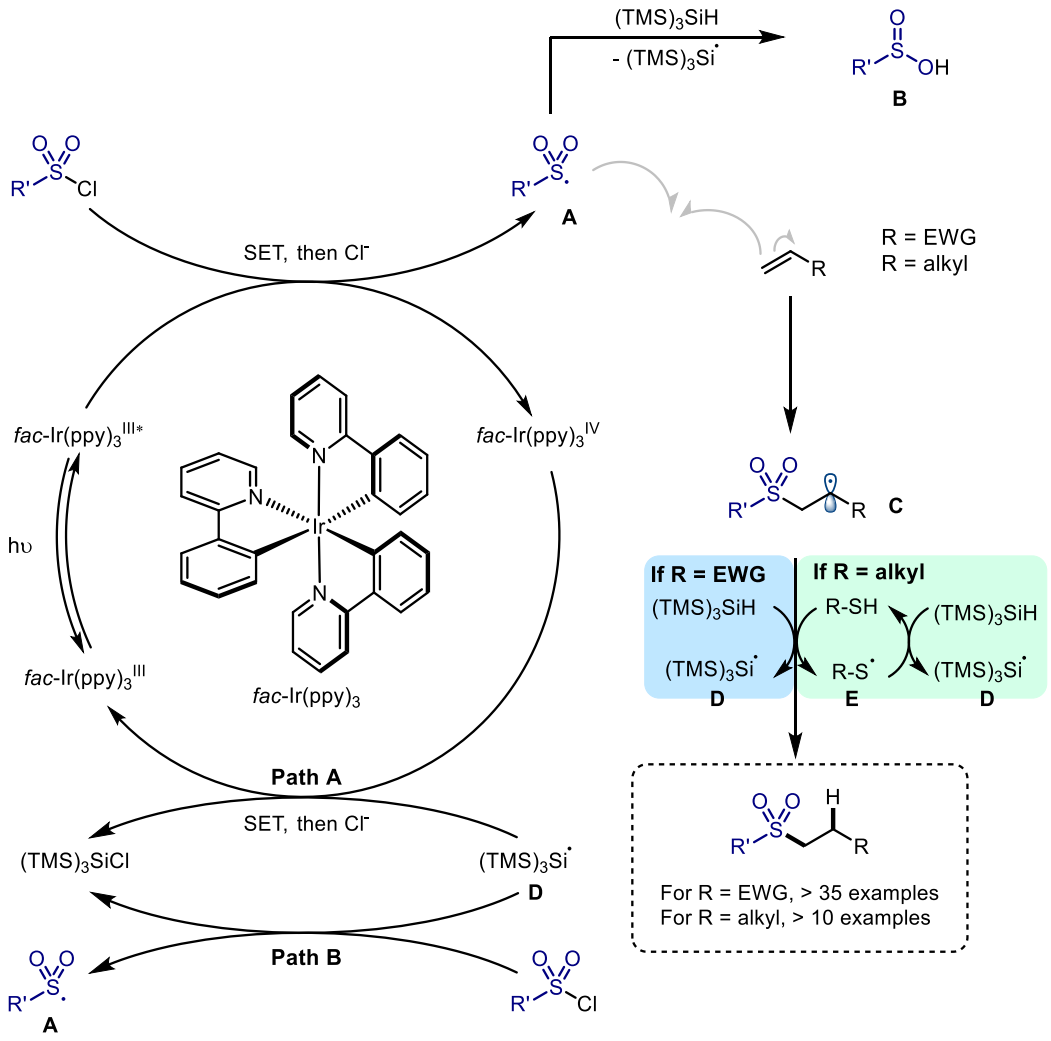


Figure 3.9: Stern-Volmer luminescence quenching experiments.

3.9.3 Proposed Mechanism

Based on the aforementioned control experiments, we propose that upon blue light irradiation, the photocatalyst *fac*-Ir(ppy)$_3$ is excited to the triplet excited state *fac*-Ir(ppy)$_3^*$ which can undergo SET with the sulfonyl chloride (**Scheme 3.27**).



Scheme 3.27: Proposed mechanism for the hydrosulfonylation of alkenes.

This forms a sulfonyl radical anion, which spontaneously dissociates to the free sulfonyl radical **A** and the chloride anion. This radical **A** can react with the nucleophilic HAD, $(TMS)_3SiH$, generating the sulfinic acid **B** byproduct, a suitable but less efficient reagent for hydrosulfonylation under our reaction conditions. In contrast, addition of **A** to the alkene furnishes the carbon-centred radical intermediate **C**. When the reaction is performed on an electron-deficient alkene (R = EWG), a direct HAT between the nucleophilic HAD, $(TMS)_3SiH$ and the electrophilic carbon-centred radical intermediate occurs. This affords the desired hydrosulfonylated product, along with a silyl radical **D**. For unactivated alkenes (R = alkyl), the nucleophilic carbon-centred radical intermediate reacts with the thiol polarity-reversal catalyst forming the desired product as well as a

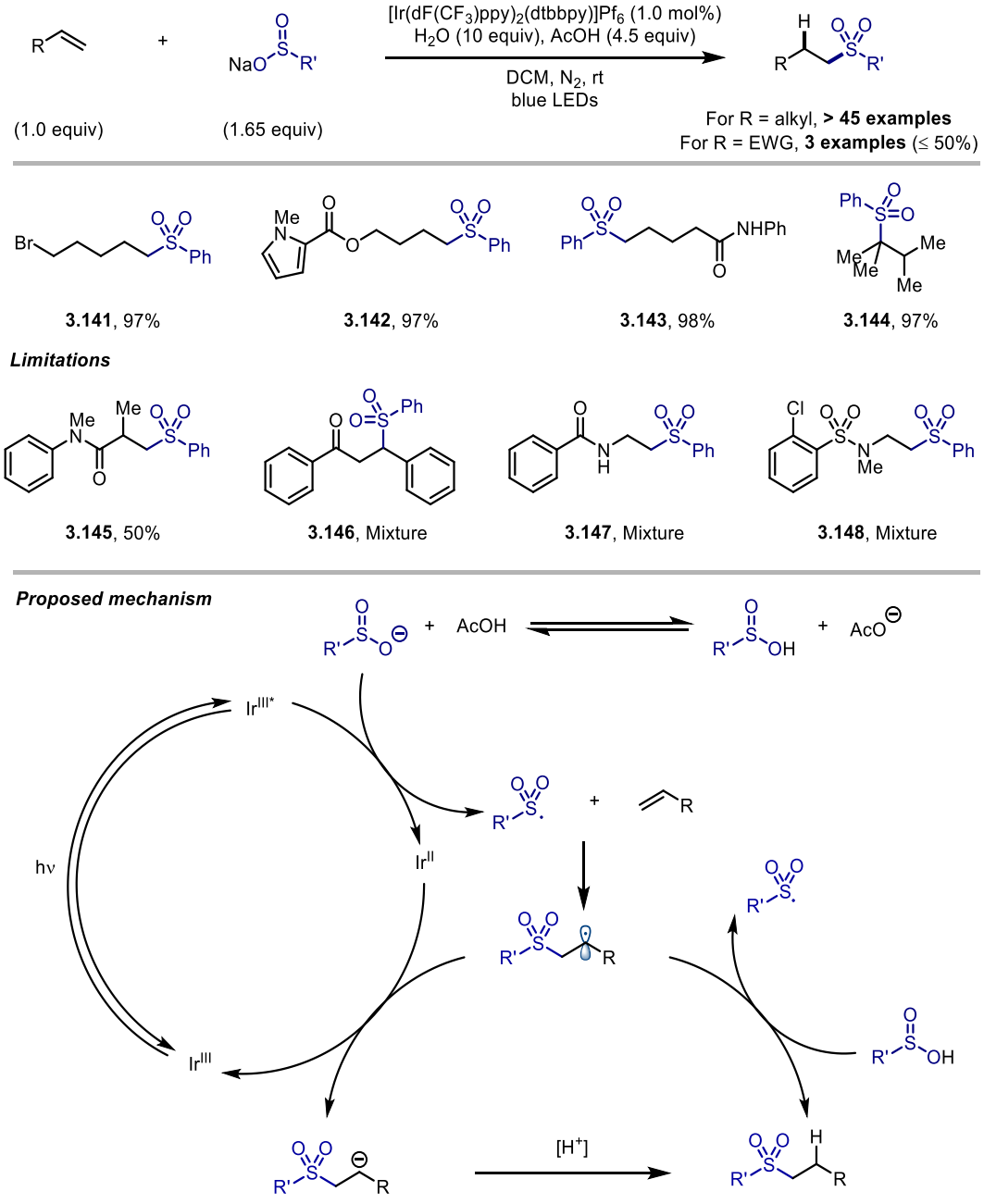
thiyl radical **E**. The thiyl radical can undergo HAA from $(TMS)_3SiH$ to afford **D** along with the regenerated thiol catalyst. Oxidation of **D** with *fac*-$Ir(ppy)_3^{IV}$ regenerates the ground state of *fac*-$Ir(ppy)_3$ and a siliconium ion, which can be quenched by chloride to form $(TMS)_3SiCl$ (**Path A**). Alternatively, a second pathway involving the direct chlorine atom abstraction from the sulfonyl chloride by the silyl radical **D** cannot be ruled out. Indeed, the formation of the hydrosulfonylated product in absence of photocatalyst (although more effective in its presence) advocates in favour of a photoinitiation-radical chain propagation pathway (**Path B**). Based on our previous work on the hydrosulfamoylation of electron-deficient alkenes as well as our mechanistic investigation, this transformation likely operates *via* a chain propagation mechanism. The presence of a chain propagation pathway could also be assessed by quantum yield experiment. However, at the time of this study no suitable equipment for the determination of the quantum yield was available.

3.10 Comparison of this Methodology to a Recently Disclosed Radical Sulfonylation using Sodium Sulfinates

In the course of our investigation, Yu and co-workers reported an anti-Markovnikov photoredox-catalysed hydrosulfonylation of unactivated alkenes (**Scheme 3.28**).[99] In this procedure, sodium sulfinates are employed as sulfonyl radical precursors. This protocol is suitable for a wide range of unactivated alkenes and displays a broad functional tolerance. Remarkably, tri- and tetra- substituted alkenes are suitable substrates and gave the desired hydrosulfonylated products in good to excellent yields. Mechanistically, sulfonyl radicals are generated by single-electron oxidation of sodium sulfinates by the triplet excited state of the photocatalyst upon exposure to blue light irradiation. The sulfonyl radical can add to an alkene, forming a carbon-centred radical intermediate. The authors suggest that the desired hydrosulfonylated product can be obtained by a second SET to generate a carbanion, followed by protonation. Alternatively, a radical chain propagation mechanism can also be envisioned, whereby the sulfinic acid acts as a HAD. In this scenario, acetic acid plays a key role to form the corresponding sulfinic acid from the corresponding sodium sulfinate.

Sulfinate salts are often not commercial and commonly synthesised from the corresponding sulfonyl chlorides in a two-step process. Although easy to prepare, the use of sulfinate salts limits the applicability of such a protocol in terms of introduction of complex sulfonyl fragments. In comparison to our work, the late-stage functionalisation of alkenes using this protocol was not demonstrated. Whilst this procedure is powerful for the hydrosulfonylation of unactivated alkenes, limitations with electron-deficient and electron-rich alkenes have been observed. Using Yu's protocol, these substrates are less reactive and often result in a mixture of products. This lack of reactivity likely stems

from a polarity mismatch between the electrophilic carbon-centred radical intermediate (e.g. α-carbonyl radical) and the electrophilic HAD (acetic acid or sulfinic acid) under these reaction conditions. Aside from our work, this protocol represents a rare example of radical-mediated hydrosulfonylation of unactivated alkenes.



Scheme 3.28: Hydrosulfonylation of unactivated alkenes under photoredox catalysis.

3.11 Conclusion

In conclusion, we developed a robust and general one-step procedure for the hydrosulfonylation of alkenes, a reaction that has received very little attention despite the well-established generation of sulfonyl radicals *via* single-electron reduction of sulfonyl chlorides. Under visible light activation, a wide range of alkenes underwent net hydrosulfonylation using commercial and readily available sulfonyl chlorides in the presence of an iridium photocatalyst and tris(trimethylsilyl)silane as the HAD. Under our reaction conditions, numerous sulfonyl chlorides were added to various electron-deficient alkenes. The reaction exhibited remarkable functional group compatibility and allowed for the late-stage hydrosulfonylation of alkene-containing drug compounds. This reaction was expanded to the functionalisation of unactivated alkenes using a thiol polarity reversal catalyst, demonstrating the diverse reactivity of this methodology. These new conditions were applied to the direct hydrosulfonylation of biologically active molecules. Noteworthy, styrenes did not perform well under the optimised reaction conditions, resulting in a complex mixture of products.

By comparison with our previous work on the hydrosulfamoylation of electron-deficient alkenes (**Chapter 2**), the differences in reduction potentials between sulfonyl chlorides and sulfamoyl chlorides (E_{red} Me_2NSO_2Cl = -1.59 V vs SCE in MeCN; E_{red} $MeSO_2Cl$= -1.30 V vs SCE in MeCN)[71] allude to the different reactivity profiles for hydrosulfonylation and hydrosulfamoylation: sulfonyl radicals can be generated by direct single-electron reduction from the excited state of *fac*-$Ir(ppy)_3$, a scenario which is not applicable to sulfamoyl chlorides. Stern-Volmer luminescence quenching experiments demonstrated unambiguously the mechanistically distinct behaviour of sulfamoyl and sulfonyl chlorides towards *fac*-$Ir(ppy)_3$.

3.12 Future Work

Future developments should focus on the radical-mediated activation of other sulfur-containing reagents such as sulfoximidoyl chlorides to generate sulfoximines. Sulfoximines have rarely been employed in drug discovery despite their powerful biological effects. This might likely be due to the challenging synthesis of such fragments. However, owing to their high stability and ability to engage in hydrogen-bond interactions (acceptor/donor functionalities), these functionalities deserve more attention. The development of a novel radical-mediated methodology for the late-stage introduction of sulfoximines might be of interest to the pharmaceutical industry, and thus prompt the generation of chemical libraries leading to efficient SAR explorations and enhancement of target potency.

Although vicinal sulfonylation procedures have been reported, there is no example of fluorosulfonylation, namely the introduction of a sulfonyl group and a fluorine atom. Owing to the unique properties of fluorine, the mild introduction of such an atom across a double bond would be a powerful strategy to expand existing chemical space. One could envision that the carbon-centred radical intermediate generated upon radical addition to the alkene, could be intercepted with a metal (e.g. copper) and undergo reductive elimination with fluorine or fluorinated motifs. On the other hand, the carbon-centred radical intermediate (alkyl radical) could react with an electrophilic fluorine source (e.g. NFSI, Selectfluor®) to form vicinal fluorosulfonylated fragments.

3.13 References

[1] K. A. Scott, J. T. Njardarson, *Top. Curr. Chem.* **2018**, *376*, 5–39.
[2] W. Xu, J. He, M. He, F. Han, X. Chen, Z. Pan, J. Wang, M. Tong, *Molecules* **2011**, *16*, 9129–9141.
[3] M. Ueda, H. Toyota, T. Ouchi, J. I. Suciyama, K. Yonetake, T. Masuko, T. Teramoto, *J. Polym. Sci. Polym. Chem. Ed.* **1993**, *31*, 853–858.
[4] J. M. Harris, *Isolatable, Water Soluble, and Hydrolytically Stable Active Sulfones of Poly(Ethylene Glycol) and Related Polymers for Modification of Surfaces and Molecules*, **1995**, US5446090A.
[5] I. Ahmad, A. Khaimah, R. Al Khaimah, *Int. J. Pharm. Pharm. Sci.* **2015**, *7*, 9–27.
[6] M. Feng, B. Tang, S. H. Liang, X. Jiang, *Curr Top Med Chem* . **2016**, *16*, 1200–1216.
[7] A. V. Ivachtchenko, E. S. Golovina, M. G. Kadieva, V. M. Kysil, O. D. Mitkin, S. E. Tkachenko, I. M. Okun, *J. Med. Chem.* **2011**, *54*, 8161–8173.
[8] C. Zhao, K. P. Rakesh, L. Ravidar, W. Y. Fang, H. L. Qin, *Eur. J. Med. Chem.* **2019**, *162*, 679–734.
[9] P. S. Fier, K. M. Maloney, *J. Am. Chem. Soc.* **2019**, *141*, 1441–1445.
[10] K. A. Scott, J. T. Njardarson, *Top. Curr. Chem.* **2018**, *376*, DOI 10.1007/s41061-018-0184-5.
[11] B. M. Trost, *Bull. Chem. Soc. Jpn.* **1988**, *61*, 107–124.
[12] B. M. Trost, C. A. Kalnmals, *Chem. Eur. J.* **2019**, *25*, 11193–11213.
[13] B. Tozkoparan, E. Küpeli, E. Yeşilada, M. Ertan, *Bioorg. Med. Chem.* **2007**, *15*, 1808–1814.
[14] M. Catarinella, T. Grüner, T. Strittmatter, A. Marx, T. U. Mayer, *Angew. Chem. Int. Ed.* **2009**, *48*, 9072–9076.
[15] R. J. Griffin, A. Henderson, N. J. Curtin, A. Echalier, J. A. Endicott, I. R. Hardcastle, D. R. Newell, M. E. M. Noble, L. Z. Wang, B. T. Golding, *J. Am. Chem. Soc.* **2006**, *128*, 6012–6013.
[16] A. B. Pritzius, B. Breit, *Angew. Chem. Int. Ed.* **2015**, *54*, 3121–3125.
[17] J. L. Baihua Hu, Vishal Verma, Matthew Volgraf, Anthony Estrada, *Sulfonylcycloalkyl Carboxamide Compounds*, **2019**, US 2019 / 0144430 A1.
[18] E. Voutyritsa, I. Triandafillidi, C. G. Kokotos, *Synthesis* **2017**, *49*, 917–924.
[19] M. Jereb, *Green Chem.* **2012**, *14*, 3047–3052.
[20] A. Shaabani, P. Mirzaei, S. Naderi, D. G. Lee, *Tetrahedron* **2004**, *60*, 11415–11420.
[21] N. Fukuda, T. Ikemoto, *J. Org. Chem.* **2010**, *75*, 4629–4631.
[22] N. K. Jana, J. G. Verkade, *Org. Lett.* **2003**, *5*, 3787–3790.
[23] B. Karimi, M. Ghoreishi-Nezhad, J. H. Clark, *Org. Lett.* **2005**, *7*, 625–628.
[24] R. S. Varma, K. P. Naicker, *Org. Lett.* **1999**, *1*, 189–191.
[25] M. Kirihara, A. Itou, T. Noguchi, J. Yamamoto, *Synlett* **2010**, *2010*, 1557–1561.
[26] K. Bahrami, M. M. Khodaei, M. Sheikh Arabi, *J. Org. Chem* **2010**, *75*, 6208–6213.
[27] N. W. Liu, S. Liang, G. Manolikakes, *Synthesis* **2016**, *48*, 1939–1973.
[28] S. Liang, R. Y. Zhang, G. Wang, S. Y. Chen, X. Q. Yu, *European J. Org. Chem.* **2013**, 7050–7053.
[29] V. G. Pandya, S. B. Mhaske, *Org. Lett.* **2014**, *16*, 3836–3839.
[30] M. Jegelka, B. Plietker, *Org. Lett.* **2009**, *11*, 3462–3465.
[31] M. Jegelka, B. Plietker, *Chem. Eur. J.* **2011**, *17*, 10417–10430.
[32] W. Zhu, D. Ma, *J. Org. Chem.* **2005**, *70*, 2696–2700.
[33] G. Nie, X. Deng, X. Lei, Q. Hu, Y. Chen, *RSC Adv.* **2016**, *6*, 75277–75281.
[34] M. Ueda, J. F. Hartwig, *Org. Lett.* **2010**, *12*, 92–94.
[35] H. Suzuki, H. Abe, *Tetrahedron Lett.* **1995**, *36*, 6239–6242.
[36] H. Eichelmann, H. J. Gais, *Tetrahedron: Asymmetry* **1995**, *6*, 643–646.
[37] J. A. Wolfe, S. R. Hitchcock, *Tetrahedron: Asymmetry* **2010**, *21*, 2690–2695.
[38] N. Margraf, G. Manolikakes, *J. Org. Chem.* **2015**, *80*, 2582–2600.
[39] J. P. Wu, J. Emeigh, X. P. Su, *Org. Lett.* **2005**, *7*, 1223–1225.
[40] D. Marković, C. M. R. Volla, P. Vogel, A. Varela-Álvarez, J. A. Sordo, *Chem. Eur. J.* **2010**, *16*, 5969–5975.
[41] E. J. Emmett, B. R. Hayter, M. C. Willis, *Angew. Chem. Int. Ed.* **2014**, *53*, 10204–10208.
[42] C. C. Chen, J. Waser, *Org. Lett.* **2015**, *17*, 736–739.
[43] E. J. Emmett, B. R. Hayter, M. C. Willis, *Angew. Chem. Int. Ed.* **2013**, *52*, 12679–12683.
[44] A. S. Deeming, C. J. Russell, A. J. Hennessy, M. C. Willis, *Org. Lett.* **2014**, *16*, 150–153.
[45] B. N. Rocke, K. B. Bahnck, M. Herr, S. Lavergne, V. Mascitti, C. Perreault, J. Polivkova, A. Shavnya, *Org. Lett.* **2014**, *16*, 154–157.
[46] A. Shavnya, K. D. Hesp, V. Mascitti, A. C. Smith, *Angew. Chem. Int. Ed.* **2015**, *54*, 13571–13575.
[47] M. W. Johnson, S. W. Bagley, N. P. Mankad, R. G. Bergman, V. Mascitti, F. D. Toste, *Angew. Chem. Int. Ed.* **2014**, *53*, 4404–4407.
[48] B. Ge, D. Wang, W. Dong, P. Ma, Y. Li, Y. Ding, *Tetrahedron Lett.* **2014**, *55*, 5443–5446.
[49] Y. H. Xu, M. Wang, P. Lu, T. P. Loh, *Tetrahedron* **2013**, *69*, 4403–4407.
[50] C. Xia, Z. Wei, C. Shen, J. Xu, Y. Yang, W. Su, P. Zhang, *RSC Adv.* **2015**, *5*, 52588–52594.
[51] X. Zhao, V. M. Dong, *Angew. Chem. Int. Ed.* **2011**, *50*, 932–934.
[52] X. Zhao, E. Dimitrijević, V. M. Dong, *J. Am. Chem. Soc.* **2009**, *131*, 3466–3467.
[53] Z. Wu, H. Song, X. Cui, C. Pi, W. Du, Y. Wu, *Org. Lett.* **2013**, *15*, 1270–1273.
[54] H. W. Liang, K. Jiang, W. Ding, Y. Yuan, L. Shuai, Y. C. Chen, Y. Wei, *Chem. Commun.* **2015**, *51*,

16928–16931.
[55] J. Liu, L. Yu, S. Zhuang, Q. Gui, X. Chen, W. Wang, Z. Tan, *Chem. Commun.* **2015**, *51*, 6418–6421.
[56] R. V Kupwade, *J. Chem. Rev.* **2019**, *1*, 99–113.
[57] S. Matavos-Aramyan, S. Soukhakian, M. H. Jazebizadeh, *Phosphorus, Sulfur Silicon Relat. Elem.* **2020**, *195*, 181–193.
[58] K. Hofman, N. W. Liu, G. Manolikakes, *Chem. Eur. J.* **2018**, *24*, 11852–11863.
[59] F. Lovering, J. Bikker, C. Humblet, *J. Med. Chem.* **2009**, *52*, 6752–6756.
[60] F. Lovering, *Med. Chem. Commun.* **2013**, *4*, 515–519.
[61] K. Kingwell, *Nat. Rev. Drug Discov.* **2009**, *8*, 931.
[62] F. W. Goldberg, J. G. Kettle, T. Kogej, M. W. D. Perry, N. P. Tomkinson, *Drug Discov. Today* **2015**, *20*, 11–17.
[63] S. Caddick, D. Hamza, S. N. Wadman, *Tetrahedron Lett.* **1999**, *40*, 7285–7288.
[64] J. E. Brumwell, N. S. Simpkins, N. K. Terrett, *Tetrahedron* **1994**, *50*, 13533–13552.
[65] A. S. Gozdz, P. Maslak, *J. Org. Chem* **1991**, *56*, 2179–2189.
[66] A. Hossain, S. Engl, E. Lutsker, O. Reiser, *ACS Catal.* **2019**, *9*, 1103–1109.
[67] M. Alkan-Zambada, X. Hu, *J. Org. Chem.* **2019**, *84*, 4525–4533.
[68] X. J. Tang, W. R. Dolbier, *Angew. Chem. Int. Ed.* **2015**, *54*, 4246–4249.
[69] X. Zeng, L. Ilies, E. Nakamura, *Org. Lett.* **2012**, *14*, 954–956.
[70] C.-J. Wallentin, J. D. Nguyen, P. Finkbeiner, C. R. J. Stephenson, *J. Am. Chem. Soc.* **2012**, *134*, 8875–8884.
[71] S. M. Hell, C. F. Meyer, G. Laudadio, A. Misale, M. C. Willis, T. Noël, A. A. Trabanco, V. Gouverneur, *J. Am. Chem. Soc.* **2020**, *142*, 720–725.
[72] J. Aziz, S. Messaoudi, M. Alami, A. Hamze, *Org. Biomol. Chem.* **2014**, *12*, 9743–9759.
[73] V. Nair, A. Augustine, S. B. Panicker, T. D. Suja, S. Mathai, *Res. Chem. Intermed.* **2003**, *29*, 213–226.
[74] C.-P. Chuang, *Synth. Commun.* **1993**, *23*, 2371–2380.
[75] M. María, J. Jes´, J. Cabrera-Afonso, Z.-P. Lu, C. B. Kelly, S. B. Lang, R. Dykstra, O. Gutierrez, G. A. Molander, *Chem. Sci.* **2018**, *9*, 3186–3191.
[76] P. James, F. X. Felpin, Y. Landais, K. Schenk, *J. Org. Chem.* **2005**, *70*, 7985–7995.
[77] P. James, K. Schenk, Y. Landais, *J. Org. Chem.* **2006**, *71*, 3630–3633.
[78] T. J. He, W. Q. Zhong, J. M. Huang, *Chem. Commun.* **2020**, *56*, 2735–2738.
[79] X. Li, X. Xu, C. Zhou, *Chem. Commun.* **2012**, *48*, 12240–12242.
[80] T. Taniguchi, A. Idota, H. Ishibashi, *Org. Biomol. Chem.* **2011**, *9*, 3151–3153.
[81] N. Mantrand, P. Renaud, *Tetrahedron* **2008**, *64*, 11860–11864.
[82] I. W. Harvey, E. D. Phillips, G. H. Whitham, *Tetrahedron* **1997**, *53*, 6493–6508.
[83] L. Quebatte, K. Thommes, K. Severin, *J. Am. Chem. Soc.* **2006**, *128*, 7440–7441.
[84] C. S. Gloor, F. Dénès, P. Renaud, *Angew. Chem. Int. Ed.* **2017**, *129*, 13514–13517.
[85] S. Ye, D. Zheng, J. Wu, G. Qiu, *Chem. Commun.* **2019**, *55*, 2214–2217.
[86] X. Wang, M. Yang, W. Xie, X. Fan, J. Wu, *Chem. Commun.* **2019**, *55*, 6010–6013.
[87] C. F. Meyer, S. M. Hell, J. B. I. Sap, A. Misale, A. Peschiulli, D. Oehlrich, A. A. Trabanco, V. Gouverneur, *Tetrahedron* **2019**, 130679.
[88] C. F. Meyer, S. M. Hell, A. Misale, A. A. Trabanco, V. Gouverneur, *Angew. Chem. Int. Ed.* **2019**, *131*, 8921–8925.
[89] S. Mizuta, S. Verhoog, K. M. Engle, T. Khotavivattana, M. O'Duill, K. Wheelhouse, G. Rassias, M. Médebielle, V. Gouverneur, *J. Am. Chem. Soc.* **2013**, *135*, 2505–2508.
[90] N. Ignat'ev, A. Kucherina, S. P., *Acta Chem. Scand.* **1999**, *53*, 1110–1116.
[91] L. B. Johansson, P. Bjorn, *Acta Chem. Scand. B* **1978**, *32*, 431–436.
[92] C.-J. Wallentin, J. D. Nguyen, P. Finkbeiner, C. R. J. Stephenson, *J. Am. Chem. Soc.* **2012**, *134*, 8875–8884.
[93] X. Liu, T. Cong, P. Liu, P. Sun, *Org. Biomol. Chem.* **2016**, *14*, 9416–9422.
[94] S. K. Pagire, S. Paria, O. Reiser, *Org. Lett.* **2016**, *18*, 2106–2109.
[95] S. K. Pagire, A. Hossain, O. Reiser, *Org. Lett.* **2018**, *20*, 648–651.
[96] R. Chaudhary, P. Natarajan, *ChemistrySelect* **2017**, *2*, 6458–6479.
[97] A. A. Ermoshkin, A. N. Kasatochkin, V. P. Boyarskii, *Russ. J. Org. Chem.* **2007**, *43*, 996–1000.
[98] M. P. Bertrand, *Org. Prep. Proced. Int.* **1994**, *26*, 257–290.
[99] J. J. Wang, W. Yu, *Org. Lett.* **2019**, *21*, 9236–9240.
[100] T. J. Burkey, M. Majewski, D. Griller, *J. Am. Chem. Soc.* **1986**, *108*, 2218–2221.
[101] C. Chatgilialoglu, C. Ferreri, Y. Landais, V. I. Timokhin, *Chem. Rev.* **2018**, *118*, 6516–6572.
[102] J. Lalevée, X. Allonas, J. P. Fouassier, *J. Org. Chem.* **2007**, *72*, 6434–6439.
[103] T. H. Wright, B. J. Bower, J. M. Chalker, J. L. Bernardes, R. Wiewiora, W.-L. Ng, R. Raj, S. Faulkner, M. Robert, J. Vallée, et al., *Science* **2016**, *354*, 1465–1475.
[104] A. Dowine De Bruijn, G. Oelfes, *Chem. Eur.J.* **2018**, *24*, 12728–12733.
[105] J. Dadová, S. Bastien, R. G. Galan, B. G. Davis, *Curr. Opin. Chem. Biol.* **2018**, *46*, 71–81.
[106] E. Lønning, E. Bajetta, R. Murray, M. Tubiana-Hulin, P. D. Eisenberg, E. Mickiewicz, L. Celio, P. Pitt, M. Mita, N. K. Aaronson, et al., *J. Clin. Oncol.* **2000**, *18*, 2234–2244.
[107] C. Sambiagio, T. Noël, *Trends Chem.* **2020**, *2*, 92–106.
[108] F. Politano, G. Oksdath-Mansilla, *Org. Process Res. Dev.* **2018**, *22*, 1045–1062.
[109] C. Sambiagio, T. Noël, *Trends Chem.* **2020**, *2*, 92–106.

[110] J. P. Knowles, L. D. Elliott, K. I. Booker-Milburn, *Beilstein J. Org. Chem.* **2012**, *8*, 2025–2052.
[111] H. A. Sakai, W. Liu, C. Le, D. W. C. MacMillan, *J. Am. Chem. Soc.* **2020**, *142*, 11691–11697.
[112] S. Kim, M. J. Goldfogel, M. M. Gilbert, D. J. Weix, *J. Am. Chem. Soc.* **2020**, *142*, 9902–9907.
[113] T. Besset, T. Poisson, X. Pannecoucke, *European J. Org. Chem.* **2015**, *2015*, 2765–2789.
[114] Y. Fang, Z. Luo, X. Xu, *RSC Adv.* **2016**, *6*, 59661–59676.
[115] D. C. Meadows, J. Gervay-Hague, *Med. Res. Rev.* **2006**, *26*, 793–814.
[116] T. P. M. Goumans, K. Van Alem, G. Lodder, *Eur. J. Org. Chem.* **2008**, *2008*, 435–443.
[117] C. Galli, A. Guarnieri, H. Koch, P. Mencarelli, Z. Rappoport, *J. Org. Chem.* **1997**, *62*, 4072–4077.
[118] B. Giese, *Angew. Chem. Int. Ed.* **1989**, *28*, 969–980.
[119] D. Cristina Silva Costa, *Arab. J. Chem.* **2020**, *13*, 799–834.
[120] B. Chan, C. J. Easton, L. Radom, *J. Phys. Chem. A* **2018**, *122*, 1741–1746.
[121] B. P. Roberts, *Chem. Soc. Rev.* **1999**, *28*, 25–35.
[122] L. Li, Y. Liu, Y. Peng, L. Yu, X. Wu, H. Yan, *Angew. Chem. Int. Ed.* **2016**, *128*, 339–343.
[123] N. A. Romero, D. A. Nicewicz, *Chem. Rev.* **2016**, *116*, 10075–10166.

Chapter 4

Efficient Generation of the Fluoromethyl Radical *via* a Silyl Radical-Mediated Activation of Fluoroiodomethane

This chapter discusses the radical-mediated hydrofluoromethylation of electron-deficient alkenes, an unsolved challenge in the literature. Fluoroiodomethane, a simple and commercially available fluoroalkyl halide, is harnessed as an effective source of the fluoromethyl radical *via* a silyl radical-mediated halogen atom abstraction. The utility of this methodology was showcased in the late-stage functionalisation of complex biologically active molecules. To demonstrate the applicability of our method, the procedure was adapted to the ^{18}F-hydrofluoromethylation of structurally complex molecules using easily accessible [^{18}F]CH_2FI. A manuscript is in preparation.

Author contributions: Reactions were designed by Sandrine M. Hell, Claudio F. Meyer and Prof. Véronique Gouverneur. The reaction conditions were optimised by Sandrine M. Hell. Scope and mechanistic experiments were performed by Sandrine M. Hell, Claudio F. Meyer and Sebastiano Ortalli. The scale-up experiment was performed by Sebastiano Ortalli. Competition experiments were performed by Claudio F. Meyer and Sandrine M. Hell. Robustness screen was performed by Sandrine M. Hell. ^{18}F-radiolabeling was conducted by Claudio F. Meyer and Dr. Jeroen Sap. Cyclic voltammetry measurements of fluoroiodomethane and methyl iodide were performed by Xuanxiao Chen (joint PhD student in the research group of Prof. Ben Davis and Prof. Jason Davis, Oxford University, United-Kingdom). Dr. Andrés A. Trabanco provided helpful comments.

4.1 Introduction to Fluorine

The selective introduction of fluorinated methyl groups, including trifluoromethyl (CF_3), difluoromethyl (CF_2H) and fluoromethyl (CH_2F), can significantly influence the biological activity of organic molecules.[1–8] Nowadays, fluorine-containing molecules account for about 30% of all pharmaceuticals and have been used in the treatment of various diseases (**Figure 4.1**).[3,9]

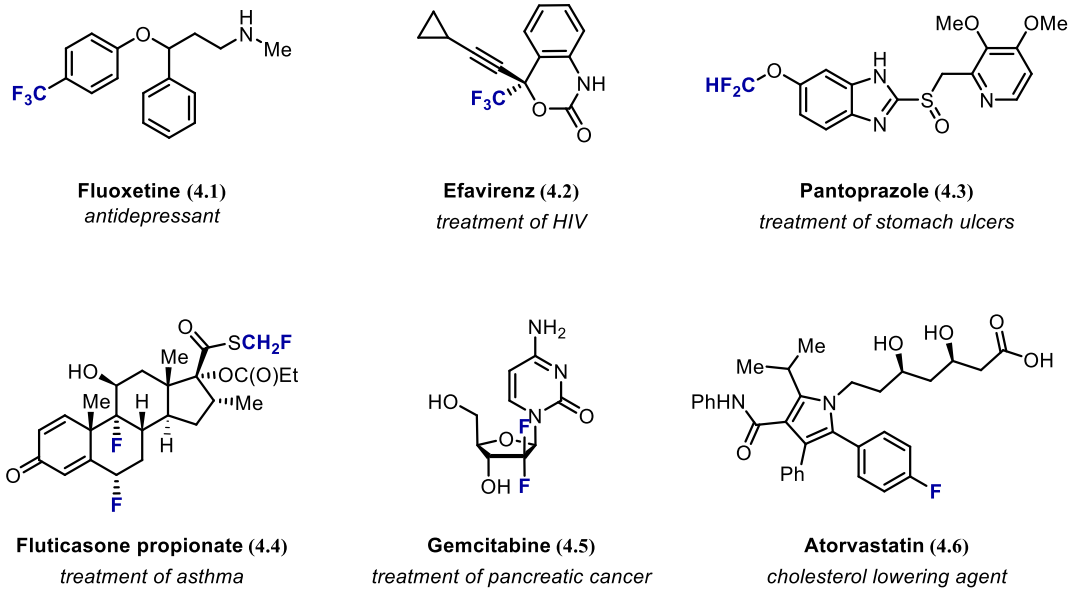


Figure 4.1: Fluorine-containing pharmaceuticals.

The high electronegativity of fluorine (Pauling scale: $\chi(F) = 4.0$ vs $\chi(C) = 2.55$)[10] combined with its small size (van der Waals radius: 1.47 Å) result in the C-F bond being one of the strongest single bonds in organic chemistry (BDE = 108 kcal/mol).[11] This unique property renders the C-F bond extremely stable towards various chemical and biological processes.

Furthermore, the high electronegativity of fluorine can induce significant changes in the pKa of surrounding functional groups (**Table 4.1**).[12] This effect is well represented by the introduction of fluorine atoms to amines or carboxylic acids, where the pKa is lowered with increasing fluorine content.[10]

Table 4.1: Influence of fluorine on pKa (in water).

Ammonium	pKa	Carboxylic acid	pKa
$CH_3CH_2NH_3^+$ (4.7)	10.7	**CH_3CO_2H (4.11)**	4.7
$CH_2FCH_2NH_3^+$ (4.8)	9.0	**CH_2FCO_2H (4.12)**	2.6
$CHF_2CH_2NH_3^+$ (4.9)	7.3	**CHF_2CO_2H (4.13)**	1.2
$CF_3CH_2NH_3^+$ (4.10)	5.7	**CF_3CO_2H (4.14)**	0.2

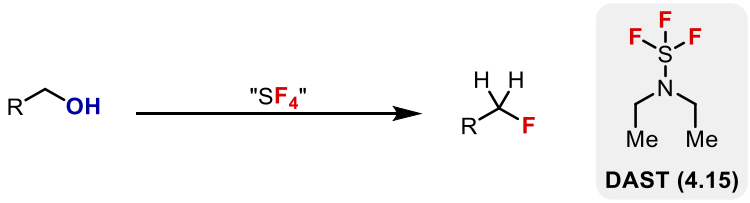
The lipophilicity of molecules can also be modulated by the introduction of fluorine atoms, often enhancing the ability to permeate cell membranes by 1–70 fold,[13] and increasing binding affinity to the target protein.[14] The selective incorporation of a fluorine atom into biologically relevant organic molecules also influences the metabolic stability of drug candidates. Indeed, fluorine prevents oxidative metabolism of specific C−H bonds by the liver cytochrome P450 monooxygenase enzymes, as C−F bonds have much higher bond dissociation energies than C−H bonds (BDE (C−H): 81 kcal/mol vs. BDE (C−F): 108 kcal/mol).[15] This improved metabolic stability often results in increased bioavailability as well as prolonged biological half-life. Owing to these unique properties, fluorine and fluoroalkyl groups have been considered as potential bioisosteres for a variety of functionalities, and as such have been used in a plethora of drug molecules to improve absorption, distribution, metabolism and excretion (ADME) properties.[16–20]

Given its favourable nuclear and chemical propertiesm the radionuclide fluorine-18 (F-18) has been widely employed in PET imaging for *in vivo* studies of biological processes.[21–24] F-18 is often represented as the ideal radionuclide for the synthesis of radiopharmaceuticals, as its half-life (109.7 minutes) allows for off-site synthesis and subsequent distribution to imaging centres. The use of fluorine-18 in PET imaging will be further discussed in **Section 4.10**.

4.2 Synthesis of the Fluoromethyl Groups

4.2.1 Common Methods

Nucleophilic fluorination is one of the most efficient method for the preparation of C(sp^3) fluoroalkyl groups.[25–28] Nowadays, the deoxyfluorination of alcohols, employing sulphur tetrafluoride or its derivatives (e.g. DAST (**4.15**)) has been extensively investigated for the synthesis of various fluorinated building blocks (**Scheme 4.1**).[25,29]



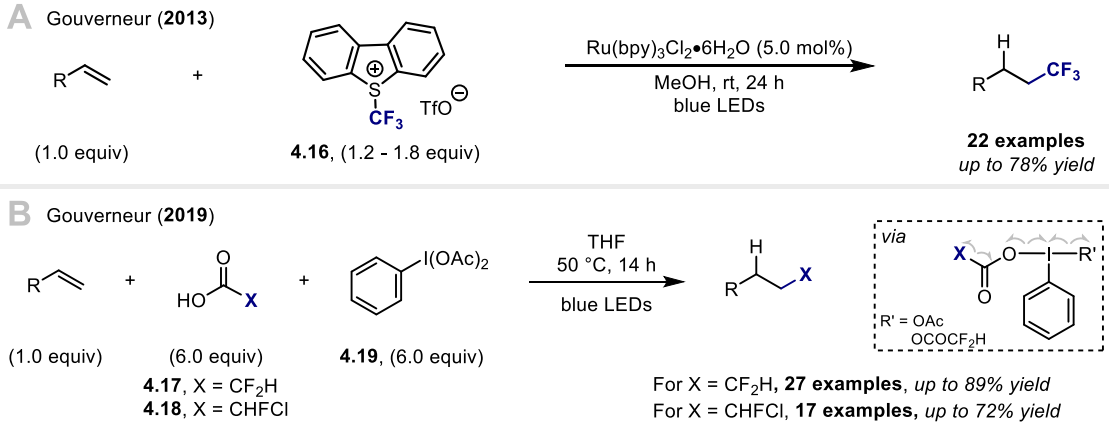
Scheme 4.1: Deoxyfluorination strategy for the synthesis of the fluoromethyl group.

However, deoxyfluorination reagents are often hygroscopic, highly toxic and explosive at higher temperatures. The limited functional group tolerance of these reagents often requires extensive protecting group chemistry, and therefore longer synthetic routes. In the last decades, conceptual advances have been made in the field of synthetic organofluorine chemistry for the preparation of fluoroalkyl groups. These methods have been addressed in several reviews and will not be the focus in this chapter.[25,29–35]

4.2.2 Hydrofluoroalkylation of Alkenes

With the development of radical fluoroalkylation reagents and the recent emergence of photochemistry, numerous radical-mediated strategies have allowed for the late-stage introduction of various fluorinated groups into drug-like molecules under mild reaction conditions.[36–40] Fluoroalkyl radicals can react with various functional groups, the most common ones being alkenes and heteroarenes *via* Minisci-type chemistry.[41] Within the realm of alkene functionalisation, hydrotrifluoromethylation and

hydrodifluoromethylation are well established.[42–49] Often, the generation of fluoroalkyl radicals relies on a single-electron reduction strategy using a photocatalyst to activate electrophilic fluoroalkylating reagents, such as fluoroalkyl sulfonyl chlorides[50] and fluoroalkyl halides.[44] More elaborated reagents, such as the Langlois,[51] Umemoto[52,53] and Togni[54] reagents, have recently been utilised for challenging transformations (e.g. trifluoromethylation of alkyl halides).[55] In 2013, Gouverneur and co-workers reported a broadly applicable catalytic hydrotrifluoromethylation of alkenes and alkynes under visible light activation using Umemoto reagent (**4.16**, **Scheme 4.2A**).[48] The generation of the trifluoromethyl radical relied on a single-electron transfer between the visible light-activated photocatalyst $Ru(bpy)_3Cl_2$ (E_{ox} (Ru^{2+*}/Ru^{3+} = − 0.81 V vs SCE in MeCN) and **4.16** (E_{red} (**4.16**/**4.16**$^{\bullet-}$) = − 0.25 V vs SCE in MeCN).



Scheme 4.2: Catalytic hydrofluoroalkylation of alkenes, Gouverneur 2013 and 2019.

Later, the same group disclosed an operationally simple protocol for the hydrodifluoromethylation of alkenes using difluoroacetic acid (**4.17**), as a commercially available and inexpensive difluoromethyl radical source (**Scheme 4.2B**).[56] In combination with the mild oxidant diacetoxy(iodo)benzene (PIDA, **4.19**), a difluoroacetoxy-containing hypervalent iodine complex was formed *in situ*. This intermediate undergoes spontaneous homolytic iodine-oxygen bond cleavage to form the

desired CF_2H radical upon decarboxylation. This strategy was later extended to the hydrochlorofluoromethylation of alkenes using chlorofluoroacetic acid (**4.18**).[57]

In contrast, the addition of a fluoromethyl radical to an alkene remains underdeveloped. To the best of our knowledge, there is no example of hydrofluoromethylation of alkenes to date. An early report of the fluoromethyl radical was disclosed by Andrews and co-workers in 1971, describing its nonplanar and slightly pyramidal geometry, with a pyramidal angle determined to be 5° or less. This distortion from planarity becomes increasingly apparent with higher degrees of fluorine substitution (**Figure 4.2**).[58]

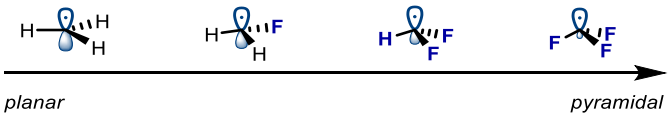


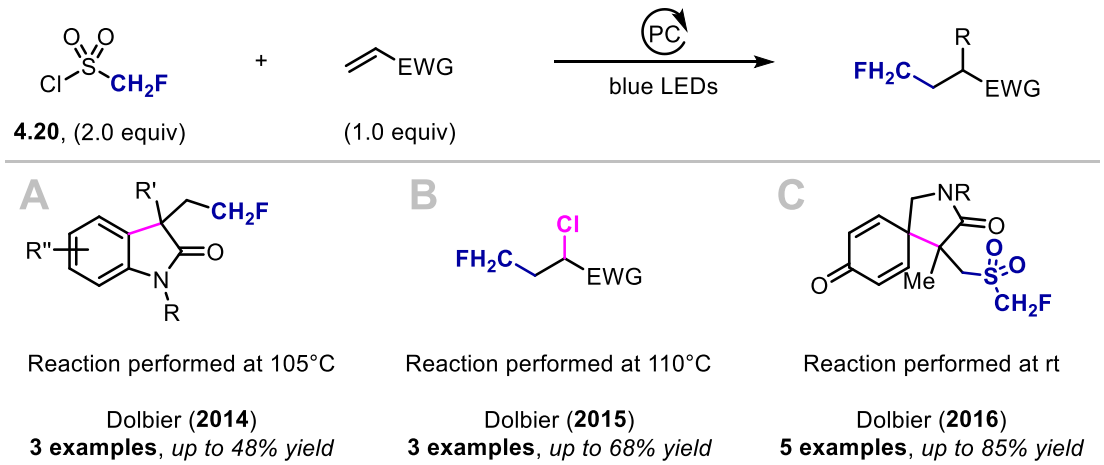
Figure 4.2: Geometry of fluoroalkyl radicals.

Two parameters can influence the reactivity of fluoroalkyl radicals, namely (i) the electron-donating resonance effect of lone pair electrons (increasing nucleophilicity) and (ii) the inductive effect of α-fluorine substituents (increasing electrophilicity). Owing to the high electronegativity of fluorine ($\chi(F) = 4.0$), the trifluoromethyl radical (sum of electronegativities ($\Sigma\chi$) = 12.0, strong inductive effect)[58] is considered to be more electrophilic than the methyl radical ($\Sigma\chi = 6.6$), and therefore readily reacts with electron-rich substrates (e.g. electron-rich benzene derivatives).[59] However, despite the fluoromethyl radical having more electronegative substituents ($\Sigma\chi = 8.4$) than the methyl radical ($\Sigma\chi = 6.6$), this effect is outweighed by the π-donating effect of fluorine, rendering the fluoromethyl radical more nucleophilic in comparison to the methyl radical.[9] This enhanced nucleophilic allows the fluoromethyl radical to react with more electrophilic substrates, such as pyridine derivatives.[60]

The fluoromethyl radical has previously been generated from a wide set of reagents. The reactivity of this radical has been harnessed in the context of vicinal difunctionalisation of alkenes (e.g. electron-deficient alkenes, styrenes) and in Minisci-type chemistry.[60]

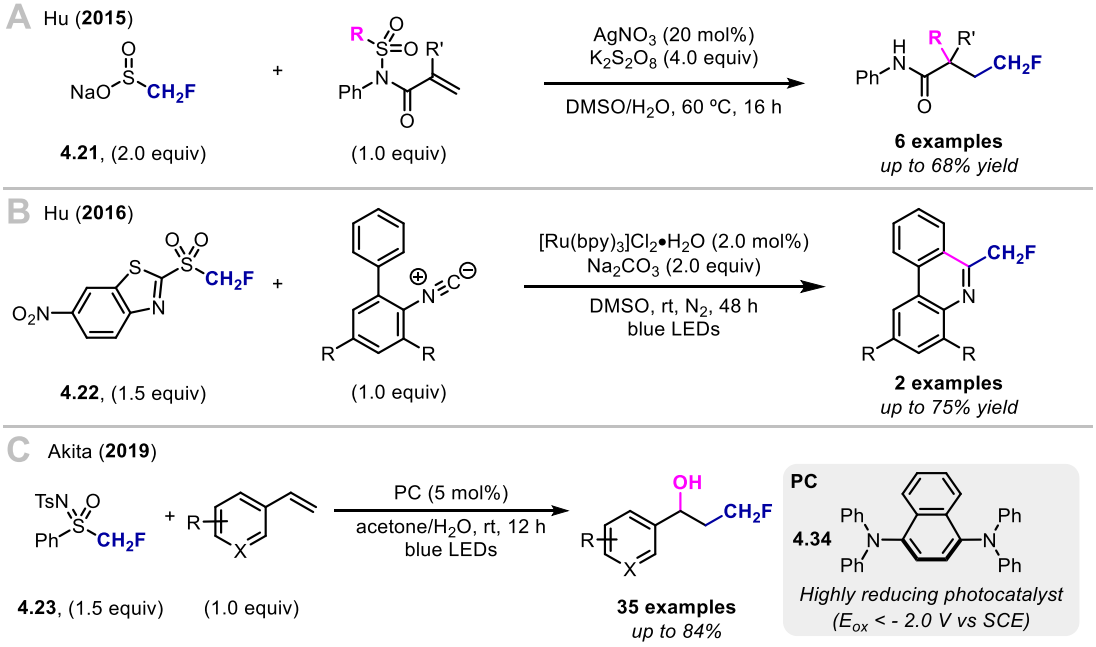
4.2.3 Radical Fluoromethylation of Alkenes

Dolbier and co-workers disclosed the use of fluoromethylsulfonyl chloride (**4.20**) as fluoromethyl radical precursor for the preparation of oxindoles and for the vicinal chlorofluoromethylation of alkenes (**Scheme 4.4A,B**).[61,62] The fluoromethyl radical was generated upon single-electron reduction of the corresponding sulfonyl chloride using a suitable photocatalyst (e.g. *fac*-Ir(ppy)$_3$). Interestingly, the reaction was performed at higher temperatures (105 - 110 °C), compared to the corresponding trifluoromethylation, which occurs at room temperature. This result showcases that the generation of fluoromethyl radicals can be more challenging and requires harsher reaction conditions in comparison to the generation of other fluoroalkyl radicals. Interestingly, when using fluoromethylsulfonyl chloride **4.20** at room temperature in the context of a fluoromethylation-cyclisation of *N*-benzylacrylamides, SO_2 extrusion was not observed (**Scheme 4.4C**).[63]



Scheme 4.4: Fluoromethylsulfonyl chloride as fluoromethyl radical precursor.

Simultaneously, Hu and co-workers reported the generation of fluoroalkyl radicals from sodium fluoromethanesulfinate **4.21,** a reagent which was prepared from the corresponding benzothiazole sulfone derivative (**Scheme 4.5A**).[64] Similar to Dolbier's work, the difluoromethylation and difluorophenylmethylation of conjugated arylsulfonyl amides proceeded in good yields using mild reaction conditions (i.e. room temperature). However, the introduction of the fluoromethyl radical required higher temperatures (60 °C).



Scheme 4.5: Radical-mediated fluoromethylation of alkenes.

In 2016, Hu and co-workers achieved the direct fluoromethylation of isocyanides from heteroaryl sulfones, avoiding the preparation of sulfinate salts (**Scheme 4.5B**).[65] Under the reaction conditions optimised for the photoredox-catalysed difluoromethylation, the corresponding monofluoromethylation resulted in no desired product. Instead, the development of a new reagent with a lower reduction potential was required to enable monofluoromethylation to occur. This was achieved by introducing a nitro group on the heteroaryl ring (**4.22**).

More recently, Akita and co-workers disclosed a metal-free photocatalytic hydroxyfluoromethylation of styrenes using a sulfoximine-based fluoromethyl radical precursor (**4.23**, **Scheme 4.5C**).[66] Given the high reduction potential of the CH_2F radical precursor **4.23** ($E_{red} = -2.43$V vs SCE in MeCN), the use of a novel and strongly reducing photocatalyst was required (**4.34**, $E_{ox} < -2.0$ V vs SCE).

Compared to the corresponding difluoro- and trifluoromethylation, the reports described above demonstrate that radical fluoromethylation is more challenging and often require harsher reaction conditions, namely high temperatures and strongly reducing photocatalysts. Hence, we became interested in developing a novel methodology that would allow for the hydrofluoromethylation of alkenes under mild reaction conditions and using commercially available reagents.

4.3 Fluoroiodomethane as an Ideal Fluoromethyl Radical Precursor

As part of our growing interest in developing "minimalistic" procedures for the late-stage hydrofluoroalkylation of alkene-containing biologically active molecules, we sought to identify the ideal fluoromethyl radical precursor. To achieve this, we aimed at fulfilling two criterias: 1) the fluoromethyl radical precursor needs to be commercially available and relatively inexpensive; and 2) generation of the corresponding radical would occur under mild reaction conditions and ideally using a metal-free protocol. To address these criteria, we initially examined the fluoromethyl radical precursors described in the literature (**Figure 4.3**, **4.20 - 4.27**). Most of these reagents are either expensive, non-commercial or require multistep synthesis for their preparation.

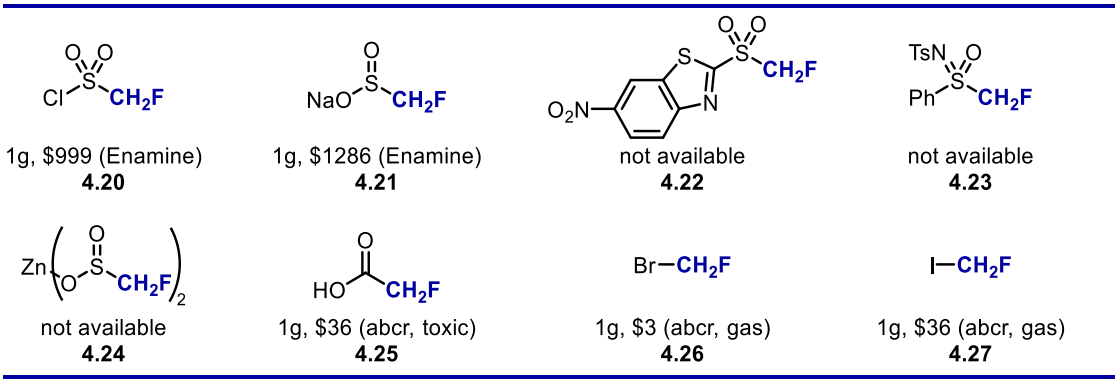
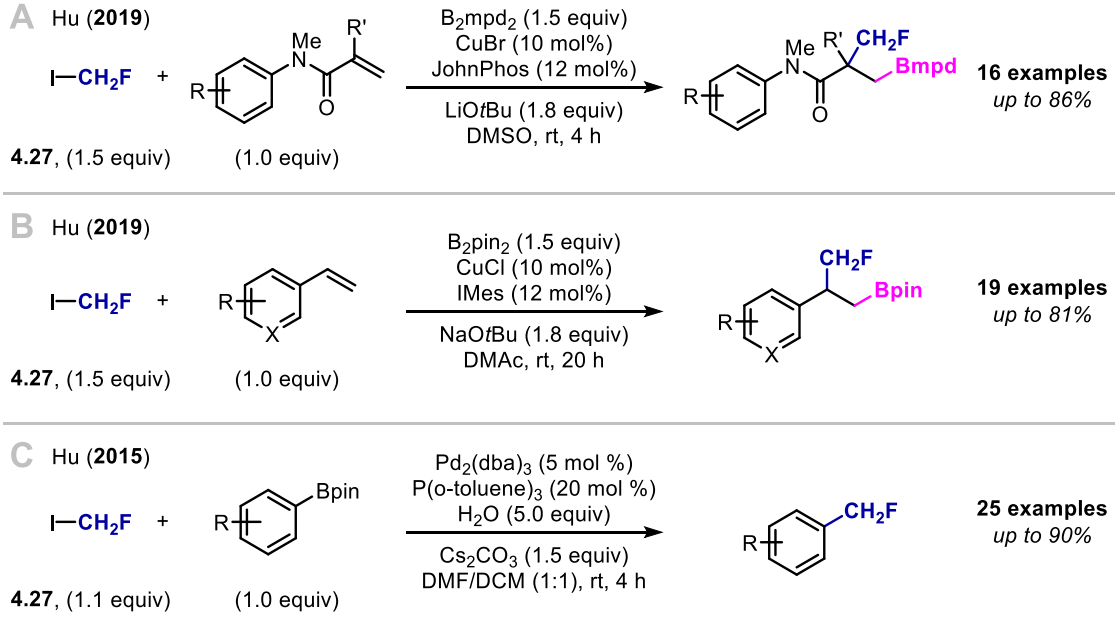


Figure 4.3: Potential fluoromethyl radical precursors.

Encouraged by previous work in our group on the hydrodifluoromethylation[56] and hydrochlorofluoromethylation[57] of alkenes, we considered fluoroacetic acid (**4.25**) as a potential alternative fluoromethyl radical precursor. However, fluoroacetic acid (**4.25**) is notoriously toxic (LD_{50} (FCH_2CO_2Na) = 0.2 mg/kg in rats)[67,68] and therefore, not an ideal reagent. We then focused on the use of inexpensive commercial fluoroiodomethane (**4.27**). In contrast to bromofluoromethane (**4.26**), which is a gas,[69,70] fluoroiodomethane **4.27** represents an ideal reagent as it is easier to handle (b.p. 53.4 °C). Another advantage of this reagent is its accessibility as an ^{18}F reagent for application in PET radiochemistry. Fluoroiodomethane has previously found applications as an electrophilic fluoromethylating reagent, allowing for the direct and chemoselective electrophilic monofluoromethylation of heteroatoms (O-, S-, N-, P-, Se-) under basic conditions.[71] Hu and co-workers also employed fluoroiodomethane **4.27** for the copper-catalysed borylfluoromethylation of electron-deficient alkenes (**Scheme 4.6A**).[72] Compared to previous methods, the CH_2F group was introduced to the more substituted carbon, providing the Markovnikov product. This reaction could also be applied to the borylfluoromethylation of styrenes and unactivated alkenes using bis(pinacolato)diboron, albeit in low yield (**Scheme 4.6B**). This methodology was successfully applied to the preparation of a CH_2F-ibuprofen derivative. Under palladium-catalysed conditions, Hu and co-worker also reported the preparation of

fluoromethylarenes from readily available fluoroiodomethane **4.27** and arylboronic esters, providing a useful method for the formation of C(sp^2)-CH_2F bonds (**Scheme 4.6C**).[73]



Scheme 4.6: Metal-catalysed C-CH_2F bond formation using fluoroiodomethane (**4.27**).

To the best of our knowledge, fluoroiodomethane (**4.27**) has not been explored in the context of radical chemistry. At the onset, we investigated if the direct activation of CH_2FI by single-electron reduction would be feasible. Since the reduction potential of fluoroiodomethane **4.27** has not been reported in the literature, our collaborators at the University of Oxford (Prof. Jason Davis and Xuanxiao Chen) performed cyclic voltammetry measurements of CH_2FI (**Figure 4.4**). From the shape of the voltammetric response, the electrochemical reduction of CH_2FI is irreversible as no anodic peak was observed. The voltammogram reveals a cathodic peak potential (V vs SCE) of – 2.19 V for CH_2FI. This result indicates that the single-electron reduction of CH_2FI is significantly more challenging compared to CF_3I (E_{red} = – 1.22 V vs SCE in MeCN)[74] and therefore, not within reach of common photocatalysts.

Fluoroiodomethane (4.27): *E* (V *vs.* SCE) = − 2.19 V

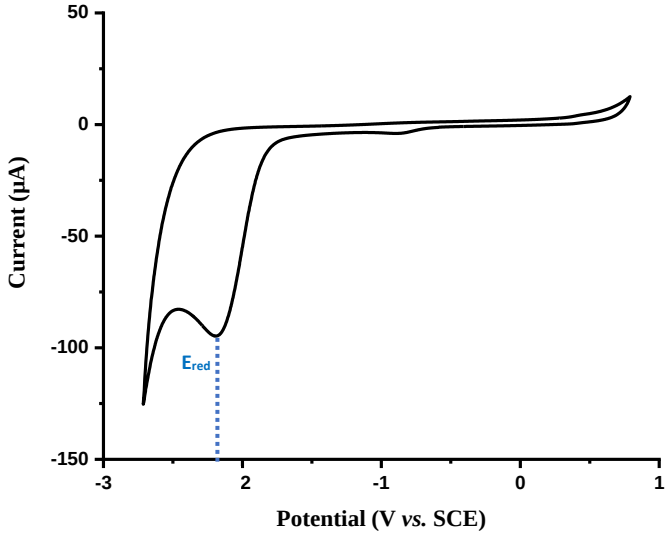


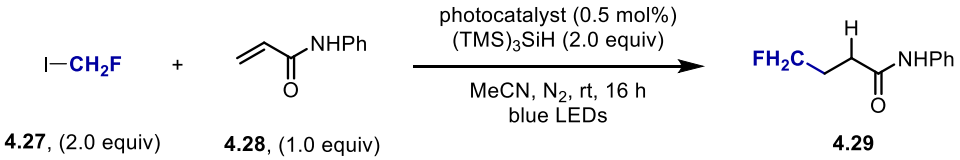
Figure 4.4. Voltammetric response of 3 mM fluoroiodomethane (**4.27**) in anhydrous CH_3CN and 0.1 M $LiClO_4$. Experiment conducted by Xuanxiao Chen.

4.4 Optimisation of the Reaction Conditions

Due to the high absolute reduction potential of fluoroiodomethane (**4.27**), we sought to pursue an alternative mode of activation for the generation of the fluoromethyl radical. Building on our previously disclosed hydrosulfamoylation of electron-deficient alkenes,[75,76] we considered a silyl radical-mediated halogen abstraction for the generation of the fluoromethyl radical from fluoroiodomethane. To test the feasibility of this approach, *N*-phenylacrylamide (**4.28**) was elected as ideal model substrate for reaction development and optimisation, as the formation of the fluoromethylalkane product **4.29** can be detected by its characteristic signal in ^{19}F NMR (**^{19}F NMR** (377 MHz, $CDCl_3$) δ -220.5 (tt, $^2J_{H\text{-}F}$ = 47.4, $^3J_{H\text{-}F}$ = 27.0 Hz)).

We initially exposed **4.28** to the reaction conditions we developed in **Chapter 2**, employing Eosin Y as the photocatalyst, $(TMS)_3SiH$ as the HAD and MeCN as the solvent. After 16 hours, the desired hydrofluoromethylated product **4.29** was obtained in 56% yield (**Table 4.2**, **entry 1**).

Table 4.2: Screening of photocatalysts for the hydrofluoromethylation of *N*-phenylacrylamide (**4.28**).[a]



4.27, (2.0 equiv) **4.28**, (1.0 equiv) **4.29**

entry	photocatalyst	yield[b]
1	Eosin Y	56%
2	*fac*-Ir(ppy)$_3$	76%
3	MesAcrBF$_4$	73%
4	Benzophenone	75%
5	-	71%

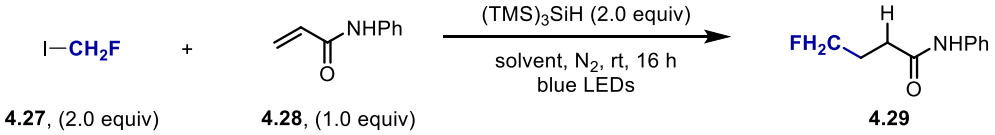
[a] Reaction conditions: **4.27** (0.1 mmol), **4.28** (0.2 mmol), photocatalyst (1.0 mol%), $(TMS)_3SiH$ (0.2 mmol), MeCN (0.6 mL) under nitrogen atmosphere and blue light (λ_{max} = 470 nm) irradiation for 16 hours. [b] The yield was determined by quantitative ^{19}F NMR spectroscopy using α,α,α-trifluorotoluene as the internal standard.

Alternative photocatalysts such as MesAcrBF$_4$, *fac*-Ir(pppy)$_3$ and benzophenone resulted in higher yields (**entries 2-4**). A control experiment revealed that the reaction is also efficient in absence of photocatalyst, yielding the fluoromethyl alkane product **4.29** in 71% (**entry 5**). Aiming at developing an operationally simple and metal-free protocol, we opted to optimise the reaction conditions in the absence of photocatalyst.

The reaction was successful in other polar and non-polar aprotic solvents, such as *N*,*N*-dimethylformamide (DMF), dichloroethane (DCE) or tetrahydrofuran (THF), but in all cases, lower yields were obtained compared to MeCN (**Table 4.3**, **entries 1-4**). The use of DMSO, nitromethane ($MeNO_2$) or trifluorotoluene ($PhCF_3$) resulted in low to no conversion towards the desired product (**entries 5-7**). MeCN was chosen as the optimum

solvent for this transformation, with DMF being a viable alternative for less soluble substrates.

Table 4.3: Screening of solvents for the hydrofluoromethylation of *N*-phenylacrylamide (**4.28**).[a]



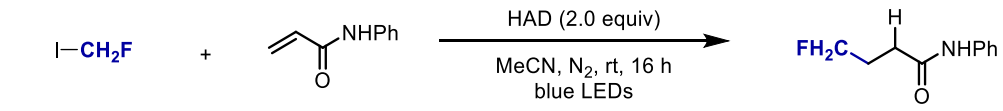
4.27, (2.0 equiv) **4.28**, (1.0 equiv) **4.29**

entry	solvent	yield[b]
1	MeCN	71%
2	DCE	60%
3	THF	55%
4	DMF	68%
5	DMSO	0%
6	$MeNO_2$	17%
7	$PhCF_3$	6%

[a] Reaction conditions: **4.28** (0.1 mmol), **4.27** (0.2 mmol), $(TMS)_3SiH$ (0.2 mmol), solvent (0.6 mL) under blue light (λ_{max} = 470 nm) irradiation for 16 hours. [b] The yield was determined by quantitative ^{19}F NMR spectroscopy using α,α,α-trifluorotoluene as the internal standard.

As with our previous transformations, no other silanes or HAD allowed for efficient hydrofluoromethylation of electron-deficient alkenes (**Table 4.4**, **entries 1-5**), likely due to the higher BDE of these reagents as well as the ineffective activation of CH_2FI (**see Chapter 2**).

Table 4.4: Screening of HAD for the hydrofluoromethylation of *N*-phenylacrylamide (**4.28**).[a]



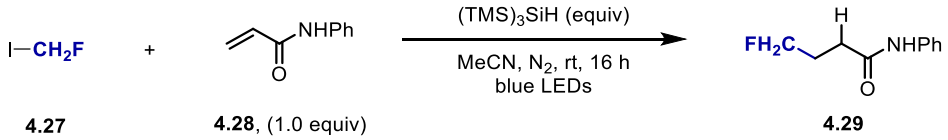
4.27, (2.0 equiv) **4.28**, (1.0 equiv) **4.29**

entry	HAD	yield[b]
1	$(TMS)_3SiH$	71%
2	Ph_3SiH	0%
3	Et_3SiH	traces
4	Hantzsch ester	7%
5	Ph_3CH	0%

[a] Reaction conditions: **4.28** (0.1 mmol), **4.27** (0.2 mmol), HAD (0.2 mmol), solvent (0.6 mL) under nitrogen atmosphere and blue light (λ_{max} = 470 nm) irradiation for 16 hours. [b] The yield was determined by quantitative ^{19}F NMR spectroscopy using α,α,α-trifluorotoluene as the internal standard.

Further screening revealed that the amount on silane could be reduced to 1.2 equivalents, with no drop in yield (**Table 4.5**, **entry 3**). Furthermore 2.0 equivalents of CH_2FI was shown to be optimal for this hydrofluoromethylation protocol (**entries 4-6**).

Table 4.5: Screening of reagent equivalents for the hydrofluoromethylation of *N*-phenylacrylamide (**4.28**).[a]



4.27 **4.28**, (1.0 equiv) **4.29**

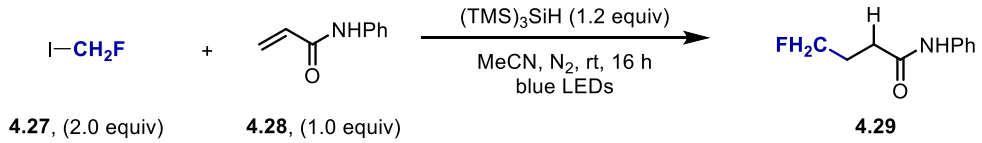
entry	$(TMS)_3SiH$ (equiv)	CH_2FI (equiv)	yield[b]
1	2.0	2.0	71%
2	1.5	2.0	75%
3	1.2	2.0	76% (71%)[c]
4	1.2	1.5	68%
5	1.2	1.0	64%

[a] Reaction conditions: **4.28** (0.1 mmol), **4.27** (x mmol), $(TMS)_3SiH$ (y mmol), solvent (0.6 mL) under nitrogen atmosphere and blue light (λ_{max} = 470 nm) irradiation for 16 hours. [b] The yield was determined by quantitative ^{19}F NMR spectroscopy using α,α,α-trifluorotoluene as the internal standard. [c] Yield of the isolated product is depicted in brackets.

Control experiments revealed that no conversion towards the desired product was observed in absence of $(TMS)_3SiH$ (**Table 4.6**, **entry 1**). This result is in accordance with a silyl radical-mediated activation of fluoroiodomethane for the efficient generation of the fluoromethyl radical. Furthermore, the reaction is drastically hampered in absence of light giving only trace amount of the desired product (**Table 4.6**, **entry 2**). Removal of residual oxygen is not crucial for the reaction to proceed in moderate yield but proved to be beneficial (**Table 4.6**, **entry 3**).

Optimal conditions for the hydrofluoromethylation of electron-deficient alkenes thus employed 2.0 equivalents of CH_2FI (**4.27**), 1.2 equivalents of $(TMS)_3SiH$ and MeCN (0.16 M). The reaction was run at room temperature (using a fan) for 16 h in a SynLED Parallel Photoreactor with a 12 W blue LED lamp (λ_{max} = 470 nm).

Table 4.6: Control experiments for the hydrofluoromethylation of *N*-phenylacrylamide **4.28**.[a]



4.27, (2.0 equiv) **4.28**, (1.0 equiv) **4.29**

entry	conditions	yield[b]
1	no $(TMS)_3SiH$	0%
2	no light	7%
3	no nitrogen	56%

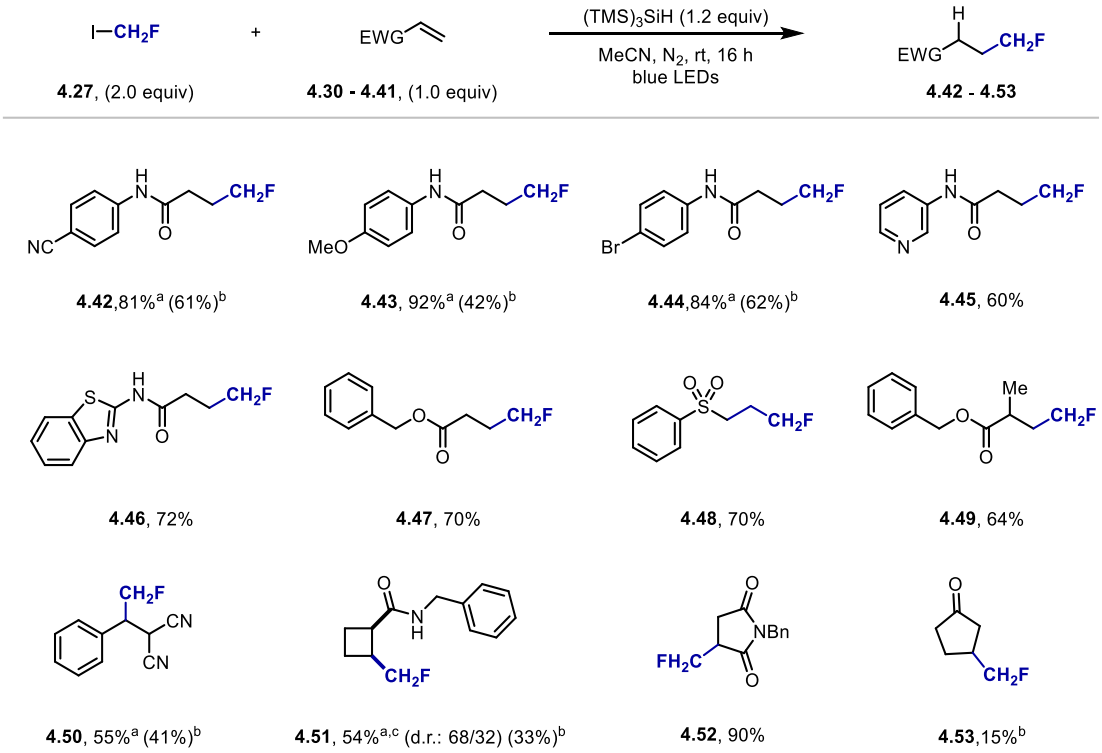
[a] Reaction conditions: **4.28** (0.1 mmol), **4.27** (0.2 mmol), $(TMS)_3SiH$ (0.12 mmol), solvent (0.6 mL) under nitrogen atmosphere and blue light (λ_{max} = 470 nm) irradiation for 16 hours. The yield was determined by quantitative ^{19}F NMR spectroscopy using α,α,α-trifluorotoluene as internal standard.

4.5 Hydrofluoromethylation of Alkenes

4.5.1 Scope of Electron-Deficient Alkenes

With the optimised conditions in hand, we examined the scope of electron-deficient alkenes. Aryl acrylamides bearing electron-withdrawing or electron-donating groups underwent hydrofluoromethylation and gave the corresponding products in good to excellent yields (**Scheme 4.7**, **4.42** - **4.44**). Notably, an aryl bromide was well tolerated, and no side-product resulting from the formation of an aryl radical *via* a silyl radical halogen abstraction was observed (**4.44**).[77] This result demonstrates the chemoselectivity of this transformation, where the silyl radical preferentially abstracts the iodine atom from fluoroiodomethane. In contrast, alkyl iodides undergo competitive silyl radical-mediated iodine atom abstraction under these reaction conditions (see **Chapter 4**, **Section 4.8**). Heteroaryl-containing acrylamides, such as a pyridyl and a benzothiazyl, reacted with high chemoselectivity to produce the desired product in good yields (**4.45**, **4.46**), with no competitive Minisci-type C−H fluoromethylation of the heteroarene.[60] Treatment of other electron-deficient alkenes, such as an acrylic ester and

a vinyl sulfone, under our standard reaction conditions, resulted in 70% yield of the desired products (**4.47**, **4.48**).



4.42,81%[a] (61%)[b] **4.43**, 92%[a] (42%)[b] **4.44**,84%[a] (62%)[b] **4.45**, 60%

4.46, 72% **4.47**, 70% **4.48**, 70% **4.49**, 64%

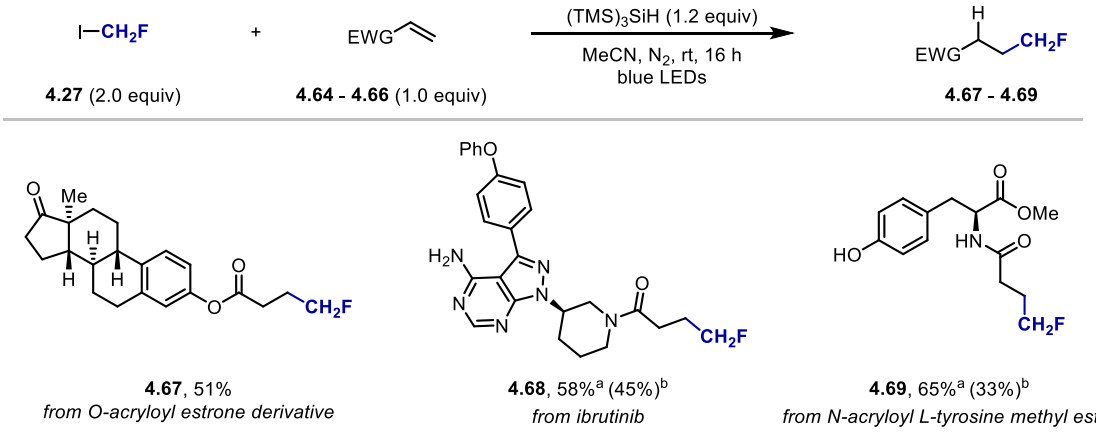
4.50, 55%[a] (41%)[b] **4.51**, 54%[a,c] (d.r.: 68/32) (33%)[b] **4.52**, 90% **4.53**,15%[b]

Scheme 4.7: Substrate scope of the hydrofluoromethylation of electron-deficient alkenes. Reaction conditions: alkene **4.30** - **4.41** (0.5 mmol), $(TMS)_3SiH$ (0.6 mmol), **4.27** (1.0 mmol) in MeCN (3.0 mL), N_2 atmosphere, blue LEDs, room temperature, 16 h. Yields of isolated products. a) The reaction was performed with *fac*-$Ir(ppy)_3$ (0.5 mol%). b) The yield was determined by quantitative ^{19}F NMR spectroscopy using α,α,α-trifluorotoluene as the internal standard (reaction performed in absence of photocatalyst). c) The product was isolated as a mixture of diastereomers.

A representative geminal disubstituted alkene provided the fluoroalkane product **4.49** in slightly lower yield (64%). Trisubstituted alkenes containing two geminal electron-withdrawing groups, such as malononitrile yielded a benzylic fluoromethyl derivative in moderate yield (55%, **4.50**). A cyclobutene carboxamide provided the 1,2-disubsituted cyclobutane product in 54% (**4.51**). The product was isolated as a mixture of diastereoisomers, as separation by silica gel chromatography was not possible. This fluoroalkyl-containing 1,2-disubstituted cyclobutane is of particular interest as similar building blocks previously required 16 steps for their preparation.[78] Furthermore, *N*-benzylmaleimide was a suitable substrate and underwent hydrofluoromethylation in 90%

yield (**4.52**). In contrast, the hydrofluoromethylation of cyclopentenone gave the desired product in low yield (15%, **4.53**). For specific substrates, the addition of the iridium-based photocatalyst *fac*-Ir(ppy)$_3$ (0.5 mol%) resulted in higher yields and easier purification due to full consumption of the starting material.

This strategy was further investigated on the late-stage functionalisation of biologically active molecules (**Scheme 4.8**). Hydrofluoromethylation of an *O*-acryloyl estrone and the anti-cancer drug ibrutinib proceeded in good yields (**4.67**, **4.68**). The successful introduction of the fluoromethyl group in a molecule as complex as ibrutinib demonstrates the tolerance of this transformation.



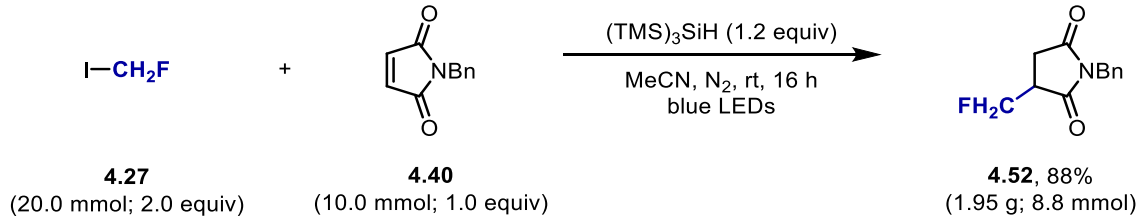
Scheme 4.8: Substrate scope of the hydrofluoromethylation of biologically active molecules. Reaction conditions: Alkene **4.64** - **4.66** (0.5 mmol), $(TMS)_3SiH$ (0.6 mmol), **4.27** (1.0 mmol) in MeCN (3.0 mL), N_2 atmosphere, blue LEDs, room temperature, 16 h. Yields of isolated products. a) The reaction was performed with *fac*-Ir(ppy)$_3$ (0.5 mol%). b) The yield was determined by quantitative ^{19}F NMR spectroscopy using α,α,α-trifluorotoluene as the internal standard (reaction performed in absence of photocatalyst).

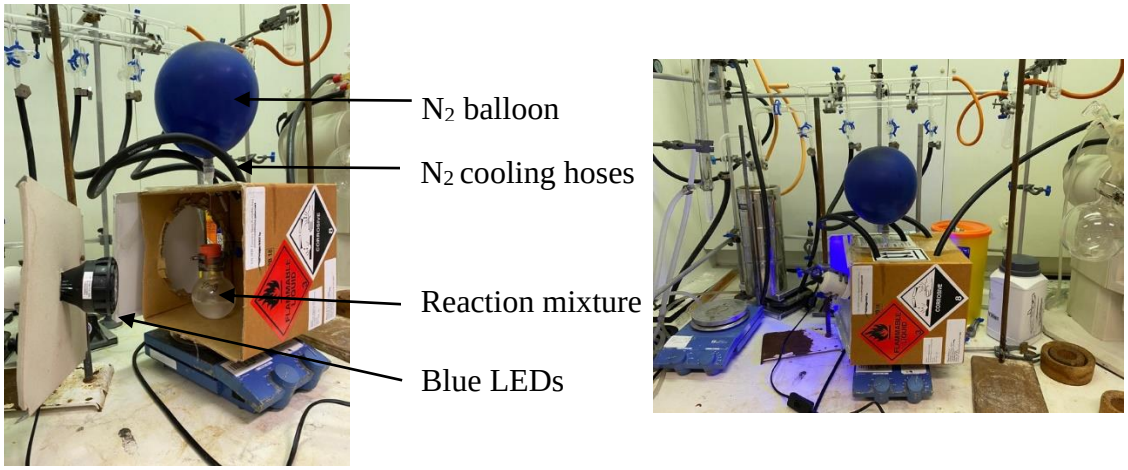
The functionalisation of amino acids is of high importance to drug discovery, allowing for the modification of drug targets and thus improving SAR.[79–83] Our hydrofluoromethylation strategy provides a simple method for incorporating the fluoromethyl group into amino acid derivatives, as witnessed with the successful fluoromethyl radical addition to *N*-acryloyl *L*-tyrosine methyl ester (**4.69**). No fluoromethylether side-product of the phenol ring was observed. The late-stage

hydrofluoromethylation of these drug-like molecules confirms the wide functional group tolerance of this protocol (e.g. ethers, amides, anilines, ketones, esters, phenols). Cyclic alkenes (e.g. cyclopentenone), Michael acceptors bearing ketones, aldehydes, and carboxylic acids were less reactive (less than 20 % yield) under our standard reaction conditions. For such alkenes, either starting material was recovered or hydrosilylation of the alkene was identified as a side product.

4.5.2 Scale-up Experiment

Considering the importance of fluoromethylated building blocks in medicinal chemistry, we sought to investigate if this protocol would be amenable to scale-up (**Scheme 4.9**). We therefore performed a multigram synthesis on the hydrofluoromethylation of **4.40** (10 mmol) for the preparation of **4.52**.





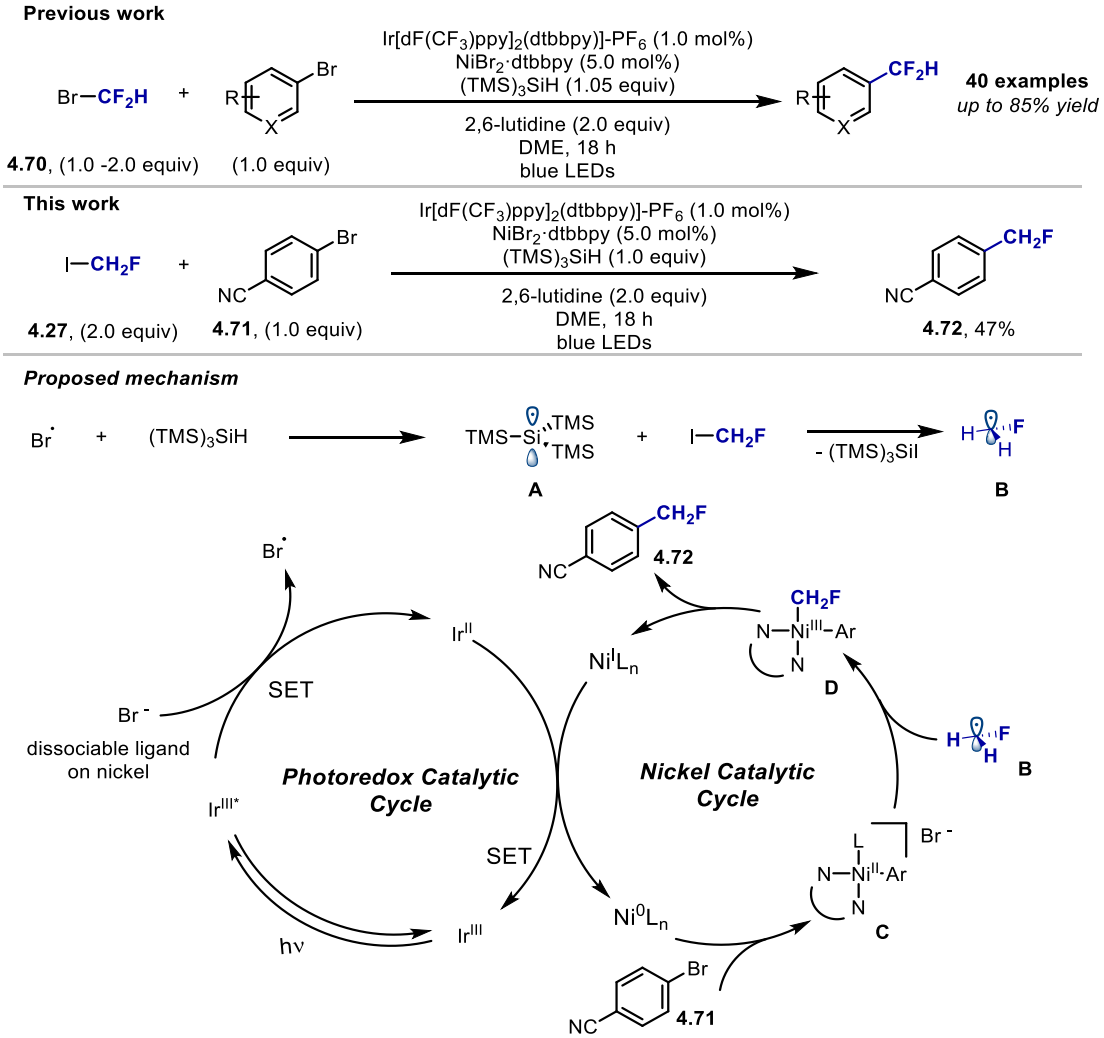
Scheme 4.9: Scale-up experiment of benzyl-3-(fluoromethyl)pyrrolidine-2,5-dione. Yield of isolated product. Experiment conducted by Sebastiano Ortalli.

3-Substituted pyrrolidine-2,5-diones are useful intermediates towards 3-substituted pyrrolidines, a highly desirable substrate class for medicinal chemistry that traditionally requires multi-step synthesis. The reaction was performed in a round bottom flask irradiated by a blue LED light (12 W blue HepatoChem LED lamp, λ_{max} = 470 nm). A cardboard box was added to reduce the light emission into the lab and nitrogen cooling hoses were used to keep the reaction mixture at room temperature. The reaction scaled well and the alkene starting material was fully consumed after 16 hours. Due to the potentially high toxicity of **4.27**, we performed an aqueous work-up to quench ant remaining fluoroiodomethane. Upon purification by silica gel column chromatography, 1.95 g of **4.52** was obtained (88%).

4.5.3 Metallaphotoredox Fluoromethylation of Aryl Bromides

More recently, the merger of photoredox and transition-metal catalysis has appeared as a powerful alternative to traditional C-C cross-coupling reactions.[84,85] Major advances in metallaphoredox catalysis are the mild reaction conditions employed (typically room temperature) allowing for novel and unprecedented disconnections. Encouraged by a previous report from the MacMillan group on the silyl radical-mediated metallaphotoredox difluoromethylation of aryl bromides,[86] we hypothesised that fluoroiodomethane could be employed as a radical precursor for the fluoromethylation of aryl bromides by merging photoredox and nickel catalysis (**Scheme 4.10**). The metallaphotoredox-catalysed fluoromethylation of 4-bromobenzonitrile (**4.71)** afforded product **4.72** in 47% yield. We hypothesised that the reaction would proceed through a mechanism similar to that described by MacMillan and co-workers.[86] Upon blue-light irradiation, the triplet excited state of the iridium photocatalyst (E_{red} (Ir^{III*}/Ir^{II}]= + 1.21 V vs SCE in MeCN) can readily oxidise bromide to the corresponding bromine radical

(E_{ox}= + 0.80 V vs. SCE in DME). The bromine radical can participate in HAT with $(TMS)_3SiH$ to yield a nucleophilic silyl radical **A**, which is then able to undergo iodine atom abstraction from fluoroiodomethane to afford the corresponding fluoromethyl radical **B**. Simultaneously, the aryl bromide undergoes oxidative addition with the Ni^0 catalyst to generate a Ni^{II}–aryl intermediate **C**. At this stage, the fluoromethyl radical **B** is trapped by intermediate **C** to form an aryl–Ni^{III}–CH_2F complex **D**. Upon reductive elimination, the desired fluoromethylarene **4.79** is formed along with a Ni^I species. Finally, the nickel catalyst as well as the photocatalyst are regenerated by single-electron transfer.

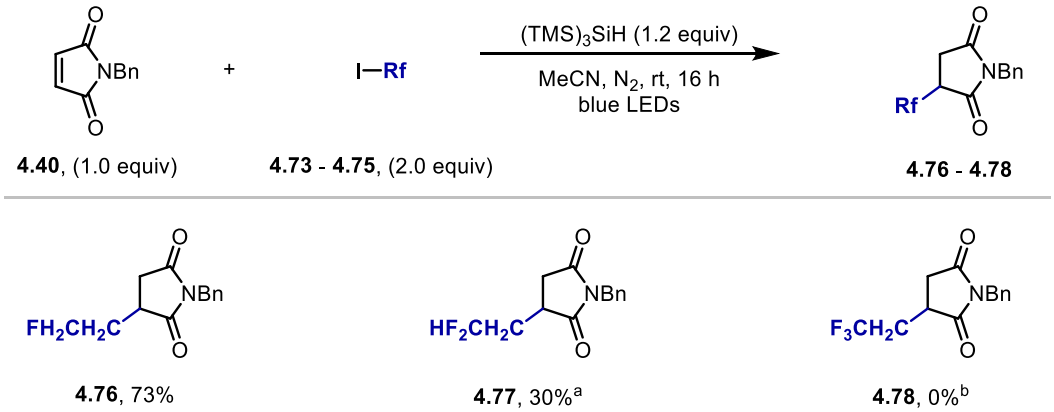


Scheme 4.10: Metallaphotoredox-catalysed fluoromethylation of aryl bromides. Yield of isolated product.

4.6 Generation of Fluorinated Ethyl Radicals

We next turned our attention to the generation of (poly)fluoroethyl radicals under our silyl radical-mediated reaction conditions (**Scheme 4.11**). Trifluoroethyl and difluoroethyl radicals have been previously generated from the corresponding fluoroiodoethane derivatives in the context of alkene functionalisation *via* photoredox catalysis or other metal-catalysed protocols.[87–94] Contrastingly, the generation of the fluoroethyl radical remains underdeveloped.

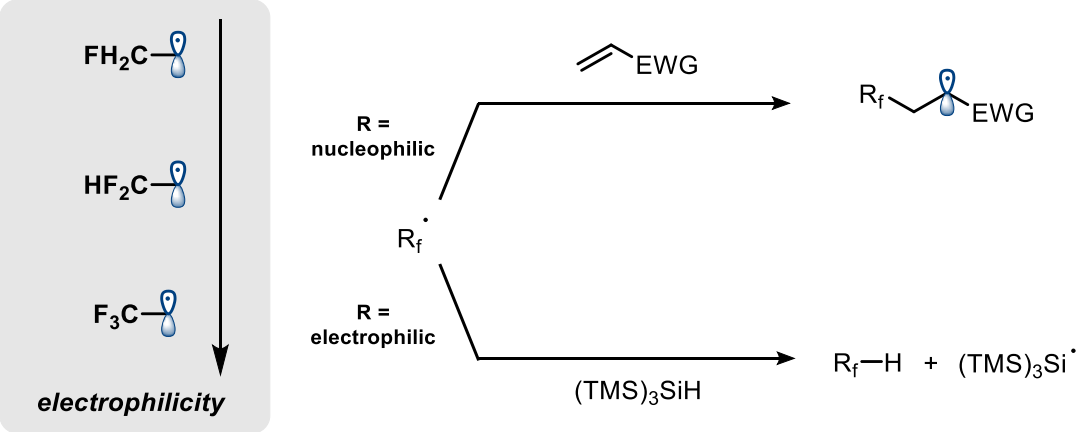
Under our standard reaction conditions, the fluoroethyl radical could be efficiently generated using the same silyl radical activation mode, providing the corresponding hydrofluoroethylated product **4.76** in good yield. The consecutive introduction of more fluorine atoms resulted in a significant loss of reactivity, with only 30% of the difluoroethylated product **4.77** isolated, whereas no reactivity towards the trifluoroethylated product **4.78** was observed.



Scheme 4.11: Substrate scope of the hydrofluoroethylation of *N*-benzylmaleimide **4.40**. Reaction conditions: *N*-benzylmaleimide **4.40** (0.5 mmol), $(TMS)_3SiH$ (0.6 mmol), R_fI **4.73** - **4.75** (1.0 mmol) in MeCN (3.0 mL), N_2 atmosphere, blue LEDs, room temperature, 16 h. Yields of isolated products. a) 44% of CH_3CF_2H observed by quantitative ^{19}F NMR using α,α,α-trifluorotoluene as the internal standard. b) 28% of CH_3CF_3 observed by quantitative ^{19}F NMR using α,α,α-trifluorotoluene as the internal standard.

Owing to the high electronegativity of fluorine ($\chi = 4.0$),[10] the difluoroethyl radical ($\Sigma\chi = 17.2$) is expected to be slightly more electrophilic than the fluoroethyl radical ($\Sigma\chi =$

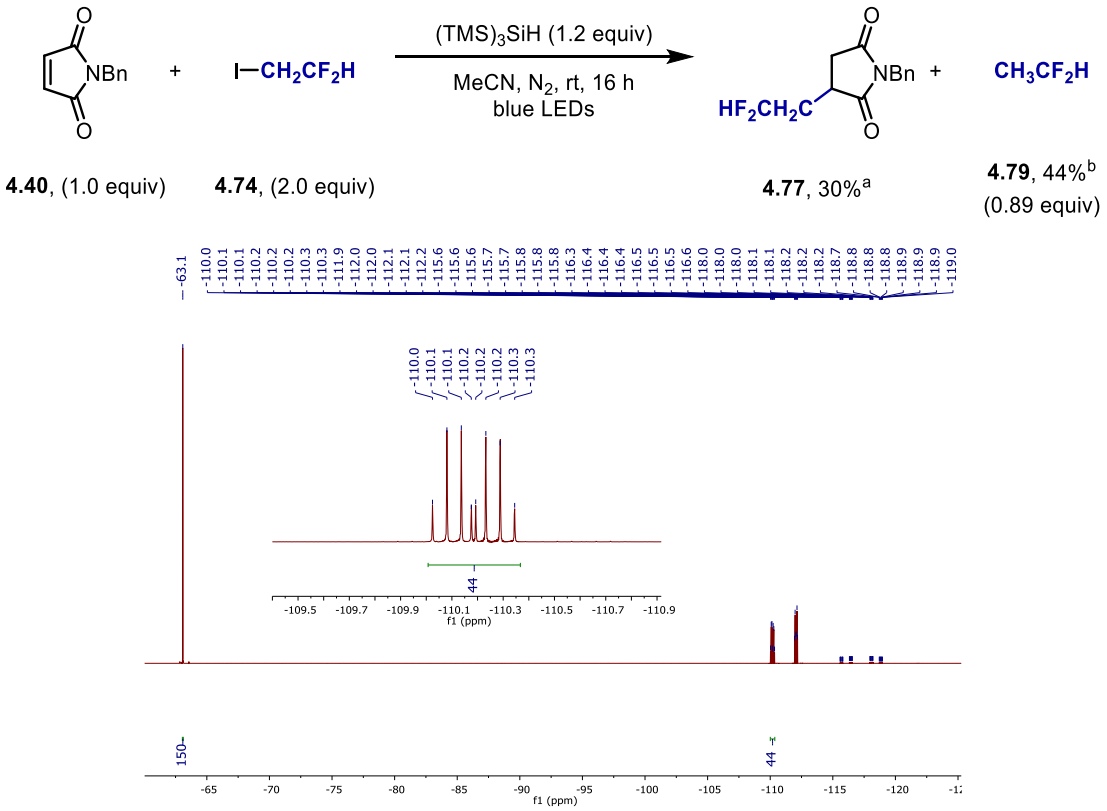
15.4), and similarly with the trifluoroethyl radical ($\Sigma\chi$ = 19.0) being more electrophilic than the difluoroethyl radical. In this transformation, two challenges have been identified for the addition of fluoroethyl radicals to *N*-benzylmaleimide (**Scheme 4.12**).



Scheme 4.12: Reactivity of fluoroethyl radicals.

The first challenge relies on a polarity match between the radical and the electron-deficient alkene in the Giese addition step; nucleophilic radicals undergo faster addition to an electron-deficient alkene than electrophilic radicals. It is therefore expected that the addition of the trifluoroethyl radical to an electron-deficient alkene would be more challenging. Furthermore, the *in situ* generated electrophilic radicals could undergo competitive HAT with the nucleophilic $(TMS)_3SiH$, quenching the reactive radical and forming the corresponding fluoroethane derivative.

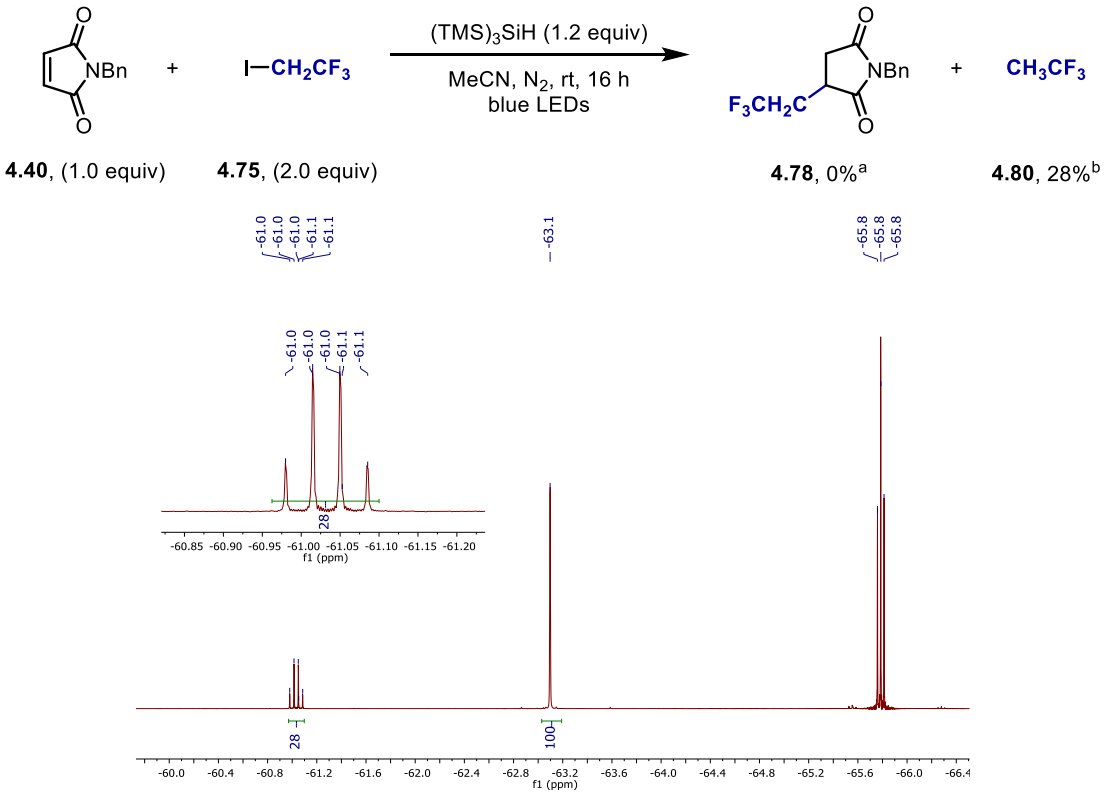
Analysis of the crude reaction mixtures by quantitative ^{19}F NMR spectroscopy (using α,α,α-trifluorotoluene as the internal standard) showed evidence of HAT (**Scheme 4.13**). With regard to the difluoroethyl radical, 0.89 equivalents of the reduced radical, difluoroethane **4.79**, was observed. Specifically, a characteristic doublet of quartets was identified (**^{19}F NMR** (377 MHz, $CDCl_3$) δ -110.2 (dq, $^2J_{H\text{-}F}$ = 57.2, $^3J_{H\text{-}F}$ = 21.3 Hz).



Scheme 4.13: Quantitative ^{19}F NMR spectra of the crude reaction mixture using **4.74**. a) Yields of isolated products. b) The yield was determined by quantitative ^{19}F NMR spectroscopy using α,α,α-trifluorotoluene as the internal standard.

Similarly, we examined the crude reaction mixture using trifluoroiodoethane **4.75** as radical precursor (**Scheme 4.14**). A characteristic quartet was assigned to trifluoroethane **4.80**, demonstrating the higher reactivity of trifluoroethyl radicals towards nucleophilic HAD (**^{19}F NMR** (377 MHz, $CDCl_3$) δ -61.0 (q, $^3J_{H\text{-}F}$ = 13.3 Hz). Under these reaction conditions, no desired hydrotrifluoroethylated product was observed, suggesting that the trifluoroethyl radical is too electrophilic and does not undergo Giese addition under our standard reaction conditions.

On the other hand, no side product arising from the reduction of the fluoroethyl radical to fluoroethane was observed. These data confirms that the fluoroethyl radical is more nucleophilic than the difluoro- and trifluoroethyl radicals. Overall, our method offers an attractive metal-free strategy for the introduction of fluoroethyl and difluoroethyl groups into electron-deficient alkenes in moderate to good yields.



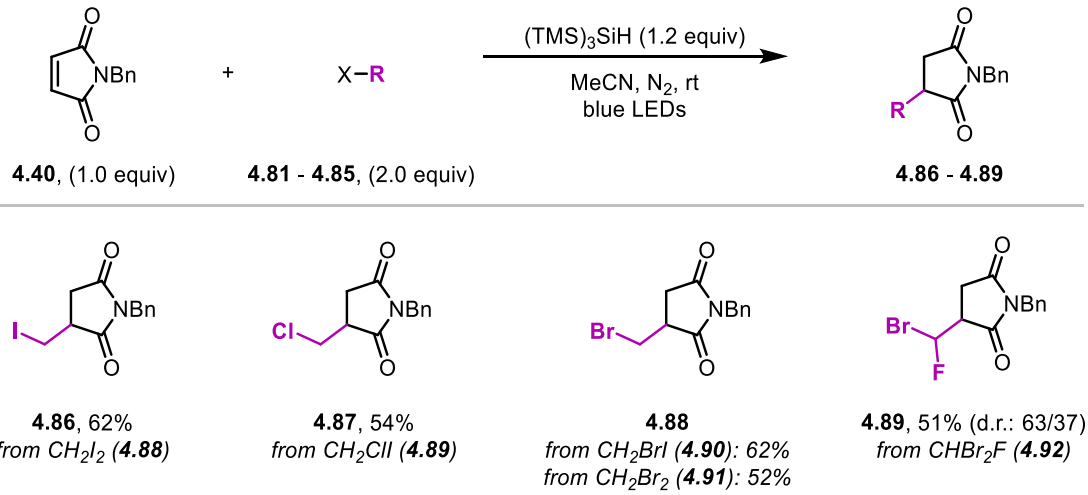
Scheme 4.14: Quantitative ^{19}F NMR spectra of the crude reaction mixture using **4.75**. a) Yields of isolated products. b) The yield was determined by quantitative ^{19}F NMR spectroscopy using α,α,α-trifluorotoluene as the internal standard.

4.7 Generation of Other Halomethyl Radicals

Next, we examined whether other halomethyl derivatives were suitable radical precursors, allowing for the one-step introduction of terminal alkyl halides on alkenes. To date, only few examples have been reported for the generation of other halomethyl radicals.[95–99] Encouraged by our previous work on silyl radical-mediated halogen atom abstraction, we propose herein a streamlined approach for the efficient generation of halomethyl radicals from commercially available and cost-effective reagents (**Scheme 4.15**). When diiodomethane was employed, the iodomethyl radical was efficiently generated and added to *N*-benzylmaleimide, affording the desired iodomethylated product **4.86** in 62% yield. The iodomethyl radical has previously been generated from diiodomethane in the context of a cyclopropanation reaction of substituted styrenes

reported by Suero and co-workers.[95,96] Notably, only one example using an α-substituted styrene afforded the corresponding hydroiodomethylated product in low yield. Our protocol offers an attractive metal-free and operationally simple alternative for the introduction of the iodomethyl radical on electron-deficient alkenes.

The chloromethyl radical,[97] generated from chloroiodomethane, could also undergo Giese-addition to afford the corresponding chloromethylated products **4.87** in 54%. Interestingly, the corresponding bromomethyl radical could be efficiently generated from two different sources: bromoiodomethane and dibromomethane to afford product **4.88** in similar yields. Furthermore, a bromofluoromethylalkane **4.89** was prepared from dibromofluoromethane in 51% yield.[99] This one-step procedure for the introduction of a wide set of different halomethyl groups is highly advantageous, as all methods available to date rely either on a multistep procedure, on toxic chemicals, or suffer from a limited substrate scope. These haloalkanes could be further employed as reactive synthons for homologation, cross-coupling, organometallic reactions and others.



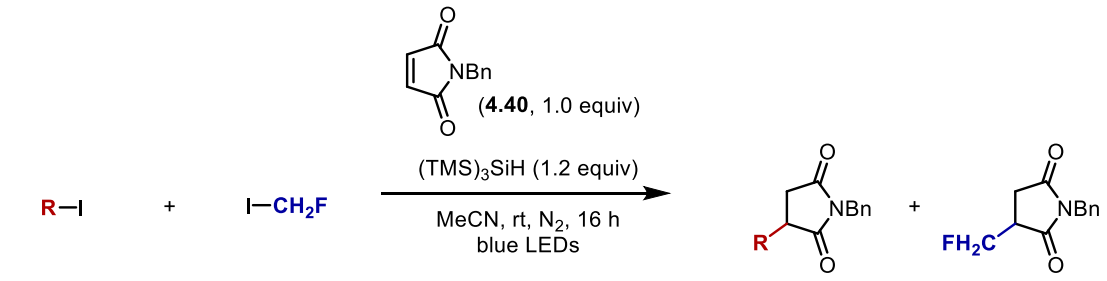
Scheme 4.15: Substrate scope of the hydrohalomethylation of **4.40**. Reaction conditions: **4.40** (0.5 mmol), $(TMS)_3SiH$ (0.6 mmol), radical precursor **4.81** - **4.85** (1.0 mmol) in MeCN (3.0 mL), N_2 atmosphere, blue LEDs, room temperature, 16 h. Yields of isolated products.

These products were unstable under silica gel column chromatography purification and afforded a mixture of the desired product as well as the elimination product (homologated

exo-alkene). To circumvent this issue, fast purification by preparative thin layer chromatography (prep TLC) (using Pentane/Et_2O: 70/30 as eluent) was required to isolate these products in moderate yields.

4.8 Competition Experiment

To compare the reactivity of the fluoromethyl radical with other alkyl radicals, the following competition experiments were carried out using *N*-benzylmaleimide **4.40** as model substrate (**Scheme 4.16**).



Me—I (**4.90**)	vs	I—CH_2F (**4.39**)	25% (**4.94**)	74%
Et—I (**4.91**)	vs	I—CH_2F (**4.39**)	43% (**4.95**)	51%
*i*Pr—I (**4.92**)	vs	I—CH_2F (**4.39**)	62% (**4.96**)	36%
*t*Bu—I (**4.93**)	vs	I—CH_2F (**4.39**)	73% (**4.97**)	19%

Scheme 4.16: Competition experiments subjecting equimolar amount of different alkyl iodides. Reaction conditions: **4.40** (0.5 mmol), $(TMS)_3SiH$ (0.6 mmol), alkyl iodide **4.90** - **4.93** (1.0 mmol), **4.27** (1.0 mmol) in MeCN (3.0 mL), N_2 atmosphere, blue LEDs, room temperature, 16 h. Yields of isolated products.

First, when equimolar amounts (2.0 equivalents) of methyl iodide **4.90** and fluoroiodomethane **4.27** were subjected to the standard reaction conditions, product **4.52** resulting from the fluoromethyl radical addition was obtained in 64% yield, and only 25% of the methylated product **4.94** was observed. This initial result suggests that the fluoromethyl radical is more reactive than the methyl radical under our reaction

conditions. This result is in accordance with literature reports describing the stabilising π-donating effect of fluorine by resonance in the fluoromethyl radical, resulting in a more nucleophilic radical compared to the methyl radical.[9] When the reaction was carried out with ethyl iodide (**4.91**), both products (**4.52** and **4.95**) were isolated in moderate yield, demonstrating the similar reactivity between the ethyl and the fluoromethyl radicals. Additional competition experiments showed that the isopropyl (**4.96**) and *tert*-butyl (**4.97**) adducts were formed preferentially to the fluoromethylated product. Together, these results suggest that under our reaction conditions the reactivity of these alkyl iodides decreases in the following order: ***t*BuI > *i*PrI > CH_2FI > EtI > MeI**.

4.9 Robustness Screening

The synthesis of structurally complex molecules is a costly, timely and challenging procedure. This process often involves iterative screening and optimisation of reactions for the successful preparation of a single compound. Although powerful synthetic reactions have been developed in recent years for the late-stage functionalisation of complex molecules,[100] medicinal chemists noticed a high risk of failure at the late-stage of a multistep synthesis. Commonly, new synthetic procedures reported by academic groups showcase high yielding transformations, albeit with poor functional group tolerance. In some cases, these methodologies are not compatible with functional groups that are commonly found in medicinal chemistry, such as heterocycles and polar functionalities (acidic and basic). To address this challenge, Glorius and co-workers disclosed in 2013 a robustness screen, enabling the rapid assessment of functional group tolerance of a given chemical reaction.[101,102] This approach is of particular interest to medicinal chemists, who strive to predict the compatibility of complex scaffolds. The

concept is operationally simple and consists of adding one molar equivalent of an additive containing a specific chemical functionality or structural motif. The outcome of the reaction is assessed by determining the yield of the desired transformation and thus evaluating the tolerance of the reaction towards given functionalities. The result is quantified by the functional group robustness factor:

$$\textbf{Robustness factor}: 100\ x\ \frac{Yield\ in\ presence\ of\ additive}{Yield\ in\ absence\ of\ additive}$$

Given the relevance of our hydrofluoromethylation to drug discovery, we conducted a robustness screening to evaluate the likely success of our transformation in presence of a variety of pharmacophores and reactive functional groups, commonly found in drug-like molecules (**Figure 4.5**).

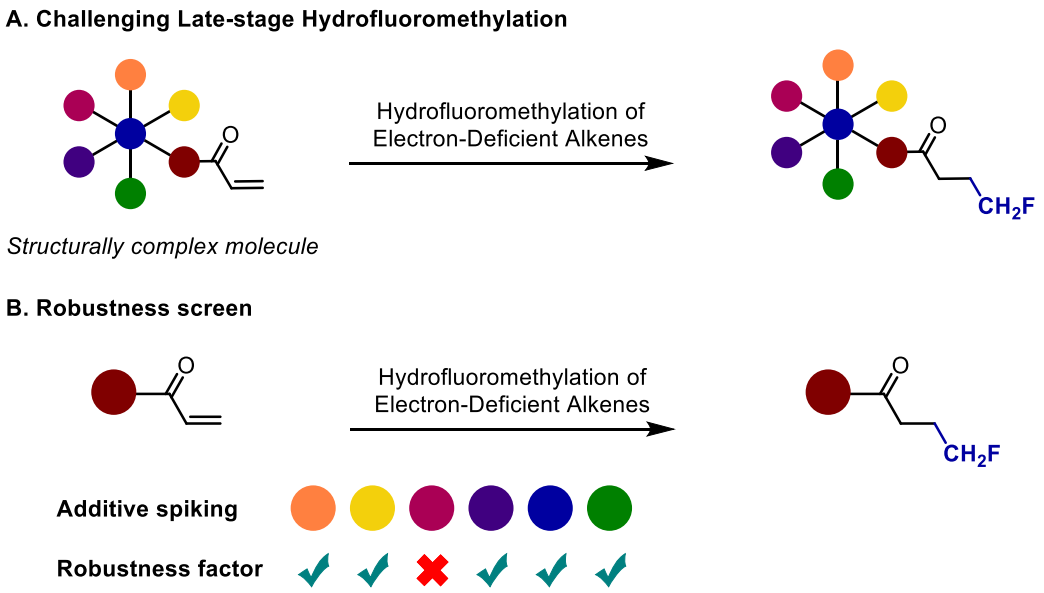
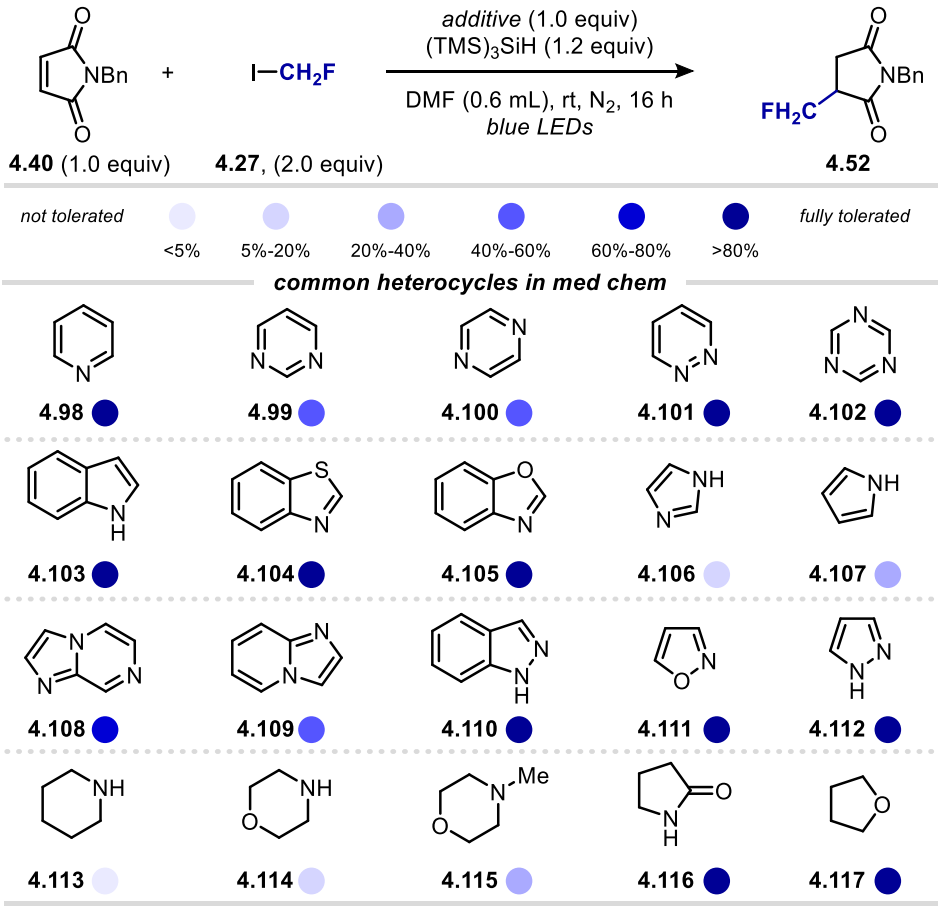


Figure 4.5: A. Challenging late-stage hydrofluoromethylation of a structurally complex molecule. B. Robustness screen allowing for the assessment of the functional group tolerance of this transformation.

The screening was performed by spiking one equivalent of an additive, such as a heterocycle (**Scheme 4.17**), or a molecule containing a specific functional group (**Scheme 4.18**) under our standard reaction conditions. Due to the relevance of amino acid functionalisation in medicinal chemistry, we also performed a robustness screen on

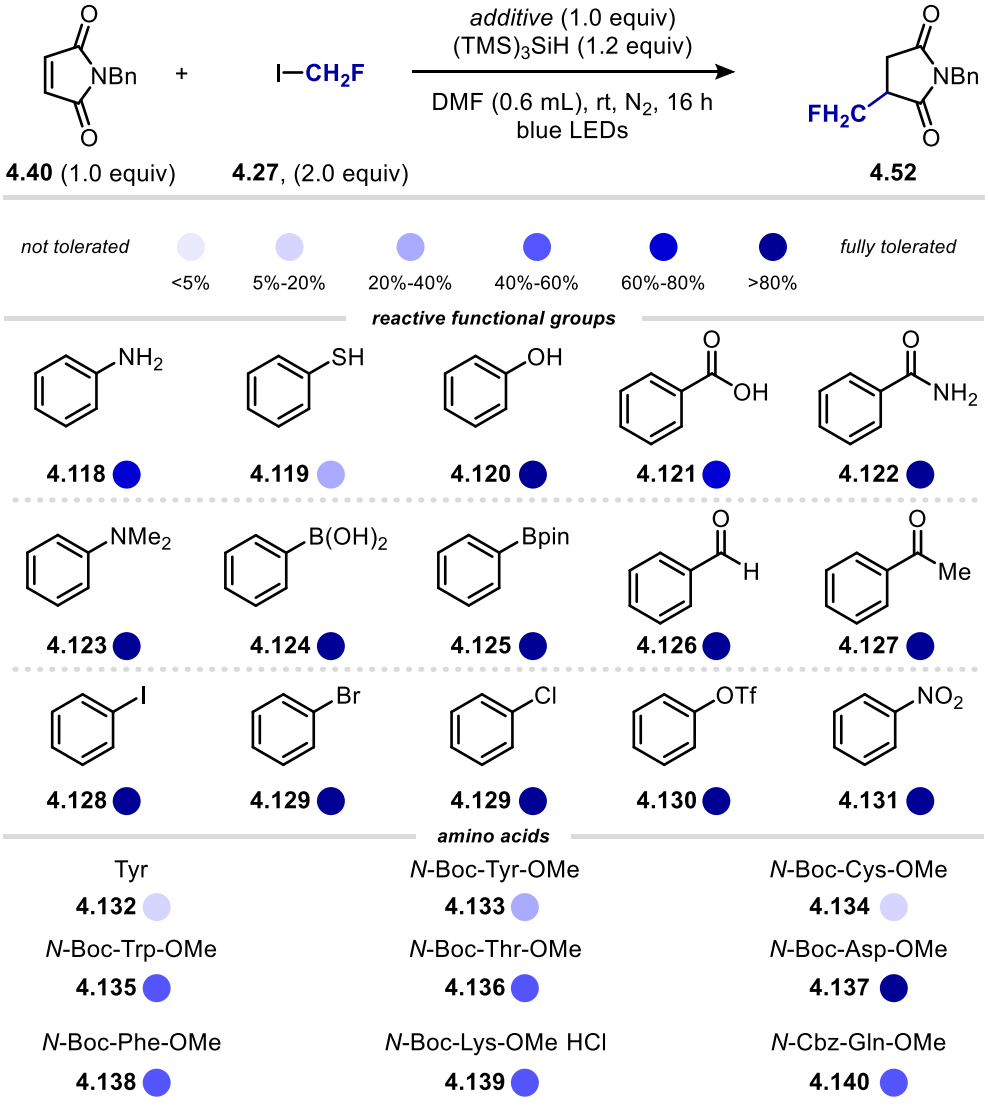
a range of amino acids (**Scheme 4.18**). In contrast to our standard reaction conditions, screenings were performed in DMF to allow for homogenous reaction mixtures. All reactions were performed on 0.1 mmol scale of model substrate **4.40** and the crude reaction mixtures were analysed by quantitative ^{19}F NMR using α,α,α-trifluorotoluene as the internal standard.



Scheme 4.17: Robustness screen on common heterocycles in medicinal chemistry. Reaction conditions: **4.40** (0.1 mmol), $(TMS)_3SiH$ (0.12 mmol), **4.27** (0.2 mmol), additive **4.98** - **4.117** (0.1 mmol) in DMF (0.6 mL), N_2 atmosphere, blue LEDs, room temperature, 16 h.

Initially, we exposed our model reaction to common heterocycles in medicinal chemistry (**Scheme 4.17**). Pyridine (**4.98**), pyridazine (**4.101**), 1,3,5-triazine (**4.102**), indole (**4.103**) or benzo-thiazole and oxazole (**4.104, 4.105**) were broadly tolerated and did not significantly affect the outcome of the reaction. However, other heteroarenes, such as imidazole (**4.106**) and pyrrole (**4.107**) prevented partly the hydrofluoromethylation of our model substrate. Other fused (**4.108** - **4.110**) and five-membered heterocycles (**4.111**,

4.112, **4.116**, **4.117**) were well tolerated. However, cyclic aliphatic amines, like piperidine (**4.113**), morpholine (**4.114**) or *N*-methyl morpholine (**4.115**) resulted in lower yields. We speculated that this reduced yield is partially due to the nucleophilicity of the nitrogen, which can readily attack and consume the reagent, fluoroiodomethane, as similar reactions have been described in the literature.[103] Although cyclic aliphatic amines are not that well tolerated, the broad tolerance to the other heterocycles is substantial, particularly considering the ubiquity of these motifs in drug discovery.



Scheme 4.18: Robustness screen on reactive functional groups and amino acids. Reaction conditions: **4.40** (0.1 mmol), $(TMS)_3SiH$ (0.12 mmol), **4.27** (0.2 mmol), additive (0.1 mmol) in DMF (0.6 mL), N_2 atmosphere, blue LEDs, room temperature, 16 h.

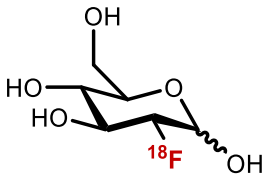
Next, we investigated the tolerance of reactive functional groups commonly found in complex molecules (**Scheme 4.18**). All functionalities, including primary and secondary amines (**4.118**, **4.123**), alcohol (**4.120**), carboxylic acid (**4.121**), amide (**4.122**), boronic acid (**4.124**), ester (**4.125**), aldehyde (**4.126**), ketone (**4.127**), halogens (**4.128 - 4.129**), as well as triflate (**4.130**) and nitro groups (**4.131**) were extremely well tolerated, with little to no effect on the reaction yield. Thiols (**4.119**), however, significantly reduced the reaction yield, presumably due to its nucleophilic character. Finally, we were also interested in investigating the tolerance of amino acids under our reaction conditions (**Scheme 4.18**). The data collected demonstrated that unprotected amino acids, such as *L*-tyrosine (**4.132**) for example, are not well tolerated by the reaction conditions. In contrast, reactions in the presence of fully protected (protection of the carboxylic acid and the amine) amino acids proceeded in higher yields. Most amino acids, except cysteine derivatives (**4.134**), gave the desired product in moderate to excellent yield.

The hydrofluoromethylation of ibrutinib **4.65** and *N*-acryloyl *L*-tyrosine methyl ester **4.66**, which gave the desired products in 58% and 64% respectively, correlate with our robustness screen, as complex fused heterocycles (e.g. 1*H*-pyrazolo[3,4-d]pyrimidin-4-amine), phenols and protected amino acids were shown to be tolerated under our reaction conditions. Potential side reactivity of the additive during the reaction was not assessed in this screening. These experimental robustness data provide an overview of the heterocycles, functional groups or amino acids that are likely to be tolerated under our reaction conditions. This screening demonstrates that our methodology is robust enough to be considered as a valuable transformation for the chemoselective late-stage hydrofluoromethylation of complex molecules.

4.10 ^{18}F-Fluoromethylation of Alkenes

4.10.1 Introduction to PET Imaging

Positron emission tomography (PET) is a non-invasive and quantitative imaging technique which allows for the *in vivo* analysis of biological events.[22,23,104] This detection method is often used in oncology, neuroscience, and cardiology.[104–106] It is also employed in drug discovery for the quantification of pharmacodynamic and pharmacokinetic properties of lead candidates. To date, most radiopharmaceutical tracers have employed F-18 and C-11 as positron-emitting radioactive isotopes. Owing to the shorter half-life of C-11 ($t_{1/2}$ = 20.4 min), F-18 ($t_{1/2}$ = 110 min) is a superior radionuclide for PET imaging enabling the synthesis of multiple patient doses in one radiosynthesis.[105] The most widely used ^{18}F-radiopharmaceutical is [^{18}F]fluoro-2-deoxyglucose ([^{18}F]FDG, **4.141**), which allows for the detection of cancer metastases (**Figure 4.6**).[107,108]



[^{18}F]FDG (4.141)

Figure 4.6: ^{18}F-labeled fluoro-2-deoxyglucose ([^{18}F]FDG).

The principle of PET relies on the detection of radiation emitted from a radiotracer, which is injected intravenously. Fluorine-18 decays by positron (β^+) emission (**Figure 4.7**). The released positron travels a short distance until it annihilates with a free electron. This event leads to the emission of two anti-parallel gamma ray photons. These high energy gamma rays (511 keV) are detected by several rings of detectors in the PET instrument.

Fluorine-18 possesses a low positron energy (633 keV), which results in a high-resolution image of the PET scan.[109] [^{18}F]Fluoride is produced in a cyclotron by bombardment of O-18 enriched water with high energy protons (~18 MeV).[110] The solution of [^{18}F]F^- in ^{18}O-water can then be delivered to chemistry laboratories for the preparation of a given tracer. A typical protocol begins with the trapping of [^{18}F]fluoride on an anion exchange cartridge to remove any radioactive impurities, such as tritium enriched water or transition-metal impurities. [^{18}F]fluoride is then eluted from the cartridge using a solution containing a suitable counter ion to afford most commonly [^{18}F]potassium fluoride ([^{18}F]KF) or [^{18}F]tetraethylammonium fluoride ([^{18}F]TEAF), before engaging in chemical reactions to prepare the radiotracer.

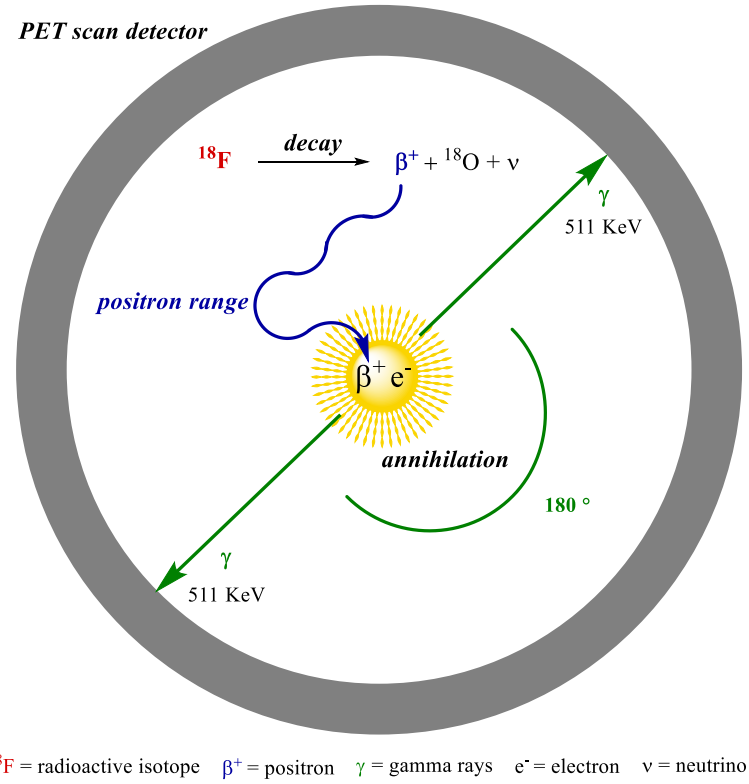


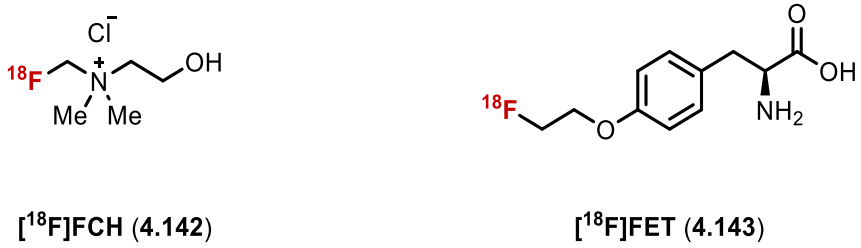
Figure 4.7: Principle of positron emission tomography.

In contrast to traditional ^{19}F reactions, yields in radiochemistry, so-called radiochemical yield (RCY), are therefore always based on the conversion from [^{18}F]fluoride.[111] In the

context of PET imaging, high activity yield (AY, the amount of isolated radioactive product obtained as a ratio of the starting activity) and high molar activity (MA, the ratio of ^{18}F-material to its ^{19}F isotopologue) are highly desirable. These factors enable administration of radiotracers in low doses (preventing pharmacologic side-effects), while still maintaining high quality images. Hence, there is a continuous effort from radiochemists to develop novel synthetic routes that meet these requirements.

4.10.2 ^{18}F-Hydrofluoromethylation of Electron-Deficient Alkenes

Aiming to develop new routes towards the late-stage ^{18}F-labeling of alkenes, we sought to translate our methodology to F-18 radiochemistry using [^{18}F]CH_2FI as the radical precursor. [^{18}F]Fluoroiodomethane as well as other derivatives, such as [^{18}F]fluoroiodoethane and [^{18}F]fluoromethyltosylate, have been widely explored in the context of ^{18}F-alkylation of (thio)phenols and amines.[112–115] The radiolabelling procedure for preparing these reagents is well-established, enabling their application for the synthesis of various ^{18}F-labelled probes. An illustrative example of a radiotracer synthesised *via* ^{18}F-fluoroalkylation is the oncological PET tracer [^{18}F]fluorocholine ([^{18}F]FCH, **Figure 4.8**, **4.142**)[116] as well as the neuro-oncological PET tracer [^{18}F]fluoroethyl-*L*-tyrosine ([^{18}F]FET, **4.143**).[117]

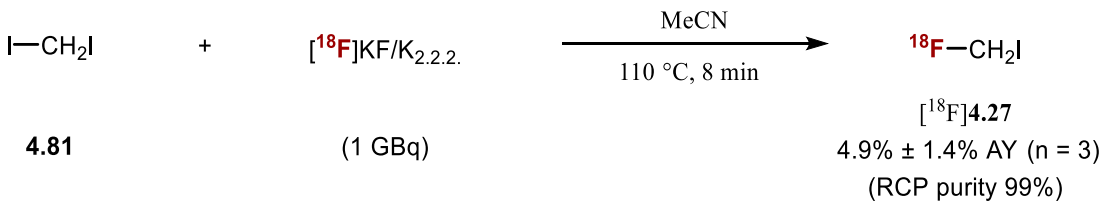


[^{18}F]FCH (4.142) **[^{18}F]FET (4.143)**

Figure 4.8: ^{18}F-Fluoroalkyl radiotracers.

Most importantly, in contrast to radical ^{18}F-reagents available to date,[118–120] [^{18}F]CH_2FI is synthesised in high MA and AY, making this reagent extremely powerful for radical F-18 radiolabeling. Furthermore, the 18F equivalent of this reagent is readily accessible *via* a simple halogen exchange reaction of commercial diiodomethane **4.81**.

[^{18}F]Fluoroiodomethane (**[^{18}F]4.27**) was prepared by reacting diiodomethane **4.81** and [^{18}F]KF in presence of the cryptand kryptofix 2.2.2 ($K_{2.2.2.}$). The cryptand is used to sequester the potassium cation, generating a more reactive fluoride, and increase the solubility of [^{18}F]F^- in organic solvents (**Scheme 4.19**). [^{18}F]Fluoroiodomethane **[^{18}F]4.27** was distilled over a P_2O_5/NaOH cartridge using a polyether ether ketone (PEEK) tubing, into a vessel containing DMF cooled to -20 °C. With this procedure, [^{18}F]**4.39** was obtained in 5% AY and a radiochemical purity (RCP) of 99%.

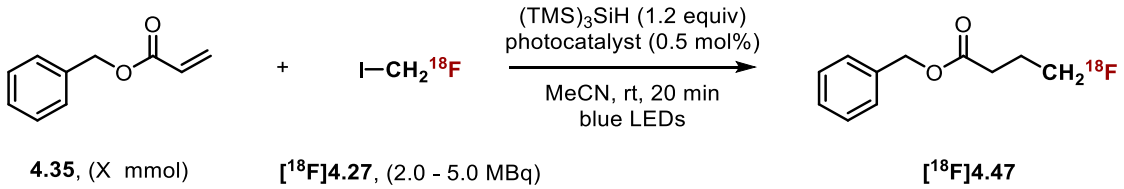


Scheme 4.19: Synthesis of **[^{18}F]4.27** from diiodomethane **4.81**. This reaction was conducted by Claudio F. Meyer with the assistance of Dr. Jeroen Sap.

The key difference between the protocols for ^{19}F- and ^{18}F-hydrofluoromethylation of electron-deficient alkenes relies on the reagent stoichiometry. Whilst fluoroiodomethane is used in excess in ^{19}F-fluorination, the F-18 protocol employs the reagent as a limiting reagent. Preliminary hydrofluoromethylation experiments were conducted using 0.05 mmol of benzyl acrylate **4.35** as model substrate and **[^{18}F]4.27** as radical precursor in MeCN (300 µL) under blue light irradiation. Under the standard reaction conditions, 33% of the desired ^{18}F-hydrofluoromethylated product (**[^{18}F]4.47**) was obtained (**Table 4.7**, **entry 1**). Screening of different photocatalysts revealed that employing *fac*-$Ir(ppy)_3$

slightly improved the RCY to 36% (**entries 3-5**). When the reaction was performed on 0.1 mmol scale the RCY was increased to 70% in presence of the photocatalyst *fac*-Ir(ppy)$_3$ (**entry 6**). Further increasing the substrate loading to 0.2 mmol did not improve the yield (**entries 7**,**8**). Interestingly, the reaction also worked in absence of the iridium photocatalyst in good yield (**entry 9**).

Table 4.7: Optimisation of ^{18}F-hydrofluoromethylation of benzyl acrylate.[a]

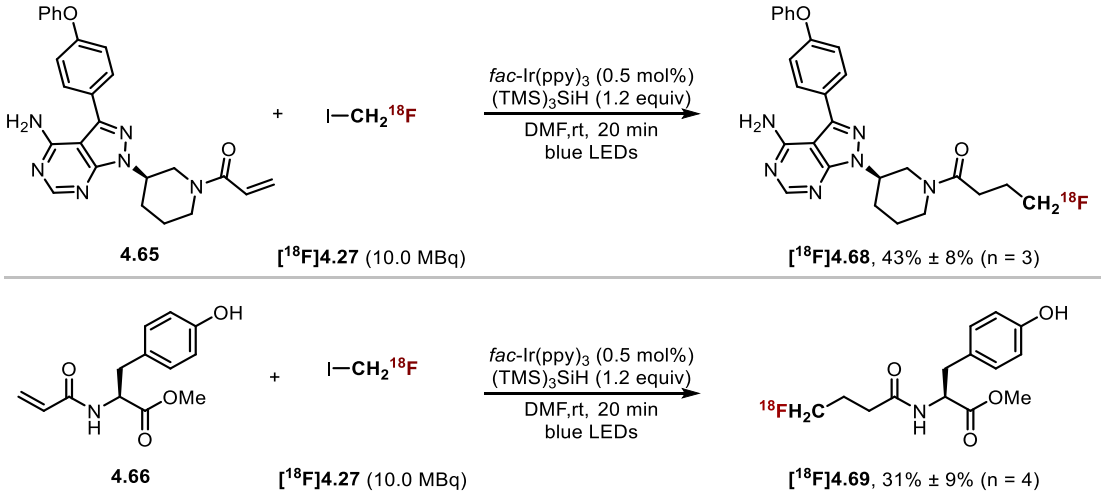


entry	scale (X)	photocatalyst	MeCN	RCY
1	0.05 mmol	-	300 µL	33%
2	0.05 mmol	$MesAcrClO_4$	300 µL	33%
3	0.05 mmol	Eosin Y	300 µL	30%
4	0.05 mmol	*fac*-Ir(ppy)$_3$	300 µL	36%
5	0.1 mmol	*fac*-Ir(ppy)$_3$	600 µL	55%
6[a]	0.1 mmol	*fac*-Ir(ppy)$_3$	600 µL	70%
7[a]	0.1 mmol	*fac*-Ir(ppy)$_3$	1200 µL	62%
8[a]	0.2 mmol	*fac*-Ir(ppy)$_3$	1200 µL	66%
9[a]	0.1 mmol	-	600 µL	68%

[a] Reaction conditions: To a 1.75 mL vial containing benzyl acrylate **4.35** (given mmol), $(TMS)_3SiH$ (1.2 equiv), photocatalyst (0.5 mol%) and MeCN was added freshly distilled [^{18}F]**4.27** (2 MBq in MeCN). The mixture was placed in a photoreactor and irradiated with blue LEDs for 20 min. An aliquot of this mixture was analysed by analytical radio-HPLC. These reactions were conducted by Claudio F. Meyer with the assistance of Dr. Jeroen Sap.

The conditions developed for the ^{18}F-hydrofluoromethylation of electron-deficient alkenes were applied to the anti-cancer agent ibrutinib **4.65** and *N*-acryloyl *L*-tyrosine methyl ester **4.66** (**Scheme 4.20**). Both alkenes underwent ^{18}F-hydrofluoromethylation in moderate RCY ([^{18}F]**4.68,** [^{18}F]**4.69**). The introduction of the [^{18}F]fluoromethyl group has previously been achieved on phenols[115] (*via* electrophilic fluoromethylation) and

arenes[121] (*via* palladium-mediated cross-coupling). Our radical-mediated strategy represents an alternative $C(sp^3)$-$C(sp^3)$ bond disconnection for the introduction of the [^{18}F]fluoromethyl group.

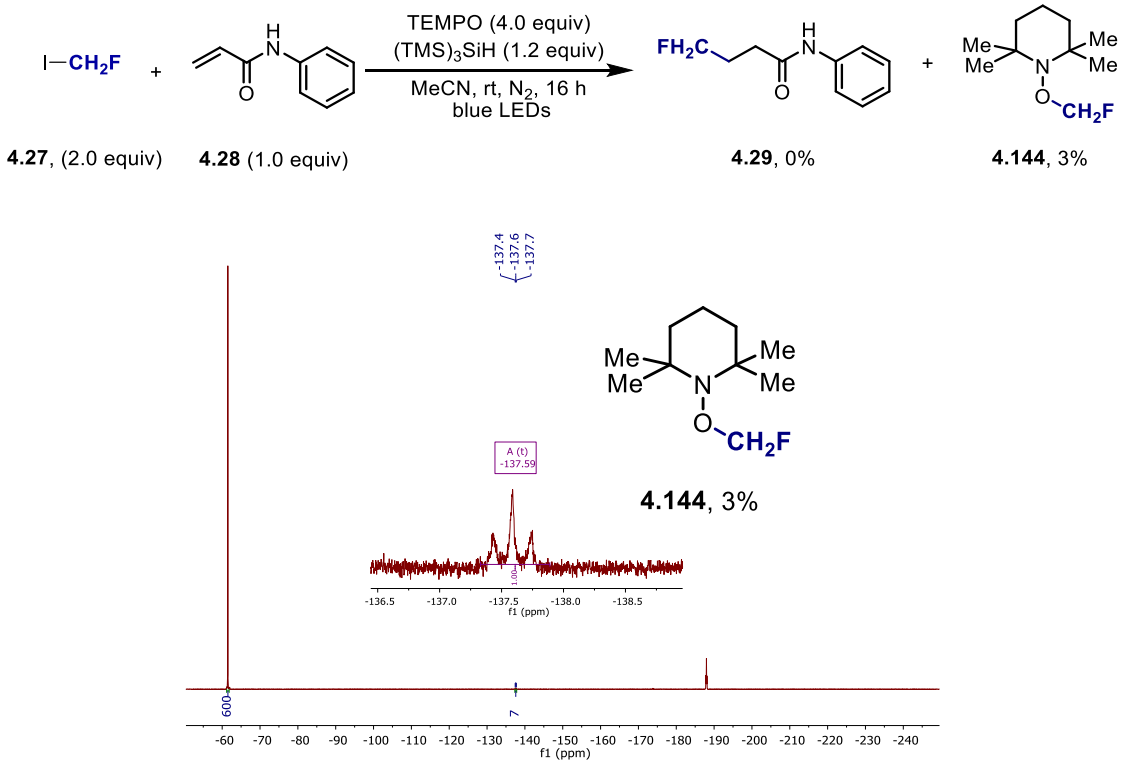


Scheme 4.20: ^{18}F-hydrofluoromethylation of **4.65**. Radiochemical yield calculated on crude mixture *via* radio-HPLC. n = number of reactions. These reactions were conducted by Claudio F. Meyer with the assistance of Dr. Jeroen Sap.

4.11 Mechanistic Investigations

To gain further insight into the mechanism of this transformation, a series of control experiments were pursued. When the radical scavenger TEMPO (4.0 equivalents) was added under our standard reaction conditions, the hydrofluoromethylation did not proceed and the alkene was fully recovered (**Scheme 4.21**). Analysis of the crude reaction mixture by quantitative ^{19}F NMR spectroscopy revealed the presence of a product corresponding to the recombination of the fluoromethyl radical with TEMPO (product **4.144**). A characteristic triplet was observed in the quantitative ^{19}F NMR spectrum (377 MHz, $CDCl_3$) δ -137.6 (t, J = 57.0 Hz). This result advocates in favour of a radical

pathway. As previously disclosed in **Section 4.3**, optimisation of the reaction conditions revealed that no photocatalyst is required for this reaction to proceed in good yield.

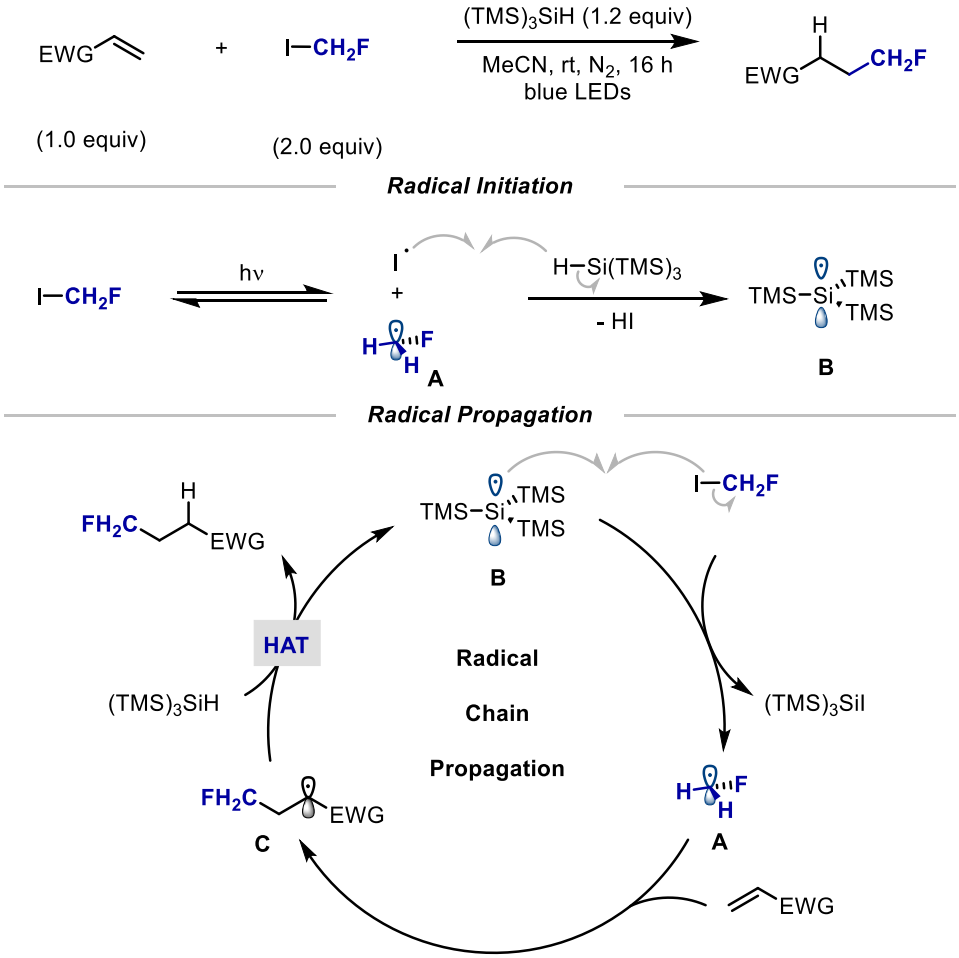


Scheme 4.21: Quantitative ^{19}F NMR spectrum of the TEMPO experiment using α,α,α-trifluorotoluene as the internal standard.

Proposed mechanism

Based on this observation, we suggest that a radical chain propagation mechanism is operating in this transformation. We propose the following reaction mechanism for the hydrofluoromethylation of electron-deficient alkenes (**Scheme 4.22**): upon blue-light irradiation, the reaction is initiated by homolytic bond cleavage of the carbon-iodine bond of fluoroiodomethane to generate trace amounts of the fluoromethyl radical **A**, along with an iodine radical. The latter radical can undergo hydrogen atom abstraction with $(TMS)_3SiH$ to afford hydrogen iodide and the corresponding nucleophilic tris(trimethylsilyl)silyl radical **B**. Subsequent iodine atom abstraction from fluoroiodomethane would then yield radical **A**. This fluoroalkyl radical undergoes Giese-

addition to the electron-deficient alkene and furnishes an electrophilic carbon-centred radical intermediate **C**. HAT between the carbon-centred radical and $(TMS)_3SiH$ affords the desired hydrofluoromethylated product, along with a new silyl radical **B**, which can reinitiate the chain reaction.



Scheme 4.22: Proposed radical chain propagation mechanism for the hydrofluoromethylation of electron-deficient alkenes.

4.12 Limitations

This hydrofluoromethylation protocol is best suited for electron-deficient alkenes. A representative unactivated alkene (**4.145**) was less reactive and afforded only 13% of the desired hydrofluoromethylated product **4.146**. To be applicable to alkenes with different electronic profiles, we sought to investigate polarity reversal catalysis.[122] We initially screened different HAD in the hope to further increase the yield of this transformation. However, the use of a thiol polarity reversal catalyst or other electrophilic HAD only afforded the desired product in trace amounts (**Table 4.8**, **entries 1-6**).

Table 4.8: Screening of HAD for the hydrofluoromethylation of *N*-allyl-4-bromobenzamide **4.145**.[a]



4.145, (1.0 equiv) **4.27**, (2.0 equiv) **4.146**

entry	HAD	yield[b]
1	-	0%
2	$(TMS)_3SiH$	13%
3	Hantzsch ester	0%
4	4-mercaptophenol	traces
5	cyclohexanethiol	traces
6	*N*-hydroxyphtalimide	9%

[a] Reaction conditions: **4.109** (0.1 mmol), **4.39** (0.2 mmol), HAD (0.02 mmol), $(TMS)_3SiH$ (0.2 mmol), solvent (0.6 mL) under nitrogen atmosphere and blue light (λ_{max} = 470 nm) irradiation for 16 hours. [b] The yield was determined by quantitative ^{19}F NMR spectroscopy using α,α,α-trifluorotoluene as internal standard.

Furthermore, styrenes also proved unreactive under our standard reaction conditions and ^{19}F NMR analysis of the crude mixture showed a mixture of various products, potentially resulting from polymerisation side reactions. As mentioned in **Section 4.5**, limitations in the purification process have been observed with non-polar substrates and in case of incomplete conversion of the alkene starting material.

4.13 Conclusion

In conclusion, we have developed the first protocol enabling late-stage radical hydrofluoromethylation of electron-deficient alkenes. CH_2FI has been identified as an ideal fluoromethyl radical precursor, as it is commercially available, not expensive and easy-to-handle. Although the direct single-electron reduction of CH_2FI was identified to be challenging ($E_{red} = -2.19V$ vs SCE in MeCN), an alternative activation mode relying on a silyl radical-mediated halogen abstraction was employed for the generation of the fluoromethyl radical. The utility of this protocol has been demonstrated on a wide range of different electron-deficient alkenes, including complex biological active molecules, such as the anti-cancer agent ibrutinib and *N*-acryloyl *L*-tyrosine methyl ester. This protocol is amenable to multigram synthesis of fluoromethyl building blocks for drug discovery. Our silyl radical-mediated activation of organohalide strategy has been extended to the formation of other halomethyl radicals, allowing for the preparation of terminal alkyl halides on readily available alkenes. These synthons could prove valuable for further functionalisation for various applications.

Further investigations revealed the more nucleophilic character of the fluoroethyl radical, compared to the corresponding difluoroethyl and trifluoroethyl radicals. Additionally, competition experiments demonstrated the similar reactivity between the ethyl and the fluoromethyl radical in the context of hydrofunctionalisation of alkenes.

A robustness screen revealed that this operationally simple protocol tolerates a wide range of heterocycles, functional groups and protected amino acids often present in pharmaceutically relevant molecules. This powerful hydrofluoromethylation protocol has been translated to F-18 radiochemistry for the site-selective ^{18}F-fluoromethylation of alkenes, *via* the *in situ* generation of the $[^{18}F]CH_2F$ radical.

4.14 Future Work

In medicinal chemistry, the methyl group is an important fragment in small molecule drug compounds.[123–125] Nowadays, 70% of the top-selling drugs contain a methyl group, modulating both biological and physical properties.[126] Having illustrated the ability of the tris(trimethylsilyl)silyl radical to efficiently activate a wide set of different organohalides, we sought to investigate next the generation of the methyl radical from methyl iodide, a commercially available, cost-effective, easy-to-handle and readily available reagent in a myriad of radioactive and isotopic labelled forms.[127–131] Owing to the myriad of radioactive and stable isotopically labelled forms of MeI that are readily available, the introduction of the methyl group with many permutations is highly desirable. Cyclic voltammetry experiments revealed a cathodic potential of − 2.39V (vs. SCE in MeCN), suggesting that the single-electron reduction of methyl iodide is even more challenging compared to CH_2FI (E_{red} = − 2.19V vs SCE in MeCN, **Figure 4.9**). We will therefore attempt to implement a silyl radical-mediated iodine abstraction strategy for the methylation of alkenes.

Methyl iodide: *E* (V *vs.* SCE) = − 2.39 V

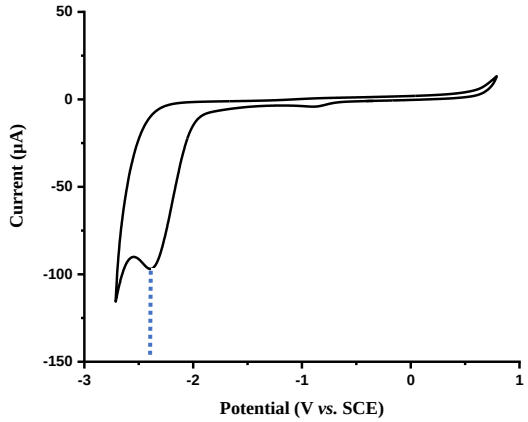


Figure 4.9: Voltammetric response of 3 mM methyl iodide in anhydrous CH_3CN and 0.1 M $LiClO_4$. Experiment conducted by Xuanxiao Chen.

4.15 References

[1] B. M. Johnson, Y. Z. Shu, X. Zhuo, N. A. Meanwell, *J. Med. Chem.* **2020**, *63*, 6315–6386.
[2] M. Cheng, C. Guo, M. L. Gross, *Angew. Chem. Int. Ed.* **2020**, *59*, 5880–5889.
[3] J. Wang, M. Sánchez-Roselló, J. L. Aceña, C. Del Pozo, A. E. Sorochinsky, S. Fustero, V. A. Soloshonok, H. Liu, *Chem. Rev.* **2014**, *114*, 2432–2506.
[4] H. Mei, J. Han, S. Fustero, M. Medio-Simon, D. M. Sedgwick, C. Santi, R. Ruzziconi, V. A. Soloshonok, *Chem. Eur. J.* **2019**, *25*, 11797–11819.
[5] D. E. Yerien, S. Bonesi, A. Postigo, *Org. Biomol. Chem.* **2016**, *14*, 8398–8427.
[6] Y. Zhou, J. Wang, Z. Gu, S. Wang, W. Zhu, J. L. Acenã, V. A. Soloshonok, K. Izawa, H. Liu, *Chem. Rev.* **2016**, *116*, 422–518.
[7] E. P. Gillis, K. J. Eastman, M. D. Hill, D. J. Donnelly, N. A. Meanwell, *J. Med. Chem.* **2015**, *58*, 8315–8359.
[8] J. Wang, M. Sánchez-Roselló, J. L. Aceña, C. Del Pozo, A. E. Sorochinsky, S. Fustero, V. A. Soloshonok, H. Liu, *Chem. Rev.* **2014**, *114*, 2432–2506.
[9] C. Ni, J. Hu, *Chem. Soc. Rev.* **2016**, *45*, 5441–5454.
[10] S. Swallow, *Prog. Med. Chem.* **2015**, *54*, 65–133.
[11] R. K. Hanson, R. M. Spearrin, C. S. Goldenstein, R. K. Hanson, R. M. Spearrin, C. S. Goldenstein, *Spectrosc. Opt. Diagnostics Gases* **2016**, 51–57.
[12] M. B. Van Niel, I. Collins, M. S. Beer, H. B. Broughton, S. K. F. Cheng, S. C. Goodacre, A. Heald, K. L. Locker, A. M. MacLeod, D. Morrison, et al., *J. Med. Chem.* **1999**, *42*, 2087–2104.
[13] P. Shah, A. D. Westwell, *J. Enzyme Inhib. Med. Chem.* **2007**, *22*, 527–540.
[14] B. E. Smart, *J. Fluor. Chem.* **2001**, *109*, 3–11.
[15] S. B. Rosenblum, T. Huynh, A. Afonso, H. R. Davis, N. Yumibe, J. W. Clader, D. A. Burnett, *J. Med. Chem.* **1998**, *41*, 973–980.
[16] N. A. Meanwell, *J. Med. Chem.* **2018**, *61*, 5822–5880.
[17] Y. Zafrani, D. Yeffet, G. Sod-Moriah, A. Berliner, D. Amir, D. Marciano, E. Gershonov, S. Saphier, *J. Med. Chem.* **2017**, *60*, 797–804.
[18] G. A. Patani, E. J. Lavoie, *Chem. Rev.* **1996**, *96*, 3147− 3176.
[19] C. Ballatore, D. M. Huryn, A. B. Smith, *ChemMedChem* **2013**, *8*, 385–395.
[20] C. D. Sessler, M. Rahm, S. Becker, J. M. Goldberg, F. Wang, S. J. Lippard, *J. Am. Chem. Soc.* **2017**, *139*, 9325–9332.
[21] M. G. Campbell, J. Mercier, C. Genicot, V. Gouverneur, J. M. Hooker, T. Ritter, *Nat. Chem.* **2016**, *9*, 1–3.
[22] S. Preshlock, M. Tredwell, V. Gouverneur, *Chem. Rev.* **2016**, *116*, 719–766.
[23] M. Tredwell, V. Gouverneur, *Angew. Chem. Int. Ed.* **2012**, *51*, 11426–11437.
[24] L. Cai, S. Lu, V. W. Pike, *Eur. J. Org. Chem.* **2008**, *2008*, 2853–2873.
[25] M. R. C. Gerstenberger, A. Haas, *Angew. Chem. Int. Ed.* **1981**, *20*, 647–667.
[26] C. L. Liotta, H. P. Harris, *J. Am. Chem. Soc.* **1974**, *96*, 2250–2252.
[27] D. Phillip Cox, J. Terpinski, W. Lawrynowicz, *J. Org. Chem.* **1984**, *49*, 3216–3219.
[28] A. S. Pilcher, H. L. Ammon, P. DeShong, *J. Am. Chem. Soc.* **1995**, *117*, 5166–5167.
[29] T. Liang, C. N. Neumann, T. Ritter, *Angew. Chem. Int. Ed.* **2013**, *52*, 8214–8264.
[30] G. C. Finger, *J. Chem. Educ.* **1951**, *28*, 49–52.
[31] C. N. Neumann, T. Ritter, *Angew. Chem. Int. Ed.* **2015**, *54*, 3216–3221.
[32] X. Li, X. Shi, X. Li, D. Shi, *Beilstein J. Org. Chem.* **2019**, *15*, 2213–2270.
[33] P. A. Champagne, J. Desroches, J. D. Hamel, M. Vandamme, J. F. Paquin, *Chem. Rev.* **2015**, *115*, 9073–9174.
[34] D. E. Yerien, S. Bonesi, A. Postigo, *Org. Biomol. Chem.* **2016**, *14*, 8398–8427.
[35] R. Szpera, D. F. J. Moseley, L. B. Smith, A. J. Sterling, V. Gouverneur, *Angew. Chem. Int. Ed.* **2019**, *58*, 14824–14848.
[36] C. Ni, M. Hu, J. Hu, *Chem. Rev.* **2015**, *115*, 765–825.
[37] X. H. Xu, K. Matsuzaki, N. Shibata, *Chem. Rev.* **2015**, *115*, 731–764.
[38] S. Barata-Vallejo, B. Lantano, A. Postigo, *Chem. Eur. J.* **2014**, *20*, 16806–16829.
[39] A. Studer, *Angew. Chem. Int. Ed.* **2012**, *51*, 8950–8958.
[40] S. Barata-Vallejo, S. M. Bonesi, A. Postigo, *Org. Biomol. Chem.* **2015**, *13*, 11153–11183.
[41] T. Koike, *Asian J. Org. Chem.* **2020**, *9*, 529–537.
[42] H. Egami, Y. Usui, S. Kawamura, S. Nagashima, M. Sodeoka, *Chem. Asian J.* **2015**, *10*, 2190–2199.

[43] A. L. Barthelemy, G. Dagousset, E. Magnier, *Eur. J. Org. Chem.* **2020**, *2020*, 1429–1432.
[44] S. Choi, Y. J. Kim, S. M. Kim, J. W. Yang, S. W. Kim, E. J. Cho, *Nat. Commun.* **2014**, *5*, 1–7.
[45] Y. Cheng, S. Yu, *Org. Lett.* **2016**, *18*, 2962–2965.
[46] T. Koike, M. Akita, *Chem* **2018**, *4*, 409–437.
[47] C. F. Meyer, S. M. Hell, A. Misale, A. A. Trabanco, V. Gouverneur, *Angew. Chem. Int. Ed.* **2019**, *131*, 8921–8925.
[48] S. Mizuta, S. Verhoog, K. M. Engle, T. Khotavivattana, M. O'Duill, K. Wheelhouse, G. Rassias, M. Médebielle, V. Gouverneur, *J. Am. Chem. Soc.* **2013**, *135*, 2505–2508.
[49] J. Rong, C. Ni, J. Hu, *Asian J. Org. Chem.* **2017**, *6*, 139–152.
[50] X. J. Tang, Z. Zhang, W. R. Dolbier, *Chem. Eur. J.* **2015**, *21*, 18961–18965.
[51] B. R. Langlois, E. Laurent, N. Roidot, *Tetrahedron Lett.* **1991**, *32*, 7525–7528.
[52] T. Umemoto, *Chem. Rev.* **1996**, *96*, 1757–1777.
[53] T. Umemoto, B. Zhang, T. Zhu, X. Zhou, P. Zhang, S. Hu, Y. Li, *J. Org. Chem.* **2017**, *82*, 7708–7719.
[54] J. Charpentier, N. Früh, A. Togni, *Chem. Rev.* **2015**, *115*, 650–682.
[55] D. J. P. Kornfilt, D. W. C. MacMillan, *J. Am. Chem. Soc.* **2019**, *141*, 6853–6858.
[56] C. F. Meyer, S. M. Hell, A. Misale, A. A. Trabanco, V. Gouverneur, *Angew. Chem. Int. Ed.* **2019**, *58*, 8829–8833.
[57] C. F. Meyer, S. M. Hell, J. B. I. Sap, A. Misale, A. Peschiulli, D. Oehlrich, A. A. Trabanco, V. Gouverneur, *Tetrahedron* **2019**, 130679.
[58] M. Schwartz, L. R. Peebles, R. J. Berry, P. Marshall, *J. Chem. Phys.* **2003**, *118*, 557–564.
[59] F. O'Hara, D. G. Blackmond, P. S. Baran, *J. Am. Chem. Soc.* **2013**, *135*, 12122–12134.
[60] Y. Fujiwara, J. A. Dixon, F. O'hara, E. D. Funder, D. D. Dixon, R. A. Rodriguez, R. D. Baxter, B. Herlé, N. Sach, M. R. Collins, et al., *Nature* **2012**, *492*, 95–99.
[61] X. J. Tang, C. S. Thomoson, W. R. Dolbier, *Org. Lett.* **2014**, *16*, 4594–4597.
[62] X. J. Tang, W. R. Dolbier, *Angew. Chem. Int. Ed.* **2015**, *54*, 4246–4249.
[63] Z. Zhang, X. J. Tang, W. R. Dolbier, *Org. Lett.* **2016**, *18*, 1048–1051.
[64] Z. He, P. Tan, C. Ni, J. Hu, *Org. Lett.* **2015**, *17*, 1838–1841.
[65] J. Rong, L. Deng, P. Tan, C. Ni, Y. Gu, J. Hu, *Angew. Chem. Int. Ed.* **2016**, *55*, 2743–2747.
[66] N. Noto, T. Koike, M. Akita, *ACS Catal.* **2019**, *9*, 4382–4387.
[67] G. W. Gribble, *J. Chem. Educ.* **1973**, *50*, 460–462.
[68] K. Uneyama, S. Watanabe, Y. Tokunaga, K. Kitagawa, Y. Sato, *Bull. Chem. Soc. Jpn.* **1992**, *65*, 1976–1981.
[69] L. An, Y. L. Xiao, Q. Q. Min, X. Zhang, *Angew. Chem. Int. Ed.* **2015**, *54*, 9079–9083.
[70] J. Sheng, H. Q. Ni, H. R. Zhang, K. F. Zhang, Y. N. Wang, X. S. Wang, *Angew. Chem. Int. Ed.* **2018**, *57*, 7634–7639.
[71] R. Senatore, M. Malik, M. Spreitzer, W. Holzer, V. Pace, *Org. Lett.* **2020**, *22*, 1345–1349.
[72] N. Y. Wu, X. H. Xu, F. L. Qing, *ACS Catal.* **2019**, *9*, 5726–5731.
[73] J. Hu, B. Gao, L. Li, C. Ni, J. Hu, *Org. Lett.* **2015**, *17*, 3086–3089.
[74] Y. Y. Volodin, A. A. Stepanov, L. I. Denisovich, V. A. Grinberg, *Russ. J. Electrochem.* **2000**, *36*, 1026–1028.
[75] S. M. Hell, C. F. Meyer, G. Laudadio, A. Misale, M. C. Willis, T. Noël, A. A. Trabanco, V. Gouverneur, *J. Am. Chem. Soc.* **2020**, *142*, 720–725.
[76] S. M. Hell, C. F. Meyer, A. Misale, J. B. I. Sap, K. E. Christensen, M. C. Willis, A. A. Trabanco, V. Gouverneur, *Angew. Chem. Int. Ed.* **2020**, *59*, 11620–11626.
[77] C. Le, T. Q. Chen, T. Liang, P. Zhang, D. W. C. MacMillan, *Science* **2018**, *360*, 1010–1014.
[78] A. Skreminskiy, D. M. Volochnyuk, O. Oleksandr, *Chem. Eur. J.* **2020**, DOI 10.1016/s0740-5472(96)90021-5.
[79] L. Gentilucci, R. De Marco, L. Cerisoli, *Curr. Pharm. Des.* **2010**, *16*, 3185–3203.
[80] J. Q. Liu, A. Shatskiy, B. S. Matsuura, M. D. Kärkäs, *Synth.* **2019**, *51*, 2759–2791.
[81] M. Imiołek, G. Karunanithy, W. L. Ng, A. J. Baldwin, V. Gouverneur, B. G. Davis, *J. Am. Chem. Soc.* **2018**, *140*, 1568–1571.
[82] J. Dadová, S. Bastien, R. G. Galan, B. G. Davis, *Curr. Opin. Chem. Biol.* **2018**, *46*, 71–81.
[83] T. H. Wright, B. J. Bower, J. M. Chalker, G. J. L. Bernardes, R. Wiewiora, W. L. Ng, R. Raj, S. Faulkner, M. R. J. Vallée, A. Phanumartwiwath, et al., *Science* **2016**, *354*, 597–608.
[84] A. Lipp, S. O. Badir, G. A. Molander, *Angew. Chem. Int. Ed.* **2020**, *59*, doi.org/10.1002/anie.202007668.
[85] J. Twilton, C. C. Le, P. Zhang, M. H. Shaw, R. W. Evans, D. W. C. MacMillan, *Nat. Rev. Chem.* **2017**, *1*, 0052.
[86] V. Bacauanu, S. Cardinal, M. Yamauchi, M. Kondo, D. F. Fernández, R. Remy, D. W. C.

MacMillan, *Angew. Chem. Int. Ed.* **2018**, *57*, 12543–12548.
[87] B. He, Q. Pan, Y. Guo, Q. Y. Chen, C. Liu, *Org. Lett.* **2020**, *22*, 6552–6556.
[88] L. Fritsche, A. Bach, P. Chen, *J. Chem. Phys.* **2018**, *148*, 084306.
[89] Y. Chen, A. Rauk, E. Tschuikow-Roux, *J. Chem. Phys.* **1991**, *94*, 7299–7310.
[90] X. Y. Pan, Y. Zhao, H. A. Qu, J. H. Lin, X. C. Hang, J. C. Xiao, *Org. Chem. Front.* **2018**, *5*, 1452–1456.
[91] N. Yi, H. Zhang, C. Xu, W. Deng, R. Wang, D. Peng, Z. Zeng, J. Xiang, *Org. Lett.* **2016**, *18*, 1780–1783.
[92] R. Adamik, T. Földesi, Z. Novák, *Org. Lett.* **2020**, DOI 10.1021/acs.orglett.0c03043.
[93] L. Li, M. Huang, C. Liu, J. C. Xiao, Q. Y. Chen, Y. Guo, Z. G. Zhao, *Org. Lett.* **2015**, *17*, 4714–4717.
[94] L. M. Kreis, S. Krautwald, N. Pfeiffer, R. E. Martin, E. M. Carreira, *Org. Lett.* **2013**, *15*, 1634–1637.
[95] A. M. del Hoyo, M. García Suero, *European J. Org. Chem.* **2017**, *2017*, 2122–2125.
[96] A. M. del Hoyo, A. G. Herraiz, M. G. Suero, *Angew. Chem. Int. Ed.* **2017**, *56*, 1610–1613.
[97] Q. Zhu, D. G. Nocera, *J. Am. Chem. Soc.* **2020**, *142*, 17913–17918.
[98] S. Bailleux, P. Dréan, Z. Zelinger, S. Civiš, H. Ozeki, S. Saito, *J. Chem. Phys.* **2005**, *122*, 134302 134306.
[99] A. Tressaud, C. Wakselman, *J. Fluor. Chem.* **2001**, *107*, 183–184.
[100] J. Boström, D. G. Brown, R. J. Young, G. M. Keserü, *Nat. Rev. Drug Discov.* **2018**, *17*, 709–727.
[101] K. D. Collins, F. Glorius, *Nat. Chem.* **2013**, *5*, 597–601.
[102] K. D. Collins, A. Rühling, F. Glorius, *Nat. Protoc.* **2014**, *9*, 1348–1353.
[103] X. N. Hua, W. Q. Liao, Y. Y. Tang, P. F. Li, P. P. Shi, D. Zhao, R. G. Xiong, *J. Am. Chem. Soc.* **2018**, *140*, 12296–12302.
[104] P. W. Miller, N. J. Long, R. Vilar, A. D. Gee, *Angew. Chem. Int. Ed.* **2008**, *47*, 8998–9033.
[105] J. I. Andrés, M. Schmidt, *Drug Discov. Today Technol.* **2017**, *25*, 11–17.
[106] M. Piel, I. Vernaleken, F. Rösch, *J. Med. Chem.* **2014**, *57*, 9232–9258.
[107] N. A. Gomzina, D. A. Vasil'ev, R. N. Krasikova, *Radiochemistry* **2002**, *44*, 403–409.
[108] S. Yu, *Biomed. Imaging Interv. J.* **2006**, *2*, e57.
[109] G. B. Saha, W. J. MacIntyre, R. T. Go, *Semin. Nucl. Med.* **1992**, *22*, 150–161.
[110] M. R. Kilbourn, J. T. Hood, M. J. Welch, *Int. J. Appl. Radiat. Isot.* **1984**, *35*, 599–602.
[111] H. H. Coenen, A. D. Gee, M. Adam, G. Antoni, C. S. Cutler, Y. Fujibayashi, J. M. Jeong, R. H. Mach, T. L. Mindt, V. W. Pike, et al., *Nucl. Med. Biol.* **2017**, *55*, 5–11.
[112] L. Zheng, M. S. Berridge, *Appl. Radiat. Isot.* **2000**, *52*, 55–61.
[113] R. Iwata, C. Pascali, A. Bogni, S. Furumoto, K. Terasaki, K. Yanai, *Appl. Radiat. Isot.* **2002**, *57*, 347–352.
[114] T. R. Neal, S. Apana, M. S. Berridge, *J. Label. Compd. Radiopharm.* **2005**, *48*, 557–568.
[115] M. R. Zhang, M. Ogawa, K. Furutsuka, Y. Yoshida, K. Suzuki, *J. Fluor. Chem.* **2004**, *125*, 1879–1886.
[116] C. Stegmayr, G. Stoffels, C. Filß, A. Heinzel, P. Lohmann, A. Willuweit, J. Ermert, H. H. Coenen, F. M. Mottaghy, N. Galldiks, et al., *Nucl. Med. Biol.* **2020**, DOI 10.1016/j.nucmedbio.2020.02.006.
[117] M. E. Rodnick, A. F. Brooks, B. G. Hockley, B. D. Henderson, P. J. H. Scott, *Appl. Radiat. Isot.* **2013**, *78*, 26–32.
[118] S. Verhoog, C. W. Kee, Y. Wang, T. Khotavivattana, T. C. Wilson, V. Kersemans, S. Smart, M. Tredwell, B. G. Davis, V. Gouverneur, *J. Am. Chem. Soc.* **2018**, *140*, 1572–1575.
[119] C. W. Kee, O. Tack, F. Guibbal, T. C. Wilson, P. G. Isenegger, M. Imiołek, S. Verhoog, M. Tilby, G. Boscutti, S. Ashworth, et al., *J. Am. Chem. Soc.* **2020**, *142*, 1180–1185.
[120] L. Trump, A. Lemos, B. Lallemand, P. Pasau, J. Mercier, C. Lemaire, A. Luxen, C. Genicot, *Angew. Chem. Int. Ed.* **2019**, *58*, 13149–13154.
[121] H. Doi, I. Ban, A. Nonoyama, K. Sumi, C. Kuang, T. Hosoya, H. Tsukada, M. Suzuki, *Chem. - A Eur. J.* **2009**, *15*, 4165–4171.
[122] B. P. Roberts, *Chem. Soc. Rev.* **1999**, *28*, 25–35.
[123] Y. Chen, *Adv. Synth. Catal.* **2020**, *362*, 998–1014.
[124] H. Schönherr, T. Cernak, *Angew. Chem. Int. Ed.* **2013**, *52*, 12256–12267.
[125] E. J. Barreiro, A. E. Kümmerle, C. A. M. Fraga, *Chem. Rev.* **2011**, *111*, 5215–5246.
[126] S. Sun, J. Fu, *Bioorganic Med. Chem. Lett.* **2018**, *28*, 3283–3289.
[127] R. D. Finn, T. E. Boothe, M. M. Vora, J. C. Hildner, A. L. M. Emran, P. J. Kothari, *Int. J. Appl. Radiat. Isot.* **1984**, *35*, 323–335.

[128] F. Wuest, M. Berndt, T. Kniess, in *PET Chem.*, **2007**, pp. 183–213.
[129] K. Dahl, C. Halldin, M. Schou, *Clin. Transl. Imaging* **2017**, *5*, 275–289.
[130] R. Bolton, *J. Label. Compd. Radiopharm.* **2001**, *44*, 701–736.
[131] H. Doi, *J. Label. Compd. Radiopharm.* **2015**, *58*, 73–85.

Chapter 5

Experimental and Analysis

5.1 General Informations

All NMR spectra were recorded on a Bruker AVIIIHD 400, Bruker DPX-400 or on a Bruker Avance II HD spectrometer with standard pulse sequences operating at 400 and 500 MHz, respectively, using $CDCl_3$, DMSO-d_6 and Acetone-d_6 as solvent. ^{1}H and ^{13}C NMR spectral data are reported as chemical shifts (δ) in parts per million (ppm) relative to the solvent peak using the Bruker internal referencing procedure (edlock). ^{19}F NMR spectra are referenced relative to $CFCl_3$ in $CDCl_3$. Coupling constants (J) are measured in hertz (Hz). The following abbreviations are used to describe multiplicities s=singlet, d=doublet, t=triplet, q=quartet, quint=quintet, m=multiplet, dd=doublet of doublets, dt=doublet of triplets, td=triplet of doublets, tt=triplet of triplets, br=broad. NMR spectra were processed with MestReNova 11.0 or higher. High resolution mass spectra (HRMS, m/z) were recorded on a Thermo Exactive HighResolution Orbitrap FTMS instrument equipped with Waters Acquity liquid chromatography system using either the heated electrospray (HESI-II) probe for positive electrospray ionization (ESI+); or on a Bruker MicroTOF spectrometer using positive electrospray ionization (ESI). Melting points of solids were measured on a Griffin apparatus and are uncorrected; or on a DSC823^{e} (Differential Scanning Analysis) Mettler Toledo apparatus. Infrared spectra were recorded as the neat compound or in solution using a Bruker tensor 27 FT-IR spectrometer. Absorptions are reported in wavenumber (cm^{-1}). IUPAC names were obtained using the ChemDraw service. Weighing was performed with a 4 decimal place balance. If the purity of the compounds was not satisfying, an analytical sample was further purified by reverse phase HPLC. The yields were determined by isolation on SiO_2 gel column chromatography.

5.2 Experimental Procedures and Characterisation of Compounds from Chapter 2

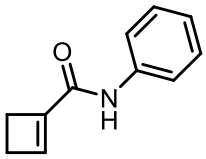
All reactions for the hydrosulfamoylation of electron-deficient alkenes were conducted in non-dried glassware with magnetic stirring. All solvents were used as received without further purification. $(TMS)_3SiH$ was purchased from Sigma-Aldrich, Fluorochem, TCI and Combi-blocks. Eosin Y was purchased from Sigma-Aldrich. Sulfamoyl chlorides were purchased from Sigma-Aldrich, Combi-blocks, ChemBridge and Enamine. Reactions were performed in 7 mL vials in a SynLED Parallel Photoreactor with a 12W blue LED lamp (λ_{max} = 470 nm). The scale-up experiment was performed using two Kessil LEDSs (35W, 450 nm, approximately 5 cm away from the reaction vessel. Additional analytical data (^1H, ^{13}C, ^{19}F, NOESY spectra) are available at https://pubs.acs.org/doi/10.1021/jacs.9b13071.

[a]: Experiments were conducted by Claudio F. Meyer (PhD student, University of Oxford).
[b]: Experiments were conducted by Dr. Gabriele Laudadio (former PhD student in the research group of Prof. Timothy Noël, Eindhoven University, Netherlands).

5.2.1 Synthesis of Starting Materials

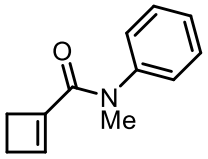
Compounds **2.43**, **2.73**, **2.74**, **2.75**, **2.76**, **2.77**, **2.79**, **2.80**, **2.84**, **2.102**, **2.103**, and **2.105** were synthesised according to literature procedures and spectroscopic data were in accordance with previous reports.[1–6]

***N*-phenylcyclobut-1-ene-1-carboxamide** (**2.104**)



Aniline (502 µL, 5.5 mmol, 1.1 equiv) was added to a solution of cyclobut-1-ene-1-carboxylic acid (490 mg, 5.0 mmol, 1.0 equiv), HATU (2.10 g, 5.5 mmol, 1.1 equiv), and *N*,*N*-diisopropylethylamine (1.75 mL, 10.0 mmol, 2.0 equiv) in DCM (50 mL). The reaction was stirred at room temperature for 16 h, after which time the reaction mixture was diluted with DCM (30 mL) and washed with an aqueous solution of HCl (1M, 30 mL) and brine (sat., 30 mL). The organic layer was dried (Na2SO4), filtered and concentrated *in vacuo*. The crude product was purified by flash chromatography (silica, EtOAc in heptane, 0/100 to 40/60). The desired fractions were collected and concentrated in vacuo to give **2.104** (424 mg, 2.5 mmol, 49%) as a white solid. **^{1}H NMR** (400 MHz, $CDCl_3$) δ 7.61 – 7.54 (m, 2H), 7.46 (br s, 1H), 7.35 – 7.28 (m, 2H), 7.14 – 7.07 (m, 1H), 6.73 (s, 1H), 2.79 (dd, J = 3.1, 2.9 Hz, 2H), 2.51 – 2.47 (m, 2H); **^{13}C NMR** (101 MHz, $CDCl_3$) δ 160.7, 141.8, 137.7, 129.1, 124.4, 120.0, 28.8, 26.2; **HRMS** (ESI-TOF) calculated for $C_{11}H_{12}ON$ $[M+H]^+$: 174.0913; found 174.0911; **IR** (neat) 2981, 1650, 1599, 1579, 1531, 1440, 1384, 1339, 1323, 1253, 1156, 1117, 1076, 1030, 957, 749, 687, 617; **m.p.**: 139 – 143 °C.

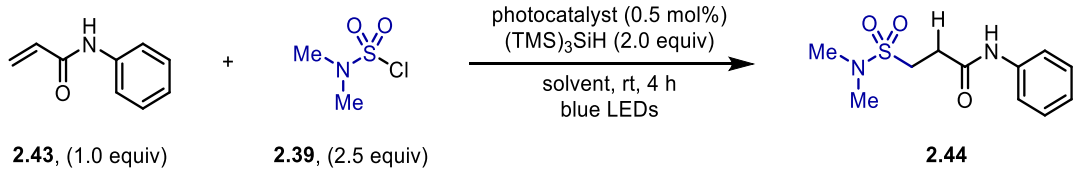
_N_-methyl-_N_-phenylcyclobut-1-ene-1-carboxamide (2.110)



N-Methylaniline (596 µL, 5.5 mmol, 1.1 equiv) was added to a solution of cyclobut-1-ene-1-carboxylic acid (490 mg, 5.0 mmol, 1.0 equiv), HATU (2.1 g, 5.5 mmol, 1.1 equiv), and *N*,*N*-Diisopropylethylamine (1.75 mL, 10.0 mmol, 2.0 equiv) in DCM (50 mL). The reaction was stirred at room temperature for 16 h, after which time the reaction mixture was diluted with DCM (30 mL) and washed with an aqueous solution of HCl (1M, 30 mL) and brine (sat., 30 mL). The organic layer was dried (Na_2SO_4), filtered and concentrated *in vacuo*. The crude product was purified by flash chromatography (silica, EtOAc in heptane, 0/100 to 40/60). The desired fractions were collected and concentrated *in vacuo* to give the **2.110** (605 mg, 3.2 mmol, 64%) as a white solid. **^{1}H NMR** (400 MHz, $CDCl_3$) δ 7.40 – 7.28 (m, 3H), 7.21 – 7.17 (m, 2H), 5.66 (s, 1H), 3.27 (s, 3H), 2.24 – 2.08 (m, 4H); **^{13}C NMR** (101 MHz, $CDCl_3$) δ 162.8, 143.8, 143.3, 141.4, 129.5, 128.0, 127.9, 37.8, 31.0, 26.8; **HRMS** (ESI-TOF) calculated for $C_{12}H_{14}ON$ $[M+H]^+$: 188.1075; found 188.1075; **IR** (neat) 2981, 2360, 1625, 1593, 1574, 1493, 1417, 1379, 1305, 1256, 1169, 1108, 1072, 1032, 1010, 951, 910, 878, 862, 842, 777, 740, 705, 682; **m.p.**: 63 – 67 °C.

5.2.2 Optimisation of the Reaction Conditions

Procedure for the optimisation studies:



2.43, (1.0 equiv) **2.39**, (2.5 equiv) **2.44**

To a 7 mL vial equipped with a magnetic stir bar, was added *N*-phenylacrylamide **2.43** (74 mg, 0.50 mmol, 1.0 equiv), photocatalyst (0.0025 mmol, 0.5 mol%), solvent (3.0 mL), HAD (1.0 mmol, 2.0 equiv) and *N*,*N*-dimethylsulfamoyl chloride **2.39** (1.25 mmol, 2.5 equiv) under air. The vial was equipped with a Teflon septum and stirred in a SynLED Parallel Photoreactor with a 12W blue LED lamp (λ_{max} = 470 nm) at room temperature for 4 hours. The solvent was removed *in vacuo* and the residue was purified by column chromatography (silica, EtOAc in heptane 0/100 to 100/0) to yield the sulfonamide product **2.44**.

5.2.3 General Procedures

General procedure A: To a 7 mL vial equipped with a magnetic stir bar, was added alkene (0.50 mmol, 1.0 equiv), Eosin Y (1.7 mg, 0.0025 mmol, 0.5 mol%), MeCN (3.0 mL), $(TMS)_3SiH$ (309 uL, 1.0 mmol, 2.0 equiv) and sulfamoyl chloride (1.25 mmol, 2.5 equiv) under air. The vial was equipped with a Teflon septum and stirred in a SynLED Parallel Photoreactor with a 12W blue LED lamp (λ_{max} = 470 nm) at room temperature for 4 hours. The solvent was removed *in vacuo* and the residue was purified by column chromatography (silica, EtOAc in heptane 0/100 to 100/0) to yield the desired product(s).

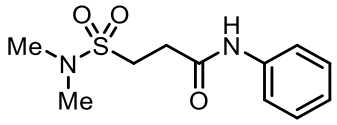
General procedure B: To a 7 mL vial equipped with a magnetic stir bar, was added alkene (0.50 mmol, 1.0 equiv), Eosin Y (1.7 mg, 0.0025 mmol, 0.5 mol%), MeCN (3.0 mL), $(TMS)_3SiH$ (309 uL, 1.0 mmol, 2.0 equiv) and sulfamoyl chloride (1.25 mmol, 2.5 equiv) under air. The vial was equipped with a Teflon septum and stirred in a SynLED Parallel Photoreactor with a 12W blue LED lamp (λ_{max} = 470 nm) at room temperature for 16 hours. The solvent was removed *in vacuo* and the residue was purified by column chromatography (silica, EtOAc in heptane 0/100 to 100/0) to yield the desired product(s).

General procedure C: To a 7 mL vial equipped with a magnetic stir bar, was added alkene (0.50 mmol, 1.0 equiv), $[Ir\{dF(CF_3)ppy\}_2(dtbpy)]PF_6$ (2.8 mg, 0.0025 mmol, 0.5 mol%), MeCN (3.0 mL), $(TMS)_3SiH$ (309 uL, 1.0 mmol, 2.0 equiv) and sulfamoyl chloride (1.25 mmol, 2.5 equiv) under air. The vial was equipped with a Teflon septum and stirred in a SynLED Parallel Photoreactor with a 12W blue LED lamp (λ_{max} = 470 nm) at room

temperature for 4 hours. The solvent was removed *in vacuo* and the residue was purified by column chromatography (silica, EtOAc in heptane 0/100 to 100/0) to yield the desired product(s).

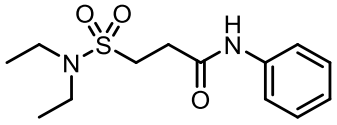
5.2.4 Characterisation: Hydrosulfamoylation of Electron-Deficient Alkenes

3-(*N*,*N*-dimethylsulfamoyl)-*N*-phenylpropanamide (2.44)[a]



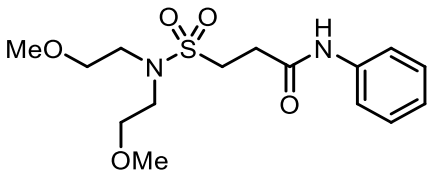
General procedure A was followed to obtain **2.44** (106 mg, 0.41 mmol, 83%) as a white solid. **^{1}H NMR** (400 MHz, $CDCl_3$) δ 8.20 (s, 1H), 7.51 (d, J = 7.6 Hz, 2H), 7.29 (dd, J = 7.9 Hz, 2H), 7.09 (dd, J = 7.4 Hz, 1H), 3.35 (t, J = 7.5 Hz, 2H), 2.91 (t, J = 7.5 Hz, 2H), 2.87 (s, 6H); **^{13}C NMR** (101 MHz, $CDCl_3$) δ 167.9, 137.9, 129.1, 124.6, 120.0, 43.5, 37.5, 30.5; **HRMS** (ESI-TOF) calculated for $C_{11}H_{15}O_3N_2{}^{32}S$ $[M-H]^-$: 255.0809; found 255.0806; **IR** (neat) 1681, 1619, 1551, 1491, 1443, 1336, 1314, 1258, 1186, 1147, 952, 760, 742, 684; **m.p.**: 120 – 122 °C.

3-(*N*,*N*-diethylsulfamoyl)-*N*-phenylpropanamide (2.59)[a]



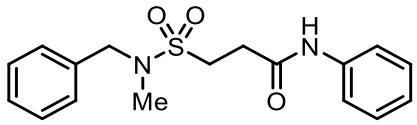
General procedure A was followed to obtain **2.59** (101 mg, 0.36 mmol, 71%) as a white solid. **^{1}H NMR** (400 MHz, $CDCl_3$) δ 8.33 (s, 1H), 7.52 (d, J = 7.6 Hz, 2H), 7.28 (t, J = 7.6 Hz, 2H), 7.08 (t, J = 7.4 Hz, 1H), 3.34 (t, J = 7.3 Hz, 2H), 3.29 (q, J = 7.1 Hz, 4H), 2.91 (t, J = 7.9, 7.4 Hz, 2H), 1.20 (t, J = 7.1 Hz, 6H); **^{13}C NMR** (101 MHz, $CDCl_3$) δ 168.0, 138.0, 129.0, 124.4, 120.0, 47.5, 41.9, 30.9, 14.5; **HRMS** (ESI-TOF) calculated for $C_{13}H_{21}O_3N_2{}^{32}S$ $[M+H]^+$: 285.1267; found 285.1273; **IR** (neat) 1696, 1603, 1547, 1499, 1424, 1311, 1259, 1172, 1014, 938, 761, 731, 697, 668; **m.p**: 70 – 72 °C.

3-(*N*,*N*-bis(2-methoxyethyl)sulfamoyl)-*N*-phenylpropanamide (2.60)



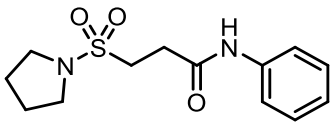
General procedure B was followed to obtain **2.60** (100 mg, 0.29 mmol, 58%) as a colourless oil. **^{1}H NMR** (400 MHz, $CDCl_3$) δ 8.16 (s, 1H), 7.51 (d, J = 7.4 Hz, 2H), 7.30 (t, J = 8.0 Hz, 2H), 7.08 (t, J = 7.4 Hz, 1H), 3.56 – 3.46 (m, 10H), 3.33 (s, 6H), 2.88 (t, J = 7.5 Hz, 2H); **^{13}C NMR** (101 MHz, $CDCl_3$) δ 168.1, 138.1, 129.0, 124.4, 120.0, 71.2, 58.9, 47.9, 47.6, 31.2; **HRMS** (ESI-TOF) calculated for $C_{15}H_{25}O_5N_2{}^{32}S$ $[M+H]^+$: 345.1479; found 345.1486; **IR** (neat) 2981, 1689, 1600, 1543, 1382, 1317, 1252, 1148, 1118, 1090, 954, 820, 756, 694.

3-(*N*-benzyl-*N*-methylsulfamoyl)-*N*-phenylpropanamide (2.61)



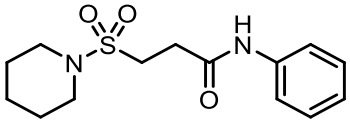
General procedure A was followed to obtain **2.61** (124 mg, 0.37 mmol, 75%) as a white solid. **^{1}H NMR** (400 MHz, $CDCl_3$) δ 8.15 (s, 1H), 7.53 (d, J = 7.7 Hz, 2H), 7.38 – 7.27 (m, 7H), 7.11 (t, J = 7.4 Hz, 1H), 4.34 (s, 2H), 3.44 (t, J = 7.4 Hz, 2H), 2.96 (t, J = 7.4 Hz, 2H), 2.78 (s, 3H); **^{13}C NMR** (101 MHz, $CDCl_3$) δ 167.8, 137.9, 135.7, 129.1, 128.9, 128.3, 128.2, 124.6, 120.1, 53.8, 45.5, 34.3, 30.8; **HRMS** (ESI-TOF) calculated for $C_{17}H_{21}O_3N_2{}^{32}S$ $[M+H]^+$: 333.1267; found 333.1271; **IR** (neat) 2981, 1668, 1597, 1527, 1456, 1385, 1323, 1135, 1077, 987, 777, 734, 701; **m.p.**: 111 – 113 °C.

***N*-phenyl-3-(pyrrolidin-1-ylsulfonyl)propenamide (2.62)**



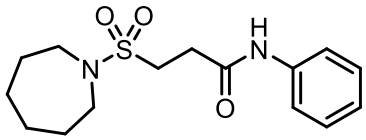
General procedure A was followed to obtain **2.62** (99 mg, 0.35 mmol, 70%) as a white solid. **^{1}H NMR** (400 MHz, $CDCl_3$) δ 8.26 (s, 1H), 7.52 (d, J = 7.6 Hz, 2H), 7.29 (t, J = 7.9 Hz, 2H), 7.09 (t, J = 7.4 Hz, 1H), 3.40 (t, J = 7.3 Hz, 2H), 3.37 – 3.32 (m, 4H), 2.91 (t, J = 7.3 Hz, 2H), 1.92 – 1.84 (m, 4H); **^{13}C NMR** (101 MHz, $CDCl_3$) δ 168.0, 138.0, 129.1, 124.5, 119.9, 47.9, 44.7, 30.9, 25.9; **HRMS** (ESI-TOF) calculated for $C_{13}H_{19}O_3N_2{}^{32}S$ $[M+H]^+$: 283.1111; found 283.1119; **IR** (neat) 2981, 1682, 1601, 1542, 1382, 1311, 1260, 1138, 1081, 1016, 958, 749, 710, 605; **m.p.**: 115 – 117 °C.

***N*-phenyl-3-(piperidin-1-ylsulfonyl)propenamide (2.63)**



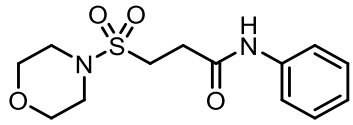
General procedure A was followed to obtain **2.63** (102 mg, 0.34 mmol, 69%) as a white solid. **^{1}H NMR** (400 MHz, $CDCl_3$) δ 8.31 (s, 1H), 7.52 (d, J = 7.2 Hz, 2H), 7.28 (t, J = 7.9 Hz, 2H), 7.08 (t, J = 7.4 Hz, 1H), 3.31 (t, J = 7.5 Hz, 2H), 3.29 – 3.26 (m, 4H), 2.90 (t, J = 7.5 Hz, 2H), 1.66 – 1.58 (m, 4H), 1.57 – 1.49 (m, 2H); **^{13}C NMR** (101 MHz, $CDCl_3$) δ 168.0, 138.0, 129.0, 124.4, 120.0, 46.6, 44.5, 30.6, 25.6, 23.7; **HRMS** (ESI-TOF) calculated for $C_{14}H_{19}O_3N_2{}^{32}S$ $[M-H]^-$: 295.1122; found 295.1118; **IR** (neat) 2981, 1692, 1603, 1547, 1498, 1425, 1310, 1256, 1162, 1133, 951, 742, 688; **m.p.**: 138 – 140 °C.

3-(azepan-1-ylsulfonyl)-*N*-phenylpropanamide (2.64)



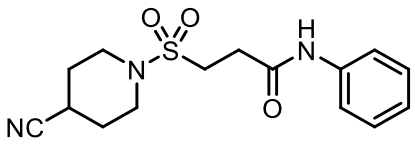
General procedure A was followed to obtain **2.64** (126 mg, 0.41 mmol, 81%) as a white solid. **^{1}H NMR** (400 MHz, $CDCl_3$) δ 8.24 (s, 1H), 7.53 (d, J = 7.6 Hz, 2H), 7.29 (t, J = 7.9 Hz, 2H), 7.09 (t, J = 7.4 Hz, 1H), 3.41 – 3.32 (m, 6H), 2.91 (t, J = 7.5 Hz, 2H), 1.77 – 1.69 (m, 4H), 1.66 – 1.58 (m, 4H); **^{13}C NMR** (101 MHz, $CDCl_3$) δ 168.0, 138.0, 129.1, 124.4, 120.0, 48.4, 46.0, 31.0, 29.6, 27.0; **HRMS** (ESI-TOF) calculated for $C_{15}H_{23}O_3N_2{}^{32}S$ $[M+H]^+$: 311.1424; found 311.1433; **IR** (neat) 2981, 1687, 1603, 1546, 1498, 1443, 1382, 1312, 1258, 1133, 1055, 955, 944, 745, 689; **m.p.**: 139 – 142 °C.

3-(morpholinosulfonyl)-*N*-phenylpropanamide (2.65)



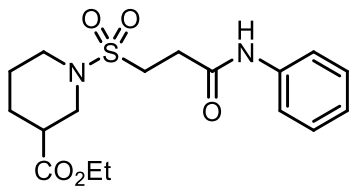
General procedure A was followed to obtain **2.65** (122 mg, 0.41 mmol, 82%) as a white solid. **^{1}H NMR** (400 MHz, DMSO-d_6) δ 10.12 (s, 1H), 7.59 (d, J = 7.6 Hz, 2H), 7.30 (t, J = 7.9 Hz, 2H), 7.05 (t, J = 7.9 Hz, 1H), 3.64 – 3.58 (m, 4H), 3.39 (t, J = 7.3 Hz, 2H), 3.18 – 3.14 (m, 4H), 2.78 (t, J = 7.3 Hz, 2H); **^{13}C NMR** (101 MHz, DMSO-d_6) δ 167.9, 139.0, 128.8, 123.3, 119.1, 65.8, 45.3, 43.8, 29.9; **HRMS** (ESI-TOF) calculated for $C_{13}H_{19}O_4N_2{}^{32}S$ $[M+H]^+$: 299.1066; found 299.1064; **IR** (neat) 1648, 1542, 1445, 1341, 1311, 1257, 1153, 1107, 1076, 951, 738; **m.p.**: 175 – 178 °C.

3-((4-cyanopiperidin-1-yl)sulfonyl)-*N*-phenylpropanamide (2.66)



General procedure B was followed to obtain **2.66** (109 mg, 0.34 mmol, 68%) as a colourless oil. **^{1}H NMR** (400 MHz, $CDCl_3$) δ 8.24 (s, 1H), 7.49 (d, J = 7.2 Hz, 2H), 7.28 (t, J = 7.9 Hz, 2H), 7.09 (t, J = 7.4 Hz, 1H), 3.40 (ddd, J = 12.6, 7.4, 3.7 Hz, 2H), 3.33 (t, J = 7.3 Hz, 2H), 3.22 (ddd, J = 12.8, 7.1, 3.7 Hz, 2H), 2.84 (t, J = 7.3 Hz, 2H), 2.76 (tt, J = 7.2, 4.3 Hz, 1H), 1.97 – 1.78 (m, 4H); **^{13}C NMR** (126 MHz, $CDCl_3$) δ 167.7, 137.8, 129.1, 124.7, 120.6, 120.0, 45.1, 43.5, 30.4, 28.2, 25.5; **HRMS** (ESI-TOF) calculated for $C_{15}H_{18}O_3N_3{}^{32}S$ $[M-H]^-$: 320.1074; found 320.1078; **IR** (neat) 28981, 1686, 1596, 1447.7, 1410, 1310, 1268, 1224, 1201, 1142, 1132, 1058, 978, 953, 831, 760, 738, 692, 644.

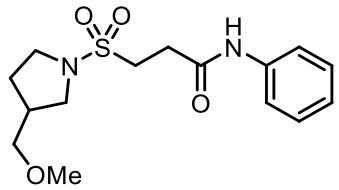
Ethyl 1-((3-oxo-3-(phenylamino)propyl)sulfonyl)piperidine-3-carboxylate (2.67)



General procedure B was followed to obtain **2.67** (118 mg, 0.32 mmol, 64%) as a white solid. **^{1}H NMR** (400 MHz, $CDCl_3$) δ 8.26 (s, 1H), 7.51 (d, J = 7.6 Hz, 2H), 7.28 (t, J = 7.4 Hz, 2H), 7.08 (t, J = 7.4 Hz, 1H), 4.12 (q, J = 7.1 Hz, 2H), 3.80 (dd, J = 12.3, 3.9 Hz, 1H), 3.57 (dt, J = 12.6, 3.9 Hz, 1H), 3.34 (t, J = 7.4 Hz, 2H), 3.05 (dd, J = 12.3, 9.8 Hz, 1H), 2.91 – 2.81 (m, 3H), 2.56 (tt, J = 9.8, 4.1 Hz, 1H), 2.07 – 1.96 (m, 1H), 1.81 – 1.71 (m, 1H), 1.65 – 1.52 (m, 2H), 1.23 (t, J = 7.1 Hz, 3H); **^{13}C NMR** (101 MHz, $CDCl_3$) δ 172.7, 167.8, 137.9, 129.0, 124.5, 120.0, 61.0, 47.3, 46.0, 45.2, 41.3, 30.7, 26.6, 24.3, 14.2; **HRMS** (ESI-TOF)

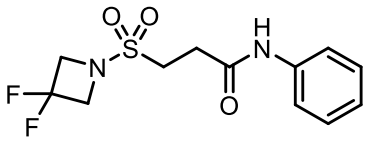
calculated for $C_{17}H_{25}O_5N_2{}^{32}S$ $[M+H]^+$: 369. 1479.; found 369. 1489; **IR** (neat) 2981, 1718, 1693, 1604, 1546, 1382, 1335, 1254, 1152, 955, 770, 694, 653; **m.p.**: 102 – 105°C.

3-((3-(methoxymethyl)pyrrolidin-1-yl)sulfonyl)-*N*-phenylpropanamide (2.68)



General procedure A was followed to obtain **2.68** (116 mg, 0.36 mmol, 71%) as a colourless oil. **^{1}H NMR** (400 MHz, $CDCl_3$) δ 8.35 (s, 1H), 7.52 (d, J = 7.6 Hz, 2H), 7.28 (t, J = 7.7 Hz, 2H), 7.08 (t, J = 7.4 Hz, 1H), 4.02 – 3.94 (m, 1H), 3.50 – 3.37 (m, 4H), 3.36 – 3.28 (m, 5H), 2.91 (t, J = 7.7, 2H), 2.03 – 1.81 (m, 4H); **^{13}C NMR** (101 MHz, $CDCl_3$) δ 168.1, 138.1, 129.0, 124.4, 119.9, 74.9, 59.1, 58.9, 48.9, 45.6, 30.8, 28.9, 24.7; **HRMS** (ESI-TOF) calculated for $C_{15}H_{23}O_4N_2{}^{32}S$ $[M+H]^+$: 327.1373; found 327.1382; **IR** (neat) 2981, 1670, 1600, 1543, 1498, 1444, 1382, 1313, 1252, 1147, 957, 756, 694.

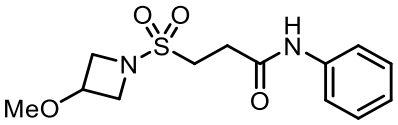
3-((3,3-difluoroazetidin-1-yl)sulfonyl)-*N*-phenylpropanamide (2.69)



General procedure B was followed to obtain **2.69** (97 mg, 0.32 mmol, 64%) as a white solid. **^{1}H NMR** (500 MHz, $CDCl_3$) δ 7.90 (s, 1H), 7.47 (d, J = 7.1 Hz, 2H), 7.31 (t, J = 7.9 Hz, 2H), 7.12 (t, J = 7.4 Hz, 1H), 4.28 (t, J = 12.0 Hz, 4H), 3.47 (t, J = 7.1 Hz, 2H), 2.83 (t, J = 7.1 Hz, 2H); **^{13}C NMR** (101 MHz, $CDCl_3$) δ 167.4, 137.5, 129.2, 124.9, 120.2, 113.7 (t, J = 74.5 Hz), 61.4 (t, J = 28.3), 47.3, 30.8; **^{19}F NMR** (471 MHz, $CDCl_3$) δ –99.3 (quint, J

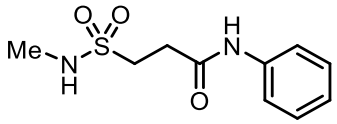
= 11.8 Hz); **HRMS** (ESI-TOF) calculated for $C_{12}H_{13}F_2O_3N_2{}^{32}S$ $[M-H]^-$: 303.0620; found 303.0614; **IR** (neat) 1684, 1606, 1551, 1499, 1459, 1445, 1352, 1306, 1246, 1208, 1178, 1145, 1024, 997, 952, 926, 903, 756, 693, 624. **m.p.**: 106 – 108 °C.

3-((3-methoxyazetidin-1-yl)sulfonyl)-*N*-phenylpropanamide (2.70)



General procedure B was followed to obtain **2.70** (69 mg, 0.23 mmol, 46%) as a white solid.**^{1}H NMR** (400 MHz, $CDCl_3$) δ 10.12 (s, 1H), 7.59 (d, J = 7.6 Hz, 2H), 7.30 (dd, J = 7.9 Hz, 2H), 7.05 (dd, J = 7.9 Hz, 1H), 4.13 – 4.06 (m, 1H), 4.06 – 4.00 (m, 2H), 3.88 (dd, J = 8.8, 4.8 Hz, 2H), 3.41 (t, J = 7.3 Hz, 2H), 3.23 (s, 3H), 2.85 (t, J = 7.3 Hz, 2H); **^{13}C NMR** (101 MHz, $CDCl_3$) δ 167.7, 137.9, 129.1, 124.6, 120.0, 67.8, 57.2, 56.2, 45.8, 30.9; **HRMS** (ESI-TOF) calculated for $C_{13}H_{19}O_4N_2{}^{32}S$ $[M+H]^+$: 299.1060; found 299.1068; **IR** (neat) 1690, 1599, 1535, 1497, 1441, 1368, 1289, 1248, 1118, 1103, 1045, 1021, 982, 959, 879, 774, 752, 692, 645; **m.p.**: 73 – 75 °C.

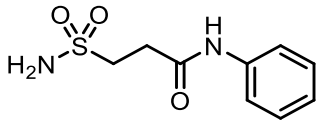
3-(*N*-methylsulfamoyl)-*N*-phenylpropanamide (2.71)



General procedure B was followed to obtain **2.71** (74 mg, 0.31 mmol, 61%) as a white solid. **^{1}H NMR** (400 MHz, DMSO-d_6) δ 10.06 (s, 1H), 7.58 (d, J = 8.6 Hz, 2H), 7.30 (t, J = 6.9 Hz, 2H), 7.04 (t, J = 7.4 Hz, 1H), 6.98 (q, J = 4.9 Hz, 1H), 3.31 (t, J = 7.5 Hz, 2H), 2.74 (t, J = 7.4 Hz, 2H), 2.60 (d, J = 4.9 Hz, 3H); **^{13}C NMR** (101 MHz, DMSO-d_6) δ 168.0, 139.0,

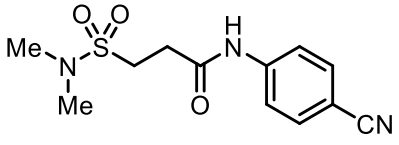
128.7, 123.3, 119.1, 45.4, 30.4, 28.6; **HRMS** (ESI-TOF) calculated for $C_{10}H_{13}O_3N_2{}^{32}S$ [M-H]$^-$: 241.0652; found 241.0644; **IR** (neat) 2981, 1662, 1601, 1549, 1501, 1444, 1308, 1263, 1152, 1127, 1097, 960, 876, 747, 689; **m.p.**: 162 – 165 °C.

_N_-phenyl-3-sulfamoylpropanamide (2.72)



General procedure B was followed to obtain **2.72** (53 mg, 0.23 mmol, 46%) as a white solid. **^{1}H NMR** (500 MHz, DMSO-d_6) δ 10.08 (s, 1H), 7.58 (d, J = 7.6 Hz, 2H), 7.30 (t, J = 8.1 Hz, 2H), 7.04 (t, J = 7.4 Hz, 1H), 6.90 (s, 2H), 3.32 – 3.27 (m, 2H), 2.80 – 2.75 (m, 2H); **^{13}C NMR** (101 MHz, DMSO-d_6) δ 168.2, 139.0, 128.7, 123.3, 119.2, 50.4, 30.9; **HRMS** (ESI-TOF) calculated for $C_9H_{13}O_3N_2{}^{32}S$ [M+H]$^+$: 229.0641; found 229.0645; **IR** (neat) 3369, 1668, 1596, 1531, 1502, 1444, 1421, 1318, 1251, 1197, 1149, 1080, 1024, 898, 822, 757, 689; **m.p.**: 148 – 152 °C.

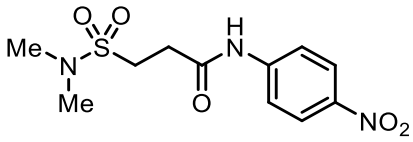
_N_-(4-cyanophenyl)-3-(_N_,_N_-dimethylsulfamoyl)propenamide (2.86)



General procedure A was followed to obtain **2.86** (110 mg, 0.39 mmol, 79%) as a white solid. **^{1}H NMR** (400 MHz, DMSO-d_6) δ 10.53 (s, 1H), 7.76 (s, 4H), 3.38 – 3.31 (m, 2H), 2.82 (t, J = 7.4 Hz, 2H), 2.78 (s, 6H); **^{13}C NMR** (101 MHz, DMSO-d_6) δ 168.9, 143.1, 133.3, 119.1, 119.0, 105.1, 42.5, 37.0, 30.1; **HRMS** (ESI-TOF) calculated for $C_{12}H_{14}O_3N_3{}^{32}S$ [M-

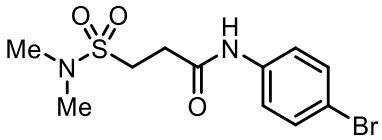
H]$^-$: 280.0761; found 280.0754; **IR** (neat) 2217, 1703, 1593, 1534, 1508, 1425, 1407, 1312, 1279, 1259, 1169, 1135, 968, 957, 852, 831, 805, 758, 716, 669; **m.p.**: 107 – 109 °C.

3-(*N*,*N*-dimethylsulfamoyl)-*N*-(4-nitrophenyl)propenamide (2.87)



General procedure B was followed to obtain **2.87** (126 mg, 0.42 mmol, 84%) as a white solid. **General procedure C** was followed to obtain **2.87** (120 mg, 0.40 mmol, 80%) as a white solid. **^{1}H NMR** (400 MHz, DMSO-d_6) δ 10.71 (s, 1H), 8.25 – 8.20 (m, 2H), 7.86 – 7.80 (m, 2H), 3.37 (t, J = 7.4 Hz, 2H), 2.85 (t, J = 7.4 Hz, 2H), 2.79 (s, 6H); **^{13}C NMR** (101 MHz, DMSO-d_6) δ 169.1, 145.1, 142.2, 125.0, 118.7, 42.4, 37.0, 30.1; **HRMS** (ESI-TOF) calculated for $C_{11}H_{14}O_5N_3{}^{32}S$ [M-H]$^-$: 300.0660; found 300.0649; **IR** (neat) 1709, 1593, 1566, 1492, 1317, 1263, 1166, 1137, 1108, 970, 860, 829, 782, 684; **m.p.**: 188 – 191 °C.

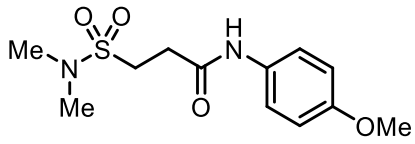
***N*-(4-bromophenyl)-3-(*N*,*N*-dimethylsulfamoyl)propenamide (2.88)**



General procedure B was followed to obtain **2.88** (133 mg, 0.40 mmol, 79%) as a white solid. **General procedure C** was followed to obtain **2.88** (133 mg, 0.40 mmol, 79%) as a white solid. **^{1}H NMR** (400 MHz, $CDCl_3$) δ 8.15 (s, 1H), 7.41 (s, 4H), 3.34 (t, J = 7.4 Hz, 2H), 2.95 – 2.85 (m, 8H); **^{13}C NMR** (101 MHz, $CDCl_3$) δ 167.9, 137.0, 132.1, 121.5, 117.2, 43.4, 37.5, 30.6; **HRMS** (ESI-TOF) calculated for $C_{11}H_{16}O_3N_2{}^{79}Br{}^{32}S$ [M+H]$^+$: 337.0039;

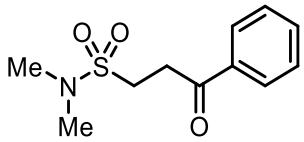
found 337.0043; **IR** (neat) 1684, 1593, 1526, 1485, 1426, 1396, 1321, 1300, 1137, 960, 815, 772, 753, 685, 630; **m.p.**: 154 – 156 °C.

3-(*N*,*N*-dimethylsulfamoyl)-*N*-(4-methoxyphenyl)propenamide (2.89)



General procedure B was followed to obtain **2.89** (110 mg, 0.38 mmol, 77%) as a white solid. **General procedure C** was followed to obtain **2.89** (113 mg, 0.40 mmol, 79%) as a white solid. **^{1}H NMR** (400 MHz, $CDCl_3$) δ 7.94 (s, 1H), 7.42 – 7.37 (m, 2H), 6.86 – 6.80 (m, 2H), 3.77 (s, 3H), 3.34 (t, J = 7.5 Hz, 2H), 2.90 – 2.82 (m, 8H); **^{13}C NMR** (101 MHz, $CDCl_3$) δ 167.7, 156.7, 130.9, 121.9, 114.3, 55.6, 43.6, 37.5, 30.5; **HRMS** (ESI-TOF) calculated for $C_{12}H_{19}O_4N_2{}^{32}S$ $[M+H]^+$: 287.1060; found 287.1068; **IR** (neat) 1669, 1526, 1513, 1409, 1326, 1281, 1248, 1131, 1026, 967, 827, 797, 776, 735, 687, 667; **m.p.**: 107 – 109 °C.

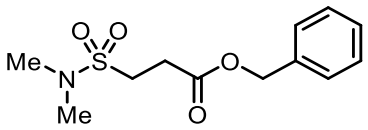
***N*,*N*-dimethyl-3-oxo-3-phenylpropane-1-sulfonamide (2.90)**



General procedure A was followed to obtain **2.90** (101 mg, 0.39 mmol, 77%) as a white solid. **^{1}H NMR** (400 MHz, $CDCl_3$) δ 8.00 – 7.94 (m, 2H), 7.63 – 7.56 (m, 1H), 7.52 – 7.45 (m, 2H), 3.55 – 3.49 (m, 2H), 3.40 – 3.34 (m, 2H), 2.88 (s, 6H); **^{13}C NMR** (101 MHz, $CDCl_3$) δ 196.3, 136.0, 133.9, 128.9, 128.2, 42.6, 37.5, 32.3; **HRMS** (ESI-TOF) calculated for

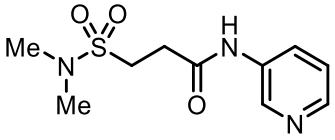
$C_{11}H_{15}O_3NNa^{32}S$ $[M+Na]^+$: 264.0665; found 264.0673; **IR** (neat) 1685, 1448, 1410, 1329, 1268, 1201, 1142, 953, 760, 737, 692, 644; **m.p.:** 155 – 159 °C.

Benzyl 3-(*N*,*N*-dimethylsulfamoyl)propanoate (2.91)



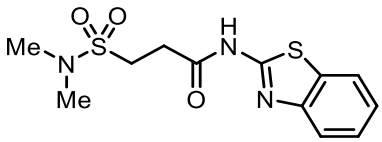
General procedure A was followed to obtain **2.91** (123 mg, 0.46 mmol, 91%) as a white solid. **^{1}H NMR** (400 MHz, $CDCl_3$) δ 7.41 – 731 (m, 5H), 5.16 (s, 2H), 3.26 (t, J = 7.5 Hz, 2H), 2.89 – 2.82 (m, 8H); **^{13}C NMR** (101 MHz, $CDCl_3$) δ 170.6, 135.4, 128.7, 128.6, 128.5, 67.2, 43.8, 37.4, 28.4; **HRMS** (ESI-TOF) calculated for $C_{12}H_{18}O_4N^{32}S$ $[M+H]^+$: 272.0951; found 272.0961; **IR** (neat) 1734, 1456, 1422, 1386, 1329, 1256, 1186, 1132, 1055, 957, 750, 698; **m.p.**: 47 – 49 °C.

3-(*N*,*N*-dimethylsulfamoyl)-*N*-(pyridin-3-yl)propenamide (2.92)



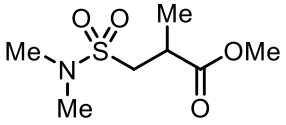
General procedure A was followed to obtain **2.92** (69 mg, 0.27 mmol, 54%) as a white solid. **^{1}H NMR** (400 MHz, DMSO-d_6) δ 10.34 (s, 1H), 8.73 (d, J = 2.3 Hz, 1H), 8.26 (dd, J = 4.7, 1.4 Hz, 1H), 8.02 (ddd, J = 8.3, 2.4, 1.5 Hz, 1H), 7.34 (dd, J = 8.3, 4.7 Hz, 1H), 3.40 – 3.33 (m, 2H), 2.84 – 2.76 (m, 8H); **^{13}C NMR** (101 MHz, DMSO-d_6) δ 168.6, 144.3, 140.7, 135.6, 126.0, 123.7, 42.6, 37.0, 29.8; **HRMS** (ESI-TOF) calculated for $C_{10}H_{16}O_3N_3{}^{32}S$ $[M+H]^+$: 258.0907; found 258.0914; **IR** (neat) 1696, 1606, 1586, 1555, 1424, 1322, 1301, 1136, 1125, 955, 813, 749, 706, 691; **m.p.**: 166 – 168 °C

_N_-(benzo[d]thiazol-2-yl)-3-(_N_,_N_-dimethylsulfamoyl)propenamide (2.93)



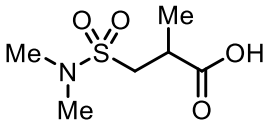
General procedure A was followed to obtain **2.93** (102 mg, 0.33 mmol, 65%) as a white solid. **^{1}H NMR** (400 MHz, DMSO-d_6) δ 12.48 (s, 1H), 7.97 (d, J = 7.8 Hz, 1H), 7.75 (d, J = 8.0 Hz, 1H), 7.46 – 7.40 (m, 1H), 7.33 – 7.27 (m, 1H), 3.42 (t, J = 7.4 Hz, 2H), 2.96 (t, J = 7.4 Hz, 2H), 2.79 (s, 6H); **^{13}C NMR** (101 MHz, DMSO-d_6) δ 169.4, 157.7, 148.5, 131.5, 126.1, 123.6, 121.7, 120.6, 42.3, 37.0, 29.1; **HRMS** (ESI-TOF) calculated for $C_{12}H_{16}O_3N_3{}^{32}S_2$ $[M+H]^+$: 314.0628; found 314.0631; **IR** (neat) 1703, 1601, 1553, 1421, 1329, 1269, 1142, 954, 761, 728, 691; **m.p.:** 197 – 199 °C.

Methyl 3-(_N_,_N_-dimethylsulfamoyl)-2-methylpropanoate (2.94)



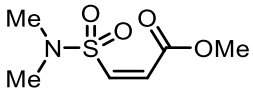
General procedure A was followed to obtain **2.94** (64 mg, 0.31 mmol, 61%) as a colourless oil. **^{1}H NMR** (400 MHz, $CDCl_3$) δ 3.72 (s, 3H), 3.46 (dd, J = 13.9, 7.3 Hz, 1H), 3.09 – 2.99 (m, 1H), 2.86 (dd, J = 14.0, 5.6 Hz, 1H), 2.83 (s, 6H), 1.34 (d, J = 7.2 Hz, 3H); **^{13}C NMR** (101 MHz, $CDCl_3$) δ 174.7, 52.4, 50.9, 37.4, 35.2, 17.8; **HRMS** (ESI-TOF) calculated for $C_7H_{16}O_4N^{32}S$ $[M+H]^+$: 210.0795; found 210.0799; **IR** (neat) 1736, 1460, 1436, 1330, 1213, 1138, 1055, 956, 832, 775, 760, 740, 711, 671.

3-(*N*,*N*-dimethylsulfamoyl)-2-methylpropanoic acid (2.95)



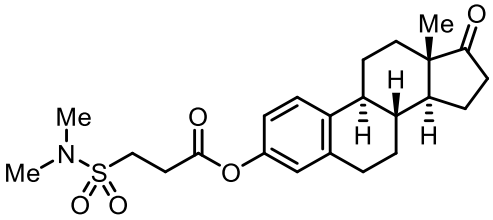
General procedure A was followed to obtain **2.95** (69 mg, 0.36 mmol, 61%) as a colourless oil. **^{1}H NMR** (400 MHz, $CDCl_3$) δ 3.49 (dd, J = 14.0, 7.4 Hz, 1H), 3.14 – 3.04 (m, 1H), 2.91 (dd, J = 14.0, 5.4 Hz, 1H), 2.86 (s, 6H), 1.42 (d, J = 7.2 Hz, 3H); **^{13}C NMR** (101 MHz, $CDCl_3$) δ 179.2, 50.8, 37.5, 35.3, 17.7; **HRMS** (ESI-TOF) calculated for $C_6H_{11}O_4N^{32}S$ $[M-H]^-$: 194.0493; found 194.0488; **IR** (neat) 2994, 1455, 1302, 1255, 1121, 1105, 1060, 1040, 1006, 873, 734, 615.

Methyl (*Z*)-3-(*N*,*N*-dimethylsulfamoyl)acrylate (2.96)



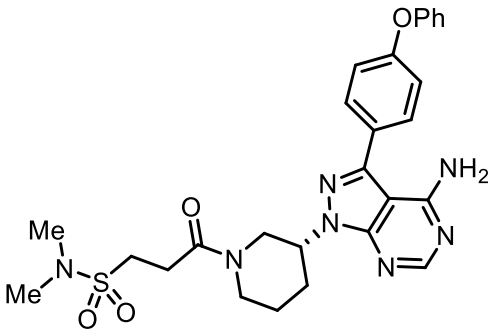
General procedure A was followed to obtain **2.96** (59 mg, 0.31 mmol, 61%) as a white solid. **^{1}H NMR** (500 MHz, DMSO-d_6) δ 7.00 (d, J = 11.6 Hz, 1H), 6.76 (d, J = 11.7 Hz, 1H), 3.69 (s, 3H), 2.73 (s, 6H); **^{13}C NMR** (126 MHz, DMSO-d_6) δ 165.3, 133.1, 127.8, 52.3, 37.1; **HRMS** (ESI-TOF) calculated for $C_6H_{12}O_4N^{32}S$ $[M+H]^+$: 194.0482; found 194.0483. The product decomposed within a few hours after isolation (melting points and IR were therefore not measured for this compound).

(8*R*,9*S*,13*S*,14*S*)-13-methyl-17-oxo-7,8,9,11,12,13,14,15,16,17-decahydro-6*H*-cyclopenta[*a*]phenanthren-3-yl 3-(*N*,*N*-dimethylsulfamoyl)propanoate (2.97)



General procedure A was followed to obtain **2.97** (169 mg, 0.39 mmol, 78%) as a white solid. **^{1}H NMR** (400 MHz, $CDCl_3$) δ 7.28 (d, J = 8.5 Hz, 1H), 6.86 (dd, J = 8.5, 2.5 Hz, 1H), 6.82 (d, J = 2.5 Hz, 1H), 3.34 (t, J = 7.4 Hz, 2H), 3.06 (t, J = 7.4 Hz, 2H), 2.94 – 2.87 (m, 7H), 2.50 (dd, J = 18.8, 8.6 Hz, 1H), 2.43 – 2.35 (m, 1H), 3.34 – 2.23 (m, 1H), 2.19 – 1.92 (m, 4H), 1.69 – 1.38 (7H), 0.90 (s, 3H); **^{13}C NMR** (101 MHz, $CDCl_3$) δ 220.8, 169.7, 148.4, 138.3, 137.9, 126.6, 121.4, 118.6, 50.5, 48.0, 44.2, 43.8, 38.1, 37.5, 35.9, 31.6, 29.5, 28.6, 26.4, 25.8, 21.7, 13.9; **HRMS** (ESI-TOF) calculated for $C_{23}H_{32}O_5N^{32}S$ $[M+H]^+$: 434.1996; found 434.1997; **IR** (neat) 1753, 1732, 1602, 1547, 1494, 1442, 1343, 1311, 1240, 1222, 1208, 1140, 1122, 1082, 957, 743; **m.p.**: 173 – 175 °C.

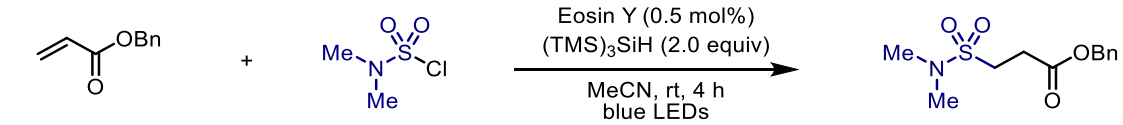
(*R*)-3-(3-(4-amino-3-(4-phenoxyphenyl)-1*H*-pyrazolo[3,4-*d*]pyrimidin-1-yl)piperidin-1-yl)-*N*,*N*-dimethyl-3-oxopropane-1-sulfonamide (2.98)



General procedure A was followed to obtain **2.98** (189 mg, 0.35 mmol, 69%) as a yellow oil. NMR analysis showed two rotamers.**^{1}H NMR** (400 MHz, $CDCl_3$) δ 8.34 (d, J = 8.5 Hz, 1H), 7.68 – 7.60 (m, 2H), 7.42 – 7.34 (m, 2H), 7.19 – 7.11 (m, 3H), 7.10 – 7.05 (m, 2H), 5.73 (br s, 2H), 4.90 – 4.72 (m, 1.5H), 4.50 – 4.40 (m, 0.5H), 4.04 (dd, J = 13.2, 3.9 Hz, 0.5H), 3.93 – 3.84 (m, 0.5H), 3.76 (dd, J = 13.3, 10.2 Hz, 0.5H), 3.36 (dd, J = 12.5, 10.5 Hz, 0.5H), 3.31 – 3.23 (m, 2H), 3.22 – 3.14 (m, 0.5H), 2.97 – 2.88 (m, 2H), 2.87 (s, 3H), 2.85 (s, 3H), 2.46 – 2.31 (m, 1H), 2.29 – 2.19 (m, 1H), 2.07 – 1.86 (m, 1.5H), 1.79 – 1.60 (m, 1H); **^{13}C NMR** (101 MHz, $CDCl_3$) δ 168.2, 168.1, 158.7, 158.7, 158.1, 158.0, 156.5, 156.4, 156.1, 155.9, 154.5, 154.4, 144.2, 144.0, 131.7, 130.1, 127.9, 127.7, 124.2, 124.2, 119.7, 119.7, 119.2, 98.8, 98.7, 53.3, 52.5, 49.6, 46.2, 45.6, 43.6, 43.5, 42.3, 37.5, 37.5, 30.2, 30.0, 27.2, 27.1, 25.1, 23.9; **HRMS** (ESI-TOF) calculated for $C_{27}H_{32}O_4N_7{}^{32}S$ $[M+H]^+$: 550.2231; found 550.2240; **IR** (neat) 1624, 1586, 1561, 1544, 1520, 1488, 1475, 1456, 1329, 1276, 1232, 1144, 957, 849, 802, 756, 731, 693.

5.2.5 Scale-up Experiment

The scale-up experiment has been performed on the synthesis of compound **2.91**.



2.78, (1.0 equiv)
5.0 g (30.9 mmol)

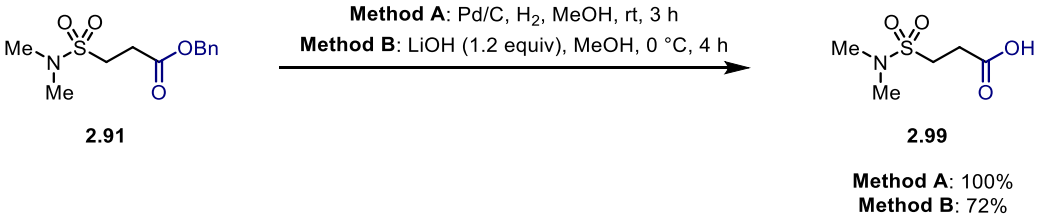
2.39, (2.5 equiv)

2.91, 80%
6.7 g (25.7 mmol)

In a 250 mL round bottom flask, equipped with a stirring bar and a thermometer, was added benzyl acrylate **2.78** (5.0 g, 30.8 mmol, 1.0 equiv), Eosin Y (100 mg, 0.154 mmol, 0.5 mol%), MeCN (130 mL), $(TMS)_3SiH$ (19.0 mL, 61.7 mmol, 2.0 equiv) and *N*,*N*-dimethylsulfamoyl chloride **2.39** (8.3 mL, 77.1 mmol, 2,5 equiv). The reaction was irradiated with two Kessil H150-Blue LED lights (34 W, 5 cm distance, see picture above) at room temperature for 4 hours. The reaction mixture was concentrated *in vacuo* and the crude product was purified by flash column chromatography (silica, EtOAc in heptane, 0/100 to 100/0). The desired fractions were collected and concentrated *in vacuo* to give the desired hydrosulfamoylated product **2.91** as an off-white solid (6.7 g, 24.7 mmol, 80%).

5.2.6 Further Transformations of Sulfonamide 2.91

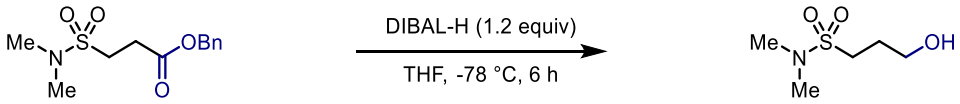
3-(*N*,*N*-dimethylsulfamoyl)propanoic acid (2.99)



Method A: A suspension of benzyl 3-(*N*,*N*-dimethylsulfamoyl)propanoate **2.91** (81.4 mg, 0.3 mmol, 1.0 equiv) and Pd/C (31.9 mg, 0.03 mmol, 10 mol%, 10 wt. %) in MeOH (3 mL) was equipped with a hydrogen containing balloon (approx. 1 mbar). The mixture was stirred at room temperature for 3 hours, filtered over a Celite® pad and the filtrate was concentrated *in vacuo* to give carboxylic acid **2.99** as a white solid (54 mg, 0.3 mmol, 100%).

Method 2: LiOH (8.6 mg, 0.36 mmol, 1,2 equiv) was added to a stirred solution of benzyl 3-(*N*,*N*-dimethylsulfamoyl)propanoate **2.91** (81.4 mg, 0.3 mmol, 1.0 equiv) in MeOH (3 mL) at 0 °C. The reaction mixture was warmed to room temperature and stirred for 4 hours. The mixture was treated with an aqueous solution of HCl (1M) and extracted with EtOAc. The organic layer was dried (Na_2SO_4), filtered and concentrated *in vacuo.* The crude product was purified by flash column chromatography (silia, EtOAc in heptane, 0/100 to 100/0) to afford carboxylic acid **2.99** as a white solid (39 mg, 0.22 mmol, 72%). **^{1}H NMR** (400 MHz, DMSO-d_6) δ 3.25 (t, J = 7.3 Hz, 2H), 2.77 (s, 6H), 2.61 (t, J = 7.4 Hz, 2H); **^{13}C NMR** (101 MHz, DMSO-d_6) δ 171.8, 42.9, 37.0, 28.0; **HRMS** (ESI-TOF) calculated for $C_5H_{12}O_4N^{32}S$ $[M+H]^+$: 182.0482; found 182.0497; **IR (neat)** 2981, 1692, 1458, 1395, 1329, 1291, 1263, 1143, 1112, 956, 940, 794, 770, 742, 709, 661, 636, 608; **m.p.**: 133 − 139 °C.

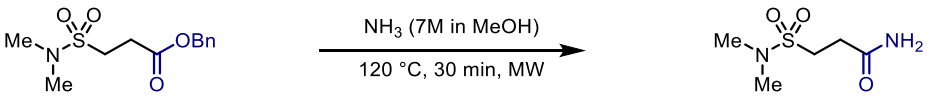
3-hydroxy-*N*,*N*-dimethylpropane-1-sulfonamide (2.100)



2.91, (1.0 equiv) **2.100**, 62%

DIBAL-H (0.75 mL, 0.8 mmol, 1M in Hexane, 2.5 equiv) was added dropwise to a stirred solution of benzyl 3-(*N*,*N*-dimethylsulfamoyl)propanoate **2.91** (81.4 mg, 0.3 mmol, 1.0 equiv) in DCM (3 mL) at -78 °C under nitrogen atmosphere. The reaction mixture was warmed to room temperature and stirred for 6 hours. An aqueous solution of potassium sodium tartrate (10 mol%) was added. Upon formation of a white precipitate (30 minutes), the suspension was extracted with DCM. The organic layers were dried (Na_2SO_4), filtered and concentrated *in vacuo*. The crude product was purified by flash column chromatography (silica, EtOAc in heptane, 0/100 to 100/0) to give the corresponding alcohol **2.100** as a colourless oil (31 mg, 0.19 mmol, 62%). **^{1}H NMR** (500 MHz, $CDCl_3$) δ 3.71 (q, J = 5.7 Hz, 2H), 3.05 – 3.00 (m, 2H), 2.84 (s, 6H), 2.60 (t, J = 5.3 Hz, 1H), 2.03 – 1.96 (m, 2H); **^{13}C NMR** (126 MHz, $CDCl_3$) δ 60.5, 44.9, 37.5, 26.1; **HRMS** (ESI-TOF) calculated for $C_5H_{13}O_3NNa^{32}S$ $[M+Na]^+$: 190.0508; found 190.0507; **IR (neat)** 2981, 1647, 1559, 1461, 1383, 1320, 1266, 1137, 1058, 956, 908, 782, 745, 709, 668.

3-(*N*,*N*-dimethylsulfamoyl)propenamide (2.101)



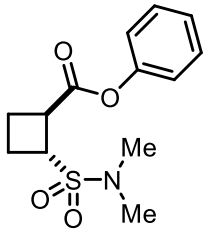
2.91 **2.101**, 76%

A solution of benzyl 3-(*N*,*N*-dimethylsulfamoyl)propanoate **2.91** (81.4 mg, 0.3 mmol, 1.0 equiv) in NH_3 (7M in MeOH, 3 mL) was stirred at 120 °C under microwave irradiation for

30 minutes. The reaction mixture was concentrated *in vacuo* and purified by flash column chromatography (silica, MeOH in DCM, 0/100 to 20/80) to give amide **2.101** as a white solid (41 mg, 0.23 mmol, 76%). **^{1}H NMR** (400 MHz, DMSO-d_6) δ 7.48 (br s, 1H), 6.98 (br s, 1H), 3.24 – 3.18 (m, 2H), 2.76 (s, 6H), 2.49 – 2.45 (m, 2H); **^{13}C NMR** (101 MHz, DMSO-d_6) δ 171.0, 42.8, 37.0, 28.4; **HRMS** (ESI-TOF) calculated for $C_5H_{12}O_3N_2Na^{32}S$ $[M+Na]^+$: 203.0461; found 203.0466; **IR (neat)** 1665, 1418, 1319, 1308, 1223, 1190, 1147, 1128, 1062, 1025, 987, 957, 799, 777, 623; **m.p.**: 196 – 200 °C.

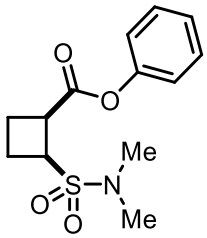
5.2.7 Hydrosulfamoylation of Cyclobutenes

Phenyl *trans*-2-(*N*,*N*-dimethylsulfamoyl)cyclobutane-1-carboxylate (*trans*-2.106)



General procedure A was followed to obtain ***trans*-2.106** (20 mg, 0.07 mmol, 14%) as a colourless oil. **^{1}H NMR** (400 MHz, $CDCl_3$) δ 7.43 – 7.36 (m, 2H), 7.28 – 7.23 (m, 1H), 7.11 – 7.05 (m, 2H), 4.22 – 4.13 (m, 1H), 3.87 – 3.77 (m, 1H), 2.89 (s, 6H), 2.65 – 2.55 (m, 1H), 2.53 – 2.43 (m, 1H), 2.42 – 2.26 (m, 2H); **^{13}C NMR** (101 MHz, $CDCl_3$) δ 171.2, 150.5, 129.7, 126.4, 121.4, 52.6, 40.5, 37.5, 22.0, 20.8; **HRMS** (ESI-TOF) calculated for $C_{13}H_{18}O_4N^{32}S$ $[M+H]^+$: 284.0951; found 284.0956; **IR** (neat) 1750, 1593, 1487, 1458, 1326, 1272, 1242, 1187, 1137, 1070, 1024, 961, 926, 839, 760, 690.

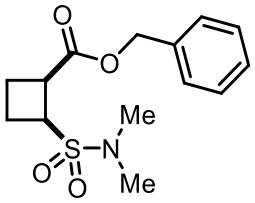
Phenyl *cis*-2-(*N*,*N*-dimethylsulfamoyl)cyclobutane-1-carboxylate (*cis*-2.106)



General procedure A was followed to obtain ***cis*-2.106** (56 mg, 0.20 mmol, 40%) as a white solid. **^{1}H NMR** (400 MHz, $CDCl_3$) δ 7.40 – 7.3 (m, 2H), 7.28 – 7.17 (m, 3H), 4.18 (q, J = 8.5 Hz, 1H), 3.74 – 3.64 (m, 1H), 2.87 (s, 6H), 2.83 – 2.69 (m, 1H), 2.69 – 2.59 (m, 1H), 2.39 – 2.29 (m, 1H), 2.27 – 2.14 (m, 1H); **^{13}C NMR** (101 MHz, $CDCl_3$) δ 169.6, 151.0,

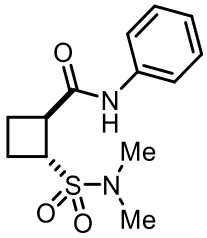
129.4, 125.9, 121.8, 54.3, 41.9, 37.7, 23.7, 21.0; **HRMS** (ESI-TOF) calculated for $C_{13}H_{18}O_4N^{32}S$ $[M+H]^+$: 284. 0951; found 284.0945; **IR** (neat) 1745, 1592, 1485, 1456, 1351, 1329, 1196, 1166, 1132, 962, 806, 776, 745, 711, 693; **m.p.**: 103 – 106 °C.

cis-Benzyl (1S,2S)-2-(_N_,_N_-dimethylsulfamoyl)cyclobutane-1-carboxylate (_cis_-2.107)



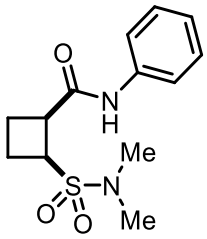
General procedure A was followed to obtain ***cis*-2.107** (67 mg, 0.23 mmol, 45%) as a colourless oil. **^{1}H NMR** (400 MHz, $CDCl_3$) δ 7.45 – 7.28 (m, 5H), 5.27 (d, J = 12.2 Hz, 1H), 5.13 (d, J = 12.2 Hz, 1H), 4.08 (dtt, J = 9.2, 8.5, 0.7 Hz, 1H), 3.55 – 3.45 (m, 1H), 2.84 (s, 7H), 2.80 – 2.65 (m, 1H), 2.62 – 2.51 (m, 1H), 2.34 – 2.23 (m, 1H), 2.18 – 2.06 (m, 1H); **^{13}C NMR** (101 MHz, $CDCl_3$) δ 170.9, 135.8, 128.8, 128.6, 128.3, 67.7, 54.3, 42.1, 37.7, 23.8, 21.0; HRMS (ESI-TOF) calculated for $C_{14}H_{19}NNaO_4{}^{32}S$ $[M+Na]^+$: 320.0927; found 320.0927; **IR** (neat) 2981, 2818, 1663, 1357, 1323, 1279, 1236, 1175, 1086, 1029, 992, 951, 847, 740, 729, 699, 628.

***trans*-2-(*N*,*N*-dimethylsulfamoyl)-*N*-phenylcyclobutane-1-carboxamide (*trans*-2.108)**



General procedure A was followed to obtain ***trans*-2.108** (38 mg, 0.14 mmol, 27%) as a white solid. **^{1}H NMR** (400 MHz, $CDCl_3$) δ 8.30 (s, 1H), 7.56 – 7.51 (m, 2H), 7.33 – 7.27 (m, 2H), 7.11 – 7.06 (m, 1H), 4.10 – 4.00 (m, 1H), 3.73 – 3.63 (m, 1H), 2.87 (s, 6H), 2.56 – 2.37 (m, 2H), 2.31 – 2.12 (m, 2H); **^{13}C NMR** (101 MHz, $CDCl_3$) δ 169.5, 138.0, 129.1, 124.4, 119.7, 53.6, 42.2, 37.7, 21.1, 20.6; **HRMS** (ESI-TOF) calculated for $C_{13}H_{19}O_3N_2{}^{32}S$ $[M+H]^+$: 283.1111; found 283.1125; **IR** (neat) 1745, 1660, 1598, 1531, 1442, 1323, 1197, 1136, 1029, 897, 755, 717, 692; **m.p.**: 126 – 128 °C.

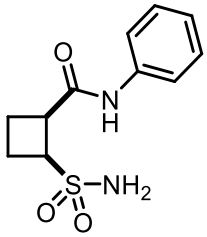
***cis*-2-(*N*,*N*-dimethylsulfamoyl)-*N*-phenylcyclobutane-1-carboxamide (*cis*-2.108)**



General procedure A was followed to obtain ***cis*-2.108** (38 mg, 0.14 mmol, 27%) as a white solid. **^{1}H NMR** (400 MHz, $CDCl_3$) δ 7.88 (s, 1H), 7.58 – 7.51 (m, 2H), 7.33 – 7.27 (m, 2H), 7.12 – 7.05 (m, 1H), 4.15 (q, J = 8.2 Hz, 1H), 3.62 – 3.52 (m, 1H), 2.85 (s, 6H), 2.77 – 2.67 (m, 1H), 2.67 – 2.56 (m, 1H), 2.35 – 2.25 (m, 1H), 2.24 – 2.13 (m, 1H); **^{13}C NMR** (101 MHz, $CDCl_3$) δ 167.8, 138.1, 129.0, 124.4, 120.3, 55.2, 43.6, 37.7, 23.3, 21.0; **HRMS** (ESI-

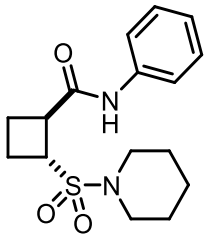
TOF) calculated for $C_{13}H_{19}O_3N_2{}^{32}S$ $[M+H]^+$: 283.1111; found 283.1114; **IR** (neat) 1658, 1550, 1495, 1445, 1328, 1198, 1104, 1024, 993, 825, 763; **m.p.**: 130 – 133°C.

***cis*-*N*-phenyl-2-sulfamoylcyclobutane-1-carboxamide (*cis*-2.110)**



General procedure A was followed to obtain ***cis*-2.110** (37 mg, 0.15 mmol, 29%) as a colourless oil. **^{1}H NMR** (400 MHz, DMSO-d_6) δ 9.82 (s, 1H), 7.57 – 7.53 (m, 2H), 7.32 – 7.26 (m, 2H), 7.11 – 6.99 (m, 1H), 6.70 (s, 2H), 4.08 – 3.99 (m, 1H), 3.67 (dt, J = 8.6 Hz, 1H), 2.55 – 2.44 (m, 1H), 2.40 – 2.30 (m, 2H), 2.09 – 1.98 (m, 1H); **^{13}C NMR** (101 MHz, DMSO-d_6) δ 169.2, 138.9, 128.5, 123.4, 119.8, 59.0, 41.5, 21.4, 20.4; **HRMS** (ESI-TOF) calculated for $C_{11}H_{15}O_3N_2{}^{32}S$ $[M+H]^+$: 255.0798; found 255.0808; **IR** (neat) 2981, 2259, 1671, 1618, 1600, 1542, 1494, 1473, 1444, 1417, 1382, 1326, 1253, 1194, 1150, 1025, 1002, 847, 758,695, 621.

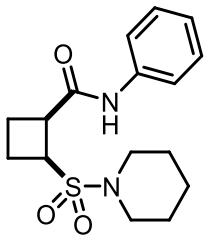
***trans*-*N*-phenyl-2-(piperidin-1-ylsulfonyl)cyclobutane-1-carboxamide (*trans*-111)**



General procedure A was followed to obtain ***trans*-2.111** (66 mg, 0.21 mmol, 41%) as a white solid. **^{1}H NMR** (400 MHz, $CDCl_3$) δ 8.50 (s, 1H), 7.58 – 7.52 (m, 2H), 7.32 – 7.24 (m, 2H), 7.10 – 7.04 (m, 1H), 4.08 – 3.98 (m, 1H), 3.70 – 3.62 (m, 1H), 3.28 – 3.165 (m,

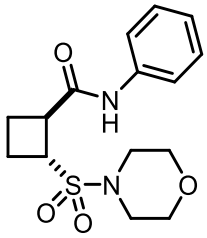
4H), 2.50 – 2.32 (m, 2H), 2.27 – 2.10 (m, 2H), 1.65 – 1.48 (m, 6H); **^{13}C NMR** (101 MHz, $CDCl_3$) δ 167.8, 138.2, 129.0, 124.3, 120.3, 55.7, 47.0, 43.5, 25.9, 23.8, 23.2, 20.8; **HRMS** (ESI-TOF) calculated for $C_{16}H_{23}O_3N_2{}^{32}S$ $[M+H]^+$: 323.1424; found 323.1439; **IR** (neat) 3334, 2937, 1663, 1599, 1536, 1500, 1440, 1373, 1301, 1274, 1253, 1204, 1160, 1139, 1104, 1079, 1055, 1027, 965, 934, 897, 862, 840, 795, 753, 719, 691, 658, 608; **m.p.**: 165 – 170 °C.

***trans*-*N*-phenyl-2-(piperidin-1-ylsulfonyl)cyclobutane-1-carboxamide (*cis*-111)**



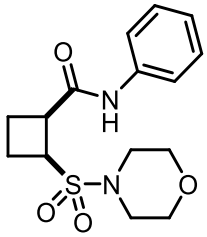
General procedure A was followed to obtain ***cis*-2.111** (66 mg, 0.21 mmol, 41%) as a white solid. **^{1}H NMR** (400 MHz, $CDCl_3$) δ 8.02 (s, 1H), 7.57 – 7.51 (m, 2H), 7.32 – 7.24 (m, 2H), 7.10 – 7.03 (m, 1H), 4.06 (dt, J = 8.6 Hz, 1H), 3.48 – 3.49 (m, 1H), 3.27 – 3.15 (m, 4H), 2.74 – 2.62 (m, 1H), 2.60 – 2.48 (m, 1H), 2.30 – 2.20 (m, 1H), 2.18 – 2.07 (m, 1H), 1.61 – 1.44 (m, 6H); **^{13}C NMR** (101 MHz, $CDCl_3$) δ 169.7, 138.1, 129.0, 124.2, 119.7, 54.1, 46.8, 42.0, 25.7, 23.7, 21.0, 20.4; **HRMS** (ESI-TOF) calculated for $C_{16}H_{23}O_3N_2{}^{32}S$ $[M+H]^+$: 323.1424; found 323.1428; **IR** (neat) 3345, 2940, 1677, 1603, 1543, 1499, 1439, 1369, 1328, 1319, 1307, 1251, 1210, 1182, 1158, 1130, 1045, 1024, 947, 901, 851, 829, 768, 754, 718, 692, 669; **m.p.**: 160 – 161 °C.

***trans*-2-(morpholinosulfonyl)-*N*-phenylcyclobutane-1-carboxamide (*trans*-2.112)**



General procedure A was followed to obtain ***trans*-2.112** (73 mg, 0.23 mmol, 45%) as a white solid. **^{1}H NMR** (400 MHz, $CDCl_3$) δ 8.26 (s, 1H), 7.57 – 7.51 (m, 2H), 7.35 – 7.28 (m, 2H), 7.14 – 7.07 (m, 1H), 4.11 – 4.01 (m, 1H), 3.73 – 3.61 (m, 1H), 3.29 – 3.21 (m, 4H), 2.52 – 2.36 (m, 2H), 2.30 – 2.12 (m, 2H); **^{13}C NMR** (101 MHz, $CDCl_3$) δ 169.4, 137.9, 129.1, 124.5, 119.8, 66.6, 53.8, 46.0, 42.0, 21.0, 20.6; **HRMS** (ESI-TOF) calculated for $C_{15}H_{21}O_4N_2{}^{32}S$ $[M+H]^+$: 325.1217; found 325.1226; **IR** (neat) 2981, 2890, 1618, 1598, 1544, 1533, 1499, 1490, 1472, 1457, 1389, 1357, 1339, 1279, 1236, 1203, 1143, 1029, 952, 741, 724, 676, 619; **m.p.**: 108 – 110 °C.

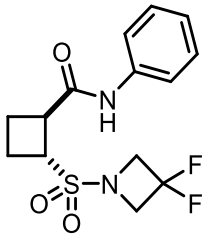
***cis*-2-(morpholinosulfonyl)-*N*-phenylcyclobutane-1-carboxamide (*cis*-2.112)**



General procedure A was followed to obtain ***cis*-2.112** (60 mg, 0.18 mmol, 37%) as a white solid. **^{1}H NMR** (400 MHz, $CDCl_3$) δ 7.78 (s, 1H), 7.58 – 7.49 (m, 2H), 7.31 (t, J = 8.0 Hz, 2H), 7.10 (t, J = 7.4 Hz, 1H), 4.12 (dt, J = 8.5 Hz, 1H), 3.66 (t, J = 4.7 Hz, 4H), 3.63 – 3.54 (m, 1H), 3.32 – 3.20 (m, 4H), 2.79 – 2.69 (m, 1H), 2.67 – 2.56 (m, 1H), 2.39 – 2.28 (m, 1H), 2.26 – 2.15 (m, 1H); **^{13}C NMR** (101 MHz, $CDCl_3$) δ 167.4, 138.0, 129.1, 124.6, 120.3, 66.8, 66.3, 55.8, 46.3, 43.7, 23.3, 21.0; **HRMS** (ESI-TOF) calculated for $C_{15}H_{21}O_4N_2{}^{32}S$ $[M+H]^+$:

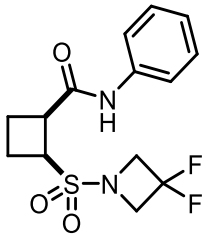
325.1225; found 325.1217; **IR** (neat) 2981, 1652, 1599, 1570, 1537, 1492, 1464, 1443, 1412, 1374, 1326, 1271, 1255, 1193, 1166, 1120, 1098, 1078, 1019, 989, 934, 809, 789, 676, 610; **m.p.**: 156 – 157 °C.

trans-2-((3,3-difluoroazetidin-1-yl)sulfonyl)-_N_-phenylcyclobutane-1-carboxamide (_trans_-2.113)



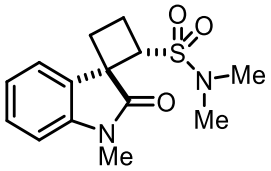
General procedure A was followed to obtain ***trans*-2.113** (21 mg, 0.07 mmol, 13%) as a white solid. **^{1}H NMR** (500 MHz, $CDCl_3$) δ 7.90 (s, 1H), 7.54 – 7.50 (m, 2H), 7.35 – 7.30 (m, 2H), 7.15 – 7.09 (m, 1H), 4.35 (t, J = 12.0 Hz, 4H), 4.12 – 4.00 (m, 1H), 3.64 – 3.51 (m, 1H), 2.52 – 2.38 (m, 2H), 2.33 – 2.21 (m, 2H); **^{19}F NMR** (471 MHz, $CDCl_3$) δ –98.95 (p, J = 11.6 Hz, 2F); **^{13}C NMR** (101 MHz, $CDCl_3$) δ 168.8, 137.8, 129.2, 124.7, 119.8, 113.8 (t, $J_{C\text{-}F}$ = 272.2 Hz), 62.0 (t, $J_{C\text{-}F}$ = 28.4 Hz), 56.4, 41.6, 20.4, 19.8; **HRMS** (ESI-TOF) calculated for $C_{14}H_{17}F_2O_3N_2{}^{32}S$ $[M+H]^+$: 331.0922; found 331.0932; **IR** (neat) 2981, 1660, 1603, 1531, 1508, 1491, 1473, 1460, 1443, 1382, 1350, 1337, 1303, 1273, 1249, 1222, 1166, 1146, 1072, 927, 889, 757, 729, 697, 646, 617; **m.p.:** 125 – 129 °C.

cis-2-((3,3-difluoroazetidin-1-yl)sulfonyl)-_N_-phenylcyclobutane-1-carboxamide (_cis_-2.113)



General procedure A was followed to obtain ***cis*-2.113** (28 mg, 0.09 mmol, 17%) as a white solid. **^{1}H NMR** (500 MHz, $CDCl_3$) δ 7.60 (s, 1H), 7.56 – 7.52 (m, 2H), 7.36 – 7.30 (m, 2H), 7.15 – 7.09 (m, 1H), 4.30 – 4.19 (m, 4H), 4.19 – 4.12 (m, 1H), 3.63 – 3.57 (m, 1H), 2.80 – 2.69 (m, 1H), 2.52 – 2.39 (m, 2H), 2.24 – 2.14 (m, 1H); **^{19}F NMR** (471 MHz, $CDCl_3$) δ – 99.43 (p, J = 11.9 Hz, 2F); **^{13}C NMR** (101 MHz, $CDCl_3$) δ 167.2, 137.8, 129.3, 124.7, 119.8, 113.9 (t, $J_{C\text{-}F}$ = 274.1 Hz), 62.4 (t, $J_{C\text{-}F}$ = 28.5 Hz), 58.6, 42.9, 22.5, 20.6; **HRMS** (ESI-TOF) calculated for $C_{14}H_{17}F_2O_3N_2{}^{32}S$ $[M+H]^+$: 331.0922; found 331.0927; **IR** (neat) 2981, 1660, 1597, 1540, 1490, 1474, 1457, 1443, 1373, 1347, 1329, 1294, 1276, 1249, 1223, 1207, 1152, 1133, 1063, 1010, 956, 901, 811, 754, 730, 698, 668, 646; **m.p.:** 136 – 138°C.

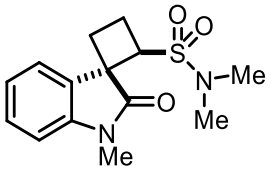
***trans*-_N_,_N_,1'-trimethyl-2'-oxospiro[cyclobutane-1,3'-indoline]-2-sulfonamide (*trans*-2.115)**



General procedure A was followed to obtain ***trans*-2.115** (57 mg, 0.19 mmol, 39%) as a white solid. **General procedure C** was followed to obtain ***trans*-2.115** (81 mg, 0.28 mmol, 55%) as a white solid. **^{1}H NMR** (500 MHz, $CDCl_3$) δ 7.79 (dd, J = 7.5, 1.3 Hz, 1H), 7.30 (td, J = 7.8 Hz, 1.2, 1H), 7.13 (td, J = 7.6 Hz, 1.1, 1H), 6.81 (d, J = 7.7 Hz, 1H), 4.33 (t, J =

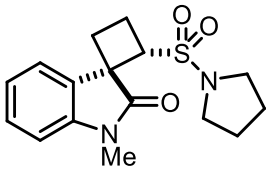
8.9, 1H), 3.21 (s, 3H), 2.99 – 2.89 (m, 1H), 2.67 – 2.57 (m, 7H), 2.56 – 2.46 (m, 1H), 2.33 – 2.25 (m, 1H); **^{13}C NMR** (126 MHz, $CDCl_3$) δ 177.1, 143.3, 128.9, 128.3, 126.2, 122.8, 108.1, 56.8, 51.3, 37.2, 29.0, 26.6, 22.1; **HRMS** (ESI-TOF) calculated for $C_{14}H_{19}O_3N_2{}^{32}S$ $[M+H]^+$: 295.1111; found 295.1117; **IR** (neat) 1704, 1614, 1494, 1472, 1417, 1377, 1350, 1331, 1312, 1274, 1232, 1193, 1146, 1103, 1086, 1054, 1023, 1011, 985, 924, 899, 811, 745, 693, 680, 610; **m.p.**: 149 – 151 °C.

***cis*-*N*,*N*,1'-trimethyl-2'-oxospiro[cyclobutane-1,3'-indoline]-2-sulfonamide (*cis*-2.115)**



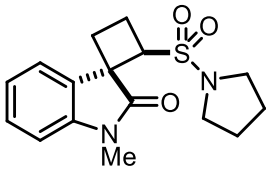
General procedure A was followed to obtain ***cis*-2.115** (25 mg, 0.08 mmol,17%) as a white solid. **General procedure C** was followed to obtain ***cis*-2.115** (35 mg, 0.12 mmol, 24%) as a white solid. **^{1}H NMR** (500 MHz, $CDCl_3$) δ 7.35 – 7.27 (m, 2H), 7.09 (td, J = 7.5, 1.0 Hz, 1H), 6.80 (d, J = 7.7 Hz, 1H), 4.13 – 4.07 (m, 1H), 3.27 – 3.18 (m, 4H), 2.60 (s, 6H), 2.51 – 2.44 (m, 1H), 2.40 – 2.30 (m, 2H); **^{13}C NMR** (126 MHz, $CDCl_3$) δ 176.2, 143.7, 130.0, 129.4, 122.7, 122.3, 108.2, 60.5, 52.4, 37.1, 28.4, 26.6, 22.0; **HRMS** (ESI-TOF) calculated for $C_{14}H_{19}O_3N_2{}^{32}S$ $[M+H]^+$: 295.1111; found 295.1118; **IR** (neat) 1706, 1615, 1494, 1461, 1417, 1376, 1348, 1333, 1313, 1274, 1252, 1234, 1191, 1146, 1120, 1094, 1012, 988, 897, 812, 792, 780, 707, 696, 680, 661, 607; **m.p.**: 134 – 137 °C.

***trans*-1'-methyl-2-(pyrrolidin-1-ylsulfonyl)spiro[cyclobutane-1,3'-indolin]-2'-one (*trans*-2.116)**



General procedure A was followed to obtain ***trans*-2.116** (37 mg, 0.12 mmol, 23%) as a white solid. **General procedure C** was followed to obtain ***trans*-2.116** (53 mg, 0.17 mmol, 33%) as a white solid. **^{1}H NMR** (400 MHz, $CDCl_3$) δ 7.79 (ddd, J = 7.6, 1.3, 0.6 Hz, 1H), 7.29 (td, J = 7.7, 1.3 Hz, 1H), 7.13 (td, J = 7.6, 1.1 Hz, 1H), 6.81 (d, J = 7.6 Hz, 1H), 4.39 (t, J = 9.3 Hz, 1H), 3.20 (s, 3H), 3.14 – 3.06 (m, 2H), 3.03 – 2.89 (m, 3H), 2.66 – 2.57 (m, 1H), 2.56 – 2.49 (m, 1H), 2.32 – 2.23 (m, 1H), 1.79 – 1.68 (m, 4H); **^{13}C NMR** (101 MHz, $CDCl_3$) δ 177.3, 143.3, 128.9, 128.4, 126.4, 122.8, 107.9, 57.9, 51.3, 47.4, 28.7, 26.6, 25.9, 21.7; **HRMS** (ESI-TOF) calculated for $C_{16}H_{21}O_3N_2{}^{32}S$ $[M+H]^+$: 321.1267; found 321.1274; **IR** (neat) 2957, 1712, 1613, 1493, 1470 1377, 1331, 1314, 1273, 1250, 1195, 1145, 1122, 1090, 1060, 1007, 929, 910, 857, 797, 779, 754, 625C; **m.p.**: 176 – 179 °C.

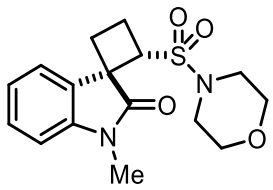
***cis*-1'-methyl-2-(pyrrolidin-1-ylsulfonyl)spiro[cyclobutane-1,3'-indolin]-2'-one (*cis*-2.116)**



General procedure A was followed to obtain ***cis*-2.116** (24 mg, 0.08 mmol, 15%) as a white solid. **General procedure C** was followed to obtain ***cis*-2.116** (35 mg, 0.11 mmol, 22%) as a white solid. **^{1}H NMR** (400 MHz, $CDCl_3$) δ 7.34 – 7.26 (m, 2H), 7.08 (td, J = 7.6, 1.0 Hz, 1H), 6.79 (d, J = 7.7, 1H), 4.20 – 4.11 (m, 1H), 3.32 – 3.17 (m, 4H), 2.52 – 2.41 (m, 1H),

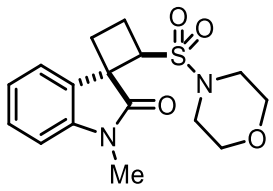
2.41 – 2.28 (m, 2H), 1.73 – 1.61 (m, 4H); **^{13}C NMR** (101 MHz, $CDCl_3$) δ 176.2, 143.7, 130.2, 129.3, 122.7, 122.3, 108.1, 61.6, 52.4, 47.5, 28.3, 26.6, 25.8, 21.9; **HRMS** (ESI-TOF) calculated for $C_{16}H_{21}O_3N_2{}^{32}S$ $[M+H]^+$: 321.1267; found 321.1270; **IR** (neat) 2963, 1713, 1618, 1492, 1467, 1414, 1375, 1344, 1330, 1313, 1272, 1250, 1237, 1193, 1144, 1120, 1091, 1062, 1046, 1008, 755, 696, 660, 625, 618; **m.p.**: 166 – 170 °C.

***trans*-1'-methyl-2-(morpholinosulfonyl)spiro[cyclobutane-1,3'-indolin]-2'-one (*trans*-2.117)**



General procedure A was followed to obtain ***trans*-2.117** (51 mg, 0.15 mmol, 31%) a white solid. **General procedure C** was followed to obtain ***trans*-2.117** (83 mg, 0.25 mmol, 49%) as a white solid. **^{1}H NMR** (500 MHz, $CDCl_3$) δ 7.79 – 7.76 (m, 1H), 7.31 (td, J = 7.7, 1.2 Hz, 1H), 7.13 (td, J = 7.6, 1.0 Hz, 1H), 6.83 (d, J = 7.9 Hz, 1H), 4.36 (t, J = 9.7 Hz, 1H), 3.54 – 3.43 (m, 4H), 3.23 (s, 3H), 3.00 – 2.88 (m, 5H), 2.67 – 2.59 (m, 1H), 2.58 – 2.50 (m, 1H), 2.31 – 2.24 (m, 1H); **^{13}C NMR** (101 MHz, $CDCl_3$) δ 177.1, 143.4, 129.1, 128.1, 126.3, 122.9, 108.1, 66.7, 57.5, 51.2, 45.6, 28.9, 26.7, 21.6; **HRMS** (ESI-TOF) calculated for $C_{16}H_{21}O_4N_2{}^{32}S$ $[M+H]^+$: 337.1217; found 3337.1223; **IR** (neat) 1704, 1614, 1532, 1494, 1466, 1445, 1418, 1374, 1439, 1330, 1313, 1301, 1256, 1152, 1116, 1074, 1050, 1014, 995, 945, 753, 715, 609; **m.p.**: 174 – 176 °C.

***cis*-1'-methyl-2-(morpholinosulfonyl)spiro[cyclobutane-1,3'-indolin]-2'-one (*cis*-2.117)**



General procedure A was followed to obtain ***cis*-2.117** (34 mg, 0.10 mmol, 20%) as a white solid. **General procedure C** was followed to obtain ***cis*-2.117** (55 mg, 0.16 mmol, 33%) as a white solid. **^{1}H NMR** (500 MHz, $CDCl_3$) δ 7.35 – 7.29 (m, 2H), 7.10 (td, J = 7.6, 1.0 Hz, 1H), 6.81 (d, J = 7.8, 1H), 4.15 – 4.08 (m, 1H), 3.55 – 3.46 (m, 4H), 3.28 – 3.17 (m, 4H), 3.04 – 2.94 (m, 4H), 2.51 – 2.45 (m, 1H), 2.41 – 2.32 (m, 2H); **^{13}C NMR** (101 MHz, $CDCl_3$) δ 175.9, 143.8, 130.0, 129.5, 122.8, 122.3, 108.2, 66.5, 60.6, 52.3, 45.6, 28.4, 26.6, 21.8; **HRMS** (ESI-TOF) calculated for $C_{16}H_{21}O_4N_2{}^{32}S$ $[M+H]^+$: 337.1217; found 337.1234; **IR** (neat) 1699, 1613, 1494, 1473, 1454, 1377, 1343, 1311, 1295, 1278, 1254, 1210, 1192, 1153, 1125, 1110, 1087, 1072, 1022, 1009, 950, 752, 694, 680, 607; **m.p.**: 230 – 231 °C.

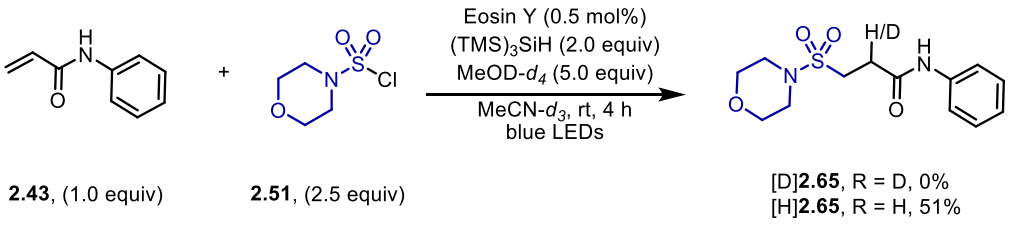
5.2.8 Mechanistic Investigations

5.2.8.1 Radical-Trapping Experiment with TEMPO



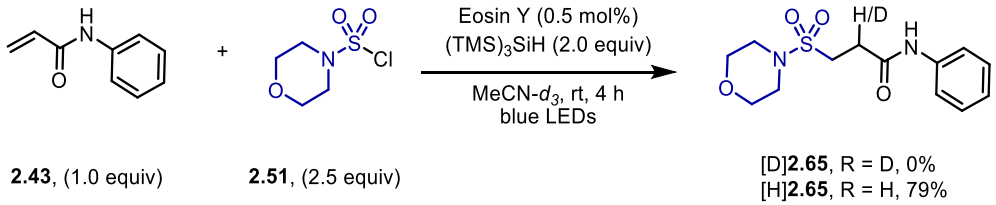
A suspension of *N*-phenylacrylamide **2.43** (74 mg, 0.5 mmol, 1.0 equiv), Eosin Y (1.7 mg, 0.5 mol%, 0.005 equiv), MeCN (3.0 mL), $(TMS)_3SiH$ (309 µL, 1.0 mmol, 2.0 equiv), morpholine-4-sulfonyl chloride (232 mg, 1.25 mmol, 2.5 equiv) and TEMPO (313 mg, 2.0 mmol, 4.0 equiv) was stirred under blue LED (λ_{max} = 470 nm) irradiation for 4 hours at room temperature. LCMS analysis of the crude reaction mixture showed no desired hydrosulfonylation product **2.65** and alkene starting material **2.43** remaining.

5.2.8.2 Deuteration Experiments



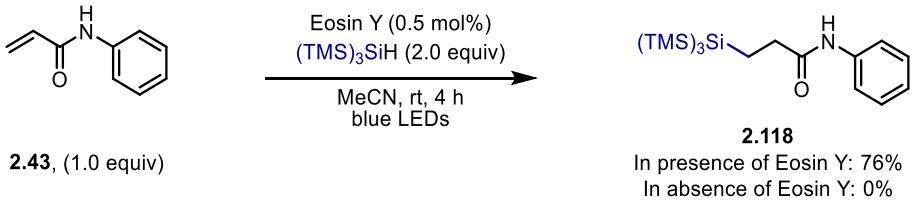
Morpholine-4-sulfonyl chloride **2.51** (232 mg, 1.3 mmol, 2.5 equiv) was added to a stirred solution of *N*-phenylacrylamide **2.43** (74 mg 0.5 mmol, 1.0 equiv), Eosin Y (1.7 mg, 0.0025 mmol, 0.005 equiv), $(TMS)_3SiH$ (309 µL, 1.0 mmol, 2.0 equiv) and MeOD (102 µL, 2.5 mmol, 5.0 equiv) in MeCN (3.0 mL). The reaction mixture was stirred at room temperature under blue LED irradiation for 4 hours. The solution was concentrated *in vacuo* and purified

by flash column chromaography (silica, EtOAc in heptane, 0/100 to 100/0) to afford sulfonamide [H]**2.65** in 51% yield (76 mg, 0.26 mmol).



Morpholine-4-sulfonyl chloride **2.51** (232 mg, 1.25 mmol, 2.5 equiv) was added to a stirred solution of *N*-phenylacrylamide **2.43** (74 mg 0.5 mmol, 1.0 equiv), Eosin Y (1.7 mg, 0.0025 mmol, 0.005 equiv), $(TMS)_3SiH$ (309 µL, 1.0 mmol, 2.0 equiv) in MeCN-d_3 (3.0 mL). The reaction mixture was stirred at room temperature under blue LED irradiation for 4 hours. The solution was concentrated *in vacuo* and purified by flash column chromaography (silica, EtOAc in heptane, 0/100 to 100/0) to afford sulfonamide [H]**2.65** in 79% yield (118 mg, 0.40 mmol).

5.2.8.3 Hydrosilylation of Electron-Deficient Alkenes



$(TMS)_3SiH$ (309 µL, 1.0 mmol, 2.0 equiv) was added to a stirred suspension of *N*-phenylacrylamide **2.43** (74 mg, 0.5 mmol, 1.0 equiv) and Eosin Y (1.7 mg, 0.5 mol%, 0.005 equiv) in MeCN (3.0 mL). The reaction mixture was stirred at room temperature under blue LED irradiation (λ_{max} = 470 nm) for 4 hours. The reaction mixture was concentrated *in vacuo*

and purified by flash column chromatography (silica, EtOAc in heptane 0/100 to 20/80) to afford 3-(1,1,1,3,3,3-hexamethyl-2-(trimethylsilyl)trisilan-2-yl)-*N*-phenylpropanamide **2.118** as a white solid (150 mg, 0.38 mmol, 76%). **^{1}H NMR** (400 MHz, $CDCl_3$) δ 7.54 – 7.52 (m, 2H), 7.34 – 7.32 (m, 2H), 7.15 – 7.06 (m, 2H), 2.44 – 2.35 (m, 2H), 1.26 – 1.16 (m, 2H), 0.20 (s, 27H); **^{13}C NMR** (101 MHz, $CDCl_3$) δ 172.2, 138.1, 129.1, 124.3, 119.8, 36.8, 3.5, 1.3; **HRMS** (ESI-TOF) calculated for $C_{18}H_{36}ONSi_4$ $[M-H]^-$: 394.1879; found 394.1870; **IR (neat)** 1660, 1602, 1550, 1499, 1442, 1358, 1308, 1243, 1210, 828, 749, 688, 622; **m.p.**: 155 – 158 °C.

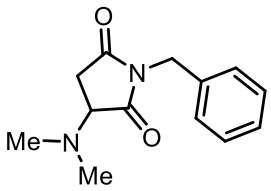
5.2.8.4 Isolation of Chlorotris(trimethylsilyl)silane (2.119)



A suspension of *N*-phenylacrylamide **2.43** (74 mg, 0.5 mmol, 1.0 equiv), Eosin Y (1.7 mg, 0.5 mol%, 0.005 equiv), MeCN (3.0 mL), $(TMS)_3SiH$ (309 µL, 1.0 mmol, 2.0 equiv), *N*,*N*-dimethylsulfamoyl chloride **2.39** (309 µL, 1.25 mmol, 2.5 equiv) and TEMPO (313 mg, 2.0 mmol, 4.0 equiv) was stirred under blue LED (λ_{max} = 470 nm) irradiation for 4 hours at room temperature. The reaction mixture was concentrated *in vacuo* and purified by flash column chromatography (silica, EtOAc in heptane 0/100 to 20/80) to afford **2.119** (98 mg, 0.35 mmol, 69%) as a colourless oil. **^{1}H NMR** (400 MHz, $CDCl_3$) δ 0.23 (s, 27H); **^{13}C NMR** (101 MHz, $CDCl_3$) δ –0.6. Spectroscopic data were in accordance with a commercial sample.

5.2.9 Limitations

1-benzyl-3-(dimethylamino)pyrrolidine-2,5-dione (2.125)

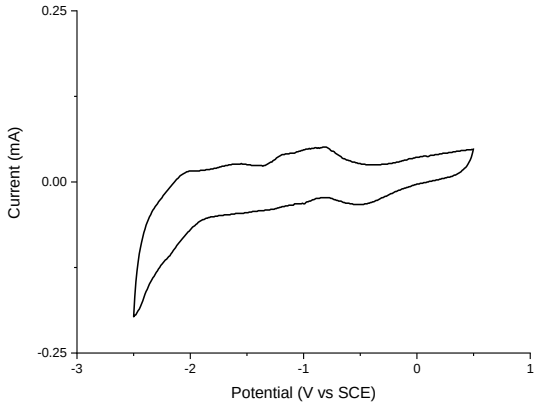


General procedure A was followed to obtain **2.125** as an orange oil (36 mg, 0.16 mmol, 49%). **^{1}H NMR** (400 MHz, $CDCl_3$) δ 7.39 – 7.34 (m, 2H), 7.33 – 7.27 (m, 3H), 4.66 (d, J = 3.6 Hz, 2H), 3.78 (dd, J = 8.9, 4.9 Hz, 1H), 2.79 (dd, J = 18.5, 8.9 Hz, 1H), 2.62 (dd, J = 18.5, 4.8 Hz, 1H), 2.34 (s, 6H).; **^{13}C NMR** (101 MHz, $CDCl_3$) δ 176.3, 174.9, 135.9, 128.9, 128.8, 128.1, 62.8, 42.3, 41.5, 31.1; **HRMS** (ESI-TOF) calculated for $C_{13}H_{17}O_2N_2$ $[M+H]^+$: 233.1285; found 233.1292; **IR** (neat) 2981, 1696, 1393, 1342, 1164, 1082, 1008, 944, 888, 827, 759, 706, 629.

5.2.10 Cyclic Voltammetry[b]

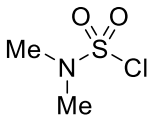
The cyclic voltammetry experiments were performed in a batch setup. The analyses were performed with an IVIUM CompactStat equipped with a platinum working electrode, a nickel counter electrode and a SCE reference electrode. All measurement were carried out at a concentration of 0.05 M in anhydrous CH_3CN with an electrolyte ($LiClO_4$, 0.1M), with a scan rate of 100 mV/s.

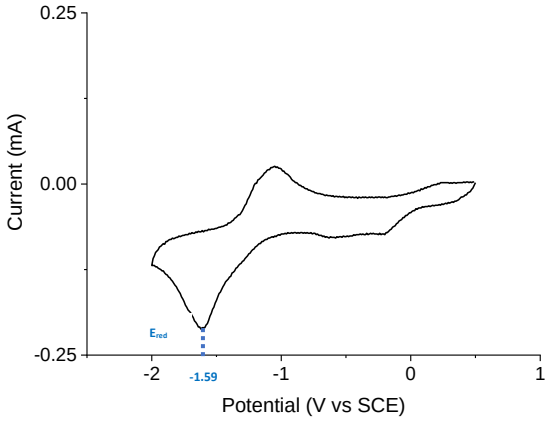
Blank:



Cyclic Voltammetry of $LiClO_4$ in anhydrous CH_3CN.

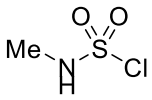
***N*,*N*-Dimethylsulfamoyl chloride:** *E* (V *vs* SCE): − 1.59 V

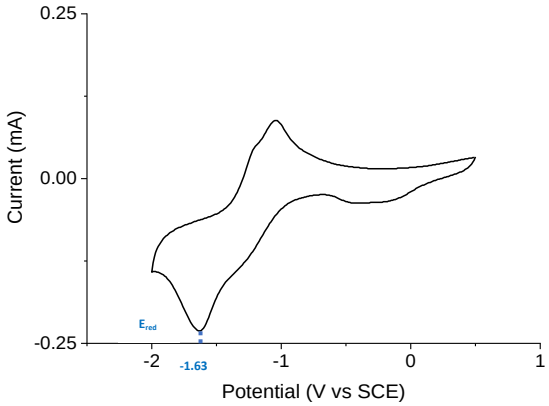




Cyclic voltammetry of *N*,*N*-dimethylsulfamoyl chloride in anhydrous CH_3CN.

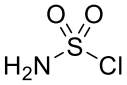
Methylsulfamoyl chloride: *E* (V *vs* SCE): − 1.63 V

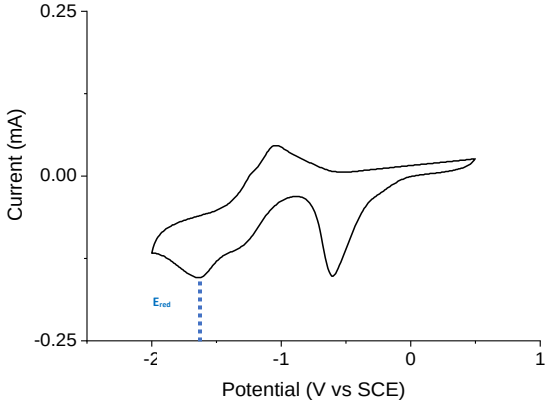




Cyclic voltammetry of methylsulfamoyl chloride in anhydrous CH_3CN.

Sulfamoyl chloride: *E* (V *vs.* SCE): − 1.65 V





Cyclic voltammetry of sulfamoyl chloride in anhydrous CH_3CN.

5.3 Experimental Procedures and Characterisation of Compounds from Chapter 3

All reactions for the hydrosulfonylation of alkenes were conducted in non-dried glassware with magnetic stirring. All solvents were used as received without further purification. $(TMS)_3SiH$ was purchased from Sigma-Aldrich, TCI and Combi-blocks. Photocatalyst *fac*-$Ir(ppy)_3$ was purchased from Sigma-Aldrich. Sulfonyl chlorides were purchased from Sigma-Aldrich, Combi-blocks, TCI and Enamine. Reactions were performed in 7 mL vials with two Kessil LEDSs (35W, 450 nm, approximately 4 cm away from the light source). The scale-up experiment in batch was performed using a Radleys Reactor Ready of 1 or 2 Liters and the temperature controlled using a Julabo A80 unit. The scale-up experiment in continuous flow was performed in a Vapourtec photoreactor (fluoropolymer tube, 1.3 mm i.d., 10 mL). Low temperature single crystal X-ray diffraction data were collected using a (Rigaku) Oxford Diffraction SuperNova A diffractometer. Data were reduced using CrysAlisPro, solved using SuperFlip[7] and refined using CRYSTALS.[8,9] Full crystallographic data (in CIF format) is available as ESI and has been deposited with the Cambridge Crystallographic Data Centre (CCDC 1973291). Additional analytical data (^1H, ^{13}C, ^{19}F, NOESY spectra) are available at https://onlinelibrary.wiley.com/action/downloadSupplement?doi=10.1002%2Fanie.202004070&file=anie202004070-sup-0001-misc_information.pdf.

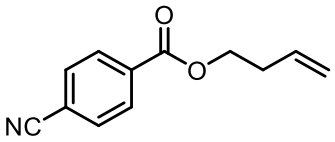
[a]: Experiments were conducted by Claudio F. Meyer (PhD student, University of Oxford).

[b]: Experiments were conducted by Dr. Jeroen Sap (former PhD student).

5.3.1 Synthesis of Starting Materials

Compounds **3.22**, **3.53**, **3.55**, **3.56**, **3.63**, **3.65**, **3.86**, **3.87**, **3.88**, **3.102**, **3.108**, **3.113**, **3.114**, **3.115**, **3.120**, **3.121**, **3.122**, **3.124**, **3.125**, **3.126**, **3.127**, and **3.128** were synthesised according to literature procedures and spectroscopic data were in accordance with previous reports.[1,3,10–15] For the preparation of compounds **3.85** and **3.108,** ***see*** **Chapter 5**, **Section 5.2.1**.

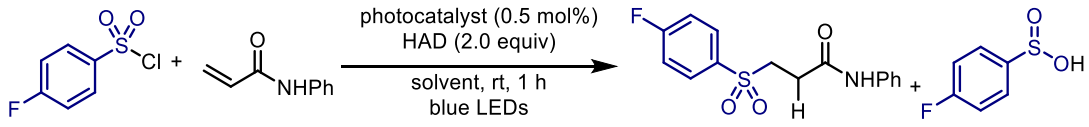
But-3-en-1-yl 4-cyanobenzoate (3.123)[a]



4-Cyanobenzoyl chloride (2.0 g, 12.1 mmol, 1.0 equiv) was added to a stirred solution of 3-buten-1-ol (870 mg, 12.1 mmol, 1.0 equiv) and triethylamine (2.5 mL, 18.1 mmol, 1.5 equiv) in DCM (25 mL) at 0 °C. The reaction mixture was warmed to room temperature and stirred for 72 hours., quenched by dropwise addition of a saturated aqueous solution of NH_4Cl and extracted with DCM. The organic layer was separated, dried (Na_2SO_4), filtered and concentrated *in vacuo.* The crude product was purified by flash column chromatography (silica, EtOAc in Heptane, 0/100 to 25/75). The desired fractions were collected and concentrated in vacuo to yield but-3-en-1-yl 4-cyanobenzoate **3.123** (1.86 g, 9.2 mmol, 77%) as a colourless oil. **^{1}H NMR** (400 MHz, $CDCl_3$) δ 8.15 − 8.10 (m, 2H), 7.76 − 7.71 (m, 2H), 5.92 − 5.78 (m, 1H), 5.21 − 5.08 (m, 2H), 4.43 − 4.37 (m, 2H), 2.57 − 2.49 (m, 2H); **^{13}C NMR** (101 MHz, $CDCl_3$) δ 165.0, 134.3, 133.8, 132.3, 130.2, 118.1, 117.8, 116.5, 64.8, 33.2; **HRMS** (ESI-TOF) calculated for $C_{12}H_{12}NO_2$ $[M+H]^+$: 202.0863; found 202.0865; **IR** (neat) 2232, 1720, 1407, 1269, 1177, 1105, 1019, 920, 862, 766, 691, 642.

5.3.2 Optimisation of the Reaction Conditions

Procedure for the optimisation studies:



3.21, (2.5 equiv) **3.22**, (1.0 equiv) **3.23** **3.24**

To a 7 mL vial equipped with a magnetic stir bar, was added *N*-phenylacrylamide **3.22** (0.50 mmol, 1.0 equiv), photocatalyst (0.0025 mmol, 0.5 mol%), solvent (3.0 mL), HAD (1.0 mmol, 2.0 equiv) and 4-fluorobenzenesulfonyl chloride **3.21** (1.25 mmol, 2.5 equiv) under air. The vial was equipped with a Teflon septum and stirred under blue LED irradiation with two Kessil LEDs (35W, 450 nm, approximately 4 cm away from the reaction mixture) for 1 hour. After this time, internal standard was added (0.1 mmol of α,α,α-trifluorotoluene as internal standard) to the crude reaction mixture, further diluted with $CDCl_3$ and analysed by quantitative ^{19}F NMR spectroscopy.

5.3.3 General Procedures

General procedure A: To a 7 mL vial equipped with a magnetic stir bar, was added alkene (0.50 mmol, 1.0 equiv), *fac*-Ir(ppy)$_3$ (1.70 mg, 0.0025 mmol, 0.5 mol%), MeCN (3.0 mL), (TMS)$_3$SiH (309 uL, 1.0 mmol, 2.0 equiv) and sulfonyl chloride (1.25 mmol, 2.5 equiv) under air. The vial was equipped with a Teflon septum and stirred under blue LED irradiation with two Kessil LEDs (35W, 450 nm, approximately 4 cm away from the reaction mixture) for 1 hour. The solvent was removed *in vacuo* and the residue was purified by column chromatography (silica, EtOAc in heptane 0/100 to 100/0) to yield the desired product(s).

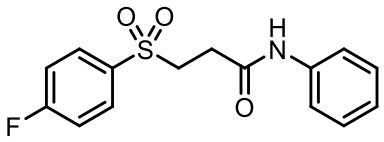
General procedure B: To a 7 mL vial equipped with a magnetic stir bar, was added alkyne (0.50 mmol, 1.0 equiv), *fac*-Ir(ppy)$_3$ (1.70 mg, 0.0025 mmol, 0.5 mol%), MeCN (3.0 mL), (TMS)$_3$SiH (309 uL, 1.0 mmol, 2.0 equiv) and sulfonyl chloride (1.25 mmol, 2.5 equiv) under air. The vial was equipped with a Teflon septum and stirred under blue LED irradiation with two Kessil LEDs (35W, 450 nm, approximately 4 cm away from the reaction mixture) for 16 hours. The solvent was removed *in vacuo* and the residue was purified by column chromatography (silica, EtOAc in heptane 0/100 to 100/0) to yield the desired product(s).

General procedure C: To a 7 mL vial equipped with a magnetic stir bar, was added alkene (0.50 mmol, 1.0 equiv), *fac*-Ir(ppy)$_3$ (1.70 mg, 0.0025 mmol, 0.5 mol%), 4-mercaptophenol (13 mg, 0.1 mmol, 0.2 equiv), MeCN (3.0 mL), (TMS)$_3$SiH (309 uL, 1.0 mmol, 2.0 equiv) and sulfonyl chloride (1.25 mmol, 2.5 equiv) under air. The vial was equipped with a Teflon septum and stirred under blue LED irradiation with two Kessil LEDs (35W, 450 nm,

approximately 4 cm away from the reaction mixture) for 16 hours. The solvent was removed *in vacuo* and the residue was purified by column chromatography (silica, EtOAc in heptane 0/100 to 100/0) to yield the desired product(s).

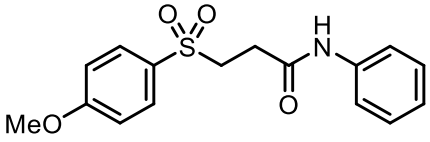
5.3.4 Characterisation: Hydrosulfonylation of Electron-Deficient Alkenes

3-((4-fluorophenyl)sulfonyl)-*N*-phenylpropanamide (3.23)



General procedure A was followed to obtain **3.23** (126 mg, 0.41 mmol, 82%) as a white solid. **^{1}H NMR** (500 MHz, $CDCl_3$) δ 8.12 (s, 1H), 7.99 − 7.94 (m, 2H), 7.47 − 7.43 (m, 2H), 7.31 − 7.27 (m, 2H), 7.26 − 7.21 (m, 2H), 7.13 − 7.09 (m, 1H), 3.58 (t, J = 8.1 Hz, 2H), 2.95 (t, J = 8.1 Hz, 2H); **^{13}C NMR** (126 MHz, $CDCl_3$) δ 167.1, 166.5 (d, $J_{C\text{-}F}$ = 257.8 Hz), 137.65, 134.8 (d, $J_{C\text{-}F}$ = 3.2 Hz), 131.1 (d, $J_{C\text{-}F}$ = 9.7 Hz), 129.1, 124.7, 120.1, 117.0 (d, $J_{C\text{-}F}$ = 22.6 Hz), 52.2, 29.8; **^{19}F NMR** (471 MHz, $CDCl_3$) δ − 102.5 (m, 1F); **HRMS** (ESI-TOF) calculated for $C_{15}H_{15}FO_3N^{32}S$ $[M+H]^+$: 308.0751; found 308.0759; **IR** (neat): 2981, 1689, 1661, 1594, 1527, 1493, 1445, 1399, 1312, 1292, 1256, 1226, 1180, 1157, 1139, 1084, 1055, 1015, 966, 951, 904, 839, 821, 794, 774, 752, 727, 693, 670, 651; **m.p.**: 143 − 144 °C.

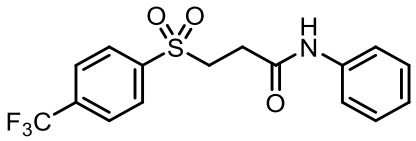
3-((4-methoxyphenyl)sulfonyl)-*N*-phenylpropanamide (3.39)



General procedure A was followed to obtain **3.39** (137 mg, 0.43 mmol, 86%) as a white solid. **^{1}H NMR** (400 MHz, $CDCl_3$) δ 8.45 (s, 1H), 7.85 − 7.80 (m, 2H), 7.45 − 7.39 (m, 2H), 7.25 − 7.18 (m, 2H), 7.06 − 7.00 (m, 1H), 6.97 − 6.92 (m, 2H), 3.78 (s, 3H), 3.53 (t, J = 7.9 Hz, 1H), 2.89 (t, J = 7.8 Hz, 1H); **^{13}C NMR** (101 MHz, $CDCl_3$) δ 167.5, 164.1, 137.9, 130.3,

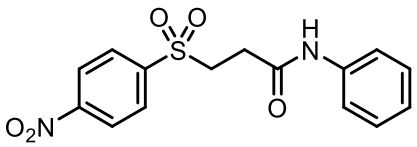
129.9, 128.9, 124.4, 120.0, 114.7, 55.7, 52.2, 30.1; **HRMS** (ESI-TOF) calculated for $C_{16}H_{18}NO_4{}^{32}S$ $[M+H]^+$: 320.0951; found 320.0956; **IR** (neat) 2981, 1690, 1595, 1545, 1496, 1445, 1425, 1315, 1292, 1264, 1172, 1138, 1087, 1051, 1027, 952, 835, 804, 804, 760, 728, 697, 653; **m.p.**: 111 − 113 °C.

***N*-phenyl-3-((4-(trifluoromethyl)phenyl)sulfonyl)propenamide (3.40)**



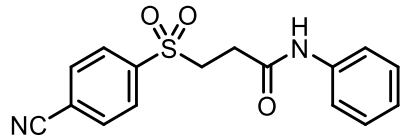
General procedure A was followed to obtain **3.40** (164 mg, 0.46 mmol, 92%) as a white solid. **^{1}H NMR** (500 MHz, DMSO-d_6) δ 10.02 (s, 1H), 8.15 (d, J = 8.1 Hz, 2H), 8.02 (d, J = 8.2 Hz, 2H), 7.45 (d, J = 7.2 Hz, 2H), 7.26 (t, J = 8.3 Hz, 2H), 7.02 (t, J = 7.4 Hz, 1H), 3.73 (t, J = 7.3 Hz, 2H), 2.71 (t, J = 7.3 Hz, 2H); **^{13}C NMR** (126 MHz, DMSO-d_6) δ 167.0, 142.5, 138.8, 133.5 (q, $J_{C\text{-}F}$ = 32.4 Hz), 129.0, 128.7, 126.6 (q, $J_{C\text{-}F}$ = 3.8 Hz), 123.3, 123.3 (q, $J_{C\text{-}F}$ = 273.0 Hz), 119.0, 50.5, 29.4; **^{19}F NMR** (471 MHz, DMSO-d_6) δ −61.8 (s, 3F); **HRMS** (ESI-TOF) calculated for $C_{16}H_{15}F_3NO_3{}^{32}S$ $[M+H]^+$: 358.0718; found 358.0728; **IR** (neat) 2981, 2889, 1656, 1531, 1498, 1319, 1271, 1258, 1169, 1147, 1109, 1062, 1018, 849, 792, 776, 735, 696; **m.p.**: 112 − 114 °C.

3-((4-nitrophenyl)sulfonyl)-*N*-phenylpropanamide (3.41)



General procedure A was followed to obtain **3.41** (150 mg, 0.45 mmol, 90%) as a white solid. **^{1}H NMR** (400 MHz, DMSO-d_6) δ 10.01 (s, 1H), 8.45 − 8.39 (m, 2H), 8.22 − 8.16 (m, 2H), 7.48 − 7.42 (m, 2H), 7.28 − 7.22 (m, 2H), 7.04 − 6.98 (m, 1H), 3.76 (t, J = 7.3 Hz, 2H), 2.72 (t, J = 7.3 Hz, 2H); **^{13}C NMR** (101 MHz, DMSO-d_6) δ 167.0, 150.5, 143.9, 138.7, 129.8, 128.7, 124.6, 123.3, 119.0, 50.6, 29.3; **HRMS** (ESI-TOF) calculated for $C_{15}H_{13}N_2O_5{}^{32}S$ [M-H]$^-$: 333.0551; found 333.0548; **IR** (neat) 2981, 2889, 1692, 1543, 1527, 1495, 1442, 1383, 1353, 1303, 1250, 1142, 1083, 1011, 957, 854, 815, 773, 759, 737, 704, 693, 655, 606; **m.p.**: 185 − 188 °C.

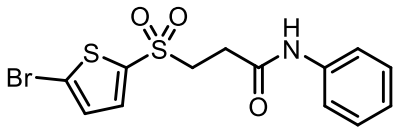
3-((4-cyanophenyl)sulfonyl)-*N*-phenylpropanamide (3.42)[a]



General procedure A was followed to obtain **3.42** (131 mg, 0.42 mmol, 83%) as a white solid. **^{1}H NMR** (400 MHz, DMSO-d_6) δ 10.01 (s, 1H), 8.16 − 8.07 (m, 4H), 7.48 − 7.44 (m, 2H), 7.31 − 7.24 (m, 2H), 7.07 − 7.00 (m, 1H), 3.72 (t, J = 7.3 Hz, 2H), 2.69 (t, J = 7.4 Hz, 2H); **^{13}C NMR** (101 MHz, DMSO-d_6) δ 167.0, 142.6, 138.8, 133.5, 128.7, 128.7, 123.3, 119.0, 117.5, 116.3, 50.4, 29.3; **HRMS** (ESI-TOF) calculated for $C_{16}H_{13}N_2O_3{}^{32}S$ [M-H]$^-$: 313.0652; found 313.0648; **IR** (neat) 2981, 2889, 1693, 1600, 1538, 1496, 1439, 1394, 1356,

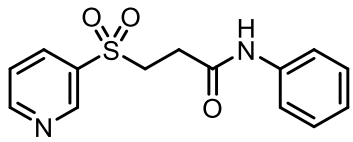
1315, 1249, 1177, 1149, 1132, 1083, 1024, 985, 968, 954, 845, 818, 788, 761, 747, 721, 691, 655; **m.p.**: 157 − 159 °C.

3-((5-bromothiophen-2-yl)sulfonyl)-*N*-phenylpropanamide (3.43)



General procedure A was followed to obtain **3.43** (159 mg, 0.43 mmol, 85%) as a white solid. **^{1}H NMR** (400 MHz, $CDCl_3$) δ 7.67 (s, 1H), 7.47 (d, J = 4.0 Hz, 1H), 7.43 (d, J = 7.7 Hz, 2H), 7.30 (t, J = 7.9 Hz, 2H), 7.15 − 7.08 (m, 2H), 3.65 (t, J = 7.7 Hz, 2H), 2.90 (t, J = 7.8 Hz, 2H); **^{13}C NMR** (101 MHz, $CDCl_3$) δ 166.7, 140.3, 137.5, 134.9, 131.4, 129.2, 124.9, 123.0, 120.1, 53.4, 30.4; **HRMS** (ESI-TOF) calculated for $C_{13}H_{13}NO_3{}^{79}Br^{32}S_2$ $[M+H]^+$: 375.9515; found 375.9497; **IR** (neat) 2981, 2889, 1674, 1600, 1535, 1497, 1474, 1462, 1442, 1396, 1318, 1253, 1198, 1149, 1129, 1078, 1019, 989, 967, 955, 808, 778, 751, 709, 688, 665; **m.p.**: 139 − 142 °C.

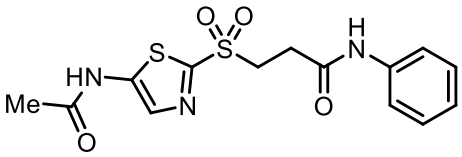
***N*-phenyl-3-(pyridin-3-ylsulfonyl)propenamide (3.44)**



General procedure A was followed to obtain **3.44** (107 mg, 0.37 mmol, 74%) as a white solid. **^{1}H NMR** (400 MHz, DMSO-d_6) δ 10.04 (s, 1H), 9.06 (dd, J = 2.4, 0.9 Hz, 1H), 8.90 (dd, J = 4.9, 1.6 Hz, 1H), 8.32 (ddd, J = 8.0, 2.4, 1.6 Hz, 1H), 7.69 (ddd, J = 8.2, 4.8, 0.8 Hz, 1H), 7.50 − 7.45 (m, 2H), 7.31 − 7.24 (m, 2H), 7.06 − 6.99 (m, 1H), 3.73 (t, J = 7.4 Hz, 2H),

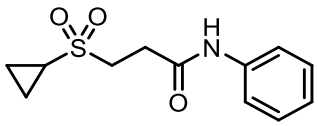
2.73 (t, *J* = 7.4 Hz, 2H); **^{13}C NMR** (101 MHz, DMSO-d_6) δ 167.1, 154.4, 148.5, 138.8, 136.2, 135.1, 128.7, 124.4, 123.3, 119.1, 50.9, 29.4; **HRMS** (ESI-TOF) calculated for $C_{14}H_{15}N_2O_3{}^{32}S$ $[M+H]^+$: 291.0798; found 291.0804; **IR** (neat) 2981, 2889, 1687, 1599, 1546, 1489, 1444, 1383, 1301, 1255, 1155, 1103, 1083, 956, 828, 809, 776, 753, 701, 688, 623; **m.p.**: 181 − 183 °C.

3-((5-acetamidothiazol-2-yl)sulfonyl)-*N*-phenylpropanamide (3.45)



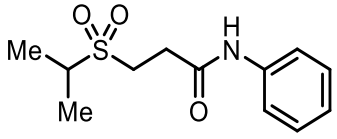
General procedure A was followed to obtain **3.45** (134 mg, 0.38 mmol, 76%) as a white solid. **^{1}H NMR** (500 MHz, DMSO-d_6) δ 12.78 (s, 1H), 10.04 (s, 1H), 8.08 (s, 1H), 7.51 − 7.47 (m, 2H), 7.30 − 7.25 (m, 2H), 7.05 − 7.00 (m, 1H), 3.69 (t, *J* = 7.3 Hz, 2H), 2.76 (t, *J* = 7.3 Hz, 2H), 2.19 (s, 3H); **^{13}C NMR** (126 MHz, DMSO-d_6) δ 169.8, 167.2, 163.7, 145.7, 138.8, 128.7, 126.8, 123.3, 119.1, 52.7, 30.0, 22.4; **HRMS** (ESI-TOF) calculated for $C_{14}H_{14}N_3O_4{}^{32}S_2$ $[M-H]^-$: 352.0431; found 352.0434; **IR** (neat) 2981, 2889, 1687, 1675, 1552, 1498, 1443, 1381, 1316, 1300, 1277, 1255, 1229, 1178, 1142, 1126, 1958, 1025, 1004, 956, 797, 772, 753, 706, 691, 671; **m.p.**: 238 − 240 °C.

3-(cyclopropylsulfonyl)-*N*-phenylpropanamide (3.46)



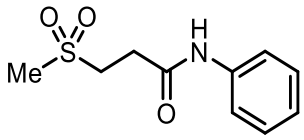
General procedure A was followed to obtain **3.46** (99 mg, 0.39 mmol, 78%) as a white solid. **^{1}H NMR** (400 MHz, $CDCl_3$) δ 8.12 (s, 1H), 7.53 − 7.48 (m, 2H), 7.34 − 7.27 (m, 2H), 7.13 − 7.07 (m, 1H), 3.52 (t, J = 7.4 Hz, 2H), 2.95 (t, J = 7.5 Hz, 2H), 2.47 (tt, J = 7.9, 4.8 Hz, 1H), 1.30 −1.21 (m, 2H), 1.12 − 1.02 (m, 2H); **^{13}C NMR** (101 MHz, $CDCl_3$) δ 167.6, 137.8, 129.2, 124.7, 120.1, 49.5, 30.1, 29.5, 5.1; **HRMS** (ESI-TOF) calculated for $C_{12}H_{16}NO_3{}^{32}S$ $[M+H]^+$: 254.0845; found 254.0849; **IR** (neat) 2981, 2889, 1689, 1596, 1541, 1500, 1488, 1442, 1422, 1383, 1307, 1269, 1252, 1186, 1128, 1084, 1072, 1040, 956, 887, 829, 752, 739, 698, 681; **m.p.**: 128 − 130 °C.

3-(isopropylsulfonyl)-*N*-phenylpropanamide (3.47)



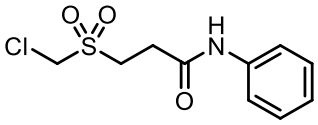
General procedure A was followed to obtain **3.47** (108 mg, 0.43 mmol, 85%) as a white solid. **^{1}H NMR** (400 MHz, $CDCl_3$) δ 8.31 (s, 1H), 7.51 (d, J = 7.4 Hz, 2H), 7.32 − 7.26 (m, 2H), 7.12 − 7.06 (m, 1H) 3.40 (t, J = 7.8 Hz, 2H), 3.18 (hept, J = 6.8 Hz, 1H), 2.97 (t, J = 7.8 Hz, 2H), 1.42 (d, J = 6.9 Hz, 6H); **^{13}C NMR** (101 MHz, $CDCl_3$) δ 167.8, 137.9, 129.1, 124.6, 120.1, 54.1, 44.8, 28.4, 15.4; **HRMS** (ESI-TOF) calculated for $C_{12}H_{18}NO_3{}^{32}S$ $[M+H]^+$: 256.1002; found 256.1013; **IR** (neat) 2981, 1672, 1602, 1547, 1499, 1462, 1440, 1422, 1383, 1307, 1253, 1154, 1139, 1125, 1081, 1060, 953, 908, 878, 804, 753, 726, 694, 664; **m.p.**: 120 − 122 °C.

3-(methylsulfonyl)-*N*-phenylpropanamide (3.48)



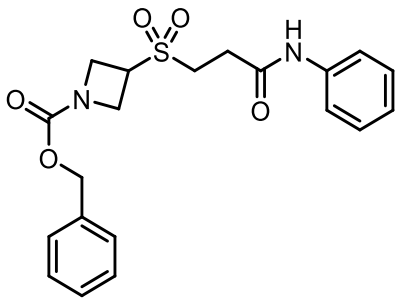
General procedure A was followed to obtain **3.48** (90 mg, 0.40 mmol, 79%) as a white solid. **^{1}H NMR** (400 MHz, DMSO-d_6) δ 10.11 (s, 1H), 7.60 − 7.55 (m, 2H), 7.34 − 7.27 (m, 2H), 7.07 − 7.02 (m, 1H), 3.43 (t, J = 7.6 Hz, 2H), 3.02 (s, 3H), 2.81 (t, J = 7.6 Hz, 2H); **^{13}C NMR** (101 MHz, DMSO-d_6) δ 167.9, 139.0, 128.7, 123.3, 119.1, 49.5, 40.5, 28.4; **HRMS** (ESI-TOF) calculated for $C_{10}H_{14}NO_3{}^{32}S$ $[M+H]^+$: 228.0689; found 228.0693; **IR** (neat) 2981, 2889, 1671, 1598, 1543, 1503, 1491, 1448, 1431, 1382, 1296, 1269, 1249, 1190, 1130, 1081, 1026, 995, 057, 918, 813, 753, 700, 676; **m.p.**: 120 − 122 °C.

3-((chloromethyl)sulfonyl)-*N*-phenylpropanamide (3.49)



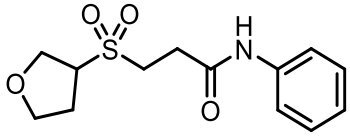
General procedure A was followed to obtain **3.49** (81 mg, 0.31 mmol, 62%) as a white solid. **^{1}H NMR** (400 MHz, DMSO-d_6) δ 10.15 (s, 1H), 7.60 − 7.55 (m, 2H), 7.34 − 7.27 (m, 2H), 7.08 − 7.02 (m, 1H), 5.15 (s, 2H), 3.58 (t, J = 7.4 Hz, 2H), 2.86 (t, J = 7.5 Hz, 2H); **^{13}C NMR** (101 MHz, DMSO-d_6) δ 167.5, 138.9, 128.8, 123.4, 119.1, 55.8, 45.7, 28.2; **HRMS** (ESI-TOF) calculated for $C_{10}H_{13}ClNO_3{}^{32}S$ $[M+H]^+$: 262.0299; found 262.0299; **IR** (neat) 2981, 2889, 1676, 1604, 1544, 1489, 1440, 1392, 1307, 1277, 1250, 1160, 1121, 1081, 1050, 1024, 991, 954, 878, 827, 798, 766, 745, 699, 676; **m.p.**: 141 − 145 °C.

Benzyl 3-((3-oxo-3-(phenylamino)propyl)sulfonyl)azetidine-1-carboxylate (3.50)[a]



General procedure A was followed to obtain **3.50** (195 mg, 0.49 mmol, 97%) as a white solid. **^{1}H NMR** (400 MHz, DMSO-d_6) δ 10.12 (br s, 1H), 7.59 − 7.54 (m, 2H), 7.40 − 7.27 (m, 7H), 7.08 − 7.01 (m, 1H), 5.06 (s, 2H), 4.41 − 4.32 (m, 1H), 4.31 − 4.19 (br s, 2H), 4.18 − 4.03 (br s, 2H), 3.47 (t, J = 7.4 Hz, 2H), 2.80 (t, J = 7.4 Hz, 2H) ; **^{13}C NMR** (101 MHz, DMSO-d_6) δ 167.6, 155.6, 138.9, 136.5, 128.8, 128.4, 128.0, 127.7, 123.4, 119.1, 66.1, 49.5 (br s), 49.0 (br s), 48.2, 46.4, 28.3; **HRMS** (ESI-TOF) calculated for $C_{20}H_{23}N_2O_5{}^{32}S$ $[M+H]^+$: 403.1322; found 403.1327; **IR** (neat) 2981, 2889, 1704, 1663, 1601, 1545, 1440, 1408, 1381, 1356, 1316, 1299, 1284, 1254, 1202, 1138, 1115, 1080, 1054, 1026, 998, 968, 951, 820, 758, 739, 696, 673, 629, 608; **m.p.**: 146 − 148 °C.

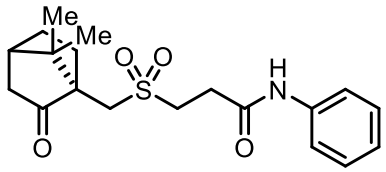
***N*-phenyl-3-((tetrahydrofuran-3-yl)sulfonyl)propanamide (3.51)**



General procedure A was followed to obtain **3.51** (115 mg, 0.41 mmol, 81%) as a white solid. **^{1}H NMR** (500 MHz, $CDCl_3$) δ 7.92 (s, 1H), 7.49 (d, J = 7.3 Hz, 2H), 7.34 − 7.29 (m, 2H), 7.14 − 7.09 (m, 1H), 4.25 (dd, J = 10.2, 5.1 Hz, 1H), 4.06 (dd, J = 10.2, 7.9 Hz, 1H), 4.03 − 3.97 (m, 1H), 3.85 − 3.79 (m, 1H), 3.78 − 3.71 (m, 1H), 3.46 − 3.38 (m, 2H), 2.96 (t,

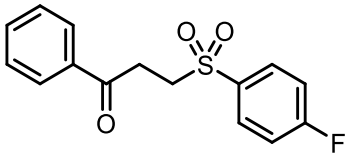
J = 7.2 Hz, 2H), 2.45 − 2.36 (m, 1H), 2.35 − 2.28 (m, 1H); **^{13}C NMR** (126 MHz, $CDCl_3$) δ 167.5, 137.7, 129.2, 124.8, 120.1, 68.5, 67.2, 61.9, 47.4, 28.7, 27.3; **HRMS** (ESI-TOF) calculated for $C_{13}H_{18}NO_4{}^{32}S$ $[M+H]^+$: 284.0951; found 284.0956; **IR** (neat) 2981, 2888, 1660, 1600, 1541, 1443, 1382, 1302, 1252, 1137, 1075, 968, 924, 742, 717, 691; **m.p.**: 125 − 128 °C.

3-((((*1S*)-7,7-dimethyl-2-oxobicyclo[2.2.1]heptan-1-yl)methyl)sulfonyl)-*N*-phenylpropanamide (3.52)



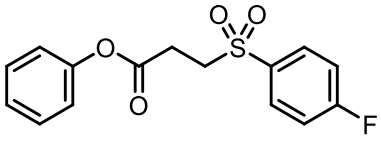
General procedure A was followed to obtain **3.52** (163 mg, 0.45 mmol, 90%) as a white solid. **^{1}H NMR** (400 MHz, $CDCl_3$) δ 8.40 (s, 1H), 7.56 − 7.51 (m, 2H), 7.31 − 7.25 (m, 2H), 7.11 − 7.05 (m, 1H), 3.61 (ddd, *J* = 7.8, 6.7, 3.2 Hz, 2H), 3.53 (d, *J* = 14.9 Hz, 1H), 3.07 − 2.91 (m, 2H), 2.86 (d, *J* = 14.9 Hz, 1H), 2.45 − 2.32 (m, 2H), 2.11 (t, *J* = 4.5 Hz, 1H), 2.06 − 1.96 (m, 1H), 1.92 (d, *J* = 18.5 Hz, 1H), 1.79 (ddd, *J* = 14.0, 9.3, 4.7 Hz, 1H), 1.41 (td, *J* = 9.2, 4.7 Hz, 1H), 1.02 (s, 3H), 0.85 (s, 3H); **^{13}C NMR** (101 MHz, $CDCl_3$) δ 215.4, 167.8, 138.0, 129.0, 124.4, 120.1, 58.8, 51.3, 50.9, 48.8, 42.7, 42.5, 29.7, 27.1, 24.9, 19.7, 19.6; **HRMS** (ESI-TOF) calculated for $C_{19}H_{26}NO_4{}^{32}S$ $[M+H]^+$: 364.1577; found 364.1584; **IR** (neat) 2980, 2889, 1704, 1667, 1599, 1545, 1491, 1462, 1441, 1381, 1299, 1251, 1132, 1082, 952, 879, 816, 740, 698, 673.

3-((4-fluorophenyl)sulfonyl)-1-phenylpropan-1-one (3.69)



General procedure A was followed to obtain **3.69** (129 mg, 0.44 mmol, 88%) as a white solid. **^{1}H NMR** (500 MHz, $CDCl_3$) δ 8.02 − 7.97 (m, 2H), 7.96 − 7.92 (m, 2H), 7.65 − 7.60 (m, 1H), 7.52 − 7.48 (m, 2H), 7.30 − 7.24 (m, 2H), 3.59 (ddd, J = 8.3, 6.4, 1.8 Hz, 2H), 3.53 (ddd, J = 8.3, 6.4, 1.8 Hz, 2H); **^{13}C NMR** (126 MHz, $CDCl_3$) δ 195.4, 166.1 (d, $J_{C\text{-}F}$ = 256.9 Hz), 135.9, 135.3 (d, $J_{C\text{-}F}$ = 3.2 Hz), 134.0, 131.1 (d, $J_{C\text{-}F}$ = 9.5 Hz), 129.0, 128.2, 116.9 (d, $J_{C\text{-}F}$ = 22.6 Hz), 51.3, 31.5; **^{19}F NMR** (471 MHz, $CDCl_3$) δ −102.9 - −103.0 (m, 1F); **HRMS** (ESI-TOF) calculated for $C_{15}H_{14}FO_3{}^{32}S$ $[M+H]^+$: 293.0642; found 293.0646; **IR** (neat) 1679, 1590, 1493, 1415, 1356, 1315, 1290, 1270, 1258, 1235, 1200, 1161, 1143, 1131, 1084, 1059, 1014, 973, 946, 832, 817, 743, 695, 673, 637; **m.p.**: 143 − 145 °C.

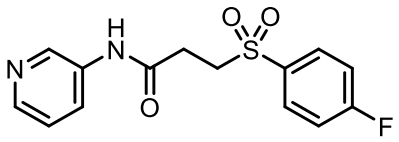
Phenyl 3-((4-fluorophenyl)sulfonyl)propanoate (3.70)



General procedure A was followed to obtain **3.70** (146 mg, 0.48 mmol, 95%) as a white solid. **^{1}H NMR** (400 MHz, $CDCl_3$) δ 8.00 − 7.93 (m, 2H), 7.39 − 7.32 (m, 2H), 7.29 − 7.19 (m, 3H), 7.06 − 7.01 (m, 2H), 3.53 (t, J = 7.5 Hz, 2H), 3.00 (t, J = 7.5 Hz, 2H); **^{13}C NMR** (101 MHz, $CDCl_3$) δ 168.7, 166.1 (d, $J_{C\text{-}F}$ = 257.1 Hz), 150.4, 134.7 (d, $J_{C\text{-}F}$ = 3.2 Hz), 131.2 (d, $J_{C\text{-}F}$ = 9.7 Hz), 129.6, 126.3, 121.3, 116.9 (d, $J_{C\text{-}F}$ = 22.6 Hz), 51.7, 28.1; **^{19}F NMR** (471

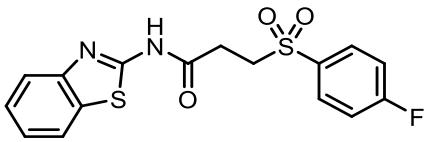
MHz, $CDCl_3$) δ −102.6 - −102.7 (m, 1F); **HRMS** (ESI-TOF) calculated for $C_{15}H_{14}FO_4{}^{32}S$ $[M+H]^+$: 309.0591; found 309.0593; **IR** (neat) 2981, 2889, 1750, 1591, 1492, 1462, 1381, 1310, 1291, 1251, 1193, 1155, 1085, 1022, 954, 902, 819, 803, 773, 751, 713, 697; **m.p.**: 104 − 106 °C.

3-((4-fluorophenyl)sulfonyl)-*N*-(pyridin-3-yl)propenamide (3.71)



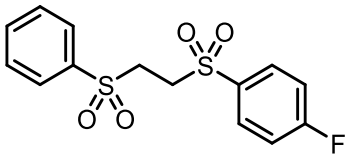
General procedure A was followed to obtain **3.71** (85 mg, 0.28 mmol, 55%) as a white solid. **^{1}H NMR** (400 MHz, DMSO-d_6) δ 10.26 (s, 1H), 8.63 (dd, J = 2.7, 0.8 Hz, 1H), 8.24 (dd, J = 4.7, 1.5 Hz, 1H), 8.03 − 7.96 (m, 2H), 7.91 (ddd, J = 8.3, 2.6, 1.5 Hz, 1H), 7.52 − 7.44 (m, 2H), 7.31 (ddd, J = 8.4, 4.7, 0.8 Hz, 1H), 3.65 (t, J = 7.4 Hz, 2H), 2.72 (t, J = 7.4 Hz, 2H); **^{13}C NMR** (101 MHz, DMSO-d_6) δ 167.9, 165.2 (d, $J_{C\text{-}F}$ = 252.9 Hz), 144.3, 140.7, 135.5, 134.9 (d, $J_{C\text{-}F}$ = 3.0 Hz), 131.17 (d, $J_{C\text{-}F}$ = 9.9 Hz), 126.0, 123.6, 116.7 (d, $J_{C\text{-}F}$ = 22.8 Hz), 50.7, 29.5; **^{19}F NMR** (377 MHz, DMSO-d_6) δ −102.4 - −102.5 (m, 1F); **HRMS** (ESI-TOF) calculated for $C_{14}H_{14}FN_2O_3{}^{32}S$ $[M+H]^+$: 309.0704; found 309.0714; **IR** (neat) 1589, 1496, 1446, 1308, 1291, 1222, 1149, 1120, 1099, 1083, 1012, 839, 808, 767, 749, 733, 706, 686; **m.p.**: 156 − 159 °C.

***N*-(benzo[*d*]thiazol-2-yl)-3-((4-fluorophenyl)sulfonyl)propenamide (3.72)**



General procedure A was followed to obtain **3.72** (158 mg, 0.43 mmol, 87%) as a white solid. **^{1}H NMR** (400 MHz, DMSO-d_6) δ 8.02 − 7.97 (m, 2H), 7.97 − 7.93 (m, 1H), 7.74 − 7.71 (m, 1H), 7.53 − 7.46 (m, 2H), 7.45 − 7.39 (m, 1H), 7.32 − 7.26 (m, 1H), 3.70 (t, J = 7.2 Hz, 2H), 2.88 (t, J = 7.3 Hz, 2H); **^{13}C NMR** (101 MHz, DMSO-d_6) δ 168.7, 165.2 (d, $J_{C\text{-}F}$ = 252.9 Hz), 157.7, 148.5, 134.8 (d, $J_{C\text{-}F}$ = 2.9 Hz), 131.4, 131.2 (d, $J_{C\text{-}F}$ = 9.9 Hz), 126.1, 123.6, 121.7, 120.6, 116.7 (d, $J_{C\text{-}F}$ = 22.9 Hz), 50.3, 28.8; **^{19}F NMR** (471 MHz, DMSO-d_6) δ −104.6 - −104.7 (m, 1F); **HRMS** (ESI-TOF) calculated for $C_{16}H_{12}FN_2O_3{}^{32}S_2$ $[M\text{-}H]^-$: 363.0279; found 363.0278; **IR** (neat) 1698, 1592, 1546, 1492, 1455, 1445, 1319, 1288, 1268, 1238, 1149, 1086, 1046, 1024, 983, 877, 832, 759, 727, 706, 667; ; **m.p.**: 200 −204 °C.

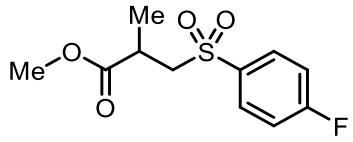
1-fluoro-4-((2-(phenylsulfonyl)ethyl)sulfonyl)benzene (3.73)



General procedure A was followed to obtain **3.73** (112 mg, 0.34 mmol, 68%) as a white solid. **^{1}H NMR** (500 MHz, $CDCl_3$) δ 7.92 − 7.86 (m, 4H), 7.73 − 7.69 (m, 1H), 7.62 − 7.57 (m, 2H), 7.29 − 7.24 (m, 2H), 3.45 (s, 4H); **^{13}C NMR** (126 MHz, $CDCl_3$) δ 166.4 (d, $J_{C\text{-}F}$ = 258.2 Hz), 138.1, 134.7, 134.2 (d, $J_{C\text{-}F}$ = 3.2 Hz), 131.2 (d, $J_{C\text{-}F}$ = 9.7 Hz), 129.9, 128.2, 117.2 (d, $J_{C\text{-}F}$ = 22.9 Hz), 49.7, 49.5; **^{19}F NMR** (471 MHz, $CDCl_3$) δ −101.5 - −101.6 (m, 1F); **HRMS** (ESI-TOF) calculated for $C_{14}H_{13}FNaO_4{}^{32}S_2$ $[M+H]^+$: 351.0131; found

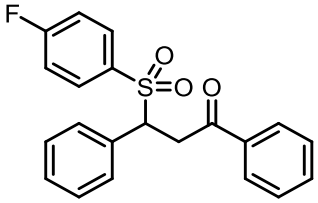
351.0132; **IR** (neat) 1589, 1496, 1446, 1308, 1291, 1222, 1149, 1120, 1099, 1083, 1012, 839, 808, 767, 749, 733, 706, 686; **m.p.**: 177 − 178 °C. Compound **3.73** was found to be unstable under various ionization techniques and HRMS could therefore not be obtained.

Methyl 3-((4-fluorophenyl)sulfonyl)-2-methylpropanoate (3.74)



General procedure A was followed to obtain **3.74** (101 mg, 0.39 mmol, 78%) as a white solid. **^{1}H NMR** (400 MHz, $CDCl_3$) δ 7.93 − 7.85 (m, 2H), 7.25 − 7.18 (m, 2H), 3.66 (dd, J = 14.2, 7.7 Hz, 1H), 3.59 (s, 3H), 3.06 (dd, J = 14.2, 5.1 Hz, 1H), 3.02 − 2.92 (m, 1H), 1.28 (d, J = 7.1 Hz, 3H); **^{13}C NMR** (101 MHz, $CDCl_3$) δ 173.9, 166.0 (d, $J_{C\text{-}F}$ = 256.6 Hz), 135.3 (d, $J_{C\text{-}F}$ = 3.2 Hz), 131.1 (d, $J_{C\text{-}F}$ = 9.7 Hz), 116.7 (d, $J_{C\text{-}F}$ = 22.7 Hz), 58.9, 52.4, 34.8, 17.9; **^{19}F NMR** (471 MHz, $CDCl_3$) δ −103.1 - −103.2 (m, 1F); **HRMS** (ESI-TOF) calculated for $C_{11}H_{14}FO_4{}^{32}S$ $[M+H]^+$: 261.0591; found 261.0602; **IR** (neat) 1735, 1591, 1493, 1459, 1405, 1320, 1290, 1230, 1141, 1085, 837, 758, 673.

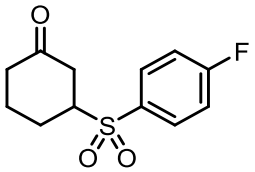
3-((4-fluorophenyl)sulfonyl)-1,3-diphenylpropan-1-one (3.75)



General procedure A was followed to obtain **3.75** (162 mg, 0.44 mmol, 88%) as a white solid. **^{1}H NMR** (400 MHz, $CDCl_3$) δ 7.97 − 7.92 (m, 2H), 7.61 − 7.50 (m, 3H), 7.49 − 7.43 (m, 2H), 7.29 − 7.17 (m, 5H), 7.08 − 7.01 (m, 2H), 4.93 (dd, J = 9.6, 3.6 Hz, 1H), 4.14 (dd,

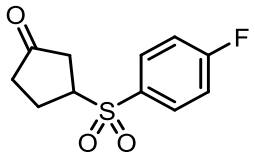
J = 17.9, 3.6 Hz, 1H), 3.93 (dd, *J* = 17.9, 9.6 Hz, 1H); **^{13}C NMR** (101 MHz, $CDCl_3$) δ 194.9, 165.9 (d, $J_{C\text{-}F}$ = 256.6 Hz), 136.2, 133.9, 133.1 (d, $J_{C\text{-}F}$ = 3.2 Hz), 132.6, 132.0 (d, $J_{C\text{-}F}$ = 9.7 Hz), 129.9 129.1, 128.9, 128.7, 128.3, 116.2 (d, $J_{C\text{-}F}$ = 22.6 Hz), 66.8, 36.9; **^{19}F NMR** (471 MHz, $CDCl_3$) δ −103.1 - −103.2 (m, 1F); **HRMS** (ESI-TOF) calculated for $C_{21}H_{18}FO_3{}^{32}S$ $[M+H]^+$: 369.0955; found 369.0962; **IR** (neat) 2981, 2888, 1688, 1591, 1492, 1449, 1382, 1314, 1289, 1235, 1142, 1085, 1015, 957, 832, 817, 778, 750, 730, 698, 688, 672, 641, 615; **m.p.**: 170 − 172 °C.

3-((4-fluorophenyl)sulfonyl)cyclohexan-1-one (3.76)



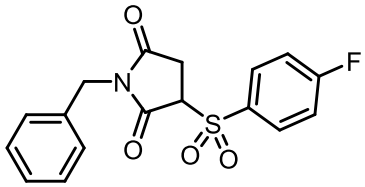
General procedure A was followed to obtain **3.76** (97 mg, 0.36 mmol, 71%) as a white solid. **^{1}H NMR** (400 MHz, $CDCl_3$) δ 7.93 − 7.87 (m, 2H), 7.39 − 7.32 (m, 2H), 3.36 − 3.25 (m, 1H), 2.64 − 2.54 (m, 2H), 2.47 − 2.39 (m, 1H), 2.37 − 2.18 (3H), 1.99 − 1.86 (m, 1H), 1.72 − 1.59 (m, 1H); **^{13}C NMR** (101 MHz, $CDCl_3$) δ 206.2, 166.2 (d, $J_{C\text{-}F}$ = 257.4 Hz), 132.8 (d, $J_{C\text{-}F}$ = 3.2 Hz), 131.9 (d, $J_{C\text{-}F}$ = 9.7 Hz), 116.9 (d, $J_{C\text{-}F}$ = 22.7 Hz), 62.5, 40.5, 40.4, 23.8, 23.4; **^{19}F NMR** (471 MHz, $CDCl_3$) δ −102.4 - −102.5 (m, 1F); **HRMS** (ESI-TOF) calculated for $C_{12}H_{17}FNO_3{}^{32}S$ $[M+NH_4]^+$: 274.0908; found 274.0910; **IR** (neat) 1713, 1590, 1493, 1311, 1286, 1267, 1227, 1138, 1084, 1058, 843, 818, 776, 720, 674; **m.p.**: 84 − 87 °C.

3-((4-fluorophenyl)sulfonyl)cyclopentan-1-one (3.77)



General procedure A was followed to obtain **3.77** (92 mg, 0.38 mmol, 76%) as a white solid. **^{1}H NMR** (400 MHz, $CDCl_3$) δ 7.98 − 7.90 (m, 2H), 7.34 − 7.25 (m , 2H), 3.76 (p, J = 7.7 Hz, 1H), 2.72 − 2.62 (m, 1H), 2.60 − 2.37 (m, 3H), 2.35 − 2.20 (m, 2H); **^{13}C NMR** (101 MHz, $CDCl_3$) δ 212.5, 166.3 (d, $J_{C\text{-}F}$ = 257.5 Hz), 133.6 (d, $J_{C\text{-}F}$ = 3.3 Hz), 131.6 (d, $J_{C\text{-}F}$ = 9.6 Hz), 117.1 (d, $J_{C\text{-}F}$ = 22.6 Hz), 61.0, 38.7, 37.0, 23.3; **^{19}F NMR** (471 MHz, $CDCl_3$) δ − 102.3 - − 102.4 (m, 1F);**HRMS** (ESI-TOF) calculated for $C_{11}H_{11}O_3F^{23}Na^{32}S$ $[M+Na]^+$: 265.0305; found 265.0307; **IR** (neat) 2981, 1738, 1700, 1589, 1493, 1473, 1462, 1383, 1323, 1287, 1253, 1227, 1141, 1081, 1014, 954, 903, 850, 837, 819, 789, 754, 124, 691, 655, 635; **m.p.**: 99 − 101 °C.

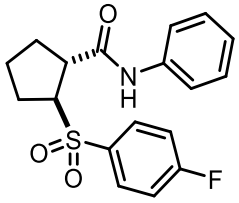
1-benzyl-3-((4-fluorophenyl)sulfonyl)pyrrolidine-2,5-dione (3.78)



General procedure A was followed to obtain **3.78** (130 mg, 0.38 mmol, 75%) as a white solid. **^{1}H NMR** (500 MHz, $CDCl_3$) δ 7.86 − 7.81 (m, 2H), 7.30 − 7.24 (m, 5H), 7.20 − 7.14 (m, 2H), 4.59 (d, J = 4.5 Hz, 2H), 4.30 (dd, J = 9.6, 3.8 Hz, 1H), 3.32 (dd, J = 19.1, 3.8 Hz, 1H), 3.07 (dd, J = 19.1, 9.6 Hz, 1H); **^{13}C NMR** (101 MHz, $CDCl_3$) δ 172.5, 168.4, 166.6 (d, $J_{C\text{-}F}$ = 258.7 Hz), 134.7, 132.5 (d, $J_{C\text{-}F}$ = 10.0 Hz), 132.3 (d, $J_{C\text{-}F}$ = 3.2 Hz), 128.8, 128.8, 128.4, 116.9 (d, $J_{C\text{-}F}$ = 22.8 Hz), 63.6, 43.2, 30.0; **^{19}F NMR** (471 MHz, $CDCl_3$) δ −100.7 - −

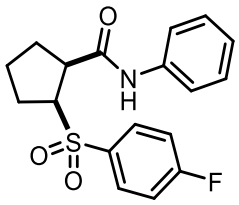
100.8 (m, 1F); **HRMS** (ESI-TOF) calculated for $C_{17}H_{13}FO_4N^{32}S$ $[M-H]^-$: 346.0555; found 346.0550; **IR** (neat) 2981, 2914, 1699, 1588, 1492, 1447, 1399, 1356, 1324, 1293, 1237, 1214, 1157, 1136, 1084, 1011, 955, 908, 836, 788, 754, 701, 655, 632, 614; **m.p.**: 181 − 183 °C.

***trans*-2-((4-fluorophenyl)sulfonyl)-*N*-phenylcyclopentane-1-carboxamide (*trans*-3.79)**



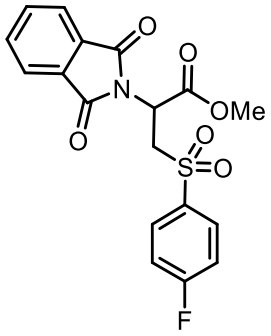
General procedure A was followed to obtain ***trans*-3.79** (113 mg, 0.33 mmol, 65%) as a white solid. **^{1}H NMR** (500 MHz, DMSO-d_6) δ 9.95 (s, 1H), 7.98 − 7.92 (m, 2H), 7.44 − 7.36 (m, 4H), 7.29 − 7.23 (m, 2H), 7.04 − 7.00 (m, 1H), 4.09 (dt, J = 9.1, 7.2 Hz, 1H), 3.23 (dt, J = 9.1, 8.1 Hz, 1H), 2.16 − 2.07 (m, 1H), 2.06 − 1.97 (m, 2H), 1.79 − 1.71 (m, 1H), 1.71 − 1.59 (m, 2H); **^{13}C NMR** (126 MHz, DMSO-d_6) δ 170.6, 165.1 (d, $J_{C\text{-}F}$ = 253.1 Hz), 138.7, 134.4 (d, $J_{C\text{-}F}$ = 3.0 Hz), 131.5 (d, $J_{C\text{-}F}$ = 9.9 Hz), 128.6, 123.3, 119.1, 116.6 (d, $J_{C\text{-}F}$ = 22.8 Hz), 65.2, 46.8, 32.8, 27.0, 25.6; **^{19}F NMR** (471 MHz, DMSO-d_6) δ −104.7 - −104.8 (m); **HRMS** (ESI-TOF) calculated for $C_{18}H_{19}FO_3N^{32}S$ $[M+H]^+$: 348.1064; found 348.1070; **IR** (neat) 1727, 1589, 1493, 1452, 1408, 1365, 1319, 1295, 1225, 1174, 1157, 1144, 1099, 1082, 1024, 955, 857, 844, 832, 820, 732, 709, 697, 647; **m.p.**: 175 − 178 °C.

***cis*-2-((4-fluorophenyl)sulfonyl)-*N*-phenylcyclopentane-1-carboxamide (*cis*-3.79)**



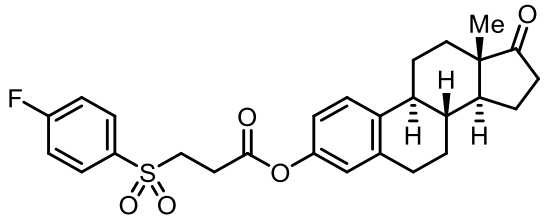
General procedure A was followed to obtain ***cis*-3.79** (61 mg, 0.18 mmol, 35%) as a white solid. **^{1}H NMR** (400 MHz, DMSO-d_6) δ 9.77 (s, 1H), 7.88 − 7.82 (m, 2H), 7.50 − 7.45 (m, 2H), 7.37 − 7.30 (m, 2H), 7.29 − 7.23 (m, 2H), 7.05 − 6.99 (m, 1H), 4.09 (dt, J = 7.7 Hz, 1H), 3.16 (dt, J = 7.1 Hz, 1H), 2.34 − 2.21 (m, 1H), 2.04 − 1.76 (m, 4H), 1.71 − 1.58 (m, 1H); **^{13}C NMR** (101 MHz, DMSO-d_6) δ 169.0, 164.9 (d, $J_{C\text{-}F}$ = 252.3 Hz), 139.0, 135.7 (d, $J_{C\text{-}F}$ = 2.9 Hz), 131.2 (d, $J_{C\text{-}F}$ = 9.9 Hz), 128.4, 123.0, 119.2, 116.3 (d, $J_{C\text{-}F}$ = 22.9 Hz), 66.6, 46.8, 28.2, 26.3, 22.2; **^{19}F NMR** (471 MHz, DMSO-d_6) δ −105.2 - −105.3 (m, 1F); **HRMS** (ESI-TOF) calculated for $C_{18}H_{19}FO_3N^{32}S$ $[M+H]^+$: 348.1064; found 348.1069; **IR** (neat) 1662, 1590, 1547, 1491, 1445, 1395, 1317, 1292, 1253, 1238, 1203, 1193, 1145, 1129, 1098, 1080, 1013, 963, 932, 905, 885, 850, 823, 792, 755, 722, 695, 632, 616; **m.p.**: 188 − 191 °C.

Methyl 2-(1,3-dioxoisoindolin-2-yl)-3-((4-fluorophenyl)sulfonyl)propanoate (3.80)



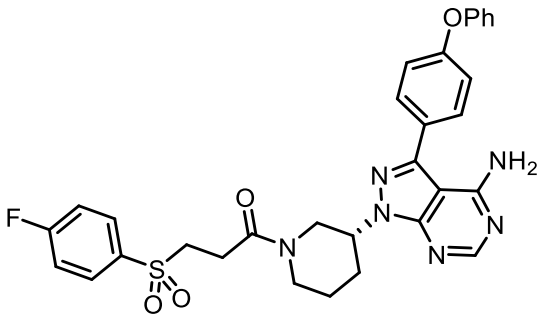
General procedure A was followed to obtain **3.80** (119 mg, 0.31 mmol, 61%) as a white solid. **^{1}H NMR** (400 MHz, $CDCl_3$) δ 7.90 − 7.83 (m, 2H), 7.83 − 7.78 (m, 2H), 7.77 − 7.71 (m, 2H), 7.11 − 7.03 (m, 2H), 5.33 (dd, J = 11.5, 2.4 Hz, 1H), 4.29 (dd, J = 15.2, 11.5 Hz, 1H), 3.98 (dd, J = 15.2, 2.5 Hz, 1H), 3.72 (s, 3H); **^{13}C NMR** (101 MHz, $CDCl_3$) δ 167.2, 167.2, 165.8 (d, $J_{C\text{-}F}$ = 224.8 Hz), 134.6, 134.5 (d, $J_{C\text{-}F}$ = 3.1 Hz), 131.5, 131.2 (d, $J_{C\text{-}F}$ = 9.8 Hz), 123.8, 116.7 (d, $J_{C\text{-}F}$ = 22.8 Hz), 53.8, 53.1, 46.9; **^{19}F NMR** (471 MHz, $CDCl_3$) δ −102.6 - −102.7 (m, 1F); **HRMS** (ESI-TOF) calculated for $C_{18}H_{15}FNO_6{}^{32}S$ $[M+H]^+$: 392.0599; found 392.0599; **IR** (neat) 2981, 2889, 1775, 1735, 1718, 1589, 1492, 1470, 1438, 1383, 1309, 1291, 1256, 1142, 1085, 1072, 1014, 1002, 956, 911, 873, 853, 839, 820, 806, 787, 756, 712, 656; **m.p.**: 155 − 159 °C.

(8*R*,9*S*,13*S*,14*S*)-13-methyl-17-oxo-7,8,9,11,12,13,14,15,16,17-decahydro-6*H*-cyclopenta[*a*]phenanthren-3-yl 3-((4-fluorophenyl)sulfonyl)propanoate (3.81)



General procedure A was followed to obtain **3.81** (189 mg, 0.39 mmol, 78%) as a white solid. **^{1}H NMR** (500 MHz, $CDCl_3$) δ 7.97 − 7.92 (m, 2H), 7.25 − 7.22 (m, 3H), 6.77 (dd, J = 8.5, 2.6 Hz, 1H), 6.71 (d, J = 2.5 Hz, 1H), 3.50 (t, J = 7.5 Hz, 2H), 2.97 (t, J = 7.5 Hz, 2H), 2.88 − 2.84 (m, 2H), 2.51 − 2.44 (m, 1H), 2.39 − 2.32 (m, 1H), 2.28 − 2.19 (m, 1H), 2.17 − 2.06 (m, 1H), 2.06 − 1.90 (m, 3H), 1.65 − 1.35 (m, 6H), 0.87 (s, 3H); **^{13}C NMR** (126 MHz, $CDCl_3$) δ 220.8, 169.0, 166.2 (d, $J_{C\text{-}F}$ = 257.3 Hz), 148.3, 138.4, 138.0, 134.7 (d, $J_{C\text{-}F}$ = 3.1 Hz), 131.3 (d, $J_{C\text{-}F}$ = 9.6 Hz), 126.7, 121.4, 118.5, 117.0 (d, $J_{C\text{-}F}$ = 22.8 Hz), 51.8, 50.6, 48.1, 44.3, 38.1, 36.0, 31.7, 29.5, 28.1, 26.4, 25.9, 21.7, 14.0; **^{19}F NMR** (471 MHz, $CDCl_3$) δ − 102.5 - −102.6 (m, 1F); **HRMS** (ESI-TOF) calculated for $C_{27}H_{33}FO_5N^{32}S$ $[M+NH_4]^+$: 502.2058; found 502.2065; **IR** (neat) 2971, 1692, 1589, 1520, 1489, 1467, 1440, 1380, 1342, 1315, 1295, 1234, 1159, 1130, 1085, 1051, 951, 838, 816, 789, 757, 707, 690, 669, 617.

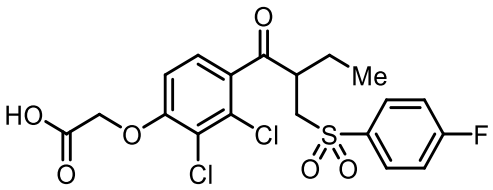
(*R*)-1-(3-(4-amino-3-(4-phenoxyphenyl)-1*H*-pyrazolo[3,4-*d*]pyrimidin-1-yl)piperidin-1-yl)-3-((4-fluorophenyl)sulfonyl)propan-1-one (3.82)



General procedure A was followed to obtain **3.82** (219 mg, 0.37 mmol, 73%) as a white solid. NMR analysis showed two rotamers. **^{1}H NMR** (500 MHz, $CDCl_3$) δ 8.38 (s, 0.5H), 8.33 (s, 0.5H), 7.97 − 7.88 (m, 2H), 7.67 − 7.60 (m, 2H), 7.42 − 7.36 (m, 2H), 7.29 − 7.19 (m, 2H), 7.18 − 7.12 (m, 3H), 7.11 − 7.06 (m, 2H), 5.91 − 5.55 (m, 2H), 4.88 − 4.76 (m, 1H), 4.73 − 4.63 (m, 0.5H), 4.40 − 4.33 (m, 0.5H), 4.03 − 3.97 (m, 0.5H), 3.89 − 3.82 (m, 0.5H), 3.74 (br dd, J = 13.3, 10.1 Hz, 0.5H), 3.54 − 3.40 (m, 2H), 3.32 (dd, J = 12.8, 10.7 Hz, 0.5H), 3.23 − 3.14 (m, 0.5H), 2.96 − 2.84 (m, 2H), 2.83 − 2.75 (m, 0.5H), 2.44 − 2.27 (m, 1H), 2.27 − 2.19 (m, 1H), 2.06 − 1.99 (m, 0.5H), 1.97 − 1.90 (m, 0.5H), 1.77− 1.68 (m, 0.5H), 1.68 − 1.57 (m, 0.5H); **^{13}C NMR** (126 MHz, $CDCl_3$) δ 167.4, 167.3, 166.0 (d, $J_{C\text{-}F}$ = 255.0 Hz), 165.7 (d, $J_{C\text{-}F}$ = 255.7 Hz), 158.7, 158.6, 158.2, 158.0, 156.4, 156.4, 156.1, 155.9, 154.5, 154.3, 144.2, 144.0, 135.4 (d, $J_{C\text{-}F}$= 3.2 Hz), 135.3 (d, J = 3.2 Hz), 131.0 (dd, $J_{C\text{-}F}$ = 9.0 Hz), 131.0 (d, $J_{C\text{-}F}$ = 9.0 Hz), 130.1, 130.1, 130.1, 130.1, 127.9, 127.7, 124.2, 124.2, 119.7, 119.7, 119.3, 119.2, 116.9 (d, $J_{C\text{-}F}$ = 22.9 Hz), 116.8 (d, $J_{C\text{-}F}$ = 22.8 Hz), 98.8, 98.6, 53.2, 52.4, 52.4, 52.3, 49.6, 46.2, 45.6, 42.3, 30.2, 30.0, 26.3, 26.2, 25.0, 23.8; **^{19}F NMR** (471 MHz, $CDCl_3$) δ −103.0 - −103.0 (m, 0.5F), −103.0 - −103.0 (m, 0.5F); **HRMS** (ESI-TOF) calculated for $C_{31}H_{30}FO_4N_6{}^{32}S$ $[M+H]^+$: 601.2028; found 601.2028; **IR** (neat) 2981, 2361, 2341, 1697,

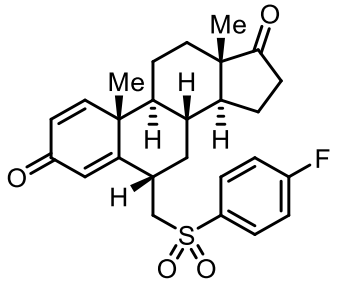
1632, 1589, 1522, 1491, 1444, 1395, 1356, 1322, 1292, 1237, 1148, 1085, 1010, 954, 837, 802, 788, 755, 693, 669, 655.

-(2,3-dichloro-4-(2-(((4-fluorophenyl)sulfonyl)methyl)butanoyl)phenoxy)acetic acid (3.83)



General procedure A was followed to obtain **3.83** (97 mg, 0.21 mmol, 42%) as a white solid. **^{1}H NMR** (500 MHz, $CDCl_3$) δ 7.93 − 7.87 (m, 2H), 7.60 (d, J = 8.6 Hz, 1H), 7.22 (t, J = 8.5 Hz, 2H), 6.84 (d, J = 8.5 Hz, 1H), 4.76 (s, 2H), 3.99 − 3.84 (m, 2H), 3.20 − 3.13 (m, 1H), 1.87 − 1.76 (m, 1H), 1.63 − 1.52 (m, 1H), 0.86 (t, J = 7.4 Hz, 3H); **^{13}C NMR** (101 MHz, $CDCl_3$) δ 199.9, 171.7, 166.1 (d, $J_{C\text{-}F}$ = 257.0 Hz), 156.5, 135.7 (d, $J_{C\text{-}F}$ = 3.2 Hz), 132.7, 132.5, 130.9 (d, $J_{C\text{-}F}$ = 9.6 Hz), 128.5, 124.3, 116.9 (d, $J_{C\text{-}F}$ = 22.7 Hz), 110.8, 65.9, 56.1, 45.5, 24.9, 10.7; **^{19}F NMR** (471 MHz, $CDCl_3$) δ −102.8 - −102.9 (m, 1F); **HRMS** (ESI-TOF) calculated for $C_{19}H_{16}{}^{35}Cl_2FO_6{}^{32}S$ $[M\text{-}H]^-$: 461.0034; found 461.0024; **IR** (neat) 2980, 2888, 2360, 2342, 2160, 2034, 1693, 1633, 1589, 1526, 1492, 1463, 1441, 1381, 1316, 1293, 1236, 1149, 1085, 1011, 951, 837, 817, 788, 756, 692, 669, 655, 631, 617.

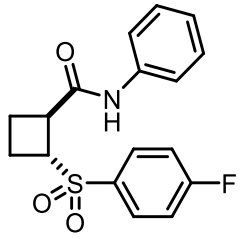
(6*S*, 8*R*, 9*S*, 10*R*, 13*S*, 14*S*)-6-(((4-fluorophenyl)sulfonyl)methyl)-10,13-dimethyl-7,8,9,10,11,12,13,14,15,16-decahydro-3*H*-cyclopenta[*a*]phenanthrene-3,17(6*H*)-dione (3.84)



General procedure A was followed to obtain **3.84** (114 mg, 0.25 mmol, 50%) as a white solid. **^{1}H NMR** (400 MHz, $CDCl_3$) δ 7.99 − 7.92 (m, 2H), 7.32 − 7.24 (m, 2H), 7.05 (d, J = 10.2 Hz, 1H), 6.22 (dd, J = 10.2, 1.7 Hz, 1H), 5.81 (t, J = 1.6 Hz, 1H), 3.44 (dd, J = 13.5, 3.4 Hz, 1H), 3.36 − 3.26 (m, 1H), 3.13 (dd, J = 13.5, 8.9 Hz, 1H), 2.64 (dt, J = 12.6, 4.1 Hz, 1H), 2.48 (dd, J = 19.5, 8.6 Hz, 1H), 2.08 (dt, J = 19.2, 9.0 Hz, 1H), 2.01 − 1.91 (m, 2H), 1.90 − 1.80 (m, 2H), 1.77 − 1.58 (m, 2H), 1.31 (s, 3H), 1.30 − 1.19 (m, 2H), 1.12 − 0.98 (m, 2H), 0.95 (s, 3H); **^{13}C NMR** (126 MHz, $CDCl_3$) δ 219.6, 185.3, 167.2, 166.3 (d, $J_{C\text{-}F}$ = 256.7 Hz), 156.1, 136.4 (d, $J_{C\text{-}F}$ = 3.6 Hz), 130.8 (d, $J_{C\text{-}F}$ = 9.6 Hz), 127.3, 121.6, 117.1 (d, $J_{C\text{-}F}$ = 22.8 Hz), 58.4, 53.6, 50.3, 47.8, 44.2, 39.2, 35.7, 35.1, 34.2, 31.2, 22.4, 22.0, 18.9, 14.0; **^{19}F NMR** (471 MHz, $CDCl_3$) δ −102.5 - −102.6 (m, 1F); **HRMS** (ESI-TOF) calculated for $C_{26}H_{30}FO_4{}^{32}S$ $[M+H]^+$: 457.1843; found 457.1846; **IR** (neat) 2981, 2889, 2361, 2341, 1735, 1660, 1621, 1590, 1494, 1462, 1381, 1312, 1291, 1239, 1146, 1086, 1010, 953, 888, 818, 717, 669.

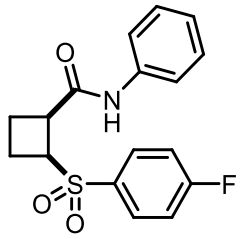
3.5.5 Hydrosulfonylation of cyclobutenes

trans-2-((4-fluorophenyl)sulfonyl)-_N_-phenylcyclobutane-1-carboxamide (_trans_-3.89)



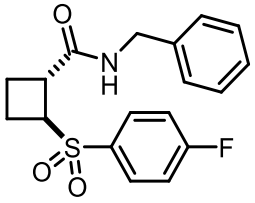
General procedure A was followed to obtain ***trans*-3.89** (60 mg, 0.18 mmol, 36%) as a white solid. **^{1}H NMR** (500 MHz, $CDCl_3$) δ 8.35 (s, 1H), 7.94 − 7.89 (m, 2H), 7.57 − 7.52 (m, 2H), 7.35 − 7.30 (m, 2H), 7.28 − 7.23 (m, 2H), 7.13 − 7.09 (m, 1H), 4.05 − 3.98 (m, 1H), 3.82 − 3.75 (m, 1H), 2.50 − 2.38 (m, 2H), 2.26 − 2.16 (m, 1H), 2.07 – 1.98 (m, 1H); **^{13}C NMR** (126 MHz, $CDCl_3$) δ 169.1, 166.3 (d, $J_{C\text{-}F}$ = 257.6 Hz), 137.9, 133.3 (d, $J_{C\text{-}F}$ = 3.1 Hz), 131.2 (d, $J_{C\text{-}F}$ = 9.7 Hz), 129.1, 124.4, 119.8, 117.1 (d, $J_{C\text{-}F}$ = 22.7 Hz), 59.8, 40.2, 20.1, 19.5; **^{19}F NMR** (471 MHz, $CDCl_3$) δ −102.17 (s, 1F); **HRMS** (ESI-TOF) calculated for $C_{17}H_{17}FO_3N^{32}S$ $[M+H]^+$: 334.0908; found 334.0922; **IR** (neat) 2981, 2889, 2160, 2022, 1977, 1681, 1633, 1592, 1548, 1492, 1446, 1297, 1274, 1147, 1034, 937, 837, 746, 672, 631; **m.p.**: 144 − 146 °C.

***cis*-2-((4-fluorophenyl)sulfonyl)-*N*-phenylcyclobutane-1-carboxamide (*cis*-3.89)**



General procedure A was followed to obtain ***cis*-3.89** (75 mg, 0.23 mmol, 45%) as a white solid. **^{1}H NMR** (500 MHz, $CDCl_3$) δ 7.90 (s, 1H), 7.86 − 7.81 (m, 1H), 7.57 − 7.54 (m, 1H), 7.36 − 7.31 (m, 1H), 7.18 − 7.11 (m, 1H), 4.18 − 4.11 (m, 1H), 3.67 − 3.60 (m, 1H), 2.74 − 2.64 (m, 1H), 2.60 − 2.49 (m, 1H), 2.23 − 2.09 (m, 1H); **^{13}C NMR** (126 MHz, $CDCl_3$) δ 167.3, 166.0 (d, $J_{C\text{-}F}$ = 256.9 Hz), 138.0, 134.0 (d, $J_{C\text{-}F}$ = 3.2 Hz), 131.42 (d, $J_{C\text{-}F}$= 9.7 Hz), 129.0, 124.5, 120.3, 116.6 (d, $J_{C\text{-}F}$ = 22.6 Hz), 59.9, 42.6, 22.3, 20.6; **^{19}F NMR** (471 MHz, $CDCl_3$) δ −102.85 (s, 1F); **HRMS** (ESI-TOF) calculated for $C_{17}H_{17}FO_3N^{32}S$ $[M+H]^+$: 334.0908; found 334.0915; **IR** (neat) 2981, 2888, 2181, 1717, 1660, 1634, 1593, 1437, 1443, 1382, 1321, 1289, 1269, 1252, 1145, 1086, 954, 846, 821, 753, 705, 678, 615; **m.p. :** 149 − 152 °C.

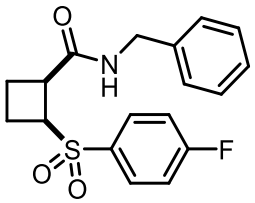
***trans*-*N*-benzyl-2-((4-fluorophenyl)sulfonyl)cyclobutane-1-carboxamide (*trans*-3.90)**



General procedure A was followed to obtain ***trans*-3.90** (26 mg, 0.08 mmol, 15%) as a white solid. **^{1}H NMR** (500 MHz, $CDCl_3$) δ 7.87 − 7.80 (m, 2H), 7.35 − 7.30 (m, 2H), 7.29 − 7.18 (m, 5H), 6.54 (br t, J = 5.9 Hz, 1H), 4.44 − 4.34 (m, 2H), 4.02 − 3.96 (m, 1H), 3.60 −

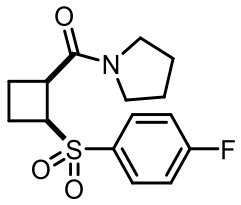
3.53 (m, 1H), 2.46 − 2.29 (m, 2H), 2.21 − 2.12 (m, 1H), 2.06 − 1.98 (m, 1H); **^{13}C NMR** (126 MHz, $CDCl_3$) δ 170.8, 166.2 (d, $J_{C\text{-}F}$ = 257.2 Hz), 138.1, 133.6 (d, $J_{C\text{-}F}$ = 3.2 Hz), 131.2 (d, $J_{C\text{-}F}$ = 9.7 Hz), 128.8, 127.8, 127.6, 117.0 (d, $J_{C\text{-}F}$ = 22.6 Hz), 59.5, 43.8, 39.5, 20.1, 19.7; **^{19}F NMR** (471 MHz, $CDCl_3$) δ −102.46 - −102.53 (m, 1F); **HRMS** (ESI-TOF) calculated for $C_{18}H_{19}FO_3N^{32}S$ $[M+H]^+$: 348.1064; found 348.1072; **IR** (neat) 3350, 2957, 2225, 1657, 1590, 1533, 1493, 1376, 1313, 1276, 1228, 1180, 1101, 987, 948, 871, 841, 821, 698, 643; **m.p.**: 144 − 146 °C.

***cis*-*N*-benzyl-2-((4-fluorophenyl)sulfonyl)cyclobutane-1-carboxamide (*cis*-3.90)**



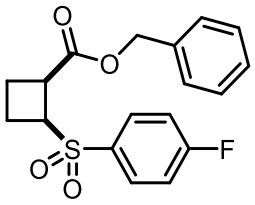
General procedure A was followed to obtain ***cis*-3.90** (108 mg, 0.31 mmol, 62%) as a white solid. **^{1}H NMR** (500 MHz, $CDCl_3$) δ 7.87 − 7.81 (m, 2H), 7.40 − 7.31 (m, 4H), 7.30 − 7.25 (m, 1H), 7.22 − 7.16 (m, 2H), 6.45 (t, J = 5.5 Hz, 1H), 4.59 (dd, J = 14.6, 6.1 Hz, 1H), 4.42 (dd, J = 14.6, 5.0 Hz, 1H), 4.06 − 3.98 (m, 1H), 3.54 − 3.46 (m, 1H), 2.66 − 2.57 (m, 1H), 2.56 − 2.46 (m, 1H), 2.18 − 2.04 (m, 2H); **^{13}C NMR** (126 MHz, $CDCl_3$) δ 168.9, 166.0 (d, $J_{C\text{-}F}$ = 256.5 Hz), 138.1, 134.4 (d, $J_{C\text{-}F}$ = 3.2 Hz), 131.4 (d, $J_{C\text{-}F}$ = 9.6 Hz), 128.7, 128.2, 127.6, 116.6 (d, $J_{C\text{-}F}$ = 22.6 Hz), 59.9, 44.4, 41.8, 22.4, 21.0; **^{19}F NMR** (471 MHz, $CDCl_3$) δ −103.06 - −103.14 (m, 1F); **HRMS** (ESI-TOF) calculated for $C_{18}H_{19}FO_3N^{32}S$ $[M+H]^+$: 348.1064; found 348.1091; **IR** (neat) 3294, 2161, 1632, 1589, 1542, 1492, 1454, 1492, 1454, 1311, 1249, 1221, 1161, 1144, 1080, 834, 814, 747, 716, 696, 672; **m.p.**: 130 − 132 °C.

cis-2-((4-fluorophenyl)sulfonyl)cyclobutyl)(pyrrolidin-1-yl)methanone (_cis_-3.91)



General procedure A was followed to obtain ***cis*-3.91** (96 mg, 0.31 mmol, 62%) as a white solid. **^{1}H NMR** (500 MHz, DMSO-d_6) δ 7.92 − 7.86 (m, 2H), 7.52 − 7.46 (m, 2H), 4.49 − 4.43 (m, 1H), 3.65 (ddd, J = 8.8 Hz, 1H), 3.28 − 3.19 (m, 2H), 3.09 − 3.02 (m, 1H), 2.96 − 2.90 (m, 1H), 2.65 − 2.55 (m, 1H), 2.28 − 2.18 (m, 2H), 1.83 − 1.76 (m, 1H), 1.76 − 1.68 (m, 1H), 1.68 − 1.61 (m, 1H), 1.61 − 1.53 (m, 1H), 1.53 − 1.44 (m, 1H); **^{13}C NMR** (126 MHz, DMSO-d_6) δ 166.0, 165.4 (d, J = 252.7 Hz), 134.8 (d, J = 3.0 Hz), 131.5 (d, J = 9.8 Hz), 116.4 (d, J = 22.7 Hz), 59.3, 45.2, 45.1, 39.4, 25.2, 23.5, 20.7, 20.6; **^{19}F NMR** (471 MHz, DMSO-d_6) δ −104.9 - −104.9 (m, 1F); **HRMS** (ESI-TOF) calculated for $C_{15}H_{19}FO_3N^{32}S$ $[M+H]^+$: 312.1064; found 312.1069; **IR** (neat) 2981, 2889, 1737, 1702, 1617, 1590, 1493, 1380, 1349, 1316, 1292, 1231, 1193, 1141, 1084, 1048, 1024, 996, 822, 763, 752, 718, 690, 669; **m.p.**: 155 − 159 °C.

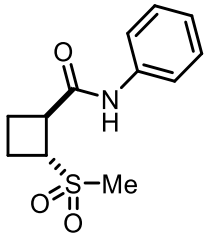
Benzyl-_cis_-2-((4-fluorophenyl)sulfonyl)cyclobutane-1-carboxylate (_cis_-3.92)



General procedure A was followed to obtain ***cis*-3.92** (103 mg, 0.30 mmol, 59%) as a white solid. **^{1}H NMR** (500 MHz, $CDCl_3$) δ 7.88 − 7.82 (m, 2H), 7.45 − 7.41 (m, 2H), 7.40 − 7.32 (m, 3H), 7.17 − 7.11 (m, 2H), 5.29 (d, J = 12.2 Hz, 1H), 5.15 (d, J = 12.1 Hz, 1H), 4.08 (dt,

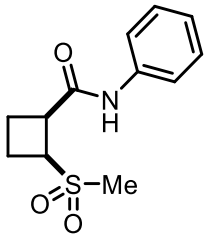
J = 9.1, 8.4 Hz, 1H), 3.51 − 3.43 (m, 1H), 2.76 − 2.66 (m, 1H), 2.63 − 2.54 (m, 1H), 2.23 − 2.14 (m, 1H), 2.14 − 2.05 (m, 1H); **^{13}C NMR** (126 MHz, $CDCl_3$) δ 170.4, 165.9 (d, *J* = 256.4 Hz), 135.6, 134.9 (d, *J* = 3.2 Hz), 131.3 (d, *J* = 9.6 Hz), 128.8, 128.7, 128.5, 116.5 (d, *J* = 22.5 Hz), 67.7, 59.2, 40.9, 22.5, 20.6; **^{19}F NMR** (471 MHz, $CDCl_3$) δ −103.4 - −103.5 (m, 1F); **HRMS** (ESI-TOF) calculated for $C_{18}H_{21}FO_4N^{32}S$ $[M+NH_4]^+$: 366.1170; found 366.1173; **IR** (neat) 2981, 2889, 1726, 1586, 1383, 1349, 1317, 1269, 1251, 1233, 1181, 1145, 1081, 1030, 1009, 956, 847, 821, 772, 752, 740, 704, 673, 654, 606; **m.p.**: 114 − 118 °C.

cis-2-(methylsulfonyl)-_N_-phenylcyclobutane-1-carboxamide (_trans_-3.93)



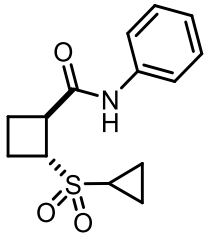
General procedure A was followed to obtain ***trans*-3.93** (33 mg, 0.13 mmol, 26%) as a white solid. **^{1}H NMR** (400 MHz, $CDCl_3$) δ 8.10 (s, 1H), 7.54 − 7.49 (m, 2H), 7.33 − 7.28 (m, 2H), 7.14 − 7.07 (m, 1H), 4.10 − 4.01 (m, 1H), 3.78 − 3.68 (m, 1H), 2.90 (s, 3H), 2.54 − 2.41 (m, 2H), 2.32 − 2.18 (m, 2H); **^{13}C NMR** (101 MHz, $CDCl_3$) δ 169.1, 137.8, 129.2, 124.6, 119.8, 58.1, 39.7, 39.0, 19.7, 19.4; **HRMS** (ESI-TOF) calculated for $C_{12}H_{16}O_3N^{32}S$ $[M+H]^+$: 254.0845; found 254.0855; **IR** (neat) 3246, 2956, 1736, 1659, 1597, 1547, 1492, 1446, 1297, 1223, 1158, 1024, 965, 751, 130, 676; **m.p.**: 106 − 109 °C.

***trans*-2-(methylsulfonyl)-*N*-phenylcyclobutane-1-carboxamide (*cis*-3.93)**



General procedure A was followed to obtain ***cis*-3.93** (80 mg, 0.32 mmol, 63%) as a white solid. **^{1}H NMR** (400 MHz, $CDCl_3$) δ 7.91 (s, 1H), 7.52 − 7.48 (m, 2H), 7.32 − 7.26 (m, 2H), 7.13 − 7.08 (m, 1H), 3.99 (td, J = 8.8, 5.3 Hz, 1H), 3.70 − 3.61 (m, 1H), 2.99 (s, 3H), 2.71 − 2.50 (m, 2H), 2.46 − 2.35 (m, 1H), 2.24 − 2.13 (m, 1H); **^{13}C NMR** (101 MHz, $CDCl_3$) δ 168.4, 137.5, 129.1, 124.9, 120.7, 59.6, 42.8, 40.2, 21.9, 20.8; **HRMS** (ESI-TOF) calculated for $C_{12}H_{16}O_3N^{32}S$ $[M+H]^+$: 254.0845; found 254.0860; **IR** (neat) 3329, 2926, 1729, 1672, 1538, 1494, 1441, 1294, 1122, 985, 755, 693; **m.p.**: 110 − 114 °C.

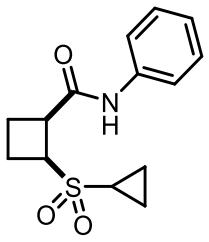
***trans*-2-(cyclopropylsulfonyl)-*N*-phenylcyclobutane-1-carboxamide (*trans*-3.94)**



General procedure A was followed to obtain ***trans*-3.94** (31 mg, 0.11 mmol, 22%) as a white solid. **^{1}H NMR** (400 MHz, $CDCl_3$) δ 8.30 (s, 1H), 7.56 − 7.50 (m, 2H), 7.34 − 7.27 (m, 2H), 7.12 − 7.06 (m, 1H), 4.14 − 4.04 (m, 1H), 3.80 − 3.69 (m, 1H), 2.57 − 2.39 (m, 2H), 2.38 − 2.29 (m, 1H), 2.28 − 2.19 (m, 2H), 1.32 − 1.20 (m, 2H), 1.13 − 1.00 (m, 2H); **^{13}C NMR** (101 MHz, $CDCl_3$) δ 169.3, 138.0, 129.1, 124.4, 119.7, 57.9, 40.1, 27.9, 20.1, 19.9, 4.7, 4.3; **HRMS** (ESI-TOF) calculated for $C_{14}H_{18}O_3N^{32}S$ $[M+H]^+$: 280.1002; found

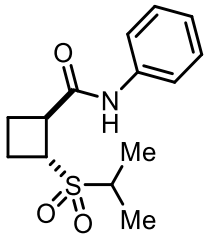
280.1007; **IR** (neat) 2981, 1976, 1719, 1682, 1660, 1596, 1546, 1473, 1445, 1380, 1295, 1158, 1091, 961, 890, 836, 755, 696; **m.p**: 132 − 134 °C.

cis-2-(cyclopropylsulfonyl)-_N_-phenylcyclobutane-1-carboxamide (_cis_-3.94)



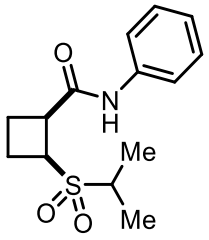
General procedure A was followed to obtain ***cis*-3.94** (75 mg, 0.27 mmol, 54%) as a white solid. **^{1}H NMR** (400 MHz, $CDCl_3$) δ 8.04 (s, 1H), 7.55 − 7.48 (m, 2H), 7.32 − 7.25 (m, 2H), 7.12 − 7.06 (m, 1H), 4.09 − 4.01 (m, 1H), 3.71 − 3.62 (m, 1H), 2.75 − 2.56 (m, 3H), 2.43 − 2.31 (m, 1H), 2.24 − 2.13 (m, 1H), 1.25 − 2.09 (m, 2H), 1.03 − 0.90 (m, 2H); **^{13}C NMR** (101 MHz, $CDCl_3$) δ 168.5, 137.7, 129.0, 128.9, 128.9, 128.9, 124.7, 120.6, 120.5, 58.9, 43.0, 28.6, 21.9, 21.9, 21.9, 21.8, 21.8, 21.4, 4.9, 4.7; **HRMS** (ESI-TOF) calculated for $C_{14}H_{18}O_3N^{32}S$ $[M+H]^+$: 280.1002; found 280.1012; **IR** (neat) 2981, 2181, 1719, 1693, 1664, 1597, 1544, 1495, 1474, 1445, 1380, 1270, 1126, 1040, 888, 828, 755, 755, 694; **m.p**: 136 − 138 °C.

***trans*-2-(isopropylsulfonyl)-*N*-phenylcyclobutane-1-carboxamide (*trans*-3.95)**



General procedure A was followed to obtain ***trans*-3.95** (55 mg, 0.20 mmol, 39%) as a white solid. **^{1}H NMR** (200 MHz, $CDCl_3$) δ 8.59 (s, 1H), 7.57 − 7.48 (m, 2H),7.34 − 7.22 (m, 2H), 7.12 − 7.02 (m, 1H), 4.21 − 4.03 (m, 1H), 3.84 − 3.67 (m, 1H), 3.09 (hept, J = 6.9 Hz, 1H), 2.59 − 2.33 (m, 2H), 2.29 − 2.05 (m, 2H), 1.35 (d, J = 6.9 Hz, 6H); **^{13}C NMR** (101 MHz, $CDCl_3$) δ 169.4, 138.0, 129.0, 124.3, 119.6, 54.1, 52.8, 39.7, 20.5, 20.3, 15.4, 15.1; **HRMS** (ESI-TOF) calculated for $C_{14}H_{20}O_3N^{32}S$ $[M+H]^+$: 282.1158; found 282.1173; **IR** (neat) 3291, 2957, 2161, 1667, 1598, 1549, 1499, 1442, 1306, 1257, 1120, 1053, 763, 747, 690, 624; **m.p.**: 87 − 93°C.

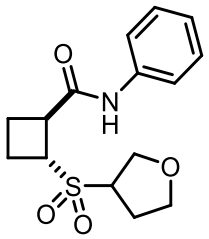
***cis*-2-(isopropylsulfonyl)-*N*-phenylcyclobutane-1-carboxamide (*cis*-3.95)**



General procedure A was followed to obtain ***cis*-3.95** (55 mg, 0.20 mmol, 39%) as a white solid. **^{1}H NMR** (400 MHz, $CDCl_3$) δ 7.89 (s, 1H), 7.53 − 7.49 (m, 2H), 7.34 − 7.29 (m, 2H), 7.14 − 7.09 (m, 1H), 4.18 − 4.09 (m, 1H), 3.74 − 3.65 (m, 1H), 3.37 (hept, J = 6.9 Hz, 1H), 2.80 − 2.62 (m, 2H), 2.44 − 2.34 (m, 1H), 2.33 − 2.23 (m, 1H), 1.33 (dd, J = 6.9, 3.3 Hz, 7H); **^{13}C NMR** (101 MHz, $CDCl_3$) δ 168.1, 137.7, 129.1, 124.8, 120.6, 54.7, 52.8, 42.9, 22.7,

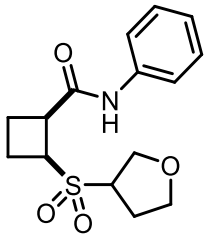
21.0, 15.9, 14.8; **HRMS** (ESI-TOF) calculated for $C_{14}H_{20}O_3N^{32}S$ $[M+H]^+$: 282.1158; found 282.1177; **IR** (neat) 3291, 2957, 2161, 1667, 1598, 1549, 1499, 1442, 1306, 1257, 1190, 1120, 1053, 763, 762, 690, 624; **m.p.**: 95 − 97°C.

***trans*-*N*-phenyl-2-((tetrahydrofuran-3-yl)sulfonyl)cyclobutane-1-carboxamide (*trans*-3.96)**



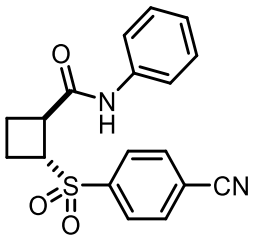
General procedure A was followed to obtain ***trans*-3.96** (52 mg, 0.17 mmol, 34%) as a colourless oil. **^{1}H NMR** (400 MHz, $CDCl_3$) δ 8.29 (s, 0.5H), 8.27 (s, 0.5H), 7.55 − 7.48 (m, 2H), 7.34 − 7.27 (m, 2H), 7.13 − 7.06 (m, 1H), 4.19 (dd, J = 10.2, 5.1 Hz, 1H), 4.13 − 3.93 (m, 3H), 3.83 − 3.70 (m, 2H), 3.69 − 3.60 (m, 1H), 2.58 − 2.39 (m, 2H), 2.38 − 2.13 (m, 4H); **^{13}C NMR** (101 MHz, $CDCl_3$) δ 169.2, 169.1, 137.9, 137.8, 129.1, 124.5, 124.5, 119.8, 119.8, 68.4, 68.3, 67.2, 66.9, 60.7, 60.5, 55.8, 40.1, 40.0, 27.2, 26.9, 20.4, 20.3, 20.0, 20.0; **HRMS** (ESI-TOF) calculated for $C_{15}H_{20}O_4N^{32}S$ $[M+H]^+$: 310.1108; found 310.1122 ; **IR** (neat) 3454, 2161, 2029, 1656, 1601, 1538, 1499, 1443, 1377, 1308, 1267, 1205, 1130, 1075, 1055, 1026, 981, 807, 691, 753, 691.

***cis*-*N*-phenyl-2-((tetrahydrofuran-3-yl)sulfonyl)cyclobutane-1-carboxamide (*cis*-3.96)**



General procedure A was followed to obtain ***cis*-3.96** (70 mg, 0.23 mmol, 45%) as a colourless oil. **^{1}H NMR** (500 MHz, $CDCl_3$) δ 7.85 (s, 0.5H), 7.84 (s, 0.5H), 7.51 − 7.46 (m, 2H), 7.33 − 7.28 (m, 2H), 7.14 − 7.08 (m, 1H), 4.20 (dd, J = 9.8, 5.3 Hz, 0.5H), 4.12 − 4.05 (m, 1H), 4.05 − 3.88 (m, 4H), 3.81 − 3.73 (m, 1H), 3.70 − 3.61 (m, 1H), 2.72 − 2.59 (m, 2H), 2.43 − 2.32 (m, 1.5H), 2.31 − 2.14 (m, 2H); **^{13}C NMR** (126 MHz, $CDCl_3$) δ 168.3, 168.3, 137.5, 137.5, 129.1, 124.9, 124.9, 120.7, 120.7, 68.5, 67.6, 66.8, 60.7, 60.6, 57.2, 43.0, 43.0, 27.7, 26.9, 22.4, 22.2, 21.0, 20.6; **HRMS** (ESI-TOF) calculated for $C_{15}H_{20}O_4N^{32}S$ $[M+H]^+$: 310.1108; found 310.1119 ; **IR** (neat) 3322, 2964, 1673, 1619, 1541, 1496, 1371, 1307, 1254, 1192, 1128, 1077, 951, 915, 755, 693, 616.

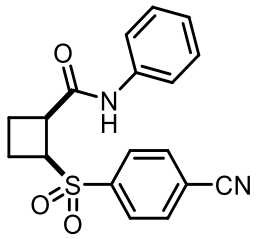
***trans*-2-((4-cyanophenyl)sulfonyl)-*N*-phenylcyclobutane-1-carboxamide (*trans*-3.97)[a]**



General procedure A was followed to obtain ***trans*-3.97** (60 mg, 0.18 mmol, 35%) as a white solid. **^{1}H NMR** (400 MHz, DMSO-d_6) δ 9.87 (s, 1H), 8.07 (s, 4H), 7.46 − 7.41 (m, 2H), 7.31 − 7.24 (m, 2H), 7.07 − 7.00 (m, 1H), 4.40 − 4.32 (m, 1H), 3.64 − 3.56 (m, 1H), 2.42 − 2.29 (m, 1H), 2.25 − 2.02 (m, 3H); **^{13}C NMR** (101 MHz, DMSO-d_6) δ 168.6, 141.5,

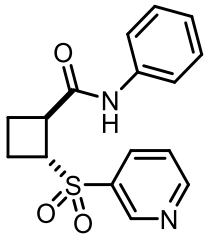
138.4, 133.4, 128.8, 128.6, 123.5, 119.2, 117.3, 116.4, 56.3, 40.1, 20.9, 18.7; **HRMS** (ESI-TOF) calculated for $C_{18}H_{17}O_3N_2{}^{32}S$ $[M-H]^-$: 339.0809; found 339.0810; **IR** (neat) 3301, 2161, 1655, 1620, 1600, 1529, 1497, 1442, 1398, 1304, 1179, 1106, 982, 956, 889, 837, 756, 691, 643; **m.p.**: 163 − 166 °C.

cis-2-((4-cyanophenyl)sulfonyl)-_N_-phenylcyclobutane-1-carboxamide (_cis_-3.97) [a]



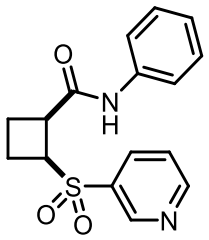
General procedure A was followed to obtain ***cis*-3.97** (79 mg, 0.23 mmol, 47%) as a colourless oil. **^{1}H NMR** (400 MHz, DMSO-d_6) δ 9.55 (s, 1H), 7.90 (s, 4H), 7.44 − 7.38 (m, 2H), 7.30 − 7.24 (m, 2H), 7.07 − 7.00 (m, 1H), 4.59 − 4.50 (m, 1H), 3.66 − 3.56 (m, 1H), 2.56 − 2.39 (m, 2H), 2.38 − 2.25 (m, 1H), 2.03 − 1.93 (m, 1H); **^{13}C NMR** (101 MHz, DMSO-d_6) δ 166.7, 142.7, 138.8, 133.0, 128.6, 128.5, 123.1, 118.9, 117.5, 115.8, 58.7, 41.7, 20.7, 20.1; **HRMS** (ESI-TOF) calculated for $C_{18}H_{17}O_3N_2{}^{32}S$ $[M+H]^+$: 341.0954; found 341.0955; **IR** (neat) 1719, 1675, 1599, 1533, 1494, 1441, 1378, 1313, 1141, 1084, 828, 186, 160, 123, 689, 631.

***trans*-*N*-phenyl-2-(pyridin-3-ylsulfonyl)cyclobutane-1-carboxamide (*trans*-3.98)**



General procedure A was followed to obtain ***trans*-3.98** (34 mg, 0.11 mmol, 22%) as a white solid. **^{1}H NMR** (400 MHz, $CDCl_3$) δ 9.10 (dd, J = 2.3, 0.6 Hz, 1H), 8.90 (dd, J = 4.9, 1.7 Hz, 1H), 8.23 − 8.15 (m, 2H), 7.55 − 7.50 (m, 3H), 7.35 − 7.29 (m, 2H), 7.14 − 7.09 (m, 1H), 4.14 − 4.04 (m, 1H), 3.85 − 3.76 (m, 1H), 2.56 − 2.40 (m, 2H), 2.33− 2.20 (m, 1H), 2.12 − 2.00 (m, 1H); **^{13}C NMR** (101 MHz, $CDCl_3$) δ 168.7, 155.0, 149.3, 137.8, 136.1, 134.1, 129.2, 124.6, 124.2, 119.8, 60.1, 40.1, 20.1, 19.5; **HRMS** (ESI-TOF) calculated for $C_{16}H_{17}O_3N_2{}^{32}S$ $[M+H]^+$: 317.0954; found 317.0962; **IR** (neat) 3301, 2981, 1652, 1599, 1570, 1537, 1492, 1464, 1443, 1412, 1374, 1327, 1309, 1271, 1238, 1166, 1148, 1120, 1078, 989, 934, 809, 789, 755, 743, 697, 676, 630; **m.p.**: 126 − 129 °C.

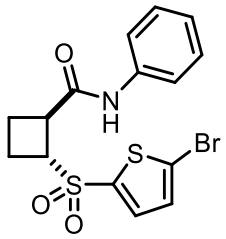
***cis*-*N*-phenyl-2-(pyridin-3-ylsulfonyl)cyclobutane-1-carboxamide (*cis*-3.98)**



General procedure A was followed to obtain ***cis*-3.98** (51 mg, 0.16 mmol, 32%) as a white solid. **^{1}H NMR** (400 MHz, $CDCl_3$) δ 9.04 (dd, J = 2.4, 0.9 Hz, 1H), 8.84 (dd, J = 4.9, 1.6 Hz, 1H), 8.10 (ddd, J = 8.0, 2.3, 1.6 Hz, 1H), 7.83 (s, 1H), 7.57 − 7.51 (m, 2H), 7.42 (ddd, J = 8.0, 4.9, 0.9 Hz, 1H), 7.37 − 7.31 (m, 2H), 7.17 − 7.11 (m, 1H), 4.18 (dt, J = 9.3, 8.4 Hz,

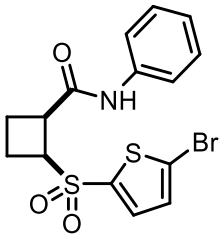
1H), 3.70 – 3.61 (m, 1H), 2.77 − 2.55 (m, 2H), 2.31 − 2.12 (m, 2H); **^{13}C NMR** (101 MHz, $CDCl_3$) δ 166.9, 154.5, 149.5, 137.8, 136.5, 134.7, 129.2, 124.8, 123.9, 120.4, 60.3, 42.8, 22.3, 20.9; **HRMS** (ESI-TOF) calculated for $C_{16}H_{17}O_3N_2{}^{32}S$ $[M+H]^+$: 317.0954; found 317.0964; **IR** (neat) 2981, 1676, 1620, 1599, 1570, 1541, 1493, 1472, 1464, 1443, 1415, 1382, 1310, 1252, 1195, 1150, 1056, 806, 754, 695, 620; **m.p.**: 153 − 144 °C .

trans-2-((5-bromothiophen-2-yl)sulfonyl)-_N_-phenylcyclobutane-1-carboxamide (_trans_-3.99)



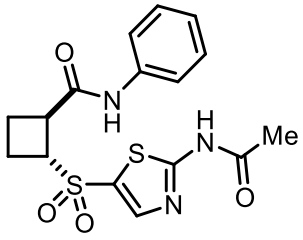
General procedure A was followed to obtain ***trans*-3.99** (60 mg, 0.15 mmol, 30%) as a white solid. **^{1}H NMR** (400 MHz, $CDCl_3$) δ 8.15 (s, 1H), 7.55 − 7.50 (m, 2H), 7.46 (d, J = 4.0 Hz, 1H), 7.34 − 7.28 (m, 2H), 7.15 (d, J = 4.0 Hz, 1H), 7.14 − 7.08 (m, 1H), 4.17 − 4.09 (m, 1H), 3.77 − 3.68 (m, 1H), 2.51 − 2.37 (m, 2H), 2.27 − 2.08 (m, 2H); **^{13}C NMR** (101 MHz, $CDCl_3$) δ 168.8, 138.3, 137.9, 135.1, 131.6, 129.2, 124.6, 123.4, 119.8, 60.9, 40.5, 20.3, 19.2; **HRMS** (ESI-TOF) calculated for $C_{15}H_{15}BrO_3N^{32}S_2$ $[M+H]^+$: 401.9651; found 401.9659; **IR** (neat) 2981, 1720, 16670, 1619, 1599, 1542, 1492, 1473, 1443, 1398, 1310, 1252, 1139, 1081, 1022, 969, 857, 758, 694, 674, 617; **m.p.**: 154 − 158 °C.

cis-2-((5-bromothiophen-2-yl)sulfonyl)-_N_-phenylcyclobutane-1-carboxamide (_cis_-3.99)



General procedure A was followed to obtain ***cis*-3.99** (102 mg, 0.26 mmol, 51%) as a white solid. **^{1}H NMR** (400 MHz, $CDCl_3$) δ 7.82 (s, 1H), 7.56 − 7.52 (m, 2H), 7.37 (d, J = 4.1 Hz, 1H), 7.35 − 7.31 (m, 2H), 7.15 − 7.10 (m, 1H), 7.06 (d, J = 4.0 Hz, 1H), 4.24 − 4.14 (m, 1H), 3.69 − 3.62 (m, 1H), 2.74 − 2.54 (m, 2H), 2.34 − 2.23 (m, 1H), 2.22 − 2.11 (m, 1H); **^{13}C NMR** (101 MHz, $CDCl_3$) δ 166.8, 139.2, 137.8, 135.4, 131.2, 129.1, 124.7, 123.2, 120.4, 61.1, 42.8, 22.7, 20.6; **HRMS** (ESI-TOF) calculated for $C_{15}H_{15}BrO_3N^{32}S_2$ $[M+H]^+$: 401.9651; found 401.9654; **IR** (neat) 2981, 1734, 1668, 1618, 1599, 1542, 1491, 1462, 1442, 1382, 1309, 1253, 1185, 1155, 1126, 1076, 966, 914, 757, 695, 620; **m.p.**: 149 − 152 °C;

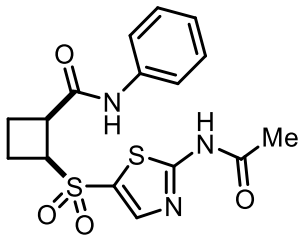
trans-2-((2-acetamidothiazol-5-yl)sulfonyl)-_N_-phenylcyclobutane-1-carboxamide (_trans_-3.100)



General procedure A was followed to obtain ***trans*-3.100** (69 mg, 0.18 mmol, 37%) as a white solid. **^{1}H NMR** (400 MHz, DMSO-d_6) δ 9.96 (s, 1H), 8.00 (s, 1H), 7.51 − 7.46 (m, 2H), 7.30 − 7.24 (m, 2H), 7.06 − 7.01 (m, 1H), 4.24 (dt, J = 8.5, 7.9 Hz, 1H), 3.59 (dt, J = 9.1, 8.6 Hz, 1H), 2.38 − 2.25 (m, 1H), 2.22 − 2.12 (m, 2H), 2.11 (s, 3H), 2.09 − 1.97 (m, 1H); **^{13}C NMR** (101 MHz, DMSO-d_6) δ 171.5, 169.1, 166.8, 146.1, 138.7, 128.7, 123.5, 123.0,

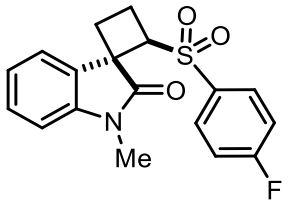
119.4, 58.1, 40.4, 23.4, 20.6, 19.2; **HRMS** (ESI-TOF) calculated for $C_{16}H_{18}O_4N_3{}^{32}S_2$ $[M+H]^+$: 380.0733; found 380.0740; **IR** (neat) 3356, 2166, 1698, 1665, 1601, 1528, 1489, 1439, 1376, 1308, 1249, 1221, 1178, 1116, 1019, 689, 620; **m.p.**: 157 − 161 °C.

cis-2-((2-acetamidothiazol-5-yl)sulfonyl)-_N_-phenylcyclobutane-1-carboxamide (_cis_-3.100)



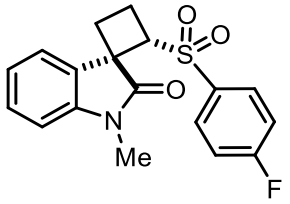
General procedure A was followed to obtain ***cis*-3.100** (92 mg, 0.24 mmol, 48%) as a white solid. **^{1}H NMR** (400 MHz, DMSO-d_6) δ 9.75 (s, 1H), 7.84 (s, 1H), 7.53 − 7.49 (m, 2H), 7.30 − 7.24 (m, 2H), 7.05 − 7.00 (m, 1H), 4.47 − 4.39 (m, 1H), 3.68 − 3.59 (m, 1H), 2.48 − 2.35 (m, 2H), 2.34 − 2.21 (m, 1H), 2.18 (s, 3H), 2.03 − 1.91 (m, 1H); **^{13}C NMR** (101 MHz, DMSO-d_6) δ 169.6, 166.8, 163.4, 145.3, 139.0, 128.5, 126.9, 123.0, 119.2, 60.5, 41.8, 22.3, 21.7; **HRMS** (ESI-TOF) calculated for $C_{16}H_{18}O_4N_3{}^{32}S_2$ $[M+H]^+$: 380.0733; found 380.0737; **IR** (neat) 3356, 2919, 2161, 1698, 1680, 1601, 1531, 1492, 1440, 1366, 1311, 1251, 1227, 1187, 1127, 1065, 1039, 1026, 797, 689, 632, 621; **m.p.**: 245 − 247 °C.

cis-2-((4-fluorophenyl)sulfonyl)-1'-methylspiro[cyclobutane-1,3'-indolin]-2'-one (_cis_-3.109)



General procedure A was followed to obtain ***cis*-3.109** (64 mg, 0.19 mmol, 37%) as a white solid. **^{1}H NMR** (400 MHz, $CDCl_3$) δ 7.69 − 7.64 (m, 2H), 7.24 − 7.19 (m, 2H), 7.05 − 6.99 (m, 3H), 6.64 (d, J = 7.8 Hz, 1H), 4.27 − 4.20 (m, 1H), 3.23 − 3.14 (m, 1H), 3.13 (s, 3H), 2.50 − 2.28 (m, 3H); **^{13}C NMR** (101 MHz, $CDCl_3$) δ 175.2, 165.8 (d, $J_{C\text{-}F}$ = 256.3 Hz), 143.21, 134.7 (d, $J_{C\text{-}F}$ = 3.2 Hz), 131.1 (d, $J_{C\text{-}F}$ = 9.7 Hz), 129.5, 129.3, 122.7, 122.3, 115.9 (d, $J_{C\text{-}F}$ = 22.6 Hz), 108.0, 65.3, 51.9, 28.4, 26.4, 21.0; **^{19}F NMR** (471 MHz, $CDCl_3$) δ −103.6 - −103.7 (m, 1F); **HRMS** (ESI-TOF) calculated for $C_{18}H_{17}FO_3N^{32}S$ $[M+H]^+$: 346.0908; found 346.0915; **IR** (neat) 2981, 2889, 1737, 1702, 1615, 1590, 1493, 1474, 1429, 1380, 1350, 1331, 1316, 1286, 1258, 1230, 1192, 1140, 1099, 1084, 1014, 954, 884, 849, 820, 775, 751, 713, 698, 669; **m.p.**: 144 − 146 °C.

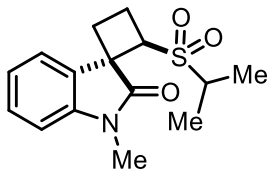
trans-2-((4-fluorophenyl)sulfonyl)-1'-methylspiro[cyclobutane-1,3'-indolin]-2'-one (_trans_-3.109)



General procedure A was followed to obtain ***trans*-3.109** (64 mg, 0.19 mmol, 37%) as a white solid. **^{1}H NMR** (400 MHz, $CDCl_3$) δ 7.83 − 7.79 (m, 1H), 7.34 − 7.28 (m, 3H), 7.18 (td, J = 7.6, 1.1 Hz, 1H), 6.99 − 6.92 (m, 2H), 6.62 (d, J = 7.7 Hz, 1H), 4.48 − 4.41 (m, 1H), 3.16 − 3.03 (m, 1H), 2.89 (s, 3H), 2.72 − 2.60 (m, 1H), 2.58 − 2.48 (m, 1H), 2.31 − 2.24 (m,

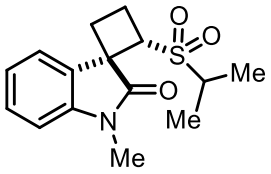
1H); **^{13}C NMR** (101 MHz, $CDCl_3$) δ 176.1, 165.8 (d, $J_{C\text{-}F}$ = 256.4 Hz), 143.5, 134.0 (d, $J_{C\text{-}F}$ = 3.2 Hz), 131.0 (d, $J_{C\text{-}F}$ = 9.6 Hz), 129.1, 127.0, 126.5, 122.8, 116.0 (d, $J_{C\text{-}F}$ = 22.6 Hz), 107.9, 61.9, 50.4, 28.6, 26.3, 20.0; **^{19}F NMR** (471 MHz, $CDCl_3$) δ −103.73 - −103.81 (m, 1F); **HRMS** (ESI-TOF) calculated for $C_{18}H_{17}FO_3N^{32}S$ $[M+H]^+$: 346.0908; found 346.0908; **IR** (neat) 1713, 1614, 1588, 1493, 1468, 1427, 1406, 1376, 1348, 1310, 1292, 1271, 1240, 1128, 1188, 1143, 1105, 1084, 1053, 1024, 1009, 970, 937, 846, 816, 807, 793, 742, 711, 698, 655, 626; **m.p.**: 164 − 166 °C.

***cis*-2-(isopropylsulfonyl)-1'-methylspiro[cyclobutane-1,3'-indolin]-2'-one (*cis*-3.110)**



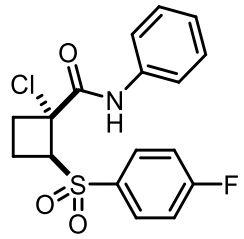
General procedure A was followed to obtain ***cis*-3.110** (32 mg, 0.11 mmol, 22%) as a white solid. **^{1}H NMR** (400 MHz, $CDCl_3$) δ 7.34 − 7.27 (m, 2H), 7.08 (td, J = 7.5, 1.0 Hz, 1H), 6.80 (d, J = 7.7 Hz, 1H), 4.16 − 4.07 (m, 1H), 3.38 − 3.26 (m, 1H), 3.23 (s, 3H), 2.99 (h, J = 6.9 Hz, 1H), 2.54 − 2.44 (m, 1H), 2.42 − 2.30 (m, 2H), 1.22 (d, J = 6.8 Hz, 3H), 1.18 (d, J = 6.9 Hz, 3H); **^{13}C NMR** (101 MHz, $CDCl_3$) δ 176.4, 143.8, 130.0, 129.5, 122.7, 122.3, 108.3, 60.7, 54.1, 51.9, 28.3, 26.6, 21.6, 15.3, 15.1; **HRMS** (ESI-TOF) calculated for $C_{15}H_{20}O_3N^{32}S$ $[M+H]^+$: 294.1158; found 294.1162; **IR** (neat) 2980, 2889, 1704, 1611, 1491, 1470, 1418, 1378, 1349, 1307, 1264, 1220, 1140, 1130, 1115, 1099, 1059, 1020, 1009, 972, 938, 898, 879, 855, 811, 789, 754, 692, 666, 609; **m.p.**: 186 − 188 °C.

trans-2-(isopropylsulfonyl)-1'-methylspiro[cyclobutane-1,3'-indolin]-2'-one (_trans_-3.110)



General procedure A was followed to obtain ***trans*-3.110** (79 mg, 0.27 mmol, 54%) as a white solid. **^{1}H NMR** (400 MHz, $CDCl_3$) δ 7.83 − 7.79 (m, 1H), 7.31 (td, J = 7.7, 1.2 Hz, 1H), 7.13 (td, J = 7.6, 1.0 Hz, 1H), 6.82 (dt, J = 7.7, 0.8 Hz, 1H), 4.34 (t, J = 8.7 Hz, 1H), 3.21 (s, 4H), 3.08 − 2.95 (m, 1H), 2.73 − 2.61 (m, 2H), 2.58 − 2.48 (m, 1H), 2.39 − 2.30 (m, 1H), 1.20 (d, J = 6.8 Hz, 3H), 1.19 (d, J = 6.9 Hz, 3H); **^{13}C NMR** (101 MHz, $CDCl_3$) δ 177.1, 143.3, 129.1, 127.9, 126.3, 122.9, 108.2, 56.9, 53.4, 50.5, 29.3, 26.7, 21.0, 15.5, 14.4; **HRMS** (ESI-TOF) calculated for $C_{15}H_{20}O_3N^{32}S$ $[M+H]^+$: 294.1158; found 294.1163; **IR** (neat) 2981, 2889, 1704, 1611, 1491, 1470, 1418, 1377, 1348, 1292, 1260, 1140, 1127, 1093, 1051, 1018, 955, 939, 898, 880, 855, 805, 789, 755, 690, 666, 611; **m.p.**: 166 − 168 °C.

trans-1-chloro-2-((4-fluorophenyl)sulfonyl)-_N_-phenylcyclobutane-1-carboxamide (3.111)



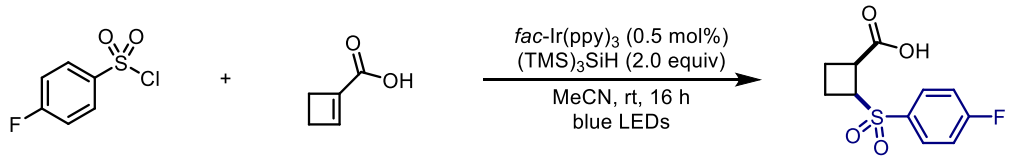
4-fluorobenzenesulfonyl chloride (243 mg, 1.3 mmol, 2.5 equiv) was added to a stirred suspension of *N*-phenylacrylamide (74 mg, 0.5 mmol, 1.0 equiv), *fac*-$Ir(ppy)_3$ (1.70 mg, 0.0025 mmol, 0.5 mol%), MeCN (3.0 mL) and K_2HPO_4 (17.4 mg, 0.1 mmol, 0.2 equiv). The reaction mixture was stirred under blue LED irradiation for 1 hour. The solution was concentrated *in vacuo* and purified by flash column chromaography (silica, EtOAc in

Heptane, 0/100 to 100/0) to afford sulfone **3.111** (134 mg, 0.37 mmol, 73%) as a white solid. **^{1}H NMR** (500 MHz, $CDCl_3$) δ 8.32 (s, 1H), 7.85 − 7.79 (m, 2H), 7.59 − 7.55 (m, 2H), 7.39 − 7.34 (m, 2H), 7.19 − 7.14 (m, 3H), 4.31 (t, J = 9.7 Hz, 1H), 3.31 − 3.22 (m, 1H), 2.52 (dt, J = 20.0, 10.3 Hz, 1H), 2.36 (dt, J = 11.5, 9.7 Hz, 1H), 2.25 − 2.16 (m, 1H); **^{13}C NMR** (126 MHz, $CDCl_3$) δ 166.2 (d, $J_{C\text{-}F}$ = 257.7 Hz), 163.4, 137.2, 133.9 (d, $J_{C\text{-}F}$ = 3.2 Hz), 131.4 (d, $J_{C\text{-}F}$ = 9.7 Hz), 129.1, 125.2, 120.6, 116.8 (d, $J_{C\text{-}F}$ = 22.8 Hz), 69.3, 66.1, 33.1, 20.9; **^{19}F NMR** (471 MHz, $CDCl_3$): δ − 102.0 - − 102.1 (m, 1F); **HRMS** (ESI-TOF) calculated for $C_{17}H_{14}FO_3NCl^{32}S$ $[M\text{-}H]^-$: 366.0372; found 366.0365; **IR** (neat) 2981, 1691, 1588, 1488, 1439, 1400, 1321, 1298, 1257, 1233, 1150, 1095, 1051, 1021, 990, 973, 903, 839, 814, 757, 707, 668; **m.p.**: 103 − 106 °C. Single Crystal Data for **6**: $C_{17}H_{15}ClFNO_3S$, Mr =367.83. 150 K – orthorhombic, P21/n, a = 6.8699(2) Å, b = 27.6557(7) Å, c = 8.8183(2) Å, V = 1644.22(7) Å, Data/restraints/parameters – 3403/0/217.

5.3.6 Scale-up experiments

The scale-up experiments (in batch and in continuous flow) have been performed on the synthesis of sulfone **3.107**.

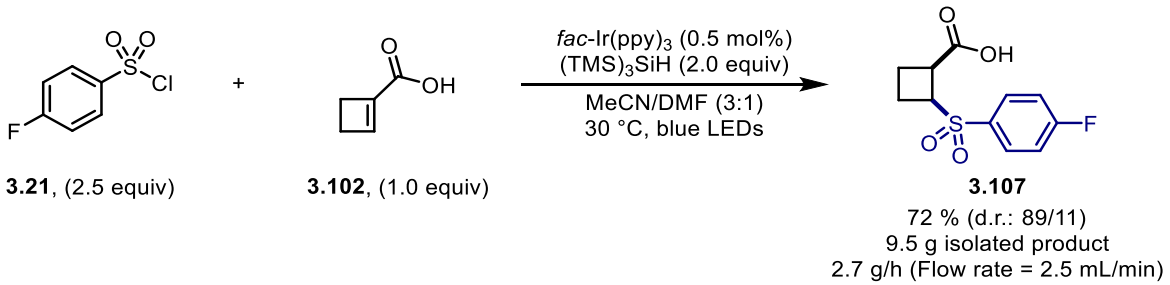
5.3.6.1 Scale-up experiment in batch



3.21, (2.5 equiv) **3.102**, (1.0 equiv) **3.107**
81% (d.r.: 89/11)
10.7 g isolated product

A stock solution of cyclobut-1-ene-1-carboxylic acid **3.102** in MeCN (185 mL, 0.276 M, 50.97 mmol, 1.0 equiv)* was added to a 500 mL round bottom flask. To that solution was added 4-fluorobenzenesulfonyl chloride (24.8 g, 127.4 mmol, 2.5 equiv) and *fac*-Ir(ppy)$_3$ (167.6 mg, 0.25 mmol, 0.5 mol%). This suspension was transfered to the Radley 1L reactor, followed by the addition of (TMS)Si$_3$H (31.4 mL, 101.9 mmol, 2.0 equiv) and MeCN (115 mL). The reactor was irradiated with two Kessil H150-Blue LED lights (34 W, 5 cm distance, see picture above) for 16 h at 30 °C. The reaction mixture was collected from the outlet and concentrated *in vacuo*. The crude was purified by flash column chromatography (silica, sample dry-loading with Celite®, EtOAc in Heptane with 1% acetic acid, 0/100 to 100/0). The desired fractions were collected and concentrated *in vacuo* to give the desired hydrosulfonylated product **3.107** as mixture of diastereoisomers (89/11, *cis*/*trans*) and as an off-white solid (10.7 g, 41.5 mmol, 81%). Trituration with Et$_2$O afforded exclusively the *cis*-diastereoisomer as a white solid (9.1 g, 35.3 mmol, 69%).

5.3.6.2 Scale-up experiment in continuous flow

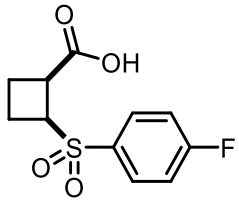


A stock solution of cyclobut-1-ene-1-carboxylic acid **3.102** in MeCN (185 mL, 0.276M, 50.97 mmol, 1.0 equiv)* was added to a 500 mL round bottom flask. To that solution was added 4-fluorobenzenesulfonyl chloride (24.8 g, 127.4 mmol, 2.5 equiv), *fac*-Ir(ppy)$_3$ (167.6 mg, 0.25 mmol, 0.5 mol%), (TMS)Si$_3$H (31.4 mL, 101.9 mmol, 2.0 equiv), MeCN (100 mL) and DMF (170 mL). The solution was pumped through a Vapourtec photoreactor (fluoropolymer tube, 1.3 mm i.d., 10 mL) and the liquid flowrate was set at 2.5 mL/min (4 min residence time). The reactor was irradiated with 54 blue LEDs (410 nm, total power 24 W) at 30 °C (internal temperature of the photoreactor: 35 °C). The reaction mixture collected from the outlet was concentrated *in vacuo*. The crude was purified by flash column chromatography (silica, EtOAc in Heptane with 1% acetic acid, 0/100 to 100/0). The desired fractions were collected and concentrated *in vacuo* to give the desired hydrosulfonylated product **3.107** as a mixture of diastereoisomers (89/11, *cis*/*trans*) as an off-white solid (9.5 g, 36.8 mmol, 72%). Trituration with Et$_2$O afforded exclusively the *cis*-diastereoisomer as white solid (7.3 g, 28.3 mmol, 56%).

* The approximate concentration of the solution was calculated using quantitative ^{1}H NMR. To a sample of the solution containing **3.102** in MeCN (20 µL) was added CH_2Br_2 (7.0 µL,

0.1 mmol) and $CDCl_3$ (ca. 0.5 mL). The concentration of the **3.102** stock solution was determined by ^{1}H NMR spectroscopy to be 0.276 M (n = 3).

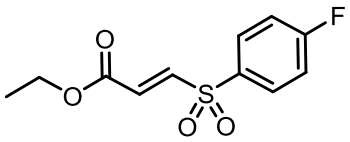
***cis*-2-((4-fluorophenyl)sulfonyl)cyclobutane-1-carboxylic acid (3.107)**



^{1}H NMR (400 MHz, DMSO-d_6) δ 12.43 (s, 1H), 7.96 − 7.89 (m, 2H), 7.50 − 7.42 (m, 2H), 4.50 − 4.40 (m, 1H), 3.48 − 3.40 (m, 1H), 2.39 − 2.26 (m, 2H), 2.20 − 2.09 (m, 1H), 2.02 − 1.91 (m, 1H); **^{13}C NMR** (101 MHz, DMSO-d_6) δ 171.9, 165.5 (d, $J_{C\text{-}F}$ = 252.5 Hz), 135.8 (d, $J_{C\text{-}F}$ = 3.0 Hz), 131.6 (d, $J_{C\text{-}F}$ = 9.9 Hz), 116.8 (d, $J_{C\text{-}F}$ = 22.7 Hz), 58.6, 40.2, 21.3, 20.9; **^{19}F NMR** (471 MHz, DMSO-d_6) δ −105.1 - −105.2 (m, 1F); **HRMS** (ESI-TOF) calculated for $C_{11}H_{10}FO_4{}^{32}S$ $[M\text{-}H]^-$: 257.0289; found 257.0288; **IR** (neat) 2981, 2888, 1744, 1587, 1493, 1440, 1382, 1312, 1285, 1269, 1237, 1204, 1165, 1132, 1084, 1013, 955, 847, 836, 818, 779, 759, 718, 689, 650; **m.p.**: 185 − 187 °C.

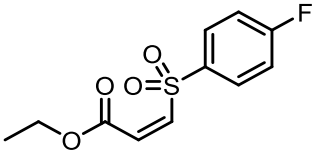
5.3.7 Characterisation: Hydrosulfonylation of alkynes

Ethyl (*E*)-3-((4-fluorophenyl)sulfonyl)acrylate ((*E*)-3.116)



General procedure B was followed to obtain **(*E*)-3.116** (14 mg, 0.04 mmol, 8%) as a colourless oil. **^{1}H NMR** (400 MHz, $CDCl_3$) δ 7.91 − 7.84 (m, 2H), 7.24 − 7.15 (m, 3H), 6.77 (d, J = 15.2 Hz, 1H), 4.19 (q, J = 7.1 Hz, 2H), 1.24 (t, J = 7.1 Hz, 3H); **^{13}C NMR** (101 MHz, $CDCl_3$) δ 166.4 (d, $J_{C\text{-}F}$ = 257.9 Hz), 163.5, 143.1, 134.7 (d, $J_{C\text{-}F}$ = 3.2 Hz), 131.5 (d, $J_{C\text{-}F}$ = 9.8 Hz), 131.4, 117.2 (d, $J_{C\text{-}F}$ = 22.7 Hz), 62.3, 14.2; **^{19}F NMR** (471 MHz, $CDCl_3$) δ −101.8 - −101.9 (m, 1F); **HRMS** (ESI-TOF) calculated for $C_{11}H_{12}FO_4{}^{32}S$ $[M+H]^+$: 359.0435; found 359.0436; **IR** (neat) 1787, 1632, 1486, 1328, 1305, 1289, 1271, 1225, 1196, 1111, 1093, 1039, 963, 905, 857, 842, 805, 784, 753, 688, 631.

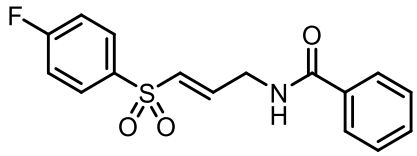
Ethyl (*Z*)-3-((4-fluorophenyl)sulfonyl)acrylate ((*Z*)-3.116)



General procedure B was followed to obtain **(*Z*)-3.116** (112 mg, 0.31 mmol, 62%) as a white solid. **^{1}H NMR** (400 MHz, $CDCl_3$) δ 8.07 − 8.00 (m, 2H), 7.28 − 7.21 (m, 2H), 6.53 (s, 2H), 4.36 (q, J = 7.2 Hz, 2H), 1.39 (t, J = 7.2 Hz, 3H); **^{13}C NMR** (101 MHz, $CDCl_3$) δ 167.4, 164.5 (d, $J_{C\text{-}F}$ = 87.0 Hz), 135.6 (d, $J_{C\text{-}F}$ = 3.1 Hz), 135.2, 132.3, 131.4 (d, $J_{C\text{-}F}$ = 9.6 Hz), 116.8 (d, $J_{C\text{-}F}$ = 22.6 Hz), 62.4, 14.1; **^{19}F NMR** (471 MHz, $CDCl_3$) δ −102.7 - −102.7 (m, 1F); **HRMS** (ESI-TOF) calculated for $C_{11}H_{12}FO_4{}^{32}S$ $[M+H]^+$: 359.0435; found

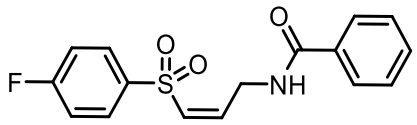
359.0439; **IR** (neat) 1726, 1625, 1589, 1494, 1367, 1340, 1317, 1294, 1232, 1166, 1142, 1100, 1083, 1024, 942, 867, 841, 819, 760, 742, 703, 657, 629; **m.p.**: 99 − 101 °C.

(*E*)-4-((4-fluorophenyl)sulfonyl)-*N*-phenylbut-3-enamide ((*E*)-3.117)[a]



General procedure B was followed to obtain **(*E*)-3.117** (18 mg, 0.06 mmol, 11%) as a colourless oil. **^{1}H NMR** (400 MHz, DMSO-d_6) δ 8.80 (t, J = 5.6 Hz, 1H), 7.98 − 7.91 (m, 2H), 7.88 − 7.84 (m, 2H), 7.58 − 7.43 (m, 5H), 6.98 (dt, J = 15.2, 4.4 Hz, 1H), 6.82 (dt, J = 15.1, 1.8 Hz, 1H), 4.17 − 4.12 (m, 2H); **^{13}C NMR** (101 MHz, $CDCl_3$) δ 167.6, 165.8 (d, $J_{C\text{-}F}$ = 256.5 Hz), 143.60, 136.0 (d, $J_{C\text{-}F}$ = 3.2 Hz), 133.5, 132.0, 130.8, 130.6 (d, $J_{C\text{-}F}$ = 9.6 Hz), 128.7, 127.2, 116.8 (d, $J_{C\text{-}F}$ = 22.7 Hz), 40.0; **^{19}F NMR** (377 MHz, DMSO-d_6) δ −104.9 - − 105.0 (m, 1F); **HRMS** (ESI-TOF) calculated for $C_{16}H_{15}FO_3N^{32}S$ $[M+H]^+$: 320.0751; found 320.0752; **IR** (neat) 2981, 2680, 1640, 1591, 1493, 1384, 1313, 1290, 1233, 1192, 1141, 1084, 1026, 956, 934, 865, 837, 818, 737, 716, 691, 671, 617.

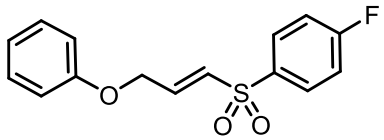
(*Z*)-4-((4-fluorophenyl)sulfonyl)-*N*-phenylbut-3-enamide ((*Z*)-3.117)[a]



General procedure B was followed to obtain **(*Z*)-3.117** (106 mg, 0.33 mmol, 66%) as a white solid. **^{1}H NMR** (400 MHz, DMSO-d_6) δ 8.86 (t, J = 5.5 Hz, 1H), 8.10 − 8.03 (m, 2H), 7.87 − 7.83 (m, 2H), 7.56 − 7.43 (m, 5H), 6.64 (dt, J = 11.2, 2.3 Hz, 1H), 6.43 (dt, J = 11.4, 5.8 Hz, 1H), 4.51 (td, J = 5.7, 2.2 Hz, 2H); **^{13}C NMR** (101 MHz, DMSO-d_6) δ 166.5, 165.0

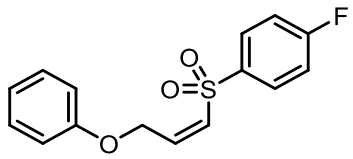
(d, $J_{C\text{-}F}$ = 253.1 Hz), 145.4, 137.1 (d, $J_{C\text{-}F}$ = 2.9 Hz), 133.9, 131.3, 130.2 (d, $J_{C\text{-}F}$ = 9.9 Hz), 129.4, 128.2, 127.1, 116.8 (d, $J_{C\text{-}F}$ = 22.9 Hz), 36.8; **^{19}F NMR** (377 MHz, DMSO-d_6) δ − 104.5 - − 104.7 (m, 1F); **HRMS** (ESI-TOF) calculated for $C_{16}H_{15}FO_3N^{32}S$ $[M+H]^+$: 320.0751; found 320.0777; **IR** (neat) 2981, 1633, 1589, 1578, 1535, 1492, 1428, 1374, 1330, 1307, 1292, 1264, 1221, 1181, 1158, 1141, 1085, 1065, 1031, 1011, 983, 954, 839, 814, 756, 737, 717, 703, 691, 675, 652, 631, 616; **m.p.**: 99 − 103 °C.

(*E*)-1-fluoro-4-((3-phenoxyprop-1-en-1-yl)sulfonyl)benzene ((*E*)-3.118)



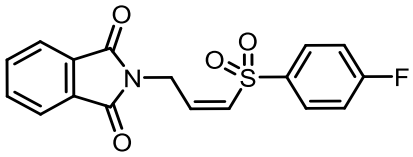
General procedure B was followed to obtain **(*Z*)-3.118** (43 mg, 0.15 mmol, 30%) as a white solid. **^{1}H NMR** (500 MHz, $CDCl_3$) δ 8.00 − 7.95 (m, 2H), 7.36 − 7.30 (m, 2H), 7.30 − 7.24 (m, 2H), 7.18 (dt, *J* = 15.0, 3.3 Hz, 1H), 7.06 − 7.01 (m, 1H), 6.94 − 6.90 (m, 2H), 6.81 (dt, *J* = 15.0, 2.2 Hz, 1H), 4.79 (dd, *J* = 3.4, 2.2 Hz, 2H); **^{13}C NMR** (126 MHz, $CDCl_3$) δ 165.8 (d, $J_{C\text{-}F}$ = 256.3 Hz), 157.6, 141.0, 136.3 (d, $J_{C\text{-}F}$ = 3.2 Hz), 131.2, 130.8 (d, $J_{C\text{-}F}$ = 9.6 Hz), 129.8, 121.9, 116.8 (d, $J_{C\text{-}F}$ = 22.6 Hz), 114.7, 65.6; **^{19}F NMR** (471 MHz, $CDCl_3$) δ −103.6 - −103.7 (m, 1F); **HRMS** (ESI-TOF) calculated for $C_{15}H_{12}FO_3{}^{32}S$ $[M-H]^-$: 291.0497; found 291.0490; **IR** (neat) 2981, 2889, 1767, 1702, 1638, 1587, 1491, 1446, 1385, 1315, 1294, 1286, 1254, 1236, 1159, 1141, 1087, 1025, 998, 958, 890, 872, 845, 834, 817, 777, 751, 711, 691, 668; **m.p.**: 105 − 107 °C.

(*Z*)-1-fluoro-4-((3-phenoxyprop-1-en-1-yl)sulfonyl)benzene ((*Z*)-3.118)



General procedure B was followed to obtain **(*Z*)-3.118** (74 mg, 0.25 mmol, 50%) as a white solid. **^{1}H NMR** (500 MHz, $CDCl_3$) δ 8.01 − 7.94 (m, 2H), 7.35 − 7.25 (m, 4H), 7.04 − 6.99 (m, 1H), 6.95 − 6.90 (m, 2H), 6.56 (dt, J = 11.5, 4.9 Hz, 1H), 6.36 (dt, J = 11.5, 2.4 Hz, 1H), 5.26 (dd, J = 5.0, 2.4 Hz, 2H); **^{13}C NMR** (126 MHz, $CDCl_3$) δ 166.0 (d, $J_{C\text{-}F}$ = 256.9 Hz), 157.8, 143.2, 136.7 (d, $J_{C\text{-}F}$ = 3.2 Hz), 130.5 (d, $J_{C\text{-}F}$ = 9.6 Hz), 130.1, 129.8, 121.6, 116.9 (d, $J_{C\text{-}F}$ = 22.6 Hz), 114.8, 64.0; **^{19}F NMR** (377 MHz, $CDCl_3$) δ −102.9 - −102.9 (m, 1F); **HRMS** (ESI-TOF) calculated for $C_{15}H_{12}FO_3{}^{32}S$ $[M\text{-}H]^-$: 291.0497; found 291.0492; **IR** (neat) 2981, 2888, 1588, 1494, 1446, 1383, 1317, 1294, 1236, 1206, 1178, 1162, 1149, 1138, 1083, 1044, 1012, 956, 840, 817, 770, 755, 713, 702, 690, 656, 632; **m.p.**: 82 − 83 °C.

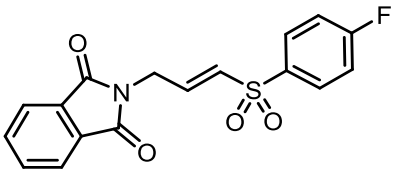
(*Z*)-2-(3-((4-fluorophenyl)sulfonyl)allyl)isoindoline-1,3-dione ((*Z*)-3.119)



General procedure B was followed to obtain **(*Z*)-3.119** (91 mg, 0.26 mmol, 53%) as a white solid. **^{1}H NMR** (500 MHz, $CDCl_3$) δ 8.12 − 8.06 (m, 2H), 7.85 (dd, J = 5.4, 3.1 Hz, 2H), 7.74 (dd, J = 5.5, 3.0 Hz, 2H), 7.27 (t, J = 8.6 Hz, 2H), 6.32 (dt, J = 11.2, 2.0 Hz, 1H), 6.19 (dt, J = 11.5, 6.0 Hz, 1H), 5.07 (dd, J = 6.0, 2.1 Hz, 2H); **^{13}C NMR** (126 MHz, $CDCl_3$) δ 167.7, 166.0 (d, $J_{C\text{-}F}$ = 256.5 Hz), 140.4, 136.5 (d, $J_{C\text{-}F}$ = 3.2 Hz), 134.4, 131.9, 131.3, 130.8 (d, $J_{C\text{-}F}$ = 9.7 Hz), 123.6, 116.8 (d, $J_{C\text{-}F}$ = 22.6 Hz), 35.0; **^{19}F NMR** (471 MHz, $CDCl_3$) δ −

103.1 - − 103.2 (m, 1F); **HRMS** (ESI-TOF) calculated for $C_{17}H_{13}FNO_4{}^{32}S$ $[M+H]^+$: 346.0544; found 346.0551; **IR** (neat) 3658, 2981, 2888, 1766, 1702, 1591, 1495, 1471, 1417, 1395, 1372, 1316, 1294, 1252, 1221, 1144, 1113, 1084, 952, 842, 832, 815, 796, 762, 738, 718, 692, 654; **m.p.**: 128 − 130 °C.

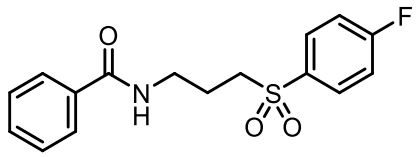
(*E*)-2-(3-((4-fluorophenyl)sulfonyl)allyl)isoindoline-1,3-dione ((*E*)-3.119)



General procedure B was followed to obtain **(*Z*)-3.119** (35 mg, 0.10 mmol, 20%) as a white solid. **^{1}H NMR** (500 MHz, $CDCl_3$) δ 7.89 − 7.83 (m, 4H), 7.76 (dd, J = 5.5, 3.1 Hz, 2H), 7.20 (t, J = 8.5 Hz, 2H), 6.96 (dt, J = 15.1, 5.3 Hz, 1H), 6.43 (dt, J = 15.1, 1.7 Hz, 1H), 4.47 (dd, J = 5.3, 1.7 Hz, 2H); **^{13}C NMR** (126 MHz, $CDCl_3$) δ 167.4, 165.9 (d, $J_{C\text{-}F}$ = 256.4 Hz), 139.6, 136.0 (d, $J_{C\text{-}F}$ = 3.2 Hz), 134.6, 132.8, 131.9, 130.8 (d, $J_{C\text{-}F}$ = 9.6 Hz), 123.8, 116.9 (d, $J_{C\text{-}F}$ = 22.8 Hz), 37.6; **^{19}F NMR** (471 MHz, $CDCl_3$) δ −103.4 - − 103.5 (m, 1F); **HRMS** (ESI-TOF) calculated for $C_{17}H_{13}FNO_4{}^{32}S$ $[M+H]^+$: 346.0544; found 346.0544; **IR** (neat) 3658, 2981, 2888, 1767, 1703, 1590, 1494, 1471, 1393, 1318, 1292, 1252, 1145, 1114, 1084, 952, 832, 815, 762, 738, 718, 691, 655; **m.p.**: 162 − 166 °C.

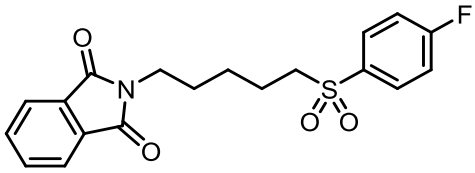
5.3.8 Characterisation: Hydrosulfonylation of unactivated alkenes

4-((4-fluorophenyl)sulfonyl)-*N*-phenylbutanamide (3.130)[a]



General procedure B was followed to obtain **3.130** (64 mg, 0.20 mmol, 40%) as a white solid. **General procedure C** was followed to obtain **3.130** (132 mg, 0.41 mmol, 82%) as a white solid. **^{1}H NMR** (400 MHz, $CDCl_3$) δ 7.93 − 7.87 (m, 2H), 7.77 − 7.73 (m, 2H), 7.50 − 7.45 (m, 1H), 7.42 − 7.37 (m, 2H), 7.25 − 7.18 (m, 2H), 6.81 − 6.72 (m, 1H), 3.58 (q, J = 6.4 Hz, 2H), 3.22 − 3.16 (m, 2H), 2.08 (p, J = 6.7 Hz, 2H); **^{13}C NMR** (101 MHz, $CDCl_3$) δ 167.9, 166.1 (d, $J_{C\text{-}F}$ = 256.8 Hz), 135.2 (d, $J_{C\text{-}F}$ = 3.2 Hz), 134.2, 131.8, 131.0 (d, $J_{C\text{-}F}$ = 9.5 Hz), 128.7, 127.1, 116.9 (d, $J_{C\text{-}F}$ = 22.6 Hz), 54.3, 38.4, 23.2; **^{19}F NMR** (377 MHz, $CDCl_3$) δ −103.0 - −103.1 (m, 1F); **HRMS** (ESI-TOF) calculated for $C_{16}H_{17}FO_3N^{32}S$ $[M+H]^+$: 322.0908; found 322.0916; **IR** (neat) 1640, 1592, 1579, 1543, 1489, 1459, 1450, 1286, 1234, 1185, 1158, 1141, 1087, 1036, 1012, 999, 977, 858, 835, 818, 801, 771, 731, 717, 694, 672, 658, 619; **m.p.**: 136 − 138 °C.

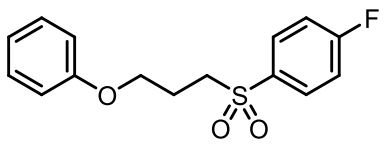
12-(5-((4-fluorophenyl)sulfonyl)pentyl)isoindoline-1,3-dione (3.131)



General procedure C was followed to obtain **3.131** (143 mg, 0.38 mmol, 76%) as a white solid. **^{1}H NMR** (500 MHz, $CDCl_3$) δ 7.95 − 7.89 (m, 2H), 7.84 − 7.80 (m, 2H), 7.74 − 7.70

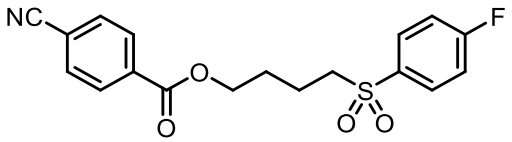
(m, 2H), 7.28 − 7.22 (m, 2H), 3.65 (t, *J* = 7.1 Hz, 2H), 3.13 − 3.07 (m, 2H), 1.81 − 1.72 (m, 2H), 1.71 − 1.63 (m, 2H), 1.48 − 1.39 (m, 2H); **^{13}C NMR** (126 MHz, $CDCl_3$) δ 168.3, 165.7 (d, $J_{C\text{-}F}$ = 256.1 Hz), 135.1 (d, $J_{C\text{-}F}$ = 3.2 Hz), 134.0, 131.9, 130.9 (d, $J_{C\text{-}F}$ = 9.6 Hz), 123.1, 116.6 (d, $J_{C\text{-}F}$ = 22.6 Hz), 56.0, 37.3, 28.0, 25.4, 22.3; **^{19}F NMR** (471 MHz, $CDCl_3$) δ −103.6 - −103.7 (m, 1F); **HRMS** (ESI-TOF) calculated for $C_{19}H_{19}FO_4N^{32}S$ $[M+H]^+$: 376.1013; found 376.1025; **IR** (neat): 1771, 1707, 1640, 1592, 1543, 1494, 1466, 1441, 1400, 1378, 1340, 1319, 1286, 1255, 1230, 1199, 1187, 1162, 1145, 1087, 1074, 1049, 1014, 1000, 959, 941, 873, 835, 817, 794, 766, 721, 712, 693, 671, 622; **m.p.**: 120 − 122 °C.

1-fluoro-4-((3-phenoxypropyl)sulfonyl)benzene (3.132)



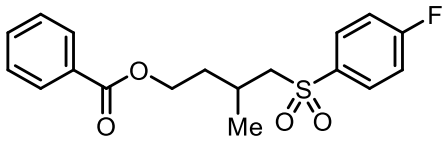
General procedure C was followed to obtain **3.132** (116 mg, 0.40 mmol, 79%) as a colourless oil. **^{1}H NMR** (500 MHz, $CDCl_3$) δ 7.97 − 7.91 (m, 2H), 7.29 − 7.19 (m, 4H), 6.94 (t, *J* = 7.4 Hz, 1H), 6.84 − 6.78 (m, 2H), 4.01 (t, J = 5.9 Hz, 2H), 3.34 − 3.28 (m, 2H), 2.25 − 2.16 (m, 2H); **^{13}C NMR** (126 MHz, $CDCl_3$) δ 165.9 (d, $J_{C\text{-}F}$ = 256.5 Hz), 158.3, 135.2 (d, $J_{C\text{-}F}$ = 3.3 Hz), 131.0 (d, $J_{C\text{-}F}$ = 9.6 Hz), 129.6, 121.3, 116.8 (d, $J_{C\text{-}F}$ = 22.7 Hz), 114.5, 65.3, 53.5, 23.1; **^{19}F NMR** (471 MHz, $CDCl_3$) δ −103.3 - −103.4 (m, 1F); **HRMS** (ESI-TOF) calculated for $C_{15}H_{14}FO_3{}^{32}S$ $[M-H]^-$: 293.0653 found 293.0659; **IR** (neat): 1589, 1493, 1473, 1405, 1316, 1288, 1237, 1172, 1140, 1085, 1040, 1014, 930, 886, 838, 819, 781, 755, 729, 692, 672, 634.

4-((4-fluorophenyl)sulfonyl)butyl 4-cyanobenzoate (3.133)



General procedure C was followed to obtain **3.133** (147 mg, 0.41 mmol, 82%) as a colourless oil. **^{1}H NMR** (400 MHz, $CDCl_3$) δ 8.10 − 8.05 (m, 2H), 7.95 − 7.89 (m, 2H), 7.76 − 7.72 (m, 2H), 7.26 − 7.19 (m, 2H), 4.38 − 4.29 (m, 2H), 3.21 − 3.08 (m, 2H), 1.96 − 1.82 (m, 4H); **^{13}C NMR** (101 MHz, $CDCl_3$) δ 165.5 (d, $J_{C\text{-}F}$ = 258.7 Hz), 164.8, 135.1 (d, $J_{C\text{-}F}$ = 3.2 Hz), 133.8, 132.3, 131.0 (d, $J_{C\text{-}F}$ = 9.6 Hz), 130.1, 118.0, 116.7 (d, $J_{C\text{-}F}$ = 22.6 Hz), 116.5, 64.5, 55.8, 27.3, 19.6; **^{19}F NMR** (377 MHz, $CDCl_3$) δ −103.0 - −103.1 (m, 1F); **HRMS** (ESI-TOF) calculated for $C_{18}H_{15}FO_4N^{32}S$ $[M+H]^+$: 360.0711; found 360.0696; **IR** (neat) 2232, 1715, 1591, 1492, 1472, 14004, 1313, 1272, 1221, 1178, 1141, 1123, 1111, 1085, 1034, 1020, 961, 905, 868, 838, 778, 765, 738, 694.

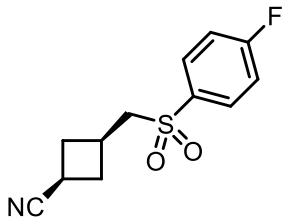
4-((4-fluorophenyl)sulfonyl)-3-methylbutyl benzoate (3.134)



General procedure C was followed to obtain **3.134** (151 mg, 0.43 mmol, 86%) as a white solid. **^{1}H NMR** (400 MHz, $CDCl_3$) δ 7.99 − 7.94 (m, 2H), 7.92 − 7.86 (m, 2H), 7.56 (ddt, J = 7.9, 6.9, 1.3 Hz, 1H), 7.46 − 7.40 (m, 2H), 7.18 − 7.11 (m, 2H), 4.37 − 4.28 (m, 2H), 3.18 (dd, J = 14.2, 5.3 Hz, 1H), 3.01 (dd, J = 14.2, 7.3 Hz, 1H), 2.35 − 2.23 (m, 2H), 2.06 − 1.96 (m, 2H), 1.79 − 1.67 (m, 2H), 1.18 (d, J = 6.8 Hz, 3H); **^{13}C NMR** (101 MHz, $CDCl_3$) δ 166.8 (d, $J_{C\text{-}F}$ = 263.2 Hz), 164.6, 136.0 (d, $J_{C\text{-}F}$ = 3.3 Hz), 133.2, 130.8 (d, $J_{C\text{-}F}$ = 9.6 Hz), 130.1, 129.6, 128.5, 116.7 (d, $J_{C\text{-}F}$ = 22.6 Hz), 62.4, 62.1, 35.2, 26.3, 19.9; **^{19}F NMR** (471 MHz,

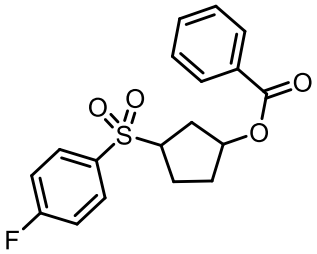
$CDCl_3$) δ −103.3 - −103.4 (m, 1F); **HRMS** (ESI-TOF) calculated for $C_{18}H_{20}FO_4{}^{32}S$ $[M+H]^+$: 351.1061; found 351.1065; **IR** (neat): 1712, 1588, 1491, 1469, 1455, 1405, 1390, 1359, 1310, 1278, 1243, 1230, 1194, 1178, 1142, 1123, 1097, 1083, 1072, 1032, 1000, 954, 854, 843, 820, 801, 765, 713, 690, 677, 632, 618; **m.p.**: 63 − 65 °C.

3-(((4-fluorophenyl)sulfonyl)methyl)cyclobutane-1-carbonitrile (3.135)



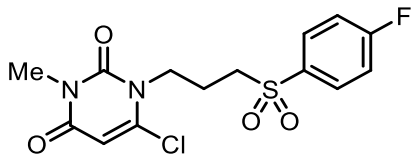
General procedure C was followed to obtain **3.135** (118 mg, 0.47 mmol, 93%) as a white solid (mixture of both diastereomers, d.r: 60/40). **^{1}H NMR** (400 MHz, $CDCl_3$) δ 7.94 − 7.87 (m, 2H), 7.30 − 7.23 (m, 2H), 3.26 (d, J = 7.3 Hz, 1H), 3.25 (d, J = 7.4 Hz, 1H), 3.15 − 3.07 (m, 0.4H), 3.07 − 2.96 (m, 1H), 2.87 − 2.73 (m, 0.6H), 2.61 − 2.47 (m, 2H), 2.23 − 2.12 (m, 2H); **^{13}C NMR** (101 MHz, $CDCl_3$) δ 166.5 (d, $J_{C\text{-}F}$ = 257.1 Hz), 166.0 (d, $J_{C\text{-}F}$ = 257.1 Hz), 135.3 (d, $J_{C\text{-}F}$ = 3.2 Hz), 135.1 (d, $J_{C\text{-}F}$ = 3.2 Hz), 130.9 (d, $J_{C\text{-}F}$ = 9.5 Hz), 130.9 (d, $J_{C\text{-}F}$ = 9.6 Hz), 122.2, 121.2, 117.0 (d, $J_{C\text{-}F}$ = 22.5 Hz), 116.9 (d, $J_{C\text{-}F}$ = 22.6 Hz), 61.3, 60.7, 32.8, 31.4, 27.7, 27.2, 20.2, 19.3; **^{19}F NMR** (471 MHz, $CDCl_3$) δ −102.6 - −102.8 (m, 1F); **HRMS** (ESI-TOF) calculated for $C_{12}H_{16}FO_2N_2{}^{32}S$ $[M+NH_4]^+$: 271.0911; found 271.0915; **IR** (neat): 2947, 2360, 2341, 1587, 1493, 1406, 1310, 1287, 1225, 1142, 1099, 1085, 1012, 844, 818, 780, 754, 671; **m.p.**: 100 − 102 °C.

3-((4-fluorophenyl)sulfonyl)cyclopentyl benzoate (3.136)



General procedure C was followed to obtain **3.136** (137 mg, 0.38 mmol, 75%) as a white solid. **^{1}H NMR** (500 MHz, $CDCl_3$) δ 7.99 − 7.93 (m, 4H), 7.60 − 7.55 (m, 1H), 7.47 − 7.41 (m, 2H), 7.30 − 7.25 (m, 2H), 5.57 − 5.52 (m, 1H), 3.83 − 3.74 (m, 1H), 2.44 (ddd, J = 14.5, 8.9, 5.4 Hz, 1H), 2.36 − 2.27 (m, 1H), 2.26 − 2.17 (m, 3H), 2.08 − 1.98 (m, 1H); **^{13}C NMR** (126 MHz, $CDCl_3$) δ 166.0 (d, $J_{C\text{-}F}$ = 256.2 Hz), 165.9, 134.7 (d, $J_{C\text{-}F}$ = 3.4 Hz), 133.3, 131.4 (d, $J_{C\text{-}F}$ = 9.6 Hz), 130.1, 129.6, 128.5, 116.83 (d, $J_{C\text{-}F}$ = 22.6 Hz), 76.6, 62.9, 34.4, 32.0, 25.0; **^{19}F NMR** (471 MHz, $CDCl_3$) δ −103.2 - −103.3 (m, 1F); **HRMS** (ESI-TOF) calculated for $C_{18}H_{21}FO_4N^{32}S$ $[M+NH_4]^+$: 366.1170; found 366.1178; **IR** (neat): 1713, 1590, 1493, 1451, 1404, 1359, 1314, 1271, 1233, 1142, 1112, 1084, 1070, 1026, 1014, 967, 911, 839, 711, 685, 671; **m.p.**: 120 − 122 °C. Stereochemistry of **3.136** could not be assigned.

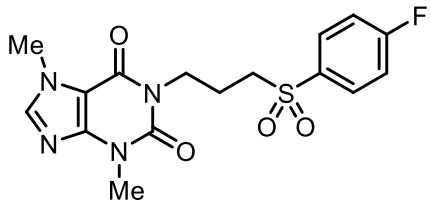
6-chloro-1-(3-((4-fluorophenyl)sulfonyl)propyl)-3-methylpyrimidine-2,4(*1H*,*3H*)-dione (3.137)



General procedure C was followed to obtain **3.137** (131 mg, 0.37 mmol, 73%) as a white solid. **^{1}H NMR** (400 MHz, $CDCl_3$) δ 7.99 − 7.92 (m, 2H), 7.31 − 7.24 (m, 2H), 5.94 (s, 1H), 4.21 (t, J = 7.3 Hz, 2H), 3.30 (s, 3H), 3.20 (t, J = 7.6 Hz, 2H), 2.22 − 2.11 (m, 2H); **^{13}C NMR** (101 MHz, $CDCl_3$) δ 166.1 (d, $J_{C\text{-}F}$ = 257.0 Hz), 160.6, 151.1, 145.0, 134.8 (d, $J_{C\text{-}F}$ = 3.2

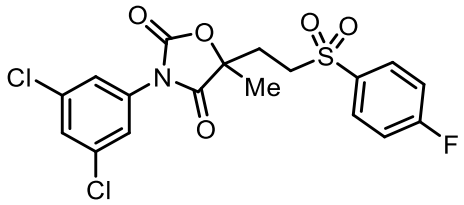
Hz), 131.1 (d, $J_{C\text{-}F}$ = 9.7 Hz), 116.93 (d, $J_{C\text{-}F}$ = 22.6 Hz), 102.5, 53.7, 45.4, 28.4, 22.4;**^{19}F NMR** (471 MHz, $CDCl_3$) δ −102.7 (tt, J = 8.7, 4.5 Hz, 1F); **HRMS** (ESI-TOF) calculated for $C_{14}H_{15}ClFO_4N_2{}^{32}S$ $[M+H]^+$: 361.0420; found 361.0428.; **IR** (neat): 1701, 1665, 1605, 1591, 1494, 1438, 1418, 1401, 1376, 1351, 1314, 1284, 1237, 1204, 1158, 1140, 1085, 1030, 962, 861, 819, 774, 756, 690, 667, 652, 634; **m.p.**: 136 − 138 °C.

1-(3-((4-fluorophenyl)sulfonyl)propyl)-3,7-dimethyl-3,7-dihydro-*1H*-purine-2,6-dione (3.138)



General procedure C was followed to obtain **3.138** (74 mg, 0.21 mmol, 41%) as a white solid. **^{1}H NMR** (400 MHz, $CDCl_3$) δ 7.93 − 7.88 (m, 2H), 7.51 − 7.50 (m, 1H), 7.24 − 7.18 (m, 2H), 4.07 (t, J = 6.7 Hz, 2H), 3.95 (s, 3H), 3.53 (s, 3H), 3.21 − 316 (m, 2H), 2.11 − 2.02 (m, 2H); **^{13}C NMR** (101 MHz, $CDCl_3$) δ 166.0 (d, $J_{C\text{-}F}$ = 256.3 Hz), 155.2, 152.0, 149.1, 141.9, 135.0 (d, $J_{C\text{-}F}$ = 3.2 Hz), 131.2 (d, $J_{C\text{-}F}$ = 9.6 Hz), 116.7 (d, $J_{C\text{-}F}$ = 22.6 Hz), 107.6, 54.5, 39.6, 33.7, 29.9, 22.1; **^{19}F NMR** (471 MHz, $CDCl_3$) δ −103.5 (s, 1F); **HRMS** (ESI-TOF) calculated for $C_{16}H_{18}FO_4N_4{}^{32}S$ $[M+H]^+$: 381.1027; found 381.1030; **IR** (neat): 1710, 1656, 1587, 1548, 1489, 1445, 1406, 1376, 1354, 1310, 1281, 1229, 1197, 1182, 1142, 1112, 1097, 1085, 1028, 1010, 1001, 898, 879, 838, 822, 804, 784, 748, 731, 635, 611; **m.p.**: 159 − 161 °C.

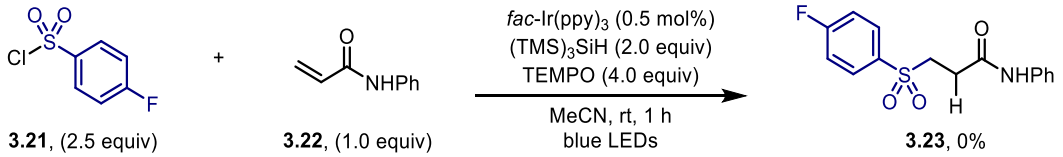
3-(3,5-dichlorophenyl)-5-(2-((4-fluorophenyl)sulfonyl)ethyl)-5-methyloxazolidine-2,4-dione (3.139)



General procedure C was followed to obtain **3.139** (148 mg, 0.34 mmol, 67%) as a colourless oil. **^{1}H NMR** (400 MHz, $CDCl_3$) δ 7.97 − 7.91 (m, 2H), 7.45 − 7.42 (m, 3H), 7.32 − 7.27 (m, 2H), 3.27 (ddd, J = 13.7, 10.4, 5.6 Hz, 2H), 3.16 (ddd, J = 13.7, 10.6, 5.9 Hz, 2H), 2.49 − 2.32 (m, 2H), 1.67 (s, 3H); **^{13}C NMR** (101 MHz, DMSO-d_6) δ 172.8, 165.3 (d, $J_{C\text{-}F}$ = 252.9 Hz), 152.0, 134.9 (d, $J_{C\text{-}F}$ = 3.0 Hz), 134.0, 133.1, 131.2 (d, $J_{C\text{-}F}$ = 9.9 Hz), 128.6, 125.8, 116.8 (d, $J_{C\text{-}F}$ = 22.8 Hz), 84.1, 49.3, 28.7, 20.9; **^{19}F NMR** (471 MHz, DMSO-d_6) δ − 104.4 - − 104.6 (m, 1F); **HRMS** (ESI-TOF) calculated for $C_{18}H_{13}Cl_2FO_5N^{32}S$ $[M+H]^+$: 443.9881; found 443.9873; **IR** (neat) 1816, 1730, 1577, 1492, 1455, 1397, 1379, 1307, 1232, 1179, 1138, 1085, 1053, 1027, 961, 938, 864, 834, 806, 764, 746, 677, 657, 640, 622.

5.3.9 Mechanistic investigations

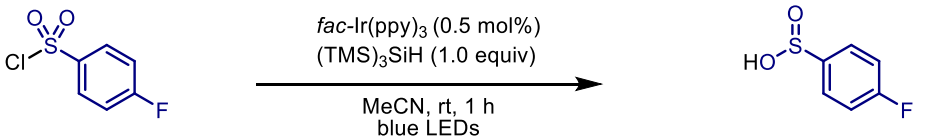
5.3.9.1 Radical-trapping experiment with TEMPO



3.21, (2.5 equiv) **3.22**, (1.0 equiv) **3.23**, 0%

4-fluorobenzenesulfonyl chloride **3.21** (243 mg, 1.3 mmol, 2.5 equiv) was added to a stirred suspension of *N*-phenylacrylamide **3.22** (74 mg, 0.5 mmol, 1.0 equiv), *fac*-Ir(ppy)$_3$ (1.70 mg, 0.0025 mmol, 0.5 mol%), MeCN (3.0 mL), (TMS)$_3$SiH (309 µL, 1.0 mmol, 2.0 equiv) and (2,2,6,6-tetramethylpiperidin-1-yl)oxyl (TEMPO) (313 mg, 2.0 mmol, 4.0 equiv). The reaction mixture was stirred under blue LED irradiation for 1 hour. LCMS analysis of the crude reaction mixture showed that no product was formed (starting material remaining).

5.3.9.2 Reduction of sulfonyl chloride to sulfinic acid 3.24

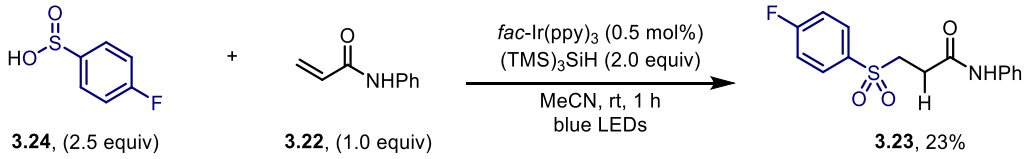


3.21, (1.0 equiv) **3.24**, *quantitative*[a]

4-fluorobenzenesulfonyl chloride **3.21** (19.4 mg, 0.1 mmol, 1.0 equiv) was added to a stirred suspension of *fac*-Ir(ppy)$_3$ (0.34 mg, 0.005 mmol, 0.5 mol%), (TMS)$_3$SiH (31 uL, 0.1 mmol, 1.0 equiv), MeCN (0.6 mL) and *α*,*α*,*α*-trifluorotoluene (12.3 uL, 0.1 mmol, 1.0 equiv; used as internal standard). The vial was stirred under blue LED irradiation with two Kessil LEDSs (35W, 450 nm, approximately 4 cm away from the light source) at 30 °C for 30 minutes.

The crude reaction mixture was analysed by quantitative ^{19}F NMR (using *α,α,α*-trifluorotoluene as internal standard).

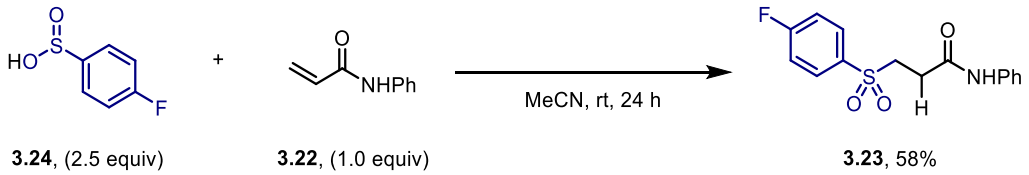
5.3.9.3 Photoredox-catalyzed hydrosulfonylation of alkenes using sulfinic acid 3.24



3.24, (2.5 equiv) **3.22**, (1.0 equiv) **3.23**, 23%

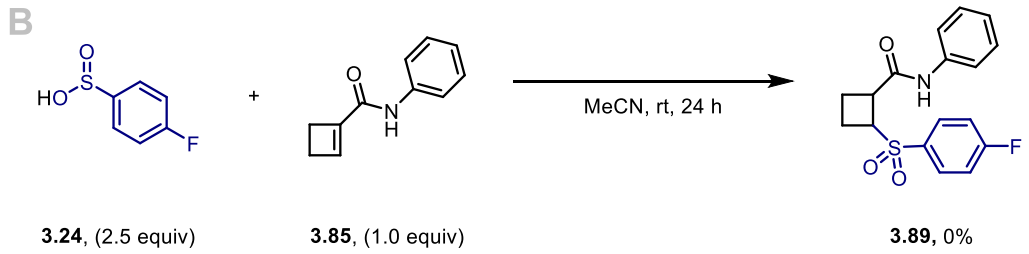
4-fluorobenzenesulfinic acid **3.24** (200 mg, 1.3 mmol, 2.5 equiv) was added to a stirred suspension of *N*-phenylacrylamide **3.22** (74 mg, 0.5 mmol, 1.0 equiv), *fac*-Ir(ppy)$_3$ (1.70 mg, 0.0025 mmol, 0.5 mol%), MeCN (3.0 mL) and (TMS)$_3$SiH (309 µL, 1.0 mmol, 2.0 equiv). The reaction mixture was stirred under blue LED irradiation for 1 hour. The solution was concentrated *in vacuo* and purified by flash column chromaography (silica, EtOAc in Heptane, 0/100 to 100/0) to afford sulfone **3.23** in 23% yield (35 mg, 0.11 mmol).

5.3.9.4 Michael addition of sulfinic acids to electron-deficient alkenes



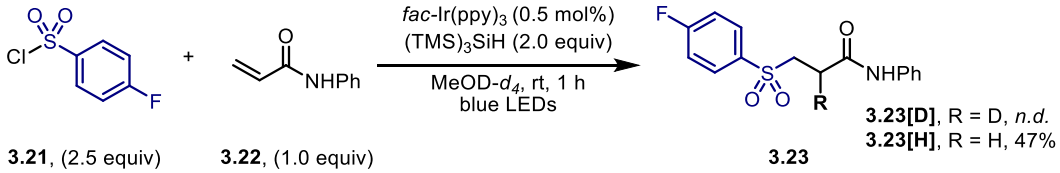
3.24, (2.5 equiv) **3.22**, (1.0 equiv) **3.23**, 58%

4-fluorobenzenesulfinic acid **3.24** (200 mg, 1.3 mmol, 2.5 equiv) was added to a stirred suspension of *N*-phenylacrylamide **3.22** (74 mg, 0.5 mmol, 1.0 equiv) in MeCN (3.0 mL). The reaction mixture was stirred under blue LED irradiation for 1 hour. The solution was concentrated *in vacuo* and purified by flash column chromaography (silica, EtOAc in Heptane, 0/100 to 100/0) to afford sulfone **3.23** in 58% yield (89 mg, 0.29 mmol).



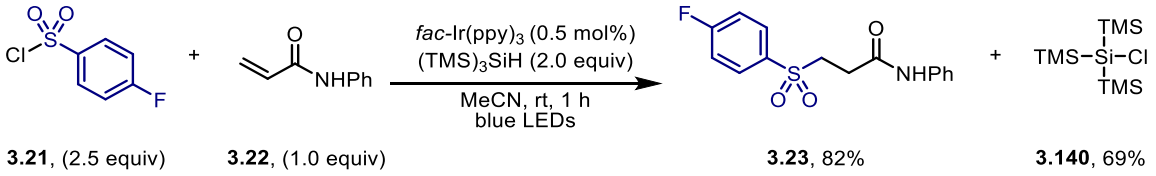
4-fluorobenzenesulfinic acid **3.24** (200 mg, 1.3 mmol, 2.5 equiv) was added to a stirred suspension of *N*-phenyl cyclobutene **3.85** (86.5 mg, 0.5 mmol, 1.0 equiv) in MeCN (3.0 mL). The reaction mixture was stirred under blue LED irradiation for 1 hour. LCMS analysis of the crude reaction mixture showed no conversion towards the desired product **3.89**.

5.3.9.5. Deuteration experiment



4-fluorobenzenesulfonyl chloride **3.21** (243 mg, 1.3 mmol, 2.5 equiv) was added to a stirred suspension of *N*-phenylacrylamide **3.22** (74 mg, 0.5 mmol, 1.0 equiv), *fac*-Ir(ppy)$_3$ (1.70 mg, 0.0025 mmol, 0.5 mol%), MeOD-d_4 (3.0 mL) and (TMS)$_3$SiH (309 µL, 1.0 mmol, 2.0 equiv). The reaction mixture was stirred under blue LED irradiation for 1 hour. The solution was concentrated *in vacuo* and purified by flash column chromaography (silica, EtOAc in Heptane, 0/100 to 100/0) to afford [H]**3.23** in 47% yield (72 mg, 0.23 mmol).

5.3.9.6 Isolation of Chlorotris(trimethylsilyl)silane (3.140)



3.21, (2.5 equiv) **3.22**, (1.0 equiv) **3.23**, 82% **3.140**, 69%

4-fluorobenzenesulfonyl chloride **3.21** (243 mg, 1.3 mmol, 2.5 equiv) was added to a stirred suspension of *N*-phenylacrylamide **3.22** (74 mg, 0.5 mmol, 1.0 equiv), *fac*-Ir(ppy)$_3$ (1.70 mg, 0.0025 mmol, 0.5 mol%), MeCN (3.0 mL) and (TMS)$_3$SiH (309 µL, 1.0 mmol, 2.0 equiv). The reaction mixture was stirred under blue LED irradiation for 1 hour. The solvent was removed *in vacuo* and the residue was purified by column chromatography (silica, EtOAc in heptane 0/100 to 20/80) to yield **3.140** (98 mg, 0.34 mmol, 69%) as a colourless oil. **^{1}H NMR** (400 MHz, $CDCl_3$) δ 0.23 (s, 27H); **^{13}C NMR** (101 MHz, $CDCl_3$) δ -0.6. Spectroscopic data were in accordance with a commercial sample.

5.3.9.7 Stern-Volmer fluorescence quenching study[a,b]

A Stern-Volmer fluorescence quenching study of *fac*-Ir(ppy)$_3$ was performed with different concentrations of reaction components in MeCN under an argon atmosphere. A solution of *fac*-Ir(ppy)$_3$ (0.01 mM) was treated with 0.2-1.0 mM of either sulfonyl chloride **3.80**, alkene **3.81**, (TMS)$_3$SiH or *N*,*N*-dimethylsulfamoyl chloride in MeCN. The samples were irradiated at 370 nm and luminescence was measured over a range of 450 – 700 nm (λ_{max} = 532 nm). I_0/I was plotted against the different concentrations of the quenchers (Figure S2).

Note: (TMS)$_3$SiH and *fac*-Ir(ppy)$_3$ are poorly insoluble in MeCN and sonication was necessary to solubilise all of the reagents.

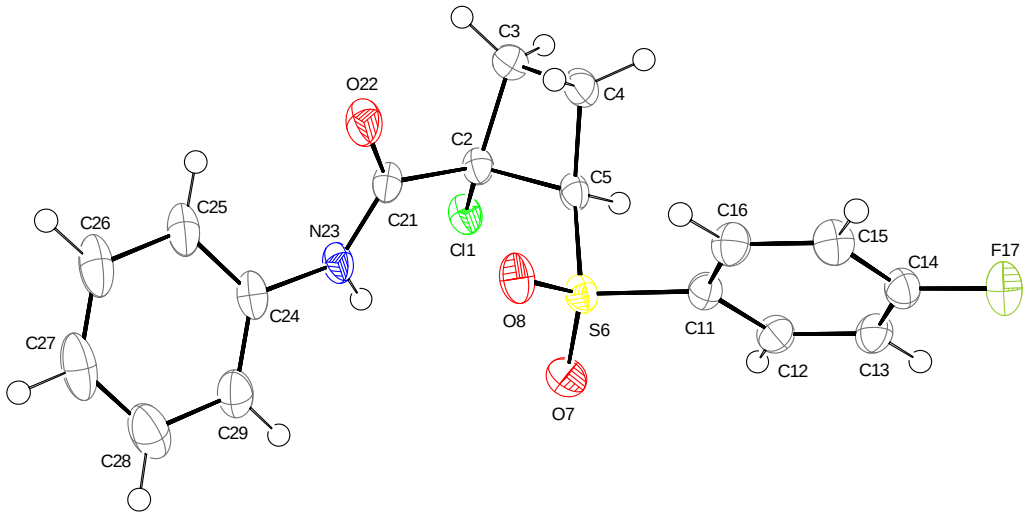
Table 5.1: Stern-Volmer fluorescence quenching experiment

c[mM]	4-F-PhSO$_2$Cl	(TMS)$_3$SiH	3.80	Me$_2$NSO$_2$Cl	TEMPO
0.0	1.000	1.000	1.000	1.000	1.000
0.2	1.508	1.068	1.087	0.941	0.993
0.4	1.905	1.055	1.004	0.910	1.086
0.6	2.402	1.064	1.039	0.910	1.166
0.8	2.842	1.104	1.054	1.060	1.166
1.0	3.318	1.080	1.106	1.068	0.986

5.3.10 X-ray - Crystallographic Data for 3.111

Empirical formula	C17 H15 Cl F N O3 S	
Formula weight	367.83	
Temperature	150 K	
Wavelength	1.54184 Å	
Crystal system	Monoclinic	
Space group	P 21/n	
Unit cell dimensions	a = 6.8699(2) Å	α = 90°.
	b = 27.6557(7) Å	β = 101.073(2)°.
	c = 8.8183(2) Å	γ = 90°.
Volume	1644.22(7) $Å^3$	
Z	4	
Density (calculated)	1.486 Mg/m^3	
Absorption coefficient	3.486 mm^{-1}	
F(000)	760	
Crystal size	0.35 x 0.22 x 0.04 mm^3	
Theta range for data collection	5.356 to 76.157°.	
Index ranges	-5<=h<=8, -34<=k<=34, -11<=l<=10	
Reflections collected	11306	
Independent reflections	3403 [R(int) = 0.042]	
Completeness to theta = 74.634°	99.6 %	
Absorption correction	Semi-empirical from equivalents	
Max. and min. transmission	0.87 and 0.50	

Refinement method	Full-matrix least-squares on F^2
Data / restraints / parameters	3403 / 0 / 217
Goodness-of-fit on F^2	1.0142
Final R indices [I>2sigma(I)]	R1 = 0.0396, wR2 = 0.0966
R indices (all data)	R1 = 0.0490, wR2 = 0.1071
Largest diff. peak and hole	0.51 and -0.35 e.$Å^{-3}$



5.4 Experimental procedures and characterisation of compounds from Chapter 4

All reactions for the hydrofluoromethylation of electron-deficient alkenes were conducted in non-dried glassware with magnetic stirring. All solvents were used as received without further purification. $(TMS)_3SiH$ was purchased from Fluorochem and Sigma-Aldrich. Fluoroiodomethane was purchased from abcr and kept at -20°C to prevent decomposition. Reactions were performed in 7 mL vials in a SynLED Parallel Photoreactor with a 12W blue LED lamp (λ_{max} = 470 nm). The scale-up experiment was performed using two Kessil LEDSs (35W, 450 nm, approximately 5 cm away from the reaction vessel). [^{18}F]Fluoride was produced by Alliance Medical (UK) *via* the 18O(p,n)18F reaction and delivered as [^{18}F]fluoride in ^{18}O-enriched-water. Radiosynthesis and azeotropic drying was performed on a NanoTek microfluidic device (Advion).

[a]: Experiments were conducted by Claudio F. Meyer (PhD student, University of Oxford).

[b]: Experiments were conducted by Sebastiano Ortalli (PhD student, University of Oxford).

[c]: Experiments were conducted by Jeroen Sap (former PhD student, University of Oxford).

[d]: Experiments were conducted by Xuanxiao Chen (joint PhD student in the research group of Prof. Ben Davis and Prof. Jason Davis, Oxford University, United-Kingdom).

5.4.1 Synthesis of starting materials

Compounds **4.28**, **4.30**, **4.31**, **4.32**, **4.33**, **4.34**, **4.35**, **4.39**, **4.64**, and **4.66** were synthesised according to literature procedures and spectroscopic data were in accordance with previous reports.[1,3,10–17]

5.4.2 Optimisation of the reaction conditions

Procedure for the optimisation studies:

To a 7 mL vial equipped with a magnetic stir bar, was added *N*-phenylacrylamide **4.28** (0.10 mmol, 1.0 equiv), photocatalyst (0.005 mmol, 1.0 mol%), solvent (0.6 mL), HAD (1.0 mmol, 2.0 equiv) and fluoroiodomethane **4.27** (1.25 mmol, 2.0 equiv). The vial was sealed with a septum, degassed by nitrogen bubbling for 10 seconds and wrapped with parafilm. The reaction mixture was stirred in a SynLED Parallel Photoreactor with a 12W blue LED lamp (λ_{max} = 470 nm) at room temperature for 16 hours. α,α,α-Trifluorotoluene (internal standard, 123 µL, 1.0 mmol, 1.0 equiv) was added, and the reaction mixture was analysed by quantitative ^{19}F NMR spectroscopy using α,α,α,-trifluorotoluene as the internal standard.

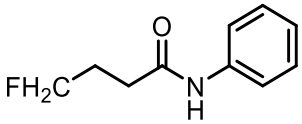
5.4.3 General procedures

General procedure A: To a 7 mL vial equipped with a magnetic stir bar, was added alkene (0.50 mmol, 1.0 equiv), MeCN (dry; 3.0 mL), $(TMS)_3SiH$ (185 uL, 0.6 mmol, 1.2 equiv) and CH_2FI (68 µL, 1.0 mmol, 2.0 equiv). The vial was sealed with a septum, degassed by nitrogen bubbling for 10 seconds and wrapped with parafilm. The reaction mixture was stirred in a SynLED Parallel Photoreactor with a 12W blue LED lamp (λ_{max} = 470 nm) at room temperature (using a fan) for 16 hours. The solvent was removed *in vacuo* and the residue was purified by column chromatography (silica, EtOAc in Pentane 0/100 to 100/0; or Et_2O in Pentane 0/100 to 100/0) to yield the desired product(s).

General procedure B: To a 7 mL vial equipped with a magnetic stir bar, was added alkene (0.50 mmol, 1.0 equiv), *fac*-$Ir(ppy)_3$ (1.6 mg, 0.0025 mmol, 0.5 mol%), MeCN (dry; 3.0 mL), $(TMS)_3SiH$ (185 uL, 0.6 mmol, 1.2 equiv) and CH_2FI (68 µL, 1.0 mmol, 2.0 equiv). The vial was sealed with a septum, degassed by nitrogen bubbling for 10 seconds and wrapped with parafilm. The reaction mixture was stirred in a SynLED Parallel Photoreactor with a 12W blue LED lamp (λ_{max} = 470 nm) at room temperature (using a fan) for 16 hours. The solvent was removed *in vacuo* and the residue was purified by column chromatography (silica, EtOAc in Pentane 0/100 to 100/0; or Et_2O in Pentane 0/100 to 100/0) to yield the desired product(s).

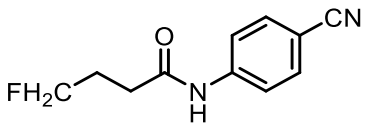
5.4.4 Characterisation: Hydrofluoromethylation of Electron-Deficient Alkenes

4-fluoro-*N*-phenylbutanamide (4.29)[a]



General procedure A was followed to obtain **4.29** (64 mg, 0.36 mmol, 71%) as a white solid. **^{1}H NMR** (400 MHz, $CDCl_3$) δ 7.57 (s, 1H), 7.50 (d, J = 7.9 Hz, 2H), 7.30 (t, J = 7.9 Hz, 2H), 7.10 (t, J = 7.4 Hz, 1H), 4.52 (dt, J = 47.3, 5.7 Hz, 2H), 2.50 (t, J = 7.3 Hz, 2H), 2.19 − 2.01 (m, 2H); **^{13}C NMR** (101 MHz, $CDCl_3$) δ 170.5, 137.9, 129.1, 124.5, 120.1, 83.3 (d, $J_{C\text{-}F}$ = 164.6 Hz), 33.1 (d, $J_{C\text{-}F}$ = 4.3 Hz), 26.3 (d, $J_{C\text{-}F}$ = 20.0 Hz); **^{19}F NMR** (377 MHz, $CDCl_3$) δ −220.5 (tt, J = 47.4, 27.0 Hz); **HRMS** (ESI-TOF) calculated for $C_{10}H_{13}FNO$ $[M+H]^+$: 182.0976, found 182.0977; **IR** (neat) 1656, 1620, 1597, 1542, 1502, 1489, 1441, 1393, 1374, 1331, 1297, 1258, 1035, 901, 758, 694, 634; **m.p.**: 76 − 78 °C.

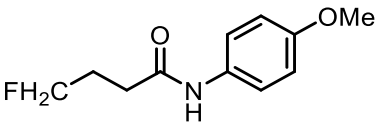
***N*-(4-cyanophenyl)-4-fluorobutanamide (4.42)**



General procedure B was followed to obtain **4.42** (83 mg, 0.41 mmol, 81%) as a white solid. **^{1}H NMR** (400 MHz, $CDCl_3$) δ 8.04 (s, 1H), 7.71 − 7.66 (m, 2H), 7.61 − 7.56 (m, 2H), 4.53 (dt, J = 47.2, 5.6 Hz, 2H), 2.56 (t, J = 7.3 Hz, 2H), 2.11 (dtt, J = 27.1, 7.2, 5.5 Hz, 2H); **^{13}C NMR** (101 MHz, $CDCl_3$) δ 171.1, 142.3, 133.4, 119.7, 119.1, 106.8, 83.1 (d, $J_{C\text{-}F}$ = 164.9 Hz), 33.2 (d, $J_{C\text{-}F}$ = 4.2 Hz), 26.0 (d, $J_{C\text{-}F}$ = 19.9

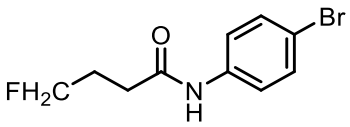
Hz); **^{19}F NMR** (377 MHz, $CDCl_3$) δ −220.6 (tt, J = 47.3, 27.1 Hz); **HRMS** (ESI-TOF) calculated for $C_{11}H_{10}FN_2O$ $[M\text{-}H]^-$: 205.0783, found 205.0777; **IR** (neat) 2237, 2220, 1703, 1677, 1596, 1523, 1437, 1409, 1377, 1324, 1254, 1174, 1174, 1079, 1061, 1035, 967, 899, 842, 733; **m.p.**: 122 − 124 °C.

4-fluoro-*N*-(4-methoxyphenyl)butanamide (4.43)



General procedure B was followed to obtain **4.43** (97 mg, 0.46 mmol, 92%) as a white solid. **^{1}H NMR** (400 MHz, $CDCl_3$) δ 7.47 (s, 1H), 7.42 − 7.35 (m, 2H), 6.87 − 6.80 (m, 2H), 4.52 (dt, J = 47.2, 5.7 Hz, 2H), 3.77 (s, 4H), 2.47 (t, J = 7.3 Hz, 2H), 2.19 − 2.01 (m, 2H); **^{13}C NMR** (101 MHz, $CDCl_3$) δ 170.2, 156.6, 131.0, 122.0, 114.3, 83.3 (d, $J_{C\text{-}F}$ = 164.7 Hz), 55.6, 32.9 (d, $J_{C\text{-}F}$ = 4.4 Hz), 26.4 (d, J = 19.9 Hz); **^{19}F NMR** (377 MHz, $CDCl_3$) δ −220.5 (tt, J = 47.3, 27.0 Hz); **HRMS** (ESI-TOF) calculated for $C_{11}H_{15}FNO_2$ $[M+H]^+$: 212.1081, found 212.1084; **IR** (neat) 1650, 1535, 1510, 1412, 1377, 1341, 1304, 1239, 1186, 1169, 1031, 981, 899, 825, 796, 759, 728, 704, 680, 606; **m.p.**: 106 − 108 °C.

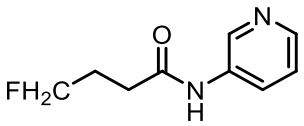
***N*-(4-bromophenyl)-4-fluorobutanamide (4.44)**



General procedure B was followed to obtain **4.44** (109 mg, 0.42 mmol, 84%) as a white solid. **^{1}H NMR** (400 MHz, $CDCl_3$) δ 7.45 − 7.38 (m, 4H), 7.32 (s, 1H), 4.53 (dt, J = 47.3, 5.6 Hz, 2H), 2.51 (t, J = 7.2 Hz, 2H), 2.11 (dtt, J = 27.1, 7.2, 5.6 Hz, 2H); **^{13}C NMR** (101 MHz, $CDCl_3$) δ 170.4, 136.9, 132.1, 121.5, 117.1, 83.2 (d, $J_{C\text{-}F}$ = 164.8

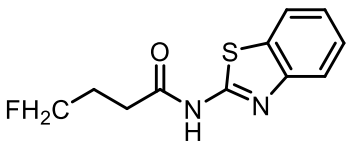
Hz), 33.2 (d, $J_{C\text{-}F}$ = 4.1 Hz), 26.2 (d, $J_{C\text{-}F}$ = 19.9 Hz); **^{19}F NMR** (377 MHz, $CDCl_3$) δ − 220.7 (tt, J = 47.5, 27.3 Hz). **HRMS** (ESI-TOF) calculated for $C_{10}H_{12}BrFNO$ $[M+H]^+$: 260.0081, found 260.0083; **IR** (neat) 1653, 1589, 1528, 1488, 1441, 1396, 1336, 1297, 1281, 1254, 1177, 1099, 1072, 1032, 1011, 980, 896, 849, 819, 785, 692, 645; **m.p.**: 87 − 89 °C

4-fluoro-*N*-(pyridin-3-yl)butanamide (4.45)



General procedure A was followed to obtain **4.45** (55 mg, 0.30 mmol, 60%) as a white solid. **^{1}H NMR** (400 MHz, $CDCl_3$) δ 7.15 (s, 1H), 6.88 − 6.83 (m, 1H), 6.77 − 6.70 (m, 1H), 5.82 (dd, J = 8.2, 4.6 Hz, 1H), 3.06 (dt, J = 47.3, 5.7 Hz, 2H), 1.10 (t, J = 7.2 Hz, 2H), 0.73 − 0.57 (m, 2H); **^{13}C NMR** (101 MHz, $CDCl_3$) δ 171.4, 144.8, 141.0, 135.4, 127.7, 124.1, 83.2 (d, $J_{C\text{-}F}$ = 164.8 Hz), 32.9 (d, $J_{C\text{-}F}$ = 4.3 Hz), 26.1 (d, $J_{C\text{-}F}$ = 20.0 Hz); **^{19}F NMR** (377 MHz, $CDCl_3$) δ −220.5 (tt, J = 47.3, 27.1 Hz); **HRMS** (ESI-TOF) calculated for $C_9H_{12}FN_2O$ $[M+H]^+$: 183.0928; found 183.0929; **IR** (neat) 1688, 1610, 1584, 1549, 1476, 1422, 1375, 1330, 1271, 1248, 1194, 1172, 1150, 1130, 1103, 1077, 1032, 967, 896, 855, 808, 750, 704, 624; **m.p.**: 70 − 72 °C.

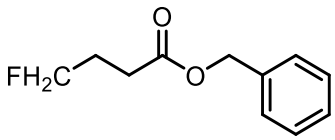
***N*-(benzo[d]thiazol-2-yl)-4-fluorobutanamide (4.46)**



General procedure A was followed to obtain **4.46** (86 mg, 0.36 mmol, 72%) as a white solid. **^{1}H NMR** (400 MHz, Acetone-d_6) δ 11.17 (s, 1H), 7.95 − 7.90 (m, 1H), 7.73 − 7.68 (m, 1H), 7.45 − 7.39 (m, 1H), 7.33 − 7.27 (m, 1H), 4.56 (dt, J = 47.4, 6.0

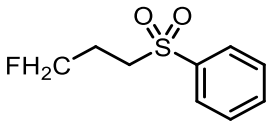
Hz, 2H), 2.77 (t, J = 7.3 Hz, 2H), 2.21 − 2.07 (m, 2H); **^{13}C NMR** (101 MHz, Acetone-d_6) δ 172.0, 158.7, 149.9, 133.1, 126.8, 124.4, 122.2, 121.7, 83.8 (d, $J_{C\text{-}F}$ = 163.5 Hz), 32.1 (d, $J_{C\text{-}F}$ = 5.5 Hz), 26.4 (d, $J_{C\text{-}F}$ = 20.2 Hz); **^{19}F NMR** (377 MHz, Acetone-d_6) δ − 220.5 (tt, J = 47.6, 25.2 Hz); **HRMS** (ESI-TOF) calculated for $C_{11}H_{12}FN_2O^{32}S$ $[M+H]^+$: 239.0649; found 239.0650; **IR** (neat) 1697, 1599, 1548, 1445, 1419, 1380, 1342, 1267, 1254, 1190, 1166, 1097, 1082, 1039, 1022, 994, 939, 906, 867, 782, 758, 683; **m.p.**: 176 − 178 °C.

Benzyl 4-fluorobutanoate (4.47)



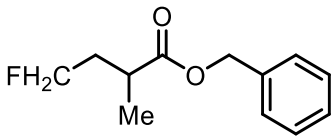
General procedure A was followed to obtain **4.47** (74 mg, 0.38 mmol, 75%) as a colourless oil. **^{1}H NMR** (400 MHz, $CDCl_3$) δ 7.41 − 7.30 (m, 5H), 5.14 (s, 2H), 4.49 (dt, J = 47.1, 5.8 Hz, 2H), 2.52 (t, J = 7.4 Hz, 2H), 2.04 (dtt, J = 26.2, 7.3, 5.7 Hz, 2H); **^{13}C NMR** (101 MHz, $CDCl_3$) δ 172.8, 136.0, 128.7, 128.4, 128.4, 83.0 (d, $J_{C\text{-}F}$ = 165.4 Hz), 66.5, 30.1 (d, $J_{C\text{-}F}$ = 5.1 Hz), 25.9 (d, $J_{C\text{-}F}$ = 20.3 Hz); **^{19}F NMR** (377 MHz, $CDCl_3$) δ −220.6 (tt, J = 47.2, 26.0 Hz). **GC-MS** (EI-TOF) calculated for $C_{11}H_{13}FO_2$ $[M]^+$: 196.0894; found 196.0891; **IR** (neat) 1734, 1498, 1456, 1422, 1384, 1351, 1317, 1247, 1213, 1165, 1083, 1037, 909, 839, 738, 697, 622. The product coeluted with silane by-products (δ: 0.19 ppm). Purification by reverse phase failed.

((3-fluoropropyl)sulfonyl)benzene (4.48)



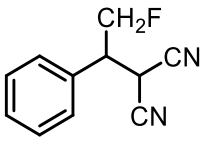
General procedure A was followed to obtain **4.48** (71 mg, 0.35 mmol, 70%) as a pale yellow oil. **^{1}H NMR** (400 MHz, $CDCl_3$) δ 7.94 − 7.88 (m, 2H), 7.70 − 7.63 (m, 1H), 7.61 − 7.53 (m, 2H), 4.50 (dt, J = 46.9, 5.7 Hz, 1H), 3.26 − 3.19 (m, 2H), 2.21 − 2.04 (m, 2H); **^{13}C NMR** (101 MHz, $CDCl_3$) δ 139.0, 134.0, 129.5, 128.1, 81.6 (d, $J_{C\text{-}F}$ = 167.8 Hz), 52.6 (d, $J_{C\text{-}F}$ = 4.2 Hz), 24.2 (d, $J_{C\text{-}F}$ = 20.8 Hz); **^{19}F NMR** (377 MHz, $CDCl_3$) δ −220.5 (tt, J = 47.1, 25.9 Hz); **HRMS** (ESI-TOF) calculated for $C_9H_{12}FO_2{}^{32}S$ $[M+H]^+$: 203.0537; found 203.0539; **IR** (neat) 1477, 1307, 1142, 1087, 1058, 1022, 889, 732, 689, 625.

Benzyl 4-fluoro-2-methylbutanoate (4.49)



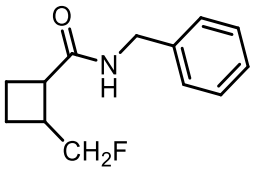
General procedure A was followed to obtain **4.49** (66 mg, 0.32 mmol, 63%) as a colourless oil. **^{1}H NMR** (400 MHz, $CDCl_3$) δ 7.43 − 7.29 (m, 5H), 5.13 (s, 2H), 4.61 − 4.36 (m, 2H), 2.72 (dq, J = 14.3, 7.1 Hz, 1H), 2.22 − 2.03 (m, 1H), 1.91 − 1.71 (m, 1H), 1.24 (d, J = 7.0 Hz, 3H); **^{13}C NMR** (101 MHz, $CDCl_3$) δ 175.9, 136.1, 128.7, 128.4, 128.2, 82.0 (d, $J_{C\text{-}F}$ = 165.0 Hz), 66.5, 36.0 (d, $J_{C\text{-}F}$ = 4.4 Hz), 34.2 (d, $J_{C\text{-}F}$ = 19.9 Hz), 17.2; **^{19}F NMR** (377 MHz, $CDCl_3$) δ 7.3 (tt, J = 47.2, 26.1 Hz); **HRMS** (ESI-TOF) calculated for $C_{12}H_{15}FNaO_2$ $[M+Na]^+$: 233.0948; found 233.0951; **IR** (neat) 2919, 1732, 1498, 1456, 1384, 1257, 1170, 1136, 1046, 992, 849, 751, 698.

2-(2-fluoro-1-phenylethyl)malononitrile (4.50)[b]



General procedure B was followed to obtain **4.50** (52 mg, 0.27 mmol, 55%) as a pale yellow oil. **^{1}H NMR** (400 MHz, $CDCl_3$) δ 7.45 (s, 3H), 7.39 − 7.34 (m, 2H), 4.87 (ddd, J = 46.3, 6.2, 2.6 Hz, 2H), 4.29 (d, J = 6.3 Hz, 1H), 3.61 (dddd, J = 17.0, 7.4, 6.4, 5.1 Hz, 1H); **^{13}C NMR** (101 MHz, $CDCl_3$) δ 132.6 (d, $J_{C\text{-}F}$ = 6.2 Hz), 129.9, 129.7, 128.3, 111.3 (d, $J_{C\text{-}F}$ = 34.8 Hz), 82.3 (d, $J_{C\text{-}F}$ = 176.7 Hz), 46.8 (d, $J_{C\text{-}F}$ = 18.3 Hz), 26.2 (d, $J_{C\text{-}F}$ = 5.0 Hz); **^{19}F NMR** (377 MHz, $CDCl_3$) δ −220.9 (td, J = 46.7, 17.0 Hz); **HRMS** (ESI-TOF) calculated for $C_{11}H_8FN$ $[M\text{-}H]^-$: 187.0677; found 187.0666; **IR** (neat) 2912, 2630, 1498 1456, 1160, 1068, 1012, 947, 815, 763, 700, 653, 620.

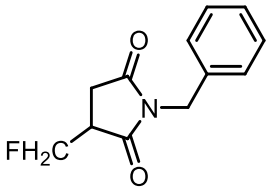
***N*-benzyl-2-(fluoromethyl)cyclobutane-1-carboxamide (4.51)**



General procedure B was followed to obtain **4.51** (60 mg, 0.27 mmol, 54%, d.r.:68/32) as a pale-yellow oil. **^{1}H NMR** (400 MHz, $CDCl_3$) δ 7.37 − 7.26 (m, 5H), 5.98 (s, 0.32H), 5.93 (s, 0.63H), 4.72 − 4.28 (m, 4H), 3.24 − 3.15 (m, 0.65H), 3.08 − 2.83 (m, 1.36H), 2.47 − 2.37 (m, 0.64H), 2.18 − 2.03 (m, 2H), 2.00 − 1.77 (m, 1.36H); **^{13}C NMR** (101 MHz, $CDCl_3$) δ 173.6, 172.4, 138.5, 138.4, 128.8, 128.8, 127.9, 127.7, 127.5, 127.5, 85.9 (d, J = 165.7 Hz), 84.1 (d, $J_{C\text{-}F}$ = 166.0 Hz), 43.6 (d, $J_{C\text{-}F}$ = 11.9 Hz), 42.0 (d, $J_{C\text{-}F}$ = 4.4 Hz), 40.8 (d, $J_{C\text{-}F}$ = 5.3 Hz), 38.9 (d, $J_{C\text{-}F}$ = 19.0 Hz), 37.5 (d, $J_{C\text{-}F}$ = 18.3 Hz), 21.4 (d, $J_{C\text{-}F}$ = 17.5 Hz), 20.4 (d, $J_{C\text{-}F}$ = 9.6 Hz), 19.2 (d, $J_{C\text{-}F}$ = 8.4 Hz); **^{19}F NMR** (377 MHz, $CDCl_3$) δ −219.7 (td, J = 47.2, 18.9 Hz), −222.2 (td, J = 47.9, 22.0

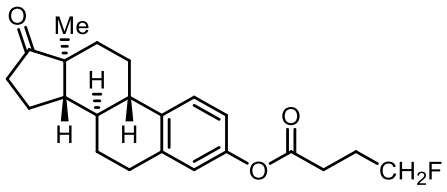
Hz); **HRMS** (ESI-TOF) calculated for $C_{13}H_{17}FNO$ $[M+H]^+$: 222.1289; found 222.1290; **IR** (neat) 1642, 1539, 1497, 1454, 1381, 1355, 1325, 1247, 1079, 1029, 992, 733, 698. *Cis*- and *trans*- products could not be separated upon purification and were isolated as a mixture of products (d.r.: 68/32).

1-benzyl-3-(fluoromethyl)pyrrolidine-2,5-dione (4.52)[a]



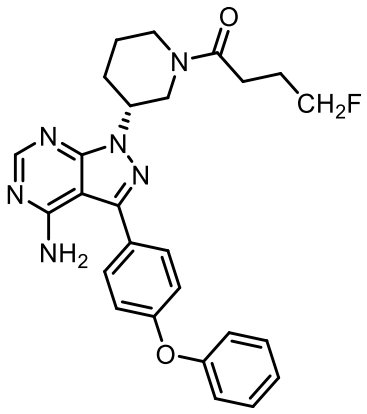
General procedure A was followed to obtain **4.52** (99 mg, 0.45 mmol, 90%) as a pale yellow oil. **^{1}H NMR** (400 MHz, $CDCl_3$) δ 7.27 − 7.09 (m, 5H), 4.75 (ddd, J = 46.4, 9.3, 3.5 Hz, 1H), 4.59 − 4.36 (m, 2H), 4.54 (d, J = 5.5 Hz, 1H), 2.98 − 2.83 (m, 1H), 2.79 − 2.58 (m, 2H); **^{19}F NMR** (377 MHz, $CDCl_3$) δ −230.1 (td, J = 46.8, 33.3 Hz); **^{13}C NMR** (101 MHz, $CDCl_3$) δ 176.2 (d, $J_{C\text{-}F}$ = 5.4 Hz), 175.4, 135.6, 128.8, 128.6, 128.1, 81.3 (d, $J_{C\text{-}F}$ = 172.4 Hz), 42.8, 41.6 (d, $J_{C\text{-}F}$ = 21.4 Hz), 30.9 (d, J = 4.0 Hz), 28.3; Mass not found, **HRMS** (ESI-TOF) calculated for $C_{12}H_{13}FNO_2$ $[M+H]^+$: 222.0925; found 222.0927; **IR** (neat) 1698, 1431, 1401, 1342, 1168, 1022, 938, 900, 755, 708, 696, 634.

(*8R*,*9S*,*13S*,*14S*)-13-methyl-17-oxo-7,8,9,11,12,13,14,15,16,17-decahydro-*6H*-cyclopenta[*a*]phenanthren-3-yl 4-fluorobutanoate (4.67)



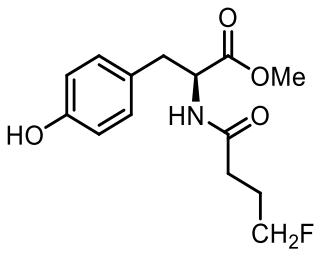
General procedure A was followed to obtain **4.67** (91 mg, 0.26 mmol, 51%) as a white solid. **^{1}H NMR** (400 MHz, $CDCl_3$) δ 7.28 (d, J = 9.7 Hz, 1H), 6.85 (dd, J = 8.5, 2.6 Hz, 1H), 6.82 − 6.80 (m, 1H), 4.56 (dt, J = 47.1, 5.7 Hz, 2H), 2.94 − 2.88 (m, 2H), 2.71 (t, J = 7.3 Hz, 2H), 2.51 (dd, J = 19.0, 8.4 Hz, 1H), 2.45 − 2.23 (m, 2H), 2.21 − 1.93 (m, 6H), 1.69 − 1.40 (m, 6H), 0.91 (s, 3H); **^{13}C NMR** (101 MHz, $CDCl_3$) δ 220.9, 171.9, 148.6, 138.2, 137.6, 126.6, 121.6, 118.8, 83.0 (d, $J_{C\text{-}F}$ = 165.5 Hz), 50.6, 48.1, 44.3, 38.1, 36.0, 31.7, 30.3 (d, $J_{C\text{-}F}$ = 4.9 Hz), 29.5, 26.5, 25.9 (d, $J_{C\text{-}F}$ = 20.3 Hz), 25.9, 21.7, 14.0; **^{19}F NMR** (377 MHz, $CDCl_3$) δ −220.7 (tt, J = 47.1, 26.3 Hz); **HRMS** (ESI-TOF) calculated for $C_{22}H_{27}FNaO_3$ $[M+Na]^+$: 381.1836; found 381.1838; **IR** (neat) 2919, 2853, 1740, 1603, 1491, 1452, 1438, 1377, 1315, 1251, 1223, 1555, 1141, 1086, 1055, 1036, 1007, 953, 9090, 875, 824, 784, 719; **m.p.**: 94 − 96 °C.

(*R*)-1-(3-(4-amino-3-(4-phenoxyphenyl)-*1H*-pyrazolo[3,4-*d*]pyrimidin-1-yl)piperidin-1-yl)-4-fluorobutan-1-one (4.68)[a]



General procedure B was followed to obtain **4.68** (137 mg, 0.29 mmol, 58%) as a yellow oil. **^{1}H NMR** (400 MHz, $CDCl_3$) δ 8.33 (d, J = 15.2 Hz, 1H), 7.63 (dd, J = 8.4, 4.0 Hz, 2H), 7.38 (t, J = 7.7 Hz, 2H), 7.20 − 7.11 (m, 3H), 7.07 (d, J = 8.0 Hz, 2H), 6.04 (s, 2H), 4.89 − 4.76 (m, 1.5H), 4.62 − 4.51 (m, 1.5H), 4.44 (dt, J = 12.6, 5.7 Hz, 1H), 4.07 (dd, J = 13.4, 4.2 Hz, 0.5H), 3.91 (d, J = 13.6 Hz, 0.5H), 3.69 (dd, J = 13.2, 10.5 Hz, 0.5H), 3.23 (dt, J = 61.6, 12.5 Hz, 2H), 2.79 (t, J = 11.7 Hz, 0.5H), 2.57 − 2.18 (m, 3H), 2.13 − 1.90 (m, 3H), 1.78 − 1.60 (m, 1H); **^{13}C NMR** (101 MHz, $CDCl_3$) δ 170.7, 170.6, 158.8, 158.8, 157.7, 157.4, 156.4, 156.4, 155.0, 154.3, 154.2, 153.9, 144.4, 130.1, 130.0, 127.6, 127.5, 124.2, 124.2, 119.7, 119.2, 98.6, 98.4, 83.6 (d, $J_{C\text{-}F}$ = 163.9 Hz), 53.5, 52.8, 49.8, 45.9, 45.6, 41.9, 30.3, 30.1, 28.8 (d, $J_{C\text{-}F}$ = 4.0 Hz), 26.2 (d, $J_{C\text{-}F}$ = 19.7 Hz), 26.1 (d, $J_{C\text{-}F}$ = 19.8 Hz), 25.2, 24.1; **^{19}F NMR** (377 MHz, $CDCl_3$) δ − 220.2 (dtt, J = 128.4, 47.3, 27.3 Hz); **HRMS** (ESI-TOF) calculated for $C_{26}H_{28}FN_6O_2$ $[M+H]^+$: 475.2252; found 475.2249; **IR** (neat) 2924, 2856, 1626, 1587, 1567, 1521, 1489, 1440, 1285, 1236, 1167, 1135, 1104, 1070, 1025, 869, 803, 803, 757, 696.

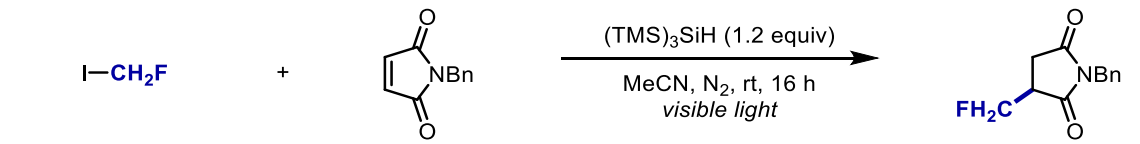
Methyl (4-fluorobutanoyl)-L-tyrosinate (4.69)[b]



General procedure B was followed to obtain **4.69** (93 mg, 0.37 mmol, 66%) as a waxy solidd; **^{1}H NMR** (400 MHz, $CDCl_3$) δ 6.93 (d, J = 8.5 Hz, 2H), 6.72 (d, J = 8.5 Hz, 2H), 6.20 (br d, J = 8.1 Hz, 1H), 4.91 − 4.82 (m, 1H), 4.52 − 4.27 (m, 2H), 3.73 (s, 3H), 3.07 (dd, J = 14.1, 5.5 Hz, 1H), 2.95 (dd, J = 14.1, 6.6 Hz, 1H), 2.31 (dd, J = 7.9, 6.7 Hz, 2H), 2.06 − 1.86 (m, 2H); **^{13}C NMR** (101 MHz, $CDCl_3$) δ 172.4, 155.7, 130.3, 127.0, 115.7, 83.1 (d, J = 164.9 Hz), 53.4, 52.6, 37.3, 32.0 (d, J = 4.6 Hz), 26.2 (d, J = 20.0 Hz) (carbonyl peaks overlapping); **^{19}F NMR** (377 MHz, $CDCl_3$) δ −220.1 - −220.9 (m); **HRMS** (ESI-TOF) calculated for $C_{14}H_{17}FNO_4$ $[M+H]^+$: 284.1293; found 282.1292; **IR** (neat) 3297, 2956, 2361, 1736, 1649, 1614, 1596, 1537, 1515, 1440, 1369, 1219, 1174, 1124, 1105, 1033, 905, 829, 802, 668.

5.4.5 Scale-up experiment[b]

The scale-up experiment was performed on the synthesis of 1-benzyl-3-(fluoromethyl)pyrrolidine-2,5-dione **4.52**.



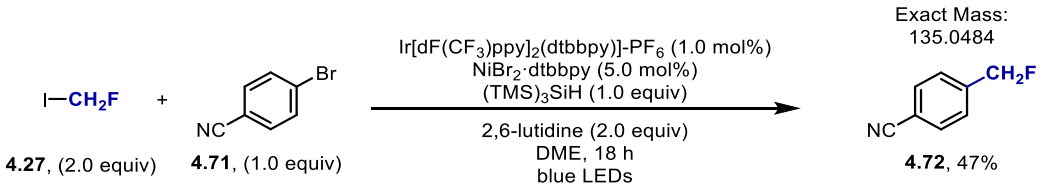
4.27
(20.0 mmol; 2.0 equiv)

4.40
(10.0 mmol; 1.0 equiv)

4.52, 88%
(1.95 g; 8.8 mmol)

To a 150 mL oven-dried round-bottomed flask equipped with a magnetic stir bar, *N*-benzylmaleimide **4.40** (1.872 g, 10 mmol, 1.0 equiv) was added, followed by dry MeCN (60 mL), $(TMS)_3SiH$ (3.70 mL, 12 mmol, 1.2 equiv) and CH_2FI **4.27** (1.35 mL, 20 mmol, 2 equiv). The flask was equipped with a Teflon septum, degassed by nitrogen bubbling for 1 minute and stirred in a custom-made photoreactor (see figures X and X) with a 12 W blue HepatoChem LED lamp (λ_{max} = 470 nm) at room temperature for 16 hours. Et_2O (100 mL) was then added to the reaction mixture, which was extracted twice with a saturated aqueous solution of $NaHCO_3$ (2 x 50 mL). The combined aqueous phases were extracted once more with Et_2O (30 mL). The combined organic phases were dried (Na_2SO_4), filtered and the solvent was removed *in vacuo*. The residue was purified by flash chromatography (SiO_2, Et_2O in Pentane, 30/70 to 60/40). The desired fractions were collected and concentrated *in vacuo* to afford the desired hydrofluoromethylated product **4.52** as a light brown oil (1.953 g, 8.8 mmol, 88.0 %). Spectroscopic data were in accordance with previous reports.

5.4.6 Metallaphotoredox fluoromethylation[a]



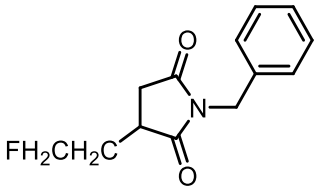
4.27, (2.0 equiv) **4.71**, (1.0 equiv) **4.72**, 47%

Modified procedure from *Angew. Chem. Int. Ed.* 2018, *57*, 12543 - 12548:

To an oven-dried 7 mL vial equipped with a magnetic stir bar were added 4-bromobenzonitrile (90.0 mg, 0.50 mmol, 1.0 equiv), $(TMS)_3SiH$ (162 µL, 0.53 mmol, 1.05 equiv.) and 2,6-Lutidine (174 µL, 1.5 mmol, 3.0 equiv). The vial was then recapped and the headspace was sparged with N_2. Then was added a solution of photocatalyst $[Ir(dF(CF_3)ppy)_2(dtbbpy)]PF_6$ (5.6 mg, 5.0 µmol, 1.0 mol%), $NiBr_2$•glyme (7.7 mg, 25 µmol, 5.0 mol%), and 4,4'-di-tert-butyl-2,2'-bipyridine (6.7 mg, 25 µmol, 5.0 mol%) in DME (5.0 mL, 0.1 M), pre-sonicated separately for 15 minutes. Next, fluoroiodomethane (68 µL, 1.0 mmol, 2.0 equiv.) was added. The reaction mixture was degassed by nitrogen bubbling for 10 seconds and wrapped with parafilm. The reaction mixture was stirred in a SynLED Parallel Photoreactor with a 12W blue LED lamp (λ_{max} = 470 nm) at room temperature (using a fan) for 16 hours. The solvent was removed *in vacuo* and the residue was purified by column chromatography (silica, EtOAc in Pentane 0/100 to 50/50) to yield 4-(fluoromethyl)benzonitrile in 47% (32 mg, 0.24 mmol, 47%). All data were in accordance with the literature.[18]

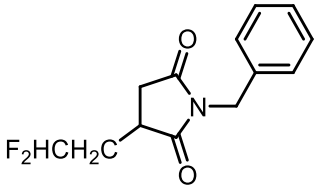
5.4.7 Generation of Fluorinated Ethyl Radicals

1-benzyl-3-(2-fluoroethyl)pyrrolidine-2,5-dione (4.76)



General procedure A was followed to obtain **4.76** (86 mg, 0.37 mmol, 73%) as a pale-yellow oil. **^{1}H NMR** (400 MHz, $CDCl_3$) δ 7.34 − 7.27 (m, 2H), 7.27 − 7.17 (m, 3H), 4.66 − 4.38 (m, 4H), 2.96 − 2.79 (m, 2H), 2.51 − 2.36 (m, 1H), 2.34 − 2.12 (m, 1H), 1.94 − 1.73 (m, 1H); **^{13}C NMR** (101 MHz, $CDCl_3$) δ 178.9, 175.8, 135.8, 128.7, 128.7, 128.0, 81.8 (d, $J_{C\text{-}F}$ = 166.5 Hz), 42.5, 37.1 (d, $J_{C\text{-}F}$ = 3.5 Hz), 34.5, 31.8 (d, $J_{C\text{-}F}$ = 19.6 Hz); **^{19}F NMR** (377 MHz, $CDCl_3$) δ −220.6 (tdd, J = 47.1, 28.7, 24.3 Hz); **HRMS** (ESI-TOF) calculated for $C_{13}H_{15}FNO_2$ $[M+H]^+$: 236.1081; found 236.1084; **IR** (neat) 1174, 1696, 1497, 1431, 1397, 1342, 1314, 1168, 1081, 1032, 1001, 949, 929, 897, 857, 707, 635.

1-benzyl-3-(2,2-difluoroethyl)pyrrolidine-2,5-dione (4.77)

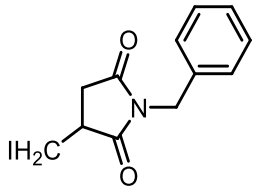


General procedure A was followed to obtain **4.77** (38 mg, 0.15 mmol, 30%) as a pale-yellow oil. **^{1}H NMR** (400 MHz, $CDCl_3$) δ 7.40 − 7.27 (m, 5H), 6.06 (tdd, J = 55.9, 4.8, 3.1 Hz, 1H), 4.66 (s, 2H), 3.10 − 2.92 (m, 2H), 2.62 − 2.41 (m, 2H), 2.10 − 1.92 (m, 1H); **^{13}C NMR** (101 MHz, $CDCl_3$) δ 178.1, 175.4, 135.6, 129.0, 128.9, 128.3,

115.6 (t, $J_{C\text{-}F}$ = 240.0 Hz), 42.8, 35.2 (t, $J_{C\text{-}F}$ = 21.7 Hz), 35.0, 34.5 (t, $J_{C\text{-}F}$ = 4.0 Hz); **^{19}F NMR** (377 MHz, $CDCl_3$) δ −115.2 (dddd, J = 285.1, 55.7, 18.7, 12.4 Hz), −118.0 (ddt, J = 285.0, 56.1, 19.3 Hz); **HRMS** (ESI-TOF) calculated for $C_{13}H_{14}F_2NO_2$ $[M+H]^+$: 254.0987; found 254.0987; **IR** (neat) 2937, 1777, 1698, 1586, 1456, 1432, 1399, 1344, 1314, 1292, 1170, 1122, 1088, 1053, 978, 964, 930, 906, 864, 825, 755, 708, 696, 650, 631.

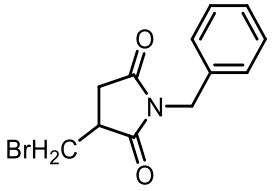
5.4.8 Generation of Other Halomethyl Radicals

1-benzyl-3-(iodomethyl)pyrrolidine-2,5-dione (4.86)[b]



This product was purified by Preparative TLC (Pentane/Et_2O, 70/30). **General procedure A** was followed to obtain **4.86** (102 mg, 0.27 mmol, 62%) as a waxy solid. **^{1}H NMR** (400 MHz, $CDCl_3$) δ 7.35 − 7.17 (m, 5H), 4.66 − 4.54 (m, 2H), 3.50 (dd, J = 10.3, 5.6 Hz, 1H), 3.32 (dd, J = 10.3, 3.7 Hz, 1H), 3.04 (dtd, J = 8.9, 5.2, 3.6 Hz, 1H), 2.82 (dd, J = 18.4, 8.9 Hz, 1H), 2.57 (dd, J = 18.4, 4.8 Hz, 1H); **^{13}C NMR** (101 MHz, $CDCl_3$) δ 177.0, 175.5, 135.3, 128.9, 128.7, 128.1, 42.9, 41.1, 35.7, 4.9; **HRMS** (ESI-TOF) calculated for $C_{12}H_{13}INO_2$ $[M+H]^+$: 329.9985, found 329.9985; **IR** (neat) 2922, 1775, 1697, 1605, 1586, 1496, 1455, 1429, 1396, 1342, 1312, 1290, 1243, 1208, 1167, 1080, 1029, 977, 929, 870, 838, 758, 707, 695, 634; **m.p.**: 72 − 74 °C.

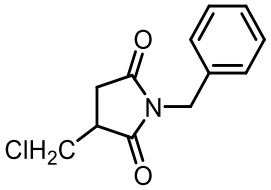
1-benzyl-3-(bromomethyl)pyrrolidine-2,5-dione (4.87)



This product was purified by Preparative TLC (Pentane/Et_2O, 70/30). **From CH_2Br_2: General procedure A** was followed to obtain **4.87** (73 mg, 0.26 mmol, 52%) as a waxy solid. **From CH_2BrI: General procedure A** was followed to obtain **4.87** (87 mg, 0.31 mmol, 62%) as a waxy solid. **^{1}H NMR** (400 MHz, $CDCl_3$) δ 7.35 – 7.16 (m,

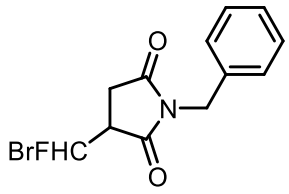
5H), 4.60 (dd, *J* = 14.2 Hz, 2H), 3.77 (dd, *J* = 10.5, 4.9 Hz, 1H), 3.53 (dd, J = 10.5, 3.5 Hz, 1H), 3.20 (dtd, *J* = 8.6, 5.0, 3.4 Hz, 1H), 2.79 (dd, *J* = 18.3, 8.9 Hz, 1H), 2.68 (dd, *J* = 18.3, 5.1 Hz, 1H); **^{13}C NMR** (101 MHz, $CDCl_3$) δ 176.4, 175.1, 135.5, 128.8, 128.7, 128.1, 42.8, 41.3, 33.3, 31.8; **HRMS** (ESI-TOF) calculated for $C_{12}H_{13}BrNO_2$ $[M+H]^+$: 282.0124, found 282.0104; **IR** (neat) 2917, 2849, 1777, 1698, 1586, 1497, 1455, 1430, 1397, 1342, 1312, 1292, 1254, 1235, 1167, 1081, 1029, 984, 933, 869, 822, 761, 708, 695, 634; **m.p.**: 50 − 52 °C.

1-benzyl-3-(chloromethyl)pyrrolidine-2,5-dione (4.88)



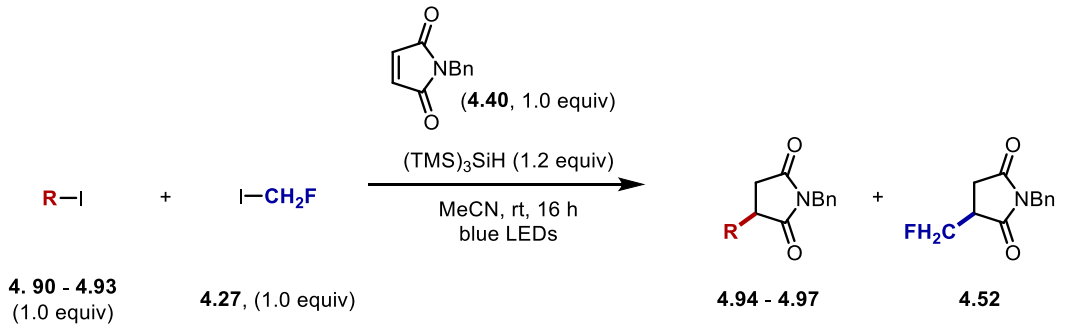
This product was purified by Preparative TLC (Pentane/Et_2O, 70/30). **General procedure A** was followed to obtain **4.88** (64 mg, 0.27 mmol, 54%) as a waxy solid. **^{1}H NMR** (400 MHz, $CDCl_3$) δ 7.33 − 7.17 (m, 5H), 4.61 (dd, *J* = 14.8, 13.4 Hz, 2H), 3.95 (dd, *J* = 11.3, 4.6 Hz, 1H), 3.68 (dd, *J* = 11.3, 3.4 Hz, 1H), 3.16 (dtd, *J* = 8.6, 4.8, 3.4 Hz, 1H), 2.80 (dd, *J* = 18.3, 8.7 Hz, 1H), 2.72 (dd, *J* = 18.3, 5.3 Hz, 1H); **^{13}C NMR** (101 MHz, $CDCl_3$) δ 176.3, 175.3, 135.5, 128.7, 128.7, 128.1, 43.4, 42.8, 41.8, 32.0; **HRMS** (ESI-TOF) calculated for $C_{12}H_{13}ClNO_2$ $[M+H]^+$: 238.0629, found 238.0630; **IR** (neat) 2918, 1777, 1698, 1586, 1497, 1455, 1432, 1398, 1341, 1313, 1244, 1168, 1082, 1029, 991, 940, 886, 790, 764, 709, 696, 673, 633, 608; **m.p.**: 75 − 77 °C.

1-benzyl-3-(bromofluoromethyl)pyrrolidine-2,5-dione (4.89)



This product was purified by Preparative TLC (Pentane/Et_2O, 70/30). **General procedure A** was followed to obtain **4.89** (66 mg, 0.26 mmol, 51%, d.r.: 63/27) as a white solid. **^{1}H NMR** (400 MHz, $CDCl_3$) δ 6.92 − 6.88 (m, 5H), 6.93 − 6.87 (m, 0.5H), 6.81 − 6.75 (m, 0.5H), 4.64 − 4.52 (m, 2H), 3.59 − 3.49 (m, 0.5H), 3.35 (dddd, J = 31.7, 9.3, 5.6, 1.8 Hz, 0.5H), 3.07 − 2.70 (m, 2H); **^{13}C NMR** (101 MHz, $CDCl_3$) δ 174.5, 174.1, 173.2, 172.9 (d, $J_{C\text{-}F}$ = 14.4 Hz), 135.2, 135.1, 128.9, 128.8, 128.7, 128.7, 128.2, 93.2 (d, $J_{C\text{-}F}$ = 256.2 Hz), 90.1 (d, $J_{C\text{-}F}$ = 254.1 Hz), 49.8 (d, $J_{C\text{-}F}$ = 21.4 Hz), 47.5 (d, $J_{C\text{-}F}$ = 22.6 Hz), 42.9 (d, $J_{C\text{-}F}$ = 6.9 Hz), 30.7, 29.8; **^{19}F NMR** (377 MHz, $CDCl_3$) δ −139.5 (dd, J = 48.0, 7.1 Hz), −147.0 (dd, J = 49.3, 31.8 Hz); The compound did not ionize; **IR** (neat) 1180, 1705, 1497, 1432, 1399, 1345, 1249, 1170, 1119, 1083, 1028, 951; **m.p.**: 64 − 66 °C. The product was isolated as a mixture of diastereomers. 5% of the elimination product was observed by quantitative ^{19}F NMR.

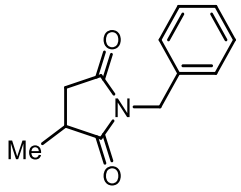
5.4.9 Competition experiments



Me—I (**4.90**)	vs	I—CH_2F (**4.39**)	25% (**4.94**)	74%
Et—I (**4.91**)	vs	I—CH_2F (**4.39**)	43% (**4.95**)	51%
*i*Pr—I (**4.92**)	vs	I—CH_2F (**4.39**)	62% (**4.96**)	36%
*t*Bu—I (**4.93**)	vs	I—CH_2F (**4.39**)	73% (**4.97**)	19%

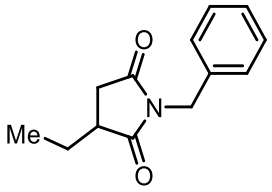
Procedure: To a 7 mL vial equipped with a magnetic stir bar, was added *N*-benzylmaleimide (0.50 mmol, 1.0 equiv), dry MeCN (3.0 mL), $(TMS)_3SiH$ (185 uL, 0.6 mmol, 1.2 equiv) CH_2FI (68 µL, 1.0 mmol, 2.0 equiv), and alkyl iodide (1.0 mmol, 2.0 equiv). The vial was sealed with a septum, degassed by nitrogen bubbling for 10 seconds and wrapped with parafilm. The reaction mixture was stirred in a SynLED Parallel Photoreactor with a 12W blue LED lamp (λ_{max} = 470 nm) at room temperature (using a fan) for 16 hours. The solvent was removed *in vacuo* and the residue was purified by column chromatography (silica, EtOAc in heptane 0/100 to 100/0) to yield the desired product(s).

1-benzyl-3-methylpyrrolidine-2,5-dione (4.94)[a]



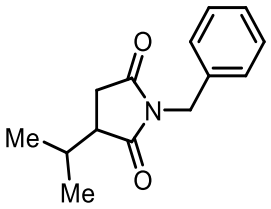
General procedure A was followed to obtain **4.94** (25 mg, 0.12 mmol, 25%) as a white solid. **^{1}H NMR** (400 MHz, $CDCl_3$) δ 7.26 – 7.22 (m, 1H), 7.22 – 7.12 (m, 1H), 4.52 (d, J = 2.1 Hz, 1H), 2.85 – 2.67 (m, 1H), 2.19 (dd, J = 21.7, 13.6 Hz, 1H), 1.20 (d, J = 7.2 Hz, 1H); **^{13}C NMR** (101 MHz, $CDCl_3$) δ 180.3, 176.1, 136.0, 128.8, 128.7, 128.0, 42.5, 36.5, 34.8, 16.8; **MS** (ESI) m/z = 204.0 $[M+H]^+$. All data were in accordance with the literature.[19]

1-benzyl-3-ethylpyrrolidine-2,5-dione (4.95)



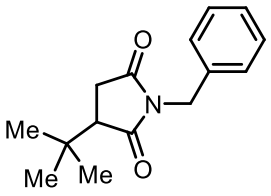
General procedure B was followed to obtain **4.95** (47 mg, 0.22 mmol, 43%) as a white solid. **^{1}H NMR** (400 MHz, $CDCl_3$) δ 7.40 − 7.19 (m, 5H), 4.62 (d, J = 1.5 Hz, 2H), 2.85 − 2.67 (m, 2H), 2.35 (dd, J = 13.6, 3.8 Hz, 1H), 1.95 − 1.81 (m, 1H), 1.56 (ddq, J = 13.7, 8.2, 7.3 Hz, 1H), 0.92 (t, J = 7.4 Hz, 3H); **^{13}C NMR** (101 MHz, $CDCl_3$) δ 179.6, 176.4, 136.0, 128.8, 128.7, 128.0, 42.4, 41.2, 33.9, 24.4, 10.9; **MS** (ESI) m/z = 218.0 $[M+H]^+$. All data were in accordance with the literature.[20]

1-benzyl-3-isopropylpyrrolidine-2,5-dione (4.96)



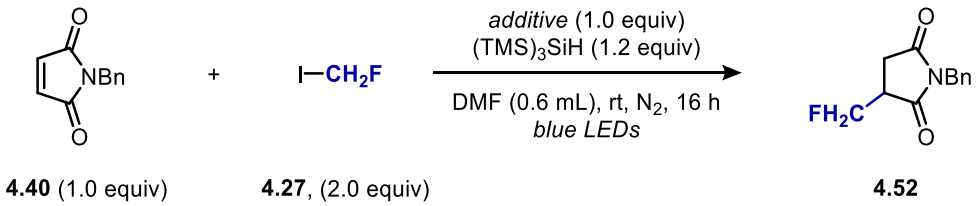
General procedure B was followed to obtain **4.96** (72 mg, 0.31 mmol, 62%) as a waxy solid. **^{1}H NMR** (400 MHz, $CDCl_3$) δ 7.35 − 7.16 (m, 5H), 4.58 (s, 2H), 2.72 (dt, *J* = 8.9, 4.3 Hz, 1H), 2.61 (dd, *J* = 18.2, 9.2 Hz, 1H), 2.39 (dd, *J* = 18.3, 4.4 Hz, 1H), 2.24 (hepd, *J* = 6.9, 4.3 Hz, 1H), 0.91 (d, *J* = 6.9 Hz, 3H), 0.75 (d, *J* = 6.8 Hz, 3zH); **^{13}C NMR** (101 MHz, $CDCl_3$) δ 179.1, 176.6, 136.0, 128.8, 128.6, 127.9, 45.7, 42.3, 30.4, 28.9, 20.0, 17.3; **HRMS** (ESI-TOF) calculated for $C_{14}H_{18}NO_2$ [M+H]+: 232.1332, found 232.1334; **IR** (neat) 2960, 1773, 1396, 1339, 1166, 1082, 695.

1-benzyl-3-(tert-butyl)pyrrolidine-2,5-dione (4.97)[a]



General procedure B was followed to obtain **4.97** (89 mg, 0.37 mmol, 73%) as a white solid. **^{1}H NMR** (400 MHz, $CDCl_3$) δ 7.34 − 7.15 (m, 5H), 4.58 (s, 2H), 2.70 − 2.41 (m, 3H), 0.95 (s, 9H); **^{13}C NMR** (101 MHz, $CDCl_3$) δ 178.2, 176.2, 136.1, 128.7, 128.6, 127.9, 49.8, 42.2, 33.5, 31.8, 27.2; **MS** (ESI) m/z = 246.0 $[M+H]^+$. All data were in accordance with the literature.[21]

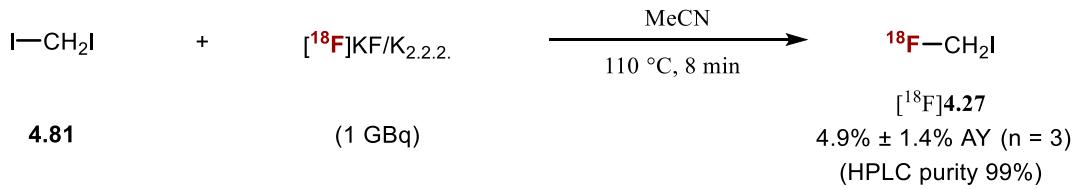
5.4.10 Robustness screen



Procedure: To an 7 mL vial equipped with a stir bar was added additive (0.1 mmol, 1.0 equiv), *N*-benzylmaleimide (18.7 mg, 0.1 mmol, 1.0 equiv.), DMF (dry; 0.6 mL), $(TMS)_3SiH$ (37 µL, 0.12 mmol, 1.2 equiv), fluoroiodomethane (CH_2FI) (13.6 µL, 0.2 mmol, 2.0 equiv.). The vial was sealed with a septum, degassed by nitrogen bubbling for 10 seconds and wrapped with parafilm. The reaction mixture was stirred in a SynLED Parallel Photoreactor with a 12W blue LED lamp (λ_{max} = 470 nm) at room temperature (using a fan) for 16 hours. α,α,α-Trifluorotoluene (internal standard, 123 µL, 1.0 mmol) was added, and the reaction mixture was analysed by quantitative ^{19}F NMR.

5.4.11 [^{18}F]-Hydrofluoromethylation of alkenes[a,c]

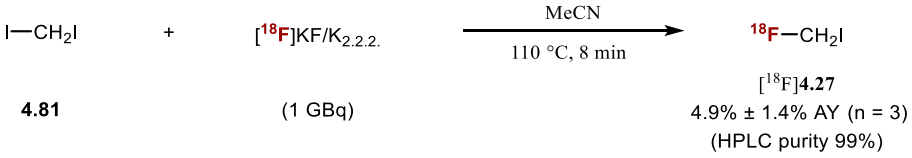
Synthesis and purification of [^{18}F]CH_2FI



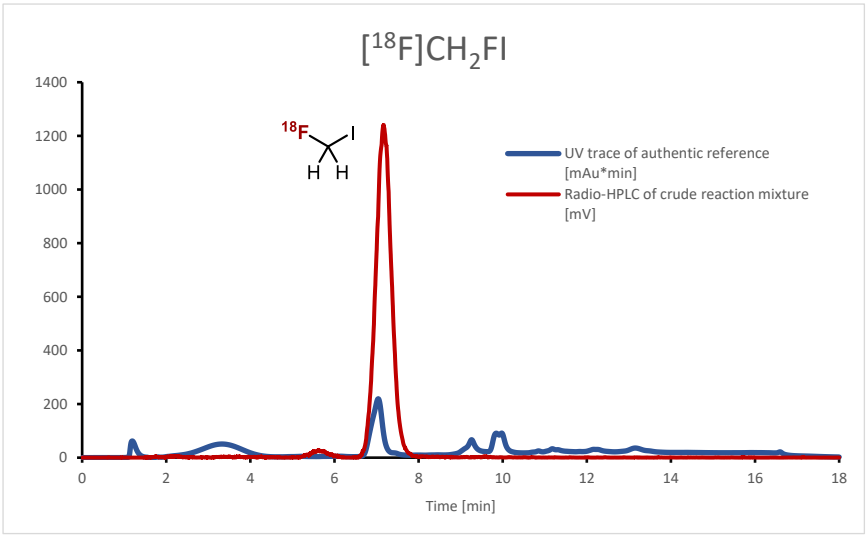
^{18}F-Fluoride was separated from ^{18}O-enriched-water using an anion exchange cartridge (Waters Sep-Pak AccellPlus QMA Carbonate Plus Light Cartridge, activated with H_2O (10.0 mL) prior to use) and released with a solution of Kryptofix (17 mg), and K_2CO_3 (3.5 mg) in MeCN/H_2O (0.75 mL, 4:1, v/v), which was concentrated by azeotropic drying. To dry [^{18}F]fluoride was added a solution of CH_2I_2 (50 µL in 1.0 mL) in dry MeCN. The vial was equipped with a PEEK line leading into a P_2O_5/NaOH cartridge. The outlet of this cartridge was leading to a v-vial containing DMF (1.0 mL) which was cooled to -20 °C. The reaction vial was heated to 110 °C for 5 minutes and the distilled product was analysed by radioHPLC. [^{18}F]CH_2FI was isolated in 4.9% ± 1.4% AY (n = 3).

^{18}F-Hydrofluoromethylation of electron-deficient alkenes

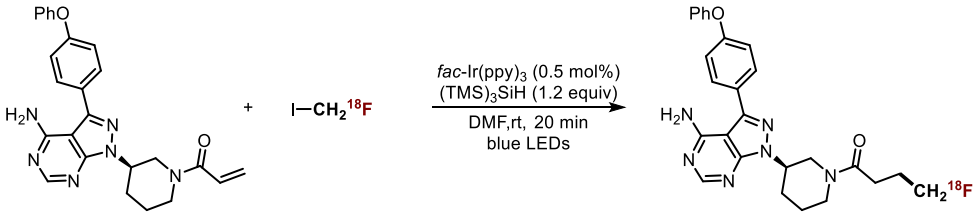
General Procedure: To a 1.75 mL vial containing alkene (0.1 mmol), $(TMS)_3SiH$ (37 µL, 0.12 mmol, 1.2 equiv), *fac*-Ir(ppy)$_3$ (0.5 mg) and DMF (300 µL) was added freshly distilled [^{18}F]CH_2FI (8 - 10 MBq) in DMF (300 µL). The mixture was placed in a photoreactor and left under blue LED irradiation for 20 min without stirring. An aliquot of this mixture was filtered and analysed by radioHPLC.



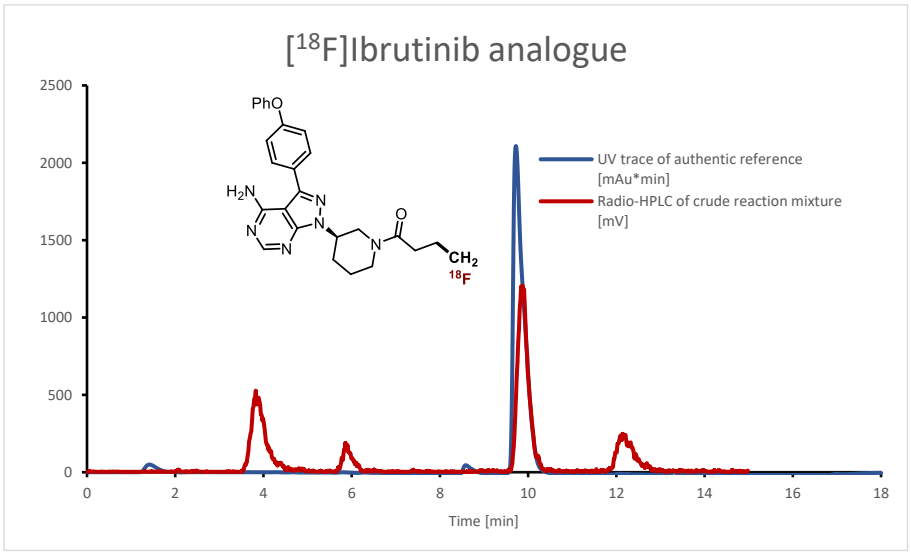
4.81 (1 GBq) [^{18}F]**4.27**
4.9% ± 1.4% AY (n = 3)
(HPLC purity 99%)



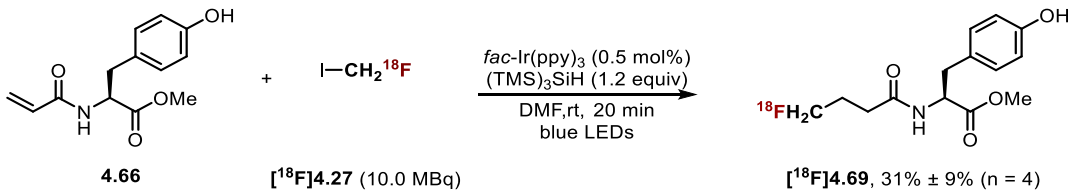
Overlay of UV and radioHPLC trace of CH_2FI

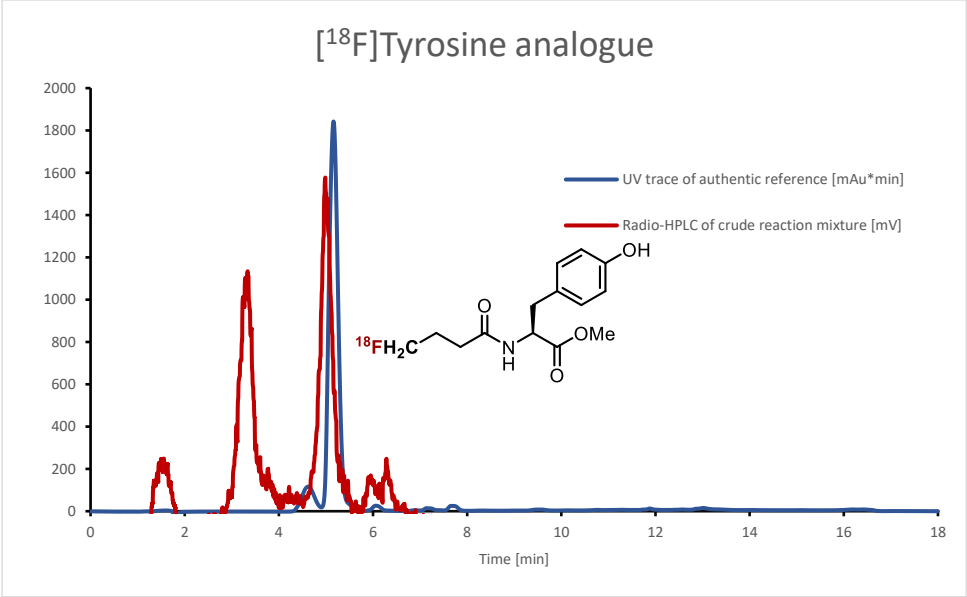


4.65 [^{18}F]**4.27** (10.0 MBq) [^{18}F]**4.68**, 43% ± 8% (n = 3)



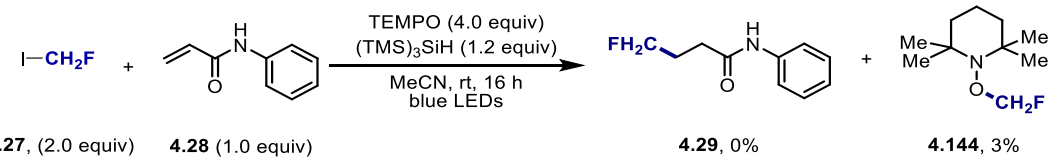
Overlay of UV and radioHPLC trace of Ibrutinib analogue





Overlay of UV and radioHPLC trace of tyrosine analogue.

5.4.12 Mechanistic investigation



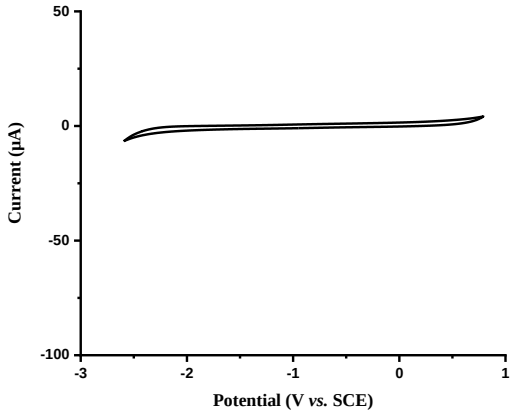
4.27, (2.0 equiv) **4.28** (1.0 equiv) **4.29**, 0% **4.144**, 3%

A suspension of *N*-phenylacrylamide **4.28** (74 mg, 0.5 mmol, 1.0 equiv), *fac*-Ir(ppy)$_3$ (3.3 mg, 0.005 mmol, 1.0 mol%), dry MeCN (3.0 mL), (TMS)$_3$SiH (185 uL, 0.6 mmol, 1.2 equiv), CH_2FI **4.27** (68 µL, 1.0 mmol, 2.0 equiv), and TEMPO (313 mg, 2.0 mmol, 4.0 equiv) was stirred under blue LED irradiation for 16 hours at room temperature. α,α,α-Trifluorotoluene (internal standard, 123 µL, 1.0 mmol) was added, and the reaction mixture was analysed by quantitative ^{19}F NMR. **^{19}F NMR** (377 MHz, $CDCl_3$) δ -137.59 (t, J = 57.0 Hz).

5.4.13 Cyclic Voltammetry[d]

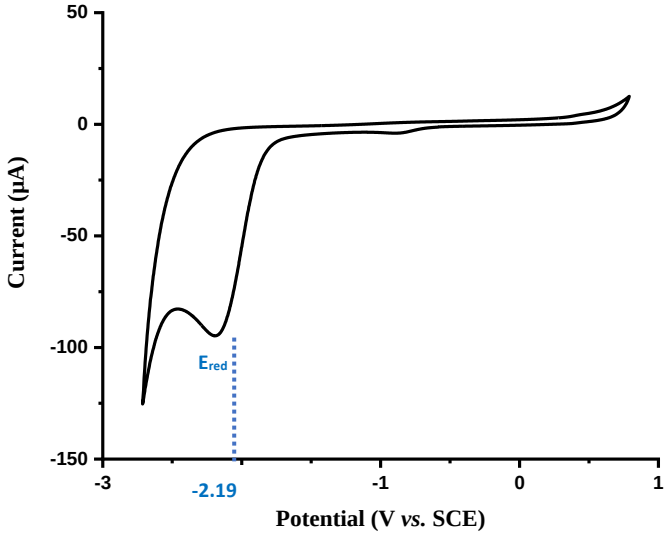
The cyclic voltammetry (CV) measurements were conducted at room temperature using an Autolab PGSTAT204 potentiostat (Metrohm, The Netherlands). Experiments were performed using a standard three-electrode setup, comprising a glassy carbon working electrode (diameter 3.0 mm, CH Instrument), an $Ag/AgNO_3$ (0.01 M) reference electrode and a Pt wire counter electrode. Before each measurement, the working electrode was mechanically polished with alumina slurries in the size 1.0 µm, 0.3 µm and 0.05 µm (purchased from Buehler Ltd, USA) respectively. All CV experiments were carried out at a concentration of 3 mM in anhydrous CH_3CN with an electrolyte $LiClO_4$ (0.1 M) at 100 mV/s scan rate. Solutions containing the compound of interest were thoroughly degassed with argon to remove oxygen prior to any measurement. The reduction potentials were measured against a ferrocene/ferrocenium (Fc/Fc^+) internal reference, and then converted to V vs. SCE (saturated calomel electrode) using the conversion $E°_{1/2}$ (Fc/Fc^+) = +0.400 V vs. SCE.

Background:



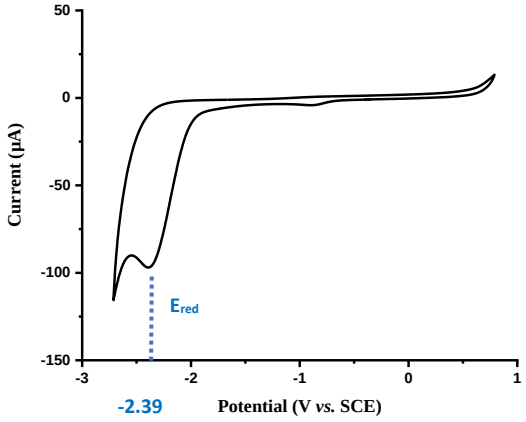
Voltammetric response of 0.1 M $LiClO_4$ in anhydrous CH_3CN. Experiment conducted by Xuanxiao Chen.

Fluoroiodomethane: *E* (V *vs.* SCE) = – 2.19 V



Voltammetric response of 3 mM fluoroiodomethane in anhydrous CH_3CN and 0.1 M $LiClO_4$. Experiment conducted by Xuanxiao Chen.

Methyl iodide: *E* (V *vs.* SCE) = – 2.39 V



Voltammetric response of 3 mM methyl iodide in anhydrous CH_3CN and 0.1 M $LiClO_4$. Experiment conducted by Xuanxiao Chen.

5.5 References

[1] X. J. Tang, W. R. Dolbier, *Angew. Chem. Int. Ed.* **2015**, *54*, 4246–4249.
[2] J. Eriksson, O. Åberg, B. Långström, *Eur. J. Org. Chem.* **2007**, 455–461.
[3] O. A. Al-Fulaij, A. Z. A. Elassar, A. F. El-Asmy, *J. Appl. Polym. Sci.* **2015**, *132*, 1–14.
[4] P. Rai, K. Maji, B. Maji, *Org. Lett.* **2019**, *21*, 3755–3759.
[5] A. Song, K. A. Parker, N. S. Sampson, *J. Am. Chem. Soc.* **2009**, *131*, 3444–3445.
[6] H. Xu, W. Zhang, D. Shu, J. B. Werness, W. Tang, *Angew. Chem. Int. Ed.* **2008**, *120*, 9065–9068.
[7] L. Palatinus, G. Chapuis, *J. Appl. Crystallogr.* **2007**, *40*, 786–790.
[8] R. I. Cooper, A. L. Thompson, D. J. Watkin, *J. Appl. Cryst.* **2010**, *43*, 1100–1107.
[9] P. W. Betteridge, J. R. Carruthers, R. I. Cooper, K. Prout, D. J. Watkin, P. W. Betteridge, J. R. Carruthers, I. Richard, K. Prout, D. J. Watkin, *Appl. Crystallogr.* **2003**, *36*, 1487-.
[10] Q. Y. Lin, X. H. Xu, K. Zhang, F. L. Qing, *Angew. Chem. Int. Ed.* **2016**, *55*, 1479–1483.
[11] Y. Xie, P. W. Sun, Y. Li, S. Wang, M. Ye, Z. Li, *Angew. Chem. Int. Ed.* **2019**, *58*, 7097–7101.
[12] H. K. Lo, F. T. Luo, *J. Chinese Chem. Soc.* **2012**, *59*, 394–398.
[13] P. J. Bhuyan, K. C. Lekhok, J. S. Sandhu, *Tetrahedron Lett.* **1999**, *40*, 1793–1794.
[14] J. E. Enholm, T. Low, D. Cooper, I. Ghivirija, *Tetrahedron* **2012**, *68*, 6920–6927.
[15] C. J. Teskey, P. Adler, C. R. Gonçalves, N. Maulide, *Angew. Chem. Int. Ed.* **2019**, *58*, 447–451.
[16] C. Descôteaux, K. Brasseur, V. Leblanc, E. Asselin, G. Bérubé, *Med. Chem. (Los. Angeles).* **2018**, *11*, 717–724.
[17] T. J. Saiegh, H. Chédotal, C. Meyer, J. Cossy, *Org. Lett.* **2019**, *21*, 8364–8368.
[18] M. Nambo, J. C. H. Yim, L. B. O. Freitas, Y. Tahara, Z. T. Ariki, Y. Maekawa, D. Yokogawa, C. M. Crudden, *Nat. Commun.* **2019**, *10*, 1–7.
[19] M. D. Barker, R. A. Dixon, S. Jones, B. J. Marsh, *Chem. Commun.* **2008**, 2218–2220.
[20] E. Dardennes, S. Labano, N. S. Simpkins, C. Wilson, *Tetrahedron Lett.* **2007**, *48*, 6380–6383.
[21] Y. X. Li, W. Y. Li, Y. Y. Jiang, L. Yang, *Tetrahedron Lett.* **2018**, *59*, 2934–2937.